IUCr Texts on Crystallography · 13

Crystal Structure Analysis

Principles and Practice

Second Edition

ALEXANDER J. BLAKE,
WILLIAM CLEGG,
JACQUELINE M. COLE,
JOHN S. O. EVANS, PETER MAIN,
SIMON PARSONS,
DAVID J. WATKIN

Edited by WILLIAM CLEGG

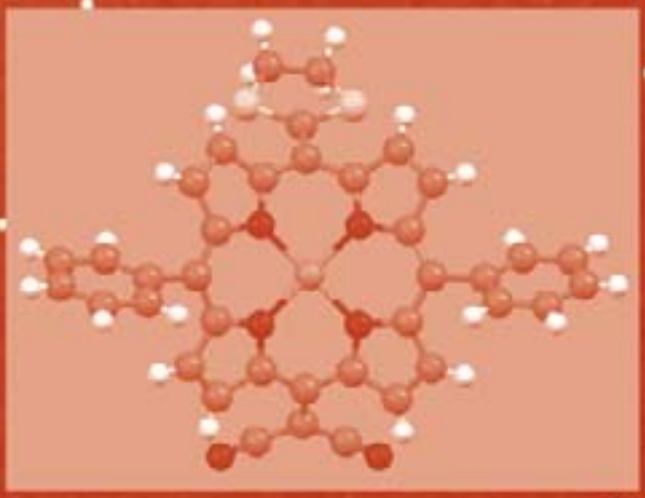

INTERNATIONAL UNION OF CRYSTALLOGRAPHY

OXFORD SCIENCE PUBLICATIONS

INTERNATIONAL UNION OF CRYSTALLOGRAPHY
BOOK SERIES

IUCr BOOK SERIES COMMITTEE

J. Bernstein, *Israel*
G. R. Desiraju, *India*
J. R. Helliwell, *UK*
T. Mak, *China*
P. Müller, *USA*
P. Paufler, *Germany*
H. Schenk, *The Netherlands*
P. Spadon, *Italy*
D. Viterbo (*Chairman*), *Italy*

IUCr Monographs on Crystallography

1 *Accurate molecular structures*
A. Domenicano, I. Hargittai, editors
2 *P.P. Ewald and his dynamical theory of X-ray diffraction*
D.W.J. Cruickshank, H.J. Juretschke, N. Kato, editors
3 *Electron diffraction techniques, Vol. 1*
J.M. Cowley, editor
4 *Electron diffraction techniques, Vol. 2*
J.M. Cowley, editor
5 *The Rietveld method*
R.A. Young, editor
6 *Introduction to crystallographic statistics*
U. Shmueli, G.H. Weiss
7 *Crystallographic instrumentation*
L.A. Aslanov, G.V. Fetisov, J.A.K. Howard
8 *Direct phasing in crystallography*
C. Giacovazzo
9 *The weak hydrogen bond*
G.R. Desiraju, T. Steiner
10 *Defect and microstructure analysis by diffraction*
R.L. Snyder, J. Fiala and H.J. Bunge
11 *Dynamical theory of X-ray diffraction*
A. Authier
12 *The chemical bond in inorganic chemistry*
I.D. Brown
13 *Structure determination from powder diffraction data*
W.I.F. David, K. Shankland, L.B. McCusker, Ch. Baerlocher, editors

14 *Polymorphism in molecular crystals*
J. Bernstein
15 *Crystallography of modular materials*
G. Ferraris, E. Makovicky, S. Merlino
16 *Diffuse x-ray scattering and models of disorder*
T.R. Welberry
17 *Crystallography of the polymethylene chain: an inquiry into the structure of waxes*
D.L. Dorset
18 *Crystalline molecular complexes and compounds: structure and principles*
F. H. Herbstein
19 *Molecular aggregation: structure analysis and molecular simulation of crystals and liquids*
A. Gavezzotti
20 *Aperiodic crystals: from modulated phases to quasicrystals*
T. Janssen, G. Chapuis, M. de Boissieu
21 *Incommensurate crystallography*
S. van Smaalen
22 *Structural crystallography of inorganic oxysalts*
S.V. Krivovichev
23 *The nature of the hydrogen bond: outline of a comprehensive hydrogen bond theory*
G. Gilli, P. Gilli
24 *Macromolecular crystallization and crystal perfection*
N.E. Chayen, J.R. Helliwell, E.H. Snell

IUCr Texts on Crystallography

1 *The solid state*
A. Guinier, R. Julien
4 *X-ray charge densities and chemical bonding*
P. Coppens
7 *Fundamentals of crystallography, second edition*
C. Giacovazzo, editor
8 *Crystal structure refinement: a crystallographer's guide to SHELXL*
P. Müller, editor
9 *Theories and techniques of crystal structure determination*
U. Shmueli
10 *Advanced structural inorganic chemistry*
Wai-Kee Li, Gong-Du Zhou, Thomas Mak
11 *Diffuse scattering and defect structure simulations: a cook book using the program DISCUS*
R. B. Neder, T. Proffen
12 *The basics of crystallography and diffraction, third edition*
C. Hammond
13 *Crystal structure analysis: principles and practice, second edition*
W. Clegg, editor

Crystal Structure Analysis

Principles and Practice

Second Edition

Alexander J. Blake

School of Chemistry, University of Nottingham

William Clegg

Department of Chemistry, University of Newcastle upon Tyne

Jacqueline M. Cole

Cavendish Laboratory, University of Cambridge

John S.O. Evans

Department of Chemistry, University of Durham

Peter Main

Department of Physics, University of York

Simon Parsons

Department of Chemistry, University of Edinburgh

David J. Watkin

Chemical Crystallography Laboratory, University of Oxford

Edited by

William Clegg

OXFORD
UNIVERSITY PRESS

OXFORD
UNIVERSITY PRESS
Great Clarendon Street, Oxford ox2 6dp

Oxford University Press is a department of the University of Oxford.
It furthers the University's objective of excellence in research, scholarship,
and education by publishing worldwide in

Oxford New York

Auckland Cape Town Dar es Salaam Hong Kong Karachi
Kuala Lumpur Madrid Melbourne Mexico City Nairobi
New Delhi Shanghai Taipei Toronto

With offices in

Argentina Austria Brazil Chile Czech Republic France Greece
Guatemala Hungary Italy Japan Poland Portugal Singapore
South Korea Switzerland Thailand Turkey Ukraine Vietnam

Oxford is a registered trade mark of Oxford University Press
in the UK and in certain other countries

Published in the United States
by Oxford University Press Inc., New York

© Alexander J. Blake, William Clegg, Jacqueline M. Cole, John S.O. Evans,
Peter Main, Simon Parsons, and David J. Watkin, 2009

The moral rights of the authors have been asserted
Database right Oxford University Press (maker)

First edition first published 2001, reprinted 2006
Second edition first published 2009

All rights reserved. No part of this publication may be reproduced,
stored in a retrieval system, or transmitted, in any form or by any means,
without the prior permission in writing of Oxford University Press,
or as expressly permitted by law, or under terms agreed with the appropriate
reprographics rights organization. Enquiries concerning reproduction
outside the scope of the above should be sent to the Rights Department,
Oxford University Press, at the address above

You must not circulate this book in any other binding or cover
and you must impose the same condition on any acquirer

British Library Cataloguing in Publication Data
Data available

Library of Congress Cataloging in Publication Data

Crystal structure analysis : principles and practice / William Clegg . . . [et al.]. — 2nd ed.
p. cm. — (International Union of Crystallography book series; 13)
ISBN 978–0–19–921946–9 (hardback) — ISBN 978–0–19–921947–6 (pbk.)
1. X-ray crystallography. 2. Crystals—Structure. I. Clegg, William, 1949–
QD945.C79 2009
548′.81—dc22 2009011644

Typeset by Newgen Imaging Systems (P) Ltd., Chennai, India
Printed in Great Britain
on acid-free paper by
CPI Antony Rowe, Chippenham, Wilts

ISBN: 978–0–19–921946–9
ISBN: 978–0–19–921947–6

1 3 5 7 9 10 8 6 4 2

Preface

The material in this book is derived from an intensive course in X-ray structure analysis organized on behalf of the Chemical Crystallography Group of the British Crystallographic Association and held every two years since 1987. As with a crystal structure derived from X-ray diffraction data, the course contents have been gradually refined over the years and they reached a stage in 1999 (the seventh course) where we considered they could be published, and hence made available to a far wider audience than can be accommodated on the course itself. The result was the first edition of this book, published in 2001. The authors were the principal lecturers on the course in 1999 and they revised and expanded the material, while converting the lecture notes into a book format. Because of its origin, the book represented a snapshot of the intensive course, which has continued to evolve, especially as the subject of chemical crystallography has undergone significant changes, mainly due to the widespread availability of area detector technology, the exponential increase in computing power and improvements in software, and greater use of synchrotron radiation and powder diffraction. Nevertheless, the underlying principles remain valid, and the particular application of those principles can be adapted to new developments for some time to come.

By the time of the eleventh course in 2007, its contents and the team of principal lecturers had changed markedly, and we were asked to consider a second edition of the book reflecting these developments. This has been encouraged and assisted by the use of a consistent template for the 2007 course notes, and these have been used as the basis for this new edition. Nevertheless, any readers who participated in the 2007 course will detect a number of changes, particularly in the inclusion of some material not covered in the lecture notes, some updating, and differences of style made necessary by a non-interactive format.

Since this book, like its first edition, owes its origins to the course, we acknowledge here our large debt to those who have dedicated much effort to the organization of the course since its inception; without them this book would never have existed, even as an idea. The first five courses were held at the University of Aston, where the local organizers Phil Lowe and Carl Schwalbe set a gold standard of course administration and smooth operation, establishing many of the enduring characteristics valued by participants ever since. Following the move to the University of Durham, Vanessa Hoy and then Claire Wilson developed these firm foundations to even further heights of excellence, presenting a

challenge to Andres Goeta, who took over for the 2009 Course. Throughout the course's history Judith Howard has provided overall guidance and expertise, particularly in fund raising, and has spared the course lecturers much concern with the practicalities of maintaining and promoting the course. Several organizations, including the EPSRC, IUCr, BCA and commercial sponsors, have been long-standing and generous supporters of the course.

The first course in 1987 was the brainchild of David Watkin, who worked extremely hard to launch it and establish it as the enduring success that it has become. His role as course director was taken over in the mid-1990s by Bob Gould, who passed on the baton to Sandy Blake after 1999; from 2011 the director will be Simon Parsons. The template for the lecture notes on which this book is based was developed by Horst Puschmann, and Amber Thompson has looked after assembling and producing the notes for the last few courses.

Many colleagues have made contributions to the course over the years, in lectures and in the crucial group tutorial sessions: a book format can never reflect the intensive interaction and lively atmosphere. These and the social aspects of the course are probably at least as important in the memories of participants as the formal lecture presentations. One aspect of the tutorial group sessions of the course has been retained in modified form in the book. Most chapters include exercises, for which answers are provided in an appendix. Readers are encouraged to tackle the exercises at leisure and not consult the answers until they are satisfied with their own efforts. In the spirit of the tutorials, these exercises may also prove beneficial as a basis for group discussion.

Over the twenty years of the course and its eleven occasions, we have seen former students return as group tutors, and tutors move on into lecturer roles. Course participants, from many countries, are established practising crystallographers in academic and industrial posts around the world. Courses elsewhere have been developed, modelled on our experience. We dedicate this book to the hundreds of students who have been the course's primary beneficiaries and whose hard work and commitment, intellectually and socially, have contributed much to its success.

Bill Clegg,
Newcastle University
November 2008
Editor, on behalf of the authors

Acknowledgements

We are grateful to authors and publishers for their permission to reproduce some of the Figures that appear in this book, as follows.

Figures 1.1, 1.8, 2.1, 2.2, 22.1, 22.2, and 22.4 from W. Clegg: *Crystal Structure Determination*. Oxford University Press, Oxford, 1998.

Figures 1.2 and 4.1 from C. Giaccovazzo, H. L. Monaco, D. Viterbo, F. Scordari, G. Gilli, G. Zanotti and M. Catti: *Fundamentals of Crystallography*. Oxford University Press, Oxford, 1992.

Figures 1.3 and 1.5 from G. Harburn, C. A. Taylor and T. R. Welberry: *Atlas of Optical Transforms*. G. Bell, London, 1975.

Figure 1.9 from J. P. Glusker and K. N. Trueblood: *Crystal Structure Analysis – A Primer*, Second Edition. Oxford University Press, Oxford, 1985.

Figures 2.3 and 2.4 from Traidcraft plc, Gateshead, UK.

Figures 5.6 and 5.7 from Rigaku Corporation, Sevenoaks, Kent, UK.

Figure 6.1 from Stoe & Cie GmbH, Darmstadt, Germany.

Figures 8.5–8.8 from W. Clegg, *J. Chem. Educ.* **81**, 908; copyright 2004. American Chemical Society.

Figure 10.1, reprinted by permission from G. N. Ramachandran and R. Srinavasan, *Nature*, **190**, 161; copyright 1961. Macmillan Magazines Ltd.

Figure 14.3 from R. B. Neder and T. Proffen: *Diffuse Scattering and Defect Structure Simulations: A Cook Book Using the Program DISCUS*. Oxford University Press, Oxford, 2008.

Figure 14.14 from *International Tables for Crystallography, Volume A*. Kluwer Academic Press, Dordrecht, The Netherlands. Copyright 1983, International Union of Crystallography.

Figure 17.2 from Panalytical Ltd, Cambridge, UK.

Figure 17.4 from R. Haberkorn, personal communication to J. S. O. Evans, 1999.

Figure 18.1 from S. Parsons, *Acta Crystallogr.* **D59**, 1995. Copyright International Union of Crystallography, 2003.

Figure 22.3 from Diamond Light Source, Didcot, Oxfordshire, UK.

This page intentionally left blank

Contents

1 Introduction to diffraction **1**
- 1.1 Introduction 1
- 1.2 X-ray scattering from electrons 1
- 1.3 X-ray scattering from atoms 1
- 1.4 X-ray scattering from a unit cell 2
- 1.5 The effects of the crystal lattice 2
- 1.6 X-ray scattering from the crystal 3
- 1.7 The structure-factor equation 4
- 1.8 The electron-density equation 5
- 1.9 A mathematical relationship 6
- 1.10 Bragg's law 6
- 1.11 Resolution 7
- 1.12 The phase problem 8

2 Introduction to symmetry and diffraction **9**
- 2.1 The relationship between a crystal structure and its diffraction pattern 9
- 2.2 Translation symmetry in crystalline solids 10
- 2.3 Symmetry of individual molecules, with relevance to crystalline solids 12
- 2.4 Symmetry in the solid state 16
- 2.5 Diffraction and symmetry 18
- 2.6 Further points 20

Exercises 24

3 Crystal growth and evaluation **27**
- 3.1 Introduction 27
- 3.2 Protect your crystals 27
- 3.3 Crystal growth 28
- 3.4 Survey of methods 28
  - 3.4.1 Solution methods 28
  - 3.4.2 Sublimation 33
  - 3.4.3 Fluid-phase growth 33
  - 3.4.4 Solid-state synthesis 34
  - 3.4.5 General comments 34

3.5 Evaluation 35
3.5.1 Microscopy 35
3.5.2 X-ray photography 36
3.5.3 Diffractometry 36
3.6 Crystal mounting 36
3.6.1 Standard procedures 36
3.6.2 Air-sensitive crystals 38
3.6.3 Crystal alignment 39

4 Space-group determination 41
4.1 Introduction 41
4.2 Prior knowledge and information other than from diffraction 42
4.3 Metric symmetry and Laue symmetry 43
4.4 Unit cell contents 43
4.5 Systematic absences 44
4.6 The statistical distribution of intensities 47
4.7 Other points 48
4.8 A brief conducted tour of some entries in International Tables for Crystallography, Volume A 50
Exercises 52

5 Background theory for data collection 53
5.1 Introduction 53
5.2 A step-wise theoretical journey through an experiment 53
5.3 The geometry of X-ray diffraction 55
5.3.1 Real-space considerations: Bragg's law 55
5.3.2 Reciprocal-space considerations: the Ewald sphere 56
5.4 Determining the unit cell: the indexing process 58
5.4.1 Indexing: a conceptual view 58
5.4.2 Indexing procedure 60
5.5 Relating diffractometer angles to unit cell parameters: determination of the orientation matrix 62
5.6 Data-collection procedures and strategies 64
5.6.1 Criteria for selecting which data to collect 64
5.6.2 How best to measure data: the need for reflection scans 65
5.7 Extracting data intensities: data integration and reduction 67
5.7.1 Background subtraction 67
5.7.2 Data integration 68
5.7.3 Crystal and geometric corrections to data 68
Exercises 72

6 Practical aspects of data collection 73
6.1 Introduction 73

6.2 Collecting data with area-detector diffractometers 73
6.3 Experimental conditions 75
6.3.1 Radiation 75
6.3.2 Temperature 76
6.3.3 Pressure 77
6.3.4 Other conditions 77
6.4 Types of area detector 77
6.4.1 Multiwire proportional chamber (MWPC) 77
6.4.2 Phosphor coupled to a TV camera 78
6.4.3 Image plate (IP) 78
6.4.4 Charge-coupled device (CCD) 78
6.5 Some characteristics of CCD area-detector systems 80
6.5.1 Spatial distortion 81
6.5.2 Non-uniform intensity response 81
6.5.3 Bad pixels 81
6.5.4 Dark current 81
6.6 Crystal screening 82
6.6.1 Unit cell and orientation matrix determination 84
6.6.2 If indexing fails 86
6.6.3 Re-harvest the reflections 86
6.6.4 Still having problems? 87
6.6.5 After indexing 87
6.6.6 Check for known cells 87
6.6.7 Unit cell volume 88
6.7 Data collection 88
6.7.1 Intensity level 88
6.7.2 Mosaic spread 89
6.7.3 Crystal symmetry 89
6.7.4 Other considerations 90
Exercises 91

7 Practical aspects of data processing 93
7.1 Data reduction and correction 93
7.2 Integration input and output 93
7.3 Corrections 94
7.4 Output 95
7.5 A typical experiment? 95
7.6 Examples of more problematic cases 96
7.7 Twinning and area-detector data 98
7.8 Some other special cases (in brief) 99
Exercises 101

8 Fourier syntheses 103
8.1 Introduction 103
8.2 Forward and reverse Fourier transforms 104
8.3 Some mathematical and computing considerations 107
8.4 Uses of different kinds of Fourier syntheses 108

8.4.1 Patterson syntheses 109
8.4.2 *E*-maps 109
8.4.3 Full electron-density maps, using (8.2) or (8.3) as they stand 109
8.4.4 Difference syntheses 110
8.4.5 $2F_o - F_c$ syntheses 111
8.4.6 Other uses of difference syntheses 112
8.5 Weights in Fourier syntheses 112
8.6 Illustration in one dimension 113
8.6.1 F_c synthesis 114
8.6.2 F_o synthesis, as used in developing a partial structure solution 114
8.6.3 $F_o - F_c$ synthesis 114
8.6.4 Full F_o synthesis 114
Exercises 115

9 Patterson syntheses for structure determination 117
9.1 Introduction 117
9.2 What the Patterson synthesis means 118
9.3 Finding heavy atoms from a Patterson map 121
9.3.1 One heavy atom in the asymmetric unit of $P\bar{1}$ 121
9.3.2 One heavy atom in the asymmetric unit of $P2_1/c$ 122
9.3.3 One heavy atom in the asymmetric unit of $P2_12_12_1$ 124
9.3.4 One heavy atom in the asymmetric unit of *Pbca* 124
9.3.5 One heavy atom in the asymmetric unit of $P2_1$ 125
9.3.6 Two heavy atoms in the asymmetric unit of $P\bar{1}$ and other space groups 125
9.4 Patterson syntheses giving more than one possible solution, and other problems 126
9.5 Patterson search methods 128
9.5.1 Rotation search 129
9.5.2 Translation search 129
Exercises 131

10 Direct methods of crystal-structure determination 133
10.1 Amplitudes and phases 133
10.2 The physical basis of direct methods 134
10.3 Constraints on the electron density 135
10.3.1 Discrete atoms 135
10.3.2 Non-negative electron density 136
10.3.3 Random atomic distribution 137
10.3.4 Maximum value of $\int \rho^3(x)dV$ 139

10.3.5 Equal atoms 139
10.3.6 Maximum entropy 140
10.3.7 Equal molecules and $\rho(x) = \text{const.}$ 140
10.3.8 Structure invariants 140
10.3.9 Structure determination 141
10.3.10 Calculation of E values 142
10.3.11 Setting up phase relationships 142
10.3.12 Finding reflections for phase determination 142
10.3.13 Assignment of starting phases 144
10.3.14 Phase determination and refinement 144
10.3.15 Figures of merit 144
10.3.16 Interpretation of maps 145
10.3.17 Completion of the structure 146
Exercises 147

11 An introduction to maximum entropy 149
11.1 Entropy 149
11.2 Maximum entropy 150
11.2.1 Calculations with incomplete data 150
11.2.2 Forming images 152
11.2.3 Entropy and probability 152
11.3 Electron-density maps 153

12 Least-squares fitting of parameters 155
12.1 Weighted mean 155
12.2 Linear regression 156
12.2.1 Variances and covariances 158
12.2.2 Restraints 158
12.2.3 Constraints 160
12.3 Non-linear least squares 162
12.4 Ill-conditioning 164
12.5 Computing time 165
Exercises 167

13 Refinement of crystal structures 169
13.1 Equations 169
13.1.1 Bragg's law 170
13.1.2 Structure factors from the continuous electron density 170
13.1.3 Electron density from the structure amplitude and phase 170
13.1.4 Structure factor from a parameterized model 172
13.2 Reasons for performing refinement 172
13.2.1 To improve phasing so that computed electron density maps more closely represent the actual electron density 172
13.2.2 To try to verify that the structure is 'correct' 173

13.2.3 To obtain the 'best' values for the parameters in the model 175
13.3 Data quality and limitations 175
13.3.1 Resolution 175
13.3.2 Completeness 176
13.3.3 Leverage 176
13.3.4 Weak reflections and systematic absences 176
13.3.5 Standard uncertainties 177
13.3.6 Systematic trends 177
13.4 Refinement fundamentals 177
13.4.1 w, the weight 178
13.4.2 Y_1, the observations 178
13.4.3 Y_2, the calculations 179
13.4.4 Issues 180
13.5 Refinement strategies 180
13.6 Under- and over-parameterization 182
13.6.1 Under-parameterization 182
13.6.2 Over-parameterization 183
13.7 Pseudo-symmetry, wrong space groups and $Z' > 1$ structures 183
13.8 Conclusion 184
Exercises 186

14 Analysis of extended inorganic structures 189
14.1 Introduction 189
14.2 Disorder 190
14.2.1 Site-occupancy disorder 191
14.2.2 Positional disorder 192
14.2.3 Limits of Bragg diffraction 193
14.3 Phase transitions 194
14.4 Structure validation 195
14.5 Case history 1 – $BiMg_2VO_6$ 196
14.6 Case history 2 – $Mo_2P_4O_{15}$ 199
Exercises 203

15 The derivation of results 205
15.1 Introduction 205
15.2 Geometry calculations 205
15.2.1 Fractional and Cartesian co-ordinates 205
15.2.2 Bond distance and angle calculations 207
15.2.3 Dot products 208
15.2.4 Transforming co-ordinates 208
15.2.5 Standard uncertainties 209
15.2.6 Assessing significant differences 211
15.3 Least-squares planes and dihedral angles 211
15.3.1 Conformation of rings and other molecular features 213
15.4 Hydrogen atoms and hydrogen bonding 213

15.5 Displacement parameters 214
15.5.1 βs, Bs and Us 215
15.5.2 'The equivalent isotropic displacement parameter' 215
15.5.3 Symmetry and anisotropic displacement parameters 216
15.5.4 Models of thermal motion and geometrical corrections: rigid-body motion 217
15.5.5 Atomic displacement parameters and temperature 218
Exercises 219

16 Random and systematic errors 221
16.1 Random and systematic errors 221
16.2 Random errors and distributions 222
16.2.1 Measurement errors 222
16.2.2 Describing data 222
16.2.3 Theoretical distributions 225
16.2.4 Expectation values 227
16.2.5 The standard error on the mean 229
16.3 Taking averages 229
16.3.1 Testing for normality using a histogram 230
16.3.2 The χ^2 test for normality 231
16.3.3 Averaging data when $\chi^2_{red} \gg 1$ 232
16.4 Weighting schemes 232
16.4.1 Weights used in least-squares refinement with single-crystal diffraction data 233
16.4.2 Robust-resistant weighting schemes and outliers 234
16.4.3 Assessing weighting schemes 235
16.5 Analysis of the agreement between observed and calculated data 238
16.5.1 R factors 238
16.5.2 Significance testing 239
16.6 Estimated standard deviations and standard uncertainties of structural parameters 240
16.6.1 Correlation and covariance 240
16.6.2 Uncertainty propagation 242
16.7 Systematic errors 242
16.7.1 Systematic errors in the data 243
16.7.2 Data thresholds 244
16.7.3 Errors and limitations of the model 244
16.7.4 Assessment of a structure determination 247
Exercises 250

17 Powder diffraction 251
17.1 Introduction to powder diffraction 251
17.2 Powder versus single-crystal diffraction 252

17.3 Experimental methods 254
17.4 Information contained in a powder pattern 258
17.4.1 Phase identification 258
17.4.2 Quantitative analysis 259
17.4.3 Peak-shape information 260
17.4.4 Intensity information 261
17.5 Rietveld refinement 261
17.6 Structure solution from powder diffraction data 264
17.7 Non-ambient studies 265
Exercises 268

18 Introduction to twinning 271
18.1 Introduction 271
18.2 A simple model for twinning 271
18.3 Twinning in crystals 272
18.4 Diffraction patterns from twinned crystals 274
18.5 Inversion, merohedral and pseudo-merohedral twins 276
18.6 Derivation of twin laws 279
18.7 Non-merohedral twinning 280
18.8 The derivation of non-merohedral twin laws 282
18.9 Common signs of twinning 283
18.10 Examples 285
Exercises 296

19 The presentation of results 299
19.1 Introduction 299
19.2 Graphics 300
19.3 Graphics programs 300
19.4 Underlying concepts 301
19.5 Drawing styles 302
19.6 Creating three-dimensional illusions 306
19.7 The use of colour 307
19.8 Textual information in drawings 307
19.9 Some hints for effective drawings 308
19.10 Tables of results 309
19.11 The content of tables 310
19.11.1 Selected results 310
19.11.2 Redundant information 311
19.11.3 Additional entries 311
19.12 The format of tables 312
19.13 Hints on presentation 312
19.13.1 In research journals 312
19.13.2 In theses and reports 313
19.13.3 On posters 313
19.13.4 As oral presentations 313
19.13.5 On the web 314
19.14 Archiving of results 315

20 The crystallographic information file (CIF) 319
20.1 Introduction 319
20.2 Basics 319
20.3 Uses of CIF 321
20.4 Some properties of the CIF format 321
20.5 Some practicalities 323
20.5.1 Strings 323
20.5.2 Text 324
20.5.3 Checking the CIF 325

21 Crystallographic databases 327
21.1 What is a database? 327
21.2 What types of search are possible? 327
21.3 What information can you get out? 328
21.4 What can you use databases for? 328
21.5 What are the limitations? 328
21.6 Short descriptions of crystallographic databases 328

22 X-ray and neutron sources 333
22.1 Introduction 333
22.2 Laboratory X-ray sources 333
22.3 Synchrotron X-ray sources 335
22.4 Neutron sources 339

A Appendix A: Useful mathematics and formulae 343
A.1 Introduction 343
A.2 Trigonometry 343
A.3 Complex numbers 344
A.4 Waves and structure factors 345
A.5 Vectors 346
A.6 Determinants 348
A.7 Matrices 348
A.8 Matrices in symmetry 349
A.9 Matrix inversion 350
A.10 Convolution 351

B Appendix B: Questions and answers 353

Index 385

This page intentionally left blank

Introduction to diffraction

1

Peter Main

1.1 Introduction

The subsequent chapters in this book will assume some basic knowledge of crystal-structure determination. As readers will be at very different levels, we wish to make sure you have available some of the fundamentals of the subject that will be developed in the book. It is not necessary to understand everything in this introduction before reading further, but we hope that it will provide helpful reference material for some of the chapters.

1.2 X-ray scattering from electrons

The scattering of X-rays from electrons is called Thomson scattering. It occurs because the electron oscillates in the electric field of the incoming X-ray beam and an oscillating electric charge radiates electromagnetic waves. Thus, X-rays are radiated from the electron at the same frequency as the primary beam. However, most electrons radiate π radians (180°) out of phase with the incoming beam, as shown by a mathematical model of the process. The motion of an electron is heavily damped when the X-ray frequency is close to the electron resonance frequency. This occurs near an absorption edge of the atom, changing the relative phase of the radiated X-rays to $\pi/2$ and giving rise to the phenomenon of anomalous (resonant) scattering.

1.3 X-ray scattering from atoms

There is a path difference between X-rays scattered from different parts of the same atom, resulting in destructive interference that depends upon the scattering angle. This reduction in X-rays scattered from an atom with increasing angle is described by the atomic scattering factor, illustrated in Fig. 1.1. The value of the scattering factor at zero scattering angle is equal to the number of electrons in the atom. The atomic scattering factors illustrated are for stationary atoms, but atoms are normally subject to thermal vibration. This movement modifies the scattering factor and must always be taken into account.

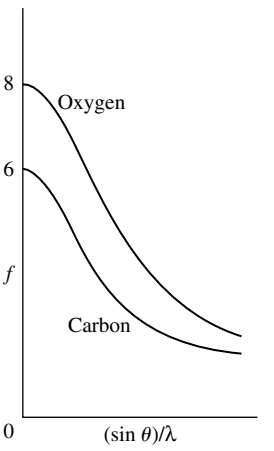

Fig. 1.1 Atomic scattering factors.

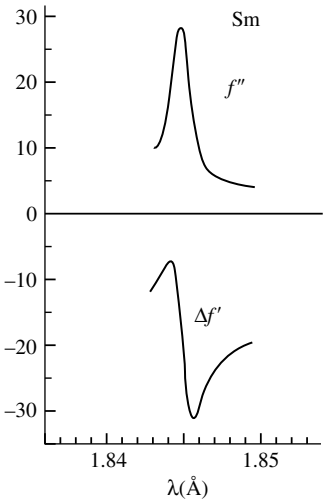

Fig. 1.2 Real ($\Delta f'$) and imaginary (f'') contributions to anomalous scattering for the example of a samarium atom.

If anomalous scattering takes place, the atomic scattering factor is altered to take this into account. This occurs when the X-ray frequency is close to the resonance frequency of an electron. Only some of the electrons in the atom are affected and they will scatter the X-rays roughly $\pi/2$ out of phase with the incident beam. Electrons scattering exactly $\pi/2$ out of phase are represented mathematically by an imaginary component of the scattering factor and they cease to contribute to the real part. The exact phase change is very sensitive to the X-ray frequency. This is shown in Fig. 1.2 that displays the real and imaginary parts of the contribution to the atomic scattering factor of the anomalously scattering electrons as a function of wavelength. The remaining electrons in the atom are unaffected by this change in wavelength. Such information on atomic scattering factors is obtained from quantum-mechanical calculations.

1.4 X-ray scattering from a unit cell

X-rays scattered from each atom in the unit cell contribute to the overall scattering pattern. Since each atom acts as a source of scattered X-rays, the waves will add constructively or destructively in varying amounts depending upon the direction of the diffracted beam and the atomic positions. This gives a complicated diffraction pattern whose amplitude and phase vary continuously, as can be seen in the two-dimensional optical analogue in Fig. 1.3.

1.5 The effects of the crystal lattice

The diffraction pattern of the crystal lattice is also a lattice, known as the reciprocal lattice. The name comes from the reciprocal relationship between the two lattices – large crystal lattice spacings result in small spacings in the reciprocal lattice and vice versa. The direct cell parameters are normally represented by $a, b, c, \alpha, \beta, \gamma$ and the reciprocal lattice parameters by $a^*, b^*, c^*, \alpha^*, \beta^*, \gamma^*$. The direction of a^* is perpendicular to the directions of b and c and its magnitude is reciprocal to the

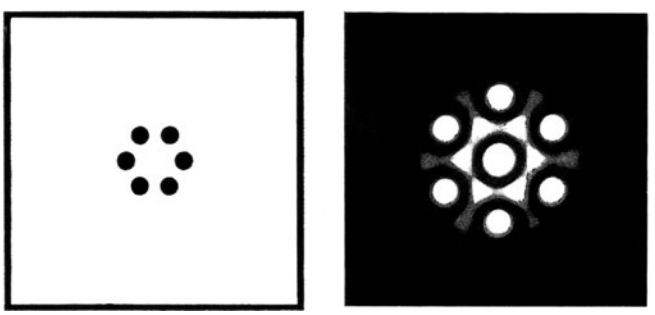

Fig. 1.3 Holes in an opaque sheet and their optical diffraction pattern.

spacing of the lattice planes parallel to b and c; similarly for b^* and c^*. A two-dimensional example of the relationship between the direct and reciprocal lattices is shown in Fig. 1.4.

1.6 X-ray scattering from the crystal

A combination (convolution) of a single unit cell with the crystal lattice gives the complete crystal. The X-ray diffraction pattern is therefore given by the product of the scattering from the unit cell and the reciprocal lattice, i.e. it is the scattering pattern of a single unit cell observed only at reciprocal lattice points. This can be seen in Fig. 1.5, which shows the unit cell of Fig. 1.3 repeated on a lattice and its corresponding diffraction pattern. The underlying intensity is the same in both patterns. The positions of the reciprocal lattice points are given by the crystal lattice; the value of the diffraction pattern at a reciprocal lattice point is given by the atomic arrangement within the unit cell.

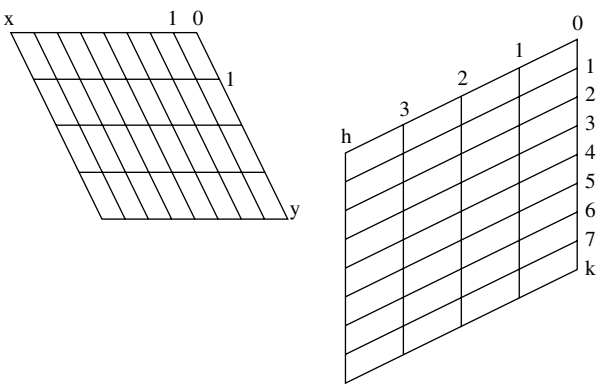

Fig. 1.4 Direct lattice (left) and the corresponding reciprocal lattice (right).

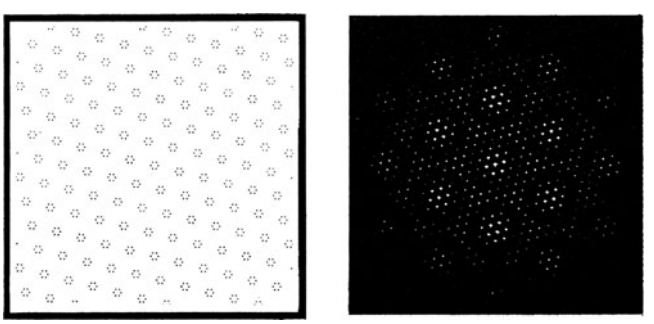

Fig. 1.5 The unit cell of Fig. 1.3 repeated on a lattice and its diffraction pattern.

1.7 The structure-factor equation

There are many factors affecting the intensity of X-rays in the diffraction pattern. The one that depends only upon the crystal structure is called the structure factor. It can be expressed in terms of the contents of a single unit cell as:

$$F(hkl) = \sum_{j=1}^{N} f_j \exp\left[2\pi \mathrm{i}(hx_j + ky_j + lz_j)\right]. \tag{1.1}$$

The position of the jth atom is given by the fractional co-ordinates (x_j, y_j, z_j), it has a scattering factor of f_j and there are N atoms in the cell. Structure factors are measured in number of electrons; they give a mathematical description of the diffraction pattern such as that illustrated in Fig. 1.6. Each structure factor represents a diffracted beam that has an amplitude, $|F(hkl)|$, and a relative phase $\phi(hkl)$. Mathematically, these are combined as $|F(hkl)| \exp[\mathrm{i}\phi(hkl)]$ and can be written as $F(hkl)$.

You may notice that the distribution of intensities in the diffraction pattern in Fig. 1.6 is centrosymmetric. This is an illustration of Friedel's Law that states that $|F(hkl)| = |F(\overline{hkl})|$. The law follows from (1.1) that shows that $F(hkl)$ is the complex conjugate of $F(\overline{hkl})$, making the magnitudes equal and relating the phases as $\varphi(hkl) = -\varphi(\overline{hkl})$. This is no longer true when the atomic scattering factor f_j is also complex. Changing the signs of the diffraction indices does not produce the complex conjugate of f_j, so Friedel's Law is not obeyed when there is anomalous scattering. However, the effect is phase dependent and for centrosymmetric structures where all the phases are 0 or π, the magnitudes of $F(hkl)$ and $F(\overline{hkl})$ are always changed by the same amount.

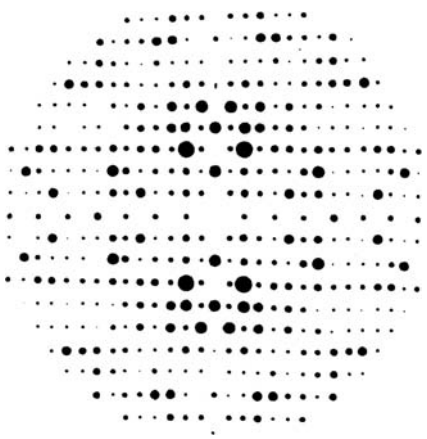

Fig. 1.6 Part of the X-ray diffraction pattern of ammonium oxalate monohydrate.

The experimental measurements consist of the intensity of each beam and its position in the diffraction pattern. After suitable correction factors are applied, the quantities recorded are h, k, l, $|F(hkl)|$ or h, k, l, $|F(hkl)|^2$.

1.8 The electron-density equation

An image of the crystal structure can be calculated from the X-ray diffraction pattern. Since it is the electrons that scatter the X-rays, it is the electrons that we see in the image, giving the value of the electron density at every point in a single unit cell of the crystal. The units of density are the number of electrons per cubic Angstrom unit – $e/Å^3$. The electron density is expressed in terms of the structure factors as:

$$\rho(xyz) = \frac{1}{V}\sum_{hkl} F(hkl)\exp\left[-2\pi i(hx + ky + lz)\right], \tag{1.2}$$

where the summation is over all the structure factors $F(hkl)$ and V is the volume of the unit cell. Note that the structure factors include the phases $\phi(hkl)$ and not just the experimentally measured amplitudes $|F(hkl)|$. Since the X-rays are diffracted from the whole crystal, the calculation yields the contents of the unit cell averaged over the whole crystal and not the contents of any individual cell. In addition, because of the finite time it takes to perform the diffraction experiment, we see a time-averaged picture of the electrons. This results in a smeared-out image of each atom because of its thermal vibration, as seen in Fig. 1.7.

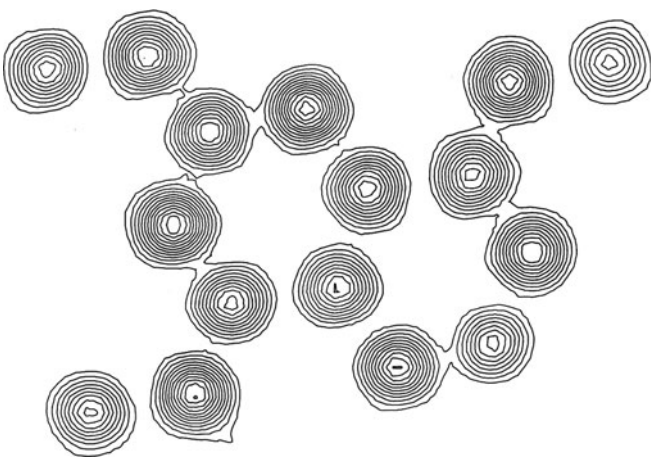

Fig. 1.7 A section of the 3D electron density map of a planar molecule.

1.9 A mathematical relationship

Notice the mathematical similarity between (1.1) and (1.2). Equation (1.1) transforms the electron density (in the form of atomic scattering factors, f_j) to the structure factors $F(hkl)$, while (1.2) transforms the structure factors back to the electron density. These are known as Fourier transforms – one equation performing the inverse transform of the other. This is a mathematical description of image formation by a lens. Light scattered by an object (Fourier transform) is collected by a lens and focused into an image (inverse transform). In the optical case, the (real) image is inverted and this is seen mathematically by the appearance of the negative sign in the exponent of (1.2).

1.10 Bragg's law

We cannot go far into X-ray diffraction without mentioning Bragg's law. This gives the geometrical conditions under which a diffracted beam can be observed. Figure 1.8 shows rays diffracted from lattice planes and, to get constructive interference, the path difference should be a whole number of wavelengths. This leads to Bragg's law which is expressed as:

$$2d \sin\theta = n\lambda, \tag{1.3}$$

where θ is known as the Bragg angle, λ is the wavelength of the X-rays and d is the plane spacing. The figure suggests the rays are reflected from the crystal planes. They are not – it is strictly diffraction – but reflection is mathematically equivalent in this context and the name X-ray reflection has stayed with us since Bragg first used it. The value of n in Bragg's law can always be taken as unity, since any multiples of the wavelength can be accounted for in the diffraction indices h, k, l of any particular reflection. For example, $n = 2$ for the planes h, k, l is equivalent to $n = 1$ for the planes $2h$, $2k$, $2l$.

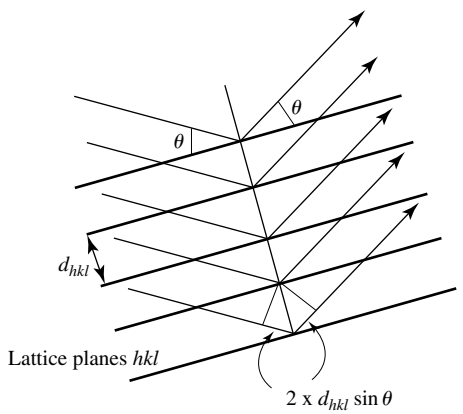

Fig. 1.8 Diffraction of X-rays from crystal lattice planes illustrating Bragg's law.

1.11 Resolution

In X-ray crystallography we have effectively a microscope that gives images of crystal structures, although its realization is different from an ordinary optical microscope. What is the resolution of the image and what is its magnification? By convention, the resolution is given by the minimum value of d that appears in Bragg's law. This will correspond to the maximum value of θ. With Mo $K\alpha$ radiation and all data collected to a maximum θ of 25°, Bragg's law gives:

$$2\,\frac{\sin(25^\circ)}{0.71} = \frac{1}{d_{\min}},$$

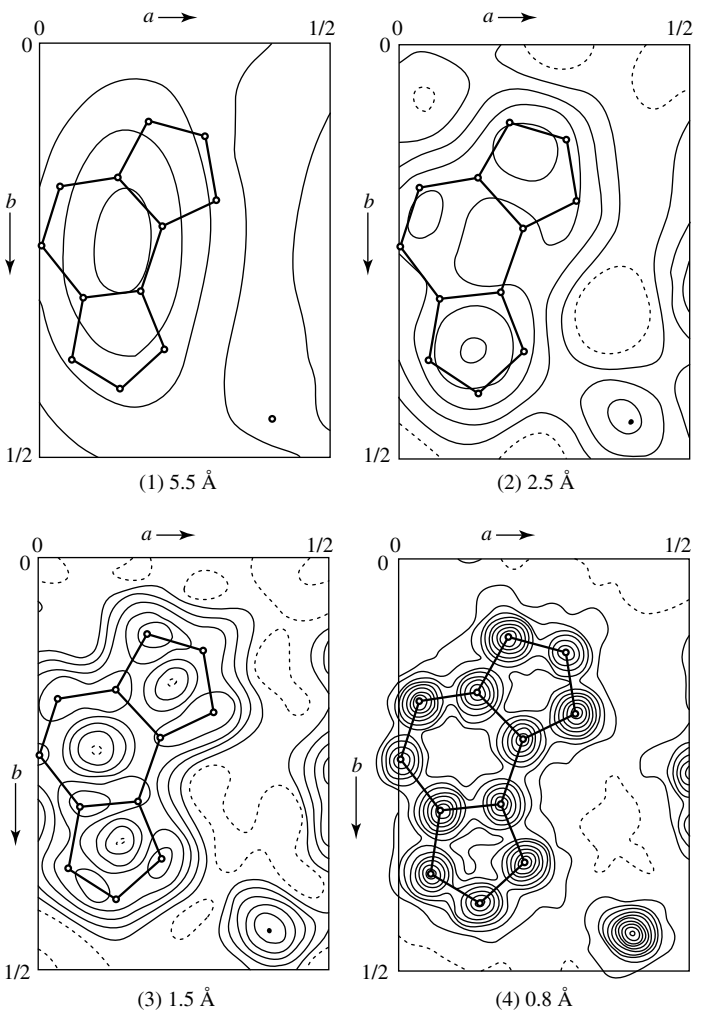

Fig. 1.9 The electron density calculated from a diffraction pattern of limited extent, indicated by the decreasing values of $d_{\min}$ from (1) to (4).

producing a resolution ($d_{\min}$) of 0.84 Å. The maximum possible resolution is $\lambda/2$, which occurs when $\sin(\theta_{\max}) = 1$. For Cu $K\alpha$ radiation this will be 0.77 Å, similar to the resolution obtained with Mo $K\alpha$ for $\theta_{\max} = 25°$. Figure 1.9 shows the effect on the electron density of imposing different limits on the extent of the diffraction pattern used to produce it.

If an electron density map is displayed on a scale of 1 cm/Å, this corresponds to a magnification of 10^8. You should be impressed by this very large number.

1.12 The phase problem

The measured X-ray intensities yield only the structure-factor amplitudes and not their phases. The calculation of the electron density can not therefore be performed directly from experimental measurements and the phases must be obtained by other means. Hence, the so-called phase problem. Methods of overcoming the phase problem include:

(i) Patterson search and interpretation techniques,
(ii) direct methods,
(iii) use of anomalous dispersion,
(iv) isomorphous replacement,
(v) molecular replacement.

Methods (i) and (ii) are the most important in small-molecule crystallography; the others feature in macromolecular crystallography.

Introduction to symmetry and diffraction

2

William Clegg

2.1 The relationship between a crystal structure and its diffraction pattern

A crystal structure and its diffraction pattern are related to each other, in both directions, by the mathematical procedure of Fourier transformation, the details of which are considered elsewhere. The diffraction pattern is the Fourier transform of the crystal structure, corresponding to the pattern of waves scattered from an incident X-ray beam by a single crystal; it can be measured by experiment (only partially, because the amplitudes are obtainable from the directly measured intensities via a number of corrections, but the relative phases of the scattered waves are lost), and it can be calculated (giving both amplitudes and phases) for a known structure. In turn, the crystal structure is the Fourier transform of the diffraction pattern and is expressed in terms of the electron-density distribution concentrated in atoms; it can not be measured by direct experiment, because the scattered X-rays can not be refracted by lenses to form an image as is done with light in an optical microscope, and it can not be obtained directly by calculation, because the required relative phases of the waves are unknown.

Part of an X-ray diffraction pattern of a single crystal is shown, as a computer-generated reproduction, in Fig. 2.1. It consists of a pattern of discrete spots with a range of intensities (represented as different sizes of spot). This pattern has a definite geometry, and a degree of symmetry in the positions and intensities of the individual spots, in this case a combination of horizontal and vertical reflection (with an inversion point at the centre of the pattern), so that only one quarter of the pattern is unique, the other three quarters being symmetry related to it. The full diffraction pattern, of course, is three-dimensional; only part of a section through it is shown here.

The geometry of the pattern can be described by measuring the distances between spots and angles between rows of spots. In this example, the pattern is rectangular, with perpendicular rows, and this is a

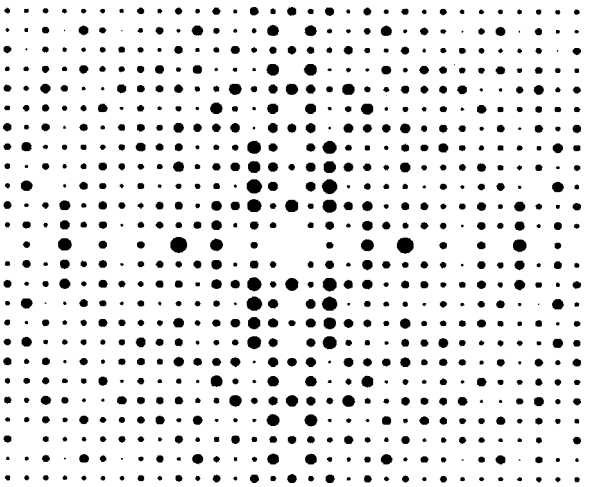

Fig. 2.1 Part of an X-ray diffraction pattern.

necessary consequence of the reflection symmetry present; the horizontal and vertical spacings are different.

Measurement of the geometry of a diffraction pattern gives information about the regular arrangement of molecules in the crystal structure. The symmetry of the pattern is related to the symmetry of the solid-state arrangement of molecules. The intensities, among which there is no obvious relationship except for the symmetry, hold information about the actual shapes and orientations of molecules, i.e. the positions of atoms in the crystal structure. The biggest task in determining a crystal structure is measuring these (usually thousands of) intensities and extracting the details of the atomic arrangement from them, but this can not be done without an understanding of the geometry and symmetry relationships as well. Here, we concentrate on symmetry aspects.

2.2 Translation symmetry in crystalline solids

Chemists are most familiar with symmetry in its application to individual molecules, as expressed in their point groups, particularly through aspects of group theory in bonding and spectroscopy. Symmetry plays a very important part in crystallography, and its application to crystalline solids includes concepts additional to those for isolated molecules.

A perfectly crystalline solid material consists of a very large (effectively infinite) number of identical molecules (or assemblies of a few molecules) arranged in a precisely regular way repeated in all directions, to give a high degree of order (theoretically zero entropy). This repetition in a regular pattern of an individual structural unit, in an identical form and orientation, is a form of symmetry, called translation, and it is the most fundamental characteristic of the crystalline solid state.

All perfect crystals display translation symmetry in three dimensions, whether or not any other symmetry elements (rotation, reflection and inversion) are also present; they are optional, but translation is necessary. The two-dimensional manifestation of translation symmetry is familiar in the form of patterns on clothing and other materials, wallpaper, etc.

A complete crystal structure can be specified by describing the contents of one repeat unit, together with the way in which this unit is repeated by translation symmetry. The translation symmetry is defined by the ***lattice*** of the structure and given numerical expression in the parameters of a ***unit cell***; here are two terms of vital importance in crystallography.

In order to obtain the lattice of a particular crystal structure, choose any single point in any repeat unit of the structure (for example, one atom), and mark it with a dot. Find all the other points in the structure that are identical to this one (i.e. with identical surroundings, in exactly the same orientation) and mark them also. Now keep the dots and remove the structure. What remains is just a regular infinite array of points in three dimensions. This is the lattice; all the points are identical, equivalent to each other by translation symmetry. The operation of translation is that of moving from one point to any equivalent one. The lattice shows the repeating nature of the structure but not the actual form (contents) of the structural repeat unit. Starting with a different point and repeating the whole process would give exactly the same result, and it is not necessary to choose the lattice points to lie on atoms (in the majority of real crystal structures they do not, because there are conventions that put them by preference on symmetry elements that lie between molecules and relate them to each other; more on this later).

Any translation from one lattice point to another can be represented as a vector, because it has a definite length and a certain direction. All such vectors, for an arbitrary choice of any two lattice points, can be constructed by putting together multiples of three basic unit vectors that are the shortest three non-coplanar vectors between pairs of adjacent lattice points:

$$\mathbf{t} = u\mathbf{a} + v\mathbf{b} + w\mathbf{c},$$

where **a**, **b**, **c** are the unit vectors for this lattice, and u, v, w are integers (positive, zero, and negative values are allowed). The complete lattice geometry can thus be defined by the three base vectors. In order to do this with pure numbers rather than vectors, it is necessary to give the lengths of the three vectors and the angles between each pair of them (three angles altogether). By standard convention, the three vector lengths are called a, b, and c, and the angles are called α, β, and γ; α is the angle between b and c, β is the angle between c and a, and γ is the angle between a and b. These three vectors and 9 others equivalent to them enclose a shape that is the three-dimensional equivalent of a two-dimensional parallelogram (called a parallelepiped), similar to a brick but not generally with 90° angles. This shape is called the unit cell of the crystal structure (and of its lattice); see Fig. 2.2. One unit cell is thus

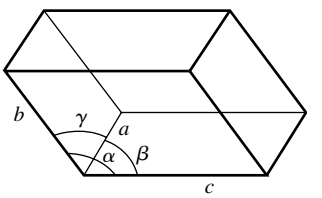

Fig. 2.2 A unit cell.

the basic building block of the whole structure, which can be regarded as being assembled by placing identical copies of the unit cell together to fill space. Each unit cell contains the equivalent of one lattice point (there are lattice points at all eight corners, but each is shared by the eight unit cells that meet there). The three basic vectors are the three different edges of the parallelepiped, and are also called the unit cell edges. Their three lengths and the three angles are often referred to as either ***unit cell parameters*** or ***lattice parameters***; these two terms are interchangeable and equivalent.

For any given lattice, many different choices of unit cell are possible, but there is always at least one for which the cell edges are the three shortest non-coplanar vectors of the lattice, and this is preferred by convention; it is called the reduced cell. (Actually, there are different definitions of the term 'reduced cell', of which this is a particular one that is probably most widely used and most clearly defined; its full name is the Niggli reduced cell. For completeness of the definition, the base vector directions are chosen to make all three cell angles $<90°$ or all three $\geq 90°$, and the axes are ordered in length, $a \leq b \leq c$.)

In the absence of any rotation or reflection symmetry in the crystal structure, the three unit cell axes are normally of different lengths and the three angles differ from each other and from special values such as 90°, although close approximation to equality or to such values may fortuitously be found sometimes.

It is the translation symmetry of crystalline materials that gives rise to X-ray diffraction. Any regularly spaced arrangement of objects can act as a diffraction grating for waves having a wavelength comparable to the repeat distance(s) between the identical objects. Thus, regularly and closely spaced parallel lines give a one-dimensional diffraction grating for infra-red and visible light in spectrometers, enabling the separation of different wavelengths, and a diffraction effect can be observed when monochromatic light from a sodium street lamp is viewed through a finely woven material such as an umbrella. Unit cell dimensions in crystals are comparable to the wavelengths of X-rays (and of electrons and neutrons moving at appropriate velocities), so crystals act as three-dimensional diffraction gratings. The basic mathematical relationships are given in the introductory chapter (Chapter 1) and in the chapter on data-collection theory (Chapter 5).

2.3 Symmetry of individual molecules, with relevance to crystalline solids

In applying point group symmetry to molecules, chemists learn about two basic types of ***symmetry operations*** and ***symmetry elements***, and these include some particularly common examples that are treated specially. Crystallographers use the same symmetry operations (they are fundamental properties of nature!), but detailed definitions and notation are different; this is unfortunate but is for good reasons.

A symmetry element is a physically identifiable point, line, or plane in a molecule (or any other individual object) about which symmetry operations are applied; a symmetry operation is an inversion through such a point, a rotation about a line, or a reflection in a plane, that leaves the molecule afterwards with an identical appearance. Each symmetry element thus provides a number of possible symmetry operations (for example, a rotation axis gives rise to rotations by any multiple of its basic minimum angle: rotations of 120°, 240° and 360° are all valid symmetry operations associated with a three-fold rotation axis; the last of these is equivalent to the identity operation, i.e. not doing anything at all, and we have just seen a similar situation for translation symmetry, where any lattice translation can be regarded as a combination of multiples of the three fundamental lattice translations for a particular crystal structure).

For individual molecules, all symmetry operations can be classified as one of two types: ***proper rotations*** (rotations by a certain fraction of 360° about a rotation axis), and ***improper rotations*** (the combination of a rotation and a simultaneous reflection in a plane perpendicular to the axis and passing through the centre of the molecule); this is the definition (known as the Schoenflies convention) used by chemists for spectroscopy and bonding applications. Because of the particular importance of the inversion centre in crystallographic symmetry (see later), we use a different convention, called the Hermann–Maugin or international convention, where an improper (or inversion) axis is the combination of a rotation and a simultaneous inversion through a point at the centre of the molecule. For the operations that can occur in crystalline solids, the correspondence between the two conventions is shown in Table 2.1, together with the conventional symbols. Note that inversion and reflection operations are just special cases of improper rotations. All improper operations involve a change of hand (a left hand is reflected

Table 2.1. Symbols for symmetry operations and elements.

Crystallography (Hermann–Maugin)	**Spectroscopy (Schoenflies)**	**Notes**
Proper rotations		
1	C_1 (or E)	identity operation
2	C_2	
3	C_3	
4	C_4	
6	C_6	
Improper rotations		
$\bar{1}$	$i\ (= S_2)$	inversion
$\bar{2}$ (or m)	$\sigma\ (= S_1)$	reflection
$\bar{3}$	S_6	
$\bar{4}$	S_4	
$\bar{6}$	$S_3\ (= C_3 + \sigma_h)$	

or inverted into a right hand), while proper rotations retain the same handedness; this has important implications for the crystal structures of chiral molecules as well as the molecules themselves.

Symmetry elements can be combined only in certain ways that are consistent with each other. For a single molecule, all symmetry elements present must pass through a common point at the centre of the molecule; if there is an inversion centre, there can be only one and it is at this point. For this reason, the total collection of all the symmetry operations for a molecule is called its ***point group***, and each point group has its own characteristic properties and a conventional symbol (again, different symbols are used by spectroscopists and by crystallographers). In principle, any order of rotation axis (the number of individual minimum rotation operations that must be repeated in order to achieve a total of 360° rotation) is possible within a molecule, although high-order rotations are rare, and two-fold rotation (C_2) is the most common. By contrast, the combination of other symmetry with translation in the crystalline state puts restrictions on the types of symmetry operation that are possible, because some orders of rotation are incompatible with the repeat nature of a lattice. Thus, the only orders possible in crystalline solids are 1, 2, 3, 4, and 6, for both proper and improper rotations. This does not mean that molecules with other symmetry elements can not crystallise! However, such symmetry elements can not apply to the surroundings of the molecules in the crystal, i.e. to the crystal structure as a whole; atoms that are symmetry-equivalent in an isolated molecule, such as all 10 carbon atoms of ferrocene, have different environments in a crystal and are no longer fully equivalent (they would give different solid-state ^{13}C NMR signals, for example). Because of this restriction, there are only 32 point groups that are relevant to crystallography; these are discussed later.

All three-dimensional lattices have inversion symmetry, whether or not the individual unit cell contents are centrosymmetric, and so the presence of inversion symmetry in a crystal structure does not put any restrictions on unit cell parameters; they can still adopt any arbitrary values that give a sensible overall packing of the molecules. Any rotation or reflection symmetry in the solid state, however, imposes restrictions and special values on the unit cell parameters. For example, four-fold rotation symmetry means that the unit cell must have two square faces exactly opposite each other with an axis perpendicular to them both (parallel to the rotation axis), so two of the cell axes are equal in length and all three angles are 90°. On the basis of these restrictions, crystal symmetry is broadly divided into seven types, called the seven crystal systems. Table 2.2 shows their names, the minimum symmetry characteristic of each one, and the restrictions on the unit cell parameters.

For some crystal structures with rotation and/or reflection symmetry, it is convenient and conventional to choose a unit cell containing more than one lattice point. For example, take an orthorhombic structure, for which each of the three unit cell axes is associated with either a two-fold rotation along the axis, a reflection perpendicular to it, or both of

Table 2.2. The seven crystal systems. For the essential symmetry, each type of rotation axis is generic; it could be a proper or improper rotation or a screw axis, and mirrors can also be glide planes. The centred cell types shown in parentheses can be converted into standard types not in parentheses by a different choice of axes, but are used in some cases in order to satisfy other conventions or conveniences regarding symmetry and geometry.

Crystal system	Essential symmetry	Unit cell restrictions	Cell types
triclinic	none	none	P
monoclinic	2 and/or m for one axis	$\alpha = \gamma = 90°$	P, C (I)
orthorhombic	2 and/or m for three axes	$\alpha = \beta = \gamma = 90°$	P, C (A), I, F
tetragonal	4 for one axis	$a = b$; $\alpha = \beta = \gamma = 90°$	P, I
trigonal	3 for one axis	$a = b$; $\alpha = \beta = 90°$, $\gamma = 120°$	P (R)
hexagonal	6 for one axis	$a = b$; $\alpha = \beta = 90°$, $\gamma = 120°$	P
cubic	3 for four directions	$a = b = c$; $\alpha = \beta = \gamma = 90°$	P, I, F

these; the unit cell is a rectangular parallelepiped with all axes mutually perpendicular, like a standard building brick; the 90° cell angles are a necessary consequence of the rotation/reflection symmetry and so are an indicator that such symmetry is probably present in the structure. Now consider a similar structure in which there is a lattice point added at the centre of the unit cell. Since lattice points are all equivalent by definition, this means the point at the centre of each unit cell is entirely equivalent to the points at the cell corners. Remember that the unit cell is just a convenient way of joining up lattice points to indicate the geometry; the lattice is a fundamental property of the structure, but the unit cell is an arbitrary definition. It would be possible to choose a smaller unit cell, since the distance from one corner to the centre of the cell is shorter than the longest of the three original unit cell axes. This cell would have half the volume of the original cell and there would be one lattice point per unit cell overall. It would, however, have some strange cell angles and the convenience of the 90° angles and rectangular cell shape are lost. In such cases, the larger unit cell with more than one lattice point is usually chosen by convention, so that the geometrical properties in Table 2.2 still apply. Unit cells with one lattice point are referred to as primitive (P), and those with more than one lattice point are called centred. Different kinds of centring are possible in the various crystal systems, and these may involve lattice points at the centres of opposite pairs of faces (A, B, or C depending on which faces are centred), at the centres of all faces (F), or at the body centre of the cell (I). We omit here consideration of alternative cell choices for some trigonal structures (R for rhombohedral); the treatment needed is more than completeness is worth. Some forms of centring are not relevant for particular crystal systems (e.g. there is no advantage in using any form of centred cell for a triclinic structure), and the essentially different possible combinations of lattice symmetry with primitive and centred cell choices leads to 14 distinct results, known as the 14 ***Bravais lattices*** (strictly speaking, this term is incorrect, as it is the unit cell and not the lattice that is centred). The appropriate combinations are included in Table 2.2 as 'cell types'.

2.4 Symmetry in the solid state

The impossibility of having some kinds of symmetry element, such as a five-fold rotation axis, in the crystalline solid state might seem to reduce the types of symmetry available in crystals compared with individual molecules. This is, however, not the case, as the presence of translation makes other kinds of symmetry possible. In a single molecule, the repeated use of one particular symmetry operation eventually reproduces the original orientation of the molecule (for example, two successive reflections in the same plane, or four 90° rotations about a four-fold axis), and this is a necessary property of any symmetry element in any point group. Imagine now a mirror plane in a crystal structure, containing two of the unit cell axes (say a and c) and perpendicular to the third axis (b), but with an operation that combines reflection with translation equal to half a unit cell repeat along one of the axes (a) instead of just reflection. Two successive operations brings the structure back, not to the same position, but exactly one unit cell removed along the a-axis, which is entirely equivalent because of the pure lattice translation symmetry. Such a symmetry operation is possible in an infinite lattice in the solid state, but not for an individual non-polymeric molecule. This is called a ***glide plane***. The glide direction in this example could equally well be along the c-axis, or along a and c simultaneously, i.e. along a unit cell face diagonal, in each case with a distance equal to half the corresponding lattice repeat, so there are different possible ways of combining reflection with translation. These are given symbols showing the glide direction: a, b, c for a glide along one of the axes, n for any diagonal glide, just as m stands for a pure reflection plane. (For centred unit cells in some crystal systems, it is possible to have glide planes with a translation component of one-quarter rather than half a unit cell repeat unit, because two successive operations correspond to translation from a cell corner to a centring lattice point instead of another corner; such glide planes are called d, and they are not common.) In a similar way, translation can be combined with rotation axes, the translation always being along the direction of the rotation axis and by an amount equal to a multiple of $1/n$ of the lattice repeat in that direction, where n is the order of the rotation axis. This gives a ***screw axis***, for which the conventional symbol is a number for the order of the axis together with a subscript for the multiple of the smallest possible translation: thus, 4_1, 4_2 and 4_3 are possible four-fold screw axes. Some screw axes, like screw threads, have handedness, so it is important to have a convention about the combined directions of rotation and translation; this occurs when the translation is not one half of the lattice repeat. A 4_1 axis is taken as a positive rotation of 90° when viewed along the axis with one-quarter translation away from the viewer, equivalent to a right-handed screw thread. Examination of the combined effects of a screw axis with pure lattice translation properties shows that the corresponding left-handed four-fold screw axis is 4_3, and there are similar pairs of left-handed and right-handed screw axes for other orders of

Table 2.3. Symmetry elements with translation components.

Rotations (screw axes)	
Two-fold	2_1
Three-fold	3_1 3_2
Four-fold	4_1 4_2 4_3
Six-fold	6_1 6_2 6_3 6_4 6_5
Reflections (glide planes)	
Translation parallel to cell axes	*a b c*
Translation parallel to diagonals	*n*
Translation half-way to centring lattice point	*d*

rotation. The full set of possible glide planes and screw axes is shown in Table 2.3.

In contrast to the situation in single molecules, symmetry elements in the solid state do not all pass through one point; instead they are regularly arranged parallel to each other, the symmetry elements of each unit cell being repeated identically in all other unit cells. Just as in molecules, however, there are only certain ways in which symmetry elements can be put together consistently. The total number of possible arrangements of symmetry elements in the crystalline solid state is exactly 230, and these arrangements are called ***space groups***, by analogy with point groups. Their symmetry properties are well established and are available in standard reference books and tables, the most important being the *International Tables for Crystallography*, Volume A, the contents of which we will look at in Chapter 4.

The notation used for space groups is an extension of that for point groups in crystallography, and this is one reason for using different notation from that followed by spectroscopists. Each space group symbol consists of a single capital letter to denote the cell centring, followed by a combination of numbers (in some cases with a horizontal bar over the top) and lower-case letters to show the presence of rotation, reflection and inversion symmetry in the structure. Because the combination of some symmetry operations necessarily implies the presence of others as well, not all the symmetry needs to be indicated, and there are conventions about which take precedence in the symbols chosen. The rules are different for each of the crystal systems, as follows.

Triclinic: no rotations or reflections, no need for centred cells, the only question is whether inversion symmetry is absent or present, giving two possible space groups $P1$ and $P\bar{1}$, respectively.

Monoclinic: there is symmetry about the unique axis, normally taken as the *b*-axis; this may be a two-fold rotation (2 or 2_1) along the axis, a reflection plane (mirror *m*, or glide *a*, *c* or *n*) perpendicular to this axis, or both of these together, e.g. $C2$, Pn, $P2_1/c$. There are 13 monoclinic space groups.

Orthorhombic: the possibilities for monoclinic symmetry apply to all three axes. Where both rotation and reflection are present for an axis, only the reflection is given. Possible combinations are rotation only for

all three axes, rotation and reflection for all three axes, and reflection for two axes with rotation for the third; in the last case, it is conventional to take the rotation axis along c. Examples are $P2_12_12_1$, $Aba2$, $Cmcm$, $Fdd2$. There are 59 orthorhombic space groups.

Tetragonal, trigonal and hexagonal: symmetry (including some kind of 4-, 3- or 6-fold rotation, possibly with perpendicular reflection) for the unique c-axis is given first, then symmetry along the a- and b-axes (equivalent to each other), then any symmetry lying between a and b, e.g. $P4_32_12$, $R\bar{3}c$, $P6_3/mmc$. There are 68 tetragonal, 25 trigonal, and 27 hexagonal space groups.

Cubic: symmetry is given first along the cell axes, then along the four body diagonals (always 3 or $\bar{3}$), then along the face diagonals, e.g. $P2_13$, $Fd\bar{3}c$. There are 36 cubic space groups.

The occurrence of the different space groups in real structures is far from equally distributed. Some space groups are extremely rare, while others are very common. Most molecular materials crystallize in triclinic, monoclinic or orthorhombic space groups, while higher symmetries are more commonly found for inorganic ionic and network structures and minerals. Around one third of all crystal structures of molecular compounds have space group $P2_1/c$, though the symbol for this space group may be $P2_1/a$ or $P2_1/n$ if the unit cell axes are chosen differently. Generally, screw axes and glide planes are more common than pure rotations and reflections in crystal structures, except where individual molecules themselves have these symmetry elements, because the presence of translation components means that the molecules, with irregular shapes and charge distributions, pack together more effectively.

Returning to a point raised earlier, in the construction of a lattice, the choice of the equivalent points in the crystal structure is arbitrary. Another way of expressing this is that the choice of origin of the unit cell (the point within one repeat unit that is assigned three zero co-ordinates) is arbitrary. In high-symmetry inorganic crystal structures such as simple ionic salts, drawings and models often show atoms or ions at the corners of unit cells, but this is not necessary and, in fact, it is unusual for the structures of molecules that have no internal symmetry elements. By convention in most space groups, the origin is chosen to lie on a symmetry element; in particular, for centrosymmetric space groups, the origin is normally placed on an inversion centre, because this simplifies the mathematics of Fourier calculations. In most cases symmetry elements lie between molecules, relating them together, rather than inside molecules.

2.5 Diffraction and symmetry

The symmetry of a diffraction pattern is closely related to the symmetry of the structure producing it, allowing us to deduce something about the space group from the observed pattern. The symmetry of a diffraction

pattern is seen in the equivalence of different regions of it, which may be related to each other by certain symmetry elements; this refers to both the positions (due to the directions of individual diffracted beams) and the intensities of the various reflections on a recorded pattern. A diffraction pattern has a central point (corresponding to the reflection with all zero indices) and so its symmetry is expressed in terms of a point group, whereas the crystal structure has a space group; how are these related? One important aspect of X-ray diffraction is that, in the absence of an effect called anomalous scattering or anomalous dispersion, which is rarely a large effect and is significant usually only when heavier elements are present in a structure, every diffraction pattern has inversion symmetry, whether or not the crystal structure is centrosymmetric; this is known as Friedel's Law. Therefore, of the 32 crystallographic point groups, only 11 are possible as the symmetry of a diffraction pattern, and these are known as the 11 ***Laue classes***. Each space group has a corresponding point group to which it is related (and is the point group symmetry that a crystal would have if grown under ideal conditions), and a corresponding Laue class. Clearly, with 230 space groups, 32 point groups, and 11 Laue classes, most of the Laue classes have a large number of related space groups.

To derive the point group from a space group, the initial capital letter is ignored (this refers to the cell centring, which is irrelevant to point group symmetry), then all screw axis symbols are replaced by the corresponding pure rotation and all glide planes are replaced by pure reflections. Thus, for example, 2_1 becomes 2, 6_5 becomes 6, and all of *a*, *b*, *c*, *n* and *d* become *m*: $P2_1/c \rightarrow 2/m$, $Aba2 \rightarrow mm2$, $I4_1/acd \rightarrow 4/mmm$. To derive the Laue class from the point group, add an inversion centre if there is not already one; in many cases, this will automatically generate further symmetry elements, and the result is just one of the 11 point groups that have inversion symmetry. For each of the three most common (and lowest-symmetry) crystal systems, there is just one Laue class; for each of the others there are two. The correspondence of different crystal systems, point groups and Laue classes is shown in Table 2.4.

We thus have the following forms of symmetry that are important in crystallography: the space group (choice of 230) is the complete symmetry of the crystal structure and is one property that has to be established as part of determining the structure by diffraction methods; the Laue class (choice of 11) is the point-group symmetry of the diffraction pattern if Friedel's Law applies, and is directly observed in the diffraction experiment; a point group is the collection of all symmetry operations (excluding any with translation components) about a particular central point in a single object. Point group symmetry can be used to refer to the shape of a crystal, the shape of a single unit cell, or any chosen point within a crystal structure, e.g. the position of an atom or the centre of a molecule. The point group symmetry of a molecule in a crystal structure, taking account not only of the molecule itself but also of its environment, may be equal to or lower than the point group symmetry of the same molecule in isolation; it can not be higher without changing

Table 2.4. Crystal systems, point groups and Laue classes. In each case, the Laue class is also one of the possible point groups. The corresponding Schoenflies point group symbols are given in the same order. In some cases a different choice of axes can lead to a different order of the symbols for a particular point group, e.g. $\bar{6}2m$ instead of $\bar{6}m2$, but these are the same point group.

System	Laue class	Other point groups	Corresponding Schoenflies	
triclinic	$\bar{1}$	1	C_i	C_1
monoclinic	$2/m$	2, m	C_{2h}	C_2, C_s
orthorhombic	mmm	$mm2$, 222	D_{2h}	C_{2v}, D_2
tetragonal	$4/m$	4, $\bar{4}$	C_{4h}	C_4, S_4
	$4/mmm$	$4mm$, 422, $\bar{4}m2$	D_{4h}	C_{4v}, D_4, D_{2d}
trigonal	$\bar{3}$	3	S_6	C_3
	$\bar{3}m$	32, $3m$	D_{3d}	D_3, D_{3d}
hexagonal	$6/m$	6, $\bar{6}$	C_{6h}	C_6, C_{3h}
	$6/mmm$	$6mm$, 622, $\bar{6}m2$	D_{6h}	C_{6v}, D_6, D_{3d}
cubic	$m\bar{3}$	23	T_h	T
	$m\bar{3}m$	432, $\bar{4}3m$	O_h	O, T_d

the shape of the molecule or by invoking structural disorder, a topic not covered here. If Friedel's Law does not apply in the presence of significant anomalous dispersion for a non-centrosymmetric structure, the symmetry of the diffraction pattern will be one of the point groups not included in the list of 11 Laue classes, the point group associated with the space group of this structure.

2.6 Further points

In pure lattice translation terms, the repeat unit of a crystal structure is either one complete unit cell (primitive cells) or a well-defined fraction of one unit cell (one half for *A*, *B*, *C* or *I* centring, one third for rhombohedral *R* structures described on a conventional trigonal unit cell, one quarter for *F* centring). If any inversion, rotation or reflection symmetry is present in the structure (including screw axes and glide planes), then these additional symmetry elements relate atoms and molecules to each other within each unit cell as well as between unit cells, so the unique, symmetry-independent part of the structure is only a fraction of the lattice repeat unit, the fraction depending on the amount of symmetry present. This unique structural portion is called the ***asymmetric unit*** of the structure, and it may consist of a single molecule, a group of more than one molecule, a fraction of a molecule possessing symmetry within itself, or a combination of different molecules and/or ions, for example including co-crystallized solvent molecules. Operation of all the space group symmetry (translation, inversion, rotation and reflection) generates the complete crystal structure from the asymmetric unit. The details of the asymmetric unit, together with the unit cell parameters and the space group, are what need to be determined in order to describe the crystal structure.

Any point in a crystal structure that does not lie on a rotation axis, a mirror plane or an inversion centre has point group symmetry 1 (C_1) and will be related by symmetry to a number of other equivalent points in the same unit cell. This is called a ***general position***, and each space group has a fixed value for the number of equivalent general positions, ranging from 1 for space group $P1$ (no symmetry other than pure lattice translation, so every point in the unit cell is unique) to 192 for the highest-symmetry cubic space groups with F unit cells. For a point on a symmetry element without translation component, operation of that element leaves the point unchanged, so the number of equivalent points in the unit cell is lower by a fraction depending on the nature of the symmetry element (2, 3, 4 or 6 for a rotation axis, 2 for reflection or inversion). Such positions are called ***special positions***, and can be occupied only by molecules that themselves possess the appropriate symmetry. In some space groups there are no special positions. In others there are special positions where two or more symmetry elements intersect; the point group symmetry of such special positions is correspondingly higher, and the number of equivalent points in the unit cell correspondingly lower. Screw axes and glide planes do not give rise to special positions, because of their translation components. Atoms on special positions may require symmetry-imposed constraints on their co-ordinates and/or displacement parameters during refinement; most of these are generated automatically by modern programs.

For a crystal structure containing just one kind of molecule (similar arguments apply to structures containing more than one kind of molecule, such as solvates and co-crystals, and to ionic crystal structures, but there are some additional complications), the number of molecules in each unit cell is conventionally known as Z. A related parameter of interest is the number of molecules in the asymmetric unit, which is given the symbol Z'. The most common value for this is 1, but it is greater than one in a significant number of structures, where there is more than one molecule (chemically identical but not related by crystallographic symmetry) in the asymmetric unit, and it is less than one if there is one independent molecule that itself lies on a crystallographic symmetry element (rotation axis, mirror plane or inversion centre).

One other symmetry term needs to be recognized before these principles are applied in trying to work out the possible space groups for a material from its observed diffraction and other properties. The ***metric symmetry*** is the observed symmetry of the unit cell of a structure without reference to its contents. It takes no account of information from the Laue symmetry and looks only at the shape of the unit cell. It can thus lead to false conclusions. For example, if a monoclinic structure fortuitously has a β angle close to 90°, the unit cell has the same shape as for genuine orthorhombic symmetry. The metric symmetry is always at least as high as the Laue symmetry, and may be higher; for the four high-symmetry crystal systems, the metric symmetry is the same as the higher of the two possible Laue classes in each case. Trigonal primitive and hexagonal unit cells are indistinguishable in terms of their basic

shape, but some trigonal crystal structures have a different (rhombohedral) lattice not discussed here in detail, so there are just seven possible different metric symmetries.

Some properties of the 32 crystallographic point groups are summarized in Table 2.5. Here, in the last column, an enantiomorphous point

Table 2.5. The 32 crystallographic point groups.

system, Laue, centring	point group	space group nos.	symm along x	symm along y	symm along z	order	E/P/C
Triclinic	1	1	1	1	1	1	E P
$\bar{1}$ P	$\bar{1}$	2	$\bar{1}$	$\bar{1}$	$\bar{1}$	2	C
monoclinic	2	3–5	1	2	1	2	E P
$2/m$ $P\,C$	m	6–9	1	m	1	2	P
	$2/m$	10–15	$\bar{1}$	$2/m$	$\bar{1}$	4	C
orthorhombic	222	16–24	2	2	2	4	E
mmm $P\,C\,I\,F$	$mm2$	25–46	m	m	2	4	P
	mmm	47–74	$2/m$	$2/m$	$2/m$	8	C
			z	x,y	xy		
tetragonal	4	75–80	4	1	1	4	E P
$4/m$ $P\,I$	$\bar{4}$	81–82	$\bar{4}$	1	1	4	
	$4/m$	83–88	$4/m$	$\bar{1}$	$\bar{1}$	8	C
tetragonal	422	89–98	4	2	2	8	E
$4/mmm$ $P\,I$	$4mm$	99–110	4	m	m	8	P
	$\bar{4}2m$	111–122	$\bar{4}$	2	m	8	
	$\bar{4}m2$		$\bar{4}$	m	2		
	$4/mmm$	123–142	$4/m$	$2/m$	$2/m$	16	C
trigonal	3	143–146	3	1	1	3	E P
$\bar{3}$ $P\,R$	$\bar{3}$	147–148	$\bar{3}$	$\bar{1}$	$\bar{1}$	6	C
trigonal	321	149–155	3	2	1	6	E
$\bar{3}m$ $P\,R$	312		3	1	2		
	$3m1$	156–161	3	m	1	6	P
	$31m$		3	1	m		
	$\bar{3}m1$	162–167	$\bar{3}$	$2/m$	$\bar{1}$	12	C
	$\bar{3}1m$		$\bar{3}$	$\bar{1}$	$2/m$		
hexagonal	6	168–173	6	1	1	6	E P
$6/m$ P	$\bar{6}$	174	$\bar{6}$	1	1	6	
	$6/m$	175–176	$6/m$	$\bar{1}$	$\bar{1}$	12	C
hexagonal	622	177–182	6	2	2	12	E
$6/mmm$ P	$6mm$	183–186	6	m	m	12	P
	$\bar{6}2m$	187–190	$\bar{6}$	2	m	12	
	$\bar{6}m2$		$\bar{6}$	m	2		
	$6/mmm$	191–194	$6/m$	$2/m$	$2/m$	24	C
			x,y,z	xyz	xy,yz,zx		
cubic	23	195–199	2	3	1	12	E
$m\bar{3}$ $P\,I\,F$	$m\bar{3}$	200–206	$2/m$	$\bar{3}$	$\bar{1}$	24	C
cubic	432	207–214	4	3	2	24	E
$m\bar{3}m$ $P\,I\,F$	$\bar{4}3m$	215–220	$\bar{4}$	3	m	24	
	$m\bar{3}m$	221–230	$4/m$	$\bar{3}$	$2/m$	48	C

group (E) means one available for the crystallization of optically pure chiral molecules; a polar point group (P) is one in which at least one particular direction is symmetrically distinct from the opposite direction; C means a centrosymmetric point group. The order of a point group is the number of equivalent general positions in each of the related space groups with *P* unit cells, and must be multiplied by 2 for *A*, *C* and *I*, by 3 for *R*, and by 4 for *F* cells. For some tetragonal, trigonal and hexagonal point groups, different arrangements of symmetry elements are possible for the *a*- and *b*-axes and the directions lying between them, leading to the use of alternative symbols so that different but related space groups are clearly distinguished; these are shown in adjacent rows.

Exercises

1. You are provided in Fig. 2.3 and Fig. 2.4 with four two-dimensional repeating patterns (Traidcraft gift wrapping paper!). For each one, identify lattice points and outline a unit cell (possible shapes are oblique, rectangular, square, and hexagonal; a rectangular unit cell can be primitive or centred). Find the symmetry elements; for a 2D pattern the following are possible: 2-, 3-, 4- and 6-fold rotations, mirror lines, and glide lines (mirrors with a half-unit-cell translation component parallel to the reflection line); in 2D inversion symmetry is the same as a 2-fold rotation. Show what fraction of the unit cell is the asymmetric unit.

(1)

(2)

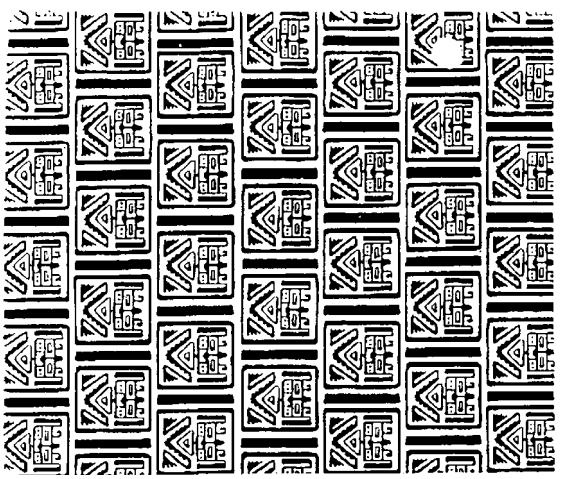

Fig. 2.3 Patterns for Exercise 1.

(3)

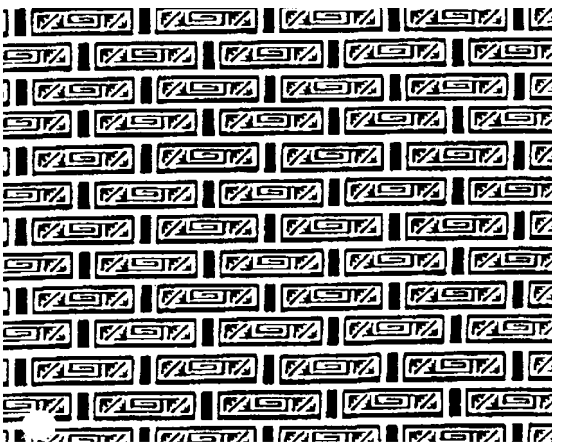

(4)

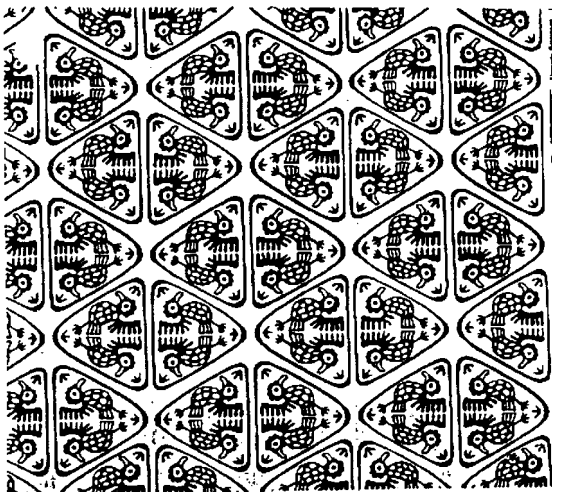

Fig. 2.4 Patterns for Exercise 1.

2. The point group of a ferrocene molecule $[Fe(C_5H_5)_2]$ is D_{5h}, assuming an eclipsed conformation of the two rings. This point group symmetry is not possible in the crystalline solid state (no 5-fold rotation axes!). The symmetry elements of D_{5h} are: a five-fold rotation axis, 5 two-fold rotation axes perpendicular to this, 5 'vertical' mirror planes each containing Fe and 2 C atoms, and one 'horizontal' mirror plane through Fe and lying between the two rings (there is also an S_5 improper rotation axis). Which of these symmetry elements could be retained in the site symmetry of a ferrocene molecule in a crystal structure, and what is the highest possible point

group symmetry for ferrocene in the crystal (the maximum number of symmetry elements that can be retained simultaneously)?

3. Why does the list of conventional Bravais lattices not include any centred unit cells in the triclinic system, tetragonal *C*, or cubic *C*?
4. Work out the point group and the Laue class corresponding to the following space groups: (a) $C2$; (b) $Pna2_1$; (c) $Fd\bar{3}c$; (d) $I4_1cd$.
5. From the space group symbols alone, what (if any) special positions would you expect to find for (a) $P\bar{1}$; (b) $C2$; (c) $P2_12_12_1$?

This page intentionally left blank

Crystal growth and evaluation

3

Alexander Blake

3.1 Introduction

Whether growing crystals or giving advice to someone else trying to do so, it is vital to remember that the quality of the crystal from which diffraction data are acquired is generally the main determinant of the final quality of the structure. The effects of a suboptimal crystal will propagate through data collection, structure solution and refinement to affect the quality of the final structure, in which unsatisfactorily high uncertainties may limit useful comparison and discussion. It may be difficult or impossible to get such a structure published.

3.2 Protect your crystals

Before you start trying to grow crystals you need to think about how they will be handled. They will need to be extracted from the vessel they grew in without suffering any damage. Less obviously, some containers make this easier than others: an oversized one like a 250-ml round-bottomed flask makes the procedure of finding and removing a small crystal unnecessarily difficult. At the other extreme, a container with a small aperture that will not admit a narrow spatula or pipette is also troublesome. You should avoid screw-top or other containers that narrow near the top, as the 'shoulders' prevent easy removal of the crystals: a small vial with straight walls works best.

Many crystals lose solvent on removal from the solution in which they have grown (mother liquor). Although the envelope of the crystals may appear intact, even a few per cent solvent loss usually renders them useless for structural analysis. This is particularly common for crystals grown from chlorocarbon solvents like dichloromethane and chloroform, but can affect crystals grown from almost any solvent, water included. If a crystal loses solvent and then does not behave well on the diffractometer, there is no way to know whether the original crystal was unsuitable, or whether the poor diffraction was due solely to

solvent loss. For this reason you should keep crystals under mother liquor whenever possible. There are other good reasons for doing this – see below.

3.3 Crystal growth

The term recrystallization has two related meanings but there are crucial differences between these. *In the synthesis and purification of compounds*, the aim is to maximize purity and yield, although these can be mutually exclusive. The material is often precipitated very rapidly (∼1 s), resulting in microcrystalline or virtually amorphous products that are useless for conventional single-crystal work. *For diffraction work* the object is to obtain a small number (one may do) of relatively large (∼0.1–0.4 mm) single crystals. As long as this is achieved, yield is irrelevant and purity is likely to be enhanced. To this end, crystals should be grown *slowly*, taking from minutes to months depending on the system. To understand why this is important, visualize the process of growth at a crystal surface. The greater the rate at which molecules arrive at the surface, the less time they have to orient themselves in relation to molecules already there: random accretion is more likely, leading to crystals that are twinned or disordered. Suitable growth conditions include the absence of dust and vibration: if these are present they can lead to small or non-singular crystals.

3.4 Survey of methods

3.4.1 Solution methods

These are by far the most flexible and widely used. They are suitable for use with molecular compounds that are the subject of most crystal structure determinations. The use of solvents means that crystals can grow separately from each other. It is therefore important not to let a solution dry out, as crystals could become encrusted and may not remain single. When choosing solvents remember the general rule that 'like dissolves like': look for a solvent that is similar to the compound (in terms of polarity, functional groups, etc.) and an antisolvent that is dissimilar to it in order to reduce its solubility (see below). Information about solvents is available from several sources (e.g. *Handbook of Physics and Chemistry*, chromatographic elution data), and the process of synthesizing and purifying a compound will often confer a knowledge of suitable solvents. Mixing solvents allows manipulation of solubility: a mixture of solvent A (in which a compound is too soluble) and antisolvent B (in which it is not sufficiently soluble) may be more useful than either alone. If crystals grown from one solvent are poor in quality, try different solvents or mixtures of solvents. Solution methods can be extremely flexible: a number of crystallizations, differing in the proportions of solvents A and B used, can be set up to run in parallel. If a particular range

of proportions appears to be more successful in producing crystals it can be investigated more closely by decreasing the difference between successive mixtures of A and B.

It is important that any vessels used for crystal growth should be free of contaminants. Older containers also tend to have a large number of scratches and other surface defects, providing multiple nucleation points and tending to give large numbers of small crystals. Two factors that favour the formation of twinned crystals are the presence of impurities and uneven thermal gradients. Conversely, if the inner surface of a container is too smooth this may inhibit crystallization. If this appears to be the case, gently scratching the surface with a metal spatula a few times may be effective. Some of the possible variations are described briefly below, and virtually all methods described can be adapted to accommodate air sensitivity.

Concentration. If the volume of a solution is reduced, for example by evaporation of a volatile solvent, the concentration of the solute will rise until it begins to crystallize. When using mixed solvents the poorer solvent should be the less volatile so that the solubility of the solute decreases upon evaporation (but see Fig. 3.1). The rate of evaporation can be controlled in various ways, for example by altering the temperature of the sample or by adjusting the size of the aperture through which the solvent vapour can escape. As solvents are frequently flammable or irritants, it is important to work on the smallest scale possible and ensure than any vapour released from the solution is safely dealt with. Avoid obvious hazards such as those that will arise if large volumes of diethyl ether or other highly volatile solvents are allowed to evaporate in a closed container such as a refrigerator.

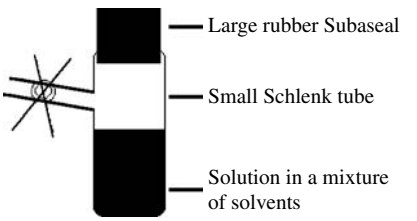

Fig. 3.1 A method of controlling solubility by selectively removing the *less* volatile solvent in which the compound is more soluble. This (chlorocarbon) solvent is absorbed by the rubber Subaseal, while the antisolvent (diethyl ether) is not, leading to a more concentrated solution and eventually to crystallization.

As noted above, it is highly undesirable to let a solution evaporate to dryness as this will allow otherwise suitable crystals to become encrusted, grow into an aggregate or be contaminated by impurities. The crystals may be degraded by loss of solvent of crystallization, especially if chlorocarbon solvents such as dichloromethane have been used. It may prove impossible to identify good crystals even if these are present, and extracting them undamaged from a mass of material may prove difficult or impossible.

Apparently sealed NMR tubes that have been forgotten at the back of a fume cupboard or fridge for weeks or months are a fruitful source of good-quality crystals: there is in fact slow evaporation of solvent and crystals are able to grow undisturbed. As long as the NMR tube is clean and relatively unscratched the smooth inner surface and narrow bore provide an excellent environment for crystal growth.

Cooling. *Either* make up a hot, nearly saturated solution and allow it to cool slowly towards room temperature *or* make up such a solution at room temperature and cool it slowly in a fridge or freezer. The cooling rate can be reduced by exploiting the fact that the larger and more massive an object, the longer it will take to lose heat. Thus, a hot solution in a large vessel (or in a small vessel within a larger one) will cool relatively slowly (Fig. 3.2, left). Similarly, a sample tube containing

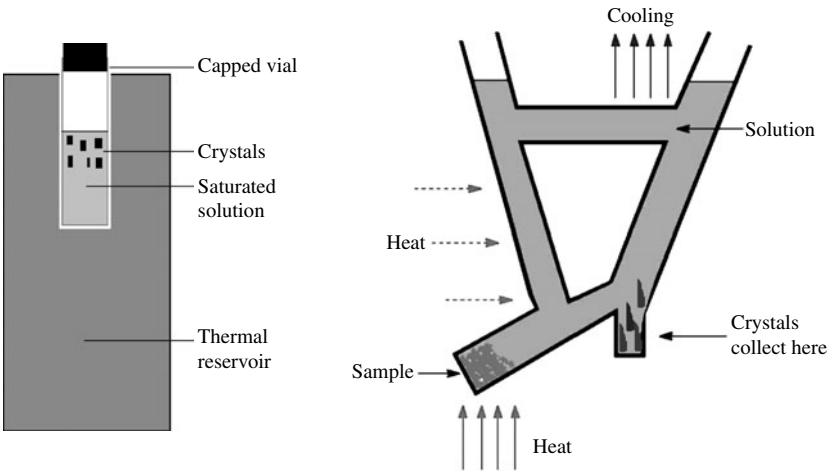

Fig. 3.2 Controlled cooling (left) and an apparatus to exploit convection (right).

a solution will cool at a slower rate if it is contained in a metal block that was originally at room temperature, or if surrounded by an effective layer of insulation. Cooling methods are based on the generally valid assumption that solubility decreases with temperature. There are rare exceptions to this (e.g. Na_2SO_4 in water) and some solubilities rise so rapidly with temperature that it can be difficult to control crystallization (e.g. of KNO_3 from water). However, it is usually possible to find a combination of solute and solvent where solubility varies slowly and controllably with temperature.

Convection. The aim here is to establish a temperature gradient across the solution, so that material dissolves in the warmer area and deposits in the colder. This gradient can be established by various means, for example (a) allow sunlight to shine on one part of the vessel; (b) put one part of the vessel against a cooler surface, such as a window at night; (c) construct an apparatus with low-power electrical heating elements in some sections (Fig. 3.2 right). A smooth concentration gradient will give the best results.

One method that combines variation of both concentration and temperature and is especially useful for sparingly soluble compounds is Soxhlet extraction (Fig. 3.3). The recycling of the solvent is the key factor here and crystals can even appear in the refluxing solvent. Failing this, they normally appear after slow cooling of the solution. There are several other methods available to control concentration. One of these is based on osmosis, where the solvent passes through a semipermeable membrane into a concentrated solution of an inert species. The resulting increase in the concentration of the solute may lead to crystal formation.

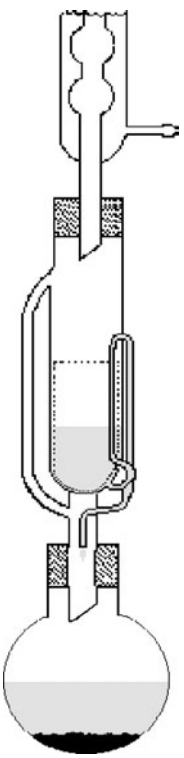

Fig. 3.3 Soxhlet apparatus.

Solvent diffusion. This method is based on the fact that a compound will dissolve well in certain solvents ('good solvents') but not in others ('poor solvents' or antisolvents), which must be co-miscible. Dissolve

the compound in the 'good solvent' and place this solution in a narrow tube. Using a syringe fitted with a fine needle, very slowly inject the neat antisolvent. If it is lighter than the solution, layer it on top; if it is denser, inject it slowly into the bottom of the tube to form a layer under the solution. Injecting the solvent is better than running it down the side of the tube. If the tube is protected from vibration, these layers will mix slowly and crystals will grow at the interface (Fig. 3.4). If necessary, cooling of the tube can be used both to lower the rate of diffusion and to reduce the solubility.

Vapour diffusion. This method is also called isothermal distillation. The antisolvent diffuses through the vapour phase into a solution of the compound in the 'good solvent', thereby reducing the solubility (Fig. 3.5). The advantages of this method include the relatively slow rate of diffusion, its controllability and its adaptability, for example in combination with Schlenk techniques to grow crystals of air-sensitive samples. It is usually worth trying vapour diffusion as it frequently succeeds where other methods have failed. A variant on this is the hanging-drop method, principally used for the growth of crystals of proteins and other macromolecules: the precipitant sits in a well and diffuses slowly into a drop of solution suspended on a glass slide covering the well.

If you are using a needle to make holes in the polythene cap of a sample vial, take particular care to remove completely any slugs of polythene formed by this procedure. They may be inside the vial or hanging loosely from the cap. If these slugs get into your sample they can look remarkably like large single crystals (Fig. 3.6), and even show plausible optical properties due to the stress of their formation. They can often be identified by the presence of a tail-like extension, but this is not always present, and they are often identified only by their diffraction pattern (Fig. 3.7). Making holes from the inside of the cap outwards makes it easier to check for the presence of slugs, but close scrutiny of vial and cap is always worthwhile.

Reactant diffusion. It is sometimes possible to combine synthesis and crystal growth. In favourable cases crystals may simply drop out of the reaction mixture, but the rate of many reactions means that crystals form rapidly and are therefore small and of low quality. If the reaction rate

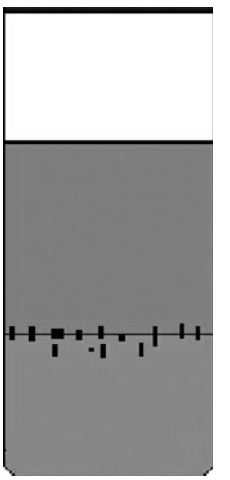

Fig. 3.4 Solvent diffusion.

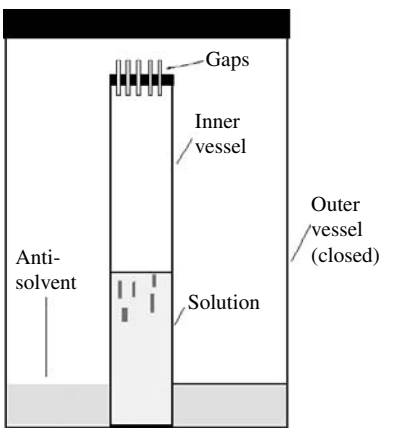

Fig. 3.5 Vapour diffusion.

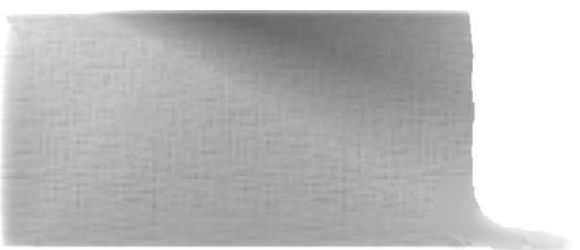

Fig. 3.6 A polythene slug produced by using a needle to make holes in the cap of a vial.

can be controlled by slow addition of one of the reactants this offers one way to overcome the problem. The best control is often achieved by controlling the rate at which reactant solutions mix, by interposing a semipermeable barrier [e.g.membrane (Fig. 3.8 left), sinter or an inert liquid such as Nujol] or by the use of gel crystallization (see below). Another variant involves placing a solid reactant at the bottom of a tube, covering it with a solvent in which it is known to dissolve slowly, and carefully adding an upper layer consisting of a solution of a second reactant (Fig. 3.8 right). The additional time required for the solid to dissolve reduces the rate at which reaction can occur.

Crystals of zeolites and of many other materials with network structures cannot be recrystallised and therefore can only be obtained from the reaction mixture. Fine tuning of the reaction conditions and the proportions and concentrations of reactants probably offer the only realistic ways to control crystal size and quality.

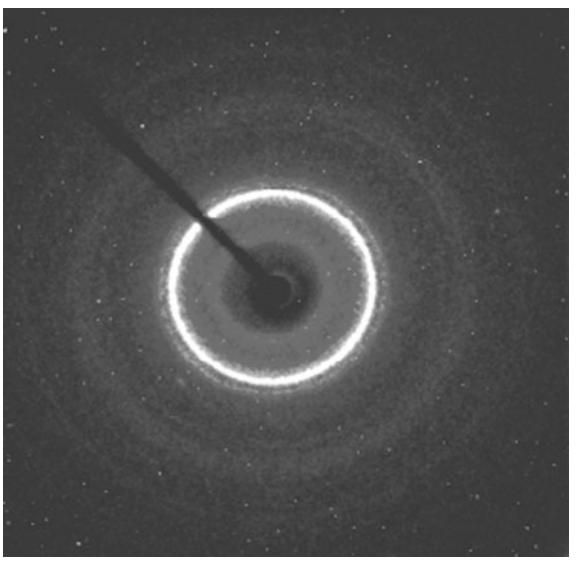

Fig. 3.7 Diffraction pattern of a polythene slug.

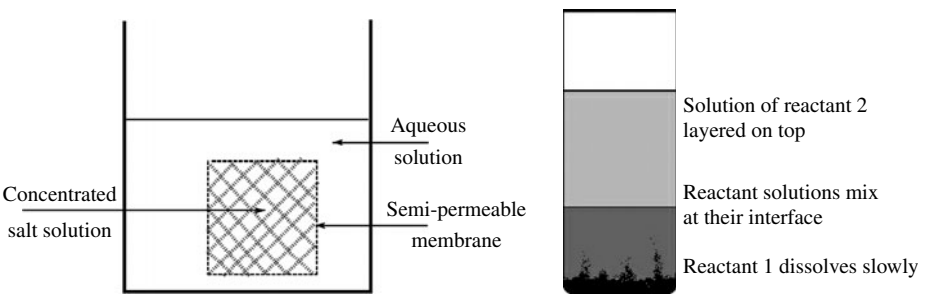

Fig. 3.8 Crystal growth by osmosis (left) and by dissolution and mixing (right).

Crystallization from gels is an under-exploited technique for obtaining single crystals of compounds of low solubility. Because the mixing of the solutions is dominated by diffusion through a viscous medium, undesirable competing processes such as convection and sedimentation are minimized. It is therefore possible to establish laboratory conditions for crystallization that closely approximate the microgravity of space. A typical arrangement is a U-tube half-filled with gel, with a solution of one reactant in the top of one arm and a solution of another reactant in the other. As gels are generally colourless, it is much easier to detect and isolate crystals if a product is strongly coloured. There are various recipes for the preparation of gels [e.g. Arend and Connelly (1982); http://www.cryst.chem.uu.nl/lutz/growing/gel.html] and it is possible to treat gels with organic solvents to produce versions suitable for use with hydrophobic or moisture-sensitive compounds.

Seed crystals. Sometimes crystallization of a compound gives crystals that, although otherwise of good quality, are clearly too small for structure analysis. A small number of these can be used as seeds by placing them into a warm saturated solution of the compound and allowing the solution to cool slowly. The hope here is that crystal growth will occur preferentially at the seed to give a suitably large single crystal. A container free of contaminants and scratches is strongly recommended here.

3.4.2 Sublimation

Sublimation (Fig. 3.9) is the direct conversion of a solid material to its gaseous state. It has been harnessed to produce solvent-free crystals of electronic materials but it is applicable to any solid with a significant vapour pressure at a temperature below its decomposition or melting point. The basic experimental arrangement is simple: a closed, usually evacuated vessel in which the solid is heated (if necessary) and a cold surface on which crystals grow. If possible, avoid heating the solid, as lower sublimation temperatures often lead to better crystals. If the solid sublimes too readily the vessel can be cooled. If a compound has a low vapour pressure, sublimation can be enhanced by evacuating the vessel or by using a cold finger containing acetone/dry ice (−78°C) rather than cold water (5−10°C).

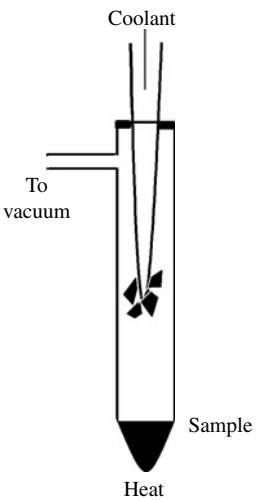

Fig. 3.9 Sublimation.

3.4.3 Fluid-phase growth

It is possible to grow crystals directly from liquids or gases, often by employing *in-situ* techniques. Fluid-phase methods encompass both high-temperature growth from melts and low-temperature growth from compounds that melt below ambient temperature (Fig. 3.10). High-temperature methods (Bridgman, Czochralski, zone refining, etc.) are used widely in the purification and growth of crystals of semiconductors and other electronic materials but are limited to compounds that melt without decomposition, thereby excluding many molecular compounds. Moreover, it is much more difficult to prevent unwanted

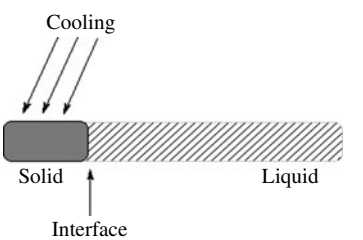

Fig. 3.10 Basic method for *in-situ* crystal growth.

phenomena such as twinning than with solution methods, and often impossible to separate overlapping or adjacent crystals.

Liquids or gases must be contained, for example in a capillary tube. One consequence of this is that crystallization conditions must be controlled to give only one crystal in that part of the tube that will be within the X-ray beam. Once crystals have grown it is usually impossible to separate them physically. Unlike crystal growth from solution there is essentially only one variable, namely the temperature of the sample. However, there are several ways to adjust this and the method can be chosen to give coarse or fine control. A typical strategy for crystal growth involves the establishment and manipulation of a stable interface between liquid and solid phases. With air-stable compounds that crystallise in a fridge or freezer it is only necessary to keep them cold until they are transferred into the cold stream of the diffractometer's low-temperature device.

3.4.4 Solid-state synthesis

In favourable circumstances it may be possible to produce adequate single crystals, but microcrystalline samples are far more typical. For example, most high-T_c superconductors do not give single crystals and their structures have been determined using powder diffraction methods. As with the synthesis of zeolites from solution, variation of synthetic conditions is likely to be the only route to better single crystals.

3.4.5 General comments

The details of crystal growth are often poorly understood, especially for new compounds, and it is important not to be discouraged if initial attempts fail. For example, microcrystalline material is not immediately useful but it does indicate that the compound is crystalline and that modification of the crystallization technique could result in larger crystals. It is always a good idea to try a range of techniques, keeping a detailed record of the exact conditions used and the results obtained. This not only allows identification of the most promising methods and conditions for the current sample but also means that in future there will be a database of procedures and their outcomes to consult. Crystal quality improves with experience, and early attempts often produce poor-quality crystals. It is important to continue until it is clear that no further improvement is likely.

In some cases, regardless of the method employed, crystals either do not form or are unsuitable. At this stage, the best way to proceed may be to modify the compound. With ionic compounds it may be practical to change the counter-ion (e.g. BF_4^- for PF_6^-, or vice versa). With neutral compounds it may be a simple matter to change some chemically unimportant peripheral group. In one case altering a piperidine substituent to morpholine, which merely involves changing one remote CH_2 group for an oxygen atom, led to a spectacular improvement in crystal quality.

3.5 Evaluation

Once crystals have appeared it is necessary to ascertain whether they are suitable for data collection. Some of the methods used are extremely rapid and can save large amounts of diffractometer time. During these procedures take care to prevent damage to the crystals, for example by loss of solvent after removal from the mother liquor. If spare crystals are available, leave one or two exposed on a microscope slide and check them regularly for signs of deterioration, using microscopy as described below. It is vital to apply the tests outlined below *optimistically* so that only crystals that are incontrovertibly unsuitable are rejected. Any that give uncertain indications of their quality should be given the benefit of the doubt.

3.5.1 Microscopy

Visual examination under a microscope takes only a few seconds or minutes, yet can identify unsuitable crystals that might otherwise occupy hours on a diffractometer. A microscope with a polarizing attachment, up to $\times 40$ magnification, a good depth of field and a strong light source is required. Crystal examination consists of three steps.

STEP ONE: With the analyzer component of the polarizing attachment out (i.e. not in use) look at the crystals in normal light to determine if they are well shaped. Reject crystals that are curved or otherwise deformed, have significant passengers that cannot be removed, or that show re-entrant angles. Be wary of rejecting crystals simply on the grounds that they are small, unless similarly sized crystals of the same type of compound have been consistently unsuccessful in the past. For organic compounds containing no element heavier than oxygen, crystals smaller than $0.1 \times 0.1 \times 0.1$ mm^3 seldom give good data with conventional laboratory instruments, although this size or smaller may be ideal for crystals of, say, an osmium cluster compound.

STEP TWO: With the analyzer in, most crystals in a typical sample will transmit polarized light. The exceptions are tetragonal and hexagonal crystals viewed along their unique *c*-axis, and cubic crystals viewed in any orientation. Tetragonal or hexagonal crystals transmit polarised light when viewed along other directions but cubic crystals cannot be distinguished from amorphous materials such as glass by this method. Fortunately, these three crystal systems together account for fewer than 5% of molecular crystals.

STEP THREE: If a crystal transmits polarized light, turn the microscope stage until the crystal turns dark (extinguishes), then light again, a phenomenon that will occur every 90° (Fig. 3.11). This extinction is the best optical indication of crystal quality, and it should be complete throughout the crystal and be relatively sharp ($\sim$1°). Any crystal that does not extinguish completely is not single and can be rejected immediately. Lack of sharpness may indicate a large mosaic spread within the crystal. A crystal that never extinguishes is almost certainly an aggregate

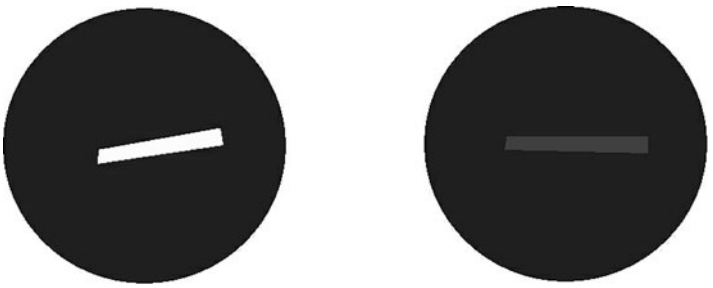

Fig. 3.11 Optical extinction observed between crossed polars.

of smaller crystals. When examining a batch of crystals, establish both the general quality of the sample and whether there are individual crystals suitable for further study.

3.5.2 X-ray photography

Photography began to decline in popularity as data collection using four-circle instruments advanced, in part because it was often quicker to record a full dataset than to obtain a complete set of photographs. Photography retained the advantage that it gave a better view of the reciprocal lattice than can be obtained from the list of reflections output by a four-circle diffractometer, and can record any diffraction occurring at other than the expected positions. Other than for specialist applications, the spread of area-detector instruments has essentially consigned X-ray photography to history. Area-detector images give much the same view of the reciprocal lattice as film, but do so much more quickly, flexibly and precisely without the need to process film.

3.5.3 Diffractometry

The ultimate test of a crystal is how it behaves on the diffractometer. Reflections must possess sufficient intensity, be well shaped (not split or excessively broadened) and index to give a sensible unit cell. Area-detector instruments combine some of the best features of photography and electronic counters and some can establish the quality of a crystal in seconds. It is worth bearing in mind that area detectors can often tolerate crystals of apparently appalling quality.

3.6 Crystal mounting

3.6.1 Standard procedures

For crystals that are stable to ambient conditions of air, moisture and light, the requirements of mounting are simple. The crystal is fixed securely with a reliable adhesive (e.g. epoxy resin) onto a glass or quartz fibre that is in turn glued into a 'pip' that fits into the well at the top of

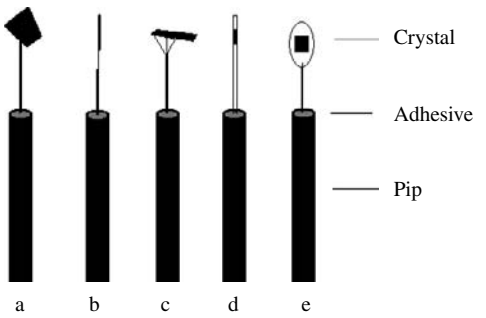

Fig. 3.12 Some methods for mounting crystals: a) on a glass fibre; b) on a two–stage fibre; c) on a fibre topped with several short lengths of glass wool; d) within a capillary tube e) in a solvent loop.

the goniometer head. The aim is to ensure that the crystal does not move with respect to this head. This means rejecting adhesives that do not set firmly (e.g. Vaseline or Evo-Stik) or mounting media that are not rigid (e.g. plasticine, Blu-tak or picene wax). On some diffractometers crystals are spun at up to 4000°/min, and an insecure mounting will lead to serious problems of crystal movement. A suitable fibre (e.g. of Pyrex glass) is just thick enough to support the crystal at a distance of about 5 mm above the pip. Fibres that are too thick add unnecessarily to errors via absorption and background effects, while those that are too thin can allow the crystal to vibrate, especially if it is being cooled in a stream of cold gas. For normal-sized crystals, the fibre should be thinner than the crystal. For small or thin crystals use a 'two-stage' fibre, which consists of a glass fibre onto which is glued approximately 1 mm of glass wool, onto which the crystal is attached. The fibre confers stability while the short length of glass wool reduces the amount of glass in the X-ray beam (Fig. 3.12).

This paragraph outlines the basic procedure for mounting a crystal. First, mix the epoxy resin, which will typically become tacky within five minutes and thereafter remain useable for a further five. Place the tip of the fibre into the resin and use the microscope to check that it has actually become coated. Ideally, the aim is to attach the tip of the fibre to the side of the crystal, thereby minimizing the amount of glass in the X-ray beam. Establish the size of the crystals, cutting them to size with a scalpel or razor blade if necessary. When picking up a crystal there is a danger of gluing it onto the slide, but this can be easily avoided: move the adhesive-tipped fibre forward until it makes contact with the side of the crystal, then continue moving the fibre forward and upwards to lift the crystal clear of the slide. [With thin plates this procedure may not be possible. If there is no alternative to mounting a crystal with a fibre along an edge or across a face of the crystal the fibre must be as thin as possible: a 'two-stage' fibre may be appropriate.] Also ensure that the crystal height can be adjusted to bring it into the X-ray beam: it is frustrating to find later that this cannot be done due to a fibre that

is too long or too short – on many instruments the X-ray beam passes 68 mm above the upper surface of the ϕ circle.

Instead of a simple fibre, some crystallographers prefer to mount the crystal on the end of a capillary tube (less glass in the beam for the same diameter); on a number of short lengths of glass wool attached to a thicker fibre (ditto); or on quartz fibres (more rigid for a given diameter). Some of the different methods for mounting crystals are shown in Fig. 3.12.

3.6.2 Air-sensitive crystals

The traditional way to protect sensitive crystals is to seal them (using a flame or epoxy resin) into a capillary tube, usually made from Lindemann glass that is composed of low-atomic-weight elements (Fig. 3.12). Even so, this puts a large volume of glass in the X-ray beam, so the tube and wall diameters should be as thin as practicable. The most sensitive crystals can be handled and encapsulated within a dry-box. When planning a low-temperature data collection, ensure that the top end of the tube is well rounded and that there are only a few millimetres of glass above the crystal position, otherwise severe icing will result (alternatively, see the second paragraph following). Crystals that desolvate may need either solvent vapour or mother liquor sealed into the tube with them. Unless crystals are mechanically robust, care must be taken when loading them into capillary tubes. With crystals that are both fragile and susceptible to solvent loss, a variant of a technique used by protein crystallographers may be helpful. Break the sealed end off a capillary tube and coat the first few millimetres of its inner surface with freshly mixed epoxy resin; place some crystals with their mother liquor in a well and isolate a good crystal; bring the open end of the tube through the surface of the solution; it may take some practice, but capillary action should draw the crystal along with some mother liquor into the tube; the crystal will stick to one side of the tube, which can then be sealed at both ends.

Many crystals can be protected by coating them with materials such as nail varnish, superglue or epoxy resin. As long as the coating confers sufficient protection and does not dissolve the crystal or react with it, this can be a simple and effective solution to air sensitivity that is applicable when cooling of the crystal is impossible. This situation can arise because an ambient-temperature dataset is required, a phase change is known or suspected to occur below ambient temperature, or because cooling causes an unacceptable degree of mechanical strain within the crystal.

A low-temperature device permits the use of an extremely flexible method for handling air-sensitive crystals. This involves transferring, examining and mounting the crystal under a suitable viscous oil. Upon cooling, the oil forms an impenetrable film around the crystal and also acts as an adhesive to attach the crystal firmly to the fibre. For crystals that do not survive room temperature, the technique can be combined with low-temperature handling, which normally involves passing a

stream of cold nitrogen gas across the microscope stage. Various oils have been used but perfluoropolyethers have the advantages of inertness and immiscibility with solvents. Suitable products are available from ABCR and Lancaster Synthesis; these have varying degrees of inertness and viscosity and some experimentation may be needed to find the most suitable. For many crystals silicone grease will be an adequate substitute.

An alternative method, popular with protein crystallographers and suitable for very thin crystals that are too fragile to be picked up on a fibre, is the solvent loop (Fig. 3.12). A small loop of a fibre such as mohair or a single strand from dental floss is used to lift the crystal in a film of solvent or oil that is then flash cooled on the diffractometer to immobilize the crystal. (For more details see Garman and Schneider, 1997.)

3.6.3 Crystal alignment

The final step is to attach the goniometer head to the ϕ circle of the diffractometer and optically adjust the crystal so that its centre does not move when it is rotated. Do not assume that the microscope crosshairs represent the true centre, although if the instrument is reasonably well set up this should be a useful starting point. Centring is an iterative procedure, and the following general outline should be possible on most instruments:

- check that the crystal is *approximately* central in X and Y by checking at $\phi = 0, 90, 180$ and $270°$ then set the height Z approximately
- view the crystal at $\phi = 0$ and $180°$, then at 90 and $270°$. At each position any lateral offset must be the same as that $180°$ away
- on instruments with fixed χ circles the height Z can be checked by rotating ω through $180°$; with a motorized χ circle the height is checked at $\chi = -90$ and $+90°$
- repeat the two previous steps until convergence is achieved.

References

Arend, H. and Connelly, J. J. (1982). *J. Cryst. Growth*, **56**, 642–644.

Buckley, H. E. (1951). *Crystal Growth*, Wiley, London.
– Very detailed, good for background and a source of alternative ideas for growing crystals, but there is almost no mention of sublimation.

Dryburgh, P. M., Cockayne, B. and Barraclough, K. G. (eds.) (1987). *Advanced Crystal Growth*, Prentice Hall, UK.

Garman, E. F. and Schneider, T. R. (1997). *J. Appl. Crystallogr.* **30**, 211–219.

Jones, P. G. (1981). *Chem. Br.* pp. 222–225.
– This article also covers aspects of crystal evaluation and is highly recommended.

Köttke, T. and Stalke, D. (1993). *J. Appl. Crystallogr.* **26**, 615–619.
– The classic paper on the use of oil films for handling sensitive crystals. It is excellent on practical aspects.

Look at the literature on related compounds. At the very least, the authors should have identified the solvent they used and the temperature at which crystals were grown.

Some crystal-growing hints and tips on the Web
http://www.nottingham.ac.uk/~pczajb2/growcrys.htm
http://www.oci.unizh.ch/service/cx/sample_prep.html
http://www.xray.ncsu.edu/GrowXtal.html
http://www.cryst.chem.uu.nl/lutz/growing/gel.html
http://www.cryst.chem.uu.nl/lutz/growing/reading.html
http://www.cryst.chem.uu.nl/growing.html

Space-group determination

4

William Clegg

4.1 Introduction

At some stage in the determination of a crystal structure by diffraction methods, it is necessary to decide which is the correct space group out of the possible 230. In many cases the choice is narrowed down quite early in the process, when the probable crystal system is indicated by the measurement of unit cell parameters, and the final choice is made once the intensity data have been collected. At this stage the information available may lead to an unambiguous choice of space group, but for other structures the space group is not completely clear until structure refinement has been successfully carried out in one of the possible space groups.

Information about the space group is obtained from a number of sources: the unit cell shape (the metric symmetry) and centring; the Laue class for the complete diffraction pattern; the systematic absence (zero intensities) of certain subgroups of reflections in the data set; the statistical distribution of intensities; other physical properties of the material being studied; and any prior knowledge of certain aspects of the structure.

There is no single universal procedure for space-group determination; the methods depend on the available information and its reliability. Although automatic computer programs are widely used, their results and the basis of their decisions should always be carefully examined, as mistakes are easily made.

At least some indication of the space group, or at least of the crystal system and preferably of the Laue class and crystal point group, is useful during the measurement of intensity data, in order to ensure that all symmetry-unique reflections are measured and none missed. With serial diffractometers, too much time spent measuring large amounts of equivalent data can be avoided, but with area detectors this is a less important consideration and, in any case, a high degree of symmetry-redundancy of data is useful for confirmation of the symmetry, for improvement of data precision, and for assessment and application of corrections for systematic errors such as absorption.

Where there is uncertainty about the symmetry, it is best to assume the lowest possible symmetry during data collection. In structure solution and refinement, however, the highest possible symmetry should be taken first, with lower symmetry considered only if necessary, avoiding the danger of missing some symmetry and describing the structure in a lower-symmetry space group than is correct; in some cases this is a poor description, but in others it leads to serious errors, particularly where an inversion centre has been missed.

Some or all of the following stages are involved in working out the correct space group for a structure, not necessarily in the order given here. In most of these descriptions, we assume ideal behaviour, and some of the problems found in real life are considered later.

4.2 Prior knowledge and information other than from diffraction

Sometimes it is possible to restrict the choice of space groups because we know something about the material being investigated. One of the best examples is the study of a compound that is known to be chiral and enantiomerically pure. This expectation may come from the known synthetic procedure, extraction of a natural product, or physical measurements. In such a case the individual molecules have no improper rotation axes (including reflection and inversion), and these symmetry elements must also be absent from the crystal structure as a whole, because all molecules are of the same hand: any improper rotation requires equal numbers of left and right hands. This immediately reduces the number of possible point groups from 32 to 11, namely those that contain only rotation symmetry (or none at all). These point groups are marked as enantiomorphous in Table 2.5.

Other indications of the absence or presence of certain symmetry elements may come from the external morphology of well-developed crystals, or from physical properties such as piezoelectricity, pyroelectricity, or non-linear optical behaviour. These measurements are not always easy or reliable, however, and are not widely used. By contrast, simple optical properties should always be examined with a microscope equipped with crossed polars and a revolving horizontal stage. Apart from anything else, this gives an indication of whether a crystal is likely to be single and of reasonable quality and makes it easier to select and mount a suitable one. Most transparent single crystals under these conditions will appear bright against a dark field of view, but will turn dark quite sharply when rotated into four orientations separated successively by 90°. This property is called optical extinction (not to be confused with X-ray extinction, a phenomenon associated with diffraction). Lack of any well-defined extinction positions usually indicates some kind of multiple crystal unsuitable for diffraction study, while amorphous materials like glass appear dark in all orientations. Other conglomerations of single crystals, including some twins, have regions that extinguish in

different orientations instead of a uniform behaviour. The exceptions to these generalizations are tetragonal, trigonal and hexagonal ('uniaxial') crystals viewed down their unique high-symmetry axis, and cubic crystals viewed in any direction; these are uniformly dark, though uniaxial crystals should become bright if tipped away from the principal axis.

4.3 Metric symmetry and Laue symmetry

Once the unit cell parameters have been determined, the crystal system can usually be selected. It is, however, possible for the unit cell to show higher metric symmetry than expected, because of fortuitous equality (within experimental uncertainties) of parameters, or angles that are close to special values not required by the true symmetry. One example is a monoclinic cell with a β angle close to 90°. From the unit cell parameters alone, this could be taken as orthorhombic, since all the angles are 90°. Similarly, an orthorhombic cell with two almost equal axis lengths appears to be tetragonal. For this reason it is important to examine the intensities of groups of reflections that should be equivalent for the assumed symmetry. Such reflections may be present in the initial set of data from which the unit cell was determined, or they may be investigated specifically at this stage. A final confirmation of the true Laue symmetry (the symmetry of the diffraction pattern with respect to both geometry and intensities) is best obtained after the complete data set has been collected.

It is also necessary to examine the intensities of related reflections in order to choose between the two possible Laue classes for each of the four higher symmetry crystal systems. These account, however, for only a few per cent of structures of molecular materials, so this will not need to be done very often. Likewise, primitive trigonal and hexagonal unit cells can not be distinguished on the basis of their geometry, and intensities of supposedly equivalent reflections must be considered.

Possible problems with this procedure include effects that make symmetry-equivalent reflections have different intensities, particularly strong absorption for crystals with extreme shapes and/or containing heavy atoms. Since many absorption correction methods are based on the measurement of equivalent reflections, this can be rather a circular argument, but in most cases a self-consistent result will be obtained if there are enough intensity data available to test the various symmetry possibilities. Final decisions should not be made until a complete data set has been measured.

4.4 Unit cell contents

Once the unit cell parameters are known, some assessment can be made of the probable contents of the cell, at least in terms of the number of atoms and molecules it can accommodate. If the density of the crystals has been measured, then the mass contents of one unit cell are easily

found from the cell volume (density = mass/volume), and the result can be compared with the proposed molecular mass for the compound.

$$D = MZ/N_0V$$

Here, D is the density, M the molecular mass, Z the number of molecules in each unit cell, N_0 Avogadro's number, and V the unit cell volume. It is important, of course, to work with consistent units in these calculations!

The usual approach is to calculate Z from the assumed value of M and the measured cell volume. If all is correct, this should be a whole number appropriate to the symmetry of the crystal system (common values are 1 or 2 for triclinic, 2, 4 or 8 for monoclinic, multiples of 4 for orthorhombic and tetragonal, and numbers with factors of 3 or 6 for other systems, unless individual molecules themselves can be of high symmetry and lie on special positions). Failure to obtain a result close to an integer, or an inappropriate value such as 5 or 7, demonstrates that the assumed value of the molecular mass is incorrect. This may be due to the presence of the solvent of crystallization, which has not been included in the overall molecular mass and leads to too high a value of Z, or it may be because the compound is not as expected! Sometimes this simple calculation helps avoid wasting time measuring the diffraction pattern of a known starting material or uninteresting decomposition product, but often the experiment proceeds anyway, in order to find out just what the material really is.

If the density has not been measured, a rather more approximate calculation can be made on the basis of an observation that, for a wide range of organic, organometallic and co-ordination compounds, each non-hydrogen atom in the unit cell requires an average volume of 18 $Å^3$; in some areas of chemistry a different value may pertain, and this is a matter of experience. Thus, the number of non-hydrogen atoms per unit cell can be estimated, and hence the number of molecules Z.

Comparison of the value of Z with the order of a point group (Table 5), in some cases, provides preliminary information about possible space groups within those associated with a particular Laue class, and may indicate that molecules are likely to lie in special positions, because Z is a fraction of the number of equivalent general positions. The most common outcome, however, is just an indication that the proposed chemical formula, possibly with some added solvent of crystallization, is compatible with the observed unit cell volume and crystal system.

4.5 Systematic absences

The intensity of each reflection in the diffraction pattern is due to interference of the waves scattered from individual atoms in that particular direction; the greater the degree to which atoms scatter in phase with each other, the higher is the intensity resulting from superposition of the waves with crests approximately aligned. The extent to which atoms

scatter in phase or out of phase relative to each other depends on their positions in the unit cell. For atoms that are related to each other by symmetry, the scattering effects are also related. In some cases this leads to either completely in-phase or strictly out-of-phase combinations of waves of equal amplitude; the former gives strong reinforcement, while the latter leads to a net contribution of zero from these atoms. At the fundamental level, of course, this is the explanation of the phenomenon of discrete diffraction maxima for X-rays scattered by single crystals: there is zero intensity in all directions except those given by the standard diffraction conditions as expressed in the reciprocal lattice and the Bragg equation, resulting from the pure translation symmetry of the crystal lattice. Similar effects, in selected parts of the diffraction pattern, are due to other symmetry elements involving translation components.

For a lattice described by a primitive unit cell, the diffraction pattern consists of reflections lying at the points of a primitive reciprocal lattice related in a well-defined way to the crystal lattice. These reflections have a range of intensities. What happens if a centred unit cell (*A*, *B* or *C*) is chosen instead of the primitive one, for the same lattice? This unit cell is twice the size of the original one, so the reciprocal unit cell is half the size and hence describes a reciprocal lattice with twice as many points. However, the structure itself has not changed as a result of this arbitrary choice of axes describing it, and so the diffraction pattern also remains the same in appearance. Therefore, half of the reciprocal lattice points for the new description do not lie on observed reflections; the intensities of these predicted 'reflections' are exactly zero, and they are called systematic absences. Which reflections are systematically absent is dictated by the choice of axes made in forming the centred unit cell, i.e. on the nature of the centring (*A*, *B* or *C*).

Each type of unit cell centring (also called lattice centring, though this is not really correct) has an associated pattern of systematic absences from which it can be uniquely identified. These are shown in Table 4.1. It is from these observed systematic absences in a diffraction pattern that the cell centring is identified as part of unit cell and space-group determination. In this and later tables, in the conditions for observed intensity, n is any integer (positive, zero or negative), so $2n$ just means any even number. Thus, for example, for a reflection to be observed for a body-centred unit cell, the sum of all three indices must be even; if the sum is odd, the reflection has zero intensity.

Centred unit cells produce systematic absences right through the whole data set; the conditions in Table 4.1 apply to all reflections. Systematic absences in selected parts of the diffraction pattern are observed when glide planes and screw axes are present in a structure, because of the translation components of these symmetry elements. If a glide plane is viewed 'face on', perpendicular to its reflection, and heights of atoms above and below this plane are ignored, the unit cell in projection appears to be centred (for n glide) or halved in one dimension (for a, b or c glide), so this produces appropriate systematic absences in

Table 4.1. Systematic absences for centred unit cells.

Centring	Points equivalent to 0,0,0	Condition for observed intensity	Fraction of observed data
P	none	none	1
A	0, ½, ½	$k + l = 2n$	½
B	½, 0, ½	$h + l = 2n$	½
C	½, ½, 0	$h + k = 2n$	½
I	½, ½, ½	$h + k + l = 2n$	½
F	0, ½, ½ and ½, 0, ½ and ½, ½, 0	h, k, l all even or all odd	¼
R	⅓, ⅔, ⅔ and ⅔, ⅓, ⅓	$-h + k + l = 3n$	⅓

Table 4.2. Systematic absences for glide planes.

Normal to glide plane	Reflections affected	Glide plane symbol	Translation vector	Condition for observed intensity
a-axis [100]	0*kl*	*b*	**b**/2	$k = 2n$
		c	**c**/2	$l = 2n$
		n	(**b**+**c**)/2	$k + l = 2n$
		d	(**b**+**c**)/4	$k + l = 4n$
b-axis [010]	*h*0*l*	*a*	**a**/2	$h = 2n$
		c	**c**/2	$l = 2n$
		n	(**a**+**c**)/2	$h + l = 2n$
		d	(**a**+**c**)/4	$h + l = 4n$
c-axis [001]	*hk*0	*a*	**a**/2	$h = 2n$
		b	**b**/2	$k = 2n$
		n	(**a**+**b**)/2	$h + k = 2n$
		d	(**a**+**b**)/4	$h + k = 4n$
[110]	*hhl*	*c*	**c**/2	$l = 2n$
		d	(**a**+**b**+**c**)/4	$2h + l = 4n$

reflections whose intensities contain no information about the heights of atoms perpendicular to the plane. The effect is to remove half the reflections within one two-dimensional section (one sheet or ***zone***) of the three-dimensional diffraction pattern; in almost all cases observed in practice these are sets of reflections with one index equal to zero. The complete set of possible systematic absences for glide planes is given in Table 4.2. The last two rows apply only in the higher-symmetry crystal systems; in the cubic system, the two directions [101] and [011] are equivalent to [110] and give similar effects.

A similar argument applies for screw axes. In this case, systematic absences occur for just one row of reflections, usually with two indices equal to zero. Table 4.3 gives the possibilities for screw axes parallel to each of the unit cell axes (there are other possible directions in higher-symmetry systems). The recognition of a screw axis from systematic

Table 4.3. Systematic absences for screw axes: conditions for observed intensity.

Parallel to	Reflections affected	Condition for $2_1, 4_2$ or 6_3	Condition for $3_1, 3_2, 6_2$ or 6_4	Condition for 4_1 or 4_3	Condition for 6_1 or 6_5
a	*h*00	$h = 2n$	$h = 3n$	$h = 4n$	$h = 6n$
b	0*k*0	$k = 2n$	$k = 3n$	$k = 4n$	$k = 6n$
c	00*l*	$l = 2n$	$l = 3n$	$l = 4n$	$l = 6n$

absences is based on only a few reflections and so is less reliable than spotting glide planes and centred unit cells.

The presence or absence of pure rotation, improper rotation, pure reflection, and inversion symmetry cannot be detected from systematic absences, as these symmetry elements have no translation components.

Some space groups can be uniquely determined from the Laue symmetry and systematic absences. Fortunately, these include the two common space groups $P2_1/c$ (alternative settings $P2_1/n$ and $P2_1/a$ by different choices of cell axes) and $P2_12_12_1$ as well as several other reasonably common space groups. In other cases two or more space groups give the same systematic absences and other information is needed in order to choose among them.

4.6 The statistical distribution of intensities

Although symmetry elements without a translation component do not cause systematic absences, they do have an effect on the distribution of intensities, which may be detected by a statistical analysis of how the intensities are distributed about their mean value. Such tests are based on a number of assumptions and approximations and must be used with due caution. At best they indicate only that something is probably true, not a certainty. In particular, the tests assume an essentially random arrangement of electron density in the unit cell apart from the symmetry elements being tested, so a structure containing atoms with widely different numbers of electrons (except for hydrogen atoms, which contribute only very weakly to X-ray diffraction) or with non-crystallographic molecular symmetry may lead to either unclear or incorrect conclusions.

Statistical tests are not made with the intensities themselves, or even with the amplitudes derived from them. Just as for direct methods of structure determination, the amplitudes are converted to 'normalized amplitudes', otherwise known as *E*-values. These represent what the amplitudes would be for point atoms at rest instead of vibrating atoms of finite size. The derivation of *E*-values from intensities and amplitudes is described in Chapter 10. They are defined in such a way that the mean value of $|E|^2$ is 1 for all data and should also be 1 for subsets of the data at different values of $\sin\theta$. However, the presence or absence of an inversion centre in the crystal structure affects the distribution of

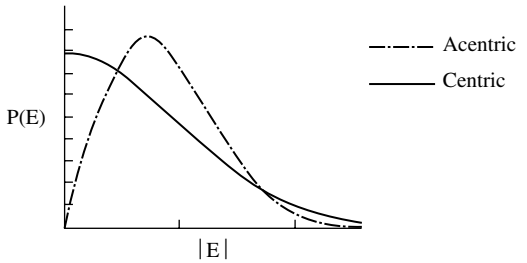

Fig. 4.1 Acentric and centric distributions.

E-values about their mean. With no inversion symmetry, particularly in the space group *P*1, *E*-values do not vary much from their mean, and the diffraction pattern does not show much variation in intensities. When there is inversion symmetry present, atoms are in pairs related by the inversion, and their combined scattering tends to give a greater proportion of strong reflections and weak reflections, so that intensities show more variation overall. The theoretical probability of a reflection having a particular value of $|E|$, $P(E)$, is quite different in the two cases, as shown in Fig. 4.1. The two distributions are called acentric and centric; these are statistical terms describing the distribution of numerical values, and should not be confused with and used interchangeably with the terms non-centrosymmetric and centrosymmetric, which apply to geometrical arrangements, for example of atoms in crystal structures.

The actual distribution of *E*-values in a particular data set can be presented in a variety of ways. The most widely used is probably the simplest: calculation of the mean value of $||E|^2 - 1|$ for all the data, giving a single value. This tends to be close to 0.74 for an acentric and 0.97 for a centric distribution of intensities, so values close to these are indicative of the probable absence or presence, respectively, of inversion symmetry.

A similar treatment can be made for rotation axes and mirror planes by using an appropriate subset of the data and looking for an acentric or centric distribution. However, with far fewer reflections in the set of data being examined, these are not generally very reliable, and they are not often used.

4.7 Other points

Even with examination of the Laue symmetry, systematic absences, and a full statistical analysis of the distribution of intensities, there remain some space groups that can not be distinguished from each other. These include a number of enantiomorphous pairs, in which one space group is the mirror image of the other and the choice between them specifies the handedness of the structure. They can be distinguished only if the true handedness is known by other means, or if there is sufficient anomalous dispersion to show that one fits the diffraction data significantly better

than the other, in which case the final choice of space group is not made until structure refinement is well advanced.

There are also two other pairs of space groups for which the correct choice can only be made by seeing which leads to successful structure solution and refinement. These are the orthorhombic pair $I222$ and $I2_12_12_1$ and the cubic pair $I23$ and $I2_13$. In both cases the two space groups have the same symmetry elements, but they are arranged differently relative to each other in space. These are unusual and subtle problems!

Various stages of the space-group determination process may be adversely affected by problems in the data collection. Poor-quality data can give unreliable statistical tests, can lead to incorrect or uncertain decisions about the Laue symmetry, and can make it difficult to work out the correct systematic absences. In particular, some effects such as multiple diffraction, the presence of wavelength harmonics, or serious underestimation of standard uncertainties of intensities can make systematically absent reflections appear to have significant and even quite substantial intensities. In such cases, reliance on fully automatic computer programs is particularly dangerous. Dealing with such problems may involve careful examination of the originally measured data, and even a partial or complete repeat of the data collection in some instances.

One complicating factor in space-group determination, and in crystal-structure determination overall, is the occurrence of pseudo-symmetry. In some structures there is an approximation to symmetry that is not exact; for example, two molecules not quite identical and with relative positions corresponding approximately to centring of the unit cell. Pseudo-symmetry can lead to various problems and ambiguities, such as metric symmetry higher than the Laue symmetry, sets of reflections that would have exactly zero intensity in recognized systematic absences but are weak rather than completely missing, and mean $||E|^2 - 1|$ values intermediate between the centric and acentric ideals. Sometimes this means the structure can be solved in more than one space group, at least for the location of some of the atoms, and the pseudo-symmetry is broken only when further atoms are found.

Some cases of metric symmetry higher than the Laue symmetry (and some other fortuitous rational geometrical relationships among unit cell parameters) can lead to unit cells being stacked together in the wrong orientations during the formation of a crystal, so that the result is a combination of two different orientations of the same structure in one apparently single crystal. This means the diffraction patterns of the two components are superimposed. This effect is called twinning. Sometimes it is obvious that the observed diffraction pattern can not be associated with a single-crystal lattice, but in other cases the reflections of the two components coincide. Depending on the precise nature of the twinning and the space group of the material, this may lead to some strange patterns of zero intensities, because systematic absences of one component overlap permitted reflections of the other. The resolution of such problems requires some skill and experience.

There are also cases where a structure can be described either with disorder in a particular space group or ordered in a lower-symmetry space group (lacking a symmetry element of inversion, reflection or pure rotation, which are not indicated by systematic absences). The correct choice is not always easy to make, though it is generally accepted that the higher symmetry, which usually has fewer parameters, is preferred unless there are strong indications otherwise. Certainly, if the lower-symmetry description involves unusual molecular geometry distortions or requires extensive use of refinement constraints or restraints, it is probably wrong.

Finally, it should be noted that the ultimate demonstration of the correct assignment of a space group is the successful refinement of the structure with no untoward features. The fact that an initial structure solution can be obtained in a lower-symmetry space group and not in a higher one does not prove that the lower symmetry is correct; the removal of inversion symmetry in particular gives direct methods programs much more freedom in their calculation of reflection phases. The possible missing symmetry should be looked for carefully in the structure solution. Various programs exist that can take a partial or completed structure and examine it for evidence of additional symmetry not noticed by the experimenter, allowing for a revised assessment and further refinement in the higher-symmetry space group. Probably the best developed and most used of these is PLATON by A. L. Spek of Utrecht University, The Netherlands. Pseudo-symmetry can also be detected and explored in this way.

4.8 A brief conducted tour of some entries in International Tables for Crystallography, Volume A

The *International Tables for Crystallography* are important standard reference works for practising crystallographers. *Volume A* is all about space group symmetry – over 800 pages of detailed information including a variety of representations and properties of each of the 230 space groups, some of them in alternative axis settings and orientations (for example, the alternatives $P2_1/c$, $P2_1/a$ and $P2_1/n$, and both primitive and obverse-centred choices for rhombohedral space groups). It should be noted that there is a much shorter volume of selected space groups available as a "teaching edition", with helpful notes, as *Brief teaching edition of Volume A: Space-group symmetry*. It currently costs about £17 from the IUCr or Springer.

Among the information are the following:

1) headings including the space group symbols in both international and (not very useful) Schoenflies notation, the former in conventional short form and also in a full form where this is different;

this full form makes explicit the association of symmetry elements with particular crystallographic axes;

2) projections of the unit cell along different axes, with the positions of the various symmetry elements, and a separate projection showing the effect of the symmetry operations on a molecule in a general position;
3) information about possible choices of origin and the size of the asymmetric unit in terms of a fraction of the unit cell;
4) a list of the symmetry-related general positions (in a form that is used by many crystallographic computer programs to represent the space group symmetry), together with lists of all the special positions (in which molecules lie on symmetry elements), with their multiplicities (Z values) and point group symmetry;
5) the systematic absences (actually expressed as positive conditions for reflections to occur, not negative ones for their absence) for the space group, and also those that arise for atoms in special positions;
6) various information about the symmetry of two-dimensional projections and of subgroups and supergroups.

In the lists of general positions, it is quite easy to work out which are generated by different kinds of symmetry elements. In the three crystal systems of lowest symmetry (no rotation symmetry higher than two-fold), the presence of one minus sign before any of x, y and z in a general position indicates reflection; two minus signs indicate rotation, and three minus signs indicate inversion. Fractions added to x, y or z are a marker of translational components of symmetry elements (centred unit cells, glide planes and screw axes). If any of x, y or z occurs without any negative signs in front of it in the list of general positions, this is a polar axis.

Exercises

1. The following unit cell volumes and densities have been measured for the given compounds. Calculate Z for the crystal, and comment on how well (or badly) the '18 Å^3 rule' works for each compound:
   a) methane (CH_4) at 70 K: $V = 215.8$ Å^3, $D = 0.492$ g cm^{-3};
   b) diamond (C): $V = 45.38$ Å^3, $D = 3.512$ g cm^{-3};
   c) glucose ($C_6H_{12}O_6$): $V = 764.1$ Å^3, $D = 1.564$ g cm^{-3};
   d) bis(dimethylglyoximato)platinum(II) ($C_8H_{14}N_4O_4Pt$): $V = 1146$ Å^3, $D = 2.46$ g cm^{-3}.
2. A unit cell has three different axis lengths and three angles all apparently equal to 90°. What is the metric symmetry? The Laue symmetry, however, does not agree with this; equivalent intensities are found to be

$$hkl \equiv hk\bar{l} \equiv \overline{\bar{h}kl} = \overline{\bar{h}k\bar{l}}$$

$$\bar{h}kl \equiv \bar{h}k\bar{l} \equiv h\bar{k}l = h\bar{k}\bar{l}.$$

   What is the true crystal system and its conventional axis setting?
3. What are the systematic absences for the space groups $I222$ and $I2_12_12_1$?
4. Deduce as much as you can about the space groups of the compounds for which the following data were obtained.
   a) Monoclinic. Conditions for observed reflections: hkl, none; $h0l$, $h + l$ even; $h00$, h even; $0k0$, k even; $00l$, l even. Centric distribution for general reflections.
   b) Orthorhombic. Conditions for observed reflections: hkl, all odd or all even; $0kl$, $k+l = 4n$ and both k and l even; $h0l$, $h + l = 4n$ and both h and l even; $hk0$, $h + k = 4n$ and both h and k even; $h00$, $h = 4n$, $0k0$, $k = 4n$; $00l$, $l = 4n$. Centric distribution for general reflections.
   c) Orthorhombic. Conditions for observed reflections: hkl, none; $0kl$, $k + l$ even; $h0l$, h even; $hk0$, none; $h00$, h even; $0k0$, k even; $00l$, l even. Acentric distribution for general reflections, centric for $hk0$.
   d) Tetragonal. Reflections hkl and khl have the same intensity. Conditions for observed reflections: hkl, none; $0kl$, none; $h0l$, none; $hk0$, none; $h00$, h even; $0k0$, k even; $00l$, $l = 4n$; $hh0$, none. Acentric distribution for general reflections; centric for $0kl$, $h0l$, $hk0$, and hhl subsets of data.

Background theory for data collection

5

Jacqueline Cole

5.1 Introduction

This chapter takes the reader through the theoretical fundamentals behind data collection and reduction methods for single-crystal structure determination. The descriptions are directed towards those using area-detector diffractometers, since these are now almost the only ones available commercially and are installed in many laboratories. However, a large part of the theory may still be relevant to older types of diffractometers.

A step-wise theoretical journey through an experiment is first presented, to illustrate the need for alternating real and reciprocal space thinking at different parts of an experiment. There follows a discussion of the geometry of X-ray diffraction in both real and reciprocal space, the sequence of procedures required to determine a unit cell, data-collection methodologies and strategies, a description of the data-integration process for diffractometers housing a standard flat-plate two-dimensional area detector, and the subsequent data-reduction corrections that are necessary to afford a list of intensities or structure factors, the starting point for data solution and refinement.

5.2 A step-wise theoretical journey through an experiment

The sequence of events that comprise an X-ray diffraction experiment is in many ways analogous to that of a microscopic investigation, as Fig. 5.1 illustrates.

When a sufficiently intense and collimated source of photons is directed at a small crystal, an inverted image of the form of that crystal can be collected on a lens or detector placed on the opposite side of the crystal. The wavelength of the photon source will dictate the scale of the contents of this image: an optical source ($\lambda \sim 1$ μm) will

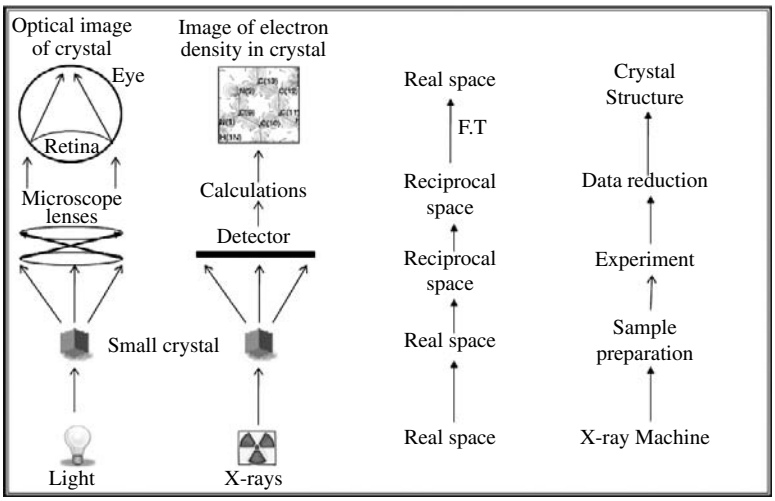

Fig. 5.1 The components of an optical and 'X-ray' microscope, revealing the real and reciprocal parts of an experiment.

present a microscopic inverted view of the exposed part of the crystal, whilst an X-ray beam ($\lambda \sim 10^{-10}$ m $= 1$ Å) will reveal an inverted image of the exposed part of the crystal on the Ångstrom scale, i.e. the scale corresponding to the size of atoms. Where X-ray diffraction (rather than absorption) occurs, the diffracted image will represent the average view of the contents of many unit cells in a reciprocal form, given the periodic nature of single crystals. Such an image would normally comprise many spots, their relative location on the image providing information about the unit cell, whilst their intensities contain all of the information about the relative positions of all atoms within the unit cell.

In the case of an optical microscope, the retina in the human eye provides a natural image-inversion process so that one can readily obtain a real-space interpretation of an optically inverted image, simply by viewing the optical lens that captured the image via objective lens with an appropriate magnification.

Realizing a real-space view of the diffracted part of an X-ray image is an entirely different matter, however; only fictional characters have 'X-ray eyes' and even they could not oblige due to the irradiation damage that they would sustain from putting their head in the X-ray beam!

An X-ray-sensitive detector, whether this is photographic film or an electronic device, can be used to obtain the reciprocal diffraction image. The positions and intensities of diffraction spots can therefore be ascertained. However, with no 'X-ray eye retina', this information still needs to be converted from reciprocal to real space. A calculation, in the form of a Fourier transformation, is needed to make this conversion. It requires the 'structure factor', F, of each spot on the image. The square of the structure factor, F^2, is proportional to the intensity of a spot, which is measurable, and so the amplitude $|F|$ can be evaluated. The phase of

each F (the sign for centrosymmetric structures) cannot be found by a normal experiment, however, since spot intensities do not directly carry phase information: there is no way of knowing the phase of an X-ray beam as it meets the detector. All intensities are positive. The phase of F is crucial, however, since the Fourier transform is based implicitly on a summation involving F. Later chapters in this book concerning structure solution explain how one can overcome this so-called 'phase problem'. Once solved, the required conversion from reciprocal to real space can be undertaken to reveal the real-space representation of a unit cell, in the form of an electron-density map.

This virtual journey through an experiment not only illustrates the analogy of an 'X-ray microscope' but hopefully also shows that one needs to look at the different stages of an experiment with different space concepts. The physical experiment itself, comprising the sample and the diffractometer, obviously exists in real space. The X-rays are fired at the crystal in real space. The diffraction patterns observed by the detector represent reciprocal space images of the crystal structure of the sample. Each spot, or 'reflection', in a diffraction pattern can be identified uniquely by Miller indices, or *hkl* values. Such indices, described in detail later, are therefore reciprocal space quantities, as are their associated structure factors. The goal of all subsequent data integration and reduction stages is to obtain the magnitudes (amplitudes) of the structure factors of each diffraction spot, via the square root of their measured intensities, corrected for various defined geometrical and physical effects. With these in hand, one can then consider the Fourier-transformation calculation to obtain the desired real-space view of a molecule via an electron-density map.

5.3 The geometry of X-ray diffraction

X-ray waves interact with electrons in a material. X-ray diffraction occurs when a crystal is oriented towards incoming X-ray waves, of a suitable wavelength (λ), such that the waves interfere non-destructively between ordered rows of electronic concentration (layers of atoms) in the crystal that are of a suitable separation (d).

The condition for diffraction can be defined mathematically by Bragg's law or geometrically by the Ewald sphere construction, in real or reciprocal space, respectively.

5.3.1 Real-space considerations: Bragg's law

Bragg's law states that $n\lambda = 2d \sin\theta$. λ and d have been defined above and θ is the angle between a plane of atoms and the line of the diffracted (or incident) beam; n is an integer. Therefore, diffraction occurs only for certain combinations of d, λ and θ. The variation of d, whilst keeping λ and θ approximately constant, results in differing magnitudes of diffraction by two lattice planes in one dimension, as illustrated in Fig. 5.2; here,

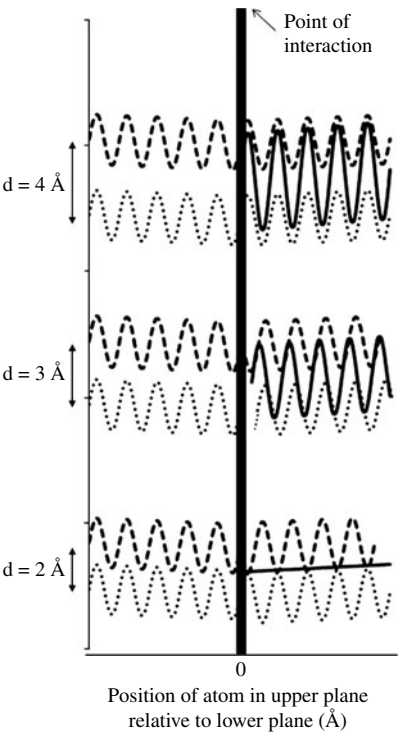

Fig. 5.2 The level of diffraction generated by interference of two X-ray waves with two planes of atoms positioned directly above each other, as a function of distance between these planes, d [d = 4 Å (top), 3 Å (middle), 2 Å (bottom); $\theta = 5°$ and $\lambda = 0.7$ Å throughout]. A fully interactive and extended version of these snapshots is given by Proffen and Neder (2008a).

where incident X-ray waves are 100% in-phase ($d = 4$) the maximum amount of diffraction occurs, whilst 100% out-of-phase ($d = 2$) will preclude diffraction; 75% in-phase waves result from $d = 3$ and so affords a moderate amount of diffraction.

Two X-ray waves diffracted from a plane will have a difference in path length, necessarily depending on d. One may notice in Fig. 5.2, for example, that the 100% in-phase interference of two waves has a path difference that corresponds to exactly one wavelength. Indeed, there exists a general relationship that the maximum amount of diffraction between two points occurs at a value of d where the path difference between two waves is an integral multiple of the X-ray wavelength, $n\lambda$. This multiplier, n, is the same integer used in Bragg's law.

Given that there are many parallel planes in a crystal, and that the diffraction condition needs to be satisfied in three dimensions simultaneously rather than in one as presented here, in practice diffraction is observed only where n is an integer. In nearly all cases of conventional X-ray diffraction, one can consider that $n = 1$, since one can always divide d by n if it is greater than 1, in order to obtain a value of d corresponding to $n = 1$.

The value of d that corresponds to 100% in-phase diffraction, in each of the three-dimensional basis-set vectors being used, is represented by vectors that relate to a, b and c and integers h, k and l, respectively, where a, b and c represent the unit cell parameters and the integers are the reciprocal-space (hkl) indices. Therefore, in practice, one can say that $\lambda = 2d_{hkl} \sin\theta$.

In conventional crystal-structure determination, our aim is to collect as many unique diffraction spots, hkl, as possible within the practical bounds of time available. The variation of d represents the orientation of a crystal with respect to the incident X-ray beam, and ideally we would want to collect diffraction data for all possible orientations of a crystal for a three-dimensional crystal-structure determination. In an experiment, d is therefore usually varied, whilst keeping λ constant (X-ray sources in a laboratory are monochromatic and λ is selected by the type of X-ray tube installed on an instrument) and stepping through θ incrementally to collect the data since 2θ, the net scattering angle, represents the angle of the detector centre relative to the incident X-ray beam, $2\theta = 0°$ being the straight-through beam.

5.3.2 Reciprocal-space considerations: the Ewald sphere

Since the diffraction patterns that we observe in an experiment relate to reciprocal space, a geometrical construct of a reciprocal space version of Bragg's law is often useful in interpreting such patterns. The Ewald sphere, illustrated in Fig. 5.3(a), provides this construct: the sample lies at the centre of a sphere whose radius is the reciprocal of the wavelength ($1/\lambda$); the diffraction condition is met when a spot touches the surface of this sphere. With an incident X-ray beam traversing the horizontal from

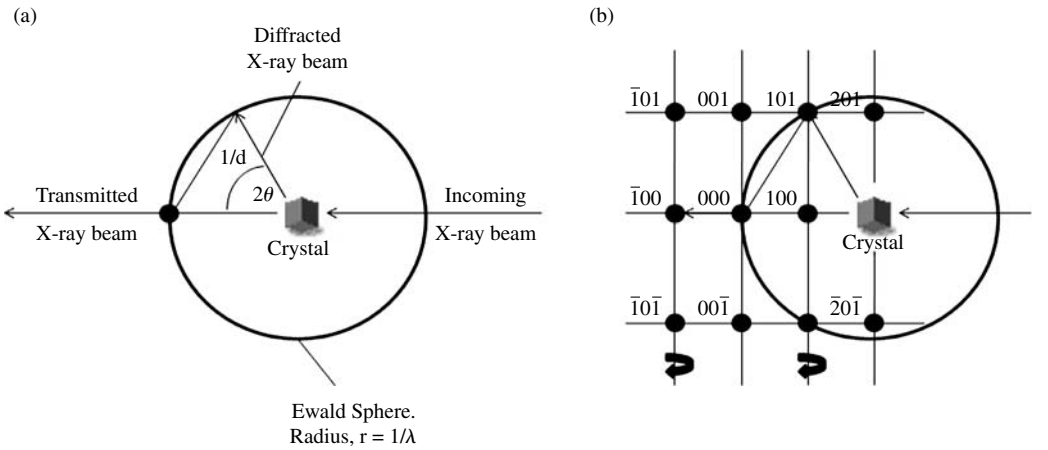

Fig. 5.3 The Ewald sphere: (a) definition of parameters; (b) the intersection of the (101) reflection with the surface of the Ewald sphere, thereby meeting the Bragg condition of diffraction.

one side of the sphere, transmitted X-rays simply continue to the other side of the sphere, whereupon the beam meets the surface to satisfy the diffraction condition for the (000) reflection that corresponds to $F(000)$. This reflection is always calculated rather than measured because the beamstop necessarily obscures the transmitted X-ray beam from the detector. Indeed, even if it could be measured, the (000) reflection would be contaminated with undiffracted direct beam and so such an intensity measurement would be inaccurate. The (000) reflection is referenced as the origin of reciprocal space.

Where diffraction occurs, one can draw a vector from the crystal centre to the surface of the Ewald sphere that subtends an angle, 2θ, (the net scattering angle) to the vector representing the transmitted X-ray beam. The point thus generated on the surface of the sphere corresponds to a reflection, *hkl*, and the chord that links this point with the reciprocal lattice origin has a length $1/d$, where d is the lattice spacing for that reflection.

As the crystal is rotated during a diffraction experiment, different lattice planes are exposed to the incident X-ray beam, and so different reflections intersect the surface of the sphere, i.e. diffract. Figure 5.3(b) shows an illustrative example of a rotating lattice plane of reflections, where diffraction at that time-captured moment derives from the (101) reflection.

A very useful demonstration of an Ewald sphere simulation is given by Proffen and Neder (2008b).

One can use the Ewald sphere construct to interpret geometrically the patterns of spots appearing on successive frames of diffraction during data collection.

If one has determined the unit cell parameters of a crystal within the diffractometer frame of reference (see Section 5.5), one can also calculate the *hkl* indices of each spot in a diffraction pattern using the appropriate

Table 5.1. Values of $1/d_{hkl}^2$ for each crystal system (Giacovazzo, 1992).

Crystal System	$\mathbf{1/d_{hkl}^2}$
Triclinic	$(1-\cos^2\alpha-\cos^2\beta-\cos^2\gamma+2\cos\alpha\cos\beta\cos\gamma)^{-1}\left(\frac{h^2}{a^2}\sin^2\alpha+\frac{k^2}{b^2}\sin^2\beta+\frac{l^2}{c^2}\sin^2\gamma+\frac{2kl}{bc}(\cos\beta\cos\gamma-\cos\alpha)+\frac{2lh}{ca}(\cos\gamma\cos\alpha-\cos\beta)+\frac{2hk}{ab}(\cos\alpha\cos\beta-\cos\gamma)\right)$
Monoclinic	$\frac{h^2}{a^2\sin^2\beta}+\frac{k^2}{b^2}+\frac{l^2}{c^2\sin^2\beta}-\frac{2hl\cos\beta}{ac\sin^2\beta}$
Trigonal (R)	$\frac{1}{a^2}\left(\frac{(h^2+k^2+l^2)\sin^2\alpha+2(hk+hl+kl)(\cos^2\alpha-\cos\alpha)}{1+2\cos^3\alpha-3\cos^2\alpha}\right)$
Hexagonal/Trigonal (P)	$\frac{4}{3a^2}(h^2+k^2+hk)+\frac{l^2}{c^2}$
Orthorhombic	$\frac{h^2}{a^2}+\frac{k^2}{b^2}+\frac{l^2}{c^2}$
Tetragonal	$\frac{h^2+k^2}{a^2}+\frac{l^2}{c^2}$
Cubic	$(h^2+k^2+l^2)/a^2$

equation in Table 5.1, thus uniquely identifying each reflection as one collects data.

The ability to identify each reflection means that one can also predict where all diffraction spots will appear in frames of data. This enables the experimenter to manipulate the diffraction geometry, via diffractometer control programs, to perform various functions: 'dial-up' certain reflections, lattice planes, time-optimize data collection strategies, and so on.

5.4 Determining the unit cell: the indexing process

There are two principal methods that are used to determine a unit cell: a real-space method, called 'autoindexing'; and a reciprocal-space method. Both methods follow a similar common procedure in that they determine the unit cell using a small portion of diffraction data taken from different parts of reciprocal space, and their methodology follows the generic flow-diagram below (Fig. 5.4).

5.4.1 Indexing: a conceptual view

If one possessed data that corresponded to every possible diffraction spot in a sufficiently large volume of reciprocal space, one could simply calculate the lattice spacings for each reflection in real space and thence build up a three-dimensional grid of periodic lattice points. This grid would contain a repeat motif, which one could identify by observation,

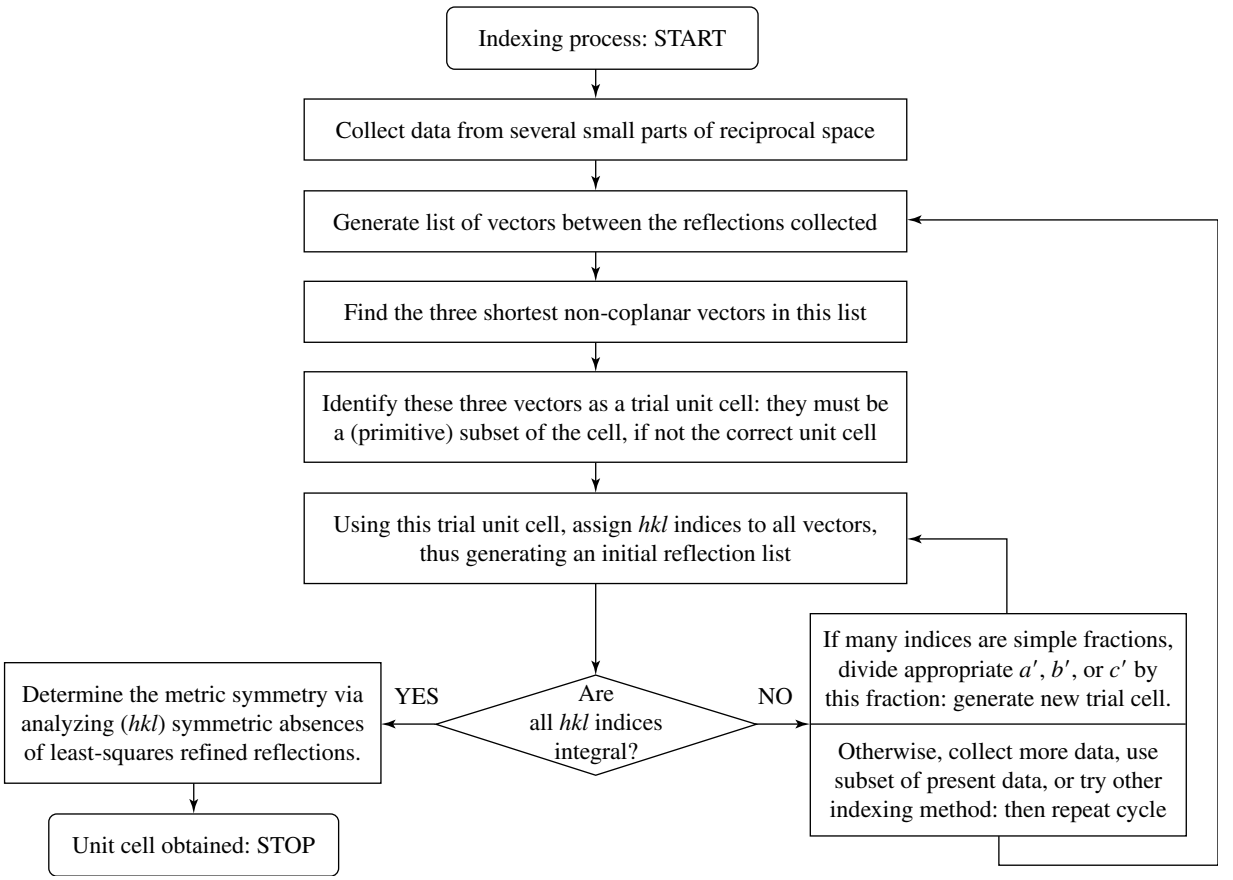

Fig. 5.4 Indexing flowchart.

and that would represent the unit cell of the sample in hand (e.g. see Fig. 5.5a).

Realizing such a situation is not practical when initially indexing a crystal and so one relies, instead, on utilizing a small portion of data collected selectively from several small volumes of reciprocal space that together will afford a representative derivation of a partial lattice in three dimensions. Whilst such a representation is rather 'patchy' (e.g. see Fig. 5.5b), as long as there are enough parts of the lattice to indicate all three unit cell parameters and corroborate them, one should be able to determine the correct unit cell of any subject material, assuming that the sample is a good-quality single crystal.

This is a rather conceptual view of indexing, but hopefully is a helpful one. In practice, one works largely with a comparison of vectors as described in the next section. That said, one can often gain an insight into the likely unit cell parameters by simply observing the frames of data collected for indexing purposes: if many diffraction spots are close

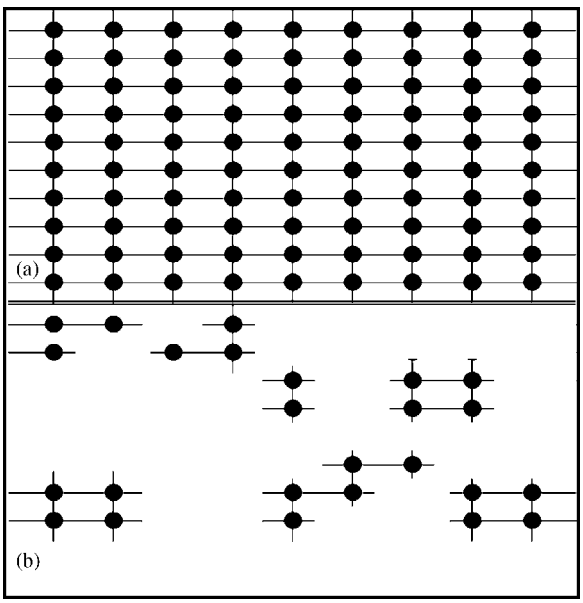

Fig. 5.5 Conceptual unit cells.

together along one direction, one would expect a long unit cell parameter in the corresponding real-space dimension. This may indicate a unit cell of a certain crystal system and thus put constraints upon some of their parameters.

5.4.2 Indexing procedure

Detailed accounts of each of the two principal indexing methods can be found in many articles (Hornstra and Vossers, 1974; Clegg, 1984; Sparks, 1976, 1982; Kabsch, 1993). However, it is instructive to consider here the basic generic procedure behind each method, via a flow diagram (Fig. 5.4) with an associated description. The first step has already been discussed in the previous section.

Each of the two indexing methodologies uses a core set of vectors, $\mathbf{x}$, that correspond to the reciprocal lattice points observed in the diffraction patterns selectively collected for indexing purposes. In the reciprocal-space method, this core set of vectors is augmented by summative or difference vectors generated from combinations of these initial vectors, $\mathbf{x}_i \pm \mathbf{x}_j$; the same difference vectors are often added to the vector set in the real-space method as well, particularly where one anticipates a large unit cell. In each case, the three shortest non-coplanar vectors for this list are then identified and used to define an initial cell, in the form of reciprocal cell axes or a real-space trial unit cell. Whilst such a trial solution does not usually correspond to the true unit cell, it will represent a subcell of the true unit cell.

By assimilating this trial cell to the true unit cell, one can calculate a trial (*hkl*) index for each of the core set of vectors, via the usual mathematical equations for a given predicted crystal system, as described in Table 5.1, Section 5.3.2, or via analogous reciprocal space axis relations. This affords a trial list of uniquely identified reflections that one can use to test the validity of the trial unit cell: the true unit cell must generate only integral values of h, k and l, for all reflections in this list, by the fundamental nature of Miller indices. One can readily tell if all (*hkl*) assignments approximate to integral quantities by simply observing the list of (*hkl*) values. In practice, one rarely finds all (*hkl*) values perfectly integral due to experimental error, spurious reflections, i.e. reflections that derive from alien reciprocal lattices, or instrumental artefacts, but one should expect most h, k and l values to be near-integer quantities if the trial cell corresponds to the primitive form of the true unit cell.

If the bulk of h, k or l values approximate to simple fractions, this may indicate that one cell parameter corresponding to this index is a corresponding multiple of the true cell parameter. In this case, there will exist a common multiplier $(2, 3, 4 \ldots)$ that will afford a list of integral *hkl* reflections when one multiplies the appropriate one of the trial unit cell parameters, a, b or c, by this common multiplier. Simple fractions are often observed when the three unit cell lengths are highly disparate.

If most reflections have non-integral *hkl* values, however, and there is no obvious numerical relationship between them, indexing fails with this core set of vectors. There are various options to consider in this scenario. Four of the most common approaches are: (i) create a new core set of vectors by collecting a new set of reflections from the same crystal and repeat the indexing process; (ii) re-index using a subset of the existing data set, typically only strong reflections defined by an intensity threshold; (iii) try another indexing method; (iv) select a new crystal for the experiment.

Where one is able to generate a list of integral *hkl* values, the trial cell can be considered to be the primitive form of the true unit cell, which will equate to the true unit cell if that is primitive. Alternatively, the true cell may possess higher metric symmetry. In order to ascertain the full metric symmetry of the sample, one first performs a full-matrix least-squares refinement on the reflection list, to remove any spurious or ill-defined reflections. Then one can determine if systematic absences are revealed that indicate a centred unit cell. If no centring is found by an automated procedure, it can be judicious to double-check for centring by considering the Laue symmetry. The metric symmetry can never be lower than the Laue symmetry but it can be higher. By checking the Laue symmetry one can, for example, identify ostensibly centred monoclinic cells that are really triclinic, or rhombohedral cells masquerading as monoclinic ones. In cases where one can not be certain if the unit cell is centred or not, at the indexing stage of data collection, one must always undertake a data-collection strategy that assumes the lower-symmetry crystal system. This is because, if higher symmetry is confirmed post-data collection (Laue symmetry is more easily distinguishable with a

full data set), equivalent reflections can be merged to afford a more reliable unique data set that one would otherwise have had. However, the converse is an unhelpful outcome: collecting data assuming too high a crystal system initially is likely to render a dataset useless because it lacks key unique data from whole segments of reciprocal space (see Section 5.6.1).

5.5 Relating diffractometer angles to unit cell parameters: determination of the orientation matrix

A modern-day area-detector-based diffractometer will typically possess three or four independent motors that, together, are able to drive the crystal sample into nearly any orientation with respect to the incident X-ray beam. The associated angular degrees of freedom for each motor are usually called $\phi, 2\theta, \omega$, and κ, where ϕ represents the rotation of the sample about the vertical axis of the goniometer head, 2θ represents the movement of the detector relative to the incident X-ray beam, ω concerns the rotation of the base of the diffractometer about its physical vertical axis and is usually constrained to 'bisecting geometry', whereby $2\theta = \omega$, and κ is the motor that provides vertical tilt of the goniometer head. Figure 5.6 illustrates these definitions in geometrical terms.

The angular positions of each motor must be defined relative to a fixed origin; the x, y, z diffractometer axes provide the co-ordinate basis set for this purpose. By convention, the z-axis is usually defined to be coincident with the diffractometer ϕ-axis. x and y are defined arbitrarily to complete a right-handed set; the definitions are not the same for all

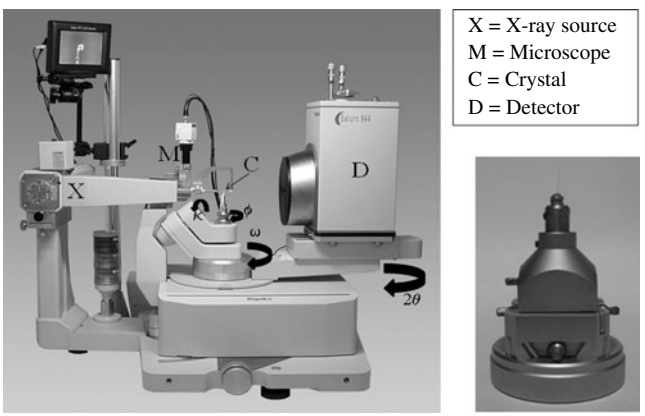

Fig. 5.6 (a) An annotated photograph of a CCD diffractometer. The crystal sample is affixed to the top of a goniometer head (b) that, in turn, is mounted onto the diffractometer at position C.

types of diffractometer, but whatever their definition, they necessarily allow a formula to define $\omega, 2\theta$ and κ in terms of x, y and z.

In order that these motors can be used to 'dial up' any (hkl) reflection during an experiment, one needs to be able to relate the diffractometer axes, x, y, z, that the motors are defined upon, with the axes that define a diffraction pattern for a given sample: the unit cell reciprocal axes; thence, one can calculate h, k, l. A 3×3 matrix, called the 'orientation matrix', enables this relation:

$$\mathbf{x} = \mathbf{A}\,\mathbf{h},$$

where $\mathbf{x}$ and $\mathbf{h}$ represent the vectors, (x, y, z) and (h, k, l), respectively, and $\mathbf{A}$ is the orientation matrix defined by:

$$\mathbf{A} = \begin{pmatrix} a_x^* & b_x^* & c_x^* \\ a_y^* & b_y^* & c_y^* \\ a_z^* & b_z^* & c_z^* \end{pmatrix},$$

the nine elements of this matrix representing the components of the reciprocal cell axes on each axis, x, y and z. See Fig. 5.7 for an illustration of these axes and relationships.

These matrix elements also contain information about the unit cell (requiring six parameters) and orientation of the crystal (three parameters). Thus, where required, the unit cell parameters can be extracted:

$$(\mathbf{A}'\mathbf{A})^{-1} = \begin{pmatrix} \mathbf{a}.\mathbf{a} & \mathbf{a}.\mathbf{b} & \mathbf{a}.\mathbf{c} \\ \mathbf{b}.\mathbf{a} & \mathbf{b}.\mathbf{b} & \mathbf{b}.\mathbf{c} \\ \mathbf{c}.\mathbf{a} & \mathbf{c}.\mathbf{b} & \mathbf{c}.\mathbf{c} \end{pmatrix},$$

where $\mathbf{A}'$ is the transpose of the orientation matrix, $\mathbf{A}$.

These interconversions also prove very useful when carried out in reverse using the inverse of the orientation matrix; for example, during the previously mentioned indexing procedure, where one wished to

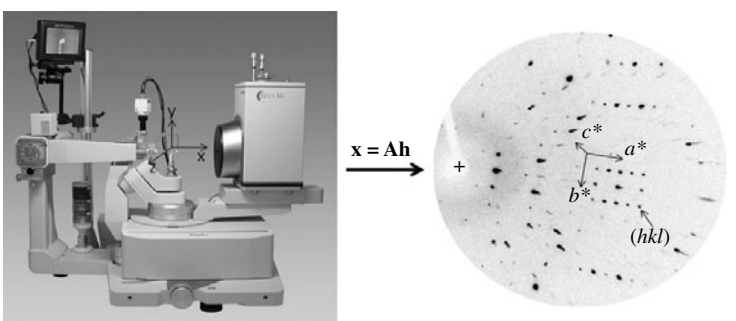

Fig. 5.7 A pictorial representation of the relationship between x, y, z and a^*, b^*, c^* and hkl.

identify (*hkl*) from a trial unit cell using a small reflection list defined only by diffractometer angles:

$$\mathbf{h} = \mathbf{A}^{-1}\mathbf{x}.$$

5.6 Data-collection procedures and strategies

5.6.1 Criteria for selecting which data to collect

The Fourier transform calculation, that permits the reciprocal-space to real-space conversion of structure factors into electron-density maps of crystal structures, requires, in principle, an infinite number of data. Naturally, such a requirement is not possible to achieve experimentally. However, one can collect sufficient data to render such a calculation viable; one usually collects data up to a certain value in 2θ (typically $2\theta = 50^\circ$ with Mo radiation) beyond which the intensities, and therefore the structure-factor magnitudes, are so low that one can approximate them to zero for all unmeasured data. Thus, the Fourier-transform calculation can still be provided with values effectively up to infinity. That said, since a series of zero-valued terms will have null effect on an integral, in practice one actually approximates the true integral, with infinite limits, to a summation with finite limits in h, k, l corresponding to the maximum values of h, k, l, collected in a dataset.

The more data collected, the better this approximation. The standard $2\theta = 50^\circ$ cut-off threshold for data collection usually proves entirely satisfactory for most crystal-structure determinations. Occasionally, one may wish to collect further in 2θ, if one perhaps wanted a particularly precise crystal-structure determination. Conversely, one might collect data with a lower 2θ cut-off threshold, where the intensity of diffraction spots becomes negligible before this default limit, $2\theta = 50^\circ$, is reached, as, for example, occurs commonly where structural disorder is present. Data-collection time restraints may also affect this default threshold choice, for example, if the unit cell is very large and so it would take too much time to collect sufficient data up to $2\theta = 50^\circ$; alternatively, if the crystal is decaying over time, it would be prudent to collect all data as fast as possible.

Crystals diffract in all directions and so it is important to collect diffraction data over a wide proportion of the scattering sphere. However, if one knows the crystal symmetry of a structure, one may not need to collect data through the complete 360° since a diffraction pattern may be replicated in octants, quadrants or hemispheres of this total sphere. Indeed, a full sphere of data would be required only if the sample possessed a non-centrosymmetric triclinic crystal structure. Where Friedel's law applies, half of a diffraction pattern should be equivalent to its other half if the crystal structure is centrosymmetric. Thus, only a hemisphere of data need be collected to obtain all unique data if one knew that

a structure was centrosymmetric and triclinic. The Laue symmetry in other crystal systems, in combination with Friedel's law, dictates what fraction of the total sphere will contain all of the unique reflections. For example, in the monoclinic crystal system, one quadrant of data will contain all unique reflections for a centrosymmetric structure, whilst only an octant of data needs to be collected for a centrosymmetric orthorhombic sample to capture all unique data.

One can therefore set up a data-collection schedule that aims to acquire only the required unique data, according to the crystal symmetry of the sample. This said, it is good practice, if time permits, to collect some duplicate reflections, so-called 'symmetry-equivalents', to improve one's data quality: symmetry-equivalents should have the same intensity and so can be averaged to provide a more statistically sound, merged dataset. It is also absolutely crucial, if one is not sure about the crystal symmetry of the sample before data collection, to collect data according to the lowest crystal symmetry possible, since one can always discard or 'merge' duplicate data after an experiment if a sample turns out to possess crystal symmetry higher than that expected, whereas one cannot restore reflections from parts of the diffraction sphere if they were never collected. The measurement of symmetry-equivalent data is very useful for other reasons in any case; e.g. confirming crystal symmetry, undertaking absorption corrections, etc.

With all of these factors in mind, one should then ensure that the order of reflections collected is the most time efficient. Fortunately, commercial area-detector diffractometers nowadays possess software to calculate automatically time-optimized schedules for data collection.

5.6.2 How best to measure data: the need for reflection scans

Due to a combination of reasons (e.g. the actual quality of a crystal sample, the intrinsic resolution of a detector), all *hkl* reflections measured are not delta functions (infinitely sharp); rather, they have a finite width. Therefore, in one dimension, a reflection profile would look like one of the curves in Fig. 5.8. The required intensity of a reflection is the area under this curve. Consequently, one cannot just orient the crystal on the diffractometer to the calculated 2θ value for a given *hkl* reflection and measure the diffraction intensity with the crystal kept stationary. One must rotate the crystal through the calculated position for each reflection as it is measured in order to capture its full intensity. There are two principal ways that one can scan through a reflection when using an area-detector diffractometer, and in either case, the axis of rotation is usually ω or ϕ.

One approach is 'narrow-frame' scans: rastering through a reflection in incremental angular steps and building up a peak profile from the sequential 'slices' obtained for each peak. Each frame of data that one collects using an area-detector diffractometer necessarily provides

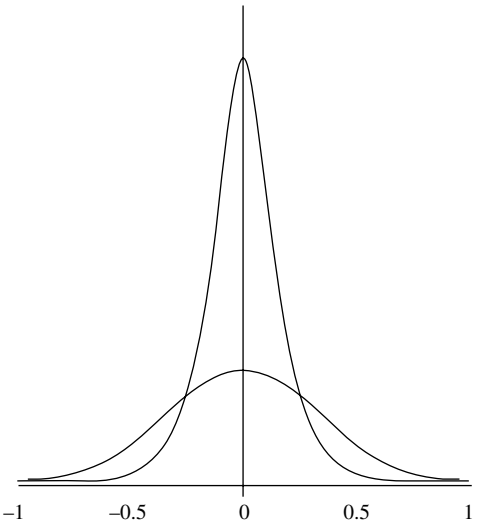

Fig. 5.8 Typical sharp and broad reflection profiles (the units are degrees).

a two-dimensional diffraction pattern. Therefore, each spot shown on a frame of data represents a two-dimensional 'slice' of a reflection. If one collects a series of such frames where only one diffractometer motor is moved, in small angular increments, between the frames of data collected, one can build up a peak profile of each reflection on these frames, assuming that there are sufficient 'slices' for each reflection observed. Figure 5.9 illustrates this process.

Alternatively, one can collect the whole intensity of a reflection in one 'wide-angle slice': sweeping through an angle greater than the angular spread of a reflection whilst acquiring one frame of data.

The decision as to whether to collect data using wide or narrow scans depends on several factors. One major advantage of wide-angle scans is the speed of data collection: far fewer frames need to be collected compared with narrow-slice data collection; moreover, both data-acquisition time and detector read-out time can represent the major contributions to the overall data-collection time. However, there is limited scope for profile analysis using wide scans; the accuracy of weak data may therefore be compromised for data-collection speed. Certainly, if reflection profiles need to be analyzed, one must collect data using the narrow-frame procedure.

When reflections appear close together in a diffraction pattern, where the sample has one or more large unit cell parameters, wide scans may become problematic, since two reflections appearing side-by-side on a diffraction pattern may be collected in one wide scan and thence interpreted as one reflection. One may overcome this barrier by extending the crystal-to-detector distance from its default position; in such cases, however, two data collections are usually required to obtain the necessary

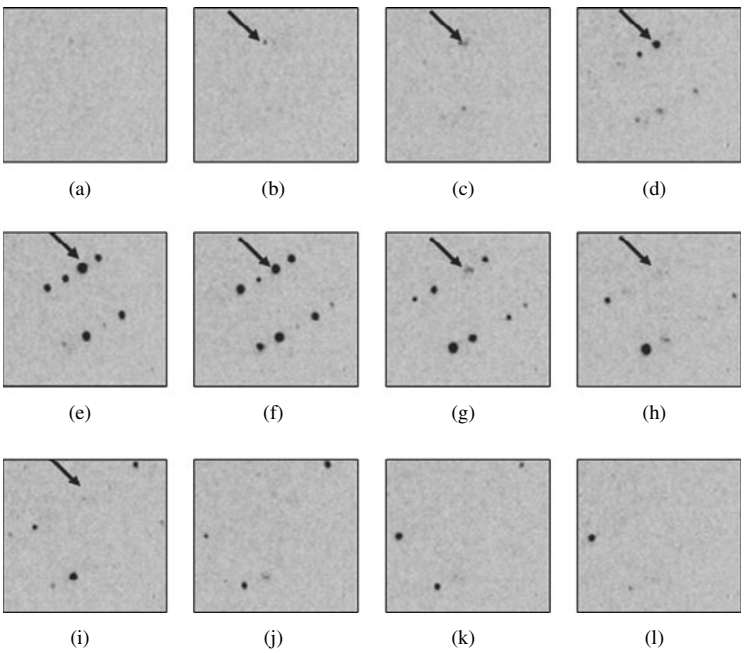

Fig. 5.9 Images of the same section of a detector from a series of data frames, collected sequentially in incremental steps. The arrow in each frame points to a particular reflection, (*hkl*), which progressively 'grows' and then 'fades' as one motor moves by an angular increment between each frame, which is about 1/6th of the full spread of the peak concerned; the reflection thus appears clearly on 6 frames and its profile can be built up by plotting the 6 discs parallel to each other and interpolating between them to create a sphere that represents the reflection intensity (the volume of the sphere).

data for structure solution, one at this extended crystal-to-detector distance and the other at the default distance (see Chapter 6).

5.7 Extracting data intensities: data integration and reduction

5.7.1 Background subtraction

Detector noise is present in all experimental data and the level of noise varies from pixel to pixel in an area detector. One must therefore subtract this from the experimental signal in order to evaluate reliable diffraction intensities. This is achieved by collecting one frame of 'data' with the X-ray shutter closed so that no signal due to X-ray diffraction can be present in this frame, only background noise. The data-acquisition time of this 'dark frame' must match that which is proposed for the data-collection frames. Then, one can simply subtract this dark frame – the detector counts due to background noise – from each frame measured.

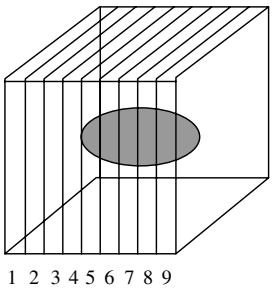

! Averaged profile: section 1–>3

| | | |

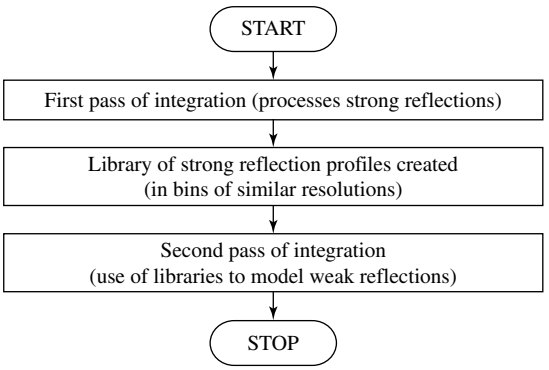

Fig. 5.11 Flow diagram of the modelling of weak reflections by profile analysis.

what we want to calculate in order to solve a structure. There are various factors that, when evaluated, allow us to correct the measured intensity thereby obtaining $|F|$, according to the equation below.

$$I_{hkl} = cL(\theta)p(\theta)A(\theta)E(\theta)d(t)m|F_{hkl}|^2.$$

Some of these factors are angle dependent (vary as a function of θ). Of these, Lorentz, $L(\theta)$, and polarization, $p(\theta)$, corrections are entirely geometric corrections, whilst absorption, $A(\theta)$, and extinction, $E(\theta)$, effects depend on the material content, crystal size and morphology and, in the case of extinction, the quality of the crystal sample. Sample decay, $d(t)$, may occur as a function of time. Multiplicity (m) is relevant only to powder diffraction and may occur if the crystal symmetry of a material dictates that certain hkl reflections must overlap at a given value of θ. c is simply a constant used for scaling.

Lorentz correction

A Lorentz correction accounts for the fact that the diffraction from some lattice planes is measured for a longer time than for others as a result of the way in which 2θ sweeps through reciprocal space.

The Ewald sphere can be used to visualize this: some reflections will intercept the surface of the Ewald sphere at a more oblique angle than others, according to the way that the crystal lattice rotates relative to the detector (2θ). The more obliquely a reflection intercepts the Ewald sphere surface, the longer the condition of diffraction is met for that reflection.

Polarization correction

The polarization correction accounts for the partial polarization of both the incident X-ray beam by the monochromator and that invoked during diffraction within the sample. In the latter case, the amount of

polarization is dependent on the value of 2θ and is given by $P = (1 + \cos^2 2\theta)/2$, whereas in the former case, the extent of polarization depends specifically on the orientation of the monochromator relative to the equatorial plane of the diffractometer and the physical nature of the monochromator crystal.

Absorption correction

A sample can absorb rather than diffract some of the X-ray beam. The level of absorbance, at a given X-ray wavelength, will depend on the absorption coefficient, μ, of a sample, which depends in turn on its elemental make-up (heavier elements generally absorb more), and the path length of X-rays through a crystal, t, according to the equation, $I_t = I_0 \exp(-\mu t)$. Absorption is also dependent upon the wavelength of the X-ray source: the longer the wavelength, the greater generally the absorption coefficient for a given sample.

Extinction correction

An X-ray beam can be diffracted by one lattice plane in a crystal, and then subsequently scatter off another, in a different part of the crystal. This effect is known as extinction and it causes a loss of intensity for a given reflection. There are two forms of extinction: primary extinction, which occurs *within* a crystal domain if the domains are sufficiently misoriented relative to others; and secondary extinction, which occurs *between* domains if they are well oriented with respect to each other. Secondary extinction is usually the dominant form of extinction, and it predominantly affects strong, low-angle reflections. These are normally corrected for approximately by including a single correction factor as a variable in the structure refinement. Secondary extinction is wavelength dependent, becoming worse with copper than with molybdenum radiation.

Decay correction

A crystal may degrade over the time of data collection, for example due to X-ray irradiation damage, chemical reaction of the crystal with air, moisture or light exposure. In such cases, the expected X-ray intensity for a given *hkl* reflection decreases over time. Corrections for progressive decay of this type may be undertaken by linear or polynomial curve fitting of certain reflections. This said, it is worth mentioning that with fast data-collection times made possible by recent area-detector technology and increasingly available cryogenic sample-cooling possibilities, crystal decay is quite rare nowadays.

Apparent crystal decay can also occur if the crystal moves in the X-ray beam during data collection. One can often correct for such movement in a similar way.

Multiplicity

All lattice planes diffracting at the same Bragg angle will be superimposed in a powder X-ray diffraction pattern. This occurs, for example, in a cubic lattice, $d_{h00} = d_{\bar{h}00} = d_{0k0} = d_{0\bar{k}0} = d_{00l} = d_{00\bar{l}}$, therefore multiplicity is 6 in this case.

Other corrections

Sometimes other effects may need to be accounted for. Particularly noteworthy are thermal diffuse scattering effects and possible variations in incident X-ray beam intensity (particularly important in some synchrotron-based X-ray diffraction experiments).

Completion of data-collection procedures

Once all of these corrections have been applied to the measured intensity, $|F_{hkl}|$ can be evaluated for each reflection in the dataset. Data reduction is then complete: the list of resulting h, k, l, and $|F|$ (or $|F|^2$) values is ready for space group determination, structure solution and onward conversion into a real-space electron-density model of the crystal structure, via the Fourier transform calculation.

References

Clegg, W. (1984). *J. Appl. Crystallogr.* **17**, 334–336.
Giacovazzo, C. (ed.) (1992). *Fundamentals of Crystallography*, Oxford University Press, Oxford, UK, p. 66.
Hornstra, J. and Vossers, H. (1974). *Philips Tech. Rundschau* **33**, 65–78.
Kabsch, W. (1988). *J. Appl. Crystallogr.* **21**, 916–924.
Kabsch, W. (1993). *J. Appl. Crystallogr.* **26**, 795–800.
Proffen, T. R. and Neder, R. B. (2008a). http://www.lks.physik.uni-erlangen.de/diffraction/iinter_bragg.html
Proffen, T. R. and Neder, R. B. (2008b). http://www.lks.physik.uni-erlangen.de/diffraction/ibasic_d.html
Sparks, R. A. (1976). *Crystallographic Computing Techniques*, ed. F. R. Ahmed. Munskgaard, Copenhagen, pp. 452–467.
Sparks, R. A. (1982). *Computational Crystallography*, ed. D. Sayre. Clarendon Press, Oxford, pp. 1–18.

Exercises

1) State which of the following represent real-space or reciprocal-space quantities:

   (a) the structure factor, F;
   (b) a space in which Miller indices, h, k, l are labelled;
   (c) the measured intensity of a diffraction spot;
   (d) unit cell parameters, $a, b, c, \alpha, \beta, \gamma$;
   (e) the representation of a part of a crystal structure via a 2D diffraction pattern;
   (f) diffractometer axes, x, y, z.

2) Below are the crystal data for a given compound. $C_{26}H_{40}N_2Mo$, $M_r = 476.54$, orange spherical crystal (0.4 mm diameter), monoclinic, space group $C2/c$, $a = 20.240(2)$, $b = 6.550(1)$, $c = 19.910(4)$ Å, $\beta = 90.101(3)$ °, $V = 2640.4(3)$ Å^3, $T = 150$ K. 2253 unique reflections were measured on a Bruker SMART CCD area diffractometer, using graphite-monochromated MoK_α radiation ($\lambda = 0.71073$ Å). Lorentz and polarization corrections were applied. Absorption corrections were made by Gaussian integration using the calculated attenuation coefficient, $\mu = 0.44$ mm^{-1}. The structure was solved using direct methods and refined by full-matrix least-squares refinement using *SHELXL97* with 2253 unique reflections. During the refinement, an extinction correction was applied. Refinement of 302 positional and anisotropic displacement parameters converged to $R_1[I > 2\sigma(I)] = 0.1654$ and $wR_2[I > 2\sigma(I)] = 0.3401$ [$w = 1/\sigma^2(F_o)^2$] with $S = 2.31$ and residual electron density, $\rho_{\min\,/\,\max} = -5.43/4.30$ eÅ^{-3}.

   (a) Calculate $F(000)$.
   (b) Using Bragg's law, calculate d when the detector lies at $2\theta = 20°$.
   (c) Confirm the result in (b) by using the Ewald construction, and the cosine rule to derive the value of d.
   (d) What percentage of the X-ray beam is absorbed by the crystal? (Assume that, on average, the X-ray path through a crystal diffracts at its centre).
   (e) When indexing the crystal, the experimenter could not be sure if the crystal was orthorhombic or monoclinic. Given this, which crystal system should the experimenter assume when setting up the data-collection strategy? Explain why.
   (f) The residual electron density is significant; indeed, the refined model is poor. Assuming that the problem lay at the data-reduction stage, describe possible causes for this.

3) From the orientation matrix:

$$\mathbf{A} = \begin{pmatrix} 0 & 0.250 & 0 \\ 0.125 & 0 & 0 \\ 0 & 0 & -0.100 \end{pmatrix}$$

calculate the unit cell parameters. About which axis is the crystal mounted? Is this desirable?

Practical aspects of data collection

6

Alexander Blake

6.1 Introduction

Unlike all other stages of a structure determination, the collection of diffraction data occurs in real time, requiring the continuous and exclusive use of valuable equipment. Whereas a refinement that has gone wrong can usually be repeated without causing significant delay, an abandoned or terminally flawed data collection has wasted instrument time irrevocably. The aim in collecting a dataset should always be to obtain the best possible quality of data from the available sample within a reasonable length of time. This requires not only preparing or demanding the best possible crystal, a topic that is covered in Chapter 3, but also choosing appropriate experimental conditions and parameters.

6.2 Collecting data with area-detector diffractometers

Until the mid-1990s, nearly all single-crystal data collection for chemical crystallography applications was carried out using four-circle (serial) diffractometers. After a slow start when image plate (IP) area-detector systems made some impact, the first commercial area-detector instruments based on charge-coupled devices (CCDs) were introduced in 1994. These have since become widely available from a number of suppliers. They have dropped markedly in price and have now totally displaced the four-circle instrument as the standard workhorse for data collection. Having said this, the large installed base of serial instruments means that, worldwide, they will be a declining source of diffraction data for some time. The replacement of single-point by area detectors has brought with it both advantages and disadvantages, but for most purposes the former greatly outweigh the latter. They are summarized below.

Advantages:

+ simultaneous recording of many reflections,
+ faster data collection possible,
+ data-collection time independent of structure size,
+ high redundancy of symmetry-equivalent data possible,
+ rapid screening of samples,
+ not necessary to obtain correct orientation matrix and unit cell before data collection,
+ complete diffraction pattern measured, not just around Bragg reflection positions,
+ reduced probability of obtaining incorrect cell from a few initially found reflections,
+ poor crystal quality and weaker diffraction can often be tolerated,
+ minimal crystal movement necessary, so easier to use low-temperature and other accessories,
+ easy visualization of the diffraction pattern, so good for teaching and training,
+ can obtain data on twinned or incommensurate crystals.

Disadvantages:

− possibly high capital and maintenance costs,
− high computing requirements, especially processing power and data storage,
− need for careful corrections for non-uniformities and other effects,
− usually poor discrimination against other X-ray wavelengths, e.g. harmonics,
− restricted detector size may lead to problems with large unit cells and with Cu $K\alpha$ X-rays,
− it may be expensive and difficult to change radiation,
− upper limit on counting time per frame for CCD detectors,
− they are not efficient for very small cells.

The major obvious feature of an electronic area detector is its ability to record diffraction data over a substantial solid angle. As far as normal Bragg diffraction is concerned, this means **the simultaneous measurement of a number of reflections**: the number of reflections measured simultaneously depends on the size of the unit cell as well as on the size of the detector. In addition, an area detector actually records the whole of the intercepted diffraction pattern and not just the Bragg reflections (i.e. the whole of reciprocal space is observed, not just the regions immediately around each reciprocal lattice point). This can be useful for special purposes, such as the detection of twinning or the study of incommensurate structures. A related advantage is that it is not actually necessary to establish the correct unit cell and crystal orientation matrix before beginning data collection – although it is highly advisable to do so whenever possible – because these can be found later from the stored images. (An invalid orientation matrix on a four-circle diffractometer usually means a useless set of data, because only the predicted reflection positions are

explored.) A corollary of this is the ability, where deemed necessary, to re-process stored images using alternative indexing and/or peak profile parameters.

6.3 Experimental conditions

6.3.1 Radiation

The crystallographer may have some choice over the conditions under which data are collected and one of these is the wavelength of the radiation used, the most common choice in the home laboratory being between copper (1.54184 Å) and molybdenum (0.71073 Å). Copper X-ray tubes produce a higher flux of incident photons (for the same power settings) and these are diffracted more efficiently than molybdenum radiation: copper radiation is therefore particularly useful for small or otherwise weakly diffracting crystals, especially if absorption effects are moderate. In addition, focusing optics provide greater enhancements for the longer wavelength. For crystals with long unit cell dimensions, reflections are further apart when the longer-wavelength copper radiation is used and this can minimize reflection overlap. If you need to determine the absolute configuration, and your crystals do not contain elements heavier than, say, silicon, then copper radiation is essential. On the other hand, absorption effects are generally less serious with molybdenum radiation and this can be crucial if elements of high atomic number are present. Molybdenum radiation allows collection of data to higher resolution and is likely to cause fewer restrictions if low-temperature or other attachments are required. Changing radiation requires some effort and skill and you lose data-collection time. The ideal situation is to have two diffractometers, one equipped with each radiation, and a supply of suitable crystals so that both may be fully utilized. Some diffractometer manufacturers offer hybrid Cu/Mo instruments with two different X-ray tubes and their associated optics but only one area detector: switching radiation takes little time and is automated, and there is substantial cost saving because the most expensive component of the diffractometer (the detector) is not duplicated.

The following illustrative examples may be helpful:

a well-diffracting organic compound containing iodine:
use Mo to minimize absorption
a poorly diffracting organic compound (CHNO):
use Cu to maximize diffracted intensity
an organic compound (CHNO) with $b > 50$ Å:
use Cu to minimize overlap
absolute configuration on $C_{19}H_{29}N_3O_7$
feasible only with Cu
most metal complexes, *etc.*
use Mo to minimize absorption
high-resolution studies
use Mo

a weakly diffracting platinum complex
a 'no-win' situation?

Where a sample diffracts too weakly on a laboratory source to yield enough observable data, and it is considered important enough, it could be taken to a synchrotron radiation facility. In this event several advantages can accrue: the wavelength can be tuned specifically to the needs of the sample; the intensity typically represents at least a 100-fold gain over that of a laboratory source; the resolution between reflections is also generally greater. The disadvantage is that there is heavy competition for such a rare resource and there is often a long wait for synchrotron beam time. For this reason, it is worth considering whether more modest enhancement would overcome the problem of weak diffraction: a longer wavelength, a lower temperature or a more powerful laboratory source may suffice.

Lastly, when considering the most appropriate wavelength for a particular experiment, you should also bear in mind the physical restrictions that will preclude data collection in some areas of reciprocal space: these limitations include where the beam stop is positioned and where accessories such as low-temperature devices, cryostats or high-pressure cells are deployed. The restrictions are generally much more serious at longer wavelengths, since higher 2θ values are required to achieve the same resolution.

6.3.2 Temperature

If a reliable low-temperature system is available it is almost always worthwhile considering data collection at low temperature (most low-temperature devices will even produce slightly elevated temperatures if this is required for a special experiment, while some have extended upper temperature limits). The benefits of low-temperature data collection can only be realized if the equipment is well aligned and correctly set up: for example, icing can lead to the crystal moving or even being lost. Reducing the temperature of the crystal can have many advantages and is essential for crystals mounted using protective oil films, compounds melting below about 50 °C and those that are thermolabile. Reactive compounds may be stabilized long enough to allow data collection. There are general advantages: at lower temperatures atomic displacements are reduced and the intensities of reflections at higher Bragg angles thereby enhanced, allowing the collection of better diffraction data at higher resolution. This reduction also minimizes librational effects that can otherwise give artificially shortened bond lengths and other systematic errors. One advantage of the reduction in temperature is the relative ease with which disorder can be modelled: for example, popular pseudo-spherical anions such as BF_4^-, PF_6^-, ClO_4^- and SO_4^{2-} are often badly disordered at room temperature but are either ordered or their disorder is much easier to model at low temperature. The actual temperature chosen is usually a compromise between the desire for the lowest temperature and the increased risk of icing as the temperature

is reduced. For routine work on molecular crystals, temperatures in the range 100–200 K are typical. Phase changes appear to be a relatively rare problem but cooling can have adverse effects on poor-quality crystals, showing up in the splitting of reflections, in poor orientation matrices and larger uncertainties on cell parameters. Sometimes the splitting can be annealed out by increasing the temperature, for example from 150 K to 200 K. Even in these apparently unfavourable cases a low-temperature determination is often better than one at ambient temperature. The fact that cooling methods typically involve rapid freezing of crystals on the diffractometer opens up the question of what proportion of such crystals are determined as metastable rather than as equilibrium phases.

6.3.3 Pressure

Although it is not used in routine experiments, the application of high pressures provides a means of inducing structural change, including the generation of new polymorphs that are inaccessible by any other means. A typical experiment involves applying pressure to material held within a high-pressure cell, then studying the product *in situ*. Such experiments are challenging, not least because the components of the high-pressure cell severely limit how much of the sample's diffraction pattern can be recorded: these components also contribute strongly to the observed diffraction pattern. Notable recent advances have included the application to chemical crystallography of techniques originally developed for mineralogy and physical crystallography (see for example Dawson *et al.*, 2004; Allan *et al.*, 2006). This has recently been recognized by an issue of *Chemical Society Reviews* (McMillan, 2006).

6.3.4 Other conditions

Considerations of crystal size, methods of mounting, choice of goniometer head and optical centring have been mentioned previously but are worth stressing again as they can seriously affect the outcome of the experiment. The collimator selected should allow the entire crystal to be immersed in the X-ray beam but its diameter should not be excessive, as this will contribute to scattering by the air, resulting in increased background levels. This scattering is more serious with copper than with molybdenum radiation. The effects of an oversized crystal are also strongly dependent on the elements in the sample: it has been shown that with only light elements (e.g., $Z \leq 8$) present, the use of large ($\sim$2 mm) crystals does not cause serious problems and may be beneficial because of the enhanced intensities that can be measured, or because the data-collection time can be reduced (Görbitz, 1999).

6.4 Types of area detector

6.4.1 Multiwire proportional chamber (MWPC)

In proportional counters each incident X-ray photon causes an ionization in the detector gas, and hence a current in a high-potential wire.

MWPCs usually have one set of parallel wires and a second set at right angles, and a current is induced in one or more wires of each set for each X-ray photon. Thus, both the time and position at which the photon arrives are known. The MWPC has the advantages over other area detectors that the output signal is instantaneous (time resolution is ideal), there is no inherent noise in the detector, and the counting efficiency is high. There is, however, a problem with parallax, particularly at shorter wavelengths, reducing the spatial precision, and the overall count rate is limited by the dead time, which affects the detector as a whole for every single recorded photon. MWPCs have not been used significantly for chemical crystallography.

6.4.2 Phosphor coupled to a TV camera

The phosphor first converts incident X-rays to visible light. Fibre optics provide the coupling that takes this light from the phosphor to the low-light-level TV camera where it is detected. This type of detector also gives an instantaneous readout, but the active area is relatively small, as is the dynamic range, and the signal-to-noise ratio is poorer than for other area detectors. The TV system most widely used was the Enraf-Nonius FAST; its principal application for chemical crystallography was in the EPSRC National Crystallography Service at Cardiff up to 1998. It is no longer commercially available, and is therefore of historical interest only.

6.4.3 Image plate (IP)

Instead of converting X-rays to visible light, the phosphor in these devices stores the image in the form of trapped electron colour centres. These are later 'read' by stimulation from visible laser light (which causes them to emit their own characteristic light for detection by a photomultiplier) and then erased by strong visible light before another exposure to X-rays. The main advantages of image plates are that they are available in large sizes and are relatively inexpensive; they also have a high recording efficiency and a high spatial resolution (Fig. 6.1). The one major disadvantage is the need for a separate read-out process, which requires minutes rather than seconds. Faster image-plate systems offer one solution but another method of increasing the time available for X-ray exposure is the use of two or more plates, so that one is recording an image while another is being read: however, this adds considerably to the cost and complexity.

6.4.4 Charge-coupled device (CCD)

This type of detector, more familiar in video cameras and other mass-market applications, is a semiconductor in which incident radiation produces electron-hole pairs; the electrons are trapped in potential wells and then read out as currents. For various reasons, direct recording of

Fig. 6.1 An image-plate system.

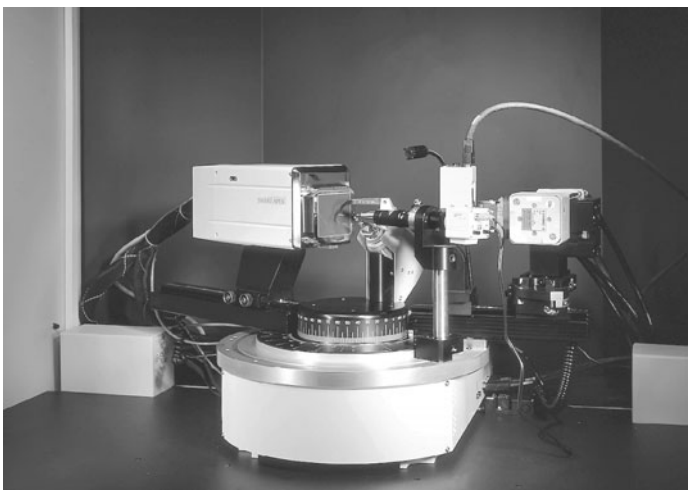

Fig. 6.2 A CCD area-detector diffractometer.

X-rays is not usually carried out: instead, a phosphor is coupled through fibre optics to the CCD chip, which is cooled to reduce the inherent electronic noise level due to thermal excitation of electrons. Efficient recording, a high dynamic range and a low noise level, and a read-out time measured in seconds or fractions of a second, combine to give the CCD some clear advantages as a rapid area detector, but the size is limited by the size and quality of chips available. Of the area-detector technologies now in use, this has the best potential for further development, and considerable effort is being made in producing larger and more sensitive chips without significantly increasing the read-out time. Commercial CCD systems for chemical crystallography are now available from several major firms (Fig. 6.2). The next few years are likely to see

the wider use of so-called 'pixel arrays', another form of solid-state detector that should be able to record X-rays directly (i.e. without conversion to visible light) and over a larger area. These detectors are under active development (see for example *http://pilatus.web.psi.ch/pilatus.htm*) and have a number of highly attractive features including no read-out noise, excellent S/N ratio, no dark current (so no need to cool the detector), read-out times of a few milliseconds per frame, very high (20 bit) dynamic range, high quantum efficiency, energy discrimination and fluorescence suppression. The X-ray shutter is open during the collection, with fine time slicing being done by the detector electronics, enabling rapid data collections (e.g., 4 s) and time-resolved studies.

Area detectors do not just offer the possibility of collecting diffraction data more quickly, although that is generally perceived as their main advantage. They also make feasible experiments that are beyond the scope of the old serial diffractometers, through higher sensitivity and the recording of the whole pattern. Much of the following applies to any type of area detector, but it will refer specifically to CCD systems, since these are the most widely used in chemical crystallography.

6.5 Some characteristics of CCD area-detector systems

An area detector, whether based on a CCD or an alternative technology, is only one component of a single-crystal X-ray diffractometer. It needs to be combined with a goniometer for mounting and moving the crystal sample, a source of X-rays, and electronic and computing control systems.

Although an area detector records a number of diffracted beams simultaneously, it is still necessary to rotate the crystal in the X-ray beam in order to access all the available reflections. In most chemical crystallography systems, the detector is offset to one side rather than being held perpendicular to the incident X-ray beam, so that a higher maximum Bragg angle can be observed for a single detector position. Typical designs and configurations give data to a maximum Bragg angle θ of around 25−30°, appropriate for a 'routine' structure determination with a more than adequate data/parameter ratio if Mo-$K\alpha$ radiation is used. The two-dimensional nature of the detector means that it is not necessary to bring all reflections into a horizontal plane (assuming the ω-axis is considered vertical and the incident X-ray beam horizontal), so less movement of the crystal is required in order to access all reflections. The relative advantages and disadvantages of different goniometer designs, with one, two or three available rotations for the crystal, can be debated. However, with only one rotation axis, for some low-symmetry crystal systems not all reflections may be measurable with the particular crystal orientation chosen. There is also no general agreement about the

choice of rotation axis. Not having a full χ-circle does give considerably more freedom for attachments such as low-temperature devices or high-pressure cells.

Corrections for a number of factors need to be applied to raw CCD images. These are usually fully integrated into commercial systems. Some of the corrections are listed here.

6.5.1 Spatial distortion

The demagnification of the diffraction image from the phosphor to the CCD chip via the fibre-optic taper used in many systems is never perfectly linear and to scale. The mapping of CCD pixels to original face-plate positions needs to be calibrated and a correction then applied to every image. The calibration can be made, for example, by recording a pattern of X-rays from an amorphous scatterer or a fluorescent sample through an accurately machined grid of fine holes placed over the detector face. It is valid until the phosphor-taper-CCD assembly is changed in some way.

6.5.2 Non-uniform intensity response

Equal incident X-ray intensity at different points on the detector face may lead to unequal numbers of electrons at the corresponding pixels on the CCD, for various reasons involving the different components of the system. Calibration involves recording a uniform intensity 'flood field' and measuring the CCD image for this.

6.5.3 Bad pixels

Minor faults in CCD production can include individual pixels or even rows of pixels that do not respond correctly to incident light. Substantial faults mean an unusable chip, but a few bad pixels can be tolerated and flagged as bad, particularly in systems in which pixels are 'binned' by combining 2×2 or other groups of pixels rather than using all pixels individually.

6.5.4 Dark current

Thermal excitation leads to the generation and trapping of electrons in the CCD pixel wells even when there is no incident light, and this slowly builds up a background 'dark image' on the detector, which will be read out superimposed on the true image. The effect is minimized by cooling the CCD (typically to a temperature between -45 and $-80\,^{\circ}\mathrm{C}$) and can be corrected by recording a dark-current image (i.e. without any X-rays) for the same time as a normal exposure and subtracting this from each measured frame. The dark-current image is temperature dependent and needs to be measured for the appropriate length of time, preferably averaged over multiple recordings to reduce statistical fluctuations. Even

with such a correction, the noise created by thermal excitation imposes a practical upper limit on the exposure time for each frame.

The steps involved in setting up and collecting data with an area detector are broadly similar irrespective of the technology used.

6.6 Crystal screening

Although area-detector data are quite tolerant of poorly centred crystals, it is obviously best to centre crystals as accurately as possible. Initial exposures can be recorded in a matter of a few seconds to give an almost instantaneous indication of the quality and intensity of diffraction by the crystal. It is a good idea to record frames at one or two different ϕ angles as this can detect crystals that look promising in one direction but show serious problems in another. Such exposures are taken with the crystal in a random orientation, and either stationary or oscillated through a small angle (Figs. 6.3 and 6.4).

At this stage, some obvious problems such as poor (or no) crystallinity, splitting of reflections and overall weak diffraction can be identified (see Figs. 6.5 to 6.9): an obviously unsuitable crystal can be quickly discarded and a hopefully better crystal selected. Note that such exposures are essentially two-dimensional and may not indicate all possible reflection splitting or other problems: these may only be detected when a series of frames have been collected for unit cell determination (and indexing may have failed – see below). The rapid screening allows more crystals to be investigated from each sample, increasing the chance of finding a useable one, or conversely increasing your level of certainty that no acceptable crystals exist in that sample. However, it should be noted that because of their greater sensitivity and efficiency overall, CCD systems

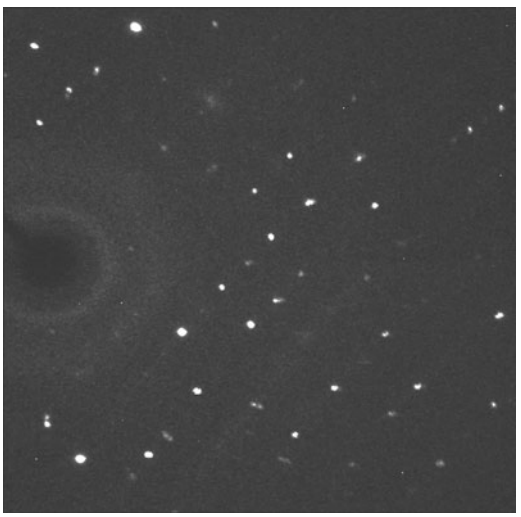

Fig. 6.3 Single frame by rotation through a small angle (0.3°).

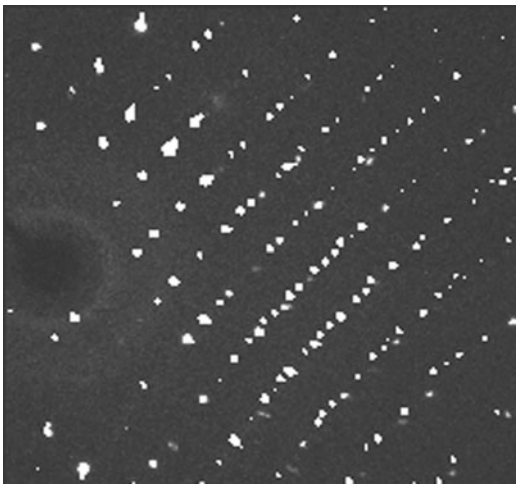

Fig. 6.4 A pseudo-oscillation photograph generated by superposition of a small number of frames.

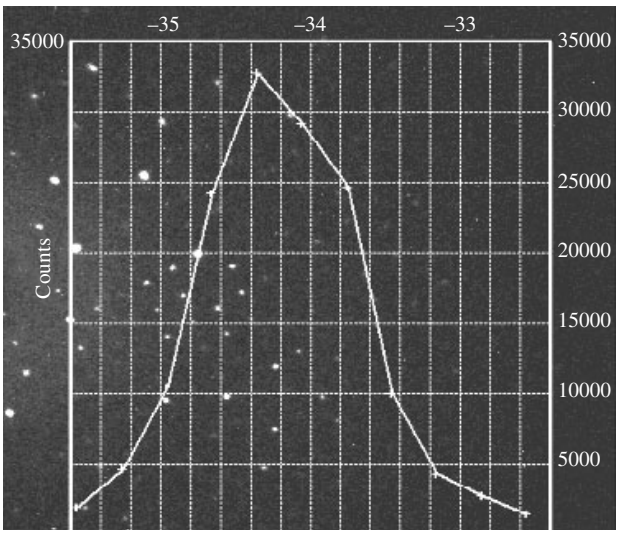

Fig. 6.5 A broad peak (FWHM ~1.3°).

can often handle samples of apparently rather poor quality and still give an acceptable structural result, so it may be worth persevering with less promising samples: experience will tell you when to give up on your own crystals.

A common problem occurs when you are faced with a crystal that is of poorer quality than you would like: do you remove it from the cold stream of the diffractometer so that you can try another crystal, potentially losing the best available crystal, or carry on with it? This can be important if either time or the supply or crystals is limited. One

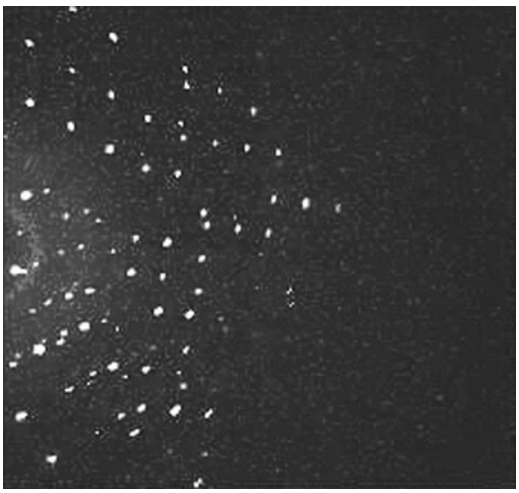

Fig. 6.6 Limited diffraction.

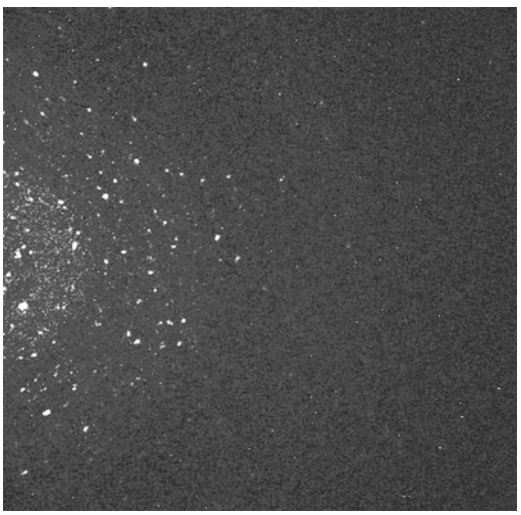

Fig. 6.7 A weak, non-single crystal.

solution is to store each crystal over liquid nitrogen after removal from the diffractometer until it is clear which one is best. However, if you have, even temporarily, access to two instruments you can try a less risky procedure whereby only the poorer of each sequential pair of crystals is removed from the diffractometer: after a few cycles of comparison it should be possible to identify the best crystal.

6.6.1 Unit cell and orientation matrix determination

Collecting a series of frames covering two or three small regions of reciprocal space takes a few minutes. After obtaining the positions of

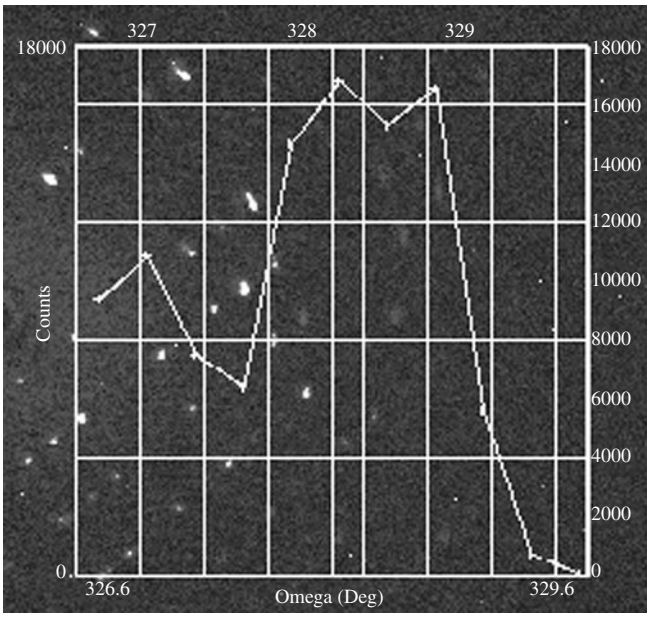

Fig. 6.8 A split/broad/poorly shaped reflection.

the reflections, including interpolation between successive frames to obtain precise setting angles, these are stored in a list by the control program. This yields co-ordinates of observed reflections in reciprocal space, referred to goniometer axes. With reasonably sized structures and moderate intensities, there may be upwards of a hundred reflections. It may be necessary in some cases to adjust the criteria for the inclusion of reflections in this list: this is most commonly done on the basis of I or I/σ for more weakly diffracting crystals, where default settings may not yield enough reflections. An incorrect (or uncertain) initial matrix and cell at this stage are not a problem, as they can be revised following the full data collection without loss of data. One advantage in obtaining a good initial matrix and unit cell is that it is possible to check whether the latter corresponds to a known phase: another is that it gives some encouragement that you will ultimately be able to index and process the full dataset.

The theory behind indexing has already been covered. Indexing of the reflections and determination of the crystal orientation matrix and unit cell parameters have the advantage of usually having many reflections available and hence a lower probability of obtaining an incorrect cell. The number of reflections can also make it easier to obtain a result from twins and other samples that are not single crystals, though the outcome then needs to be examined particularly carefully to see which reflections do not fit the proposed cell and whether there is a clear explanation for this. Assessment of the mosaic spread is usually also part of this step,

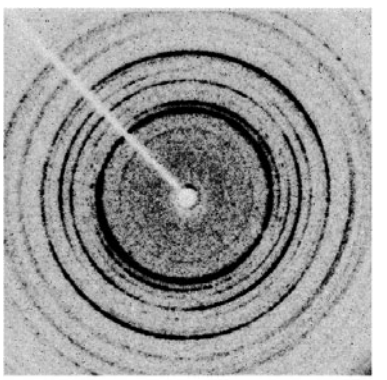

Fig. 6.9 A powder pattern from a polycrystalline sample originally thought to be a single crystal. The variation in the intensities of the individual lines indicates preferred orientation within the sample.

and is important for decisions on how to collect the full dataset and how to extract intensities from the raw data.

6.6.2 If indexing fails

If indexing fails, you should first examine the indexing parameters: these place limits on a number of factors that control the indexing, including (i) the indices that can be assigned, (ii) the lengths of the axes of the original primitive cell, (iii) how far the indices are allowed to deviate from integral values and (iv) the minimum fraction of data that must be indexed by any candidate cell. Parameters (i) and (ii) can be used to exclude ridiculously large cells, but must be reduced with care unless you know the cell beforehand. I would suggest starting off with upper and lower limits on cell axes of 3 Å and 60 Å, respectively, and indices of 15 or 20. Parameter (iii) allows less well centred reflections to be included: a value of 0.1 may be too low in many cases, but more than about 0.3–0.4 is likely to generate multiple false cells. Parameter (iv) is useful if a minor twin component is suspected and you are trying to index the major component, but there are more sophisticated and controllable methods for handling such cases. If indexing fails the first thing to try is increasing the tolerance on parameter (iii); a visual survey of the frames may indicate whether increasing (i) or (ii) is likely to help.

6.6.3 Re-harvest the reflections

If manipulation of the default list of reflections fails to provide a plausible indexing, it may be worthwhile harvesting reflections from the stored frames using your own criteria: these could include modified limits on I or I/σ, resolution or other factors. Indexing on this list may prove more successful. If indexing still fails, have a closer look at the frames, as examination of the rocking curves may show splitting or other effects not obvious on individual frames, which may mean that an initially promising crystal is in fact unsuitable. It is probably time to try another crystal if one is available. Even if indexing does work, you should always examine the rocking curves: indexing routines are robust and can often cope with split or broad reflection profiles, so a successful indexing does not automatically qualify a crystal for data collection. At the same time, you can check whether there is a good correspondence between the diffraction pattern and the reflection positions predicted from your orientation matrix: if the correspondence is poor the indexing must be regarded as questionable. Too many predicted spots may indicate that the cell is too large or that centring has been missed; too few could mean the cell is too small. Carrying out these comparisons throughout all the collected frames ensures that you can detect any crystal movement or instrumental problem that might have occurred during data collection. Such an occurrence is not usually a disaster: the data can be processed in batches using different orientation matrices, but failure to detect the

problem will give puzzling effects ranging from high merging residuals to a failure of the structure to solve or refine.

6.6.4 Still having problems?

If you are faced with a persistent failure to index, and the reasons for this are not obvious, you may be able to call on a program that can display a reciprocal lattice plot of all the reflections harvested from the frames. By rotating the lattice you should be able to decide whether the crystal is single or not. At any significant sign of non-single character the crystal should be discarded and another one examined; if all the available crystals show twinning the procedures outlined later can be adopted.

Even if indexing seems to have succeeded you should be wary of unexpectedly large, often triclinic, cells with large uncertainties on their cell dimensions. If a cell is allowed to be large and uncertain enough it will be able to accommodate almost any list of reflections. If indexing appears to succeed but some reflections have indices at or near special values such as 0.50 or 0.33, this may indicate the cell is too small in that direction and should be increased by a factor of two or three, respectively. If such a situation is unclear, it does not need to be resolved now, but can be investigated when the full area detector dataset is available.

If indexing has not worked, but there is no obvious reason for this, it may help to acquire some additional frames, preferably from a region of reciprocal space that has not yet been sampled. Because a valid orientation matrix is not mandatory for acquiring area-detector data, these additional frames can consist of a full data collection, in the hope that indexing will be successful when a selection of all available reflections can be used, but runs the risk that the indexing will still fail, giving a set of frames that cannot be processed.

6.6.5 After indexing

Successful indexing is followed by least-squares refinement of the orientation matrix and a Bravais lattice determination. The refinement also acts as a check on whether the indexing is valid: a plausible indexing that fails to give a satisfactory refinement must be discarded. In order to be accepted a refinement must end with the vast majority of significant reflections having (near)-integral indices, reasonable s.u.s on cell parameters and suitable values for various quality indicators. It may not always be possible to be certain about the Bravais lattice.

6.6.6 Check for known cells

There is probably little point in continuing if the cell from the indexing is known, either in the literature or within your own group or department. An excellent facility (CrystalWeb) for searching the relevant crystallographic databases is available to UK academic researchers via

the EPSRC Chemical Database Service at STFC Daresbury Laboratory (Fletcher *et al*., 1996; e-mail uig@dl.ac.uk; http://cds.dl.ac.uk/cweb/). In October 2006, EPSRC summarily announced that parts of this Service would close at the end of March 2007, although access to CSD and ICSD has now been secured until at least 2011.

To avoid repeating an in-house determination you should be able to search a database of your unpublished unit cells, for example by using a program such as LCELLS (Dolomanov *et al*., 2003). Finding that your unit cell is already known is not exactly good news, but at this stage you have invested only a few minutes in the crystal. If it is undetected until after data collection and structure solution such duplication could waste several hours of valuable instrument time.

6.6.7 Unit cell volume

You can calculate whether your cell volume is compatible with the expected molecular formula, using 18 $Å^3$ per non-hydrogen atom. This value is valid for a wide range of organic, metal-organic and co-ordination compounds, although some adjustment might be required for special cases (from 14 $Å^3$ for some highly condensed aromatic compounds to 23 $Å^3$ for some organosilicon compounds). It does not work for inorganic compounds like NaCl or $FeTiO_3$. A significant discrepancy may indicate that the unit cell is incorrect, that the compound is not as proposed, or that solvent molecules are present. The number of molecules present in the unit cell may warn you that, if the proposed molecular formula is correct, symmetry considerations mean that disorder must be present.

6.7 Data collection

It is necessary to set a small number of parameters to control the full data collection: their values are obtained from the preliminary screening measurements and unit cell determination. The most important factors affecting decisions concerning these parameters are the overall **intensity level** on the frames, the **mosaic spread** and the **crystal symmetry**.

6.7.1 Intensity level

The intensity level will help determine the frame measuring time, which should be long enough to give diffraction to adequate resolution: as a very crude rule of thumb, diffraction maxima should be clearly detectable to at least ½ – ⅔ of the required $2\theta_{max}$. For strongly diffracting crystals, too long an exposure time may result in detector overloads: if this happens the time should be reduced provided this does not result in the loss of higher-angle data. For special problems it may be feasible to collect low-angle data relatively rapidly, while using longer exposure times for the higher-angle data and allowing significant overlap of the

two regions. However, this requires two settings of the detector and data collection will therefore take much longer.

6.7.2 Mosaic spread

The mosaic spread is established from the widths (x, y) of the reflections on individual frames, plus an estimate of z from the width of the rocking curves. While there is little point in taking small steps through broad reflections, this may be highly advantageous for a crystal giving narrow reflections. Broad reflections are not necessarily problematic, provided they can be separated from neighbouring maxima, and a greater scan width giving fewer frames may be appropriate and deliver the dataset more rapidly. However, it is important to check that the combination of exposure time and scan width gives the required intensity. The actual scan mode and width chosen will depend on the software (and acquisition philosophy) being used, with narrow (e.g., 0.3°) frames being typical for Bruker SMART instruments, while wider 1−3° frames are used on Nonius KappaCCD diffractometers. In the former most or all reflections will be partial, and integration is carried out as part of data reduction; in the latter the detector integrates a good fraction of the reflections on each frame. As with the other factors, it is important to choose frame widths appropriate to the individual crystal being studied. A related issue occurs with larger unit cells (and usually Mo $K\alpha$ radiation), where you may have to move the detector further away from the crystal to avoid reflection overlap. Unless you have quite broad reflections, with Mo $K\alpha$ radiation you should not have to think about this until you have axes of over 30 Å, possibly longer if the cell is centred. If you have to move the detector back you should make sure that hardware and software settings are compatible, although this is a problem only if the detector distance cannot be changed under program control. A mismatch of these settings can lead to inexplicable indexing failures. As the crystal-to-detector distance is increased, the maximum value of 2θ that can be recorded is reduced, and you need to make sure that data can still be collected to the resolution you require: this may require two different 2θ settings. After you have collected your dataset, it is courteous to reinstate the normal detector settings for the next user.

6.7.3 Crystal symmetry

It is useful, but not essential, to establish crystal symmetry at this stage. The symmetry determines the minimum fraction of the whole-sphere diffraction pattern to be measured in order to achieve a complete dataset. If there is any doubt as to the correct diffraction symmetry, the lower symmetry should always be assumed. Although it is possible to calculate the optimum set of frame runs to achieve this completeness as efficiently as possible, for routine work it is sensible to collect the whole sphere of data for triclinic crystals and at least a hemisphere for all other crystal systems. Non-routine work might include higher-symmetry crystals

that diffract weakly or are prone to decay in the X-ray beam: in such cases it is important to use a data-collection strategy capable of delivering a unique set of data as quickly as possible. Another consideration is that inefficiency in achieving the unique set will give a dataset with higher redundancy (an alternative term is 'multiplicity of observations'). Despite the negative connotations of the term in other contexts, as far as data collection and processing are concerned redundancy is a very good thing: equivalent and duplicate reflections are valuable in correcting data, for example for absorption, and they can be merged to provide a unique dataset containing more precise intensity measurements.

6.7.4 Other considerations

Setting these parameters incorrectly can cause problems but area-detector systems are generally tolerant of such mistakes. In particular, collecting area-detector data without a valid orientation matrix is rarely catastrophic provided valid indexing is eventually possible. Although other data-collection parameters such as the rotation axis (e.g., ω or ϕ) can also be varied, a typical data-collection setup procedure is fairly simple and straightforward. Area-detector systems can therefore be operated by less experienced workers with minimal risk of compromising data quality or completeness.

Re-recording of some of the initial frames at the end of the main data collection and comparison of the integrated intensities allows detection of and correction for any decay, although significant decay is rare, particularly at low temperature.

At some point, record the crystal colour, shape and dimensions. If a list of indexed crystal faces is required for a numerical absorption correction, these will have to be measured. If you expect even very minor icing of your crystal during the data collection, make these measurements before you start. Finally, you could check that the X-ray generator settings are correct, that the flow of cooling water is adequate and stable and that any low-temperature device is operating at the desired temperature and has sufficient cryogenic fluid to last through the data collection.

References

Allan, D. R., Blake, A. J., Huang, D., Prior, T. J. and Schröder, M. (2006). *Chem. Commun.*, pp. 4081–4083.

Dawson, A., Allan, D. R., Parsons, S. and Ruf, M. (2004). *J. Appl. Crystallogr.* **37**, 410–416.

Dolomanov, O. V., Blake, A. J., Champness, N. R. and Schröder, M. (2003). *J. Appl. Crystallogr.* **36**, 955.

Fletcher, D. A., McMeeking, R. F. and Parkin, D. (1996). *J. Chem. Inf. Comput. Sci.* **36**, 746–749.

Görbitz, H. (1999). *Acta Crystallogr.* B**55**, 1090–1098.

McMillan, P. F. (ed.) (2006). *Chem. Soc. Rev.* **35**, 847–854.

Exercises

1. Assuming both are available, which of Cu or Mo radiation would you use to determine the following problems, and why?
   a) $C_6H_4Br_2$;
   b) $C_6Cl_4Br_2$;
   c) $C_{36}H_{12}O_{18}Ru_6$;
   d) absolute configuration of $C_{24}H_{42}N_2O_8$;
   e) absolute configuration of $C_{24}H_{40}Br_2N_2O_8$.

2. A crystal indexed to give a metrically orthorhombic unit cell. After processing the frameset, the reflection file was examined in order to establish the true diffraction symmetry, and the measurements below are representative of the pattern found. There were no significant absorption effects. Is the crystal system really orthorhombic?

h	*k*	*l*	**Intensity**
10	2	4	258.2
−10	2	4	187.4
10	−2	4	267.4
10	2	−4	216.4
−10	−2	−4	245.2
10	−2	−4	200.9
−10	2	−4	264.6
−10	−2	4	208.3

3. A compound $C_{32}H_{31}N_3O_2$ crystallized from tetrahydrofuran (C_4H_8O) solution gives a primitive monoclinic unit cell of volume 1850 Å^3. What are the likely unit cell contents?

4. Estimate the range of absorption correction factors for the following crystals with $\mu = 1.0$ mm^{-1}.
   a) a thin plate 0.02 × 0.4 × 0.4 mm
   b) a tabular crystal 0.2 × 0.4 × 0.4 mm
   c) a needle 0.06 × 0.08 × 0.40 mm, mounted parallel to the fibre
   d) a needle 0.06 × 0.08 × 0.40 mm, mounted across the fibre

   Repeat the calculations with $\mu = 0.1$ and 5.0 mm^{-1}.

5. Two estimates were made of a set of unit cell parameters $a \ldots \gamma$.
   a) 8.364(12), 10.624(16), 16.76(5) Å, 89.61(8), 90.24(8), 90.08(6)°
   b) 8.327(4), 10.622(6), 16.804(8) Å , 90, 90, 90°

   The first estimate was derived from the original orientation matrix refinement using 67 reflections, while the second was obtained by a final constrained refinement using 5965 reflections from the entire frameset. Estimate the approximate contribution in each case to the uncertainty in a C–C bond of 1.520 Å.

This page intentionally left blank

Practical aspects of data processing

7

Alexander Blake

7.1 Data reduction and correction

Once the frameset has been acquired as described in the previous chapter, integrated intensities must be extracted from the raw frames, a process that is computationally intensive and impossible without access to a sufficiently precise orientation matrix. While the matrix found from the initial indexing may be adequate, and it may even be possible to initiate data reduction to run in parallel with the acquisition of the frames, this is not always the case and the safest procedure is to harvest reflections from the entire dataset, re-index (to check the unit cell) and re-refine the matrix using this longer list. Integration software uses the orientation matrix to determine the reflection positions, and the estimation of intensities can exploit the three-dimensional information available for each reflection through some form of profile fitting. There may also be facilities for updating and refining the orientation matrix during the integration process, to allow for uncertainties or gradual changes in the crystal orientation, but if a high-quality matrix can be determined that is valid for all frames it is best to use that.

An integration program will also require the relevant calibration and correction files in order to apply any corrections (see previous chapter) that were not applied to the frames as they were being collected.

A typical integration method is that developed by Kabsch (1988). Reflection spot shapes are determined for different regions on the face of the detector. These model shapes are then used for determining the area of integration for each reflection. The model profile shapes are also used to calculate correlation coefficients that can be used to reject data and to fit profiles to weak reflections.

7.2 Integration input and output

Important input parameters include the reflection widths, which may be refined or fixed. In both cases trial integration runs can be used to

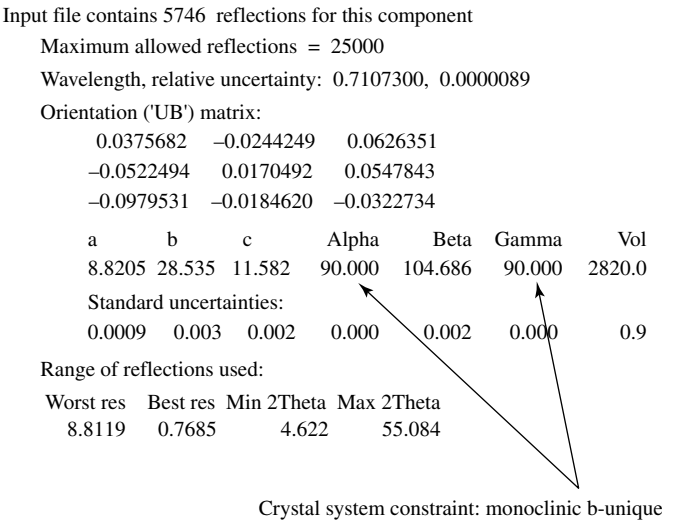

Fig. 7.1 Output from a constrained unit cell refinement.

obtain reasonable initial values. It may be better to err on the wide side but if the width is too great the integration boxes of neighbouring reflections will overlap and produce incorrect intensities. Once the integration program is running, it should produce some form of diagnostic output: examination of this (usually with the aid of a manual or other documentation) provides an indication of how the integration is proceeding. However, the volume of the raw output can be daunting, and if effective visualization tools are not available many users will only refer to the output if they subsequently encounter problems. Users are more likely to notice and act on the information if it is presented in an accessible graphical form.

A suitably constrained unit cell refinement (Fig. 7.1) should be carried out, either as part of the data reduction or separately, and should include a high proportion of the significant reflections (some software uses all reflections). Although the absolute number of reflections is always high, there may be examples where unit cells refined against a small proportion of the total data should be regarded with caution.

7.3 Corrections

A description of the required corrections to integrated data appears in Chapter 5 and these are applied during the integration procedure.[1] Lorentz and polarization factors (which are instrument specific) must be accounted for in all diffractometer measurements. There are various methods available for absorption corrections. Numerical corrections can be made on the basis of indexed faces, but routines that exploit the redundancy present in the data are more widely used (Blessing, 1995; Sheldrick, 1996–2008). Note that redundancy is often rather low

[1]Other possible corrections: (a) Extinction predominantly affects strong, low-angle reflections and is normally corrected for approximately by refining a single correction factor during structure refinement. Secondary extinction is wavelength dependent, being worse with copper than with molybdenum radiation. (b) Thermal diffuse scattering (TDS) can artificially enhance the intensity of some high-angle reflections. The fact that TDS decreases with temperature provides yet another incentive to collect low-temperature data. (c) Multiple-diffraction effects are more likely to occur if a prominent lattice vector is aligned with the rotation axis. They are most obvious where they cause significant intensity to appear at the position of a systematic absence. If their significance is not noted they can cause problems with space group determination, especially if they affect screw-axis absences. They can also be recognized by their anomalously narrow reflection profiles. (d) Some data-reduction programs will attempt to compensate for the effects of crystals that are larger than the X-ray beam. This does not appear to be problematic for crystals containing light elements, but in other cases you should avoid this situation rather than trying to correct for it.

for triclinic crystals, and in such cases the corrections need to be assessed particularly carefully. Alternatively, empirical corrections are always available if all else fails. The range of correction factors output may differ significantly from the range predicted from the cell contents and crystal dimensions, due in part to the fact that the corrections can encompass systematic effects other than absorption.

7.4 Output

Part of the output from the data-reduction routine usually includes analyses of data-significance (I/σ ratios as a function of Bragg angle and other variables), data coverage, and redundancy and consistency among equivalent data under any assumed diffraction symmetry. Examination of any such output is strongly recommended: it might cause you to question your assumptions about the diffraction symmetry, the validity of the orientation matrix, the quality of the crystal or the completeness or resolution of your data. You may decide that you need to re-process the frames. In the most serious cases, and if the crystal is fortunately still on the diffractometer, you may even decide that you would feel safer collecting some more data. However, in most cases there will be no significant problems, and the dataset is available for structure solution.

7.5 A typical experiment?

The level of detail given in the previous sections may have obscured a key feature of CCD-based diffractometers, namely their simplicity of use: below is an outline of an experiment where no particular problems are encountered. The times shown in brackets for each part of the procedure are *very* approximate.

1. Mount, orient and optically centre the crystal (1 minute).
2. Assess crystal quality using still or limited-oscillation exposures (1 minute).
3. Collect some frames and harvest reflections for indexing (several minutes).
4. Index, refine orientation matrix and determine Bravais lattice (1 minute).
5. Check whether the unit cell is known and whether its volume is sensible (1 minute).
6. Survey frames visually to check indexing and assess quality (a few minutes).
7. Determine the exposure time, frame width and fraction to collect (1 minute).
8. Record the crystal colour, shape and dimensions (1 minute); index faces if required (a few minutes).
9. Collect the data (several minutes to hours).

10. Re-determine the matrix using all available/significant reflections (a few minutes).
11. Survey frames visually as a check on the orientation matrix (a few minutes).
12. Process the data, applying corrections as required (several minutes).

Items 2–6 represent *decision points* where you have to decide whether it is worth continuing with the current crystal, and if so how the data should be collected. If indexing fails at point 4, you might decide to continue in the hope of succeeding at point 10.

Once a frameset has been processed to yield a file of reflections, you can analyze these in order to establish the likely space group(s), by looking at systematic absences and statistical intensity distributions (see Chapter 4).

7.6 Examples of more problematic cases

As noted above, it is possible to collect a frameset on very unpromising crystals: with area-detector data the challenge is to process the frames to give a useable dataset. The difficulties most commonly arise from the inherent quality of the crystal, but others may arise from the techniques used or from instrumental factors. Any circumstances that cause difficulties in defining either a single accurate, valid orientation matrix or an appropriate description of peak shapes throughout the frameset, are likely to require some special intervention.

Example 1. A frameset would not index as a whole, despite the appearance of the frames suggesting no problems.

Solution 1. It proved possible to index each run of frames individually, giving the same unit cell but slightly different orientation matrices. No decay was detected and the problem was traced to mechanical slippage of the ϕ circle while it was driving between runs. The data could be processed successfully by using a separate orientation matrix for each run.

Example 2. The symptoms were similar to Example 1, but only an approximate matrix could be defined for each run of frames. Examination of the frames suggested a systematic drift in the positions of the reflections during each run, relative to their predicted positions. These symptoms were taken as evidence of a crystal that was not securely mounted, either because of a poor bond between the crystal and fibre (or fibre and support), or because of changes occurring in the crystal.

Solution 2. In this case, a failure of the low-temperature system could be ruled out, and examination of the frames suggested the crystal was unchanged, pointing to an insecurely mounted crystal. The data were processed using a separate matrix for each run, but with each matrix being updated through the run to accommodate the movement of the

crystal. If processing had been unsuccessful, it would probably have been necessary to remount the crystal more securely and recollect all the frames.

Example 3. A crystal was coated in microcrystalline material that proved impossible to remove without damaging the crystal, and this contributed a pervasive background of weak reflections in the diffraction pattern.

Solution 3. It was possible to isolate and integrate the reflections from the main crystal by first deriving a matrix based strictly on the strongest reflections, and then extending this to include those of medium intensity. Only a small number of intensities in the final dataset were significantly affected by overlap from reflections from the small crystallites.

Example 4. A crystal indexed with a primitive unit cell with a moderately long *b*-axis of 32 Å, but with broad reflections (FWHM = 1.2°).

Solution 4. The combination of long axis and rather broad reflections could lead to reflection overlap, so the crystal-to-detector distance was increased prior to data collection. This allowed larger integration box sizes to be assessed without causing overlap.

Example 5. Examination of reflection profiles showed that their widths varied strongly as a function of goniometer angle. This pronounced anisomosaicity made it difficult to establish a single integration box size.

Solution 5. It may be possible simply to allow the box size to vary continuously during the integration, so that it always corresponds to the characteristics of the local reflections. If this option is not available in the software, or if it does not work satisfactorily, another approach is to use fixed integration box parameters that are somewhat biased towards the wider reflection profiles, followed by correction of the resulting dataset using multiscan methods (e.g., Blessing, 1995; Sheldrick, 1996–2008).

Example 6. Initial frames indicated serious problems with crystal quality, including split and poorly shaped reflections, as well as the possibility of more than one component, but it was possible to index the main component of the pattern.

Solution 6. The sample should be surveyed for better crystals but if these are not forthcoming it is probably worthwhile collecting the frames in the hope that the intensities from the main component can be extracted, giving a starting point for space group determination and structure solution. Twinning may be present in these circumstances (see below).

Example 7. Initial indexing yielded a primitive unit cell with one very long axis (85.6 Å), giving a strong likelihood of severe overlap at the standard crystal-to-detector distance.

Solution 7. The overlap problem here can be avoided by increasing the standard crystal-to-detector distance significantly, but this may mean that the highest achievable 2θ value is rather low. To achieve adequate resolution, frames will have to be collected at two different detector theta settings, chosen so that the 2θ ranges overlap. The high-angle data could be collected using a much longer exposure for each frame. A similar strategy of different detector settings and exposure times might be adopted where diffraction is strong at low angle but then falls off strongly towards higher angles.

Example 8. The output from the integration program showed good completeness, a mean redundancy of almost 4.0 and a high proportion of data with $I > 2\sigma(I)$. There were no indications of problems with crystal quality, the orientation matrix or the modelling of the reflection profiles. However, the internal agreement was terrible, with a merging R value of 0.66 under monoclinic symmetry. Unsurprisingly, structure solution failed.

Solution 8. Based on metric considerations alone, the Bravais-lattice determination had clearly indicated monoclinic C. In the light of the poor agreement between the intensties under monoclinic symmetry, this question was revisited and a smaller triclinic P cell chosen. Reprocessing gave a merging R value of 0.10 and the structure was solved at the first attempt. Clearly, the crystal possessed higher metric (pseudo)-symmetry that was inconsistent with the diffraction symmetry.

7.7 Twinning and area-detector data

A much more extensive treatment of twinning appears in Chapter 18, but some comments regarding non-merohedral twinning are appropriate here. As mentioned above, it is not necessary to have an orientation matrix before initiating data collection on an area-detector diffractometer, and one consequence of this is that framesets can sensibly be acquired on crystals that (may) have more than one component. The hope is that it will be possible to identify and index the components later, allowing the frames to be processed such that the intensity data corresponding to each component can be extracted.

At one extreme, twinning may lead to a complete failure to index using the normal indexing routines; at the other, it may not be recognized until problems are encountered with structure solution or refinement; however, the procedures required to address the problem are identical. It is obviously helpful to recognize twinning as early as possible: otherwise you might waste a lot of time, for example by pursuing other solutions to an unsatisfactory refinement. At the refinement stage, previously undetected non-merohedral twinning may generate a number of symptoms, including:

- stubbornly high R indices, with no obvious cause such as disorder,
- high-difference Fourier residuals, again with no obvious cause,

- individual reflections with $F(\text{obs})^2 \gg F(\text{calc})^2$, with certain indices most affected,
- the lowest relative $F(\text{calc})^2$ ranges show extreme values for certain indicators.

The first indications of non-merohedral twinning may be visible in the diffraction pattern (Fig. 7.2): deviations from a regular lattice of well-shaped diffraction maxima may indicate non-merohedral twinning, although they could also indicate other problems. These features might include adjacent but incompatible (i.e. mutually inclined) reciprocal lattice rows; a minority of reflections that do not correspond to the orientation matrix that fits the majority; and reflections that show splitting, overlap, irregular spacing or strange peak shapes.

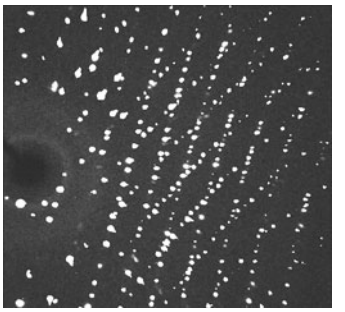

Fig. 7.2 A pattern from a crystal suspected of being a non-merohedral twin.

Although each case has to be assessed individually, the following is a general procedure for dealing with twinned area-detector data:

- examine frameset for visible indications of twinning,
- use pseudo-precession photographs or other visualization aids,
- identify major twin component, perhaps visually, or using special software such as DirAx (Duisenberg, 1992), GEMINI (Bruker, 2004), TwinSolve (Rigaku, 1999–2009), etc.,
- index the major twin component and save refined orientation matrix 1,
- identify minor twin component,
- index the minor twin component and save refined orientation matrix 2,
- repeat the last two steps for any further minor components,
- determine and view the relationships between the different matrices,
- generate predicted patterns using matrices and check these against frames,
- export orientation matrices for use by your data-reduction program,
- process the frameset using the orientation matrices,
- output separate or combined datasets for solution and refinement.

7.8 Some other special cases (in brief)

Incommensurate structures. A single unit cell and orientation matrix are not adequate in such cases because different parts of the structure exhibit different repeats. The stored frames can be processed to extract all the required data.

Collection of powder or fibre data. As the whole diffraction pattern is available, data can be extracted in different ways, for example by integrating intensity around a powder ring.

Studying phase changes. It is much easier to follow a phase transformation when the whole diffraction pattern is recorded.

Diffuse scattering. This can provide information about local structure (including disorder) in addition to conventional crystallographic data (e.g., Welberry, 2004).
Exploring lattice defects. Again, the ability to monitor what is happening between the Bragg positions is valuable.

References

Blessing, R. H. (1995). *Acta Crystallogr*. 1995, A**51**, 33–38.
Bruker (2004). GEMINI twinning program suite. Bruker AXS, Madison, WI, USA.
Duisenberg, A. J. M. (1992). *J. Appl. Crystallogr*. **25**, 92–96.
Kabsch, W. (1988). *J. Appl. Crystallogr*. **21**, 67–71.
Rigaku (1999–2009). TwinSolve. Rigaku/MSC, The Woodlands, Texas, USA.
Sheldrick, G. M. (1996–2008). SADABS. University of Göttingen, Germany.
Welberry, T.R. (2004). *Diffuse X-Ray Scattering and Models of Disorder*, Oxford University Press/IUCr, Oxford, UK.

Exercises

1. Measuring a frame for twice the time doubles the observed intensity I of the reflections on that frame. What is the effect on $\sigma(I)$ and on $I/\sigma(I)$?
2. An area detector with diameter a of 6.0 cm normally sits at a distance D of 5.0 cm from the crystal. Calculate the 2θ ranges that would be recorded with θ_c set at 28.0° if D was increased to (a) 6.0 cm; (b) 7.0 cm; (c) 8.0 cm. Assuming Mo $K\alpha$ radiation, at what point should you consider using two settings for θ_c?
3. A frameset was processed satisfactorily as orthorhombic, except for consistently high values of around 0.25 for the merging R index. Although the resulting dataset led to a plausible-looking solution, the subsequent refinement stalled at $R = 0.19$. There are no significant absorption effects. Suggest a possible solution.

This page intentionally left blank

Fourier syntheses

8

William Clegg

8.1 Introduction

The crystal structure we are trying to determine and its X-ray diffraction pattern are related to each other by the mathematical process of Fourier transformation; each is the Fourier transform of the other, as shown in the introductory material. It is worth beginning here with a summary of the fundamental relationships involved and some comments on the notation and its meaning.

X-rays are scattered by the electrons in a crystal structure, so what we are able to determine is the ***electron-density distribution***, averaged over time and hence over the vibrations of the atoms. Since the crystal structure is periodic, we need determine only the contents of one unit cell, and the presence of symmetry other than pure translation reduces this even further, to the ***asymmetric unit*** of the structure, which is a fraction of the unit cell in all cases except space group $P1$.

The electron density is a smoothly varying continuous function with a single numerical value (in units of electrons per cubic Ångstrom, e $Å^{-3}$) at each point in the structure. For many of the calculations involved in crystallography this is not a convenient function to work with, and we describe the structure instead in terms of the positions and ***displacements*** (vibrations) of discrete atoms, each with its own electron density distribution about its centre. In most studies (except for high-resolution ***charge-density*** experiments), atoms are taken to be spherical in shape when stationary, ignoring valence effects such as bonding and lone pairs of electrons, and their individual contributions to X-ray scattering, known as ***atomic scattering factors***, are calculated from electron densities derived from quantum mechanics. These atomic scattering factors are known mathematical functions, varying with Bragg angle θ, available in published tables (such as the *International Tables for Crystallography*), and incorporated in standard crystallography computer programs. The X-ray scattering effects of atoms are modified by atomic displacements, which cause the at-rest electron density to be spread out over a larger volume and usually unequally in different directions (***anisotropic***), and this effect is described by a set of ***anisotropic displacement parameters*** (adps) for each atom. The most commonly used mathematical model uses six adps and can be represented graphically as an ellipsoid. This model is a reasonable approximation to physical reality in most cases.

Thus, each symmetry-independent atom in the asymmetric unit of a crystal structure is described by the following parameters: a known atomic scattering factor (f), a set of displacement parameters (U values), and three co-ordinates (x, y, z) specifying its position. (In some cases, such as disordered structures, another parameter is used, giving the ***site occupancy factor***, because a site may be occupied by an atom in some unit cells and not in others, at random, so on average we have to specify a fraction of an atom here.) We give atomic positions relative to one corner of one unit cell chosen as the origin, and measured along each of the unit cell axes. Rather than using Å as units for the co-ordinates, we give them as fractions of the unit cell axis lengths, and these fractions do not have units. This means, for example, that the origin of the unit cell has co-ordinates 0,0,0 and the point right in the centre of the unit cell has co-ordinates ½, ½, ½. It is convenient to take most co-ordinates to lie in the range 0–1, but molecules do not generally lie conveniently within the confines of an arbitrarily defined unit cell, so some co-ordinates may be negative or be greater than 1. A majority of co-ordinates outside the range 0–1 simply means a poorly chosen unit cell origin, with the molecule lying largely or entirely outside the 'home' unit cell. This is, of course, not strictly incorrect, since all unit cells are exact copies of each other by definition, and any integer can always be added to or subtracted from all x, all y, or all z co-ordinates, but it is bad practice.

8.2 Forward and reverse Fourier transforms

The diffraction pattern (a set of discrete reflections, each a wave with its own amplitude and relative phase) is the Fourier transform of the crystal structure. The mathematical relationship for this is given by:

$$F(hkl) = \sum_{j=1}^{N} f_j \exp[2\pi \mathrm{i}(hx_j + ky_j + lz_j)]. \tag{8.1}$$

Here, f_j is the atomic scattering factor for the jth atom in the unit cell, which has co-ordinates x_j, y_j, z_j; f_j incorporates the effects of atomic displacements in this equation, in order to keep it simple. The integers h, k and l are the indices for one particular reflection, occurring in a certain direction, and this equation shows how the structure factor F for that reflection is related to the crystal structure. What this equation means in words is that each reflection in the diffraction pattern is a wave and it is made up as a sum of waves scattered by the individual atoms, each atom in accordance with its electron-density distribution (f_j); in adding up the waves scattered in this direction, their relative phases have to be allowed for, and these depend on the positions of the atoms relative to each other, as expressed in the exponential term. For mathematical convenience and compactness, complex number notation is used (hence the symbol i), allowing us to use just one symbol to represent both the amplitude and phase together for a wave. $F(hkl)$ is a complex number,

as explained in Chapter 1 and Appendix A, with an amplitude and a phase. Equation (8.1) applies once for each reflection (each direction in which a discrete diffracted beam occurs) in order to obtain the complete diffraction pattern, and each calculation involves the sum of N terms, this being the number of atoms in the unit cell. The presence of symmetry in the structure allows the calculations to be simplified further, because symmetry-equivalent reflections have the same amplitude and related phases, but we shall keep with general equations here.

Equation (8.1) can be used to calculate the expected diffraction pattern for any known structure, and it is used at various stages during a crystal-structure determination, even when the 'known structure' is incomplete. We refer to the result of this as a set of ***calculated structure factors***, $F_c(hkl)$ or just F_c.

Equation (8.1) also describes mathematically the physical process observed when X-rays are diffracted by a crystal, which is the experiment of collecting diffraction data. From the experiment, however, we obtain only the amplitudes of the reflections (derived from the measured intensities) and not their phases. Thus, we have a set of ***observed structure factors***, but they are only $|F_o|$. We do not have any observed phases, so the observed diffraction pattern is, in this sense, incomplete.

One particular F is never measured in the diffraction experiment, but is important for future use. This is the structure factor $F(000)$, corresponding to completely in-phase scattering by all atoms in the forward direction with $\theta = 0$, and it can not be physically separated from the undiffracted beam. Setting all indices to zero in (8.1) and noting that atomic displacement parameters have no effect at zero Bragg angle, we find that $F(000)$ has an amplitude equal to the total number of electrons in one unit cell, and has a phase of zero.

That is half the story, which we may call the ***forward Fourier transform***. The other half is the ***reverse Fourier transform***. The crystal structure, expressed as electron density, is the Fourier transform of the diffraction pattern. This relationship is expressed as:

$$\rho(xyz) = \frac{1}{V} \sum_{hkl} F(hkl) \exp[-2\pi \mathrm{i}(hx + ky + lz)]. \qquad (8.2)$$

There is an obvious similarity to (8.1), with the terms for the diffraction pattern and for the crystal structure exchanged between the left and right sides of the equation. The main differences otherwise are the inclusion of the unit cell volume V in (8.2) (to make sure the units are correct, since the crystal structure here is described by its electron density ρ instead of by discrete atomic scattering factors that, like structure factor amplitudes, have units of electrons rather than e Å^{-3}), and the presence of a minus sign in the exponential.

Equation (8.2) is the basis of all Fourier synthesis calculations in crystallography. It shows how the electron density in the crystal structure can, in principle, be obtained from the diffraction pattern. Like the forward Fourier transform, it describes a physical process, but this time

one that is unachievable in an experiment. It is the equivalent of the use of lenses in an optical microscope to take light scattered by an object being viewed, and recombine the scattered waves to produce a focused image of the object; unfortunately X-rays can not be bent by lenses in the same way as visible light, or we would be able to build an X-ray supermicroscope and not have so much work to do! The equation says that, in order to find the electron density at a particular point in the structure, we have to take all the individual scattered X-ray waves (the reflections F) and add them together, allowing for their different relative phases. The phase differences will vary with the position at which we are finding the electron density, because the waves will have different path lengths in converging on that point, and this is the meaning of the exponential term again; but the waves also have different phases from their initial production in the diffraction process (given by the forward Fourier transform), and these have to be included as well.

Since this physical process can not actually be carried out, we have to emulate it by calculation, using (8.2). Unfortunately, this is still not possible in a direct way, because we do not have all the information required. In (8.2), $F(hkl)$ are complex numbers, with an amplitude and a phase: although we have the structure factor amplitudes, we do not know the intrinsic relative phases of the reflections. Much of the task of solving a crystal structure is recovering the lost phase information, at least as approximate values, so that the reverse Fourier transform can be carried out.

Modified versions of (8.2) are used at various stages in a crystal-structure determination, as our knowledge of the phases develops from non-existent to essentially complete, and these are referred to as different kinds of Fourier syntheses or Fourier maps.

In order for (8.2) to give an accurate result for the electron density, it is not only necessary to have phases and to have accurate values for the reflection amplitudes (i.e. good data!); we should, in principle, also include all possible reflections with indices between $-\infty$ and $+\infty$. This is clearly unachievable, and the effect is to produce some distortions in the electron density, which may be seen as small ripples surrounding the atoms, most noticeable around atoms with high electron density. It is, however, not usually a significant problem, since the form of atomic scattering factors, together with atomic displacements, means that diffraction intensities decrease at higher Bragg angles, and the unmeasured high-index small amplitudes would not contribute much to the Fourier summations anyway. Inclusion of $F(000)$ is important in order to obtain correct electron density values, since all other terms effectively contribute no net electron density to the total in the unit cell, because they are waves consisting of equal positive and negative parts. A Fourier synthesis may be thought of as smearing out the correct total number of electrons uniformly throughout the unit cell (this is the $F(000)$ term) and then redistributing this density by successive addition of other waves, each of which will reduce the density in some regions and increase it in others by the same amount; the final result has the electron

density concentrated in discrete maxima corresponding to atoms, with low or zero (but never negative) electron-density regions in between.

8.3 Some mathematical and computing considerations

Since Fourier transform calculations, both forward and reverse, take up a very high proportion of the amount of computing involved in crystallography, they need to be carried out as efficiently as possible. The scale of the task can be illustrated easily. For the forward Fourier transformation, consider a unit cell of dimensions $10\times10\times10$ Å^3 containing 60 atoms. Typically, this will give about 7000 reflections up to a maximum θ of 25° with Mo-$K\alpha$ radiation. Calculation of the diffraction pattern F_c thus involves 7000 sums (ignoring symmetry), in each of which there are 60 terms. This makes 420 000 calculations, each of which includes exponentials, multiplications and additions. This is a relatively small structure!

For the reverse Fourier transformation, consider the same crystal structure. From (8.2) we obtain values of the electron density at discrete points in the unit cell, not a continuous function. This means calculating values at selected points on a three-dimensional grid covering the unit cell. In order to resolve adjacent atoms and make good use of the available data, a grid spacing of about 0.3 Å is reasonable, giving about 37 000 grid points. So, (8.2) has to be used 37 000 times, each one being a sum of 7000 terms, making a total of about 260 million calculations. And this is for just one Fourier synthesis.

The presence of symmetry does reduce the size of the task, of course, because symmetry-equivalent reflections have the same amplitude and related (not generally equal) phases, so the forward Fourier transformation only has to be carried out for the symmetry-unique data set. Similarly, the electron density need be calculated only for the asymmetric unit, and not for the complete unit cell.

In addition, there are various well-known mathematical procedures for simplifying the calculations involved, because of the properties of sines and cosines of sums of terms, as shown in Appendix A. The details of these do not need to concern us here; although Fourier calculations were carried out by hand in the early pioneering days of crystallography before the widespread availability of fast computers (and were often restricted to one- and two-dimensional syntheses rather than full three-dimensional studies, to provide projections of electron density, from which full structures were subsequently deduced), these calculations are now performed at very high speed in 'black boxes'.

It should be noted that the phases of reflections can take any value between 0 and 360° (0 and 2π radians) for non-centrosymmetric structures. By contrast, phases are restricted to a choice of two values, 0 and 180° (0 and π radians) when a structure is centrosymmetric. This

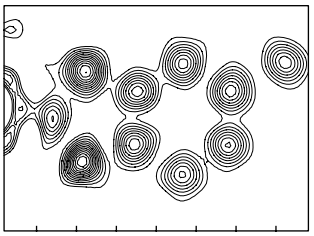

Fig. 8.1 Contoured section through a Fourier synthesis in a plane containing B, C, O and H atoms. The edge of a Pt atom bonded to B is seen at the left. H atoms are not visible; the ten clear peaks correspond to atoms.

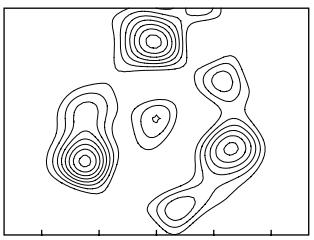

Fig. 8.2 Contoured section through a Fourier synthesis in the plane containing three methyl carbon atoms of a two-fold disordered *tert*-butyl group. The major component atoms are clearly seen as the largest peaks, but the minor components do not all give separate maxima. The small peak at the centre is the outer edge of the central carbon atom of the group, which lies below this plane, where the electron density is higher and reaches its maximum for this atom.

considerably simplifies the mathematics, since the complex exponential terms collapse to real cosines, with disappearance of the imaginary sine components. In pictorial physical terms, this means that each of the waves being added together in (8.2) can only be completely in phase (0, crest-to-crest) or completely out of phase (180°, crest-to-trough), and the problem of finding the unknown phases reduces to the smaller (but still considerable) task of finding the unknown signs, positive or negative, for the reflection amplitudes $|F|$ in order to add the waves together.

A Fourier synthesis is a three-dimensional function, usually obtained as a set of values on a three-dimensional grid. In chemical crystallography, it is rare for such a result to be presented in full. Normally, the positions of maxima (also called peaks) in the synthesis are found by interpolation between the grid points (effectively a form of curve fitting in three dimensions) as part of the computing procedure, and these positions, together with the corresponding values of the electron density, are listed and made available as potential atom sites for visual inspection or, more likely, interpretation through a molecular graphics program. In most cases, this works satisfactorily, but it causes problems when atom sites are not clearly resolved from each other, giving no discrete maximum in the synthesis. This is the norm in protein crystallography, where data often do not extend to atomic resolution, and different techniques are used. With atomic-resolution data, the most common occurrence of this problem is in cases of disorder, when the alternative sites may be too close together to give separate maxima. Inspection of the full Fourier synthesis in the region of the disorder may be necessary. This can involve taking planar sections through the three-dimensional synthesis. Sections parallel to the unit cell faces are straightforward, as these will correspond to the grid points on which the synthesis has been performed, but sections in arbitrary orientations can also be calculated, either explicitly at appropriate points or by interpolation between the points of the standard grid. The sections can be contoured with lines joining points of equal electron density, like the contours showing mountains on geographical maps, and this helps to show regions of electron density that can correspond to atom sites, even if disorder is a problem. Examples are shown in Fig. 8.1 and Fig. 8.2.

8.4 Uses of different kinds of Fourier syntheses

All Fourier syntheses are essentially variations on (8.2). This may be written in a slightly different but equivalent way to help show what the variations are.

$$\rho(xyz) = \frac{1}{V}\sum_{hkl} |F(hkl)| \exp[\mathrm{i}\phi(hkl)] \exp[-2\pi i(hx + ky + lz)]. \qquad (8.3)$$

Here, the structure factor F has been separated into its amplitude $|F|$ and its phase ϕ, both of which are needed in order to carry out the calculation.

Different kinds of Fourier syntheses use different coefficients instead of the amplitudes $|F|$, and they may also in some cases apply weights to the individual terms in the sum, so that not all reflections contribute strictly in proportion to these coefficients. These are all attempts to obtain as much useful information as possible at different stages of the structure determination, even if the phases are not well known.

8.4.1 Patterson syntheses

These are discussed in detail in the next chapter. The coefficients are $|F_o|^2$ instead of $|F_o|$, and all phases are set equal to zero. In this case all necessary information is known and the synthesis can be readily performed. The result, of course, is not the electron density distribution for the structure, but it is related to it in what is often a useful way, as is explained later. There are some slight variations even within this use, and these are covered in the Patterson synthesis chapter (Chapter 9).

8.4.2 *E*-maps

These are an important part of direct methods for solving crystal structures, and are discussed more fully in Chapter 10. The coefficients are $|E_o|$, the so-called normalized observed structure factor amplitudes, which represent the diffraction pattern expected for point atoms (with their electron density concentrated into a single point instead of spread out over a finite volume) of equal size, at rest. *E*-values are calculated, with a number of assumptions and approximations, from the observed amplitudes $|F_o|$, and only the largest values are used, weaker reflections being ignored because they contribute less to the Fourier synthesis anyway. Phases for this selected subset of the full data are estimated by a range of techniques under the general heading of 'direct methods', and usually a number of different phase sets are produced and used to calculated *E*-maps. These maps tend to contain sharper (stronger and narrower) maxima than normal Fourier syntheses (*F*-maps), and this can help to show up possible atoms, but they also tend to contain more noise (peaks, usually of smaller size, that do not correspond to genuine atoms).

8.4.3 Full electron-density maps, using (8.2) or (8.3) as they stand

These actually tend not to be used very often in chemical crystallography, except for demonstration purposes, because the other types of syntheses have particular advantages at different stages. However, let us consider how we can carry out such a synthesis without having any

experimental phases. Such a procedure can be used when some of the atoms have been located (perhaps from direct methods or a Patterson synthesis) and others still remain to be found. Once we have some atoms, we can use them as a ***model structure***, which we know is not complete, but it contains all the information we currently have. From the model structure we can use (8.1) to calculate what its diffraction pattern would be. This will not be identical to the observed diffraction pattern, but it should show some resemblance to it, the more nearly so as we include more atoms in the correct positions. There are various measures of agreement between the sets of observed and calculated amplitudes, $|F_o|$ and $|F_c|$, but the important thing is that the calculated diffraction pattern includes phases, ϕ_c as well as amplitudes $|F_c|$. Although these are not the same as the true phases we would really like to know, they are currently the nearest thing we have to them. A Fourier synthesis using coefficients $|F_c|$ with the phases ϕ_c would just reproduce the same model structure and get us nowhere, but combining the true observed amplitudes $|F_o|$ with the 'current-best-estimate' phases ϕ_c gives us a new electron-density map. If the calculated phases are not too far from the correct phases (as is usually the case if the model structure has atoms in approximately correct places and these are a significant proportion of the electron density of the structure), then this usually shows the atoms of the model structure again, together with new features not in the model structure but demanded by the diffraction data, i.e. more genuine atoms. Because of all the approximations involved in this process, there may also be peaks in the electron-density map that do not correspond to real atoms, and the results need to be interpreted in the light of chemical structural sense and what is expected. Addition of these new genuine atoms gives a better model structure, and the whole process can be repeated, giving better calculated phases and yet another new, and clearer, Fourier synthesis. This is done repeatedly until all the atoms have been found and the model structure essentially reproduces itself.

8.4.4 Difference syntheses

These are widely used in preference to full electron-density syntheses for expanding partial structures. The coefficients are $|F_o| - |F_c|$ and the phases are obtained from a model structure as described above. The result is effectively an electron-density map from which the features already in the model structure are removed, so that new features stand out more clearly, and it usually makes it easier to find new atoms. This is rather like saying that, if the tallest peaks in a range of mountains were somehow taken away, the foothills would appear to be much more impressive! Peaks lying at the positions of atoms in the model structure, or negative difference electron density there, indicate that the model has either too little or too much electron density in those places, and can indicate a wrongly assigned atom type, e.g. N instead of O or N instead of

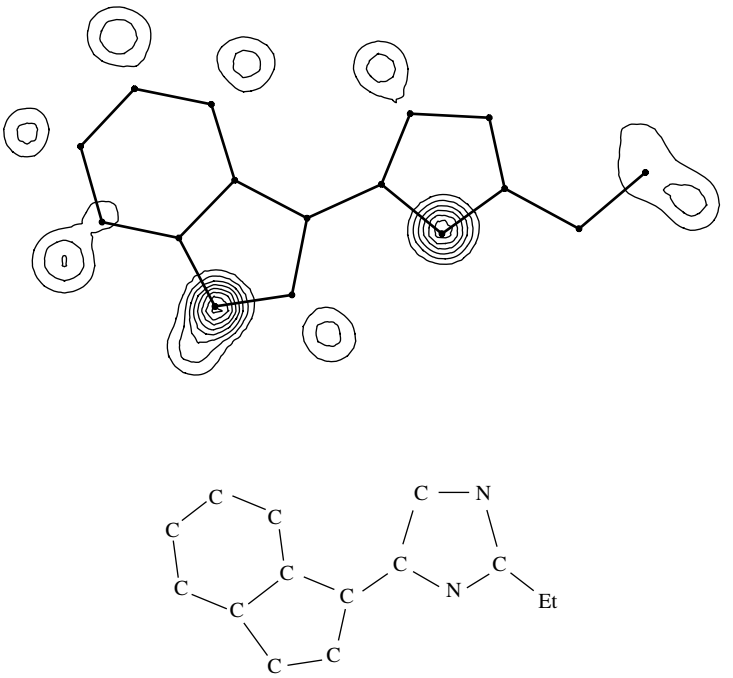

Fig. 8.3 A section through a difference synthesis showing the effect of wrongly assigned atom types and missing hydrogen atoms; the assumed model structure is shown, together with the positions of its atoms and bonds in the map.

C for these respective effects. An example is shown in Fig. 8.3. There are potentially some considerable problems with difference syntheses when the proportion of known atoms is quite small, because the calculated phases can have large errors. Also, weak reflections with relatively large uncertainties in their intensities can cause disproportionate errors, and it may be best not to use the weakest reflections; alternatively they can be given reduced weights, as discussed below. It is important to ensure that the observed and calculated data are on the same scale. Another reason why difference syntheses can be better than full F_o syntheses is that series termination errors (small ripple effects due to the lack of data beyond the measured θ_{max}) cancel out through use of the differences instead of full amplitudes.

8.4.5 $2F_o - F_c$ syntheses

The use of coefficients $2|F_o| - |F_c|$ with phases calculated from a model structure combines the advantages of standard F_o and difference syntheses. The resulting map shows both the known and the as-yet unknown features of the structures, with the new atoms emphasized, and it is less subject to some of the errors of the simple difference synthesis. It is more widely used in protein crystallography than by chemical crystallographers.

8.4.6 Other uses of difference syntheses

Towards the end of structure determination, difference maps are often used to locate hydrogen atoms. These can not usually be found until all other atoms are present and have been refined with anisotropic displacement parameters, so that their contributions are correctly represented in the model structure. This is because hydrogen atoms have very little electron density, and even that is significantly involved in bonding, so the positions found in difference maps are usually closer to the nearest atom than are the actual centres (the nuclei) of the hydrogen atoms. Unless data are of good quality, and particularly when heavy atoms are present in the structure, hydrogen atoms can easily be lost in the noise of an electron-density map. This is particularly true for non-centrosymmetric structures, where the absence of hydrogen atoms in a model structure is partially compensated by shifts in the phases from their correct values; any Fourier synthesis using calculated phases will always have a bias towards the model structure from which they were obtained. Hydrogen atoms contribute relatively more to low-angle and less to high-angle reflections, because their atomic scattering factor falls off more quickly with θ than those of other atoms, so it may help to leave out the high-angle data, or use weights that reduce their contribution to the sums. Right at the end of a structure determination, when refinement is complete, a final difference synthesis must be generated in order to see if there is any remaining electron density unexplained by the refined model. This must include all data and use no weights. Residual electron density may be an artefact of inadequate data corrections (usually absorption), or may indicate poorly modelled disorder or other problems and imperfections in the model. The sizes of the largest maxima and minima in this final difference map, together with their positions if they are of significant size, are important indicators of the quality of a structure determination, and should always be included in any summary of the results.

8.5 Weights in Fourier syntheses

It was noted above that the calculated phases, derived from the current model structure, are only an estimate of the true phases. Clearly the approximation improves as the model structure becomes more complete. In any given set of calculated phases, some will be more in error than others. For a reflection with large and almost equal $|F_o|$ and $|F_c|$ there is greater confidence in the reliability of the phase than there is when $|F_c|$ is small. This variation in reliability of the phases can be incorporated into the calculations by multiplying each contribution by a weight, which increases with expected reliability. Various weighting schemes have been developed and used, with weights calculated from the values of the observed and calculated amplitudes and the proportion of unknown electron density in the structure. Appropriately

chosen weights can help to enhance the genuine new features of Fourier syntheses and reduce noise. Weights that are θ-dependent can be used to aid the search for hydrogen atoms in the later stages, by down-weighting the higher-angle data containing less information from these atoms. No weights may be used in the final difference synthesis for checking the completeness of a refined structure; by this stage the calculated phases will be as close to the correct values as they can be.

8.6 Illustration in one dimension

For a one-dimensional structure (this direction taken as the z-axis) with inversion symmetry, (8.3) simplifies considerably:

$$\rho(z) = \frac{1}{c} \sum_{l} |F(l)|\, s(l) \cos[2\pi(lz)] \tag{8.4}$$

and the Fourier summation can easily be demonstrated pictorially. Only positive values of the index l need to be considered, each giving a double contribution to the sum, since $F(l) = F(-l)$, in addition to the single contribution of $F(0)$. The phase of each reflection is now just the (unknown) positive or negative sign, $s(l) = +1$ or -1. We use some data measured a number of years ago for a compound containing a long alkyl chain and a bromine atom (the detailed molecular structure is not important here); this crystallizes in a unit cell with one long axis (c), the molecule being stretched out so that its projection along this axis gives resolved atoms, Br and several C. There are two molecules per unit cell, appearing as inversions of each other along the two halves of the cell axis. This projection can be investigated with just the $(00l)$ reflections, with the irrelevant zero indices ignored here.

Table 8.1 lists the observed amplitudes of the measured reflections with l between 3 and 21 ($|F_o|$), and the amplitudes calculated from a model structure consisting only of the two symmetry-equivalent Br atoms ($|F_c|$, via the one-dimensional equivalent of (8.1)); how these Br atoms can be found from the data is considered in the next chapter, on Patterson syntheses. Also given are two sets of signs (reflection phases): the correct signs obtained by calculation from the complete structure once it is known (true signs), and the signs obtained from the model containing only the Br atoms (model signs). Below Table 8.1 are shown in Fig. 8.4 the individual terms $|F_o(l)|\cos[2\pi(lz)]$ that contribute to the sum in (8.4), ignoring the signs $s(l)$. Carrying out a Fourier synthesis to obtain the one-dimensional electron density just means adding up these 'electron-wave' contributions with the correct signs. Since there are 19 terms to add together, the number of possible sign combinations is 2^{19}, which is over half a million: not a good case for trial and error! Several different variants on (8.4) are shown graphically in Figs. 8.5 to 8.8.

Table 8.1. One-dimensional Fourier contributions.

l	$\lvert F_o\rvert$	$\lvert F_c\rvert$	true sign	model sign
3	8	17	+	−
4	64	51	−	−
5	56	64	−	−
6	74	55	−	−
7	15	26	−	−
8	5	9	+	+
9	46	39	+	+
10	45	53	+	+
11	43	47	+	+
12	17	26	+	+
13	9	3	−	−
14	26	28	−	−
15	31	41	−	−
16	23	39	−	−
17	12	23	−	−
18	14	1	+	−
19	20	19	+	+
20	33	31	+	+
21	63	30	+	+

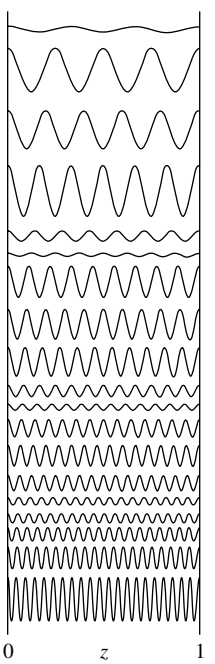

Fig. 8.4 The contributions of each of the reflections in Table 8.1 to the one-dimensional Fourier synthesis, all shown here with positive sign (zero phase angle); the reflections are in order, with $l = 3$ at the top and $l = 21$ at the bottom.

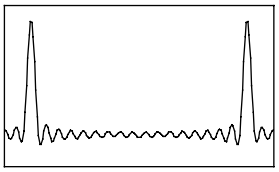

Fig. 8.5 F_c synthesis: amplitudes from Br atom, phases from Br atom.

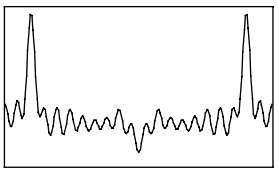

Fig. 8.6 F_o synthesis: observed amplitudes, phases from Br atom.

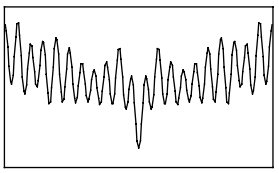

Fig. 8.7 $F_o - F_c$ synthesis: difference between observed and Br-calculated amplitudes, phases from Br atom.

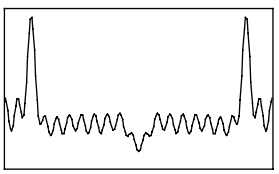

Fig. 8.8 F_o synthesis: observed amplitudes, 'correct' phases from final structure.

8.6.1 F_c synthesis

Both the amplitudes and the signs are taken from the model structure (Br atoms only). This essentially just gives back the same model structure, with two large peaks where the Br atoms were located (Fig. 8.5). However, there is significant regular ripple in the rest of the unit cell; this is caused by 'series termination', the lack of contributions from reflections with $l > 21$. If these were available and were included, most of the diagram would be essentially flat. This is not a useful Fourier synthesis!

8.6.2 F_o synthesis, as used in developing a partial structure solution

Experimental amplitudes $|F_o|$ are combined with the signs (phases) obtained from the current model structure. The resulting map (Fig. 8.6) shows the atoms of the model (2 Br), together with new atoms (a number of smaller peaks corresponding to C atoms in a chain for each molecule). Note that the model signs are mostly, but not all, correct, so this electron-density map is not perfect, but it is sufficient to locate the remaining atoms. The incorrect signs slightly distort the map, producing rather unequal peak heights for the carbon atoms and overstating the central dip.

8.6.3 $F_o - F_c$ synthesis

This is a difference map (Fig. 8.7), using the difference between the observed and calculated amplitudes together with the signs from the model structure. Comparison with the previous result shows that the Br atoms in the model no longer appear, so the new atoms stand out more clearly.

8.6.4 Full F_o synthesis

This is the same as the second result, but with all the correct phases. This gives a more even pattern of peaks for the carbon atoms (Fig. 8.8). At this stage, with the structure complete, the model structure should essentially reproduce itself in a standard $|F_o|$ synthesis, and a difference synthesis should contain no significant features.

Exercises

1. In Fig. 8.3, assign the correct atom types, the H atoms, and the appropriate bond types (single, double, or aromatic). The correct formula is $C_{13}H_{12}N_2O$. Why is there only one peak visible for the ethyl group H atoms?
2. What would be the effect on a Fourier synthesis of:
   a) omitting the term $F(000)$;
   b) omitting the 20% of reflections with highest values of $(\sin\theta)/\lambda$;
   c) omitting the 5% of reflections with lowest values of $(\sin\theta)/\lambda$;
   d) setting all phases equal to zero?

This page intentionally left blank

Patterson syntheses for structure determination

9

William Clegg

9.1 Introduction

We wish to convert a measured diffraction pattern into the corresponding crystal structure that produced it experimentally. The process involved is Fourier transformation, and the mathematical expression for this was given in the previous chapter, on Fourier syntheses.

$$\rho(xyz) = \frac{1}{V}\sum_{hkl}|F(hkl)|\exp[i\phi(hkl)]\exp[-2\pi i(hx+ky+lz)] \qquad (9.1)$$

This is the form of the equation that explicitly contains the amplitudes and phases of the structure factors as separate symbols, from which we can see the fundamental problem we face: the amplitudes $|F_o|$ are known from the diffraction experiment, but the phases ϕ are unknown, so it is not possible to carry out the Fourier synthesis directly. In the previous chapter we saw that knowledge of part of the structure can get us started, since it is then possible to calculate approximate phases and improve our knowledge of the electron density in stages through modified versions of (9.1). The question is, how do we make a start? In chemical crystallography there are two main techniques for solving the phase problem, which have complementary strengths and applications. One is the use of so-called ***direct methods***, which attempt to estimate approximate phases from relationships among the structure factors with no prior knowledge about the crystal structure itself (except for the discrete atomic nature of matter and its implications for diffraction effects), and this is considered in the next chapter. The other is the use of the ***Patterson synthesis*** (or Patterson map, or Patterson function), another variation on (9.1), which can provide information on approximate positions of some of the atoms in the structure. The Patterson synthesis finds most use either when there are a few heavy atoms (atoms with a considerably higher number of electrons) among many light atoms, such as in co-ordination complexes of most metals, or when a significant proportion of the molecular structure is expected to have a well-defined

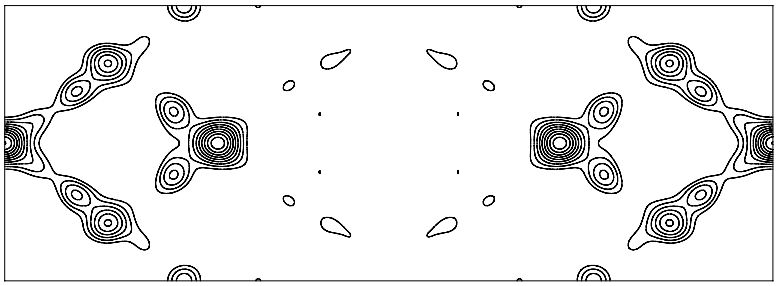

Fig. 9.1 A section through a Patterson map for an organic compound containing no heavy atoms.

and known rigid internal geometry, such as the characteristic tetracyclic framework of steroids or other fused polycyclic systems with little or no conformational flexibility.

In the Patterson synthesis (named after its inventor, A. L. Patterson), the amplitudes $|F_o|$ in (9.1) are replaced by their squares $|F_o|^2$ and the unknown phases are simply omitted (effectively all set at zero). An alternative way of expressing this is that the complex structure factors $F(hkl)$, which contain both amplitude and phase information (see (8.2) in Chapter 8) are replaced by the product of each one with its complex conjugate $F^*(hkl)$. Multiplying any complex number by its complex conjugate (which has the same cosine term but the opposite sign for its sine term) gives a real number, the imaginary terms cancelling out. In this case the complex exponential also simplifies to a real cosine.

$$P(uvw) = \frac{1}{V}\sum_{hkl} |F(hkl)|^2 \cos[2\pi(hu + kv + lw)]. \qquad (9.2)$$

Obviously, with these changes in the Fourier coefficients and omission of the phases, the result of the synthesis will no longer be the desired electron density, but it turns out to be closely related to it in what can be a useful way. The use of the co-ordinates u, v, w instead of x, y, z helps to emphasize this point; these are still fractions of the unit cell edges and the Patterson synthesis is a periodic continuous function looking rather similar to an electron-density distribution and repeated in each unit cell. Figure 9.1 is an example.

9.2 What the Patterson synthesis means

The nature of the Patterson synthesis and its relationship to the electron density can be expressed in a number of ways that look rather different but are essentially equivalent. The peaks in a Patterson map do not correspond to the positions of individual atoms (i.e. the positions of atoms relative to the unit cell origin as expressed in their co-ordinates x, y, z), but instead to vectors between pairs of atoms in the structure (i.e. the positions of atoms relative to each other). Thus, for every pair

of atoms in the structure with co-ordinates $(x_1,\ y_1,\ z_1)$ and $(x_2,\ y_2,\ z_2)$ there will be a peak in the Patterson map (a maximum in the Patterson synthesis) at the position $(x_1 - x_2,\ y_1 - y_2,\ z_1 - z_2)$ and also one at the position $(x_2 - x_1,\ y_2 - y_1,\ z_2 - z_1)$, each atom giving a vector to the other. To turn this argument the other way round, every peak observed in the Patterson map corresponds to a vector between two atoms in the crystal structure, so a Patterson peak at (u, v, w) means there must be two atoms whose x co-ordinates differ by u, y co-ordinates differ by v, and z co-ordinates differ by w. The objective is to work out some atom co-ordinates by knowing only differences between pairs of them.

Mathematically this can all be expressed in terms of Fourier transforms and convolutions. Multiplying two functions together in direct space corresponds to a convolution of their Fourier transforms in reciprocal space, and vice versa. Calculating the Patterson synthesis involves taking the product of the diffraction pattern structure factors with their complex conjugates, so the result is the convolution of the electron density with its inverse. What this convolution means can be visualized by adding together n versions of the true electron density, where n is the number of atoms in the unit cell; for each contribution to the sum, the whole structure is shifted to put this atom at the origin of the unit cell and the electron density everywhere is multiplied by the electron density of the atom at the origin.

$$P(u,v,w) = \int_{\text{cell}} \rho(x,y,z)\rho(u-x, v-y, w-z)\mathrm{d}x\mathrm{d}y\mathrm{d}z, \tag{9.3}$$

and this is the mathematical equation corresponding to the description above in terms of vectors between pairs of atoms, because the value of the Patterson function P will only be large at positions that correspond to separations between significant concentrations of electron density according to (9.3).

The practical value of this synthesis can be seen by considering some of the properties that follow from its definition.

1. There is a vector between every pair of atoms in the structure; this includes 'self-vectors' between each atom and itself, which obviously have zero length. For n atoms in the unit cell this means n^2 vectors, of which n all coincide at the position $(0, 0, 0)$, the origin of the unit cell in the Patterson map. All Patterson maps have their largest peak at the origin. There are $n^2 - n$ other peaks, many more than the number of atoms.
2. Every pair of atoms gives two vectors, A→B and A←B. These are equal and opposite, so there are two peaks related to each other by inversion through the origin. All Patterson syntheses have inversion symmetry, whether or not the crystal structure has. This consequence can also be seen from the form of (9.2): setting all phases equal to zero automatically forces an inversion centre. Perhaps less obvious, but equally true, is that screw axes and glide

planes in the crystal structure are converted into normal rotation axes and mirror planes in the Patterson synthesis, all translation components disappearing. This means the point group symmetry for a Patterson synthesis is the same as the Laue class for the diffraction pattern. The primitive or centred nature of the unit cell of the structure is retained in the Patterson synthesis, so the space group symmetry of the Patterson map is related to the true space group of the structure, but there are only 24 possible Patterson space groups, corresponding to the combinations of the 11 Laue classes with appropriate permissible unit cell centrings in each of the crystal systems.

3. Patterson peaks have a similar appearance to electron-density peaks, but they are about twice as broad as a result of the convolution effect of (9.3). Because of this and the large number of peaks resulting from the first point above, there is a considerable overlap of peaks, so they are usually not all resolved from each other like electron-density peaks. Vectors that are approximately or exactly equal in length and parallel to each other, such as opposite sides of benzene rings and metal–ligand bonds arranged *trans* to each other, will give substantial or complete overlap, further reducing the number of distinct maxima that can be seen. Symmetry in the structure also leads to exact overlap of vectors. Thus, Patterson maps often show large relatively featureless regions.
4. Each peak resulting from a vector between two atoms has a size proportional to the product of the atomic numbers Z of those two atoms, just as electron-density peaks are proportional to atomic numbers in normal Fourier syntheses (ignoring the effects of atomic displacements, which spread out the electron density somewhat). If the unit cell contains a relatively small number of heavy atoms among a majority of lighter ones, the peaks corresponding to vectors between pairs of these heavy atoms will be large and will stand out clearly from the general unresolved background level and smaller peaks.

Before going on to consider the two major ways of exploiting these properties of the Patterson function, we note some small modifications to the standard Patterson synthesis expression in (9.2) that can be used, just as there are variations in Fourier syntheses that incorporate phase information.

The first is that it is possible to remove the large ***origin peak***, so that peaks corresponding to short vectors are more clearly seen, though this is not usually a problem. In any case, the fact that the origin peak has a size proportional to the sum of Z^2 for all atoms in the unit cell, on the same scale as the sizes of other peaks described above, can help to confirm the identity of the atoms contributing to individual peaks. To remove the origin peak, $|F|^2$ in (9.2) is replaced by $|F|^2 - \langle |F|^2 \rangle_\theta$, where the term subtracted is the mean value of $|F|^2$ at this Bragg angle, obtained by some kind of curve fitting to a plot of $|F|^2$ against $(\sin\theta)/\lambda$, for example.

The second modification is to ***sharpen*** the Patterson function, reducing the width of the peaks. This is achieved by using $|E|^2$ instead of $|F|^2$ in (9.3), giving greater relative weight to the higher-angle data and effectively suppressing the effects of atomic displacements. The advantage is a better resolution of peaks from each other, but the disadvantage is introduction of more noise (spurious small peaks) because of greater uncertainty in the higher-angle data and the enhanced effects of series termination. Use of $|E|^2 - 1$ as coefficients in the synthesis gives both sharpening and origin-peak removal simultaneously. Intermediate degrees of sharpening as a compromise are obtained by using $|E||F|$ or even $\sqrt{(|E|^3|F|)}$ as coefficients.

9.3 Finding heavy atoms from a Patterson map

If a unit cell contains a small number of heavy atoms together with a majority of lighter atoms, then the Patterson map will show a relatively small number of large peaks corresponding to heavy–heavy vectors, prominent above the smaller peaks due to heavy–light vectors and (probably largely unresolved) light–light vectors. The idea is to deduce a set of heavy-atom positions that explain all the large Patterson peaks; these heavy atoms then form a model structure from which approximate phases can be calculated for Fourier syntheses to develop the model further, as already described in the previous chapter. There are generally more vectors providing information than there are atom positions to be found. Solving a Patterson map is rather like a mathematical brain-teaser or a crossword puzzle. Heavy atoms that are in symmetry-related positions often give Patterson peaks lying in special positions with co-ordinates equal to 0 or ½, which are easily recognized. This is best illustrated with specific examples in commonly occurring space groups.

9.3.1 One heavy atom in the asymmetric unit of $P\bar{1}$

In this common case, there are two heavy atoms in the unit cell, related to each other by inversion symmetry. Their unknown co-ordinates are (x, y, z) and $(-x, -y, -z)$. The largest Patterson peak is, as always, at $(0, 0, 0)$. There should be two other prominent peaks, one on each side of the origin, since the Patterson function is also centrosymmetric. One has co-ordinates $(u, v, w) = (2x, 2y, 2z)$, because this is the difference between the sets of co-ordinates of the two heavy atoms; the other has the same co-ordinates with opposite signs, $(-2x, -2y, -2z)$. It is a trivial matter to divide these by 2 and obtain the position of the unique heavy atom. Because there are two Patterson peaks, there are two possible answers, differing only in the signs of the co-ordinates; they are equally correct, corresponding to different choices of the asymmetric unit within the unit cell.

This simplicity, however, conceals the fact that these are not the only possible solutions. This is because of the periodic nature of both the crystal structure and the Patterson synthesis. A Patterson peak with a co-ordinate u is entirely equivalent to another one with co-ordinate $1+u$ lying in the next unit cell. Dividing this by 2 gives a different x co-ordinate for the heavy atom, equal to $\frac{1}{2}+x$ relative to the first solution, and this is just as valid. The same applies to the other two co-ordinates y and z, so there are 8 possible solutions from the peak (u,v,w) and a further 8 from $(-u,-v,-w)$. These actually correspond to the fact that there are 8 different inversion centres in the unit cell in space group $P\bar{1}$, so there are 8 possible choices of unit cell origin, for any of which there are then two equivalent asymmetric units consisting of half a cell. In general, when any co-ordinate is obtained from a Patterson peak for two symmetry-related atoms, this ambiguity occurs and there is an arbitrary choice to be made. When only one unique heavy atom is being located, the choice is completely unimportant. With two independent atoms in the asymmetric unit this is a possible source of error, and we have to find a self-consistent solution; we shall return to this point after looking at some other space groups.

9.3.2 One heavy atom in the asymmetric unit of $P2_1/c$

This is another very common case. There are now four symmetry-equivalent heavy atoms in the unit cell, related to each other and to those in other unit cells by screw axes, glide planes, and inversion centres. The equivalent positions can be found in the International Tables, as follows.

$$(x,y,z)\quad(-x,-y,-z)\quad(x,\tfrac{1}{2}-y,\tfrac{1}{2}+z)\quad(-x,\tfrac{1}{2}+y,\tfrac{1}{2}-z).$$

Differences of all pairs of these give 16 vectors (4×4), 4 of which are the self-vector $(0,0,0)$. The (u,v,w) co-ordinates of these can be seen in Table 9.1. Each term in the body of the table is the difference between the positions given at the column and row heads; wherever $-\frac{1}{2}$ would appear, it is replaced by $\frac{1}{2}$, since this is entirely equivalent, corresponding to a shift of one unit cell along that axis. A table of this kind, showing all possible vectors between atoms in general positions, can be constructed for any space group.

Table 9.1. Vectors between general positions in $P2_1/c$.

$P2_1/c$	x,y,z	$-x,-y,-z$	$x,\frac{1}{2}-y,\frac{1}{2}+z$	$-x,\frac{1}{2}+y,\frac{1}{2}-z$
x,y,z	$0,0,0$	$-2x,-2y,-2z$	$0,\frac{1}{2}-2y,\frac{1}{2}$	$-2x,\frac{1}{2},\frac{1}{2}-2z$
$-x,-y,-z$	$2x,2y,2z$	$0,0,0$	$2x,\frac{1}{2},\frac{1}{2}+2z$	$0,\frac{1}{2}+2y,\frac{1}{2}$
$x,\frac{1}{2}-y,\frac{1}{2}+z$	$0,\frac{1}{2}+y,\frac{1}{2}$	$-2x,\frac{1}{2},\frac{1}{2}-2z$	$0,0,0$	$-2x,2y,-2z$
$-x,\frac{1}{2}+y,\frac{1}{2}-z$	$2x,\frac{1}{2},\frac{1}{2}+2z$	$0,\frac{1}{2}-2y,\frac{1}{2}$	$2x,-2y,2z$	$0,0,0$

Inspection of Table 9.1 reveals the following relationships among the 16 vectors. The self-vector $(0,0,0)$ appears four times, along the leading diagonal. There are two appearances of $(0, ½ + 2y, ½)$ and two of its centrosymmetric opposite $(0, ½ - 2y, ½)$, with the co-ordinates u and w having special values of 0 and ½, respectively. There are also two appearances each of the centrosymmetric pairs $(2x, ½, ½ + 2z)$ and $(-2x, ½, ½-2z)$, with $v = ½$. Finally there are four entries with no special values for their co-ordinates, being $(2x, 2y, 2z)$ and three symmetry-equivalents of it with some or all signs changed. The number of separate peaks observed in the Patterson map as a result, excluding the origin peak, is 8; 4 of them are double the size of the other 4, because they each consist of two coincident peaks. The arrangement of the 8 peaks satisfies the $2/m$ monoclinic Laue group symmetry, so there are in fact only 3 peaks not related to each other by the Patterson symmetry. Each row and each column of Table 9.1 gives a version of these three peaks, and this is always the case when such a table is constructed. Only one column or one row is actually needed, and is formed by subtracting any one of the space group general positions from all of the other general positions.

For any space group having rotation and/or reflection symmetry elements (including screw axes and glide planes) there will be Patterson vectors with some special co-ordinate values in the equivalent of Table 9.1, giving two or more coincident peaks (peaks of double or higher weight, as we shall designate them). They lie, therefore, in planes or lines with a concentration of Patterson peaks, and these are known as ***Harker planes*** (or ***Harker sections***) and ***Harker lines***. They are, of course, particularly easy to recognize because of their special co-ordinate values and their preponderance of large peaks. It is worth noting that they also provide a useful indication of the presence of the corresponding symmetry elements in the structure, especially when these are not unambiguously determined from systematic absences, intensity statistics and other earlier observations, so they can play a role in space group determination; peaks in the Patterson synthesis are derived from the complete data set, not just from a particular subset, so they may be more reliable than systematic absences, especially for screw axes along short unit cell edges.

In practice, the peaks observed in the Patterson synthesis are compared with those expected from Table 9.1 and possible vectors between symmetry-equivalent heavy atoms are identified. In the Harker section $(u, ½, w)$ there should be one large unique peak, from which x and z co-ordinates can be calculated, and the y co-ordinate of the heavy atom is found from the unique peak in the Harker line $(0, v, ½)$. A peak should then also be found at the position $(2x, 2y, 2z)$ to confirm the assignment. In checking this, it is again necessary to remember that adding or subtracting any multiple of ½ is allowed (the usual Patterson ambiguity), and so is changing the sign of either y, or both of x and z simultaneously (monoclinic $2/m$ symmetry). With the single heavy atom located, we now have a first model structure.

Table 9.2. Vectors between general positions in $P2_12_12_1$.

$P2_12_12_1$	x, y, z	$\frac{1}{2}+x, \frac{1}{2}-y, -z$	$\frac{1}{2}-x, -y, \frac{1}{2}+z$	$-x, \frac{1}{2}+y, \frac{1}{2}-z$
x, y, z	$0, 0, 0$	$\frac{1}{2}, \frac{1}{2}-2y, -2z$	$\frac{1}{2}-2x, -2y, \frac{1}{2}$	$-2x, \frac{1}{2}, \frac{1}{2}-2z$
$\frac{1}{2}+x, \frac{1}{2}-y, -z$	$\frac{1}{2}, \frac{1}{2}+2y, 2z$	$0, 0, 0$	$-2x, \frac{1}{2}, \frac{1}{2}+2z$	$\frac{1}{2}-2x, 2y, \frac{1}{2}$
$\frac{1}{2}-x, -y, \frac{1}{2}+z$	$\frac{1}{2}+2x, 2y, \frac{1}{2}$	$2x, \frac{1}{2}, \frac{1}{2}-2z$	$0, 0, 0$	$\frac{1}{2}, \frac{1}{2}+2y, -2z$
$-x, \frac{1}{2}+y, \frac{1}{2}-z$	$2x, \frac{1}{2}, \frac{1}{2}+2z$	$\frac{1}{2}+2x, -2y, \frac{1}{2}$	$\frac{1}{2}, \frac{1}{2}-2y, 2z$	$0, 0, 0$

9.3.3 One heavy atom in the asymmetric unit of $P2_12_12_1$

We use the same approach as for $P2_1/c$. There are four equivalent positions in the unit cell, from which Table 9.2 can be constructed. Notice that this is a non-centrosymmetric space group, so it is our first example that does not generate a vector $(2x, 2y, 2z)$.

This gives us $4 \times 4 = 16$ vectors, of which 3 are unique together with the origin peak; the Patterson symmetry is *mmm*, so any peak in a general position in the Patterson (no special co-ordinate values) would occur single-weighted in 8 equivalent positions. There are in fact none of this kind in Table 9.2; all the non-origin peaks lie on Harker sections with one special co-ordinate (u or v or $w = \frac{1}{2}$). The peaks come in sets of 4 equivalents, all of equal single weight, because each one occurs just once in the table. The first column can be taken as representative. There should, therefore, be three prominent peaks in the asymmetric unit of the Patterson map, each having one of its co-ordinates in turn equal to $\frac{1}{2}$. The peak in the $(\frac{1}{2}, v, w)$ section provides heavy atom y and z co-ordinates; $(u, \frac{1}{2}, w)$ provides x and z, and $(u, v, \frac{1}{2})$ provides x and y. Each co-ordinate is thus given twice, so we have a consistency check, allowing as usual for the possible $\pm\frac{1}{2}$ shifts and, in the orthorhombic case, for a free choice of sign for each of the co-ordinates.

9.3.4 One heavy atom in the asymmetric unit of *Pbca*

The approach is just the same as before. This time there are eight general positions in the unit cell, so we produce a table of 64 vectors, the first column of which is shown here as Table 9.3.

Table 9.3. Vectors between general positions in *Pbca*.

Pbca	x, y, z
x, y, z	$0, 0, 0$
$\frac{1}{2}+x, \frac{1}{2}-y, -z$	$\frac{1}{2}, \frac{1}{2}+2y, 2z$
$\frac{1}{2}-x, -y, \frac{1}{2}+z$	$\frac{1}{2}+2x, 2y, \frac{1}{2}$
$-x, \frac{1}{2}+y, \frac{1}{2}-z$	$2x, \frac{1}{2}, \frac{1}{2}+2z$
$-x, -y, -z$	$2x, 2y, 2z$
$\frac{1}{2}-x, \frac{1}{2}+y, z$	$\frac{1}{2}+2x, \frac{1}{2}, 0$
$\frac{1}{2}+x, y, \frac{1}{2}-z$	$\frac{1}{2}, 0, \frac{1}{2}+2z$
$x, \frac{1}{2}-y, \frac{1}{2}+z$	$0, \frac{1}{2}+2y, \frac{1}{2}$

Note that this space group can be generated from $P2_12_12_1$ by addition of an inversion centre, the glide planes being automatically produced at the same time by combination of the other symmetry operators. The symmetry of the Patterson map is still *mmm*, as for all orthorhombic structures. Thus, the first four entries in the column of vectors here are just the same as in Table 9.2, and we now add four more. Of these, one is a general vector $(2x, 2y, 2z)$ resulting from the centrosymmetry, and the other three lie on Harker lines with two special co-ordinates each. Inspection of the complete table shows that the result overall for one heavy atom in a general position in *Pbca* is as follows: a peak of weight 8 contributing to the origin peak; 6 peaks of weight 4 on Harker lines,

a symmetry-related pair on each of three lines running parallel to the three cell axes; 12 peaks of weight 2 on Harker sections, symmetry-related to each other in sets of 4; and 8 peaks of single weight in general positions, all symmetry-related by allowing all possible combinations of + and − signs on the co-ordinates. There is a large amount of redundant information from the seven peaks in the asymmetric unit of the Patterson map, from which the three co-ordinates of the heavy atom can be found and checked. A similar situation, but with different vectors in detail, arises for all primitive centrosymmetric orthorhombic space groups.

9.3.5 One heavy atom in the asymmetric unit of $P2_1$

This is another non-centrosymmetric space group, but it differs from $P2_12_12_1$ in being ***polar***. This has a particular consequence for structure solution in such space groups, which can be seen by inspection of the general positions shown, with their vectors, in Table 9.4.

Note that the heavy atom y co-ordinate does not appear in any of the vectors in this table. This is because there are no $-y$ terms in any of the space group general positions; the space group is polar along the y (or b) axis, so y disappears from all the differences. The x and z co-ordinates of a heavy atom can be obtained from the one symmetry-independent peak that should be seen in the Harker section $(u, ½, w)$, and any arbitrary value can be assigned to its y co-ordinate. The Patterson function gives no information about this co-ordinate, because none is needed.

Table 9.4. Vectors between general positions in $P2_1$.

$P2_1$	x, y, z	$-x, ½+y, -z$
x, y, z	$0, 0, 0$	$-2x, ½, -2z$
$-x, ½+y, -z$	$2x, ½, 2z$	$0, 0, 0$

9.3.6 Two heavy atoms in the asymmetric unit of $P\bar{1}$ and other space groups

Suppose we have two heavy atoms in $P\bar{1}$ with co-ordinates (x, y, z) and (X, Y, Z), together with their centrosymmetric equivalents at $(-x, -y, -z)$ and $(-X, -Y, -Z)$. These four atoms give 16 vectors as shown in Table 9.5. Here, we use a shorthand notation in which $\Sigma x = x + X$ and $\Delta x = x - X$.

Apart from the quadruple contribution to the origin peak, this gives us pairs of double-weight peaks at $\pm(\Sigma x, \Sigma y, \Sigma z)$ and at $\pm(\Delta x, \Delta y, \Delta z)$, and pairs of single-weight peaks at $\pm(2x, 2y, 2z)$ and at $\pm(2X, 2Y, 2Z)$, a total of 4 peaks in the asymmetric unit of the Patterson map, all of them with general co-ordinates. From the expected different peak sizes and the sum and difference relationships among the various peaks, it

Table 9.5. Vectors for two atoms in $P\bar{1}$.

	x, y, z	$-x, -y, -z$	X, Y, Z	$-X, -Y, -Z$
x, y, z	$0, 0, 0$	$-2x, -2y, -2z$	$-\Delta x, -\Delta y, -\Delta z$	$-\Sigma x, -\Sigma y, -\Sigma z$
$-x, -y, -z$	$2x, 2y, 2z$	$0, 0, 0$	$\Sigma x, \Sigma y, \Sigma z$	$\Delta x, \Delta y, \Delta z$
X, Y, Z	$\Delta x, \Delta y, \Delta z$	$-\Sigma x, -\Sigma y, -\Sigma z$	$0, 0, 0$	$-2X, -2Y, -2Z$
$-X, -Y, -Z$	$\Sigma x, \Sigma y, \Sigma z$	$-\Delta x, -\Delta y, -\Delta z$	$2X, 2Y, 2Z$	$0, 0, 0$

should be easy to work out which peaks are which and so generate the co-ordinates of both unique heavy atoms.

A similar procedure can be used in other space groups when there are two independent heavy atoms. It is easier (despite the larger number of peaks present overall), however, when Harker sections and lines are present, as these provide information from which the separate atoms can first be located, and the peaks in general positions can then be used to resolve the usual ambiguities and cross-check the assignments.

9.4 Patterson syntheses giving more than one possible solution, and other problems

Is it always this easy? Unfortunately not. There are a number of things that can go wrong. To illustrate one of these, go back to the example of a single heavy atom in $P2_1/c$. Suppose this has a y co-ordinate close to $\frac{1}{4}$; this is not a special position in the unit cell. The vectors in the first column of Table 9.1 are now: $(0, 0, 0)$; $(2x, \frac{1}{2}, 2z)$; $(0, 1, \frac{1}{2})$; $(2x, \frac{1}{2}, \frac{1}{2} + 2z)$. The third of these is equivalent to $(0, 0, \frac{1}{2})$. Spotting that this is just a particular case of $(0, v, \frac{1}{2})$ is not a problem, but we have two peaks in the Harker section $(u, \frac{1}{2}, w)$, one of which is a genuine Harker peak and the other is actually a general peak that lies here by chance. How do we know which is which? A Harker section peak is expected to be twice the size, but this does not help, because inspection of the full table shows that another general position is $(2x, -\frac{1}{2}, 2z)$ and this is exactly the same place as the first general position, so the peak sizes turn out to be the same. Choosing the peaks the wrong way round (Harker versus general) gives us the same x and y co-ordinates for the heavy atom as the correct choice, but a different z co-ordinate, increased or decreased by $\frac{1}{4}$. The Patterson map can thus be interpreted to give two different possible positions for the heavy atom that are not equivalent to each other. One of them will probably serve as a good enough model structure, but the other will not, giving completely incorrect phases and no further development of the structure.

Problems of this kind can arise in many space groups when heavy atoms have one or more co-ordinates close to $\frac{1}{4}$ or some other values that give general vector peaks indistinguishable from Harker peaks. This actually occurs quite often, particularly for metal co-ordination complexes, because these tend to have the metal as the heavy atom, sitting more or less in the centre of a molecule, and the packing of the molecules around symmetry elements and at regular intervals on a lattice frequently gives rational fractions as co-ordinates. Beware of Patterson solutions with co-ordinates close to 0, $\frac{1}{4}$ and $\frac{1}{2}$ for this reason; they may not be unique solutions!

Another problem can be seen from the example (e) above, where one heavy atom is found in the polar space group $P2_1$. If this single atom is used as a model structure, then this model actually has higher symmetry than $P2_1$; its space group is $P2_1/m$, with a mirror plane passing

through the heavy atom, and this is centrosymmetric instead of non-centrosymmetric. Phases calculated from the single heavy atom will all be 0 or 180°, and the resulting Fourier synthesis based on these phases with the observed amplitudes will retain the false extra symmetry, so it will probably show some features of the correct structure together with a superimposed equally strong reflected image of it. This ***pseudo-symmetry*** has to be broken by careful selection of appropriate new atoms from only one of the two images. An alternative approach is to try to find at least one extra atom from lower peaks of the Patterson map corresponding to heavy–light vectors; inclusion of this in the first model breaks the false symmetry and should make the true structure image clearer than any superimposed mirror image.

All the above examples apply to heavy atoms in ***general positions***, so that all the expected vectors appear in the Patterson maps. In many structures, especially for co-ordination complexes, heavy atoms lie in ***special positions***: on rotation axes, mirror planes, or inversion centres. Different vector tables have to be drawn up in such cases, which contain correspondingly fewer rows and columns, and one or more of the heavy atom co-ordinates will be fixed by the known positions of the symmetry elements. Although this situation should be expected in many cases, as a result of calculating the unit cell contents when the cell and space group are determined, it can be unexpected; for example, four heavy atoms per unit cell in $P2_1/c$ usually means they lie in general positions, but they may instead be on two pairs of equivalent inversion centres, with all the co-ordinates equal to 0 or ½. This will be indicated by a Patterson map with its largest non-origin peaks at positions with all co-ordinates of 0 and ½, and no large peaks anywhere else on the Harker sections and lines or in general positions.

There are pairs (and more) of space groups that can not be distinguished from systematic absences alone and for both of which a solution may be possible from a Patterson synthesis. One of the most common examples of this is the choice between the non-centrosymmetric (and polar) space group $Pna2_1$ and the centrosymmetric space group *Pnam* (conventionally taken as *Pnma*, but this involves exchanging two of the cell axes). These both have the same systematic absences. If the unit cell contains four molecules, each with one heavy atom, then these lie either in general positions in $Pna2_1$ or in special positions in *Pnam*; one of the available special positions is on the mirror plane (assuming the molecule has a shape consistent with mirror symmetry). The set of vectors expected for four heavy atoms in general positions in $Pna2_1$ is identical to that for four heavy atoms on mirror planes in *Pnam*, so the largest Patterson peaks can not be used to decide between the two possibilities. With a heavy atom present, possibly on a special position, intensity statistics are unreliable. Examination of lower Patterson peaks may help, since the centrosymmetric space group should give plenty of vectors $(0, 0, w)$ corresponding to pairs of atoms related by reflection, but often it is necessary to try developing the structure in both space

groups and see which is successful; if they both work, the higher symmetry is taken as correct, as discussed earlier in Chapter 4 on space group determination. As a general observation, heavy atoms in special positions can lead to complications in solving Patterson syntheses.

Of course, the various procedures described above for these different space groups are all closely related and they are capable of automation to some degree in computer programs. Some such programs can also deal effectively with pseudo-symmetry problems and atoms in special positions. Human interpretation of a Patterson map remains, however, often a very effective method, and a fascinating challenge. It is a pity if this skill dies out among crystallographers through over-reliance on black-box programs.

9.5 Patterson search methods

A completely different use can be made of Patterson syntheses, for which the presence of heavy atoms is not necessary. What is needed for success here is a part of the molecule for which the shape (bond lengths, angles and conformation) is either known in advance or can be confidently predicted. Examples are rigid polycyclic systems such as the four characteristic fused rings of steroids, a norbornane bicyclic nucleus as in camphor derivatives, a porphyrin, fused polycyclic aromatics, or polyhedral cages, as illustrated in Fig. 9.2. Appropriate geometry may be known from previously determined structures (including the use of the Cambridge Structural Database) or from theoretical and molecular modelling calculations.

A molecular fragment of this kind will have a characteristic pattern of vectors for all pairs of its constituent atoms. The pattern is complex and probably contains considerable overlap of vectors, but it will vary little for structures containing this particular fragment. It should

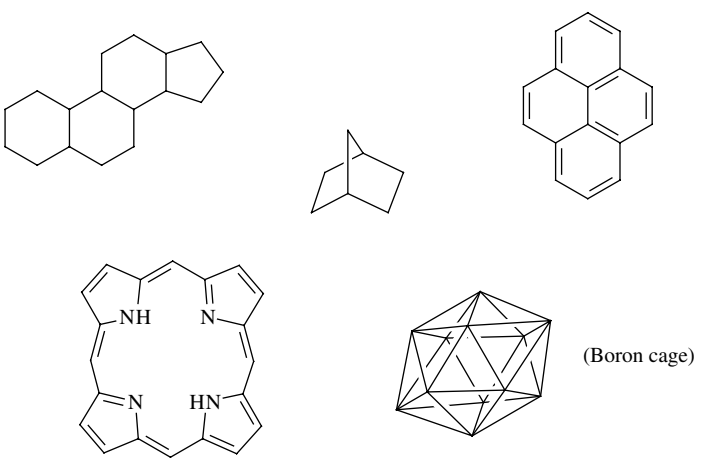

Fig. 9.2 Suitable molecular fragments for Patterson search methods.

appear, mixed up with other vectors, in the Patterson map. Finding it and deducing from it where atoms of the ***search fragment*** actually lie in the crystal structure is a pattern-matching exercise well suited to computer programming, and numerous Patterson search programs are available. The details of how they work vary considerably, they are largely automatic in operation, and they generally incorporate sophisticated extensions and variations of the basic method, but the principles are fairly simple. Two stages are involved.

9.5.1 Rotation search

This aims to find the orientation of the search fragment by matching its internal vectors to those found relatively close to the origin of the Patterson map unit cell, which contains mainly intramolecular vectors rather than intermolecular ones. Effectively, the calculated pattern of vectors for the search fragment is placed at the origin of the Patterson map and is rotated systematically in three dimensions to find the best fit to the observed vectors (large values in the Patterson function, not necessarily peak maxima, because of overlap). Various models for rotation are used, and it is not necessary to consider all possible orientations, because of symmetry in the map and in the model (this will differ from case to case). Even for a fragment with no internal symmetry and a triclinic space group, only half the total sphere of rotation needs to be searched, and this fraction reduces with higher symmetry, for example to one eighth for an orthorhombic structure. For each orientation to be tested, the values of the Patterson function at the ends of all the model vectors are examined and compared with what is expected; one simple way of doing this is to multiply together the expected and observed values at each vector end and add up the products, though there are alternative criteria. Orientations giving a large sum are good candidates for the correct orientation of the search fragment. The most promising one or a few are selected for the next stage.

9.5.2 Translation search

Except for space group $P1$, where any point can arbitrarily be chosen as the unit cell origin, it is now necessary to place the correctly oriented fragment in its right location in the unit cell, i.e. to establish its position relative to the symmetry elements. In principle (although most programs do not actually carry out the process in this way), this is done by placing the fragment successively at different points on a grid; for each position, all the symmetry equivalents are generated, intermolecular vectors (between all pairs of symmetry-related fragments) are found, and these are compared with the Patterson map in a way analogous to that used in the rotation search, but also using longer vectors. The correct position should give a high sum of products. Again, it is not necessary to search the whole unit cell, but only a fraction of it depending on the space group symmetry, and no search is needed at all along any polar

axis (e.g. all three axes in $P1$, the b-axis in $P2_1$), because the origin can be chosen arbitrarily in such directions. Positions can also be immediately discarded if they lead to impossibly short intermolecular contacts, without a full calculation.

If the search fragment constitutes a significant proportion of the total electron density of the asymmetric unit of the crystal structure, the result of this Patterson search procedure should be a model structure adequate to give reasonable approximate phases and hence develop the structure further.

Exercises

1. Generate the 4 × 4 vector table for space group $P2_1/n$. The general positions are as follows.

$$\begin{matrix} x, y, z & \tfrac{1}{2} + x, \tfrac{1}{2} - y, \tfrac{1}{2} + z \\ \tfrac{1}{2} - x, \tfrac{1}{2} + y, \tfrac{1}{2} - z & -x, -y, -z. \end{matrix}$$

2. For a compound of formula $BiBr_3(PMe_3)_2$ with $Z = 4$ in $P2_1/n$, the largest independent Patterson peaks are shown in Table 9.6. Propose co-ordinates for one Bi atom. Give the corresponding positions of the other 3 Bi atoms in the unit cell.

Table 9.6 Patterson peaks for a bismuth complex.

Peak height	Co-ordinates			Vector length (Å)
999	0.000	0.000	0.000	0.00
383	0.500	0.150	0.500	8.96
361	0.460	0.500	0.586	10.12
194	0.040	0.350	0.914	4.46

The next highest peaks in the Patterson map include some with vector lengths 2.8–3.3 Å. To what features in the molecular structure do these peaks correspond? Deduce whether the molecule is likely to be monomeric or dimeric, and give the expected co-ordination number of bismuth.

3. For a compound of formula $C_{21}H_{24}FeN_6O_3$ with $Z = 8$ in *Pbca*, the largest independent Patterson peaks are shown in Table 9.7. Propose co-ordinates for one Fe atom.

Table 9.7 Patterson peaks for an orthorhombic iron complex.

Peak height	Co-ordinates			Vector length (Å)
999	0.000	0.000	0.000	0.00
241	0.000	0.172	0.500	12.03
240	0.500	0.000	0.088	11.42
213	0.243	0.500	0.000	6.68
107	0.243	0.327	0.500	13.38
104	0.500	0.176	0.412	14.99
103	0.257	0.500	0.088	7.24
51	0.257	0.327	0.412	11.69

Table 9.8 Patterson peaks for a triclinic iron complex.

Peak height	Co-ordinates			Vector length (Å)
999	0.000	0.000	0.000	0.00
270	0.136	0.008	0.506	6.50
234	0.492	0.295	0.151	6.39
144	0.644	0.715	0.350	5.64
130	0.370	0.705	0.343	5.59

4. For a compound of formula $C_{14}H_{19}FeNO_3$ with $Z = 4$ (two molecules in the asymmetric unit) in $P\bar{1}$, the largest independent Patterson peaks are shown in Table 9.8. Propose co-ordinates for two independent Fe atoms.

This page intentionally left blank

Direct methods of crystal-structure determination

10

Peter Main

Many methods of structure determination have been termed 'direct' (e.g. Patterson function, Fourier methods) in that, under favourable circumstances, it is possible to proceed in logical steps directly from the measured X-ray intensities to a complete solution of the crystal structure. However, the term 'direct' is usually reserved for those methods that attempt to derive the structure factor phases, electron density or atomic co-ordinates by mathematical means from a single set of X-ray intensities. Of these possibilities, the determination of phases is the most important for small-molecule crystallography.

10.1 Amplitudes and phases

The importance of phases in structure determination is obvious, but it is instructive to examine their importance relative to the amplitudes. To do this, we use the convolution theorem, which is set out in Appendix A. It is not necessary to understand the mathematics in detail, but we are going to use the same relationship among the functions seen in Section A.10.

Let us regard a structure factor as the product of an amplitude $|F(\mathbf{h})|$ and a phase factor $\exp(i\phi(\mathbf{h}))$, where $\mathbf{h}$ is a reciprocal space vector, the set of three indices being represented here by a single symbol. We will call the Fourier transform of $|F(\mathbf{h})|$ the 'amplitude synthesis' and the Fourier transform of the function $\exp(i\phi(\mathbf{h}))$ the 'phase synthesis'. The convolution theorem gives:

$$\begin{array}{ccccc} |F(\mathbf{h})| & \times & \exp(i\phi(\mathbf{h})) & = & F(\mathbf{h}), \\ \Updownarrow \text{F.T.} & & \Updownarrow \text{F.T.} & & \Updownarrow \text{F.T.} \\ \textbf{amplitude synthesis} & * & \textbf{phase synthesis} & = & \textbf{electron density} \end{array} \tag{10.1}$$

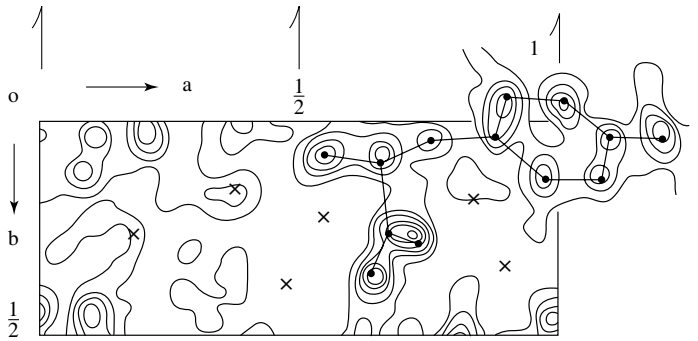

Fig. 10.1 Fourier synthesis calculated from $|F_B| \exp(i\phi A)$, where A and B are different structures. Atomic positions of structure A are marked by dots, those of B by crosses. Reprinted by permission from Macmillan Publishers Ltd: *Nature* **190**, 161, copyright 1961.

where * is the convolution operator. The amplitude synthesis must look rather like the Patterson function with a large origin peak, and its convolution with the phase synthesis will put this large peak at the site of each peak in the phase synthesis. The phase synthesis must therefore contain peaks at atomic sites for the convolution to give the electron density. It is thus the phases rather than the amplitudes that give information about atomic positions in an electron-density map. A good illustration of this was given by Ramachandran and Srinivasan (1961), who calculated an electron-density map using the phases from one structure (A) and the amplitudes from another (B). The map, in Fig. 10.1, shows the electron-density peaks corresponding to the atomic positions in structure A rather than B. Clearly, of the two problems Nature could have given us, the phase problem is much more difficult than the amplitude problem.

10.2 The physical basis of direct methods

If the amplitude and phase of a structure factor were independent quantities, direct methods could not calculate phases from observed structure amplitudes. Fortunately, structure factor amplitudes and phases are not independent, but are linked through a knowledge of the electron density. Thus, if phases are known, amplitudes can be calculated to conform to our information on the electron density and, similarly, phases can be calculated from amplitudes. If nothing at all is known about the electron density, neither phases nor amplitudes can be calculated from the other.

However, something is always known about the electron density, otherwise we could not recognize the right answer when it is obtained. Characteristics and features of the correct electron density can often be expressed as mathematical constraints on the function $\rho(\mathbf{x})$ that is to be determined. Since $\rho(\mathbf{x})$ is related to the structure factors by a Fourier transformation, constraints on the electron density impose corresponding constraints on the structure factors. Because the structure amplitudes are known, most constraints restrict the values of structure factor phases

and, in favourable cases, are sufficient to determine the phase values directly.

10.3 Constraints on the electron density

The correct electron density must always possess certain features like discrete atomic peaks (at sufficiently high resolution) and can never possess other features such as negative atoms. The electron-density constraints that may be or have been used in structure determination are set out in Table 10.1. Constraints that operate over the whole cell are generally more powerful than those that affect only a small volume.

10.3.1 Discrete atoms

The first entry in the table, that of discrete atoms, is always available, since it is the very nature of matter. To make use of this information, we remove the effects of the atomic shape from the F_o and convert them to E values, the normalized structure factors. The E values are therefore closely related to the Fourier coefficients of a point-atom structure. When they are used in the various phase-determining formulae, the effect is to strengthen the phase constraints so the electron-density map should always contain atomic peaks. The convolution theorem shows the relationships among all these quantities:

$$\begin{array}{ccccc} E(\mathbf{h}) & \times & \text{atomic scattering factor} & = & F(\mathbf{h}) \\ \Updownarrow \text{F.T.} & & \Updownarrow \text{F.T.} & & \Updownarrow \text{F.T.} \\ \text{point atom structure} & * & \text{real atom} & = & \rho(\mathbf{x}). \end{array} \tag{10.2}$$

This relationship assumes all the peaks are the same shape, which is a good approximation at atomic resolution. The deconvolution of the map to remove the peak shape can therefore be expressed as

$$|E(\mathbf{h})|^2 = |F_o(\mathbf{h})|^2 \Big/ \varepsilon_{\mathbf{h}} \sum_{i=1}^{N} f_i^2, \tag{10.3}$$

Table 10.1. Electron-density constraints.

Constraint	How Used
1. Discrete atoms	Normalized structure factors
2. $\rho(\mathbf{x}) \geq 0$	Inequality relationships
3. Random distribution of atoms	Phase relationships and tangent formula
4. $\int \rho^3(\mathbf{x}) dV = \max$	Tangent formula
5. Equal atoms	Sayre's equation
6. $-\int \rho(\mathbf{x}) \ln(\rho(\mathbf{x})/q(\mathbf{x})) \mathrm{d}V = \max$	Maximum-entropy methods
7. Equal molecules	Molecular-replacement methods
8. $\rho(\mathbf{x}) =$ constant	Density-modification techniques

where ε_h is a factor that accounts for the effect of space group symmetry on the observed intensity. If the density does not consist of atomic peaks, this operation has no proper physical meaning.

10.3.2 Non-negative electron density

The second entry in Table 10.1 expresses the impossibility of negative electron density. This gives rise to inequality relationships among structure factors, particularly those of Karle and Hauptman (1950). Expressing the electron density as the sum of a Fourier series and imposing the constraint that $\rho(\mathbf{x}) \geq 0$ leads to the requirement that the Fourier coefficients, $E(\mathbf{h})$, must satisfy

$$\begin{vmatrix} E(\mathbf{0}) & E(\mathbf{h}_1) & E(\mathbf{h}_2) & \dots & E(\mathbf{h}_n) \\ E(-\mathbf{h}_1) & E(\mathbf{0}) & E(-\mathbf{h}_1+\mathbf{h}_2) & \dots & E(-\mathbf{h}_1+\mathbf{h}_n) \\ & & \dots & & \\ E(-\mathbf{h}_n) & E(-\mathbf{h}_n+\mathbf{h}_1) & E(-\mathbf{h}_n+\mathbf{h}_2) & \dots & E(\mathbf{0}) \end{vmatrix} \geq 0. \tag{10.4}$$

The left-hand side is a Karle–Hauptman determinant, which may be of any order, and the whole expression gives the set of Karle–Hauptman inequalities. Note that the elements in any single row or column define the complete determinant. These elements may be any set of structure factors as long as they are all different. Since the normalized structure factors $E(\mathbf{h})$ and $E(-\mathbf{h})$ are complex conjugates of each other, the determinant is seen to possess Hermitian symmetry, i.e. its transpose is equal to its complex conjugate.

An example of how the inequality relationship (10.4) may restrict the values of phases is given by the order 3 determinant

$$\begin{vmatrix} E(\mathbf{0}) & E(\mathbf{h}) & E(\mathbf{k}) \\ E(-\mathbf{h}) & E(\mathbf{0}) & E(-\mathbf{h}+\mathbf{k}) \\ E(-\mathbf{k}) & E(-\mathbf{k}+\mathbf{h}) & E(\mathbf{0}) \end{vmatrix} \geq 0. \tag{10.5}$$

If the structure is centrosymmetric so that $E(-\mathbf{h}) = E(\mathbf{h})$, the expansion of the determinant gives

$$\begin{aligned} &E(\mathbf{0})[|E(\mathbf{0})|^2 - |E(\mathbf{h})|^2 - |E(\mathbf{k})|^2 - |E(\mathbf{h}-\mathbf{k})|^2] \\ &\quad + 2E(\mathbf{h})E(-\mathbf{k})E(-\mathbf{h}+\mathbf{k}) \geq 0. \end{aligned} \tag{10.6}$$

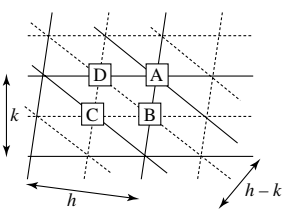

Fig. 10.2 The sign of E(–h)E(h – k)E(k)

The only term in this expression that is phase dependent is the last one on the left-hand side. Therefore, for sufficiently large *E*s, the inequality can be used to prove that the sign of $E(\mathbf{h})E(-\mathbf{k})E(-\mathbf{h}+\mathbf{k})$ must be positive.

It is instructive to see how this is expressed in terms of the electron density. Figure 10.2 shows the three sets of crystal planes corresponding to the reciprocal lattice vectors **h**, **k** and **h**–**k** drawn as full lines, the dashed lines being midway between. If the maxima of the cosine waves

Table 10.2. Signs of structure factors E(h), E(k), E(hk) when atoms are placed at the positions shown in Fig. 10.2.

Position	s(h)	s(k)	s(h–k)	s(h)s(k)s(h–k)
A	+	+	+	+
B	+	−	−	+
C	−	−	+	+
D	−	+	−	+

of the Fourier component $E(\mathbf{h})$ lie on the full lines, the minima will lie on the dashed lines and vice versa. If all three reflections $E(\mathbf{h}), E(\mathbf{k})$ and $E(\mathbf{h}–\mathbf{k})$ are strong and the electron density is to be positive, the atoms must lie in positions that are near maxima for all three components simultaneously. Examples of such positions are labelled A, B, C and D in Fig. 10.2. If most atoms in the structure are at positions of type A, $E(\mathbf{h}), E(\mathbf{k})$ and $E(\mathbf{h}–\mathbf{k})$ will all be strong and positive. If most atoms are at positions of type B, the three reflections will still be strong, but both $E(\mathbf{k})$ and $E(\mathbf{h}–\mathbf{k})$ will be negative. These results are set out in Table 10.2 together with signs obtained when most atoms are at sites of type C or D. In each case, it is seen that the product of the three signs is positive.

A useful relationship of another type can be obtained from the order 4 determinant

$$\begin{vmatrix} E(\mathbf{0}) & E(\mathbf{h}) & E(\mathbf{h}+\mathbf{k}) & E(\mathbf{h}+\mathbf{k}+\mathbf{l}) \\ E(\bar{\mathbf{h}}) & E(\mathbf{0}) & E(\mathbf{k}) & E(\mathbf{k}+\mathbf{l}) \\ E(-\mathbf{h}-\mathbf{k}) & E(-\mathbf{k}) & E(\mathbf{0}) & E(\mathbf{l}) \\ E(-\mathbf{h}-\mathbf{k}-\mathbf{l}) & E(-\mathbf{k}-\mathbf{l}) & E(\bar{\mathbf{l}}) & E(0) \end{vmatrix} \geq 0. \quad (10.7)$$

Again, for a centrosymmetric structure and under the special conditions that $|E(\mathbf{h}+\mathbf{k})| = |E(\mathbf{k}+\mathbf{l})| = 0$, the expansion of the determinant gives the mathematical form:

$$\text{terms independent of phase} - 2E(-\mathbf{h})E(-\mathbf{k})E(-\mathbf{l})E(\mathbf{h}+\mathbf{k}+\mathbf{l}) \geq 0. \quad (10.8)$$

By cyclic permutation of the indices **h**, **k** and **l**, two similar determinants can be set up. Putting $|E(\mathbf{h}+\mathbf{k})| = |E(\mathbf{k}+\mathbf{l})| = |E(\mathbf{h}+\mathbf{l})| = 0$, and with large enough amplitudes for $|E(\mathbf{h})|$, $|E(\mathbf{k})|$, $|E(\mathbf{l})|$, $|E(\mathbf{h}+\mathbf{k}+\mathbf{l})|$, these can prove that the term $E(\mathbf{h})E(\mathbf{k})E(\mathbf{l})E(-\mathbf{h}-\mathbf{k}-\mathbf{l})$ must be negative.

10.3.3 Random atomic distribution

The constraint of non-negative electron density is only capable of restricting those phases that actually make $\rho(\mathbf{x})$ negative for some $\mathbf{x}$ for some value of the phase. This will be possible if the structure factor in question represents a significant fraction of the scattering power.

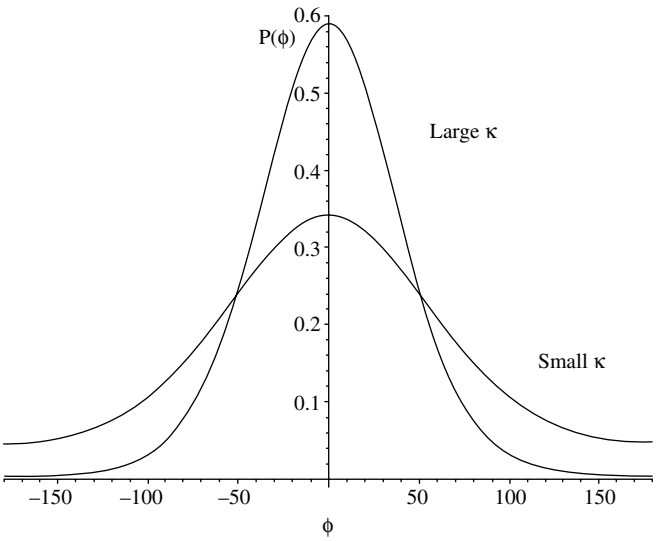

Fig. 10.3 The probability density of $\phi(\mathbf{h},\mathbf{k})$ for $\kappa(\mathbf{h},\mathbf{k}) = 2$, where $\phi(\mathbf{h},\mathbf{k}) = \phi(-\mathbf{h}) + \phi(\mathbf{h}-\mathbf{k}) + \phi(\mathbf{k})$ and $\kappa(\mathbf{h},\mathbf{k}) = 2N^{1/4}|E(-\mathbf{h})E(\mathbf{h}-\mathbf{k})E(\mathbf{k})|$.

However, this is less likely to occur the larger the structure, and a point is soon reached where no phase information can be obtained for any structure factor. A more powerful constraint is therefore required that operates on the whole of the electron density no matter what its value.

This is achieved by combining the first two constraints in Table 10.1 to produce the third entry, where the structure is assumed to consist of a random distribution of atoms. The mathematical analysis gives a probability distribution for the phases rather than merely allowed and disallowed values. The probability distribution for a non-centrosymmetric structure equivalent to the inequality (10.6) is shown in Fig. 10.3 and is expressed mathematically as

$$P(\phi(\mathbf{h},\mathbf{k})) = \frac{\exp[\kappa(\mathbf{h},\mathbf{k})\cos(\phi(\mathbf{h},\mathbf{k}))]}{2I_0(\kappa(\mathbf{h},\mathbf{k}))}, \tag{10.9}$$

where $\kappa(\mathbf{h},\mathbf{k}) = 2N^{1/4}|E(-\mathbf{h})E(\mathbf{h}-\mathbf{k})E(\mathbf{k})|$ and $\phi(\mathbf{h},\mathbf{k}) = \phi(-\mathbf{h}) + \phi(\mathbf{h}-\mathbf{k}) + \phi(\mathbf{k})$. The number of atoms in the unit cell is N and $\phi(\mathbf{h})$ is the phase of $E(\mathbf{h})$, i.e. $E(\mathbf{h}) = |E(\mathbf{h})|\exp(i\phi(\mathbf{h}))$. It can be seen that the value of $\phi(\mathbf{h},\mathbf{k})$ is more likely to be close to 0 than to π, giving rise to the phase relationship $\phi(-\mathbf{h}) + \phi(\mathbf{h}-\mathbf{k}) + \phi(\mathbf{k}) \approx 0(\textit{modulo}2\pi)$, i.e.

$$\phi(\mathbf{h}) \approx \phi(\mathbf{h}-\mathbf{k}) + \phi(\mathbf{k}), \tag{10.10}$$

where the symbol $\approx$ means 'probably equals'. The width of the distribution is controlled by the value of $\kappa(\mathbf{h},\mathbf{k})$. Large values give a narrow distribution and hence a greater likelihood that $\phi(\mathbf{h},\mathbf{k})$ is close to 0, i.e. tighter constraints on the phases.

10.3.4 Maximum value of $\int \rho^3(\mathbf{x})\mathrm{d}V$

The fourth entry in Table 10.1 is a powerful constraint. It clearly operates over the whole of the unit cell and not just over a restricted volume. It discriminates against negative density and encourages the formation of positive peaks, both expected features of the true electron density. This leads directly to probability relationships among phases and to the tangent formula, both of which have formed the basis of direct methods to the present day.

To obtain the tangent formula, the electron density in $\int \rho^3(\mathbf{x})\mathrm{d}V$ is expressed as a Fourier summation, differentiated with respect to $\phi(\mathbf{h})$ and equated to zero to obtain the maximum. A rearrangement of the result gives

$$\tan(\phi(\mathbf{h})) \approx \frac{\sum_{\mathbf{k}} |E(\mathbf{k})E(\mathbf{h}-\mathbf{k})| \sin(\phi(\mathbf{k}) + \phi(\mathbf{h}-\mathbf{k}))}{\sum_{\mathbf{k}} |E(\mathbf{k})E(\mathbf{h}-\mathbf{k})| \cos(\phi(\mathbf{k}) + \phi(\mathbf{h}-\mathbf{k}))}. \tag{10.11}$$

This is expressed more concisely and with less ambiguity as

$$\phi(h) \approx \text{ phase of } \left\{ \sum_{\mathbf{k}} E(\mathbf{k})E(\mathbf{h}-\mathbf{k}) \right\}. \tag{10.12}$$

Note that a single term in the tangent formula summation gives the phase relationship (10.10). Indeed, the tangent formula can also be derived from (10.9) by multiplying together the probability distributions with a common value of $\mathbf{h}$ and with different $\mathbf{k}$ and rearranging the result to give the most likely value of $\phi(\mathbf{h})$.

10.3.5 Equal atoms

The fifth entry in Table 10.1 has been included because of its extremely close relationship to the tangent formula in (10.11). In a large proportion of crystals, the atoms may be regarded as being equal. For example, in a crystal containing carbon, nitrogen, oxygen and hydrogen atoms only, the hydrogen atoms can be ignored and the remaining atoms are approximately equal. This constraint was used by Sayre to develop an equation that gives exact relationships among the structure factors. If the electron density is squared, it will contain equal peaks in the same positions as the original density, but the peak shapes will have changed. This is expressed in terms of structure factors as

$$F(\mathbf{h}) = \frac{\Theta(\mathbf{h})}{V} \sum_{\mathbf{k}} F(\mathbf{k})F(\mathbf{h}-\mathbf{k}), \tag{10.13}$$

where $\Theta(\mathbf{h})$ is the scattering factor of the squared atom.

Sayre's equation has had a profound influence on the development of direct methods. It is very closely related to the Karle–Hauptman

inequalities and the tangent formula mentioned earlier. It is also used as a means of phase determination and refinement for macromolecules.

10.3.6 Maximum entropy

The sixth entry in Table 10.1 gives a measure of the entropy or information content of the electron density. It operates on the whole of the electron density and completely forbids negative regions. Maximizing the entropy of the electron density is a means of dealing with incomplete information, such as missing phases. A maximum-entropy calculation produces a new map, which has made no assumptions about the missing data and is therefore an unbiased estimate of the electron density, given all available information. This very promising technique has a number of important applications in crystallography, mainly in the area of structure refinement rather than structure determination. See Chapter 11 for further information on maximum-entropy methods.

10.3.7 Equal molecules and $\rho(x) = \text{const.}$

Entries 7 and 8 in Table 10.1 have both found use in macromolecular crystallography. When the same molecule occurs more than once in the asymmetric unit of a crystal, this immediately introduces the constraint that the electron density of the two molecules should be the same. The systematic application of this constraint constitutes the standard technique of molecular replacement in macromolecular crystallography.

There is little definite structure in the solvent regions of a macromolecular crystal, making the electron density almost constant outside the molecule. This information is exploited in the solvent-flattening technique. This has been developed into a general density modification technique, which also includes Sayre's equation and other constraints and it is now in common use to improve the electron-density maps of protein molecules.

10.3.8 Structure invariants

We have seen from the inequality relationship (10.6) that electron-density constraints do not necessarily give the phases of individual structure factors. Instead, we obtain the value of a combination of phases. The same combination of phases occurs in the phase probability formula (10.9), the tangent formula (10.11) and in Sayre's equation (10.13).

The three structure factors are related such that the sum of their diffraction indices is **0** and structure-factor products that satisfy this criterion are known as structure invariants. Their special property is that the phase of the product is independent of origin position. The phase of a structure factor depends upon origin position, but its amplitude does not. Since only structure factor amplitudes feature in the phase-determining formulae, they can only define other quantities that are

independent of origin position. Hence, the phase combination must be a structure invariant. In order to determine phases for individual structure factors, both the origin and enantiomorph must be defined first.

10.3.9 Structure determination

Direct methods of structure determination have become popular because they can be fully automated and are therefore easy to use. Now that the main formulae for phase determination have been presented, it remains to see how they are used in the determination of crystal structures. Computer programs that solve crystal structures in this way are readily available, and such a program will normally carry out the following operations.

(a) Calculate normalized structure amplitudes, $|E(\mathbf{h})|$, from observed amplitudes $|F_o(\mathbf{h})|$. This is the rescaling of the F_o described in (10.3). It is normal also to use it to find the absolute scale of the Fs and produce intensity statistics as an aid to space group determination. Care must be taken in the estimation of Es for low-angle reflections.

(b) Set up phase relationships. Sets of three structure factors related as in (10.10) are identified and recorded for later use. Each such relationship is a single term in the tangent formula sum (10.11). Since this summation may be performed thousands of times, it is efficient to have all the terms already set up. In addition, 4-phase structure invariants of the type seen in (10.8) are also set up for later use.

(c) Find the reflections to be used for phase determination. The phases of only the strongest $|E|$s can be determined with acceptable accuracy. In addition, each structure factor must be present in as large a number of phase relationships as possible. These two criteria are used to choose the subset of structure factors whose phases are to be determined.

(d) Assign starting phases. In order to perform the tangent formula summation (10.11), the phases of the structure factors in the summation must be known. Initially they may be assigned random values or phases calculated from an approximate electron-density map.

(e) Phase determination and refinement. The starting phases are used in the tangent formula to determine new phase values. The process is then iterated until the phases have converged to stable values. With random starting phases, this is unlikely to yield correct phase values, so it is repeated many times as in a Monte Carlo procedure.

(f) Calculate figures of merit. Each set of phases obtained in (e) is used in the calculation of figures of merit. These are simple functions of the phases that can be calculated quickly and will give an indication of the quality of the phase set.

(g) Calculate and interpret the electron-density map. The best phase sets as indicated by the figures of merit are used to calculate electron-density maps. These are examined and interpreted in terms of the expected molecular structure by applying simple stereochemical criteria to the peaks found. Often, the best map according to the figures of merit will reveal most of the atomic positions.

10.3.10 Calculation of E values

Normalized structure amplitudes, $|E(\mathbf{h})|$s are defined in (10.3), where

$$\varepsilon_{\mathrm{h}} \sum_{i=1}^{N} f_i^2$$

is the expected intensity (also written as $\langle I \rangle$) of the **h** reflection. The best way of estimating $\langle I \rangle$ is as a spherical average of the actual intensities. In practice, the reflections are divided into ranges of $(\sin\theta)/\lambda$ and averages taken of intensity and $(\sin\theta)/\lambda$ in each range. Reflection multiplicities and also the effects of space group symmetry on intensities must be taken into account when the averages are calculated. Sampling errors can be decreased at low angles by using overlapping ranges of $(\sin\theta/\lambda)$.

Interpolation between the calculated values of $\langle I \rangle$ is aided if they can be plotted on a straight line, which is approximately true if a Wilson plot is used. Interpolation between the points on the plot can be done quite satisfactorily by fitting a curve locally to three or four points. This is repeated for different sets of points along the plot.

For best results, it is essential that the interpolated values of $\langle I \rangle$ follow the actual calculated points even if these depart greatly from a straight line. Special care must be taken in calculating Es at low angles. If these are systematically over-estimated this could easily result in failure to solve apparently simple structures. These Es are normally involved in more phase relationships than other reflections and therefore have a big influence on phase determination. The number of strong Es chosen for phase determination is normally about 4 × (number of independent atoms) + 100. More than this may be needed for triclinic or monoclinic crystals.

10.3.11 Setting up phase relationships

Care should be taken to restrict the search for phase relationships to the unique ones only. However, in space groups other than triclinic, the same relationship may be set up more than once because of the symmetry operations. Such symmetry-related relationships should be summed so that the tangent formula automatically gives the correct symmetry phase restrictions. Normally about 15 times as many phase relationships as reflections should be found. If there are fewer than 10 times as many, more can be set up by including a few extra reflections. The number of 3-phase relationships set up is roughly proportional to the cube of the number of Es used.

10.3.12 Finding reflections for phase determination

The phases of only the largest Es are usually determined and not all of these can be determined with acceptable reliability. It is therefore useful at this stage to eliminate about 10% of those reflections whose

phases are most poorly defined by the tangent formula. An estimate of the reliability of each phase is obtained from $\alpha(\mathbf{h})$:

$$\alpha(\mathbf{h}) = 2N^{-1/2}\,|E(\mathbf{h})|\left|\sum_{\mathbf{k}} E(\mathbf{k})E(\mathbf{h}-\mathbf{k})\right|. \tag{10.14}$$

The larger the value of $\alpha(\mathbf{h})$, the more reliable is the phase estimate. The relationship between $\alpha(\mathbf{h})$ and the variance of the phase, $\sigma^2(\mathbf{h})$, is given by

$$\sigma^2(\mathbf{h}) = \frac{\pi^2}{3} + 4\sum_{n=1}^{\infty}\frac{(-1)^n}{n^2}\frac{I_n(\alpha(\mathbf{h}))}{I_0(\alpha(\mathbf{h}))}, \tag{10.15}$$

and the standard deviation, $\sigma(\mathbf{h})$, is shown in Fig. 10.4. From (10.14) it can be seen that $\alpha(\mathbf{h})$ can only be calculated when the phases are known. However, an estimate of $\alpha(\mathbf{h})$ can be obtained from the known distribution of 3-phase structure invariants (10.9). A sufficiently good approximation to the estimated $\alpha(\mathbf{h})$ is given by

$$\alpha_e(\mathbf{h}) = \sum_{\mathbf{k}} K_{\mathbf{hk}}\frac{I_1(K_{\mathbf{hk}})}{I_0(K_{\mathbf{hk}})} \tag{10.16}$$

where $K_{\mathbf{hk}} = 2N^{-1/2}|E(\mathbf{h})E(\mathbf{k})E(\mathbf{h}-\mathbf{k})|$.

The reflections with the smallest values of $\alpha_e(\mathbf{h})$ can now be eliminated in turn until the desired number remain.

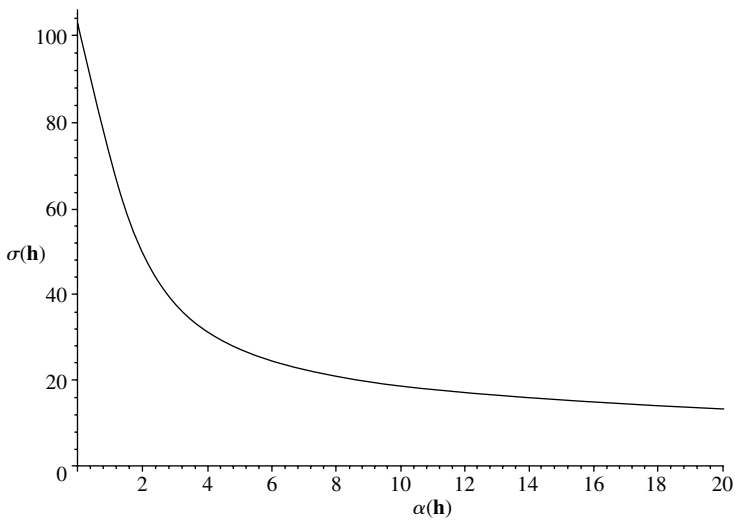

Fig. 10.4 The standard deviation of a calculated phase ($\sigma(\mathbf{h})$) as a function of $\alpha(\mathbf{h})$.

10.3.13 Assignment of starting phases

All of the phases to be determined are assigned initial random values, which also serve to define the origin and enantiomorph of the subsequent electron density. It is not expected that starting phases assigned in this way will always lead to a correct set of phases after refinement, so the procedure is repeated a number of times as in a Monte Carlo technique. The number of such phase sets is normally between 30 and 200, but many more (or fewer) may be needed for some structures. Only one of these needs to be correct (and identified) for the structure to be solved. It may sometimes help if the starting phases are calculated from a random atomic distribution or perhaps one containing parts of the molecule available from a previous calculation, thus starting closer to the correct answer than a purely random guess.

10.3.14 Phase determination and refinement

The tangent formula and associated variance (10.15) are only correct under the assumption that the phases used in the calculation are correct. This is normally far from the truth. A crude attempt at correcting for this is to weight the terms in the summation so the tangent formula becomes

$$\phi(\mathbf{h}) = \text{phase of } \sum_{\mathbf{k}} w(\mathbf{k})w(\mathbf{h}-\mathbf{k})E(\mathbf{k})E(\mathbf{h}-\mathbf{k}), \tag{10.17}$$

where $w(\mathbf{h})$ is the weight associated with $\phi(\mathbf{h})$. The correct weight is inversely proportional to the variance and, to an adequate approximation, this is proportional to $\alpha(\mathbf{h})$ defined in (10.14).

A further improvement to the tangent formula is to include additional terms whose most likely phase is π. These are the non-centrosymmetric equivalent of the relationship (10.8) and are known as 'negative quartets'. They prevent all phases from refining to zero in space groups such as $P1$ that contain no translational symmetry elements. The modified formula is

$$\phi(\mathbf{h}) = \text{phase of } \{\alpha(\mathbf{h}) - g\eta(\mathbf{h})\}, \tag{10.18}$$

with $\eta(\mathbf{h}) = N^{-1}\,|E(\mathbf{h})| \sum_{\mathbf{kl}} E(-\mathbf{k})E(-\mathbf{l})E(\mathbf{h}+\mathbf{k}+\mathbf{l})$.

$\alpha(\mathbf{h})$ is defined in (10.14) and g is an arbitrary scale factor to balance the effect of the two terms $\alpha(\mathbf{h})$ and $\eta(\mathbf{h})$. The terms in the η summation are chosen such that the amplitudes $|E(\mathbf{h}+\mathbf{k})|$, $|E(\mathbf{k}+\mathbf{l})|$ and $|E(\mathbf{h}+\mathbf{l})|$ are all extremely small or zero.

10.3.15 Figures of merit

The correct set of phases needs to be identified among the large number of incorrect phase sets. This is done by figures of merit, which are functions of the phases that can be rapidly calculated to give an indication

of their quality. Among the most useful are the following.

$$\text{(a)} \quad R_\alpha = \sum_{\mathbf{h}} |\alpha(\mathbf{h}) - \alpha_e(\mathbf{h})| \Big/ \sum_{\mathbf{h}} \alpha_e(\mathbf{h}). \tag{10.19}$$

This is a residual between the actual and the estimated α values. The correct phases should make R_α small, but so do many incorrect phase sets. This is a better discriminator against wrong phases that make R_α large.

$$\text{(b)} \quad \psi_0 = \sum_{\mathbf{h}} \left| \sum_{\mathbf{k}} E(\mathbf{k})E(\mathbf{h}-\mathbf{k}) \right| \Big/ \sum_{\mathbf{h}} \left(\sum_{\mathbf{k}} |E(\mathbf{k})E(\mathbf{h}-\mathbf{k})|^2 \right)^{1/2}. \tag{10.20}$$

The summation over $\mathbf{k}$ includes the strong Es for which phases have been determined and the indices $\mathbf{h}$ are given by those reflections for which $|E(\mathbf{h})|$ is very small. The numerator should therefore be small for the correct phases and will be much larger if the phases are systematically wrong. The denominator normalizes ψ_0 to an expected value of unity.

$$\text{(c)} \quad \text{NQUAL} = \sum_{\mathbf{h}} \alpha(\mathbf{h}).\eta(\mathbf{h}) \Big/ \sum_{\mathbf{h}} |\alpha(\mathbf{h})||\eta(\mathbf{h})|. \tag{10.21}$$

NQUAL measures the consistency between the two summations in (10.18) and should have a low value for good phases. Correct phases are expected to give a value of -1.

To enable the computer to choose the best phase sets according to the figures of merit, a combined figure of merit is normally calculated. This is a sum of the scaled versions of the separate figures of merit and is usually the best indicator of good phases.

10.3.16 Interpretation of maps

Electron-density maps are calculated using the best sets of phases as indicated by the figures of merit. The Fourier coefficients of these are normally Es rather than Fs because these are more readily available at this stage and they give sharper peaks. The slight disadvantage is that they also give a noisier background to the map. However, E-maps are usually preferred over F-maps.

Peaks in the maps should correspond to atomic positions but, because of systematic errors in the phases, there may be spurious peaks or no peaks where some atoms should be. It is normally sufficient to apply simple stereochemical criteria to identify chemically sensible molecular fragments. These may be displayed in a plot of peak positions on the least-squares plane of the molecule, from which most of the molecule will be recognized.

10.3.17 Completion of the structure

If some atoms are missing from the map, the standard method of finding them is to use Fourier refinement (see Chapter 8). Phases calculated from the known atoms are used with weighted amplitudes to obtain the next map. Usually, one or two iterations of this are sufficient to complete the structure. An alternative is to make use of all the diffraction data in Sayre's equation together with density modification to improve the map. This is normally used on macromolecular maps, but it is very successful for small molecules also. It will even convert an uninterpretable map into one in which most of the structure can be seen and the advantage is that it is all done automatically by the computer.

References

Karle, J. and Hauptman, H. (1950). *Acta Crystallogr*. **3**, 181–187.
Ramachandran, G. N. and Srinivasan, R. (1961). *Nature*, **90**, 159–161.
Robertson, J. H. (1965). *Acta Crystallogr.* **18**, 410–417.

General bibliography

Dunitz, J. D. (1995). *X-ray analysis and the structure of organic molecules.* (second corrected reprint) Verlag Helvetica Chimier Acta, Basel, Switzerland, and VCH, Weinheim, Germany.
Giacovazzo, C. (ed.) (1992). *Fundamentals of crystallography*. Oxford University Press, Oxford, UK.
Giacovazzo, C. (1998). *Direct phasing in crystallography*. Oxford University Press, Oxford, UK.
Hauptman, H. A. (1991). The phase problem of X-ray crystallography. In *Reports on Progress in Physics*, pp. 1427–1454.
Ladd, M. F. C. and Palmer, R. A. (1980). *Theory and practice of direct methods in crystallography.* Plenum, New York, USA.
Woolfson, M. M. (1987). *Acta Crystallogr*. **A43**, 593–612.
Woolfson, M. M. (1997). *An introduction to crystallography*. 2nd edn. Cambridge University Press, Cambridge, UK.

Exercises

1. Set up the order 3 Karle–Hauptman determinant for a centrosymmetric structure whose top row contains the reflections with indices **0**, **h**, and 2**h**. Hence obtain a constraint on the sign of $E(2\mathbf{h})$. What is the sign of $E(2\mathbf{h})$ if $E(\mathbf{0}) = 3$, $|E(\mathbf{h})| = |E(2\mathbf{h})| = 2$?
2. Verify (10.8). What sign information does it contain under the conditions $E(\mathbf{0}) = 3$, $|E(\mathbf{h})| = |E(2\mathbf{h})| = 2$, $|E(\mathbf{h} - \mathbf{k})| = 1$?
3. Expand the order 4 Karle–Hauptman determinant for a centrosymmetric structure whose top row contains the reflections with indices $\mathbf{0}, \mathbf{h}, \mathbf{h}+\mathbf{k}$, and $\mathbf{h}+\mathbf{k}+\mathbf{l}$ and for which $E(\mathbf{h}+\mathbf{k}) = E(\mathbf{k}+\mathbf{l}) = 0$. Interpret your expression in terms of the sign information to be obtained and under which conditions it occurs.
4. Compare the Karle–Hauptman determinants with the following reflections in the top row: $\mathbf{0}, \mathbf{h}, \mathbf{h}+\mathbf{k}, \mathbf{h}+\mathbf{k}+\mathbf{l}$; $\mathbf{0}, \mathbf{k}, \mathbf{k}+\mathbf{l}, \mathbf{k}+\mathbf{l}+\mathbf{h}$; $\mathbf{0}, \mathbf{l}, \mathbf{l}+\mathbf{h}, \mathbf{l}+\mathbf{h}+\mathbf{k}$. Summarize the sign information they contain when $E(\mathbf{h})$, $E(\mathbf{k})$, $E(\mathbf{l})$, $E(\mathbf{h}+\mathbf{k}+\mathbf{l})$ are all strong and $E(\mathbf{h}+\mathbf{k}) = E(\mathbf{k}+\mathbf{l}) = E(\mathbf{l}+\mathbf{h}) = 0$.
5. Symbolic Addition applied to a projection. Ammonium oxalate monohydrate (Robertson, 1965) gives orthorhombic crystals, $P2_12_12$, with $a = 8.017$, $b = 10.309$, $c = 3.735$ Å (at 30 K). The short c–axis projection makes this an ideal structure for study in projection, as there can be little overlap of atoms. Data for the projection have been sharpened to point atoms at rest (i.e. converted to E-values) and are shown in Fig. 10.5. Note the *mm* symmetry and the fact that data are only present for $h00$ and $0k0$ for even orders, consistent with the screw axes. Find the especially strong data 5,7; −14,5; 9,−12, which have indices summing to zero, as an example of a triple phase relationship (we omit the l index, since it is always zero for these reflections).

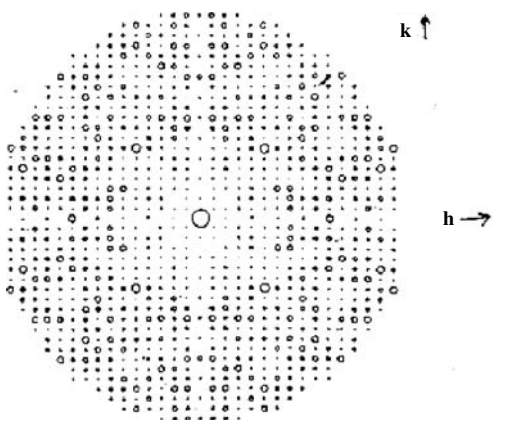

Fig. 10.5 c-Axis projection data for ammonium oxalate monohydrate.

The problem is that phases must be assigned to the structure factors before they can be added up. Since this projection is centrosymmetric, phases must be 0 or π radians (0 or 180°), i.e. E must be given a sign + or −, but there are 228 combinations of these values, and your chance of getting an interpretable map is small! Fortunately, the planes giving strong $|E|$ values are related by enough relationships to give us a unique, or almost unique, solution. The main relationship used is that for large values of $|E|$, say $|E1|$, $|E2|$ and $|E3|$ all > 1.5, if: $h1 + h2 + h3 = k1 + k2 + k3 (= l1 + l2 + l3) = 0$, then: $\phi 1 + \phi 2 + \phi \approx 0$. Additional help is given by the symmetry of the structure, illustrated in Fig. 10.6.

The plane group (two-dimensional space group) is *pgg*, with glide lines perpendicular to both axes, and there are four alternative positions for the origin: 0,0; 0,½; ½,0; and ½,½. This means that two phases may be arbitrarily fixed from any two of the parity groups g,u; u,g; or u,u (g and u mean even and odd, respectively, for the indices h and k), since, for example, shifting the origin by half a unit cell along a will shift the phase of all structure factors with h odd by π. Another result of the symmetry is that planes with indices h, k are related to $h, -k$ or $-h, k$ by the glide lines. The structure amplitudes must be the same for these, and the phases must be related, although they are not always the same. If h and k are both even or both odd, $\phi(h,k) = \phi(-h,k)$. If, however, one is odd and one even, $\phi(h,k) = \pi + \phi(-h,k)$. See the examples given for (10.23) and (10.33) in the diagrams. In other words, if we have a sign for a particular

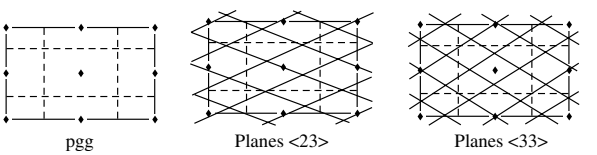

Fig. 10.6 Plane group symmetry for the ammonium oxalate monohydrate structure projection, together with two sets of lines (equivalent to planes in three dimensions).

reflection h,k and we want the sign for either $-h,k$ or $h,-k$, then we must change the sign if $h+k$ is odd, but not if $h+k$ is even. Such sign changes are marked * in the list below.

To get started, assign arbitrary signs to 5,7 and 14,5, and give 8,8 the symbol A (unknown, to be determined). Data marked * have opposite signs to those that have both indices positive. Triples are arranged from left to right and downwards in order of decreasing reliability. Note $A^2 = 1$ whatever the sign of A. For brevity, use B to stand for $-$A.

5	7	−5	7	5	7	14	5
5	−7	14	5	10	0	−9	12*
10	0	9	12	15	7	5	17
5	17	−5	7	14	−5*	5	7
5	−17	8	8	−8	8	6	−3*
10	0	3	15	6	3	11	4
−5	7	9	−12*	5	17	−5	17
6	3	−3	15	6	−3*	6	−3*
1	10	6	3	11	14	1	14
11	14	−1	14*	−1	10*	14	5
−10	0	10	0	−8	−8	−7	−2
1	14	9	14	7	2	7	3
5	7	−5	17	11	−4*	14	5
7	3	7	2	1	14	−9	14*
12	10	2	19	12	10	5	19
5	19	11	−4*	−3	15	9	9
5	−19	1	10	12	−6	−8	8
10	0	12	6	9	9	1	17
6	3	6	3	5	−7	−9	12*
6	3	7	3	13	6	1	17
12	6	13	6	8	13	10	5
−3	15	−5	7	5	−7	−7	10*
10	−5*	7	10	−2	17*	10	0
7	10	2	17	3	10	3	10
10	5	9	−9	5	19	−5	19
−9	9	−2	19*	2	−17*	13	−6*
1	14	7	10	7	2	8	13
−2	17*	−1	−10				
9	−14*	8	13				
7	3	7	3				

Determined Signs	
1	10
1	14
1	17
2	17
2	19
3	10
3	15
5	7
5	17
5	19
6	3
7	2
7	3
7	10
8	8
8	13
9	9
9	12
9	14
10	0
10	5
11	4
11	14
12	6
12	10
13	6
14	5
15	7

An introduction to maximum entropy

11

Peter Main

When crystallographers talk about maximum entropy, they are usually referring to a technique for extracting as much information as possible from incomplete data. The missing data could be structure-factor phases or perhaps some intensities where they overlap in a powder diffraction pattern. In this chapter we will look at the ideas behind the technique.

11.1 Entropy

Entropy is a concept used in thermodynamics to describe the state of order of a system. A large body of mathematics has grown up around it, and since the same mathematics occurs elsewhere in science, the vocabulary of entropy has gone with it. Apart from thermodynamics itself, the fields to benefit most from these ideas are:

1. information theory: entropy measures the amount of information in a message. The lower the entropy, the more information there is;
2. probability theory: entropy measures the change in probability upon altering the conditions under which the probability is estimated; a low value of entropy corresponds to extremes of probability;
3. image processing: entropy measures the amount of information in an image.

An increase in entropy means going from a less likely state to a more likely one. Examples of increasing entropy may be that the temperatures of two bodies become more nearly equal upon thermal contact, a message becomes slightly garbled upon transmission, or probabilities become less extreme because the information on which they are based has become outdated. In each case, you have to add something to the system to reverse the natural trend and thus decrease the entropy. Entropy naturally increases.

An illustration of this is the unlikely event portrayed in Fig. 11.1. There are many more ways of arranging lumps of wood to produce an untidy

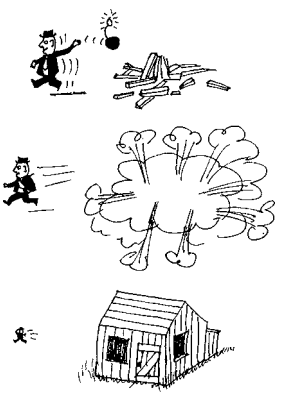

Fig. 11.1 An illustration of decreasing entropy.

pile than there are to produce a useful shed. A random rearrangement of the wood is therefore more likely to produce the high-entropy pile than the low-entropy shed.

11.2 Maximum entropy

When entropy is maximized, it implies that all information has been removed: the message tells you nothing, everything has the same probability, and the image is completely flat. This is a fairly useless state to be in, but that is not the way in which maximum entropy is used as a numerical technique.

Consider the application of maximum entropy to help form an image of a crystal structure, i.e. to produce as good an electron density map as the data will allow. Usually the data are both inaccurate (experimental error) and incomplete (low resolution, no phases, overlapped reflections), giving the possibility of an infinite number of maps that are consistent with the observed diffraction pattern.

How do you generate an acceptable map out of the infinite number of possibilities? Maximum entropy tries to do this by demanding that the map contains as little information as possible, i.e. its entropy is at a maximum, subject to the constraints imposed by the experimental data. This means that whatever information the map does contain is demanded by the data and is not there as a by-product of the numerical method or a hidden assumption. It also means that it can make no assumptions at all about the missing information and so produces as unbiased an estimate of the true map as possible.

11.2.1 Calculations with incomplete data

To illustrate how to deal with incomplete data, let us imagine we have the following information:

1. one third of all scientists make direct use of crystallographic data; let us call them crystallographers;
2. one quarter of all scientists are left-handed.

Now we pose the question: what proportion of all scientists are left-handed crystallographers?

The information given about left-handedness and crystallographic scientists is insufficient to answer the question precisely, but let us see how far we can go towards a sensible answer. The problem may be set out as in Table 11.1(a), where a is the proportion of left-handed crystallographers, d is the proportion of right-handed other scientists, and so on.

The information tells us that:

$$a + b = \frac{1}{3}; \quad a + c = \frac{1}{4}; \text{ and } a + b + c + d = 1. \tag{11.1}$$

Table 11.1. The example problem and some possible solutions.

	(a) General statement		(b) Using the information		(c) Smallest maximum		(d) Largest maximum		(e) Minimum variance		(f) Maximum entropy	
	lh	rh	lh	rh	lh	rh	lh	rh	lh	rh	lh	rh
Crystallographer	a	b	a	$1/3 - a$	0	$4/12$	$3/12$	$1/12$	$1/24$	$7/24$	$1/12$	$3/12$
Non-crystallographer	c	d	$1/4 - a$	$5/12 + a$	$3/12$	$5/12$	0	$8/12$	$5/24$	$11/24$	$2/12$	$6/12$

Using these three equations, we can eliminate b, c and d, and put everything in terms of the single variable a as in Table 11.1(b).

If we sensibly disallow a negative number of scientists, any value of a between 0 and $1/4$ will be a possible answer to the question. For example, $a = 0$ gives one extreme solution, shown in Table 11.1(c), in which there are no left-handed crystallographers at all. The other extreme is given by $a = 1/4$ (Table 11.1(d)), where all non-crystallographers are right-handed. As neither of these is very likely, we need a sensible criterion to apply to produce a plausible answer.

Let us see if it is sensible to seek a least-squares solution, i.e. find the value of a that minimizes the variance of the entries in Table 11.1(b). Such a criterion will certainly avoid the extreme solutions we have already looked at. The variance about the mean is given by:

$$V = \left(a - \frac{1}{4}\right)^2 + \left(\frac{1}{12} - a\right)^2 + a^2 + \left(\frac{1}{6} + a\right)^2, \tag{11.2}$$

and the minimum of V occurs when $\mathrm{d}V/\mathrm{d}a = 0$, giving $a = 1/24$. These results are shown in Table 11.1(e). It appears from this that $1/8$ of all crystallographers are left-handed ($1/3 \times 1/8 = 1/24$), but we see that $5/16$ of the non-crystallographers are also left-handed ($2/3 \times 5/16 = 5/24$). Why should there be this difference? The original information did not indicate this, and it seems we have made some hidden assumption that has caused it. It actually arose because of the inappropriate technique used to obtain the result; there is no good reason why all the probabilities should be as close together as possible. What we really need is a method of obtaining an unbiased estimate of the number of left-handed crystallographers. Since crystallographers are not expected to be any different from other scientists in this respect, it would be reasonable to suppose that $1/4$ of them are left-handed like the rest of the scientific population. In the absence of any further information therefore, the most plausible result should be that shown in Table 11.1(f) with $a = 1/12$.

Previously it was claimed that maximum entropy gave an unbiased estimate from incomplete data, i.e. it made no hidden assumptions about missing information. Will the maximum-entropy solution therefore correspond to our most plausible solution in Table 11.1(f)? The formula for the entropy of the quantities in Table 11.1(b) will be derived later [see (11.9)], but that does not stop us from using it here. Applying the

formula to our problem gives

$$S = -a\log(a) - \left(\frac{1}{3} - a\right)\log\left(\frac{1}{3} - a\right) + \left(\frac{1}{4} - a\right)\log\left(\frac{1}{4} - a\right) - \left(\frac{5}{12} + a\right)\log\left(\frac{5}{12} + a\right), \tag{11.3}$$

and the maximum occurs when $\mathrm{d}S/\mathrm{d}a = 0$, giving $a = 1/12$. Maximum entropy therefore does give the most plausible solution, already seen in Table 11.1(f).

11.2.2 Forming images

Maximum entropy has clearly solved the problem in a most satisfying way, but can it actually produce electron-density maps? Each array of numbers in Table 11.1 could just as easily represent an electron density map as probabilities of left-handedness among the scientific population. However, the left-handed crystallographer problem was chosen to illustrate the method because all the constraints are in the same space as the number array. With an electron-density map, information about the amplitudes is in reciprocal space. This is therefore at the wrong end of a Fourier transform as far as the map is concerned, which introduces complications in the mathematics. We have spared you this so you can see more clearly how the method works.

11.2.3 Entropy and probability

Part of the definition of entropy is that the entropy of a complicated system is the sum of the entropies of its separate parts. The state of order of a system, which is measured by entropy, has a certain probability of occurring. That is, for each value of entropy, there is a corresponding value of probability. This may be written: $S = \mathrm{f}(P)$, where S is entropy, P is probability and f is the function relating them.

Now, let us consider a system of two parts with entropies S_1 and S_2 and corresponding probabilities P_1 and P_2. If these states are independent of each other, the probability of the combined system is $P_1 \times P_2$ while its entropy is $S_1 + S_2$. That is, the entropy of the whole is

$$S = S_1 + S_2 = \mathrm{f}(P_1) + \mathrm{f}(P_2) = \mathrm{f}(P_1 \times P_2). \tag{11.4}$$

Compare this relationship with a fundamental property of logarithms that

$$\log(a) + \log(b) = \log(a \times b). \tag{11.5}$$

It is clear from this that we can write for the entropy: $S = \log(P)$ and ignore any constant factors that may multiply the log function.

11.3 Electron-density maps

If we could work out the probability of an electron-density map occurring, this would immediately give a measure of its entropy. Let us imagine building a two-dimensional map on a tray using grains of sand. The tray is divided into small boxes corresponding to the grid points at which the map is normally calculated, and the density is represented by the number of sand grains piled up in each box. Throwing the sand onto the tray at random will produce a map, though usually not a very good one. However, the number of ways in which the grains of sand can be arranged to produce the map is a measure of how likely it is to occur. If there is only one way of arranging the sand to produce the map, it will occur only very rarely with a random throw.

We now need to work out how many ways the sand can be arranged to give a particular map. Figure 11.2 shows how a one-dimensional map can be made from individual grains. Assume the sand consists of N identical grains and that the map is built up by putting in place one grain at a time. The first grain has a choice of N places to go. The next grain has $N-1$ choices, so the two together can be placed in the map in $N \times (N-1)$ different ways. The third grain has $N-2$ places to go, giving $N \times (N-1) \times (N-2)$ combinations of positions for the three grains. Thus, it can be seen that all N grains can be arranged in $N!$ ways altogether.

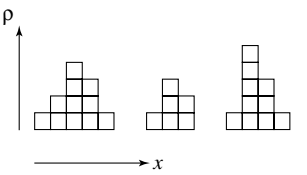

Fig. 11.2 schematic representation of a one-dimensional map.

Since the grains are identical, it does not matter how they are arranged in each box in the tray; only the *number* of grains in the box affects the shape of the map. If there are n_1 grains in the first box, they can be arranged in $n_1!$ different ways within the box without affecting the map. For example, Fig. 11.3 shows the 6 (=3!) possible arrangements of 3 grains. Therefore, the $N!$ combinations for the map must be reduced by this factor, leaving $N!/n_1!$ combinations. Each box can be treated in this way, so the final number of different combinations of position for the grains of sand is:

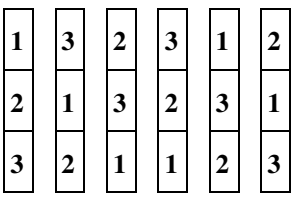

Fig. 11.3 Ways of arranging three objects in a box.

$$\frac{N!}{n_1!n_2!\cdots n_{\mathrm{m}}!}, \tag{11.6}$$

where there are m grid points in the map.

This will be proportional to the probability of occurrence of the map. We can therefore obtain a measure of the entropy, S, by taking the log of this expression:

$$S = \log\left(\frac{N!}{n_1!n_2!\cdots n_{\mathrm{m}}!}\right). \tag{11.7}$$

This is greatly simplified by making use of Stirling's approximation to the factorial of large numbers:

$$\log(N!) = N\log(N) - N. \tag{11.8}$$

Treating all the factorials in this way and remembering that $\Sigma n_i = N$ leads to the formula for the entropy of the map:

$$S = -\sum_{i=1}^{m} n_i \log(n_i). \tag{11.9}$$

If you measure electron density using electrons/Å^3 instead of counting grains of sand, the formula for entropy should be changed to

$$S = -\sum_{i=1}^{m} \rho_i \log\left(\frac{\rho_i}{q_i}\right), \tag{11.10}$$

where ρ_i is the density associated with the ith grid point and q_i is the expected density at the grid point. Initially, q_i will just be the mean density in the cell, but it can be updated as more information is obtained.

Least-squares fitting of parameters

12

Peter Main

In many scientific experiments, the experimental measurements are not the actual quantities required. Nearly always, the values of interest must be derived from those measured in the experiment. This is true in X-ray crystallography, where the atomic parameters need to be obtained from the X-ray intensities. It is this connection between parameters and experimental measurements that will be examined here.

12.1 Weighted mean

We will start with a simple situation in which only a single parameter is to be obtained, e.g. the length of a football pitch. A single measurement will not be sufficient, because it is easy to make mistakes, so we will measure it several times and take an average. Let us assume the measurements are: 86.5, 87.0, 86.1, 85.9, 86.2, 86.0, 86.4 m, giving an average of 86.3 m. How reliable is this value? Is it really close to the true value or is it just a good guess? An indication of its reliability or reproducibility is obtained by calculating the variance about the mean:

$$\sigma^2 = \frac{1}{n-1} \sum_{i=1}^{n} (x_i - \overline{x})^2, \tag{12.1}$$

where there are n measurements of value x_i whose mean is $\overline{x}$. For the measurements of the football pitch, the variance σ^2 is 0.14 m^2 and the standard deviation, σ, is about 0.4 m. For measurements that follow the Gaussian (normal) error distribution, there is a 68% chance of the true value being within one standard deviation of the derived value.

However, it may be possible to do better than this. We may know, for example, that the first two measurements were taken rather quickly and are less reliable than the others. It is sensible therefore to rely more on

the good measurements by taking a weighted average:

$$\overline{x} = \frac{\sum_{i=1}^{n} w_i x_i}{\sum_{i=1}^{n} w_i}, \tag{12.2}$$

where the weights w_i are to be defined. The weights used should be those that give us the best value for the length of the pitch. However, this depends upon how we define 'best'. A very sensible definition, and the one most often used, is to define 'best' as that value that minimizes the variance. This leads directly to making the weights inversely proportional to the variance of individual measurements, i.e. $w_i \propto 1/\sigma_i^2$ and, for independent measurements, the variance will now be

$$\sigma^2 = \frac{n}{n-1} \frac{\sum_{i=1}^{n} w_i (x_i - \overline{x})^2}{\sum_{i=1}^{n} w_i}. \tag{12.3}$$

Minimizing the sum of the squares of the deviations from the mean gives the technique its title of 'least squares'.

To apply this to the length of the pitch, we must decide on the relative reliability of the measurements. Let us say we expect the error in the first two measurements to be about three times the error in the others. Since the variance is the square of the expected error, the weights w_1 and w_2 should be $1/9$ of the other weights. Repeating the calculation using these weights gives 86.2 m for the length of the pitch with an estimated standard deviation of about 0.3 m. Notice that the estimated length has changed and that the standard deviation is smaller.

12.2 Linear regression

A common example of the determination of two parameters is the fitting of a straight line through a set of experimental points. If the equation of the line is $y = mx + c$, then the parameters are the slope, m, and the intercept, c. The experimental measurements in this case are pairs of values (x_i, y_i), which may represent, for example, the extension of a spring, y_i, due to the force x_i. Lots of measurements can be taken and, for each measurement, we can write down an ***observational equation*** $mx_i + c = y_i$. This represents a system of linear simultaneous equations in the unknown quantities m and c in that there are many more equations than unknowns. There are no values of m and c that will satisfy the equations exactly, so we seek values that satisfy the equations as well as possible, i.e. give the 'best' straight line through the points on the graph.

The residual of an observational equation is defined as $\varepsilon_i = y_i - mx_i - c$. A common definition of 'best fit' is those values of m and c that minimize $\Sigma\varepsilon_i^2$ and this gives what statisticians call the line of linear regression.

The recipe for performing the calculation is as follows. Let us write the observational equations in terms of matrices as

$$\begin{pmatrix} x_1 & 1 \\ x_2 & 1 \\ .. & . \\ x_n & 1 \end{pmatrix} \begin{pmatrix} m \\ c \end{pmatrix} = \begin{pmatrix} y_1 \\ y_2 \\ .. \\ y_n \end{pmatrix}, \tag{12.4}$$

or, more concisely, as

$$\mathbf{A}\mathbf{x} = \mathbf{b}, \tag{12.5}$$

where, with a drastic change in notation, $\mathbf{A}$ is the left-hand-side matrix containing the x values, $\mathbf{x}$ is the vector of unknowns m and c, and $\mathbf{b}$ is the right-hand-side vector containing the y values. The matrix $\mathbf{A}$ is known as the ***design matrix***. The least-squares solution of these equations is found by pre-multiplying both sides of (12.5) by the transpose of $\mathbf{A}$

$$(\mathbf{A}^{\mathrm{T}}\mathbf{A})\mathbf{x} = \mathbf{A}^{\mathrm{T}}\mathbf{b}, \tag{12.6}$$

and solving the resulting equations for $\mathbf{x}$. These are known as the normal equations of least squares, which have the same number of equations as unknowns. This is, in fact, a general recipe. The observational equations (12.5) may consist of any number of equations and unknowns. Provided there are more equations than unknowns, the least-squares solution is obtained by solving the normal equations (12.6). The least-squares solution is defined as that which minimizes the sum of the squares of the residuals of the observational equations.

The observational equations can also be given weights. As in the calculation of the weighted mean, the weights, w_i, should be inversely proportional to the (expected error)^2 of each observational equation. The error in the equation is taken as the residual, so the correct weights are $\propto$ 1/(expected residual)^2. To describe mathematically how the weights enter into the calculation, we define a ***weight matrix***, $\mathbf{W}$. It is a diagonal matrix with the weights as the diagonal elements and it pre-multiplies both sides of the observational equations (12.5), i.e.

$$\mathbf{W}\ \mathbf{A}\ \mathbf{x} = \mathbf{W}\ \mathbf{b}. \tag{12.7}$$

The normal equations of least squares are now

$$(\mathbf{A}^{\mathrm{T}}\ \mathbf{W}\ \mathbf{A})\mathbf{x} = (\mathbf{A}^{\mathrm{T}}\ \mathbf{W})\mathbf{b}, \tag{12.8}$$

which are solved for the unknown parameters $\mathbf{x}$. The weights ensure that the equations that are thought to be more accurate are satisfied more precisely. The quantity minimized is $\Sigma w_i \varepsilon_i^2$, where w_i are the diagonal elements of $\mathbf{W}$.

12.2.1 Variances and covariances

Having obtained values for m and c, we now need to know how reliable they are. That is, how do we calculate their variances? Also, since there are two parameters, we need to know their covariance, i.e. how an error in one affects the error in the other. This is important for the calculation of any quantities derived from the parameters, such as bond lengths calculated from atomic positions. If a quantity x is calculated from two parameters a and b as

$$x = \alpha a + \beta b, \tag{12.9}$$

then the variance of x is

$$\sigma_x^2 = \alpha^2\sigma_a^2 + \beta^2\sigma_b^2 + 2\alpha\beta\sigma_a\sigma_b\mu_{ab}, \tag{12.10}$$

where $\sigma_a\sigma_b\mu_{ab}$ is the covariance of a and b, and μ_{ab} is the correlation coefficient. We can calculate both variances and covariances by defining a so-called ***variance–covariance matrix***, **M**. It contains the variances as diagonal elements and the covariances as off-diagonal elements. The matrix **M** is obtained as

$$\mathbf{M} = \frac{n}{n-p}\frac{\sum_{i=1}^{n} w_i\varepsilon_i^2}{\sum_{i=1}^{n} w_i}(\mathbf{A}^{\mathrm{T}}\mathbf{W}\mathbf{A})^{-1}, \tag{12.11}$$

where $(\mathbf{A}^{\mathrm{T}}\mathbf{W}\mathbf{A})^{-1}$ is the inverse of the normal matrix of least squares and $\Sigma w\varepsilon^2/\Sigma w$ is the weighted mean (residual)^2. This is a general recipe for the case where there are n observational equations with p parameters to be derived. The quantity $n - p$ is known as the number of degrees of freedom in the equations. In the case of linear regression, $p = 2$. Notice that, as p approaches the value of n, the variances increase. If $n = p$, i.e. there are as many equations as unknowns, no estimate of variance can be made using this recipe. To make the variances as small as possible, there should be many more equations than unknowns, i.e. $n \gg p$. This means that, in crystallographic least-squares refinement, there should be many more observed reflections than parameters in the structural model.

12.2.2 Restraints

To illustrate some devices that are used in crystallographic least-squares refinement, let us see how inaccurate data can be treated in the following situation. Imagine that a totally unskilled surveyor measures the angles of a triangular field and gets the results $\alpha = 73°, \beta = 46°, \gamma = 55°$. He is so unskilled that he does not check to see if the angles add up to 180° until he gets back to the office, and by then it is too late to put things right. Can we do anything to help him? Obviously there

is no substitute for accurate measurements, but we can always try to extract the maximum amount of information from the measurements we have.

There is the additional information already alluded to, that the sum of the angles must be 180°. This information is not used in the measurement of the angles and so should help to correct the measurements in some way. If we included this as an additional equation and obtained a least-squares solution, would we get a better result? The system of equations will be:

$$\begin{aligned} \alpha &= 73^\circ \\ \beta &= 46^\circ \\ \gamma &= 55^\circ \\ \alpha + \beta + \gamma &= 180^\circ, \end{aligned} \tag{12.12}$$

and the least-squares solution is $\alpha = 74.5^\circ, \beta = 47.5^\circ, \gamma = 56.5^\circ$. The effect of using the additional information is to change the sum of the angles from its original value of 174° to a more acceptable 178.5°. This is called a ***restraint*** on the angles. Restraints are commonly used in least-squares refinement of crystal structures, such as when a group of atoms is known to be approximately planar or a particular interatomic distance is well known. Such information is included as additional observational equations. Notice that all the equations in (12.12) have the same residual of 1.5° when the least-squares solution is substituted into them.

We may be able to help our hapless surveyor even more. Upon quizzing him, it emerges that the expected error in α is probably half that of the other measurements. This allows us to apply weights to the observational equations that are inversely proportional to the variance. The restraint did not seem to be applied strongly enough either. Perhaps we would like the sum of angles to be closer to 180° than it turned out to be, so let us include the restraint with a larger weight also. The weighted observational equations now look like this:

$$\begin{pmatrix} 4 & 0 & 0 & 0 \\ 0 & 1 & 0 & 0 \\ 0 & 0 & 1 & 0 \\ 0 & 0 & 0 & 4 \end{pmatrix} \begin{pmatrix} 1 & 0 & 0 \\ 0 & 1 & 0 \\ 0 & 0 & 1 \\ 1 & 1 & 1 \end{pmatrix} \begin{pmatrix} \alpha \\ \beta \\ \gamma \end{pmatrix} = \begin{pmatrix} 4 & 0 & 0 & 0 \\ 0 & 1 & 0 & 0 \\ 0 & 0 & 1 & 0 \\ 0 & 0 & 0 & 4 \end{pmatrix} \begin{pmatrix} 73 \\ 46 \\ 55 \\ 180 \end{pmatrix}, \tag{12.13}$$

where the weight and design matrices have been written out separately. This time the least-squares solution gives $\alpha = 73.6^\circ, \beta = 48.4^\circ, \gamma = 57.4^\circ$. It is seen that the sum of the angles is closer to 180° than before, namely 179.4°, and α has moved away less from its measured value than the other angles, reflecting its greater presumed accuracy.

However, this result deserves further comment. It was stated that the expected error in α is half that of the other angles, yet its shift in value is only one quarter of the shifts applied to β and γ. Why is this? The answer lies in an unjustified assumption that was made when setting up the weight matrix. The diagonal elements are all correctly calculated as inversely proportional to the variance of the corresponding equation, but the equations were all assumed to be independent of each other, making the weight matrix diagonal. The equations are certainly not independent, since the error in α in the top equation will also appear in an identical fashion in the bottom equation. Errors in β and γ appear similarly. This is correctly dealt with by taking into account the covariances of the equations, giving rise to off-diagonal elements in the weight matrix. In crystallographic least squares this is always ignored, so it will be ignored here also.

12.2.3 Constraints

What we should have done from the very beginning is to insist that the sum of the angles is *exactly* 180°, which of course it is. Instead of using it as a restraint, which is only partially satisfied, we will now use it as a ***constraint***, which must be satisfied exactly.

There are two standard ways of applying constraints and by far the most elegant is the following. If the equations we wish to solve are expressed as

$$\mathbf{A}\mathbf{x} = \mathbf{b}, \tag{12.14}$$

and the variables $\mathbf{x}$ are subject to several linear constraints, then we can express the constraints as the equations

$$\mathbf{G}\,\mathbf{x} = \mathbf{f}. \tag{12.15}$$

In our example, the equations (12.14) are $\alpha = 73°$, $\beta = 46°$, $\gamma = 55°$ and there is only one constraint, given by the equation $\alpha + \beta + \gamma = 180°$. In the more general case, the solution of (12.14) subject to the constraints (12.15) is given by

$$\begin{pmatrix} \mathbf{A} & \mathbf{G}^T \\ \mathbf{G} & \mathbf{0} \end{pmatrix} \begin{pmatrix} \mathbf{x} \\ \boldsymbol{\lambda} \end{pmatrix} = \begin{pmatrix} \mathbf{b} \\ \mathbf{f} \end{pmatrix}, \tag{12.16}$$

where the left-hand-side matrix consists of four smaller matrices as shown, and a vector of new variables $\boldsymbol{\lambda}$ has been introduced. There is one new variable for each constraint. The technical name for these additional variables is Lagrange multipliers. These equations are now solved for $\mathbf{x}$ and $\boldsymbol{\lambda}$. Normally, the values of the λs are not required, so they can be ignored, and the $\mathbf{x}$s are now the solution of (12.14) subject to the constraints (12.15).

Let us try this on the simple example of the angles in a triangle, but this time apply the sum of the angles as a constraint. Since this is no longer a least-squares calculation (there are the same number of equations as unknowns) the square root of the previous weights must be applied, giving the equations

$$\begin{aligned} 2\alpha + \lambda &= 146^\circ \\ \beta + \lambda &= 46^\circ \\ \gamma + \lambda &= 55^\circ \\ \alpha + \beta + \gamma &= 180^\circ \end{aligned} \tag{12.17}$$

The four equations are solved for α, β, γ and λ to give $\alpha = 74.2^\circ$, $\beta = 48.4^\circ$, $\gamma = 57.4^\circ$ and $\lambda = -2.4^\circ$. It can be seen that the constraint is satisfied exactly and that the shift in the value of α is half the shifts in β and γ, as you would expect.

If there are more equations than unknowns, as is normally the case, the equations (12.16) become

$$\begin{pmatrix} \mathbf{A}^{\mathrm{T}}\mathbf{W}\mathbf{A} & \mathbf{G}^{\mathrm{T}} \\ \mathbf{G} & \mathbf{0} \end{pmatrix} \begin{pmatrix} \mathbf{x} \\ \lambda \end{pmatrix} = \begin{pmatrix} \mathbf{A}^{\mathrm{T}}\mathbf{W}\mathbf{b} \\ \mathbf{f} \end{pmatrix}, \tag{12.18}$$

where a weight matrix has also been included. You may recognize in (12.18) the normal equations of least squares along with the constraint equations.

There are more equations in (12.17) than parameters we wish to evaluate. This is always the case when constraints are applied using Lagrange multipliers. In crystallographic least-squares refinement, the number of parameters is usually large (it can easily be several thousand) and any increase in the size of the matrix by the application of constraints is avoided if possible. Normally, crystallographers use a different method of applying constraints – one that will actually decrease the size of the matrix.

In this method, the constraint equations are used to give relationships among the unknowns so that some of them can be expressed in terms of others. In general, the constraint equations may be expressed as

$$\mathbf{x} = \mathbf{C}\mathbf{y} + \mathbf{d}, \tag{12.19}$$

where $\mathbf{x}$ is the original vector of unknowns and $\mathbf{y}$ is a new set of unknowns, reduced in number by the number of independent constraints. Substituting this into (12.14) gives

$$\mathbf{A}\mathbf{C}\mathbf{y} = \mathbf{b} - \mathbf{A}\mathbf{d}, \tag{12.20}$$

from which a least-squares solution for $\mathbf{y}$ is obtained. Since there are fewer unknowns represented by the $\mathbf{y}$ vector than those in $\mathbf{x}$, this is a

smaller system of equations than we had before. The original variables **x** are then obtained from (12.19).

To illustrate this using the angles of a triangle, we can express γ in terms of α and β by the constraint $\gamma = 180 - \alpha - \beta$. We will call the reduced set of unknowns u and v such that

$$\begin{pmatrix} \alpha \\ \beta \\ \gamma \end{pmatrix} = \begin{pmatrix} 1 & 0 \\ 0 & 1 \\ -1 & -1 \end{pmatrix} \begin{pmatrix} u \\ v \end{pmatrix} + \begin{pmatrix} 0 \\ 0 \\ 180 \end{pmatrix}, \tag{12.21}$$

and substituting for α, β, γ in the observational equations gives

$$\begin{pmatrix} 1 & 0 \\ 0 & 1 \\ -1 & -1 \end{pmatrix} \begin{pmatrix} u \\ v \end{pmatrix} = \begin{pmatrix} 73 \\ 46 \\ -125 \end{pmatrix}. \tag{12.22}$$

The normal equations of least squares are

$$\begin{pmatrix} 2 & 1 \\ 1 & 2 \end{pmatrix} \begin{pmatrix} u \\ v \end{pmatrix} = \begin{pmatrix} 198 \\ 171 \end{pmatrix}, \tag{12.23}$$

which give $u = 75$, $v = 48$, so that $\alpha = 75$, $\beta = 48$ and $\gamma = 57$. No weights were used in this illustration, so all angles are shifted by the same amount and their sum is exactly 180°.

12.3 Non-linear least squares

At this point we discover that someone else in the surveyor's office has also measured the field, except he obtained the lengths of the three sides. These are $a = 21$ m, $b = 16$ m, $c = 19$ m. We can now do even better than before, because additional information is at hand. The sides are related to the angles using the sine rule. That is:

$$\frac{a}{\sin\alpha} = \frac{b}{\sin\beta} = \frac{c}{\sin\gamma}, \tag{12.24}$$

which gives additional equations that can be added to our set. The difficulty is that the new equations are non-linear and, in general, there is no direct way of solving them to obtain values of the parameters. However, we need to be able to deal with these as well, since the equations for the refinement of crystal structures are also non-linear.

Let us use the new equations first of all as restraints. That is, they are simply added to the observational equations with appropriate weights.

Our unweighted observational equations could now be:

$$\begin{aligned} 2\alpha &= 146^\circ \\ \beta &= 46^\circ \\ \gamma &= 55^\circ \\ a &= 21\,\mathrm{m} \\ b &= 16\,\mathrm{m} \\ c &= 19\,\mathrm{m} \\ a\sin\beta - b\sin\alpha &= 0\mathrm{m} \\ b\sin\gamma - c\sin\beta &= 0\mathrm{m} \\ \alpha + \beta + \gamma &= 180^\circ, \end{aligned} \tag{12.25}$$

i.e. nine equations in six unknowns. However, four of the equations give the value of an angle, while the remaining five give a length. How can you compare length measurements with angle measurements? Does it matter whether you express the angles in terms of degrees or radians? This can all be taken care of in the weights assigned to the equations. A proper weighting scheme will make the expected variance of each weighted equation numerically the same and make sure that the expected errors in the parameters all have the same effect upon the equations. However, it is unnecessary to go into such details here. The same problem arises in the refinement of crystal structures where, for example, atomic displacement parameters are determined along with atomic positional parameters. Surprisingly, not every crystallographic least-squares program does this properly.

Using the current values of the sides and angles of the triangle will not satisfy the last three equations in (12.25). Our aim is to minimize the sum of the squares of the residuals of all the equations by adjusting the values of $a, b, c, \alpha, \beta, \gamma$, thus giving the least-squares solution. Now let us see how this least-squares solution may be obtained. Let the ith non-linear equation be $f_i(x_1, x_2, \ldots, x_n) = 0$ whose jth parameter is x_j. The derivative of f_i with respect to x_j is $\partial f_i/\partial x_j$. We can set up a matrix, $\mathbf{A}$, of such derivatives so the element a_{ij} is $\partial f_i/\partial x_j$. There will be as many rows in the matrix as observational equations and as many columns as parameters. We can also calculate the residual, ε_i, of each equation using the current parameter values. The shifts $\boldsymbol{\Delta x}$ to the parameters can then be calculated from the equations $\mathbf{A}\boldsymbol{\Delta x} = -\boldsymbol{\varepsilon}$, where $\boldsymbol{\varepsilon}$ is the vector of residuals. When there are more equations than unknowns, least-squares values are obtained by solving

$$(\mathbf{A}^{\mathrm{T}}\mathbf{A})\boldsymbol{\Delta x} = -\mathbf{A}^{\mathrm{T}}\boldsymbol{\varepsilon}. \tag{12.26}$$

The shifts to the parameters are then applied to give new values

$$\mathbf{x}_{\mathrm{new}} = \mathbf{x}_{\mathrm{old}} + \boldsymbol{\Delta x}, \tag{12.27}$$

which should satisfy the observational equations better than the old values.

However, this recipe is strictly valid only for infinitesimally small shifts and is an approximation for parameter shifts of realistic size. This means the new parameter values are still only approximate and further shifts need to be calculated. A process of iteration is therefore set up, in which the latest parameter values are used to obtain new shifts and the operation is repeated until the calculated shifts are negligible.

Applying the recipe to the triangle example gives the matrix of derivatives

$$\begin{pmatrix} 1 & 0 & 0 & 0 & 0 & 0 \\ 0 & 1 & 0 & 0 & 0 & 0 \\ 0 & 0 & 1 & 0 & 0 & 0 \\ 0 & 0 & 0 & 1 & 0 & 0 \\ 0 & 0 & 0 & 0 & 1 & 0 \\ 0 & 0 & 0 & 0 & 0 & 1 \\ -b\cos\alpha & a\cos\beta & 0 & \sin\beta & -\sin\alpha & 0 \\ 0 & -c\cos\beta & b\cos\gamma & 0 & \sin\gamma & -\sin\beta \\ 1 & 1 & 1 & 0 & 0 & 0 \end{pmatrix}, \tag{12.28}$$

which is used to set up the equations for the parameter shifts.

Note that, in order to apply this method of fitting the parameters to the experimental measurements, we need to begin with approximate values that are then adjusted to improve the fit with the experimental data. There is generally no way of determining these values directly from the non-linear equations.

12.4 Ill-conditioning

You are probably very familiar with the general rule that if anything can go wrong, it will. There are many traps for the unwary in least-squares refinement, but one that everyone must know about is ill-conditioning. Consider the innocent-looking pair of equations:

$$\begin{aligned} 23.3x + 37.7y &= 14.4 \\ 8.9x + 14.4y &= 5.5. \end{aligned} \tag{12.29}$$

The exact solution is easily confirmed to be $x = -1$, $y = 1$. However, in the equations we normally deal with, the coefficients are subject to error – either experimental errors or errors in the model. Let us simulate a very small error in (12.29) by changing the right-hand side of the first equation from 14.4 to 14.39. Solving the equations this time yields the result $x = 13.4$, $y = -7.9$. The equations are, in fact, ill-conditioned and a very small change in the right-hand side has made the solution unrecognisably different. The computer will also introduce its own errors into the calculation, because it works to a limited precision. How can we

trust the solution of a system of equations ever again? We clearly need to recognize ill-conditioning when we see it.

A common way of recognizing an ill-conditioned system of equations is to calculate the determinant of the left-hand-side matrix. In this case it is -0.01. An ill-conditioned matrix always has a determinant whose value is small compared with the general size of its elements. Another, related, symptom is that the inverse matrix has very large elements. In this case, the inverse is

$$\begin{pmatrix} -1440 & 3770 \\ 890 & -2330 \end{pmatrix}. \tag{12.30}$$

Since the inverse matrix features in the formula (12.9) for calculating the variance–covariance matrix, an ill-conditioned normal matrix of least squares automatically leads to very large variances for the derived parameters.

In an extreme case, the determinant of the left-hand-side matrix may be zero. The matrix is then said to be singular and the equations no longer have a unique solution. They may have an infinite number of solutions or no solution at all. Physically, this means the equations do not contain the information required to evaluate the parameters. If the information is not there, there is no way of getting it from the equations. To make progress, it is necessary either to remove the parameters that are not defined by the observations, or to add new equations to the system so that all the parameters *are* defined. There are a number of ways of producing a singular matrix in crystallographic least-squares refinement. Easy ways are to refine parameters that should be fixed by symmetry, or to refine all atomic positional parameters in a polar space group: the symmetry does not define the origin along the polar axis, so the atomic positions in this direction can have only relative values.

12.5 Computing time

Most computing time in X-ray crystallography is spent on the least-squares refinement of the crystal structure. An appreciation of where this time goes may help crystallographers use their computing resources more efficiently.

The observational equations are mainly the structure-factor equations, e.g.

$$\left| \sum_{j=1}^{N} f_j \exp[2\pi \mathrm{i}(hx_j + ky_j + lz_j)] \right|^2 = |F_\mathrm{o}(hkl)|^2 , \tag{12.31}$$

which contain the atomic positional parameters for N atoms, and will usually also contain the atomic displacement parameters in addition to occupancy factors, scale factors etc. There will be as many equations as

observed structure factors; let this be n, with p parameters describing the structure. If the calculation proceeds by setting up the normal equations of least squares, this will be the most time-consuming part of the whole process. The matrix multiplication alone (to form $\mathbf{A}^{\mathrm{T}}\mathbf{A}$) will require about $np^2/2$ multiplication operations. With p equal to a few hundred and n equal to a few thousand, $np^2/2$ will typically be a few tens of millions ($\sim 10^7$). Efficient computer algorithms can reduce this to a few times np operations, i.e. of the order of 10^6, but it is still large.

The amount of work required to solve the normal equations is about $p^3/3$ multiplications, while it takes about p^3 multiplications to invert the matrix. Note that it is unnecessary to invert the matrix to solve the equations and so the matrix inverse should only be calculated when it is needed for the estimation of variances. Again, computer times may be reduced by using efficient algorithms, but matrix inversion will always take a lot less time than that required to set up the normal equations.

Exercises

1. Show how (12.13) was derived and verify the least-squares solution.
2. Determine the slope and intercept of the line of linear regression through the points (1, 2), (3, 3), (5, 7), giving equal weight to each point.
3. Using data from Exercise 12.2, invert the normal matrix and, from this, calculate the correlation coefficient μ_{mc} between the slope m and intercept c.
4. In the triangle problem, let the expected errors in α, β, γ be in the ratio 1:2:1.
   a) Set up the weighted observational equations for α, β, γ and include the restraint $\alpha + \beta + \gamma = 180°$ at half the weight of the equation $\alpha = 73°$.
   b) Set up the normal equations of least squares from the observational and restraint equations.
   c) Confirm that the solution of the normal equations is $\alpha = 73.6°, \beta = 48.4°, \gamma = 55.6°$.
5. In the triangle problem, let the observational equations be $\alpha = 73°$, $\beta = 46°$, $\gamma = 55°$, $a = 21\,\text{m}$, $b = 16\,\text{m}$, $c = 19\,\text{m}$, and use the two restraint equations $a^2 = b^2 + c^2 + 2bc\cos\alpha$ and $\alpha + \beta + \gamma = 180°$. Set up the matrix of derivatives needed to calculate shifts to the parameters.

This page intentionally left blank

Refinement of crystal structures

13

David Watkin

This chapter is intended to supplement the introduction to the theory of least squares given in Chapter 12, and provide crystallographic illustrations. Fourier methods (Chapter 8) provide a crucial refinement tool, especially if trial stuctures remain intransigent.

If *direct methods* are a black box, then *refinement* is a black art. There is no recipe book to deal with all situations. Difficult refinements, that is, ones where the *R*-factor does not fall as expected, or the results look anomalous, can be dealt with only by inventing strategies and trying them. An understanding of the background mathematics and physics, together with a knowledge of the literature, may enable you to use the tools provided in your software to overcome the problem.

There is a massive literature, but some selected references are given here.

Refinement on weak or problematic small molecule data using SHELXL97 (Blake, 2004).
Crystal Structure Analysis: Principles and Practice (Clegg *et al.*, 2001).
Fundamentals of Crystallography (Giacovazzo *et al.*, 2002).
Crystal Structure Refinement: A Crystallographer's Guide to SHELXL (Müller *et al.*, 2006).
The Control of Difficult Refinements (Watkin, 1994).
Current Methods and Optimisation Algorithms for the Refinement of X-ray Crystal Structures (van der Maelen, 1999).
Introduction to Macromolecular Refinement (Tronrud, 2004).

13.1 Equations

Crystal-structure analysis is built on four equations. In order to understand what is happening during refinement, and to enable you to invent ways of solving problems, it is important to understand these basics.

13.1.1 Bragg's law

$$4\sin^2\theta/\lambda^2 = h^2a^{*2}\ldots + 2klb^*c^*\cos\alpha^*. \tag{13.1}$$

Bragg's law in three dimensions. This tells us that the positions of the diffraction data in reciprocal space depend only upon the dimensions and symmetry of the unit cell. If the sample contains domains sufficiently large to cause diffraction, but randomly orientated with respect to each other, the sample is a polycrystalline powder, and the diffraction pattern will consist of randomly overlaid reciprocal lattices giving diffraction 'rings'. If the domains have simple geometric relationships between then, the sample is a twin or polytwin, and will give interpenetrating but related diffraction patterns for each component. There is generally systematic overlapping of the lattice points. If adjacent unit cells differ slightly, but the difference is periodic, the sample is modulated. Correct interpretation of the reciprocal lattice is a pre-requisite for all analyses.

13.1.2 Structure factors from the continuous electron density

$$F_{hkl} = \iiint \rho_{xyz}.e^{2\pi i(hx+ky+lz)}\partial x\,.\,\partial y.\partial z. \tag{13.2}$$

The intensity and phase of each 'reflection' in a diffraction pattern depend upon the interaction of the incident wavefront with the continuous periodic electron density throughout a mosaic block. A mosaic block is a fragment of crystal in which the alignment of the constituent unit cells is sufficiently accurate to enable interference to occur. Because diffraction is an interference phenomenon, the resulting diffracted beams have both an amplitude and a phase. Beams diffracted from adjacent mosaic blocks (or twin domains) have no rational phase relationship between them, so that the resulting intensity is just the sum of the constituent intensities. In general, the intensities can be easily measured but not the phases; their measurement requires interferometry experiments. Every point in the continuous electron density contributes to each diffracted beam (Fig. 13.1).

13.1.3 Electron density from the structure amplitude and phase

$$\rho_{xyz} = \frac{1}{V}\sum\sum\sum |F|_{hkl}\, e^{-2\pi i(hx+ky+lz-\alpha_{hkl})}\,. \tag{13.3}$$

If the intensity and phase of all the diffracted beams could be measured, then the electron density at any point in the unit cell could be computed (Fig. 13.2). Note that every reflection contributes to each point in the unit cell.

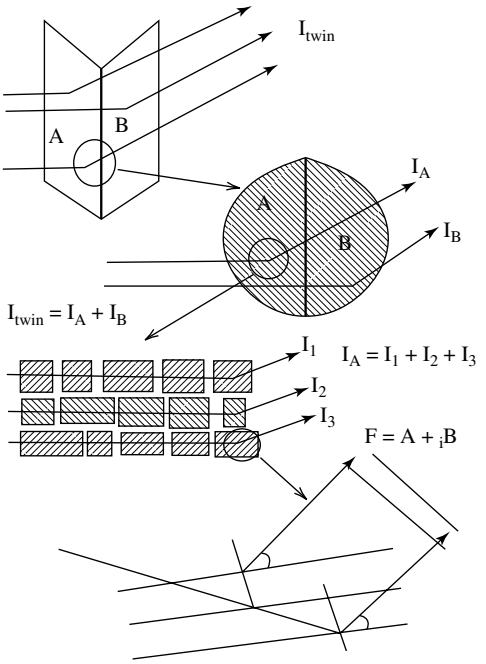

Fig. 13.1 Diffraction from crystal domains.

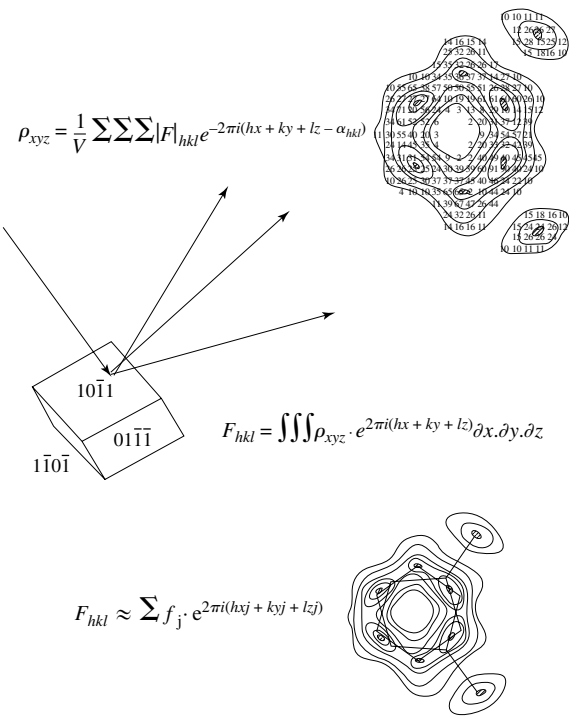

Fig. 13.2 The calculation of electron density from (13.3).

13.1.4 Structure factor from a parameterized model

$$F_{hkl} \approx \sum f_j . e^{2\pi i(hx_j+ky_j+lz_j)} . \tag{13.4}$$

The continuous electron density in a unit cell can be replaced by a parameterized model, that provides a convenient approximate representation of the true electron density. It is this model which is normally called the 'crystal structure'. Remember that X-rays do not see atoms – they see average electron density. We replace this by discrete atoms as a convenience.

13.2 Reasons for performing refinement

Refinement usually means adjustment of the values in the parameterized model according to some criteria. Both Fourier and least-squares methods are regularly applied in crystallography. Refinement is undertaken for a number of reasons, as follows.

13.2.1 To improve phasing so that computed electron density maps more closely represent the actual electron density

Commonly used variations of (13.3) are as follows.

$\boldsymbol{F = F_o, \alpha = \alpha_c}$**.** The resultant map contains features from both the observed intensities and the computed phases. It is easily demonstrated that the phases have a profound influence on the features in the map, so that their veracity is fundamental. Better phases lead to better maps, which in their turn can lead to better phases, and so on.

$\boldsymbol{F = F_o - F_c, \alpha = \alpha_c}$**.** The 'difference map'. If the structure amplitudes generated from the model lead to F_c values differing only from the observed amplitudes by their random errors, then this map will be featureless. This criterion is normally assumed to indicate that the structure has been properly parameterized, and it is assumed that, if F_c is the same as F_o, then α_c will be the same as the (unmeasured) α_o. The problem is that there are unspecified (and possibly systematic) errors in F_o. The Fourier transform of the residual $F_o - F_c$ and α_c may contain features that will enable the model to be improved. Isolated positive peaks indicate atoms missing from the model. Positive peaks adjacent to negative peaks indicate misplaced atoms, and positive or negative peaks surrounded by ripples indicate either inappropriate atomic scattering factors or inappropriate isotropic displacement parameters. Pairs of positive and negative peaks forming a 'clover leaf' indicate inappropriate anisotropic displacement parameters.

$\boldsymbol{F = 2F_o - F_c}$ ***or*** $\boldsymbol{F = 3F_o - 2F_c, \alpha = \alpha_c}$**.** Hybrid maps having properties in common with both the normal F_o map and a difference map. They reveal features from the current model, and as-yet unparameterized

features, and are commonly used in macromolecular crystallography. If the data are subject to a θ cut-off before the majority of the reflections are unobservably weak, the map will show series termination ripples with a wavelength slightly less than the resolution limit.

$\boldsymbol{F = xF_o.(1-x)E, \alpha = \alpha_c}$**.** E is the normalized structure amplitude, as used in direct methods, so that the peaks appearing in the map are accentuated. The optimal value for x is resolution dependent.

The phases, α_c, are generally obtained from the current parameterized model, which may itself have been refined by either Fourier or least-squares methods. Rarely, the computed phase may contain a contribution from the discrete Fourier transform of part of an existing map (SQUEEZE in PLATON; Spek, 2003). Interpretation of maps is the most common way of locating items missing from the parameterized model, though other forms of model building may also be applicable (addition of hydrogen atoms at their expected positions, geometric completion of other regular shapes, e.g. PF_6^- groups).

13.2.2 To try to verify that the structure is 'correct'

Because there is no way of directly and unambiguously computing the structure from the data, there is always the possibility that the proposed structure is 'wrong'. There are broadly two ways of assessing the validity of a structure.

1. From the X-ray data alone. This is the most fundamental method, and is the only one applicable to totally novel materials. It is also the most difficult method to apply. Techniques for parameter optimization that rely on fitting F_c to F_o cannot be certain that there is not another solution giving about the same goodness of fit for the amplitudes, but a better fit for the (unmeasured) phases. In addition, in reality we know little about the actual errors in the observed data, and there is the risk that over-parameterization of the model will simply result in a model that better fits the unidentified errors. In protein crystallography, where there is a very real possibility that a structure will be novel (in that there are still no reliable ways for predicting protein folding), R_{free} is used to monitor parameterization. A random subset of the data, often 10%, is excluded from the parameterization stage of the refinement, but has its value calculated whenever there is a substantial change in the modelling. If R_{free} fails to fall by a significant amount, it is probable that the change in the modelling is following noise in the data (the signal represents a common trend throughout all the data, the noise is individual to each data point, though systematic errors can be regarded as correlated noise). R_{free} is rarely used in small-molecule work since 10% of a typical data set does not contain enough reflections to give a reliable estimator.
2. From comparisons with the 'known' properties of structures. This is a Bayesian method, but requires that the analyst correctly

identify which properties are known, and what their values are. It cannot reveal if a structure is 'right', but may reveal that it is 'wrong'.

'Wrongness' comes in several forms.

(a) Correct local geometry, but the whole structure is misplaced in the cell. This phenomenon was common with early direct methods programs, and may also occur for structures solved by Patterson methods when the 'heavy' atom is not all that heavy. Symptoms include the following.
   i. The structure looks generally OK, but gives a high R factor, often as low as 20%, but failing to fall any lower.
   ii. Unusual bond lengths and adps. These rarely fall into a systematic pattern, as might be the case for refinement in a space group of too-low symmetry.
   iii. Unreasonable intermolecular contacts. Translational misplacement of a structure within a cell will generally bring it too close to a symmetry element, leading to very short non-bonded contacts.
   iv. Noisy difference maps. The difference map may be generally noisy, show some inexplicable peaks, or occasionally show ghost structural fragments.
   v. Strongly featured DIFABS map[1] or highly anisotropic R-tensors.[2] These can also be due to uncorrected systematic errors in the data, e.g. absorption, crystal decay, crystal miscentring, icing, beam inhomogeneity.

(b) Incorrect but plausible local geometry. This is relatively rare in small-molecule crystallography. The most common occurrence is generally due to disorder. Symptoms are as follows.
   i. R factor higher than anticipated, though often as deceptively low as 6–8%.
   ii. Novel molecular features. These must sometimes occur, otherwise there is little point in much structure analysis. However, if they cannot be rationalized by accepted chemical or physical reasoning, there remains the possibility that the structure is false.
   iii. Weird adps. Weird may mean unexpectedly large, small or anisotropic. Usually, if something is simply 'wrong', there is no evident relationship between the adps of adjacent atoms.
   iv. A few particularly large $F_o - F_c$ discrepancies, though the most common cause for this is some kind of failure in the data collection or pre-processing.
   v. Noisy difference maps. The maps are generally rather featureless except for a few substantial peaks, though cases are known where the maps were quite featureless even though subsequent events showed that the proposed structure was in serious error.

[1] DIFABS fits a Fourier series in polar coordinates in reciprocal space to the ratio of F_o:F_c. The value of this function can be plotted out to reveal if this ratio deviates strongly from unity in any part of reciprocal space (Walker and Stuart, 1983).

[2] The R-factor tensor is a tensor that represents the variation of local R-factor as a function of direction in reciprocal space (Parkin, 2000).

13.2.3 To obtain the 'best' values for the parameters in the model

Once the analyst is convinced that the structure is essentially correct, weighted least-squares refinement is used to optimize the parameter values.

13.3 Data quality and limitations

The quality of the data should be as high as is economically practical. Spending a little time choosing a good crystal from a mixed batch is time well spent, though it also harbours the risk that the chosen crystal is not truly representative. Spending very long times on data collection is useful only if the crystal is of excellent quality, since the signal-to-noise ratio only doubles if the counting time is increased by a factor of 4. Factors arising in data collection that can affect later refinement are as follows.

13.3.1 Resolution

With copper radiation and organic molecules, useful data can usually be measured to the instrument θ limit. With molybdenum radiation, the operator needs to use experience. If there are a few heavy elements present, they will dominate the high-angle data, and they should be measured to reduce series termination (diffraction ripple) effects. If there are only light atoms, the mean (Wilson) temperature factor B will show when reflections become indistinguishable from background. Figure 13.3 shows the variation of relative intensity as a function of Bragg angle for B values of 4 and 8.

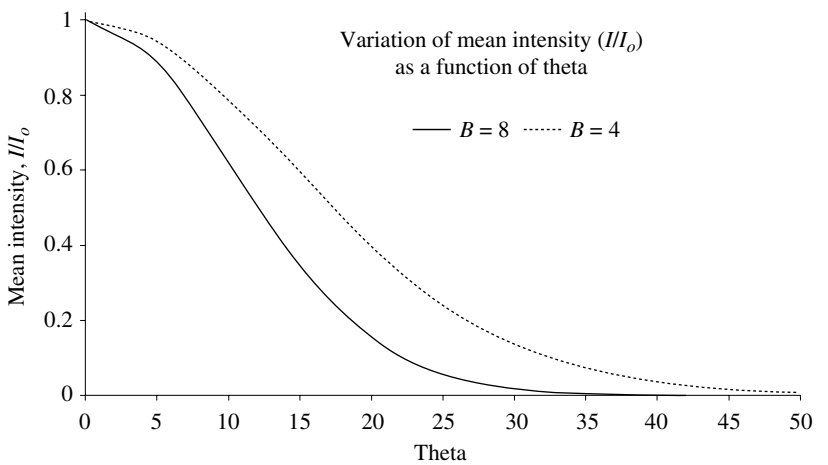

Fig. 13.3 The variation of mean intensity as a function of Bragg angle for two different B values.

Lack of properly measured high-angle data will restrict the quality of the analysis. However, if the Wilson temperature factor is unusually high, this indicates that the crystal itself is of poor quality, with substantial static or dynamic disorder. Re-collection of the data at a lower temperature should reduce dynamic disorder. Unless there is a phase change with conservation of crystallinity, struggling to work at extremely low temperatures rarely has much influence on this type of problem. The best strategy is either to try to understand the nature of the disorder, or to try growing better crystals by a different method. Simply including high-angle refections that are indistinguishable from noise into a refinement in order to achieve some required observation-to-parameter ratio is neither productive nor desirable.

13.3.2 Completeness

All kinds of refinement are to some extent sensitive to the systematic omission of substantial sections of the reciprocal lattice. Fourier methods, depending upon a summation over the whole reciprocal lattice, are most sensitive to missing reflections. Least-squares methods are more robust. Loss of data in the 'cusp' region of some diffractometers is rarely important. More serious is not collecting data to similar resolution in all directions in the asymmetric unit of reciprocal space.

13.3.3 Leverage

While all the reflections should be used to compute the electron density at any point in the unit cell, in least-squares refinement some reflections will have a particular influence on certain parameters. This effect is known as leverage. Once a structure has been approximately solved, it is possible to determine which reflections are important for which parameters. These reflections can be carefully remeasured and introduced into the refinement with appropriate weights or used as discriminators to test the effectiveness of new parameterizations.

13.3.4 Weak reflections and systematic absences

As noted above, high-angle weak reflections have very little information content. Weak lower-angle reflections can be really important, for example in deciding between a centrosymmetric or non-centrosymmetric space group. The problem is to get systematic-error-free determinations of these reflections. Programs that perform analysis of the systematic absences generally reveal that, within a given θ range, these reflections have a net positive value, i.e. are not strictly absent. Reasons for this include the Renninger effect, thermal diffuse scattering, $\lambda/2$ contamination and deviations from strict space group symmetry. These net positive values for absences suggest that all weak low-angle reflections may be systematically in error, a condition that cannot be properly handled by least-squares refinement.

13.3.5 Standard uncertainties

Even when most data were collected on serial diffractometers there were differences of opinion about the correct way to compute the standard uncertainties, particularly of the very strong and very weak reflections. With the advent of area detectors, with their very sophisticated numerical data pre-processing, the uncertainty in the uncertainty has grown. Even the massive redundancy possible with these machines creates a false sense of security (remember the parable of the Emperor of China's new robes[3]). If the errors in the individual observations are large but more or less randomly distributed about the 'true' value, then repeated measurements will yield a result approaching the true result (central limit theorem). In this case, even if $R_{\rm int}$ is large, the structure can be well refined to a reasonably trustworthy solution. If the individual observations are highly reproducible, but systematically wrong, this will lead to a low $R_{\rm int}$, but an incorrect final structure.

[3]Discussed in an article '*How precise are measurements of unit-cell dimensions from single crystals?*' (Herbstein, 2000).

13.3.6 Systematic trends

One might expect that, for a given instrument, all structures of a similar constitution would refine to about the same R value, and this is often the case. In those cases where the R value is anomalously low, we might suspect that the R factor is dominated by an anomalous feature in the structure, such as the presence of heavy atoms. In those cases where it is anomalously high, the analyst should seek an explanation. The following are possible explanations.

i. Weak data, i.e. the intensities disappear into the background at a relatively low θ angle. This can be due to static or dynamic disorder, poor crystallinity, or large solvent content.
ii. Features in the data that cannot be represented by the normal structural model. Either the experiment should be repeated, taking care to avoid these unwanted trends in the data, or some kind of 'correction' should be applied to the data to remove them. Statistically, this kind of tampering with the data is not recommended, and the statistician would prefer the model to be extended to reflect these perturbations in the data. In practice, it turns out that the tinkering works reasonably well (e.g. empirical absorption corrections, SADABS-, DIFABS- and SORTAV-like procedures).

13.4 Refinement fundamentals

For the bulk of small-molecule structures, refinement means some process related to least squares. The process seeks to minimize some function

$$M = \sum w(Y_1 - Y_2)^2. \tag{13.5}$$

13.4.1 w, the weight

For a statistically well-understood problem, it can be shown that, for uncorrelated errors in the observations, the optimal parameter values and their standard uncertainties are obtained when the weight is equal to the inverse of the variance of the observation. In crystallography, we are by no means certain about the distribution of the errors in our observations, nor can we be certain that our model is capable of fully explaining the observations; for example, there may be systematic errors in the data that should be accounted for by additional parameters in the model. Weights are now usually chosen to satisfy the criterion that there is no appreciable trend in M for any rational ranking of the data. This enables the weights to reflect errors in both the data and the model, and leads to optimal parameter values and s.u.s **for that model**. Computing these model-dependent weights when the model is substantially incorrect may lead to the error being concealed. It is therefore recommended that purely statistical or modified unit weights be used in the early stages. Note that unit weights are robust for F_o refinement, and should be replaced by $(1/2F)$ or $1/\sigma^2(F_o^2)$ for F_o^2 refinement. Note also that the assumption that the errors in observations are uncorrelated is generally unfounded, though no widely available single-crystal programs use the full data variance-covariance matrix.

Omission of data according to some s.u. threshold is a brutal way of down-weighting (to zero!) the weak reflections, and in principle cannot be justified. However, there is little justification either in including hundreds of high-angle data that are indistinguishable from noise. An appropriate θ cut-off is more acceptable than an $I/\sigma(I)$ cut-off. The small numbers of weak reflections remaining in the refinement, even if positively biased as explained above, probably do little harm, and may even be required for some kinds of analysis.

Weighting schemes can be modified in various ways to accelerate convergence, to reduce the influence of outliers, or to enhance some feature of the structure.

13.4.2 Y_1, the observations

The community is still divided as to whether Y_1 should be F_o, F_o^2 or I. The debate is finely balanced, and in practice perfectly acceptable results are obtained whichever representation is used. Traditional nomenclature, in which the structure factor is written $|F_o|$, has added to the confusion. The moduli signs were introduced to remind the reader that one can measure only the magnitude of the diffracted beam but not the phase. It has nothing to do with taking the square root of F^2. Negative F values are permitted in least-squares refinement. The application of a non-linear transformation (taking the square root) to the data raises several issues.

Rollett and Prince have independently shown that, with appropriate weighting, both F and F^2 refinements yield the same parameters and s.u.s.

Non-linear transformations of the data lead to a skewing of the error distribution. For medium and strong reflections, a $1/2F$ term successfully accommodates this, but there is an evident problem if F is ≤ 0. In the absence of a proper knowledge of the error distribution in F^2 for weak reflections, an approximate value has to be estimated for the s.u. of F_o.

Why was refinement against F_o ever introduced? Transformation of data or variables is a technique commonly used to improve the numerical stability of a calculation, which would certainly have been an issue before digital computers. In the case of transformation from F^2 to F, except for very small reflections, unit weights are close to the optimal weighting, again an advantage before computers. Neither of these considerations is important now for routine work, though F refinement remains resistant to the effects of outliers (especially partially occluded observations), particularly among the strong reflections.

Although the minima for both refinements should be the same, the paths from a given starting model will be different. There are suggestions that F^2 refinement is less influenced by false minima, but I have only seen contrived artificial examples of this.

Contrary to common belief, for the software user F^2 refinement has no advantage over F_o refinement for either determining the Flack parameter, or treating twinned data. The programmer has a little more work to do in the case of F_o refinement.

Note that the F versus F^2 debate is quite independent of the debate about the inclusion/exclusion of weak reflections.

13.4.3 Y_2, the calculations

This is generally F_c or F_c^2 to match Y_1. In maximum-likelihood refinement, the following function is minimized:

$$M = \sum \frac{1}{\sigma^2_{\mathrm{ML}}} (F_o - \langle F_o \rangle)^2. \tag{13.6}$$

$\langle F_o \rangle$ is the expected value of F_o, and is a modified form of F_c. It is intended to include a contribution to the minimization function due to the uncertainty in the phase angle, and seems to be particularly useful in protein crystallography, where the models rarely achieve the same resolution as those for small molecules. As the model improves, $\langle F_o \rangle$ approaches F_c, and such is the power of modern direct methods programs that it is generally believed that initial structures are so good that maximum-likelihood methods have little to offer small-molecule crystallographers. $1/\sigma_{ML}$ is a special weighting function. Maximum likelihood may have some role in cases of pseudo-centred cells, where a very large percentage of the data is systematically weak. Edwards (1992) has shown that maximum-likelihood least squares is unaffected by the F^2 to F transformation.

13.4.4 Issues

During least-squares refinement, (13.7) is solved. There are some important things to notice.

i. The observations of restraint are handled in the same way as the X-ray observations.
ii. The matrix of constraint is applied to the whole matrix of derivatives, so will override any conflicting restraints.
iii. The shift-limiting restraints are included as equations in the matrix work – they influence the terms in the matrix, and hence its numerical processing.

$$\delta_{x_{applied}} = P.(M'.A'.W.A.M)^{-1}.M'.A'.W.\Delta Y$$

$$A = \begin{pmatrix} \frac{\partial F_o/\partial x}{\partial R_t/\partial x} \\ 1 \end{pmatrix} \quad \begin{array}{l} A \text{ is the matrix of derivatives} \\ R_t \text{ is a restraint target value} \end{array}$$

$$\Delta Y = \begin{pmatrix} \frac{F_o - F_c}{R_t - R_c} \\ 0.0 \end{pmatrix} \quad \Delta Y \text{ is the vector of residuals}$$

$$\Delta_{x_{applied}} = P.\delta_{x_{leastsquares}} \quad P \text{ is the matrix of partial shifts}$$

$$x_{physical} = M.x_{leastsquares} + c \quad \begin{array}{l} M \text{ is the matrix of constraint} \\ c \text{ is a vector of constants.} \end{array}$$

(13.7)

iv. The matrix of partial shifts is applied after the matrix inversion, and so cannot help in the control of singularities.
v. The terms in the design matrix do not involve the values of the observations, only terms computed from the current model. If the model is seriously wrong, these terms will also be seriously wrong.
vi. The vector of residuals involves both the actual observations and values calculated from the model. If the values of F_c are hopelessly wrong, these residuals will drive the refinement towards a false minimum.

13.5 Refinement strategies

If there were a known, single, reproducible refinement strategy, it would have been programmed long ago. In the 1970s it was hoped that such a strategy was on the point of being discovered. Now, 30 years later, computerized strategies do exist for the processing of good-quality data from well-behaved structures, but there is an ever-growing number of structures requiring some kind of human insight and intervention. If a structure does not develop and refine in the normal way, some

possible actions are listed below. A refinement 'blows up' when the R factor begins to rise uncontrollably, or the displacement parameters take on nonsensical values, or massive parameter shifts make the structure unrecognizable. At later stages, it can also mean that the extinction parameter or some displacement parameters have gone substantially negative.

The crucial thing to remember about refinement is that both Fourier and least-squares methods have limited ranges of convergence. Both (13.3) and (13.7) involve the current model. The better the current model, the greater the chance of computing reliable estimates of changes to make to the parameters. In difficult cases, model development should be undertaken cautiously, with non-crystallographic information used to hold parameters at sensible values. Many cases are known where the structure solution was difficult, yet for which the final fully parameterized model refined quite stably. Exclusion of valid atoms is generally less harmful than inclusion of false ones, and in any case the valid atoms generally reappear in subsequent maps.

i. If the direct methods solution does not appear to reveal the structure, try changing some of the initial parameters, or try changing program. If SIRxx initially shows a promising structure, which falls to pieces during the automatic refinement, turn off the refinement and process the initial solution manually. Note that very poor data or data with systematic errors can yield an interpretable E-map that may never refine well.
ii. If the direct methods give a reasonable figure of merit but the structure looks wrong, try alternative programs for assembling molecules. Molecule assembly routines are affected in different ways by missing or spurious peaks. If this fails, compute a packing diagram and set the bonding criteria to a little more than their usual values. Packing diagrams are especially useful if the molecule straddles symmetry elements. A chemist, knowing what to look for, may spot molecular fragments amongst a jumble of spurious peaks.
iii. If the structure is plausible overall, but 'blows up' on normal refinement, try Fourier refinement. For Fourier refinement it is best to omit really dubious atoms from the model used to compute phases.
iv. If the main features are recognizable, use geometric model building to regularize the molecular parameter values (bonds, angles, planarity).
v. Least squares can be used to identify potentially spurious atoms. A few cycles of refinement of $U_{\rm iso}$ (with fixed x, y, z) may reveal spurious atoms as those with very high values.
vi. Least squares has no mechanism for introducing new atoms. This can be done only by Fourier methods or model building. $2F_{\rm o} - F_{\rm c}$ or $3F_{\rm o} - 2F_{\rm c}$ maps are often the easiest to interpret.
vii. If the model persists in blowing up, try increasing the effect of shift-limiting restraints. Fix the isotropic displacement parameters

at something a little below the Wilson prediction, and refine only the positions.

13.6 Under- and over-parameterization[4]

[4]Protein crystallographers often call over-parameterization 'over-fitting' or 'over-refinement'.

There is no a priori reason for believing that a given data set will adequately define any particular crystallographic parameter, though there are general trends. Set the worst-behaved parameters to reasonable values while you sort out the well-behaved ones.

Most well-behaved parameters are higher up this list:

i. unit cell
ii. space group
iii. atom positions
iv. U_{iso}
v. U_{aniso}
vi. extinction
vii. Flack parameter
viii. hydrogen atom parameters
ix. static disorder
x. mixed site occupancy

with the least-well behaved towards the bottom.

13.6.1 Under-parameterization

If important features are omitted from the model, then the remaining parameters will refine to values that try to compensate for these omissions.

The following are some examples.

i. The simplest form of under-parameterization is the omission of hydrogen atoms from organic structures. Individually they have only a small local effect, but if they are numerous, they can have a noticeable effect on the low-angle reflections, and hence on the scaling and displacement parameters. Quite approximate estimates of their positions are adequate unless the analysis has a special interest in hydrogen atoms, but many analysts are over-occupied with details of their placement.
ii. The use of isotropic adps (because of a 'shortage' of data) for residues that are clearly subject to anisotropic libration. A group adp would be a better approximation, or individual anisotropic adps plus copious appropriate adp restraints.
iii. Omission of disordered solvent. It is very rare to find an empty void in a crystal structure, but there is no reason why disordered solvent should be modelled only by partial atoms. This is a convenient model if the disorder can be rationalized, but in other cases

it may be more sensible to use models based on continuous electron distributions, or to use the discrete Fourier transform of the 'electron density' appearing in F_o maps in this region.

13.6.2 Over-parameterization

If the model is made too complex to be supported by the information contained in the X-ray data, then some parameters may refine to inappropriate values. The indeterminacy may not be concentrated in certain specific parameters, but may be distributed over a combination of parameters. Eigenvalue analysis of the normal equations should reveal this.

Here are some examples:

i. refinement of individual adps without restraints when there is a shortage of good data;
ii. refinement of the Flack parameter when the anomalous differences cannot be discerned;
iii. refinement of occupancy factors for chemically mixed sites in the absence of high-quality high-angle data.

Some analysts (and some journals!) like to use the ratio (number of observations):(number of parameters) as a measure of over/under-parameterization. This is very naive, since it takes no account of the information content or precision of the data. Dumping hundreds of unobserved high-angle data into a refinement will improve this ratio, but have no useful influence on the analysis. For non-centrosymmetric space groups it is valid to keep Friedel pairs separate if there is detectable anomalous scattering, but for most all-light atom structures with Mo radiation, it is purely cosmetic.

The 'goodness of fit', S, would be a good measure of parameterization if the weight were the inverse of the variance of the observation, but in general the weights are adjusted, and it is usual to get an S value of about 1 anyway. Note that scaling all the weights by the same factor to give an S of unity has no effect at all on the refined parameters (13.7).

$$S^2 = \Sigma(w\Delta^2)/(n-m) \tag{13.8}$$

13.7 Pseudo-symmetry, wrong space groups and $Z' > 1$ structures

Most structures contain some local non-crystallographic symmetry (e.g. phenyl groups). This is rarely harmful, and can sometimes be used as the basis for equations of restraint. More troublesome is the situation in which the pseudo-symmetry affects almost the whole of the structure. This situation is commonly found in structures with $Z' > 1$, when the independent molecules are related by the pseudo-symmetry

operator. The two most troublesome pseudo-operators are a false centre of symmetry, and a false translation of about ½ parallel to a cell axis. Both cases lead to normal matrices showing high correlation between pairs of parameters. For the pseudo-centre, the refinements often seem to proceed satisfactorily, and it is only at the evaluation stage that the problems become evident. Symptoms are adps for equivalent atoms unsatisfactory in complementary ways (e.g. one set large, the other small) and bond lengths are similarly unsatisfactory. Pseudo-translational symmetry is even more pernicious, since it leads to 50% of the data being systematically weak. The situation can generally be controlled by restraints or constraints.

There are pairs of space groups that are indistinguishable from the systematic absences alone, e.g. *Pnma* and $Pn2_1a$. Occasionally the structures will not solve in the centrosymmetric space group, but solve easily in the non-centrosymmetric group.[5] Unless one has good reason to expect the formation of a chiral crystal structure, the structure should be reviewed carefully. Symptoms that the space group symmetry is too low are as in (i) above.

[5]This is especially true for $P1/P\bar{1}$, where truly centrosymmetric structures may solve only in $P1$. The analyst then simply has to apply suitable translations to put the latent centre of symmetry at the origin, and change the space group back to $P\bar{1}$.

13.8 Conclusion

Refinement in the sense of both choosing what parameters to optimize, and obtaining the best parameter values, is frequently a tedious and a not very cost-effective procedure. Much more time can be spent fiddling about with a disordered side chain or solvent than was spent in determining the gross structure. Before getting too involved in this unrewarding task, make an effort to try to display and carefully look at the electron density in the problematic region. It may be that there is no useful atomic parameterization for the time and space averaging that occurred during the experiment. If the issue is really important, look for a better crystal, handle it carefully, cool it slowly to the lowest temperature you can achieve, and take care to optimize the data collection and pre-processing.

References

Blake, A. J. (2004). *IUCr Computing Commission Newsletter* **4**, ed. Cranswick, L. http://journals.iucr.org/iucr-top/comm/ccom/newsletters/2004aug/index.html

Clegg, W., Blake, A. J., Gould, R. O. and Main, P. (2001). *Crystal structure analysis: principles and practice*. Oxford University Press, Oxford, UK.

Edwards, A. W. F. (1992). *Likelihood*. Johns Hopkins University Press, Baltimore, USA.

Giacovazzo, C., Monaco, H. L., Artoli, G., Veterbo, D., Ferraris, G., Gilli, G., Zanotti, G. and Catti, M. (2002). *Fundamentals of crystallography*. 2nd edn, Oxford University Press, Oxford, UK.

Herbstein, F. H. (2000). *Acta Crystallogr.* **B56**, 547–557.

van der Maelen, U. (1999), *Crystallogr. Rev.*, **7**, 125–180.
Müller, P., Herbst-Irmer, R., Spek, A. L., Schneider, T. R. and Sawaya, M. R. (2006). *Crystal structure refinement: a crystallographer's guide to SHELXL*. Oxford University Press, Oxford, UK.
Parkin, S. (2000). *Acta Crystallogr.* **A56**, 157–162.
Spek, A. L. (2003). *J. Appl. Crystallogr*. **36**, 7–13.
Tronrud, D. E. (2004). *Acta Crystallogr*. **D60**, 2156–2168.
Walker, N. and Stuart, D. (1983). *Acta Crystallogr.* **A39**, 158–166.
Watkin, D. J. (1994). *Acta Crystallogr*. **A50**, 411–437.

Exercises

No one is expected to work through all these questions! They are based on frequently asked questions raised in the Chemical Crystallography Laboratory in Oxford and range from the easy to the insoluble.

General

1. List some of the important differences between $P2_1/m$, $P2_1$ and Pm.
2. Give some reasons for wishing to publish structures in $P2_1/a$ or $P2_1/n$; $Pnma$, $Pnam$ or $Pna2_1$.
3. A structure could be published in $P1$, or in $A1$ with a cell of twice the volume. Could this be valid, how many parameters would be involved in each refinement, and how might the observation to parameter ratio alter?
4. A synthetic organic material yields a good triclinic data set. The structure will not solve in $P\bar{1}$, but solves easily in $P1$. What should one do next?
5. Imagine an organometallic compound with potentially 3-fold molecular rotation symmetry. Would you be worried if the diffractometer proposed the space group $C2/c$?
6. An organolead compound crystallizes in Pc, and solves in that space group. Comment on origin-fixing techniques, and their effect on atomic and molecular parameter s.u.s.
7. Explain what happens during refinement given the following scenarios:
   a. a few structurally important C atoms have been omitted;
   b. an ethanol molecule of solvation has been omitted;
   c. an oxygen and a nitrogen atom have been interchanged;
   d. the chemist is uncertain if a terminal group is CN or NC;
   e. the crystallographer is sent some data without an indication as to whether they are F, F^2 or I;
   f. somehow the user loses 1/3 of the reflections during a file transfer without getting a warning message.
8. For a material in $P222_1$ we measure and keep separate the h and the $-h$ reflections. How does the number of independent observations we have depend upon the material and the diffraction experiment?
9. The 112 reflection for an 'ordinary' material has $F_o = 10$, $F_c = 500$. What should we do? If F_o were 400, what should we expect?
10. Suggest different restraint regimes for PF_6^- under different patterns of disorder. Suggest some suitable constraints.
11. Why do we bother fiddling with
    a) hydrogen atoms;
    b) a disordered solvent?

    Comment on different techniques available for dealing with the problems.
12. Are there any reasons why a laboratory might want both Cu and Mo data-collection capabilities?
13. For a chirally pure material in $P6_1$, the Flack parameter has an s.u. of 0.03 and a value of 0.98. What should be done?
14. Imagine a drug compound for which the diffractometer proposes the space group $I4_1$. The Flack parameter refines to about 1.0, with an s.u. of 0.01. What should you do next?
15. A novel inorganic phosphate in $P2_1$ gives a Flack parameter of 0.47 and an s.u. of 0.40. What do we know about the material? What would we know if the s.u. was 0.05?
16. Give the relationship between the number of parameters and execution time in least squares.
17. Explain the derivation of the symmetry constraints for the parameters of atoms on special positions.
18. Why does the least-squares-determined scale factor ($k.F_c = F_o$) rarely make $\Sigma F_o = \Sigma F_c$?
19. Why is the weighted R factor based on F^2 usually higher than the conventional R factor?
20. What is 'the variance of a reflection of unit weight'?
21. What is the effect of unaveraged reflections (multiple observations) on least-squares refinement?
22. What is the effect on R and bond length s.u.s of ignoring 'weak' reflections?
23. What is the effect on R and bond length s.u.s of anisotropic refinement?
24. What is the effect on R and bond length s.u.s of using block diagonal refinement?
25. What is the effect on R and bond length s.u.s of missing solvent molecules?

Matrix

26. What are the design matrix and the normal matrix?
27. What are some uses in crystallography of the eigenvalues and eigenvectors of a symmetric matrix?
28. What is the 'riding' model in parameter refinement?
29. How can the problem of pseudo-doubled cells be ameliorated?

Errors in data

Discuss:

30. the symptoms of applying the Lp correction twice, or not at all;
31. the effect of neglecting reflections with negative net intensity;
32. the effect on structural parameters of ignoring absorption effects;
33. the effect of ignoring the θ-dependent component of the absorption correction;
34. the errors introduced by ignoring anomalous dispersion;
35. 'robust-resistant' refinement.

Origin fixing

36. Give examples of space groups with origins not fixed in 1, 2 and 3 dimensions.
37. Give three methods of fixing the origin in $P1$ in least squares.
38. How do these three methods affect atomic parameter s.u.s?
39. How do these three methods affect molecular parameter (e.g. bond length) s.u.s?

Centres of symmetry

40. What is the effect of refining a centrosymmetric structure in a noncentrosymmetric space group?
41. Why are pseudosymmetric structures difficult to refine?

Refinement

42. Discuss uses in refinement of a weighting scheme that is a direct function of $(\sin\theta)/\lambda$.
43. Discuss uses in refinement of a weighting scheme that is an inverse function of $(\sin\theta)/\lambda$.
44. Under what conditions will F and F^2 refinements converge to the same parameter values?
45. What is refinement using rigid-body CONSTRAINTS?
46. List some uses of this technique.
47. List some problems with this technique.
48. What is refinement using rigid-body RESTRAINTS?
49. List some uses of this technique.
50. List some problems with this technique.
51. What are similarity restraints, and how are they used?

Absolute configuration

52. Give three methods for the determination of absolute configuration.
53. Is inverting the co-ordinates of all atoms always sufficient to correct an error in enantiomer assignment?

Standard uncertainties

54. Why can we NOT compute reliable molecular parameter s.u.s from atomic parameter s.u.s only?

This page intentionally left blank

Analysis of extended inorganic structures

14

John Evans

14.1 Introduction

Extended inorganic structures[†] frequently present a set of challenges to the crystallographer different from those encountered in small-molecule crystallography. Whilst a synthetic organic chemist might be content with a 'rough and ready' structure that tells him/her that the basic connectivity of a target molecule has been achieved, with an extended inorganic material usually 'the devil is in the detail' – it is only by understanding the most subtle features of a material's structure that one can truly understand its properties. It is vital that studies on extended systems are performed with extreme care in order that such subtleties are not overlooked.

Some of the problems that one might encounter when looking at this class of material include the following.

- *Crystal size:* extended structures often have extremely low solubilities in common solvents and precipitate rapidly during synthesis or are made by solid-state reactions such that only tiny crystals or polycrystalline samples are available.
- *Disorder:* many extended structures exhibit structural or compositional disorder.
- *Scattering power:* the contribution of, for example, an oxygen atom (8 electrons) to the diffraction pattern of an oxide containing bismuth (83 electrons) is extremely low.
- *Absorption:* extended structures frequently contain highly absorbing elements, making the use of good absorption corrections (spherical/faceted crystals), suitably sized crystals, and an appropriate choice of radiation crucial.
- *Phase transitions:* extended materials frequently undergo phase transitions as a function of temperature. These can lead to crystals shattering or twinning (see Chapter 18) or subtle departures from higher-symmetry structures.

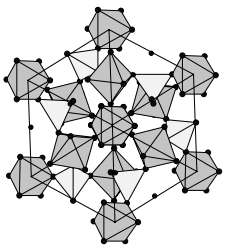

[†]Here we use the term 'extended structure' to refer to materials such as metal oxides or other 'inorganic' materials or minerals where no 'molecular' units can be identified. Similar considerations may apply to materials such as co-ordination polymers.

- *Incommensurate structures:* competing structural forces in extended materials can lead to non-periodic structures.
- *Pseudo-symmetry:* either subtle structural distortions or diffraction data being dominated by heavy elements can make space group choice difficult – symmetry-breaking reflections can often be very weak.
- *Structure solution:* many of the above problems mean that pushing the default 'solve' button in an integrated software package will fail.

This chapter contains a brief overview of some of the above areas, some case histories that illustrate several of the problems, and some information on how structures can be validated once determined.

14.2 Disorder

In many cases, the presence of disorder in small-molecule crystallography is simply an inconvenience during structure determination and not in itself of any scientific importance. If, for example, a chemist has used a conveniently sized anion such as BF_4^- or PF_6^- to crystallize a new compound, or a material contains a poorly ordered solvent molecule, one might be happy to simply 'mop up' the scattering due to the disordered portion of the structure in order to obtain better information on the part of interest. There are often a number of ways in which this can be done, some based on plausible structural models and others (e.g. SQUEEZE-type algorithms) not.

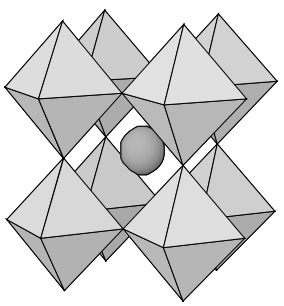

Fig. 14.1 The ideal ABO_3 perovskite structure; the 12-co-ordinate A atom is surrounded by corner-sharing BO_6 octahedra.

In contrast, there are countless problems in materials chemistry where understanding disorder is **key** to understanding structure–property relationships. As a simple example, the 1:1 binary alloy FePt can be prepared in a disordered form where Fe and Pt randomly occupy the sites of a face-centred cubic structure; this material is magnetically soft. By careful annealing, however, one can redistribute the Fe and Pt atoms such that they form ordered layers in the structure. The ordered material has one of the highest magnetocrystalline anisotropies known and is of interest for magnetic storage applications. In a material such as the perovskite $La_{1-x}Sr_xMnO_3$ (Fig. 14.1) introducing occupational disorder via Sr doping on the La site (colloquially the 'A site') dramatically changes the electronic and magnetic properties of the material. At first sight one might ascribe this merely to the changing Mn^{III}/Mn^{IV} ratio on doping and imagine that the value of x (which could be measured crystallographically by refining site occupancies) would be the only structural effect of interest. However, many other factors are crucial: changing the La:Sr ratio affects the average size of the A-site cation – this might influence Mn–O–Mn bond angles in the material, changing the width of the conduction band; oxidizing d^4 Mn^{III} to d^3 Mn^{IV} changes a Jahn–Teller-active cation into a Jahn–Teller-inactive one – this will cause different patterns of distortion in the MnO_6 octahedra and could cause

a structural phase transition. In fact, it has recently been shown that in many materials, even if one keeps the average size and average charge of an A-site cation constant (e.g. by substituting with a fixed ratio of 2+/3+ cations of different sizes), one can drastically influence a system's properties (see, e.g., Attfield *et al*., 1998). Disorder is thus a crucial parameter in determining a material's properties.

14.2.1 Site-occupancy disorder

In many cases studying occupational disorder can be relatively straightforward. For a simple system such as a cation-deficient oxide $A_{1-\delta}O$, a single diffraction experiment (which simply measures the relative scattering strength from metal and oxygen sites) would allow one to refine a fractional occupancy of the A site (along with any other free variables) to determine δ. One would want to be careful that δ does not correlate significantly with other parameters such as adps, but the problem is soluble. For a more complex oxide A_aB_bO with two cations on the same site the problem is more challenging. If one has good chemical reasons to do so (e.g. if A and B are both known to be cations that display only a +2 oxidation state), one might be able to say that $a + b = 1$ such that the problem can be rewritten as $A_{1-\delta}B_\delta O$ and is again soluble from a single diffraction measurement. Such relationships can be set up during refinement via either crystallographic constraints or, for more complex situations, restraints. If such an assumption is not possible (e.g. the true situation is $A_aB_b(\text{Vacancy})_cO$) then a single diffraction measurement will not do – one needs more information. If A and B have different neutron-scattering lengths then one might attempt a combined X-ray and neutron refinement; alternatively one might choose to perform an anomalous scattering experiment, exploiting the fact that the relative scattering power of elements can change dramatically close to an absorption edge. In some cases it might be necessary to change the isotope of the element of interest (different isotopes have different neutron-scattering lengths) to provide more information, though this can be both expensive and synthetically challenging.

It is also worth mentioning that there are some simple systems where turning to neutrons will not help. Take a simple metal oxyfluoride $MO_{1-\delta}F_\delta$, for example. Oxygen and fluorine have sufficiently similar X-ray scattering powers (8 and 9 electrons, respectively) and neutron scattering lengths (5.803 and 5.654 fm) that they are extremely difficult to distinguish by diffraction. One might have to turn to alternative experimental techniques such as solid-state NMR or theoretical calculations to probe O/F distribution in such a material.

As a final comment, it is worth noting that, despite low R factors, a structural model might be only as good as the assumptions used to derive it. Let us return to the simple example of a metal oxide, MO. As stated above, a single diffraction experiment can solve the $M_{1-\delta}O$ metal vacancy problem. Equally it could solve an $MO_{1-\varepsilon}$ oxygen vacancy problem (though the sensitivity would generally be lower with X-rays).

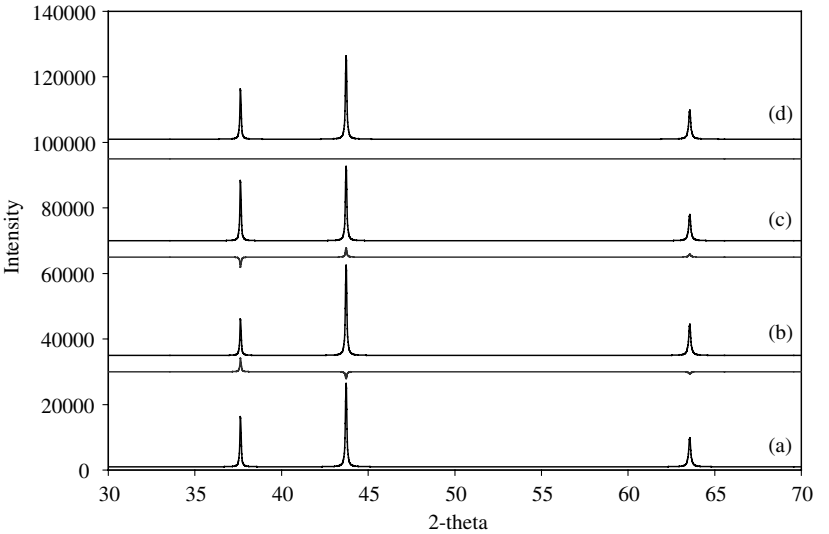

Fig. 14.2 Calculated diffraction patterns for (a) TiO, (b) $Ti_{0.8}O$, (c) $TiO_{0.8}$ and (d) $Ti_{0.8}O_{0.8}$. The line underneath each calculated pattern shows the discrepancies obtained when trying to fit the structure of stoichiometric TiO to the data, refining only an overall scale factor. Data for $Ti_{0.8}O_{0.8}$ are indistinguishable from those for TiO.

What if there are vacancies on both the metal and oxygen sites? As can be seen in Fig. 14.2, for $\delta = \varepsilon$ the diffraction pattern of a disordered $M_{1-\delta}O_{1-\varepsilon}$ material is **identical** to that of MO. This might seem an 'exotic' issue to worry about, but even a material as simple as 'stoichiometric' TiO actually contains around 1/6 vacancies on both the metal and oxygen sites. For complex disorder problems the use of other techniques (chemical analysis, density measurements, oxidation-state determination by other techniques, electron microscopy, solid-state NMR, etc.) can therefore be vital.

14.2.2 Positional disorder

A second type of disorder frequently encountered is positional disorder where an atom, or a group of atoms, can occupy one of two or more sites in a structure. In some cases this is a genuine phenomenon and can be tackled by introducing partial occupancy on several sites, often coupled with suitable constraints or restraints. In other cases, however, apparent disorder could arise due to the wrong choice of space group or twinning. It should not be forgotten that site and occupational order may be connected. If one had a material with a solid solution of La^{3+} ($r = 1.30$ Å) and Bi^{3+} ($r = 1.31$ Å) on the same site one might not be surprised if the active lone-pair cation Bi^{3+} adopted a slightly different position to La^{3+}. How does one deal with this during refinement? How does one relate adps for the two cations? Ingenuity and a critical viewpoint are required!

14.2.3 Limits of Bragg diffraction

It should be remembered that Bragg diffraction can only ever tell you about the average long-range structure of a material and that this can potentially hide significant features of its structure. Consider the two structures in Fig. 14.3. Both represent a simple material in which 30% of the available sites are vacant. The two structures can be readily distinguished visually: in one the vacancies are randomly distributed; in the second they are clustered – if one site is vacant the adjacent site is more likely to be vacant. Clearly, real-world examples of such materials could have drastically different properties. Bragg scattering is, however, completely blind to these differences and the diffracted intensities of *hkl* reflections of the two materials are identical (Fig. 14.3). The difference in the structures is revealed only by looking at the diffuse scattering between Bragg peaks. In a single-crystal experiment this is seen as streaks between *hkl* reflections; in a powder experiment it is one contribution (of several) to the background scattering. The examples in Fig. 14.3 were kindly supplied by Thomas Proffen. There is an excellent website that explores these ideas further and allows on-line simulations

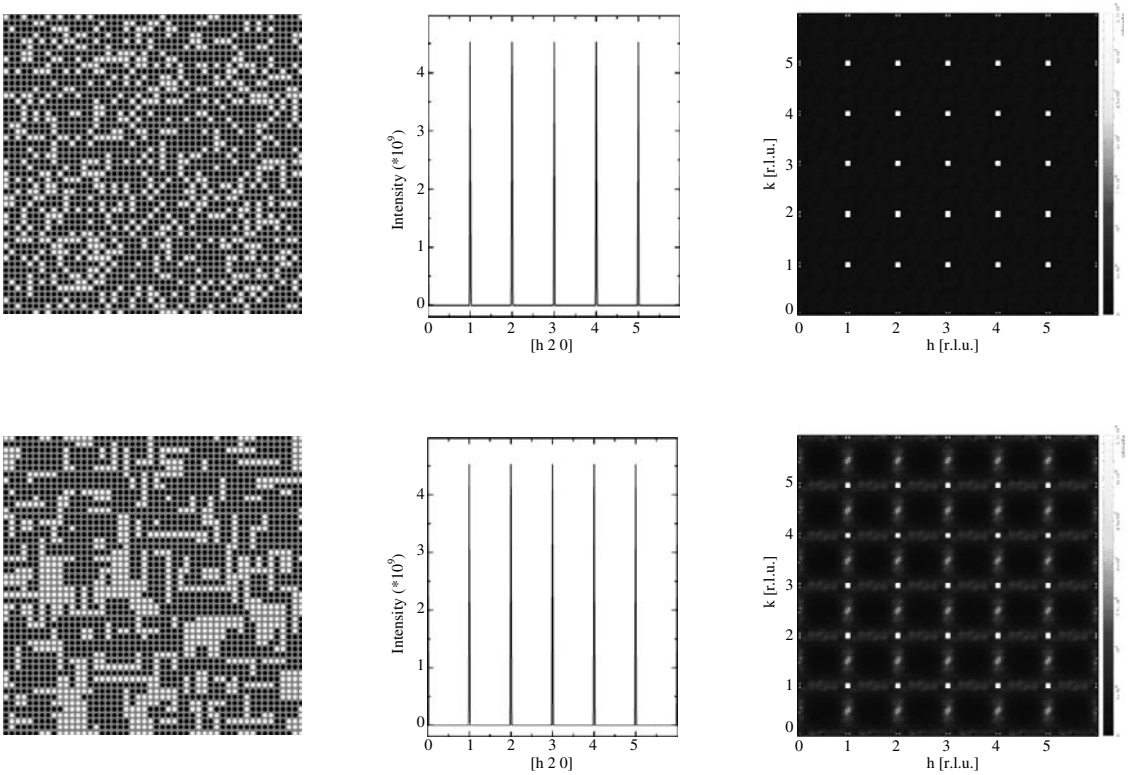

Fig. 14.3 Cross-sections of a 50 × 50 atom structure containing 30% vacancies (drawn as light dots). Bragg scattering (centre plot is of $h, 2, 0$ reflections) for a randomly disordered and a clustered model is identical. Differences can be seen only in the pattern of diffuse intensity (right).

at www.totalscattering.org/teaching (Proffen *et al.*, 2001; see also Neder and Proffen, 2008; Egami and Billinge, 2003).

14.3 Phase transitions

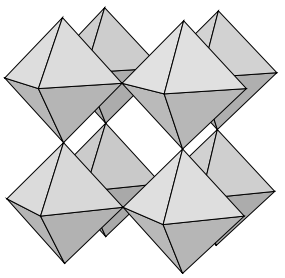

Fig. 14.4 The ideal structure of WO_3.

Phase transitions are a feature of much of the structural chemistry of extended materials. WO_3 is an apparently simple structure made up of corner-sharing WO_6 octahedra (Fig. 14.4). As such, one might expect it to have a simple ~4 Å cubic unit cell and space group $Pm\bar{3}m$. In reality, however, its structural chemistry is far more complex. Phase transitions can occur that involve coupled tiltings of the WO_6 octahedra, and/or in which W atoms move from the centres of octahedra in different directions. WO_3 is said to show more phase transitions than any other oxide and it is only recently that controversy over the true structures of some of the phases appears to have been resolved.

Part of the difficulty caused by phase transitions (particularly displacive phase transitions) is that they often lead to only subtle changes in diffraction patterns, with the relative intensities of reflections related by symmetry in the high-symmetry form showing only slight changes. Powder diffraction, in which the splitting of, e.g., a cubic 200 reflection into the 200, 020 and 002 reflections of an orthorhombic system as the cell metric changes from $a = b = c$ to $a \sim b \sim c$ can sometimes be directly observed, is often a powerful tool – particularly as it avoids the problems of twinning in single-crystal samples. Phase transitions will often lead to the formation of superstructures in which the dimensions of one or more cell edges are doubled or tripled relative to the high-symmetry structure. If the atoms that move most in the phase transition make only a small contribution to diffraction (e.g., the movement of oxygen atoms in a metal oxide), such effects can again be easily missed.

Finally, phase transitions can also lead to incommensurately modulated structures that present further structural complexity. Consider the simple structure in Fig. 14.5 that represents a one-dimensional chain of atoms with a repeat distance a. If a structural change occurs in which each atom is displaced laterally according to the magnitude of a sine

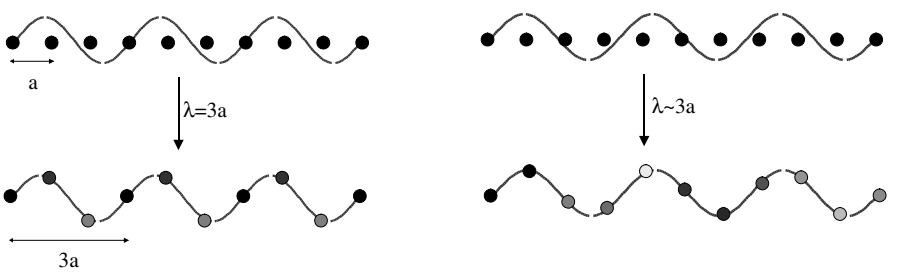

Fig. 14.5 Schematic representation of the formation of (left) a commensurate superstructure with $a = 3a_{sub}$ and (right) an incommensurate superstructure.

wave with $\lambda = 3a$, then this can easily be seen to cause a tripling of the a-axis. In a diffraction pattern one would expect extra reflections to be observed at points in reciprocal space between the original reflections (with indices $nh/3, k, l$ compared to the original subcell reflections). What if the sine wave describing the structural displacements is not exactly $\lambda = 3a$ but $\lambda \sim 3a$? The basic structure of the material produced (Fig. 14.5 right) is clearly very similar to that in Fig. 14.5 left. However, the unit cell of the material is no longer a simple multiple of the original subcell. One would again expect to see extra superstructure reflections, but they would no longer appear at simple rational positions between the subcell reflections. It might be that one can approximate the system by choosing a very large supercell. For example, in Fig. 14.5 one could approximate the superstructure using $a_{\mathrm{sup}} = 10a_{\mathrm{sub}}$. However, this is clearly a rather inelegant approach as one now has a large unit cell requiring a large number of atoms in the asymmetric unit. There is a more natural language to describe such systems – that of 'incommensurately modulated structures' – which can be used to describe either positional or compositional fluctuations in materials. This language views the periodic superstructure merely as a special case of the more general phenomenon. More detailed information can be found in a number of places, but is beyond the scope of this text.

14.4 Structure validation

Assuming that one has successfully solved the structure of an inorganic material, how can one be sure it is correct? For small-molecule work an experienced crystallographer will know that a C–C bond length should be about 1.54 Å, and C=C 1.34 Å; for more exotic distances one can easily consult the Cambridge Structural Database (Allen, 2002). Distances significantly different from those expected would immediately cause concern about the structural model. For inorganic materials such comparisons are harder. Co-ordination environments are far less regular, the range of possible environments is larger, different oxidation states of elements have different geometric preferences, and there is no direct equivalent of the CSD to consult.[†] Whilst simple structural considerations using ionic radii (the sets derived from those initially published by Shannon and Prewitt in 1969 are the the most widely used; see, for example, Shannon, 1976) are possible, they are often not desperately informative.

One relatively straightforward approach is to make use of the bond-valence concept popularized by Brown and Altermatt (1985), which builds on ideas originally applied to metals and intermetallics by Pauling in 1947. The basis of the approach is that each bond from atom i to atom j is assigned a valence v_{ij} such that the sum of valences for bonds from a given atom equals its total valence, V $(=\Sigma v_{ij})$. The most widely used expression for the dependence of bond valence on bond length is:

$$v_{ij} = \exp[(R_{ij} - d_{ij})/b]. \tag{14.1}$$

[†] There are inorganic databases available such as the ICSD, PDF-4 and Pauling file, but they are not as readily interrogated as the CSD. Inorganic structures can be read into CSD software to provide searchable databases but one should always be aware of bias in the data. How does one take account of the fact that, e.g., TiO_2 appears 113 times in the database when trying to decide an average Ti–O distance for a range of materials?

Table 14.1. Bond distances and bond valence sums for $BiMg_2VO_6$ (see case history 1). R_{ij} values taken from Brese and O'Keeffe (1991) of Bi 2.094, Mg 1.693 and V 1.803 were used.

		O1	O1	O1	O1	O2	O3	O3	O4	Sum
Bi1	d/Å	2.199	2.199	2.236	2.236					
	v_{ij}	0.75	0.75	0.68	0.68					**2.87**
Mg1	d/Å			2.066	2.066	1.980	2.038	2.038		
	v_{ij}			0.36	0.36	0.46	0.39	0.39		**1.98**
Mg2	d/Å			2.066	2.066		2.042	2.042	1.995	
	v_{ij}			0.36	0.36		0.39	0.39	0.44	**1.95**
V1	d/Å					1.688	1.733	1.733	1.684	
	v_{ij}					1.36	1.21	1.21	1.38	**5.16**
	Sum			(2 × Bi1)	**2.16**	**1.82**		**1.99**	**1.82**	

In this expression d_{ij} is the bond length, R_{ij} the so-called 'bond-valence parameter' and b a constant usually taken to be 0.37 Å. Whilst theoretical justifications of this method have been published, it is usual to treat the expression as an empirical but effective tool. Brese and O'Keeffe (1991) have taken this approach and published bond-valence parameters R_{ij} for most common cation–anion combinations using over 1000 carefully chosen crystal structures. These values can be found on a number of websites including http://www.ccp14.ac.uk/ccp/web-mirrors/i_d_brown/.

Bond-valence parameters can be used in a number of ways. The most obvious is to check the validity of a structural model. If a crystal structure is correct, then one would expect the bond-valence sum for each element to be close to its formal valency. Values for a typical inorganic structure ($BiMg_2VO_6$ of case history 1) are shown in Table 14.1. Typically, one would expect valence sums to be within a few per cent of formal valencies. Values outside this range could suggest an incorrect model, that one has used valence parameters for the wrong oxidation state of the element, that the material is highly strained, or that part of the structure is missing. In this latter context bond-valence sums are particularly useful for identifying missing H atoms in inorganic structures. Bond-valence parameters can also be used (via (14.1)) for calculating expected radii for a given element/anion configuration, or as a criterion for determining co-ordination numbers (for example, how important is an oxygen anion at 3.1 Å to the co-ordination environment of a Bi^{3+} cation? Answer: it contributes <2% of the valence sum, so not very!).

14.5 Case history 1 – $BiMg_2VO_6$

Bismuth magnesium vanadate is a material whose structure was first reported in orthorhombic space group *Cmcm* by Huang and Sleight (1992). Materials of this type have been investigated for catalytic and

non-linear optical (NLO) properties. With a material of this formula one might anticipate problems due to pseudo-symmetry (because of the heavy Bi atom) and significant absorption.

To illustrate both these potential pitfalls data have recently been collected on this material using a Bruker SMART 6000 diffractometer using Mo-$K\alpha$ radiation. A full sphere of data was collected with a frame width of 0.3° and a counting time of 20 s per frame. Using a default set of thresholding parameters the same cell and space group were found as in the published structure (though we actually chose a non-standard space group setting *Bbmm* rather than *Cmcm* for analysis). The structure would solve and refine without any difficulties. Final agreements of $R = 2.10\%$, $wR = 5.64\%$ were obtained for 552 reflections after anisotropic refinement and application of an optimal weighting scheme in the Oxford CRYSTALS suite of software. Bond distances and angles were all close to expected values and the co-ordinates were essentially as published.

However, it can be seen from Fig. 14.6 that, whilst the adps on most atoms are what one might expect for a material of this type, one oxygen atom has an adp that is physically unreasonable and might suggest that this oxygen site should be split. In fact, careful examination of the raw frames shows that additional weak reflections are present that violate the cell centring and show that the true space group of this material is *Pnma*. Refinement in this lower-symmetry space group proceeded smoothly, giving final *R*-factors for the 1054 observed reflections of $R = 2.13\%, wR = 5.27\%$, with all atoms now showing physically sensible adps. It can be seen from Fig. 14.6 that the structure is only subtly different from the *Bbmm* model. Note that in this case the correct structure has an *R* factor that is slightly higher than the incorrect structure due to the larger number of reflections.

In fact, since the original publication this material has been shown to undergo a displacive phase transition on warming above ~300 K from the primitive to the centred structure (Radosavljevic and Sleight, 2000). In the high-temperature structure the oxygen atoms of the VO_4

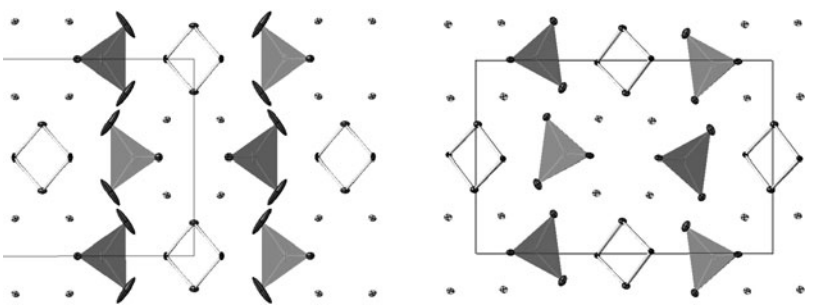

Fig. 14.6 Refinements of $BiMg_2VO_6$ in *Bbmm* (left) and *Pnma* (right); both structures are viewed down the *b*-axis with *a* running to the right. The structure contains VO_4 tetrahedra (shaded), Bi_2O_2 chains and 5-coordinate Mg (here shown without bonds for clarity). Adps have been drawn at the 50% probability level.

tetrahedra again show extended adps, which this time are indicative of dynamic disorder (Fig. 14.7).

The importance of an adequate absorption correction when working with materials of this type can be seen from Table 14.2 and Fig. 14.8.

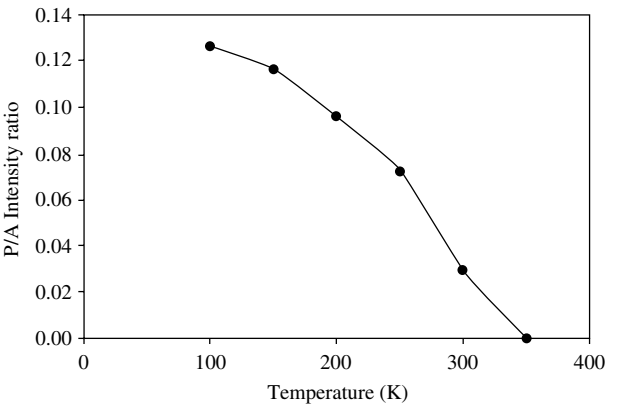

Fig. 14.7 Relative summed intensities of reflections allowed only in *Pnma* ('P' reflections) and those allowed in both space groups ('A' reflections) as a function of temperature.

Table 14.2. *R* factors for processing and refinement of $BiMg_2VO_6$ data. * failed to converge fully. ** one non-positive-definite adp.

	Untreated	**Face indexed**	**SADABS**	**FI + SADABS**
R_{int} (%)	25.8	12.8	5.2	2.9
No. reflections	8983	8983	7680	8955
R/*wR* (%), isotropic refinement	7.20/17.53	3.80/10.14	5.44/11.85	2.43/6.36
R/*wR* (%), anisotropic refinement	6.70/16.16	3.19/8.47	3.82/8.77*	2.21/6.03
R/*wR*(%), aniso ref + optimal weights	6.75/10.85	3.14/7.05	4.05/7.79**	2.13/5.27

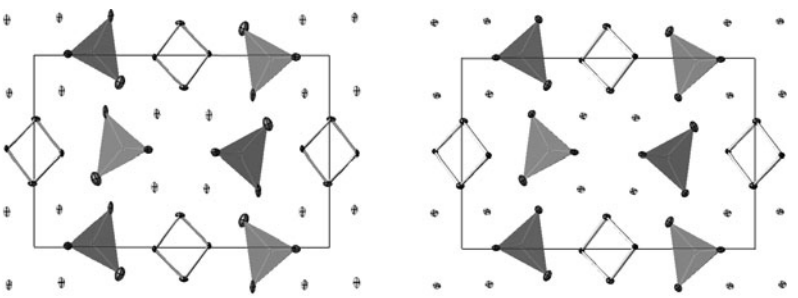

Fig. 14.8 Refinements of $BiMg_2VO_6$ using raw (left) and absorption-corrected data (right); both structures are viewed down the *b*-axis with *a* running to the right. Key as for Fig. 14.6.

The crystal used for these experiments was an elongated prism of dimensions $0.02 \times 0.03 \times 0.27$ mm. Without any absorption correction a merging R factor of 25.8% was obtained. On full anisotropic refinement final agreement factors of $R = 6.75, wR = 10.85\%$ were achieved. The best model could be obtained by application of a combined face-indexed and SADABS-type absorption correction, resulting in a merging R factor of 2.9% and final agreement factors of 2.13/5.27%. Significant improvements in the shape of adps were observed (Fig. 14.6).

14.6 Case history 2 – $Mo_2P_4O_{15}$

From its formula $Mo_2P_4O_{15}$ would appear to be a relatively simple inorganic material and one might therefore expect it to have a simple structure. In fact, the structure of the material was reported by Costentin *et al.* (1992) in space group $P2_1/c$ with unit cell parameters $a = 8.3065$, $b = 6.5154$, $c = 10.7102$ Å, $\beta = 106.695°, V = 555.20$Å^3. The cell thus contains a total of 2 formula units and can be described using 11 atoms in the asymmetric unit. The structure contains MoO_6 octahedra that share 5 of their 6 corners with PO_4 tetrahedra. The PO_4 tetrahedra themselves share corners to give P_4O_{13} groups (Fig. 14.9). However, despite the structure being chemically plausible and having an R factor of 3.6%, there were certain features that were puzzling, including (see Fig. 14.10) rather large adps on certain atoms.

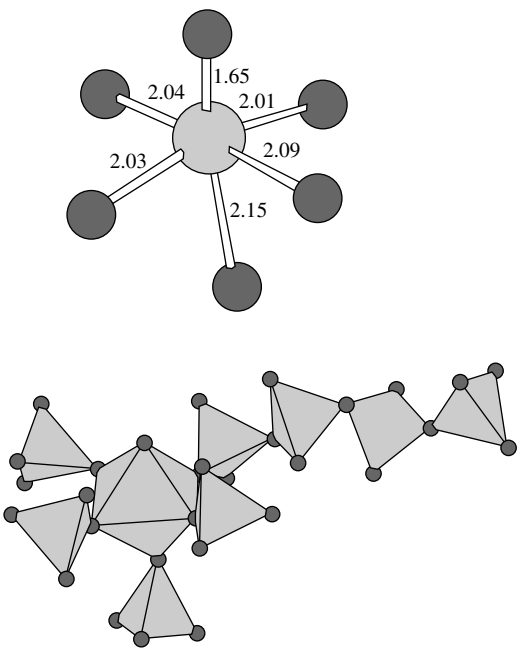

Fig. 14.9 Local MoO_6 and P_4O_{13} environments in the structure of $Mo_2P_4O_{15}$.

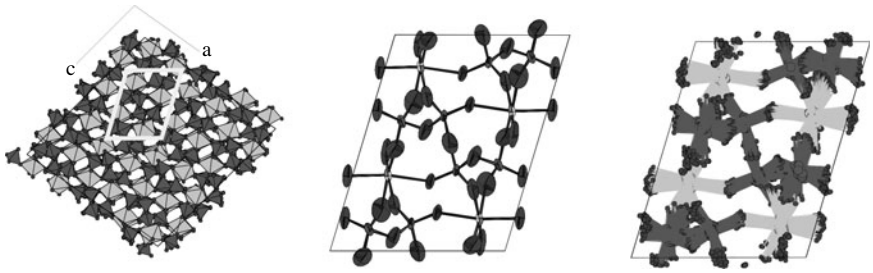

Fig. 14.10 Left: a polyhedral view of the true superstructure of $Mo_2P_4O_{15}$; the incorrect small unit cell is also shown. Middle: adps (drawn at the 70% probability level) derived from 120 K data using the incorrect subcell model. Right: true atomic positions mapped back onto the incorrect subcell. Notice the similarity between the incorrect adps and the true static displacements of atoms.

When we re-collected data on this material using a Bruker SMART 6000 it became clear that the true unit cell of this material was considerably more complex than had been initially realized. The actual cell volume was some 21 times larger than that originally reported, the true room-temperature cell parameters being $a = 24.133(2)$, $b = 19.579(2)$, $c = 25.109(2)$ Å, $\beta = 99.962(3)°$, $V = 11685.13$ Å^3. The unit cell must then contain some 42 formula units. Automated data processing using the Bruker XPREP software suggested that the space group was $P2_1/n$. However, careful manual inspection of the reflection listing revealed that reflections forbidden by the 2_1 axis were in fact present, albeit weak [the strongest $0k0$ reflection observed with $k \neq 2n$ was 070 with $I = 1.54(3)$; this ranked 13 352nd of the observed reflections ordered by intensity; by comparison the strongest reflection observed had $I = 9300(120)$], meaning that the true space group was Pn. This in turn implies that the asymmetric unit of the material must contain 441 independent atoms – some 430 more than originally thought!

Solving a structure of this complexity that displays severe pseudosymmetry is clearly challenging. We took the approach of first solving the substructure using the unit cell originally published. Using 120 K data we could refine the substructure to $R = 9.5\%$, though again adps on certain atoms were rather large. By comparing the indices hkl of certain reflections based on the (wrong) small unit cell with those of the correct larger cell we could obtain a transformation matrix to relate the two structures (see Exercise 3 at the end of this chapter). We could then transform the subcell co-ordinates to give a starting model for the high-temperature structure.

Despite now having a chemically plausible starting model, least-squares refinement is not straightforward. As described in Chapter 13, if one tries to directly refine a high-symmetry structure in a lower-symmetry space group the least-squares will invariably diverge. How then does one move forward? In this case we know a great deal of useful information about the structure: we know that it contains MoO_6 octahedra that share corners with PO_4 tetrahedra; we know from the literature that MoO_6 octahedra typically contain 4 Mo–O bonds around 2.05 Å,

1 short M=O around 1.65 Å and 1 longer M–O around 2.20 Å; we know that P–O bonds of PO_4 tetrahedra are typically around 1.5 Å; and we know that P–O bonds in P–O–P linkages are typically slightly longer, around 1.60 Å. Given this information it is possible to generate a set of distance restraints to describe the structure and to refine the structural model, not against a set of diffraction data but directly against the restraints. The quantity minimized is then the sum of the squared differences between prescribed distances and the distances in the model. Atoms are moved until these differences are minimized. This is called distance least squares or DLS refinement and has been used to great effect for many inorganic systems and particularly zeolite frameworks (see publications by Baerlocher and co-workers). By performing DLS refinement it is possible to produce plausible structural models, which can be tested against the data.

In this example it proved relatively straightforward to solve the structure by simultaneously refining against both the data and the DLS restraints (252 in total to describe Mo–O distances; 336 to describe P–O distances; 630/504, respectively, for MoO_6/PO_4 bond angles; Mo–O restraints were set up in such a way that each octahedron could have a range of distances to allow for the expected mixture of short and long bonds). We used a simulated annealing approach in which we started refinement from the subcell co-ordinates and then refined the structure against data and restraints simultaneously to convergence. At convergence, co-ordinates were automatically reset to their initial values ± a small random displacement and the refinement repeated. This process was performed on a relatively small 2θ range of data for speed, but rapidly resulted in a solution with a low R factor. This solution was then refined against the whole dataset without any restraints to give $R = 3.49\%$ and $wR = 5.99\%$ for 43783 reflections with $I > 3\sigma(I)$. It is perhaps worth noting that new charge flipping methods can solve pseudo-symmetry problems such as this far more easily.

The true structure of $Mo_2P_4O_{15}$ is necessarily complicated! Fig. 14.10 shows the structure in polyhedral representation. The figure also shows a comparison of the incorrect literature model with the true structure 'folded back' into the small unit cell (this can be done by applying the reverse of the transformation matrix used to generate the initial superstructure model). Here, each of the atomic positions in the true supercell becomes one of several closely separated positions in the subcell. It is instructive to note that the shape of the adps obtained using the incorrect small cell are closely related to the true static displacements of atoms in the larger cell.

How can one judge the quality of a structural model for an inorganic crystal structure such as this? Normally one would compare bond distances and angles with expected values or calculate bond valence sums for the various atoms in the structure. With a structure this complex (it contains 42 different MoO_6 octahedra and 84 PO_4 tetrahedra), the structure can be checked for internal self-consistency – it acts as its own database. Isotropic displacement parameters for all atoms lay

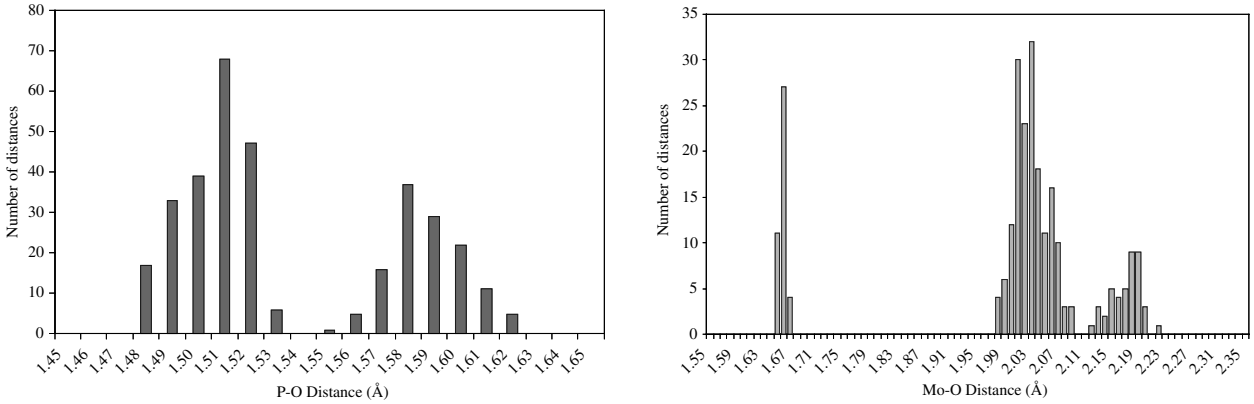

Fig. 14.11 Histograms of bond lengths for PO_4 tetrahedra and MoO_6 octahedra.

within expected ranges [minimum, maximum and average values for the 3 atom types were: 42× Mo 0.0051–0.0062, average = 0.0056 Å^2; 84× P 0.0049–0.0068, average = 0.0058 Å^2; 315 × O 0.0069–0.0170, average = 0.0097 Å^2]. Bond valence sums for the 42 MoO_6 octahedra and 84 PO_4 tetrahedra deviated by < 0.15 units (3%) from expected values. With 42 MoO_6 octahedra in the structure one would expect 42 'short' Mo–O bonds, 168 'medium' Mo–O bonds and 42 'long' Mo–O bonds. For the 84 PO_4 tetrahedra that link to form P_4O_{13} units one would expect 210 short P–O bonds and 126 longer P–O–P bonds. The histograms in Fig. 14.11 show exactly this distribution!

References

Allen, F. H. (2002). *Acta Crystallogr.* **A58**, 380–388.

Attfield, J. P., Kharlanov, A. L. and McAllister, J. A. (1998). *Nature* **394**, 157–159.

Brese, N. E. and O'Keeffe, M. (1991). *Acta Crystallogr.* **B47**, 192–197.

Brown, I. D. and Altermatt, D. (1985). *Acta Crystallogr.* **B41**, 245–247.

Costentin, G., Leclaire, A., Borel, M. M., Grandin, A. and Raveau, B. (1992). *Z. Kristallogr.* **201**, 53–58.

Egami, T. and Billinge, S. (2003). *Underneath the Bragg peaks: structural analysis and complex materials.* Pergamon Press, Oxford, UK.

Huang, H. F. and Sleight, A. W. (1992). *J. Solid State Chem.* **100**, 170–178.

Neder, B. and Proffen, T. (2008). *Diffuse scatter and defect structure simulations.* Oxford University Press, Oxford, UK.

Proffen, T., Neder, R. B. and Billinge, S. J. L. (2001). *J. Appl. Crystallogr.* **34**, 767–770.

Radosavljevic, I. and Sleight, A. W. (2000). *J. Solid State Chem.* **149**, 143–148.

Shannon, R. D. (1976). *Acta Crystallogr.* **A32**, 751–767.

Exercises

1. As part of an undergraduate practical class a student was asked to record powder diffraction patterns of the compounds BaS and SrSe, both of which have the rock salt structure (Fig. 14.12). Ionic radii (Å) are Ba 1.49, Sr 1.32, S 1.70, Se 1.84. Unfortunately the student has forgotten to label the patterns (which are shown in Fig. 14.13). Can you help?

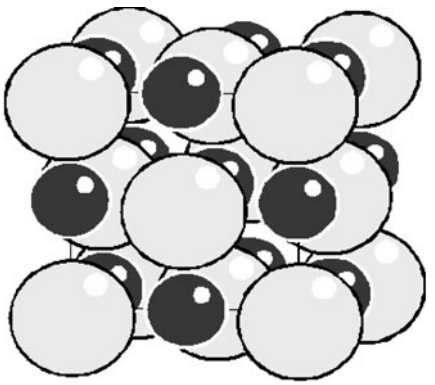

Fig. 14.12 Rock salt structure.

Table 14.3 Literature coordinates of $MnRe_2O_8$

	x	*y*	*z*
Mn1	0	0	0
Re1	1/3	2/3	0.2891
O1	0.135	0.349	0.206
O2	1/3	2/3	0.57

2. The structure of $MnRe_2O_8$ has been described in space group $P\bar{3}$ with unit cell parameters $a = b = 5.8579$, $c = 6.0665$ Å and fractional co-ordinates as shown in Table 14.3. Draw a plan view of the structure and determine the co-ordination environment of Mn and Re atoms. Given bond distances of 2.179 Å for Mn1–O1, 1.704 Å for both Re1–O1 and Re1–O2 and R_{ij} values of 1.79 and 1.97 Å for Mn^{II}/Re^{VII}, determine bond valence sums for Mn and Re. Do you think this structure is correct? What error could have been made when solving/refining the structure?
3. As described in case history 2, the structure of $Mo_2P_4O_{15}$ was originally described using an incorrect unit cell with $a = 8.3065$, $b = 6.5154$, $c = 10.7102$ Å, $\beta = 106.695°$, $V = 555.20$ Å^3. From the information below calculate the

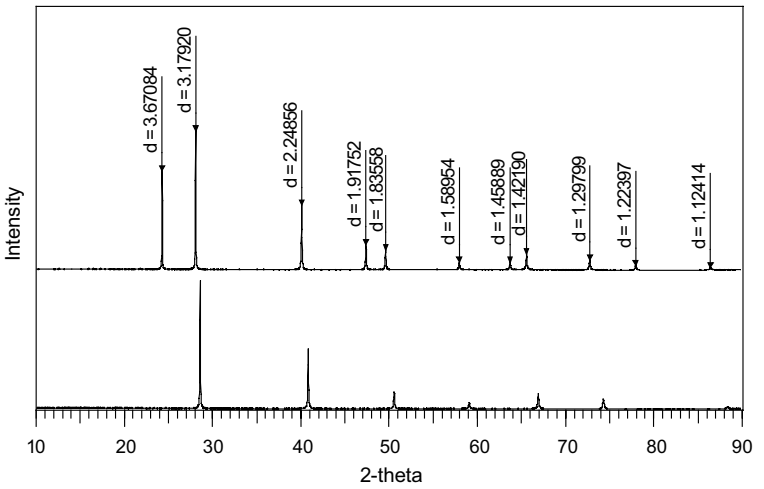

Fig. 14.13 Powder diffraction patterns of BaS and SrSe.

transformation matrix required to convert to the correct cell. Calculate the volume of the true cell.

```
Strong Supercell Reflections
-3 -3  1 d = 5.0378 2-th = 17.5904 I =  352.05 sigI =  7.90
-2  3 -4 d = 4.0281 2-th = 22.0493 I =  965.51 sigI = 28.70
 4  6 -6 d = 2.4436 2-th = 36.7491 I =  152.14 sigI =  4.46

Selected Subcell Reflections
 0  0  2 d = 5.1294 2-th = 17.2739 I =  154.96 sigI =  6.38
-1 -1  0 d = 5.0531 2-th = 17.5367 I = 2356.06 sigI = 15.64
-1  0  2 d = 5.0172 2-th = 17.6633 I =  392.77 sigI =  2.91
-2  0  1 d = 4.1308 2-th = 21.4946 I =    1.98 sigI =  0.25
 0  1 -2 d = 4.0365 2-th = 22.0030 I = 6739.94 sigI = 17.90
-1  1  2 d = 3.9811 2-th = 22.3129 I = 1233.35 sigI =  5.97
-3  0  3 d = 2.4669 2-th = 36.3908 I =    0.55 sigI =  0.30
 3  1  0 d = 2.4580 2-th = 36.5273 I = 1989.42 sigI = 11.78
 2  2 -2 d = 2.4507 2-th = 36.6401 I = 1048.92 sigI =  9.43
 3  0  1 d = 2.4059 2-th = 37.3473 I =    0.11 sigI =  0.29
```

4. A layered form of SiP_2O_7 containing corner-linked SiO_6 octahedra and P_2O_7 tetrahedra has been described in space group $P6_3$ with $a = 4.7158$, $c = 11.917$ Å and fractional co-ordinates as shown in Table 14.4. Sketch the structure. Bond distances are 3× Si–O1 1.768 Å, 3× Si–O2 1.701 Å, 3×P2–O1 1.476 Å, P2–O2 1.525 Å, P1–O2 1.585 Å and 3× P1–O3 1.481 Å. Do you think this structure is correct? See Fig. 14.14 for space group symmetry.

Table 14.4 Literature co-ordinates of SiP_2O_7.

	x	y	z
Si1	0	0	0
P1	⅔	⅓	0.394
P2	⅔	⅓	0.133
O1	0.859	0.178	0.100
O2	⅔	⅓	0.261
O3	0.93	0.261	0.422

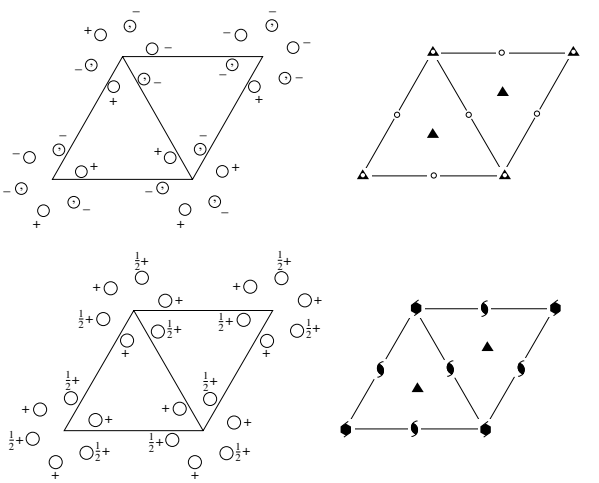

Fig. 14.14 Symmetry elements for $P\bar{3}$ (top) and $P6_3$ (bottom). Reproduced from *International Tables for Crystallography*, Vol. A, with permission of the International Union of Crystallography.

5. $RbMn[Cr(CN)_6].xH_2O$ is a framework material related to the Prussian Blues. What methods would you use to probe its structure? What are the potential problems of each approach?

The derivation of results

15

Simon Parsons and William Clegg

15.1 Introduction

The parameters obtained from the least-squares refinement are a set of co-ordinates and displacement parameters for each atom, and from these we are able to calculate geometrical parameters of interest: bond lengths, bond angles, torsion angles, least-squares planes with angles between them, intermolecular and other non-bonded distances. We can analyze the movement of the atoms and, perhaps, make some corrections to the apparent geometrical values we have calculated. To every derived result we can attach a standard uncertainty as a measure of its precision or reliability.

We must begin to *interpret* the results, to detect patterns, common features, significant differences and variations, and to make deductions on the basis of the observed geometry. We shall need to compare features within the structure, and also compare them with other related structures.

15.2 Geometry calculations

So now we have a converged refinement with which we are satisfied. The primary results include three co-ordinates for each atom. The secondary results, generally of greater interest, are parameters describing the molecular geometry.

15.2.1 Fractional and Cartesian co-ordinates

The positions of atoms in least-squares refinement are (almost) always expressed as fractional atomic co-ordinates. Familiar formulae for the calculation of distances, angles, etc., assume, however, that the co-ordinates are referred to Cartesian axes. One approach to calculating geometric parameters from crystallographic data is to transform the fractional coordinates into Cartesian co-ordinates. In order to do this the Cartesian frame (defined by vectors **X**, **Y** and **Z**) must be defined in terms of the crystallographic unit cell axes (**a**, **b** and **c**). There are an infinite number of ways in which this can be done, but one common definition is to allow the Cartesian X-axis to lie along the crystallographic a-axis

and the Cartesian Y-axis to lie in the crystallographic ab-plane, perpendicular to **X**. The Cartesian Z-axis is then parallel to **c*** (more generally it is given by the vector product $\mathbf{X} \times \mathbf{Y}$). The matrix relationship between these two sets of *axes* is

$$\begin{pmatrix} \mathbf{X} \\ \mathbf{Y} \\ \mathbf{Z} \end{pmatrix} = \begin{pmatrix} \frac{1}{a} & 0 & 0 \\ \frac{-1}{a \tan \gamma} & \frac{1}{b \sin \gamma} & 0 \\ a^* \cos \beta^* & b^* \cos \alpha^* & c^* \end{pmatrix} \begin{pmatrix} \mathbf{a} \\ \mathbf{b} \\ \mathbf{c} \end{pmatrix} = \mathbf{M} \begin{pmatrix} \mathbf{a} \\ \mathbf{b} \\ \mathbf{c} \end{pmatrix}. \tag{15.1}$$

Note that $-1/a \tan \gamma = 0$ if $\gamma = 90°$. The inverse operation is

$$\begin{pmatrix} \mathbf{a} \\ \mathbf{b} \\ \mathbf{c} \end{pmatrix} = \begin{pmatrix} a & 0 & 0 \\ b \cos \gamma & b \sin \gamma & 0 \\ c \cos \beta & \frac{-c(\cos \beta \cos \gamma - \cos \alpha)}{\sin \gamma} & \frac{1}{c*} \end{pmatrix} \begin{pmatrix} \mathbf{X} \\ \mathbf{Y} \\ \mathbf{Z} \end{pmatrix} = \mathbf{M}^{-1} \begin{pmatrix} \mathbf{X} \\ \mathbf{Y} \\ \mathbf{Z} \end{pmatrix}. \tag{15.2}$$

For transformation of *co-ordinates* between Cartesian and fractional systems the following apply (T indicates the transpose of a matrix):

$$\begin{pmatrix} x_{cart} \\ y_{cart} \\ z_{cart} \end{pmatrix} = (\mathbf{M}^{-1})^T \begin{pmatrix} x_{frac} \\ y_{frac} \\ z_{frac} \end{pmatrix} \tag{15.3}$$

$$\begin{pmatrix} x_{frac} \\ y_{frac} \\ z_{frac} \end{pmatrix} = \mathbf{M}^T \begin{pmatrix} x_{cart} \\ y_{cart} \\ z_{cart} \end{pmatrix}. \tag{15.4}$$

The following relationships are included for reference (V = volume):

$$\begin{aligned} a^* &= \frac{bc \sin \alpha}{V} \\ b^* &= \frac{ac \sin \beta}{V} \\ c^* &= \frac{ab \sin \gamma}{V} \\ \cos \alpha^* &= \frac{\cos \beta \cos \gamma - \cos \alpha}{\sin \beta \sin \gamma} \\ \cos \beta^* &= \frac{\cos \alpha \cos \gamma - \cos \beta}{\sin \alpha \sin \gamma} \\ \cos \gamma^* &= \frac{\cos \alpha \cos \beta - \cos \gamma}{\sin \alpha \sin \beta} \\ V &= abc(1 - \cos^2 \alpha - \cos^2 \beta - \cos^2 \beta + 2 \cos \alpha \cos \beta \cos \gamma)^{1/2} \\ V^* &= \frac{1}{V}. \end{aligned} \tag{15.5}$$

Once a set of Cartesian co-ordinates has been derived ordinary Cartesian geometry can be applied to calculations of distances, angles and so on. Cartesian co-ordinates are also useful when making comparisons of structures, or as a common co-ordinate framework for superposition calculations.

15.2.2 Bond distance and angle calculations

An alternative method for calculating geometric parameters, which is frequently more computationally convenient, is to apply vector methods directly to fractional co-ordinates themselves. Suppose we have two atoms with fractional co-ordinates $[x_1, y_1, z_1]$ and $[x_2, y_2, z_2]$; the interatomic vector will be:

$$\mathbf{r} = [(x_1 - x_2)\mathbf{a} + (y_1 - y_2)\mathbf{b} + (z_1 - z_2)\mathbf{c}]. \tag{15.6}$$

The length (magnitude) of this vector can be evaluated from its dot product with itself:

$$\begin{aligned} |\mathbf{r}|^2 = \mathbf{r}.\mathbf{r} &= [(x_1 - x_2)\mathbf{a} + (y_1 - y_2)\mathbf{b} + (z_1 - z_2)\mathbf{c}] \\ &\quad .[(x_1 - x_2)\mathbf{a} + (y_1 - y_2)\mathbf{b} + (z_1 - z_2)\mathbf{c}] \\ &= (a\Delta x)^2 + (b\Delta y)^2 + (c\Delta z)^2 + 2bc\cos\alpha\,\Delta y\Delta z \\ &\quad + 2ac\cos\beta\,\Delta x\Delta z + 2ab\cos\gamma\,\Delta x\Delta y. \end{aligned} \tag{15.7}$$

Bond angles, θ, can also be evaluated from dot products: if two interaction vectors **u** and **v** are represented as in (15.6), then

$$\mathbf{u}.\mathbf{v} = |\mathbf{u}||\mathbf{v}|\cos\theta. \tag{15.8}$$

Alternatively, for three atoms A–B–C the angle θ is also given by the 'cosine rule'

$$\cos\theta = \frac{r_{BA}^2 + r_{BC}^2 - r_{AC}^2}{2r_{BA}r_{BC}}. \tag{15.9}$$

Torsion angles measure the conformational twist about a series of four atoms bonded together in sequence in a chain A–B–C–D. The torsion angle is defined as the rotation about the B–C bond that is required to bring B–A into coincidence with C–D when viewed from B to C. The generally accepted sign convention is that a positive torsion angle corresponds to a **clockwise** rotation. Regrettably, this convention is opposite to that used to define positive rotations elsewhere in geometry. Note that (i) the torsion angle D–C–B–A is identical in magnitude *and* sign to the torsion angle A–B–C–D, so there is no ambiguity in the description of the angle; (ii) the torsion angles for equivalent sets of atoms in a pair of enantiomers have equal magnitudes but opposite signs, so that all torsion angles change sign if a structure is inverted. Formulae for the calculation of torsion angles are given by Dunitz (1979).

15.2.3 Dot products

The dot product **r**.**r** in (15.7) is conveniently expressed in matrix format as:

$$\begin{aligned}\begin{pmatrix}\Delta x & \Delta y & \Delta z\end{pmatrix}&\begin{pmatrix}\mathbf{a}.\mathbf{a} & \mathbf{a}.\mathbf{b} & \mathbf{a}.\mathbf{c}\\ \mathbf{b}.\mathbf{a} & \mathbf{b}.\mathbf{b} & \mathbf{b}.\mathbf{c}\\ \mathbf{c}.\mathbf{a} & \mathbf{c}.\mathbf{b} & \mathbf{c}.\mathbf{c}\end{pmatrix}\begin{pmatrix}\Delta x\\ \Delta y\\ \Delta z\end{pmatrix}\\ &= \begin{pmatrix}\Delta x & \Delta y & \Delta z\end{pmatrix}\mathbf{G}\begin{pmatrix}\Delta x\\ \Delta y\\ \Delta z\end{pmatrix}.\end{aligned} \tag{15.10}$$

Note that **G** is symmetric because **b**.**c** = **c**.**b**, and that it can be evaluated from the cell dimensions because **b**.**c** = $bc\cos\alpha$, etc. The matrix **G** is called the *metric tensor*, and is extremely important. An equivalent *reciprocal metric tensor* can be defined using the reciprocal lattice basis vectors, and this is usually given the symbol $\mathbf{G}^*$. The following relationships are often useful:

$$\mathbf{G}^{-1} = \mathbf{G}^* \tag{15.11}$$

$$V = |\mathbf{G}|^{1/2} \tag{15.12}$$

$$V^* = |\mathbf{G}^*|^{1/2}. \tag{15.13}$$

The metric tensors transform between direct and reciprocal space:

$$\begin{aligned}\begin{pmatrix}\mathbf{a}^*\\ \mathbf{b}^*\\ \mathbf{c}^*\end{pmatrix} &= \mathbf{G}^*\begin{pmatrix}\mathbf{a}\\ \mathbf{b}\\ \mathbf{c}\end{pmatrix}\\ \begin{pmatrix}\mathbf{a}\\ \mathbf{b}\\ \mathbf{c}\end{pmatrix} &= \mathbf{G}\begin{pmatrix}\mathbf{a}^*\\ \mathbf{b}^*\\ \mathbf{c}^*\end{pmatrix}\end{aligned} \tag{15.14}$$

The above formulae are very useful in computer programs, and provide a much more memorable means for evaluation of volumes and reciprocal lattice constants than the explicit formulae presented in (15.5).

15.2.4 Transforming co-ordinates

Fractional co-ordinates (x, y, z) correspond to vectors of the form

$$\mathbf{r} = x\mathbf{a} + y\mathbf{b} + z\mathbf{c},$$

which can be written in matrix format as

$$\begin{pmatrix}\mathbf{a} & \mathbf{b} & \mathbf{c}\end{pmatrix}\begin{pmatrix}x\\ y\\ z\end{pmatrix} = \mathbf{A}^T\mathbf{x}. \tag{15.15}$$

Suppose we wish to transform our unit cell using a 3×3 matrix $\mathbf{R}$ from the $\mathbf{A}$-basis to another basis, $\mathbf{B}$, where

$$\mathbf{B} = \mathbf{RA}.$$

This may be because we wish to model the structure in a different space group, or to compare one structure with another. It will be clear that we also need to transform our co-ordinates, $\mathbf{x}$, to another set, $\mathbf{y}$.

The same vector $\mathbf{r}$ can now be expressed in two ways:

$$\mathbf{r} = \mathbf{A}^T\mathbf{x}$$
$$\mathbf{r} = \mathbf{B}^T\mathbf{y},$$

so that

$$\mathbf{A}^T\mathbf{x} = \mathbf{B}^T\mathbf{y}.$$

But $\mathbf{B} = \mathbf{RA}$, and so

$$\mathbf{A}^T\mathbf{x} = (\mathbf{RA})^T\mathbf{y}.$$

Recalling that $(\mathbf{AB})^T = \mathbf{B}^T\mathbf{A}^T$,

$$\begin{aligned} \mathbf{A}^T\mathbf{x} &= \mathbf{A}^T\mathbf{R}^T\mathbf{y} \\ \mathbf{x} &= \mathbf{R}^T\mathbf{y} \\ \left(\mathbf{R}^T\right)^{-1}\mathbf{x} &= \mathbf{y}, \end{aligned} \tag{15.16}$$

which is the desired relationship: if a unit cell is transformed with a matrix $\mathbf{R}$, the co-ordinates should be transformed with $(\mathbf{R}^T)^{-1} = (\mathbf{R}^{-1})^T$. This explains why the transformations used in (15.1) and (15.2) are different from those used in (15.3) and (15.4). The same matrix $\mathbf{R}$ used to transform the direct cell axes can also be used to transform reflection indices.

15.2.5 Standard uncertainties

Although the occasional distance or angle can be calculated by hand (for example, where a non-bonded distance is required, but is not listed automatically by the refinement program because it is too long), these derivations are tedious, and are best left to automatic computer programs. Even more to the point, the correct calculation of s.u.s for the molecular geometry parameters requires inclusion of covariance terms (see Chapter 16), because atomic co-ordinates are not uncorrelated; the necessary covariances, produced automatically by a full-matrix least-squares refinement (note: refinements not based on a full matrix do not give all the covariances, and also tend to underestimate variances), are

not normally preserved and output after the refinement, so only approximate s.u.s can be calculated using parameter s.u.s alone. The approximation will be a particularly poor one when symmetry-equivalent atoms are involved, e.g. for a bond across an inversion centre, or an angle at an atom on a mirror plane.

Note that any parameter that is varied in the least-squares refinement will have an associated s.u., and any parameter that is held fixed will not. Usually, the three co-ordinates and six anisotropic U^{ij} (or one isotropic U) for each atom are refined, and each has an s.u. Symmetry may, however, require that some parameters are fixed, because atoms lie on rotation axes, mirror planes or inversion centres; in this case, the s.u. of such a fixed parameter must be zero. This has an effect on the s.u.s of bond lengths and other geometry involving these atoms, which will tend to be smaller than they would be for refined parameters. If a co-ordinate of an atom has been fixed in order to define a floating origin in a space group with a polar axis (better methods are used in most modern programs), the effect will be to produce artificially better precision for the geometry around this atom.

Parameters that are equal by symmetry must have equal s.u.s. This applies both to the primary refined parameters (for example, atoms in certain special positions in high-symmetry space groups have two or more equal co-ordinates and relationships among some of the U^{ij} components), and also to the geometrical parameters calculated from them. A good test of the correctness of the calculation of geometry s.u.s by a program is to compare the bond lengths and their s.u.s for atoms in special positions in trigonal and hexagonal space groups!

If a bond length (or other geometrical feature) has been *constrained* during refinement, the s.u. of this bond length must necessarily be zero, even though the two atoms concerned will, in general, have non-zero s.u.s for their co-ordinates; this is a consequence of correlation: the covariance terms exactly cancel the variance terms in calculating the bond length s.u. from the co-ordinate s.u.s. A good example of such a situation is the 'riding model' for refinement of hydrogen atoms, where the C–H bond is held constant in length and direction during refinement. The C and H atoms have the same s.u.s for their co-ordinates (because they are completely correlated), and the C–H bond length has a zero s.u. By contrast, *restrained* bond lengths do have an s.u., because the restraint is treated as an extra observation and the two atoms are actually refined normally. It is instructive to compare the calculated bond length and its s.u. with the imposed restraint value and its weight, to see how valid the restraint is in the light of the diffraction data.

For a group of atoms refined as a 'rigid group', all internal geometrical parameters will have zero s.u.s. The actually refined parameters are the three co-ordinates for some defined point in the group (usually one atom or the centroid) and three rotations for the group as a whole. Thus, different atoms in the group should have different co-ordinate s.u.s (this is not the case with some refinement programs, which do not calculate these s.u.s correctly), and, once again, the effects of correlation and

covariance are such as to give the required zero s.u.s for the geometry of the group.

It is often overlooked that molecular geometry depends not only on the atomic co-ordinates, but also on the unit cell parameters, and they too are subject to uncertainties. Some refinement programs make no allowance for the uncertainties in the cell parameters, and the results can be ridiculous, especially for the geometry around heavy atoms. These usually have very low co-ordinate s.u. values, so bond lengths and angles calculated without regard to cell parameter uncertainties may have s.u.s proportionately very much smaller than the cell edge s.u.s! If explicit treatment of this effect is not included in your geometry calculation program, a simple hand adjustment can be made, by increasing s.u.s by an amount depending on the ratio of the cell edges to their s.u.s [$\sigma(a)/a$, $\sigma(b)/b$ and $\sigma(c)/c$]; this usually affects only the heaviest atoms in a structure of contrasting atomic scattering powers.

15.2.6 Assessing significant differences

In crystallography we quote the standard uncertainty in parentheses, for example 1.520(4) Å, for a bond length. The figure in parentheses refers to the last quoted decimal place, and in this example the standard uncertainty on our measurement of 1.520 Å is 0.004 Å; a measurement of 1.52(4) Å is ten times less precise. See also Chapter 16 for further discussion.

Application of arguments based on the normal distribution allows us to conclude that two parameters can be considered significantly different if their difference (Δ) is more than 3 times the standard uncertainty of the difference, i.e.

$$\frac{\Delta}{\sqrt{\sigma_1^2 + \sigma_2^2}} \geq 3, \tag{15.17}$$

where σ_1 is the s.u. on the first parameter. This is called the '3σ rule', but it is important to recognize that the s.u.s from crystal-structure refinement are often thought to be underestimated by a factor of 1.5 to 2, and so perhaps a 5σ rule is safer to use in practice.

15.3 Least-squares planes and dihedral angles

It is sometimes desirable to assess whether a number of atoms are actually all in one plane and, if not, how much they deviate from coplanarity; this is particularly the case for cyclic groups of atoms and for selected atoms co-ordinating a central metal atom. When more than one exact or approximate plane can be defined in a structure, the angles between pairs of planes may also be of interest.

The usual method of assessing the planarity of a group of atoms is to fit an exact plane to the atomic positions by a least-squares calculation; the plane is chosen so as to minimize $\sum_{i=1}^{n} w_i \Delta_i^2$, where Δ_i is the perpendicular distance of the ith atom from the plane, there are n atoms to be fitted, and each has relative weight w_i in the calculation. There are various methods of actually performing the calculation, which can also be expressed as a determination of one of the principal axes of inertia for the group of atoms. In the calculation, the weights used for the atoms should be proportional to $1/\sigma^2$, where σ^2 is the variance for the atomic position in the direction perpendicular to the required plane. As a reasonable approximation, an overall average positional σ^2 may be used for each atom, but even this is often not done and unit weights are used instead. A very crude approximate scheme weights atoms proportionally to their atomic numbers or atomic masses, since the heaviest atoms usually have the smallest positional s.u. values.

Calculation of a least-squares plane also provides a 'root-mean-square deviation' of the atoms from the plane

$$\text{r.m.s.}\Delta = \left(\frac{\sum_{i=1}^{n} w_i \Delta_i^2}{n} \right)^{1/2}, \tag{15.18}$$

and this quantity may be used to assess whether the deviations from planarity are significant. A standard statistical test (the χ^2 test) can be applied, but it is rare for any set of more than three atoms to be judged truly planar by this test (except for groups that are strictly planar by symmetry, such as four atoms related in pairs by an inversion centre). It is common to quote the deviations of individual atoms from the plane; these atoms may be among those used to define the plane itself, or may be other atoms. The calculation (and even the definition) of an s.u. for such a deviation is not obvious, and various accounts have been given. Generally, these involve considerable approximations and the neglect of correlation effects.

Deviations of atoms from a least-squares plane are a much more sensitive, and hence a better, estimate of whether the co-ordination about an atom is essentially planar, than is the sum of the bond angles at that atom. This sum will be quite close to 360° even for a markedly pyramidal three-co-ordinate atom or for a square-planar coordination with significant tetrahedral distortion.

The terms 'least-squares plane' and 'mean plane' are used synonymously by most crystallographers, although some authors have distinguished between them, giving them different definitions.

The angle between two planes is sometimes called a dihedral angle, though this term may also be used to mean the same as torsion angle, so some care is needed. We must also be aware of an ambiguity in defining the interplanar angle. The correct definition is the angle between the normals to the two planes, but where two lines cross a choice can be made between two possible angles, whose sum is 180°. Where the two planes concerned have two atoms in common, the dihedral angle

represents a fold about the line joining these two atoms (a 'hinge' or 'flap' angle), and it seems sensible to choose the angle enclosed by the two hinged planes (so that the angle would be 0° for a closed hinge and 180° for a fully opened hinge), but the choice of angle is less obvious in some other situations.

15.3.1 Conformation of rings and other molecular features

It is in describing molecular features such as co-ordination, planes and ring conformations that we move from unambiguous description to interpretation. The conformation of rings can be described in many ways (Dunitz, 1979). Common quantities used to describe ring conformations are torsion angles, atomic deviations from least-squares planes, and angles between these planes, and on the basis of such measures, rings are generally classified by such terms as chair, boat, twist, envelope, etc. Ring conformations can also be analyzed in terms of linear combinations of normal atomic displacements according to irreducible representations of the D_{nh} point group symmetry appropriate to a regular planar n-membered ring. Other analyses may be in terms of asymmetry parameters and puckering parameters, variously defined.

The shapes of co-ordination polyhedra around a central atom can also be difficult to describe, and we frequently see simple expressions such as 'distorted tetrahedral' or 'approximately octahedral', which may refer to extremely unsymmetrical arrangements! Attempts to quantify these descriptions have included definitions of 'twist angles' and other measures of the degree of distortion from regular co-ordination shapes.

15.4 Hydrogen atoms and hydrogen bonding

The distance between two atoms, together with its s.u., can be calculated regardless of whether the two atoms are considered to be bonded to each other. Distances between atoms in adjacent molecules may indicate significant intermolecular interactions, if they are shorter than some 'expected' or standard value (such as the sum of van der Waals radii for the atoms concerned). Short contacts involving a hydrogen atom and an electronegative atom are often examined as potential candidates for hydrogen bonding. There are, however, some pitfalls to be avoided here.

Firstly, hydrogen atoms are not very precisely located by X-ray diffraction, because of their low electron density. Thus, freely refined hydrogen atoms will have larger positional s.u.s than other atoms. Some computer programs list bond lengths with s.u.s, but non-bonded distances without any estimate of precision. The relatively low precision of these distances should not be overlooked in interpreting the distances themselves. Weak

hydrogen bonding is sometimes postulated when the experimental precision simply does not support it.

Secondly, hydrogen atom positions determined by X-ray diffraction do not correspond to true nuclear positions, because the electron density is significantly shifted towards the atom to which the hydrogen atom is covalently bonded. Thus, typical bond lengths for freely refined atoms are around 0.95 Å for C–H and under 0.90 Å for N–H and O–H, whereas true internuclear distances, obtained by spectroscopic methods for gas-phase molecules, or by neutron diffraction, are over 0.1 Å longer. In hydrogen bonding, the hydrogen atom lies roughly between its covalently bonded atom and the electronegative atom in a D–H…A arrangement, so a significant shortening error in the D–H bond length means an incorrectly long H…A distance. This is another reason why these distances should be interpreted with caution.

Thirdly, hydrogen atoms are constrained (or restrained) in many structure determinations, and their positions are, therefore, to a large extent dictated by pre-conceived ideas. Hydrogen bonding of any significance is likely, however, to perturb hydrogen atoms from 'expected' positions.

For these reasons, the D…A distance may often be a better (or at least a safer) indication of hydrogen bonding. In any case, possible hydrogen bonding that does not fit in with widely recognized patterns should be examined very carefully before it is presented to the public (Taylor and Kennard, 1984)!

15.5 Displacement parameters

Although the major interest in a structure determination usually centres on the geometry, derived from the atomic positions, the primary results also include the so-called 'thermal parameters'. It has been suggested that these describe not only the time-averaged temperature-dependent movement of the atoms about their mean equilibrium positions (dynamic disorder), but also their random distribution over different sets of equilibrium positions from one unit cell to another, representing a deviation from perfect periodicity in the crystal (static disorder) which is not great enough to be resolved into distinct alternative sites), and so they should rather be called 'atomic displacement parameters'. A refreshingly readable account has been written for a general chemical audience, and is strongly recommended (Dunitz *et al.*, 1988). See also Downs (2000).

Interpretation and analysis of displacement parameters is not often undertaken. One reason is that various systematic errors in the data, inappropriate refinement weights, and poor aspects of the structural model all tend to affect these parameters, whereas the atomic positions are much less perturbed (fortunately!). Thus, the 'anisotropic temperature factors' of a structure are often regarded as a sort of error dustbin, and their physical significance is questionable unless the experimental work is of good quality.

15.5.1 βs, Bs and Us

It is unfortunate that atomic displacements are described by a variety of different parameters, all of which are mathematically related. Thus, for an isotropic model, a single parameter is used, but this may be called B or U. These are related by

$$f'(\theta) = f(\theta)\exp(-B\sin^2\theta/\lambda^2) = f(\theta)\exp(-8\pi^2 U\sin^2\theta/\lambda^2), \quad (15.19)$$

where $f(\theta)$ is the scattering factor for a stationary atom and $f'(\theta)$ the scattering factor for the vibrating atom. B and U both have units of Å^2 and U represents a mean-square amplitude of vibration.

For an anisotropic model, six parameters are used, and the exponent $(-B\sin^2\theta/\lambda^2)$ becomes variously

$$\begin{aligned}
&-(\beta^{11}h^2 + \beta^{22}k^2 + \beta^{33}l^2 + 2\beta^{23}kl + 2\beta^{13}hl + 2\beta^{12}hk) \text{ or}\\
&-\tfrac{1}{4}(B^{11}h^2a^{*2} + B^{22}k^2b^{*2} + B^{33}l^2c^{*2} + 2B^{23}klb^*c^* + 2B^{13}hla^*c^* + 2B^{12}hka^*b^*) \text{ or}\\
&-2\pi^2(U^{11}h^2a^{*2} + U^{22}k^2b^{*2} + U^{33}l^2c^{*2} + 2U^{23}klb^*c^* + 2U^{13}hla^*c^* + 2U^{12}hka^*b^*)
\end{aligned} \quad (15.20)$$

The first form is most compact, but the six β terms are not directly comparable (the factor 2 in the three cross-terms is sometimes omitted, adding yet more confusion to the possible definitions!); the second form is equivalent to the isotropic B, and the third to the isotropic U expression.

These parameters are often represented graphically as 'displacement ellipsoids' or 'thermal ellipsoids'. Note that this is possible only if certain inequality relationships among the six parameters are satisfied; otherwise they are said to be 'non-positive-definite' and the corresponding ellipsoid does not have three real principal axes. Such a situation may indicate a real problem in the structural model (e.g. a disordered atom), or it may just be due to imprecise (high s.u.s) U^{ij} parameters, in which case the anisotropic model for this atom is perhaps not justified.

15.5.2 'The equivalent isotropic displacement parameter'

Tables of anisotropic displacement parameters are very unlikely to be published in most chemical journals, and their significance is difficult to assess at a glance. For a simple assessment of the atomic motions, it is convenient to calculate an equivalent isotropic parameter for each atom. Different definitions of U_{eq} abound, and some of them seem to be inappropriate (Watkin, 2000). Essentially, one version of the equivalent isotropic parameter is that corresponding to a sphere of volume equal to the ellipsoid representing, on the same probability scale, the anisotropic parameters. The definition '$U_{\text{eq}} = (1/3)$(trace of the orthogonalized U^{ij} matrix)' is a commonly used one, but its meaning is, perhaps, not entirely

clear! It can be expressed mathematically as (among other equivalent forms)

$$U_{\text{eq}} = \frac{1}{3}\sum_{i=1}^{3}\sum_{j=1}^{3} U^{ij} a_i^* a_j^* \mathbf{a}_i.\mathbf{a}_j, \tag{15.21}$$

where the direct and reciprocal cell parameter terms have the effect of converting the U^{ij} parameters into a form expressed on orthogonal rather than crystal axes.

A simple calculation of the s.u. for U_{eq} can be made from the s.u.s of the U^{ij} parameters, but it has been shown that a proper inclusion of covariance terms (correlations among the U^{ij} values), which are not always available after the refinement is complete, gives lower s.u. values, so the simply calculated values are of dubious worth.

15.5.3 Symmetry and anisotropic displacement parameters

Mathematically, the β values form a tensor, whereas the U and B values do not, and so transformations of displacement parameters are most simply applied to βs. If a symmetry operation involves a point operation $\mathbf{R}$, expressed as a 3×3 matrix, the βs transform as:

$$\boldsymbol{\beta}' = \mathbf{R}\boldsymbol{\beta}\mathbf{R}^T. \tag{15.22}$$

If an atom resides on a special position $\boldsymbol{\beta}' = \boldsymbol{\beta}$, and this may impose special values on or relationships between the components of $\boldsymbol{\beta}$. For example, for two atoms related by a two-fold rotational operation (i.e. 2 or 2_1) along [010],

$$\begin{aligned}\beta' &= \begin{pmatrix} -1 & 0 & 0 \\ 0 & 1 & 0 \\ 0 & 0 & -1 \end{pmatrix} \begin{pmatrix} \beta_{11} & \beta_{12} & \beta_{13} \\ \beta_{12} & \beta_{22} & \beta_{23} \\ \beta_{13} & \beta_{23} & \beta_{33} \end{pmatrix} \begin{pmatrix} -1 & 0 & 0 \\ 0 & 1 & 0 \\ 0 & 0 & -1 \end{pmatrix} \\ &= \begin{pmatrix} \beta_{11} & -\beta_{12} & \beta_{13} \\ -\beta_{12} & \beta_{22} & -\beta_{23} \\ \beta_{13} & -\beta_{23} & \beta_{33} \end{pmatrix}.\end{aligned}$$

If an atom resides on a two-fold axis along [010], then as the atom transforms into itself

$$\begin{pmatrix} \beta_{11} & \beta_{12} & \beta_{13} \\ \beta_{12} & \beta_{22} & \beta_{23} \\ \beta_{13} & \beta_{23} & \beta_{33} \end{pmatrix} = \begin{pmatrix} \beta_{11} & -\beta_{12} & \beta_{13} \\ -\beta_{12} & \beta_{22} & -\beta_{23} \\ \beta_{13} & -\beta_{23} & \beta_{33} \end{pmatrix},$$

so that $\beta_{12} = -\beta_{12}$ and $\beta_{23} = -\beta_{23}$, which is possible only if $\beta_{12} = \beta_{23} = 0$. Physically, this means that two axes of the displacement ellipsoid must be perpendicular to [010]. Least-squares refinement will become unstable if correct relationships are not applied as a constraint during refinement. Most modern refinement programs (e.g. SHELXL and CRYSTALS) will apply this automatically, but some will not.

15.5.4 Models of thermal motion and geometrical corrections: rigid-body motion

It is well known that one effect of thermal vibration is to produce an apparent shrinkage in molecular dimensions. Analysis of this effect and correction for it is possible only in certain cases.

If a molecule has only small internal vibrations (both bond stretching and angle deformations) compared with its movement as a whole about its mean position in a crystal structure, then it can be treated approximately as a rigid body. In this case, the movements of the individual atoms are not independent and so the U^{ij} parameters of the atoms must be consistent with the overall molecular motion. This motion can be described by a combination of three tensors (3×3 matrices): the overall *translation* (oscillation backwards and forwards in three dimensions), represented by the six independent components of a symmetric tensor T (analogous to the anisotropic U tensor for an individual atom); *libration* (rotary oscillation), represented also by a symmetric tensor L; and *screw* motion, represented by an unsymmetrical tensor S. This third contribution is necessary to describe the complete motion of a molecule that does not lie on an inversion centre in the crystal structure, because there is then correlation between translational and librational motion, such that the librational axes do not all intersect at a single point. The tensor S actually has only eight independent components, because the three diagonal terms are not all independent, so the whole molecular motion can be described by 20 parameters. Except for very small molecules (and some particular geometrical shapes), the six U^{ij} values for each atom provide more than enough data for a least-squares refinement to determine these 20 parameters, and the agreement between observed and calculated U^{ij} values gives a measure of the usefulness of the rigid-body model.

From the rigid-body parameters, corrections can be calculated for bond lengths within the molecule; these depend only on the librational tensor components.

Although many molecules can not be regarded as even approximately rigid, it may be possible to treat certain groups of atoms within them as rigid bodies, and make corrections within those groups.

It is possible to test whether a molecule, or part of a molecule, might be regarded as a rigid body (Hirschfeld, 1976). If a pair of atoms (whether bonded together directly or not) behaves as part of a rigid group, then they must remain at a fixed distance apart during their concerted motion. In this case, the components of their individual anisotropic vibrations along the line joining them must be equal. Thus, a 'rigid atom-pair' test computes these components of anisotropic motion:

$$\left\langle U^2 \right\rangle = U^{11}d_1^2 + U^{22}d_2^2 + U^{33}d_3^2 + 2U^{23}d_2d_3 + 2U^{13}d_1d_3 + 2U^{12}d_1d_2, \tag{15.23}$$

where $\langle U^2 \rangle$ is the mean-square amplitude of vibration along a line that has direction cosines d_1, d_2, d_3 referred to reciprocal cell axes. Equality

or near-equality of the $\langle U^2 \rangle$ values for the two atoms is a necessary (but not sufficient) condition for rigidity. This can be used as a test for rigid bonds and for rigid bodies (the test must work for every pair of atoms in the group being tested). It can also be used as the basis of a restraint on U^{ij} values in structure refinement.

15.5.5 Atomic displacement parameters and temperature

Although the U^{ij} parameters of the atoms probably do not describe only thermal vibration effects, as noted above, they are usually strongly temperature dependent, and they can be drastically reduced by carrying out data collection at a lower temperature. With reliable low-temperature apparatus now available for X-ray diffractometers, this approach is strongly to be recommended. Low-temperature data usually give greater precision in atomic positions, more reliable molecular geometry, and an opportunity to assess and distinguish between dynamic and static disorder: the former will be reduced at lower temperature, the latter will probably not. Although we are concerned in this chapter with the analysis of results, we should bear in mind that this analysis can be greatly helped by an improvement in the experimental measurements!

References

Downs, R. T. (2000). *Rev. Min. Geochem.* **41**, 61–87.
Dunitz, J. D. (1979). *X-ray analysis and the structure of organic molecules.* Cornell University Press, Ithaca.
Dunitz, J. D., Maverick, E. F. and Trueblood, K. N. (1988). *Angew. Chem. Int. Ed. Engl.* **27**, 880–895.
Hirshfeld, F. L. (1976). *Acta Crystallogr.* **A32**, 239–244.
Taylor, R. and Kennard, O. (1984). *Acc. Chem. Res.* **17**, 320–326.
Watkin, D. J. (2000). *Acta Crystallogr.* **B56**, 747–749.

Exercises

1. The following was given in the output of CELL_NOW after indexing a twinned crystal:

```
Cell for domain 2:  6.055   5.340   7.235   89.82
113.51  90.11
Figure of merit: 0.432  %(0.1): 36.1   %(0.2): 38.9
%(0.3): 49.7
Orientation matrix:  0.03526080  0.18122675  -0.01073746
                    -0.17602921  0.03347900  -0.07420789
                    -0.01420090  0.03333605   0.13075234
Rotated from first domain by 179.9 degrees about
reciprocal axis 1.000 -0.001 0.001 and real axis
1.000 -0.001 0.334
Twin law to convert hkl from first to this domain
(SHELXL TWIN matrix):
 0.999  -0.002   0.668
-0.003  -1.000  -0.002
 0.002   0.003  -0.999
```

   The twin law is described as a two-fold rotation about the reciprocal lattice vector (1 0 0) and the direct lattice vector [3 0 1] (which is parallel to [1 0 1/3]). Show that these are equivalent descriptions of the same vector.

2. A structure has been solved in $Pna2_1$, but symmetry checking shows that the correct space group is $Pnma$. What matrices should be used to transform the reflection indices and the co-ordinates?

3. Two metal–oxygen bond lengths were found to be 2.052(5) and 2.032(4) Å. Are these significantly different?

4. Oxalyl chloride is monoclinic, with cell dimensions $a = 6.072(4)$, $b = 5.345(3)$, $c = 7.272(4)$ Å, $\beta = 113.638(7)°$. The fractional co-ordinates of the C and O atoms are:

```
O(1)    0.3854(2)   0.2109(2)   0.3029(2)
C(1)    0.5256(3)   0.1173(2)   0.4497(2)
```

   Evaluate the C(1)–O(1) distance. Do not attempt to evaluate the s.u.

5. Which of these symmetry elements make a four-membered MLML ring strictly planar? In each case, how many bond lengths are independent?

   (i) an inversion centre;
   (ii) a two-fold axis normal to the mean plane of the ring;
   (iii) a two-fold axis through the two M atoms;
   (iv) a mirror plane through the M atoms but not through the L atoms;
   (v) a mirror plane through all four atoms.

6. A six-co-ordinate atom lies on an inversion centre. How many independent bond lengths and angles are there around this atom?

7. If an atom resides on a mirror plane perpendicular to [1 0 0] (i.e. the *a*-axis) what constraints should be applied to its anisotropic displacement parameters?

8. Discuss the placement of H atoms on:

   (i) terminal hydroxyl groups ;
   (ii) ligating water molecules;
   (iii) unco-ordinated molecules of water of crystallization.

This page intentionally left blank

Random and systematic errors

16

Simon Parsons and William Clegg

16.1 Random and systematic errors

Statistics find application throughout data reduction, structure analysis and the interpretation of results. The aim of this chapter is to outline some basic statistical methods and concepts and to illustrate their importance in crystallography. This is an immense subject, and we shall not deal, for instance, with intensity statistics, or the ways in which statistics are used in direct methods. Particularly good references on the use of statistics in the physical sciences have been written by Barlow (1997), Hamilton (1964), and Bevington and Robinson (2003); these texts should be consulted for more in-depth treatments.

If we measure some quantity experimentally (for example, a bond length or a structure-factor amplitude), our observation will inevitably suffer from some sort of error. Uncertainties or random errors are introduced by random fluctuations; these can be minimized, but never eliminated, by careful experimental design. Systematic errors cause measurements to deviate from their true values because of some physical effect (which we may or may not be aware of). As an example of the contrast, consider the measurement of a distance by means of a wooden metre rule. If the distance is measured by different people, or repeatedly by one person, the separate measurements are likely to vary somewhat; this variation constitutes a random error in the measurement. If, however, the first 2 cm of the metre rule have been sawn off and this is not noticed, the measurements will be subject to a systematic error affecting all of them equally. When measuring X-ray diffraction intensities random errors might arise from the random fluctuation of a low-temperature device, or in the cooling cycle of a CCD chip, and systematic errors from the influences of absorption or crystal mis-centring. Systematic errors may also be introduced into the results of a structure determination by the models and methods used in structure determination (e.g. incorrect atomic scattering factors, inappropriate atomic displacement parameters, wrong space group symmetry).

At this stage we should also distinguish carefully between *precision* and *accuracy*. The accuracy of an experiment is a measure of how close the result is to its true value. The precision is a measure of the reproducibility of a result and therefore of how confidently the result can be defined. Truly random errors affect the precision but not the accuracy of measurements and results. Depending on their exact nature, systematic errors may or may not affect precision, but they do affect accuracy, and so high precision is not of itself an indication of a 'good' result.

The precision of a measured quantity can be expressed by its standard uncertainty, s.u. (also called its standard deviation or estimated standard deviation, e.s.d.). In crystallography we quote the standard uncertainty in parentheses, for example 1.520(4) Å for a bond length. The figure in parentheses refers to the last quoted decimal place, and in this example the standard uncertainty on our measurement of 1.520 Å is 0.004 Å; a measurement of 1.52(4) Å is ten times less precise. Instead of 1.520(4) we might have written 1.520 ± 0.004 Å, but this is an unfortunate notation as it appears to specify a strict range for the bond length. While this is what engineers *do* mean by this notation, the correct interpretation in crystallography, and the physical sciences generally, is rather more subtle.

Random errors can be treated by statistical analysis of how these errors are distributed about zero, and this is why probability distributions have assumed such importance in crystallography. Systematic errors can not be treated by such a general theory, and each source of error must be identified and its effect modelled by consideration of its physical nature.

16.2 Random errors and distributions

16.2.1 Measurement errors

The existence of random error means that whenever we make a measurement of a quantity, x, what we actually measure is

$$x_i = x_{\text{true}} + \varepsilon_i,$$

where, in the absence of systematic errors, x_{true} is the true, accurate, value of x, and ε_i is a random measurement error. If we were to measure x again, our measurement would be slightly different because the random error ε_i would not be the same as when we made our first measurement. We can never know x_{true}, but we can estimate its value, and obtain some idea of the quality of our estimate. We do this by making multiple measurements of x, and applying statistics.

16.2.2 Describing data

Consider the data below, which are the F^2 values measured for equivalents of the 114 reflection of N_2O_4 taken directly from an *hkl* data file

after application of an absorption correction. N_2O_4 is is cubic (space group $Im\bar{3}$), and the redundancy is unusually high ($N = 67$).

```
INTENSITIES OF THE 114 REFLECTION.  N=67
1684.78 1787.27 1794.81 1807.33 1819.65 1825.30 1853.30
1743.72 1788.16 1796.12 1807.53 1819.81 1826.18 1854.28
1756.32 1788.23 1798.56 1807.54 1819.88 1827.00 1856.05
1761.98 1788.50 1801.34 1808.86 1820.28 1830.38 1867.75
1767.55 1789.60 1802.79 1812.50 1821.31 1830.85 1872.35
1767.86 1789.69 1804.08 1813.05 1821.57 1832.63 1881.82
1772.06 1793.45 1804.38 1813.05 1822.44 1834.59 1902.13
1772.38 1793.93 1804.49 1813.54 1823.11 1836.25 1784.30
1794.50 1804.54 1814.43 1823.32 1837.49 1784.60 1794.52
1804.75 1819.36 1823.51 1841.55
```

A histogram illustrating these data is given in Fig. 16.1. Notice that, although the range of F^2 is 1684 to 1902, most measurements clump together in the middle of the range, with relatively few at the extremes. This is a description of the *distribution* of the data.

In some distributions the individual data can take only certain values: for example, the number of photons counted by a detector, or the number of people in a particular age group, must be integral. A case where the values that can be taken by members of the distribution are only certain discrete ones gives rise to a *discrete distribution*. By contrast, the data that make up the elements of the distribution in Fig. 16.1 can adopt any value (e.g. 1684.78 or 1787.27), and this yields a *continuous distribution*.

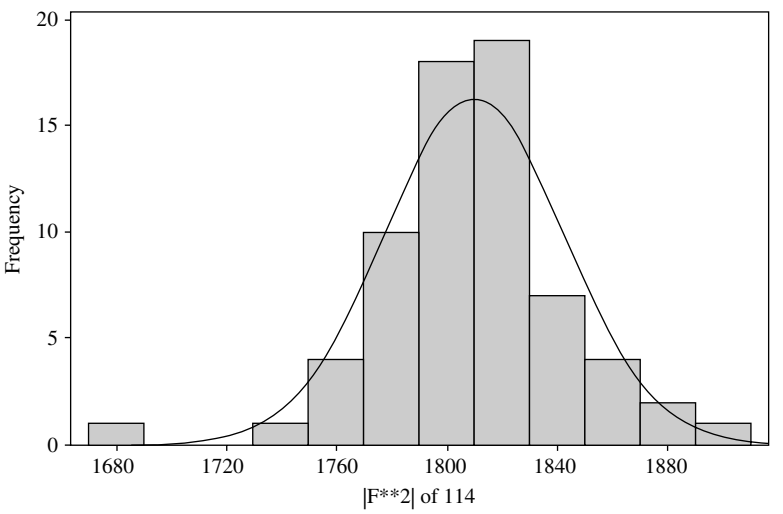

Fig. 16.1 Histogram showing intensities of the 114 reflection, superimposed on a curve of the corresponding ideal normal distribution (see Section 16.2.3).

If we measured all the x_i that it is possible to measure, which may mean making an infinite number of measurements, then we could specify exactly the form of a distribution. This is called the *parent distribution*. In general this is not possible, and the best we can do is to measure a *sample distribution*.

The two most important quantities that characterize a distribution are the *mean* $\overline{x}$ and the *variance* σ^2 (the square of the *standard deviation*). The mean is what we loosely call the 'average' value of the variable, x_i, taken from N different measurements:

$$\overline{x} = \frac{1}{N}\sum_{i=1}^{N} x_i. \tag{16.1}$$

The symbol μ is also often used for the mean, but it is best to distinguish between μ for the true (unkown) mean of the complete parent distribution and $\overline{x}$ for the sample mean. In the distribution shown in Fig. 16.1 x_i are the individual values of F^2, and $N(= 67)$ is the number of reflections in the data set. The variance of the sample distribution is defined as

$$\sigma^2 = \frac{1}{N-1}\sum_{i=1}^{N} (x_i - \overline{x})^2, \tag{16.2}$$

and is a measure of the width or spread of the distribution over the different values of x. The variance is the square of the standard deviation σ, and σ is often called the *sample standard deviation*. Equations (16.1) and (16.2) give our best estimates of the true mean and standard deviation of a parent distribution based on data taken from a sample distribution.

The term $N - 1$ appears in (16.2) because calculation of the mean has removed one *degree of freedom* from the calculation. It is sometimes replaced simply by N, though this is strictly correct only for complete distributions and not for sample distributions; on calculators these alternatives may be designated σ_{N-1} and σ_N, respectively. Press *et al.* (1991) say that *if this distinction ever matters to you, then you are probably up to no good…trying to substantiate a questionable hypothesis with marginal data*.

All observations in a set of repeated measurements will contribute equally to the mean and standard deviations given in (16.1) and (16.2). However, it is often the case that individual observations will have some measure of their precision; for example, values of $\sigma(F^2)$ are available from counting statistics or profile fitting for each reflection in a dataset, while a set of bond lengths to be averaged will also have a standard uncertainty calculated after least-squares refinement. In these cases it may be appropriate to weight the calculation of the mean:

$$\overline{x} = \frac{\sum w_i x_i}{\sum w_i}. \tag{16.3}$$

The standard deviation can be calculated using either:

$$\sigma^2 = \frac{N}{\sum w_i}, \tag{16.4}$$

or

$$\sigma^2 = \frac{N}{N-1}\frac{\sum w_i(x_i - \overline{x})^2}{\sum w_i}. \tag{16.5}$$

The first is more common, but in the crystallographic intensity data-merging program SORTAV, for example, where these quantities are referred to as σ^2_{ext} and σ^2_{int}, both are calculated and the larger of the two taken (Blessing, 1997). Choice of weights, w_i, has become something of a subdiscipline of statistics (see Section 16.4), but a common choice when averaging a set of measurements x_i with precision $\sigma(x_i)$ is to use $w_i = 1/\sigma^2(x_i)$.

Other quantities that may be quoted are the median, mode, skewness and kurtosis (or curtosis) of the data. The median of a sample of data values is the middle value of the data set when the values are placed in ascending order. If the sample size is even, then the median is defined as being half-way between the two middle values. The median is important because it is less sensitive to large *outliers* than the mean. As an illustration, suppose the set of measurements was made for a particular quantity: 0.9, 1.1, 1.2, 1.5, 10.0. The value 10.0 is obviously an outlier (a mistake). The outlier strongly affects the value of the mean: 2.94 with the outlier, 1.18 without. The median, by contrast is affected much less: 1.2 with the outlier, 1.15 without. This property is called *robustness*.

The mode is the most common value in a set of data, corresponding to the maximum in a histogram. The sample skewness is a measure of the symmetry of a distribution, and the kurtosis measures its peakiness. Formulae are given in statistics text books [e.g. Barlow (1997), p.14]. Values of the mean, sample standard deviation, median, skewness and kurtosis for the data in Fig. 16.1 are given in Table 16.1. The negative skew means that the data tail off to the left; the kurtosis value is interpreted below.

Table 16.1. Statistical descriptors for the intensities of the 114 reflection.

Mean, $\overline{x}$	1809.9
Sample standard deviation, σ	32.8
Median	1808.9
Skew	−0.39
Kurtosis	3.02
Number of data	67

The mode, skewness and kurtosis seem to be encountered rather rarely in crystallography. Indeed Barlow (1997) says: *Kurtosis is not used much by physicists, chemists, or indeed anyone else. It is a really obscure and arcane quantity whose main use is inspiring awe in demonstrators, professors or anyone else you are trying to impress.*

16.2.3 Theoretical distributions

The shape of the histogram in Fig 16.1 can be described using a mathematical function called a *probability distribution function*, or *pdf*. There are many such functions, some familiar ones being the binomial, Poisson, normal, and uniform distributions. By far the most important in

crystallography (indeed in the physical sciences generally) is the *normal distribution*, which is also called the *Gaussian distribution*.

The mathematical expression for this very important distribution is

$$P(x;\mu,\sigma) = \frac{1}{\sigma\sqrt{2\pi}} \exp\left(-\frac{(x-\mu)^2}{2\sigma^2}\right), \tag{16.6}$$

where μ and σ^2 are the mean and variance, respectively. $P(x;\mu,\sigma^2)$ is the probability of measuring a particular value x given the mean and variance. The distribution is said to be *indexed* on the mean and variance. The distribution is symmetrical about its mean, and the function calculated with $\mu = 1809.9$ and $\sigma = 32.8$ is superimposed on the histogram in Fig. 16.1. The main characteristics of a normal distribution are shown in Fig. 16.2. The values of the skew and kurtosis for a normal distribution are both 0. The fact that the data in Fig. 16.1 have a positive kurtosis (Table 16.1) means that the data are more sharply peaked than a normal distribution: they are *leptokurtic* as opposed to *platykurtic*.

Equation (16.6) can be used to evaluate the probability of measuring F^2 to be 1801 (say): it is only 0.012. This seems odd at first sight, since from the appearance of the histogram 1801 looks quite likely. But it is important to recall that we are dealing with a continuous distribution, and it is more meaningful to evaluate the probability that x lies in a specified range x_1 to x_2; this is $\int_{x_1}^{x_2} P(x)dx$. The probability of measuring F^2 between 1798 and 1804 is:

$$\frac{1}{32.8\sqrt{2\pi}} \int_{1798}^{1804} \exp\left(-\frac{(x-1809.9)^2}{2\times 32.8^2}\right) dx = 0.070,$$

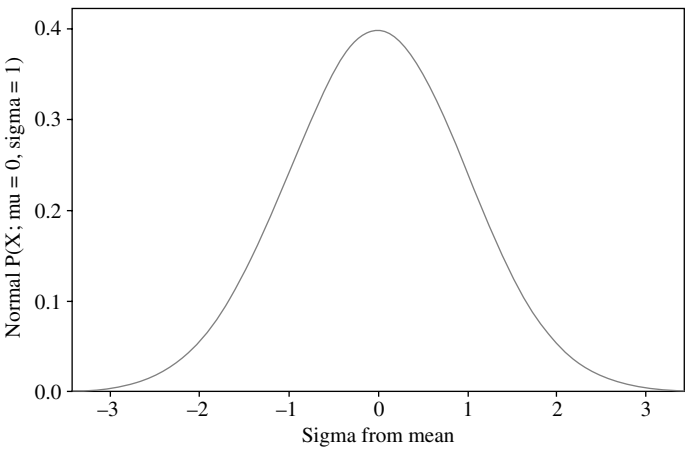

Fig. 16.2 The normal distribution calculated with a mean of 0 and a standard deviation of 1. 68.3% of a normal distribution lies within $\pm 1\sigma$ of the mean, and the interval $\pm 3\sigma$ encloses 99.7% of the total distribution.

or 7% [if we measured 100 equivalents we would expect 7 of them to lie between 1798 and 1804]. Statistics books (e.g. Barlow, 1997, p. 38) tabulate integrals of the normal distribution within $\pm(x-\mu)/\sigma$ from the mean. 1801 is $(1809.9 - 1801)/32.8 = 0.27\sigma$ from the mean, and tables give the probability of measuring a value within 0.27σ of the mean to be 21.28%. 68.27% of the area under the curve lies between $\pm 1\sigma$, and 99.73% between $\pm 3\sigma$ (this forms the basis for the '3σ rule' for assessing significant differences, see Section 15.2.6). Note that the total probability for all possible values of x is 1:

$$\int_{-\infty}^{\infty} P(x)dx = 1. \tag{16.7}$$

The normal distribution is particularly important because of an effect expressed by the *Central Limit Theorem*. Suppose we have a set of N independent variables x_i; each variable belongs to its own population with mean μ_i and variance σ_i^2. The function

$$y = \sum_{i=1}^{N} x_i \tag{16.8}$$

has a distribution that, as N becomes very large, approaches a normal distribution with mean and variance

$$\mu_y = \sum_{i=1}^{N} \mu_i \quad \text{and} \quad \sigma_y^2 = \sum_{i=1}^{N} \sigma_i^2, \tag{16.9}$$

whether the individual variables x have normal distributions or not. Figure 16.3 shows the central limit theorem in action: the top figure is a histogram of 100 random numbers taken from a uniform distribution, the lower figure is a histogram of the sum of 10 such sets of random numbers. Although each of the 10 sets of random numbers has a uniform distribution their sum has a normal distribution.

It is generally assumed that the experimental determination of the value of a particular quantity is subject to a large number of independent sources of small errors. All of these contributing errors are summed to form the ε_i in some measured quantity. Because of the central limit theorem, the ε_i values are normally distributed.

16.2.4 Expectation values

The expectation value, $\langle f(x)\rangle$, of any function $f(x)$ can be calculated provided its pdf, $P(x)$, is known:

$$\langle f(x)\rangle = \int_{-\infty}^{\infty} f(x)P(x)dx. \tag{16.10}$$

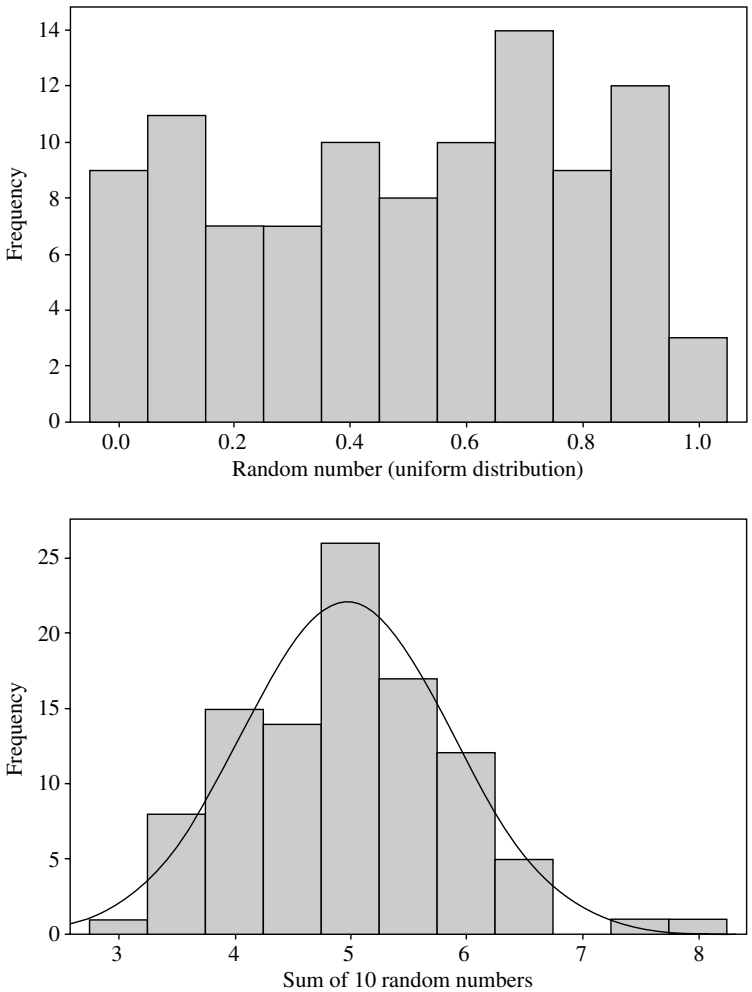

Fig. 16.3 The central limit theorem in action.

The mean of a distribution is the expectation value of x:

$$\langle x \rangle = \int_{-\infty}^{\infty} xP(x)dx, \tag{16.11}$$

and this is equal to μ for a normal distribution. The variance is the expectation value of $(x - \mu)^2$; this is σ^2 for a normal distribution. The quantity $\int_{-\infty}^{\infty} x^r P(x)dx$ is called the rth moment of a pdf.

Another illustrative example of the use of expectation values is in the calculation of E-statistics in ideal intensity distributions. For a centrosymmetric structure, Wilson (1948) showed that the values of $|E|$

follow a normal distribution:

$$P_{-1}(|E|) = \sqrt{\frac{2}{\pi}} \exp\left(\frac{-|E|^2}{2}\right).$$

Therefore

$$\langle |E^2 - 1| \rangle = \sqrt{\frac{2}{\pi}} \int_0^\infty |E^2 - 1| \exp\left(\frac{-|E|^2}{2}\right) dE = 2\sqrt{\frac{2}{\pi}} \exp\left(\frac{-1}{2}\right) = 0.968.$$

For a non-centrosymmetric structure

$$P_1(|E|) = 2|E| \exp\left(-|E|^2\right),$$

and

$$\langle |E^2 - 1| \rangle = 2 \int_0^\infty |E^2 - 1||E| \exp\left(-|E|^2\right) dE = \frac{2}{e} = 0.736.$$

Note that the integration limits here are 0 and ∞ as this is the range of $|E|$.

16.2.5 The standard error on the mean

Suppose we make N separate measurements of a quantity x. The measured values $x_1 \ldots x_N$ are a sample from all the possible measurements we could make, which follow some unknown distribution $P(x)$. For sufficiently large N, a consequence of the central limit theorem is that the mean $\overline{x}$ of our N sample values is normally distributed with the same mean μ as the parent population (all possible measurements) and with variance

$$\sigma^2(\overline{x}) = \frac{\sigma^2}{N}. \tag{16.12}$$

By 'variance of the mean $\overline{x}$' we understand the variance we would obtain by taking many such samples, calculating the mean $\overline{x}$ for each separate sample, and then looking at the distribution (mean and variance) of these individual sample means. The factor N in (16.12) means that the standard error on the mean can become very small for large numbers of observations, and it is extremely important to question the validity of the assumption that the data are drawn from the same parent distribution.

16.3 Taking averages

The mean and standard deviation can always be calculated from a set of numbers, such as a set of bond distances, and it is very tempting to do

this. Two questions arise: (i) is it better to use (16.1) or (16.3) to calculate the mean, and (ii) is such an average meaningful?

Taylor and Kennard (1983) showed that a weighted mean (16.3) is appropriate if the variation in the values to be averaged is mainly due to experimental random errors, so that the observed values are normally distributed about their mean. They illustrated their analysis using twelve C=N bond distances taken from a number of different crystal structures of adenine derivatives. The distance data were as listed in Table 16.2.

Table 16.2. Bond-distance data (in Å) for weighted mean calculation. Taken from Taylor and Kennard (1983).

1.315(3)	1.378(29)
1.311(3)	1.325(30)
1.322(12)	1.314(30)
1.329(12)	1.333(32)
1.347(21)	1.294(45)
1.301(23)	1.315(45)

The weighted mean calculated using (16.3), (16.4) and (16.12) and $w_i = 1/\sigma^2(x_i)$ is 1.314(2) Å. In order to assess whether this is valid we need to test for normality in the bond-distance data in Table 16.2.

16.3.1 Testing for normality using a histogram

One obvious test for normality is to plot the data and see if the resulting histogram looks like a normal distribution. Figure 16.4 shows this for the data in Table 16.2.

There are only 12 data here, but the histogram is highest in the middle and there is only one maximum, which is what we would expect for normally distributed data. A more quantitative test is described below.

Often, histograms can be multimodal (i.e. have two or more maxima): in such cases it is meaningless to calculate an average. An extreme example is shown in Fig. 16.5, a histogram of all the CN distances in organic molecules in the Cambridge Structural Database (Allen, 2002). We could calculate the average of these data to be 1.3967 Å, with a standard error on the mean of 0.0002 Å. This appears very precise because there are a lot of CN distances in the CSD (212 914), and so a large number goes into the denominator of (16.12). This is utterly meaningless because the

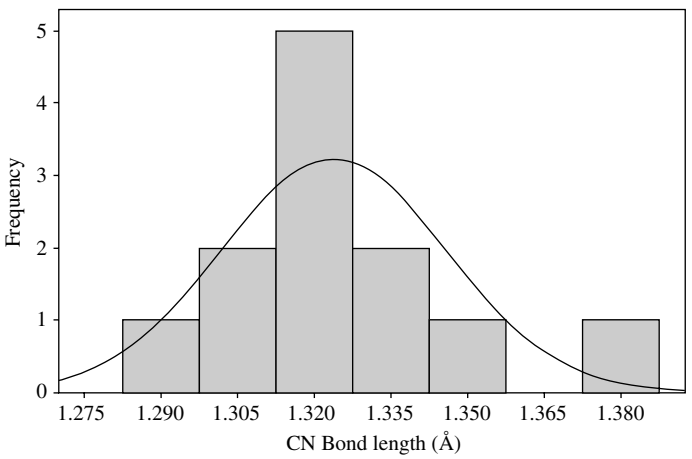

Fig. 16.4 Histogram of the data in Table 16.2; a normal distribution pdf has been superimposed.

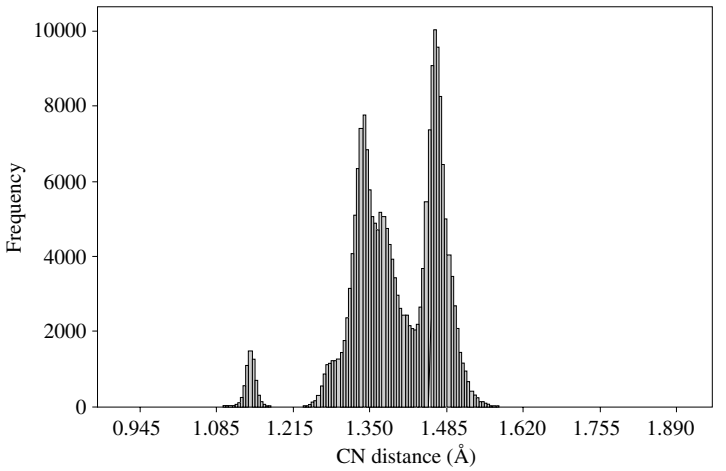

Fig. 16.5 Histogram of CN distances in the CSD.

histogram actually contains data on CN single, double, triple and delocalized bonds. It is as though we had an apple and a banana and tried to determine the average fruit. Just because we can do a calculation does not guarantee that the result is meaningful.

16.3.2 The χ^2 test for normality

A more quantitative test for normality is to calculate the value of χ^2:

$$\chi^2 = \sum w_i (x_i - \bar{x})^2, \tag{16.13}$$

where w_i are the weights used to calculate the weighted mean.

The expectation value of χ^2 is $N - P$ where N is the number of observations and P is the number of parameters that needed to be determined from the set of numbers before χ^2 could be calculated. $N - P$ is referred to as the *number of degrees of freedom*, and in the case of determining a mean, only one parameter, the mean, has had to be determined, so $P = 1$. It is convenient to define a *reduced* χ^2

$$\chi^2_{\text{red}} = \frac{\chi^2}{N - P}, \tag{16.14}$$

which has an expectation value of 1.

For Taylor and Kennard's data the value of χ^2 is 11.66, and the number of degrees of freedom $12 - 1 = 11$, therefore $\chi^2_{\text{red}} = 1.06$. The fact that this is near 1 means that we can conclude that the errors in the data are normally distributed. In fact we can assign a probability to the previous statement, and this is discussed in specialist text books on statistics (e.g. Barlow, 1997; page 150).

The normality of a distribution can also be tested with a normal probability plot, and this is discussed below in Section 16.4.3.

16.3.3 Averaging data when $\chi^2_{\mathbf{red}} \gg 1$

When the variation in a sample is mainly due to environmental effects, such as crystal-packing effects on bond distances, the mean should be calculated using (16.1). The standard deviation, σ(sample), should be calculated using (16.2), i.e. the sample standard deviation should be quoted, not the standard deviation on the mean. Taylor and Kennard (1983) argue that, if each measurement has its own standard deviation, it is better to estimate the standard deviation using

$$\sigma^2 = \sigma^2(\text{sample}) - \overline{\sigma^2(x_i)}, \tag{16.15}$$

though the second term (the average variance of the measurements) is usually so much smaller than the first that it makes little difference.

The C=N bond distances in adenine derivatives, for example, appear to be rather insensitive to crystal-packing forces, and this may be described as a 'hard' geometrical parameter. Other parameters, such as metal–metal bond lengths in clusters, bond angles, torsion angles, and intermolecular contact distances, are much more variable and subject to environmental effects. Such parameters may be described as 'soft'. It is important to remember that an average value is meaningless for a set of parameters that are not really equivalent (i.e. they do not belong to the same normal distribution). Even for bonds that appear to be chemically similar, statistical equivalence may not be found. In such cases, it is better to quote a range of values, but if you feel driven to calculate an average anyway, use (16.1) for the mean, and σ (sample) (16.2) for its standard deviation.

16.4 Weighting schemes

Weighting schemes occur throughout crystallographic calculations, such as merging of data, least-squares refinement, and analysis of results. In the following section we will discuss the use of weighting schemes in refinement.

It may seem odd to start discussing least-squares refinement in a chapter on statistics and errors. However, least squares is one form of *estimation*, a technical term used in statistics to refer to the derivation of numerical quantites from a sample set of data. The mean and standard deviation are two *estimators*, and when, for example, intensity data are merged using (16.3), we are deriving an *estimate* (using the word in its technical sense) of the intensity of a reflection given a sample set of data.

Least squares is the most important estimation procedure in physical science. In least squares we *estimate* numerical values of parameters from a dataset, including co-ordinates, displacement parameters, standard uncertainties *etc*.). We minimize a quantity

$$\chi^2 = \sum w_i(Y_\text{o} - Y_\text{c})^2 = \sum w\Delta^2, \tag{16.16}$$

where $Y = F^2$ or F. Comparison of (16.16) with (16.13) should convince you of the link that exists between refinement and statistics.

We have already seen that it is important to be sure that data belong to the same parent distribution before averaging them and calculating a standard error on the mean. It can also be shown that use of least-squares formulae implicitly assumes that the measurement errors in Y_o are normally distributed (compare (16.16) with the exponent in (16.6)). This is a fair assumption, because intensity measurements are subject to many small sources of error, and so the central limit theorem will make overall errors follow a normal distribution, as required. However, the central limit theorem works better at the centre of a distribution than in the tails, and it is common in real datasets to find data further away from the mean than would be expected if real measurement errors were truly normally distributed. This means that although the w_i are conventionally chosen to be $1/\sigma^2(Y_i)$ in data merging and refinement, the $\sigma^2(Y_i)$ may not in fact be the best estimates for the errors in our measurements.

16.4.1 Weights used in least-squares refinement with single-crystal diffraction data

Figure 16.6 shows a histogram of values of $(F_o^2 - F_c^2)/\sigma(F_o^2)$ calculated after refinement of the crystal structure of serine hydrate. According to the theory of the normal distribution, if our σs really are a good estimate of our measurement errors, there should be essentially no data with $|(F_o^2 - F_c^2)/\sigma(F_o^2)| > 3$, but in fact there are lots, including some enormous outliers.

Extra errors can come from uncorrected systematic errors (particularly absorption and extinction) that are turned into apparent random errors

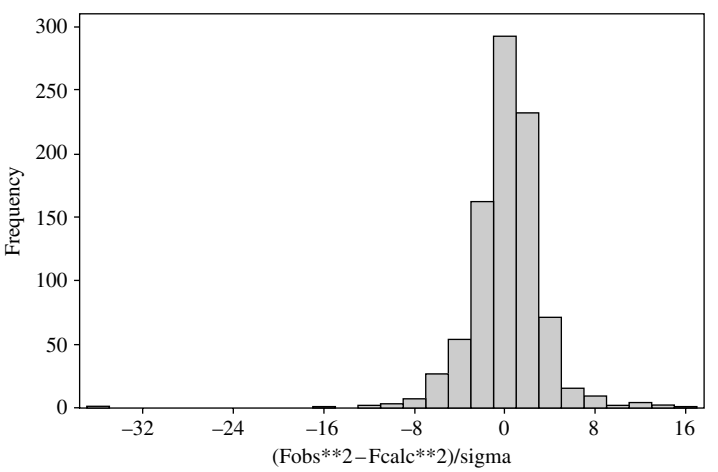

Fig. 16.6 The variation of $(F_o^2 - F_c^2)/\sigma(F_o^2)$ taken from the refinement of the crystal structure of the amino acid serine hydrate.

after merging. Conventional crystallographic models are also incapable of fully reproducing observed diffraction patterns because of the use of spherical atom scattering factors and harmonic approximations for thermal motion (see Section 16.7). If our measurement errors were really normal we could just weight on $\sigma^2(Y_i)$. Since they are not, to put no finer point on it, we fiddle the σs!

One way to modify the σs is to recognize that the biggest errors (extinction and absorption) are associated with the strong data, and to increase the $\sigma^2(F_i^2)$ according to

$$\sigma^2(F^2) + aF_o^2, \tag{16.17}$$

where a is chosen in such a way as to produce a more satisfactory plot than that shown in Fig. 16.6 (a is often between 0.1 and 0.01). Crystallographers used to do this until Wilson (1976) showed that using F_o like this induced bias in the refined parameters. Use of F_c instead also induced bias but only about half as much and in the opposite sense. To take account of this, $\sigma^2(F_i^2)$ is changed to $\sigma^2(F^2) + a(F_o^2 + 2F_c^2)/3$. This is the basis of the weighting scheme devised by Sheldrick (2008) for use in SHELXL:

$$w_i = \frac{1}{\sigma^2(F_o^2) + (aP)^2 + bP}, \tag{16.18}$$

where $P = (F_o^2 + 2F_c^2)/3$ and a and b are chosen to make χ^2_{red} constant over bins of data grouped according to intensity or resolution (a so-called *flat analysis of variance*; see Section 16.4.3).

A completely different approach (Carruthers and Watkin, 1979) is to throw away the σs altogether, and to fit a graph of $(Y_o - Y_c)^2$ versus Y_c^2 to some function. The inverted function then becomes the weighting scheme, so guaranteeing a flat analysis of variance.

16.4.2 Robust-resistant weighting schemes and outliers

Although most data in a set of measurements usually have errors that follow a normal distribution, some data will be poorly measured, and should be thrown away. Such data appear on their own well away from the centre of a distribution, and they are referred to as *outliers*. An example of such an outlier is the intensity measurement of 1684 in Fig. 16.1.

We saw above that aberrant data points can affect the value mean. They can also seriously affect parameter estimates in least-squares refinement. The mean and least-squares calculations are said not to be *robust*, and it is important therefore to remove outliers from crystallographic procedures such as merging and refinement.

One method for identifying outliers is by application of Chauvenet's criterion (Bevington and Robinson, 2003), which states that, provided the data follow a normal distribution, we should eliminate a data point if we expect less than half an event to be further from the mean than the

Table 16.3. Comparison of normal and robust-resistant weight-modifier functions. Taken from Blessing (1997).

z	$\exp(-z_i^2/2)$	$[1-\min(1,(z_i/6)^2)]^2$
0	1	1
1	0.5625	0.945
2	0.135	0.790
3	0.011	0.5625
4	3.3×10^{-4}	0.309
5	3.7×10^{-6}	0.093
6	1.5×10^{-8}	0
7	2.3×10^{-11}	0

suspect point. The most extreme point in the 114 data set is at 1684.87, or 3.81σ from the mean. How many data would we expect beyond this point? Tables that list values of the integral

$$\frac{1}{\sqrt{2\pi}}\int_{-z}^{+z}\exp\left[-\frac{z^2}{2}\right]dx \tag{16.19}$$

are available in most statistical text books. This corresponds to the area underneath a normal pdf within $\mu \pm z\sigma$, that is the probability that a measurement will fall into this range. Tables give the value of the integral for $z = 3.81$ as 0.99985530. In 67 measurements of this intensity we expect $67 \times (1 - 0.99985530) = 0.01$ measurements this far from the mean. As this is $\ll 0.5$ we should delete this point.

An alternative, more flexible, procedure that can also account for the long tails in experimentally derived distributions is to down-weight data by multiplying conventionally derived weights by a modifier function. A frequently used choice is the robust-resistant or Tukey scheme (Prince, 1994; Price and Nicolson, 1983; Press *et al.*, 1992):

$$w' = w_i\left[1-\left(\frac{z_i}{6}\right)^2\right]^2, \tag{16.20}$$

if $z_i < 6$, and $w' = 0$ otherwise. Table 16.3 (Blessing, 1997) compares the weights that would be obtained for normal and robust-resistant schemes and it can be seen how the robust-resistant scheme can accommodate the long tails of experimentally observed distributions (compare the values in Table 16.3 for a point 4σ from the mean), but also identify serious outliers.

16.4.3 Assessing weighting schemes

The most widely used test to determine whether weights are on the correct scale is the χ^2 test described above. In crystallographic refinements we tend to calculate the value of $S = \sqrt{\chi^2_{\text{red}}}$, the *goodness of fit*, instead.

A value near 1.0 implies that the weights are on the correct scale. In practice, the value of S can be manipulated to be near unity by dividing all the w_i by χ^2_{red}, and so, unless the σs derived from data processing are being used without modification in the weighting scheme, this parameter has little value.

A more useful procedure, also mentioned above, is to examine how the values of $w\Delta^2$ vary when the data are arranged in some systematic way, and this is referred to as an *analysis of variance*. In the merging procedure in SORTAV (Blessing, 1997) this analysis is based on resolution and intensity to derive more realistic estimates of the standard deviations of the merged intensities. In structure refinement, when S or χ^2_{red} is plotted against F_c^2, or $\sin\theta/\lambda$, or index, the line should be flat (Fig. 16.7).

Trends in the values of residuals across different groups (especially different ranges of resolution and of structure-factor amplitude) reveal the presence of systematic errors in the model (e.g. neglect of hydrogen atoms or of extinction effects) or imperfections in the weighting scheme. Indeed, empirical adjustments to the weighting scheme can be made on the basis of such an analysis; the weights thus obtained are supposed to reflect not only uncertainties in the data, but also shortcomings of the structural model.

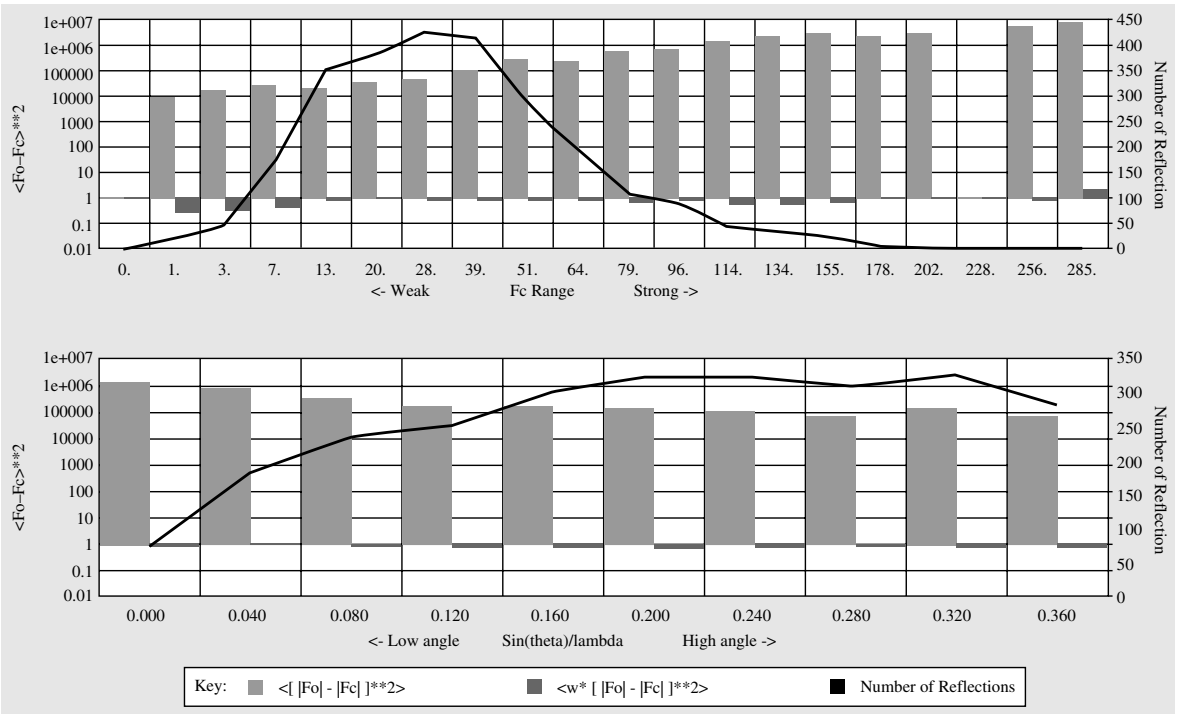

Fig. 16.7 Analysis of variance based on intensity (top) and resolution (bottom). Notice that the values of $w\Delta^2$ (bars) show a flat distribution. Data calculated using CRYSTALS (Betteridge *et al.*, 2003). Bars representing weighted residuals are very close to 1 and not easy to see.

Another method of assessing the validity of a weighting scheme is through a *normal probability plot* (Abrahams and Keve, 1971). The first stage of this analysis is to order the j observations in terms of $w^{1/2}\Delta$. If the errors in the data follow a normal distribution (and we hope that this is being reflected in our weighting scheme), then the ith data point should have a $w^{1/2}\Delta$ value of z, where z is given by the equation

$$\frac{j-2i+1}{j} = \frac{1}{\sqrt{2\pi}} \int_{-z}^{z} \exp\left(\frac{-x^2}{2}\right) dx = erf\left(\frac{z}{\sqrt{2}}\right). \qquad (16.21)$$

The values of z and $w^{1/2}\Delta$ can be plotted against each other (usually with the ideal z values on the x-axis), with $+z$ for $i > j/2$ and $-z$ for $i < j/2$.

For example, after ordering 192 $w^{1/2}\Delta$-values, the 37th had a value of $w^{1/2}\Delta = -0.95$. $192 - 74 + 1/192 = 0.62$, and consulting a table of the integral of a normal distribution (e.g. on p. 38 in Barlow), gives z for this to be 0.88. The value to be used in the normal probability analysis is -0.88 since $37 < 192/2$, and so the point to be plotted is $(-0.88, -0.95)$. In practice, of course, these calculations are accomplished using computer programs: such a facility exists in some refinement programs (e.g. CRYSTALS) and statistics packages such as MINITAB have facilities for calculating so-called *normal scores*.

A normal probability plot should be linear, pass through the origin and have a gradient of 1. An example is given in Fig. 16.8. Non-linear plots indicate some systematic error of the kind that can not be absorbed by

Fig. 16.8 Normal probability plot calculated after a refinement of data collected using a high-pressure cell. The weighting scheme used here was $w_i = 1/\sigma^2(F_i^2)$ with a robust-resistant modifier. The overall gradient is near 1, indicating that the scale of the weights is reasonable. The slight non-linearity suggests that there are still some systematic errors present in the data, most likely uncorrected cell-absorption errors. Data calculated using CRYSTALS (Betteridge *et al.*, 2003).

the model; a gradient of less than 1.0 would indicate that the weights are too small (or the σs are too large if these are being used in the weighting scheme). If the intercept of the plot is not zero, this may indicate a scaling problem.

Such plots are useful, not only in assessing weighting schemes and the agreement between observed and calculated set of data, but in any comparison of two sets of quantities (e.g. two independently measured datasets for the same structure, or two sets of parameters refined from them). For the comparison of two independent sets of measured data, for example, we would use

$$\delta_i = \frac{F_{1,i} - F_{2,i}}{\sqrt{\sigma^2(F_{1,i}) + \sigma^2(F_{2,i})}}, \tag{16.22}$$

and then sort the deviations δ_i into order of increasing value from the most negative to the most positive. Probability plots can also be adapted for testing *any* probability distribution function.

16.5 Analysis of the agreement between observed and calculated data

16.5.1 *R* factors

Before we are able to calculate the desired geometrical information from the refined atomic parameters, refinement must reach convergence. But is this convergence the best that can be achieved for our structure? At several stages during a typical structure determination, refinement converges, but the introduction of more parameters (a change in the model being refined) allows further refinement to take place, giving convergence again, this time (we hope) to an even better agreement with the observed data. Such developments of the model are, for example, the replacement of isotropic by anisotropic atomic displacement parameters, and the inclusion of hydrogen atoms. Other changes that can be made are the refinement of parameters for effects such as extinction or absorption, the addition of models of disorder, and changes to the weighting scheme. Any change in the model will produce a different set of refined parameters. How do we assess the agreement with the observed data and choose the 'best' model?

Overall 'residuals' (single-value measures of the agreement) commonly used and quoted are:

$$\begin{aligned} R &= \frac{\sum_i |\Delta|_i}{\sum_i |F_\mathrm{o}|_i} \\ wR &= \left(\frac{\sum_i w_i \Delta_i^2}{\sum_i w_i F_{\mathrm{o,i}}^2} \right). \end{aligned} \tag{16.23}$$

R is long established as *the* traditional 'R factor', accorded a general reverence far in excess of its real significance. The 'generalized R factor',

called wR here in accordance with current *Acta Crystallographica* usage, is variously referred to as RG, R' and R_w as well.

All of these residuals can be manipulated and massaged in various ways to produce an apparently better fit to the data. Both R and wR can be reduced dramatically by omitting some reflections, especially the weak ones and a few that give particularly poor agreement between $|F_o|$ and $|F_c|$ (perhaps on grounds such as 'they are strongly affected by extinction'). A much better assessment of the fit of observed and calculated data comes from an analysis of variance or normal probability plots as described above.

16.5.2 Significance testing

Increasing the number of refined parameters will always (given suitable weights) reduce the residuals and produce a better fit to the observed data. It does not follow that any such reduction is significant and meaningful.

The standard test for assessing statistically the improvement in fit when the model is changed is by analysis of χ^2 values from the different models. Ratios of pairs of χ^2 values follow a so-called F-distribution, but Hamilton (1971) adapted this for ratios of the wR residuals:

$$\Re = \frac{wR(1)}{wR(2)} \tag{16.24}$$

for comparison with tabulated values. The tables are constructed for different 'dimensions' (the difference in number of parameters for models 1 and 2) and 'degrees of freedom' ($N - P$ for model 2) and according to various 'levels of significance' α. Thus, if the value of $\Re$ is greater than a tabulated value appropriate to the degrees of freedom and dimension of the test, this means that the probability that this apparent improvement could arise by chance from two equally good models is less than α; model 2 is said to be better than model 1 at the α significance level (α is often expressed as a percentage). So a significance level of $\alpha = 0.01$ (1%), for example, indicates that there is a 1% risk of accepting the second model as better when it actually is not.

Interpolation is often necessary between tabulated values, because the available tables do not cover exactly the dimension and degrees of freedom required. In practice, it is rare for these tests to indicate that improvement is not significant, and there are some doubts as to their true statistical validity.

Note that the s.u.s of the refined parameters do not necessarily decrease when the residuals decrease. Although they do depend on the minimization function $\sum_i w_i \Delta_i^2$, they also depend *inversely* on the excess of data to parameters, $N - P$. A very simple assessment of the significance of the improvement of a model on introducing extra parameters is, then, to see whether the parameter s.u. values are reduced.

16.6 Estimated standard deviations and standard uncertainties of structural parameters

In crystal-structure determinations we do not usually determine a structure several times in order to obtain mean values of the atomic parameters and estimates of the variance of these parameters. Instead we obtain 'estimated standard deviations' (e.s.d.s or s.u.s) *from a single experiment*. This is possible because our experimentally measured data (diffraction intensities) greatly outnumber the parameters to be derived: the problem is said to be over-determined. The value obtained for the parameter is our best estimate of the true value. The s.u. is a measure of the precision or statistical reliability of this value; it is our best estimate of the variation we would expect to find for this parameter if we were to repeat the whole experiment many times. The s.u. we obtain from refinement is analogous to the standard error on the mean defined in (16.12).

In structure refinement by least squares, a number of parameters are determined from a larger number of observed data. The quantity minimized is

$$\sum_{i=1}^{N} w_i \Delta_i^2, \tag{16.25}$$

where Δ_i is usually either $|F_o|_i - |F_c|_i$ or $F_{o,i}^2 - F_{c,i}^2$ and each of the N reflections has a weight w_i. The s.u. values of the refined parameters depend on (i) the minimized function; (ii) the numbers of data and parameters; (iii) the diagonal elements of the inverse least-squares matrix $\mathbf{A}^{-1}$

$$\sigma(p_j) = \left((\mathbf{A}^{-1})_{jj} \frac{\sum_{i=1}^{N} w_i \Delta_i^2}{N - P} \right)^{1/2}, \tag{16.26}$$

where p_j is the jth of the P parameters (16.26). Note that low s.u. values (high precision) are achieved with a combination of good agreement between observed and calculated data (small numerator) and a large excess of data over parameters (large denominator).

16.6.1 Correlation and covariance

The parameters describing a crystal structure are not independent. When we derive further results from a combination of several parameters (such as calculating a bond length from the six co-ordinates of two atoms), it is important to recognize this interrelationship in order to calculate the correct s.u.s for the secondary results.

When variables are not statistically independent, they are said to be *correlated*. Just as individual variables have *variances*, so correlated

variables have *covariances*. For a discrete distribution of two correlated variables x and y, the covariance is defined as

$$\mathrm{cov}(x,y) = \frac{1}{N-1}\sum_{i=1}^{N}(x_i - \overline{x})(y_i - \overline{y}), \tag{16.27}$$

which should be compared with the variances

$$\sigma^2(x) = \frac{1}{N-1}\sum_{i=1}^{N}(x_i - \overline{x})^2 \quad \text{and} \quad \sigma^2(y) = \frac{1}{N-1}\sum_{i=1}^{N}(y_i - \overline{y})^2, \tag{16.28}$$

thus, $\mathrm{cov}(x,x) = \sigma^2(x)$ by definition. For a continuous distribution, similarly

$$\mathrm{cov}(x,y) = \frac{\int_a^b \int_c^d (x-\overline{x})(y-\overline{y})P(x,y)dxdy}{\int_a^b \int_c^d P(x,y)dxdy}, \tag{16.29}$$

where c and d are the lower and upper limits of the variable y.

In both cases, the *correlation coefficient* of x and y is

$$r(x,y) = \frac{\mathrm{cov}(x,y)}{\sigma(x)\sigma(y)}, \tag{16.30}$$

and this must lie in the range ± 1. A correlation coefficient of exactly $+1$ or -1 means that x and y are perfectly correlated – each is an exact linear function of the other, and only one variable is actually required to describe them both. If x and y are completely independent, their covariance and correlation coefficient are both zero, though the converse is not necessarily true (a covariance of zero does not have to mean independent variables).

Covariances (and hence correlation coefficients) of all pairs of refined parameters for a crystal structure are obtained together with the variances from the inverse matrix:

$$\mathrm{cov}(p_j, p_k) = (\mathbf{A}^{-1})_{jk}\frac{\sum_{i=1}^{N} w_i \Delta_i^2}{N-P}. \tag{16.31}$$

Once we have all the variances and covariances of a set of quantities (such as the refined atomic parameters), we can calculate the variances and covariances of any functions of these quantities (such as molecular geometry parameters).

16.6.2 Uncertainty propagation

For a function $f(x_1, x_2, x_3, \ldots, x_n)$

$$\sigma^2(f) = \sum_{i,j=1}^{N} \frac{\partial f}{\partial x_i} \cdot \frac{\partial f}{\partial x_j} \cdot \mathrm{cov}(x_i, x_j), \tag{16.32}$$

where $\mathrm{cov}(x_i, x_i)$ is the same as $\sigma^2(x_i)$, as we saw before.

For two functions f_1 and f_2

$$\mathrm{cov}(f_1, f_2) = \sum_{i,j=1}^{N} \frac{\partial f_1}{\partial x_i} \cdot \frac{\partial f_2}{\partial x_2} \cdot cov(x_i, x_j), \tag{16.33}$$

but this is not often needed.

Note that, if the variables x are all independent, the covariances are zero except for the variance terms themselves, so in such a simple case

$$\sigma^2(f) = \sum_{i=1}^{N} \left(\frac{\partial f}{\partial x_i} \right)^2 \sigma^2(x_i), \tag{16.34}$$

and thus, the variance of f is just a weighted sum of the variances of the individual independent variables.

The full variance–covariance matrix following the final least-squares refinement must, therefore, be used in calculating molecular geometry s.u. values. Calculation using the co-ordinate s.u. values alone, with neglect of correlation effects between atoms, does not give the correct geometry s.u.s: it is equivalent to using (16.34) instead of (16.32), and potentially important terms are missing. This is particularly evident when calculating the bond length between two atoms related by a symmetry element, because the co-ordinates of these atoms are completely correlated.

Such calculations are normally performed automatically together with the least-squares refinement. Proper calculation in a separate step later would require that the refinement program output the full variance–covariance matrix.

16.7 Systematic errors

The preceding sections have largely discussed the effects of random errors in a data set. Systematic errors usually lead to a reduction in both precision and accuracy in a structure determination if they are not corrected.

16.7.1 Systematic errors in the data

(a) Absorption
Absorption reduces the observed intensities of diffraction, but by different factors for different reflections. The effect is greatest at low Bragg angle, so that there is a systematic error even for a spherical crystal. Uncorrected significant absorption causes atomic displacement parameters to be too low, in an attempt to compensate for the effect. Anisotropic absorption (for a non-spherical crystal) affects the apparent atomic vibration differently in different directions, so that elongated 'thermal ellipsoids' are produced for the atoms in a needle crystal. The atomic co-ordinates are generally not significantly affected, but the s.u.s are increased because the observed and calculated data do not agree so well; the atomic displacement parameters can not completely mop up the absorption errors.

(b) Extinction
This also attenuates the observed intensities, and it is most severe for low-angle, strong reflections. Like absorption, it reduces overall precision and systematically affects atomic displacement parameters, while having much less effect on atomic co-ordinate values.

(c) Thermal diffuse scattering
TDS, produced as a result of co-operative lattice vibrations, has the effect of increasing observed intensities. The effect, however, increases with $\sin^2\theta$, so the net effect, if no correction is made, is once again to reduce atomic displacement parameters from their true values. TDS effects have received little attention in routine crystal-structure determination, and they are generally believed to be small. Data collection at reduced temperature is an advantage here, as well as in other ways.

(d) A poorly aligned diffractometer
Several errors can be introduced into the diffraction data by this fault, including an improper measurement of intensities if the reflections are not completely received by the counter aperture. The most common error, however, is probably in unit cell parameters. If a badly aligned instrument involves systematic errors in the zero points of the circles (especially 2θ), there will be a corresponding error in refined cell parameters, which may well be much greater than their supposed s.u.s. This, in turn, leads to systematic errors in molecular geometry, and no indication of these can be seen in the commonly quoted measures of the 'quality' of the structure determination (structure factor residuals, goodness of fit, etc.), which refer only to diffraction intensities and not to diffraction geometry. Such errors as this, therefore, are the most invidious, because it is difficult to detect them.

(e) Anomalous dispersion
This may be considered as a systematic effect (and, hence, a potential source of systematic error) in the data, or as a possible fault in the structural model if properly corrected atomic scattering factors are not used.

Neglect of the correction in a non-centrosymmetric structure with a polar axis or, even worse, a 'correction' with the wrong sign, results in a systematic shift, along the polar axis, of all atoms displaying significant anomalous scattering effects, because this shift, relative to the rest of the atoms, mimics the phase shift produced by the anomalous scattering (Cruickshank and McDonald, 1967). In a centrosymmetric or a non-polar non-centrosymmetric structure, atomic positions are not affected, but atomic displacement parameters are.

Of course, anomalous dispersion effects can be used for determining the correct 'handedness' of a non-centrosymmetric structure (see Chapter 18 on twinning), and also for determining phases of reflections in structure solution, but these are really separate subjects and not directly concerned with errors and results.

16.7.2 Data thresholds

It is fairly common for the weakest reflections not to be used in least-squares refinement, though there is considerable controversy over this. The inclusion or omission of weak reflections usually makes no significant difference to the derived parameter values. Weak reflections tend to increase the residuals R and (to a lesser extent if they are correctly weighted) wR, but this is compensated somewhat by the larger excess of data over parameters ($N - P$), so it is not clear how final s.u.s will be affected. In fact, it has been demonstrated that they, too, are scarcely altered by the inclusion or omission of weak reflections or by the decision of just where to set the threshold (Stenkamp and Jensen, 1975). Thus, the difference in the results is to a large degree just a cosmetic one. On the other hand, the weak reflections can play a crucial role in deciding between centrosymmetric and non-centrosymmetric space groups in ambiguous cases, because their omission tends to bias statistical tests towards a decision against centrosymmetry. If no sigma cut-off is to be used during refinement, it is essential to examine critically the resolution at which the data vanish into the background. In general, there seems to be little to recommend the exclusion of weak data in resolution shells where there are plenty of strong data – their weakness conveys important information. The inclusion of swathes of weak high-angle data just because the data reduction software has written them to a file only degrades the quality of a structure determination.

16.7.3 Errors and limitations of the model

The parameters refined by least squares are an attempt to describe the structure we are trying to determine. They represent an approximation to the actual X-ray scattering power of the structure. No such model can be a perfect representation, and there are various limitations on the simple models we use, and various errors that may be made in choosing the elements of the model.

(a) Atomic scattering factors

The tabulated scattering factors commonly used are reasonably accurate representations of the scattering power of individual, isolated atoms at rest. They have spherical symmetry, and probably their greatest limitation is the lack of allowance for distortion of this spherical electron density when atoms are placed together and bonded to each other. The greatest effects of this approximation are seen in the low-angle data, and an analysis of variance of the observed and calculated data after refinement commonly shows the worst agreements for such reflections. In careful work, some of the largest peaks in a final-difference electron-density synthesis are found between atoms (bonding electron density) and in regions where lone pairs of non-bonding electrons are expected to lie. This is, of course, one reason why bonds to hydrogen atoms are found to be systematically shortened in X-ray diffraction studies.

An incorrect assignment of atom types, so that a wrong scattering factor is used for an atom, scarcely affects atomic co-ordinates in most cases, although there are circumstances under which these may be subject to a systematic error. In an attempt to compensate for the wrong scattering factor, refinement will adjust the atomic displacement parameters, often to a very considerable degree; an incorrectly assigned atom may be recognized in many cases by its anomalous displacement parameter, especially at the early isotropic stage of refinement when there is a single parameter for each atom.

(b) Constraints and restraints

Properly used, these are valuable tools in refinement, allowing us to deal with problems of parameters that are not well determined from the diffraction data alone. We must, however, be quite sure of the validity of any constraints or restraints we apply. Any that strongly oppose the course of unconstrained/unrestrained refinement, rather than gently guiding it, prevent convergence to the data-determined minimum and so force a different result. This will, in particular, significantly affect the geometry around the regions in the structure where the constraints are being applied.

A common example is the use of a constrained C–H bond length of 1.08 Å, chosen because it is the 'true' value determined spectroscopically for simple hydrocarbons. Since C–H bonds are systematically shortened in X-ray work, the effect of the constraint will be to push both atoms further apart than the diffraction data alone would indicate. Although the hydrogen-atom position will be most affected, there will be a small, but possibly significant, effect on the carbon atom. Misplacing the atoms in this way will also affect their displacement parameters.

Other cases of inappropriate constraints include the imposition of too high a symmetry on a group of atoms that is genuinely perturbed to a less regular shape by bonding or packing interactions. Phenyl groups are systematically distorted from regular hexagonal symmetry, and the use of such a simple model, frequently used in refinement, may not be appropriate.

(c) Incorrect symmetry

Space group determination is based on several experimental measurements and deductions: (i) the metric symmetry of the reciprocal and direct lattices; (ii) the Laue symmetry of the observed diffraction pattern; (iii) systematically absent reflections; (iv) statistical tests for the presence or absence of symmetry elements, especially an inversion centre; (v) ultimately, a 'successful' refinement. Reports appear relatively frequently in the literature of space groups that are reputed to have been incorrectly assigned by previous workers. In many cases, the problem is not a serious one, in that two molecules, actually equivalent by unnoticed symmetry, are refined as independent, and their geometries are not significantly different: the results are reliable, but contain unnecessary redundancies. Where the missing symmetry is an inversion centre, however, there is a real problem, in that refinement is unstable (strictly speaking, the matrix is singular), but this may be masked by the particular refinement technique used. The geometrical results in this case are quite unreliable: parameters that should be equal by symmetry may be found to differ by a large amount, and the molecular geometry often displays considerable distortions.

(d) High thermal motion and static disorder

It is not always easy to distinguish these two situations, except by carrying out the data collection at a reduced temperature (which reduces dynamic disorder but not usually static disorder unless there is actually an order-disorder phase transition at an intermediate temperature). High thermal motion increases the foreshortening of interatomic distances generally observed in X-ray diffraction, so there is a considerable systematic error in bond lengths, which was discussed in Chapter 14. The usual six-parameter (ellipsoidal) model of thermal motion becomes increasingly inadequate as the motion increases in amplitude, so the displacement parameters are of dubious value and their precision is generally poor.

The presence of disorder in a structure, unless it is very simple and can be well modelled, reduces to some extent the overall precision of the whole structure, not just of the particular atoms affected. For this reason, certain atomic groupings notorious for disorder are best avoided if possible: these include ClO_4^-, BF_4^- and PF_6^- anions.

High thermal motion and/or disorder can make the geometrical interpretation of a structure difficult, and may lead to incorrect deductions about the molecular geometry and conformation. A classic case is that of ferrocene, $(C_5H_5)_2Fe$, which appears to be staggered because of unresolved disorder at room temperature, but that (contrary to statements in some standard inorganic chemistry text-books!) is actually eclipsed.

(e) Wrong structures

Such errors as those just mentioned, with an incorrect molecular geometry, are bad enough, but it is possible, though very uncommon and unlikely, to find a completely incorrect structure, in the sense of identifying the wrong chemical compound. A case of mistaken identity caused

by 30-fold disorder involves the supposed structure of dodecahedrane (Ermer, 1983). Wrongly assigned atom types were suspected in the structure of '$[ClF_6][CuF_4]$', which in reality is probably $[Cu(H_2O)_4][SiF_6]$ (von Schnering and Vu, 1983); the original workers were misled by the similarity in scattering powers of Si and Cl, and of O and F, and perhaps by some wishful thinking!

16.7.4 Assessment of a structure determination

The above discussion should encourage us to take a critical view of crystal-structure determination in general (Jones, 1984; Ibers, 1974), and to seek to evaluate carefully any particular reported structure. Several research journals issue detailed instructions for authors of crystal-structure reports, and some provide separate checklists for referees. These can provide a useful framework for assessing a structure, whether it be one reported in the literature, or one of your own.

Below is a summary of some useful points for checking the quality of a structure determination. It is derived from a number of sources, including standard tests applied by *Acta Crystallographica Sections B/C/E*, and a list distributed by David Watkin at a British Crystallographic Association Intensive School.

Check for consistency of the crystal data. If you have a suitable computer program, you can input the cell parameters and chemical formula and check the volume, Z (number of chemical formula units in the unit cell), density, absorption coefficient μ, etc. For a quick check by hand calculation:

(a) count the non-hydrogen atoms (N) in the molecule or formula unit;
(b) check that $abc \sin\delta \approx V$, where δ is the most removed of α, β, γ from 90°;
(c) calculate the average volume per non-H atom ($= V/NZ$), which is usually about 18 Å^3 for organic and many other compounds.

Assess the description of the data collection.

(a) Check that $|h|_{max}/a \approx |k|_{max}/b \approx |l|_{max}/c$, and that at least the correct minimum fraction of reciprocal space has been covered.
(b) $2\theta_{max}$ should be at least 45° (better, 50°) for Mo radiation, 110° (better, 130°) for Cu radiation.
(c) Look at the number of unique data, the number of 'observed' data, and the threshhold [which may be expressed in terms of $\sigma(I)$ or $\sigma(F)$: $I \geq 2\sigma(I)$ corresponds to $F \geq 4\sigma(F)$]; check for a low value of R_{int} if equivalent reflections are merged.
(d) Calculate and compare μt_{min} and μt_{max} (dimensionless!) for the minimum and maximum crystal dimensions. If $\mu t_{max} < 2$, absorption is probably no problem. If $\mu t_{max} > 5$ or $(\mu t_{max} - \mu t_{min}) > 2$, an absorption correction is necessary (or there will be significant effects on the U^{ij} values). More detailed tests

are described in the *Notes for Authors* of *Acta Crystallographica Section C*.

Assess the refinement and results.

(a) The number of *observed* data should be greater than the number of refined parameters by a factor of at least 5 (and preferably 10). Anisotropic refinement gives 9 parameters per atom, isotropic gives 4. *Constrained* H atoms do not count unless U is refined for them.
(b) Examine carefully the description of any constraints/restraints, the treatment of H atoms, and any disorder.
(c) Look for strange U or U^{ij} values; high values may indicate disorder, low values may indicate uncorrected absorption (unless low temperature was used); either of these could be due to misassigned atom types.
(d) Check for convergence (shift/s.u. values preferably < 0.01).
(e) Examine the fit of observed and calculated data, if possible, not only by the value of R.
(f) Difference electron density outside about ± 1 eÅ^{-3} may be due to missing, misplaced, or misassigned atoms, systematic errors such as absorption (especially if large peaks appear close to heavy atoms), or unmodelled disorder.
(g) Check for 'absolute structure' determination if the space group does not have a centre of symmetry.
(h) Assess the s.u.s (i) of the refined parameters; (ii) of the molecular geometry parameters. Watch out for low s.u.s ignoring cell parameter uncertainties. Check for s.u.s on values that should be constrained, symmetry-equivalent, etc.
(i) Check for strange results: unusual geometry, impossibly short intermolecular contacts, etc.

Many of these tests have been incorporated into the CHECKCIF procedure in PLATON (Spek, 2003), and *all structures should be validated with this program as a matter of routine*.

References

Abrahams, S. C. and Keve, E. T. (1971) *Acta Crystallogr.* **A27**, 157–165. *Erratum*: (1972) **A28**, 215.
Barlow, R. J. (1997). *Statistics*. John Wiley: Chichester.
Betteridge, P. W., Carruthers, J. R., Cooper, R. I., Prout, K. and Watkin, D. J. (2003). *J. Appl. Crystallogr.* **36**, 1487.
Bevington, P. R. and Robinson, D. K. (2003). *Data reduction and error analysis for the physical sciences*, 3rd edn. McGraw Hill, New York.
Blessing, R. H. (1997). *J. Appl. Crystallogr.* **30**, 421–426.
Carruthers, J. R. and Watkin D. J. (1979). *Acta Crystallogr.* **A35**, 698–699.

Cruickshank, D. W. J. and McDonald, W. S. (1967) *Acta Crystallogr*. **23**, 9–11.
Ermer, O. (1983). *Angew. Chem. Int. Ed. Engl.*, **22**, 251–252.
Hamilton, W. C. (1964). *Statistics in physical science*. Ronald Press, New York. [This is out of print, and can be difficult to find].
Hamilton, W. C. (1965). *Acta Crystallogr.* **18**, 502–510. See also Pawley, G. S. (1970) *Acta Crystallogr.* **A26**, 691–692.
Ibers, J. A. (1974). *Problem crystal structures* and Donohue, J. *Incorrect crystal structures: can they be avoided*? In *Critical evaluation of chemical and physical structural information*, (eds) D. R. Lide Jr. and M. A. Paul. Nat. Acad. Sci: Washington D.C.
Jones, P. G. (1984). *Chem. Soc. Rev*. **13**, 157–172.
Press, W. H., Teukolsky, S. A., Vetterling, W. T. and Flannery, B. P. (1991). *Numerical recipes in Fortran*. Cambridge University Press, Cambridge, UK.
Prince, E. (1994). *Mathematical techniques in crystallography and materials science*, 2nd edn. Springer: New York.
Prince, E. and Nicolson, W. L. (1983). *Acta Crystallogr.* **A39**, 407–410.
Sheldrick, G. M. (2008). *Acta Crystallogr*. **A64**, 112–122.
Spek, A. L. (2003). *J. Appl. Crystallogr.* **36**, 7–13.
Stenkamp, R. E. and Jensen, L. H. (1975) *Acta Crystallogr*. **B31**, 1507–1509.
Taylor, R. and Kennard, O. (1983). *Acta Crystallogr.* **B39**, 517–525.
von Schnering, H. G. and Dong Vu (1983). *Angew. Chem. Int. Ed. Engl*. **22**, 408.
Wilson, A. J. C. (1949). *Acta Crystallogr.* **2**, 315–321.
Wilson, A. J. C. (1976). *Acta Crystallogr.* **A32**, 994–996.

Exercises

1. Show that (16.1) and (16.2) can be derived from (16.3) and (16.5) if unit weights are used.
2. The data in Table 16.4 are H…O distances taken from structures determined with neutron diffraction, containing a certain type of hydrogen bond.
   (a) Calculate the weighted value of χ^2 and χ^2_{red} using $w_i = 1/\sigma^2(x_i)$.
   (b) Is calculation of a mean justified for these data? Discuss your answer in terms of the likely effects of environmental factors on hydrogen bonds.
   (c) Your supervisor looks blank when you tell him about χ^2, and says that you must calculate an average. What standard deviation should you quote?

Table 16.4 H…O distances from neutron-diffraction data.

x_i	$\sigma(x_i)$
1.814	0.0015
1.844	0.003
1.728	0.003
1.832	0.003
2.121	0.003
1.997	0.0075
1.808	0.0075
1.833	0.009
1.739	0.009
1.772	0.009
1.742	0.0105
1.877	0.012
1.948	0.012

3. The data in Table 16.5 were measured at points x giving measured values y.

Table 16.5 Data points for Exercise 3.

x	y
1	7.1
2	34.9
3	111.2
4	258.7

   (a) Fit these data to an equation of the form $y = a + bx^3$, finding the values of a and b by least-squares.
   (b) Work out an R factor.
   Hint: The crystallographic R factor is $R = \frac{\sum |F_o - F_c|}{\sum |F_o|}$
   (c) Work out the standard uncertainties of a and b.
   (d) For a particular application the quantity

$$c = a + b^2$$

   is important. Compare the standard uncertainties in c obtained if covariance terms are included or excluded.
   Note: For a function $f(x_1, x_2, x_3, \ldots, x_n)$ the full propagation of error formula is

$$\sigma^2(f) = \sum_{i,j=1}^{N} \frac{\partial f}{\partial x_i} \cdot \frac{\partial f}{\partial x_j} \cdot \text{cov}(x_i, x_j),$$

   where $\text{cov}(x_i, x_i)$ are variances $[\sigma^2(x_i)]$, and $\text{cov}(x_i, x_j)$ are covariances.
4. The following ALERT was issued by CHECKCIF after a refinement where restraints had been applied:

```
732_ALERT_1_B Angle   Calc        105(4),  Rep
104.9(8)        5.00 su-Rat

N2   -O1   -H1      1.555   1.555   1.555
```

   What response might be given?
5. In a particular structure determination the bond angles in a nitrate anion were found to be
   120.1(2), 119.4(2), 119.5(2)°.
   What is the sum of the angles and its s.u.?
6. Bond angles in a substituted cyclopropane ring are reported as:
   59.3(2), 59.6(2), 61.0(2)°.
   What is the sum of the angles and its s.u.?

Powder diffraction

17

John Evans

17.1 Introduction to powder diffraction

X-ray and neutron powder diffraction are extremely powerful tools for probing the structural chemistry of materials in the solid state. Both techniques can be used to gain information about the composition of a bulk material, the degree of crystallinity of its components, information about its unit cell size and symmetry and, in favourable cases, full 3-dimensional structural information comparable to that obtained from single-crystal methods. Powder diffraction experiments can be readily performed under the influence of external factors such as temperature, pressure or applied magnetic field, under laser illumination of a sample, and even as a function of time or chemical environment during the synthesis of materials, giving valuable kinetic and mechanistic insight into their formation.

The primary focus of this book and the BCA crystallography school on which it is based is on single-crystal methods as applied to 'small molecules'. There is no doubt that if one's primary goal is the elucidation of high-quality structural data, single-crystal diffraction will always be the method of choice. Nevertheless, the opportunities offered by powder diffraction methods should not be forgotten. In many cases single crystals of interesting materials of sufficient size/quality for single-crystal methods simply can not be prepared (though increasingly small microcrystals can now be studied at a synchrotron source; see Chapter 22). This is particularly true for the extended materials discussed in Chapter 14, where low solubility, phase transitions leading to multiple twinning, or the specific synthetic conditions required make single crystals hard or impossible to obtain. For many categories of technologically exploited materials (zeolites, high-T_c superconductors, structural materials, magnetic materials, conducting oxides, multiferroics, ionically conducting polymers, etc.) the key structural insights came from powder diffraction studies since single crystals were not available.

In other applications powder diffraction may provide complementary information (such as bulk sample composition) to single-crystal techniques. Non-ambient studies (under extremes of temperature, pressure, magnetic field or optical irradiation) are often simpler to perform on powdered samples than single crystals, allowing the potential to study functional materials under 'real' operating conditions; powder studies

become essential when phenomena such as phase transitions cause single crystals to shatter under working conditions. Recent advances in the speed of powder diffraction studies (whole patterns being collected in a matter of minutes, seconds or less) using advanced sources/detectors mean that phenomena such as host-guest inclusion reactions, chemical transformations in the solid state and crystallization can now be followed in real time, allowing valuable kinetic and mechanistic insight into the process of chemical transformations (Evans and Evans, 2004). Despite powder diffraction being seen as a 'poor cousin' to single-crystal techniques by many, it is a key member of the family of analytical methods that can be brought to bear on understanding structural problems. This chapter highlights areas of potential interest to the small-molecule community; for more in-depth and mathematical descriptions of powder diffraction the reader should look elsewhere (Klug and Alexander, 1974; Jenkins and Snyder, 1996; Cullity and Stock, 2001; Pecharsky and Zavalij, 2003; Dinnebier and Billinge, 2008). Specialist schools on structural and magnetic Rietveld refinement are organised biennially by the Physical Crystallography Group of the BCA (see www.crystallography.org.uk).

17.2 Powder versus single-crystal diffraction

In a conventional single-crystal experiment a beam of monochromatic X-rays/neutrons is incident on a suitably mounted and oriented single crystal. The phenomenon of diffraction leads to diffracted beams being produced in certain directions in space (see earlier chapters). The positions and intensities of these beams are recorded by film, point-detector or (most commonly nowadays) area-detector methods. After crystal selection and data collection the analysis is usually broken down into four essentially separate stages that are described in detail in other chapters:

1. indexing to find the unit cell;
2. integration of raw images to produce a single data file listing intensities and *hkl* values for each reflection;
3. structure solution (typically by direct methods or Patterson synthesis);
4. structure completion and refinement.

In a powder experiment (Fig. 17.1), instead of a single crystal one has a collection of randomly oriented polycrystallites exposed to the beam. Each of these polycrystallites can be thought of as giving rise to its own diffraction pattern, and individual 'spots' on a film become spread out into rings of diffracted intensity (these rings are the intersections of cones of diffracted intensity with the film). The intensity of these rings can be recorded using film/area-detector methods, but are most commonly measured by scanning a point detector or 1D line detector across a narrow strip of the rings. In either case one can represent

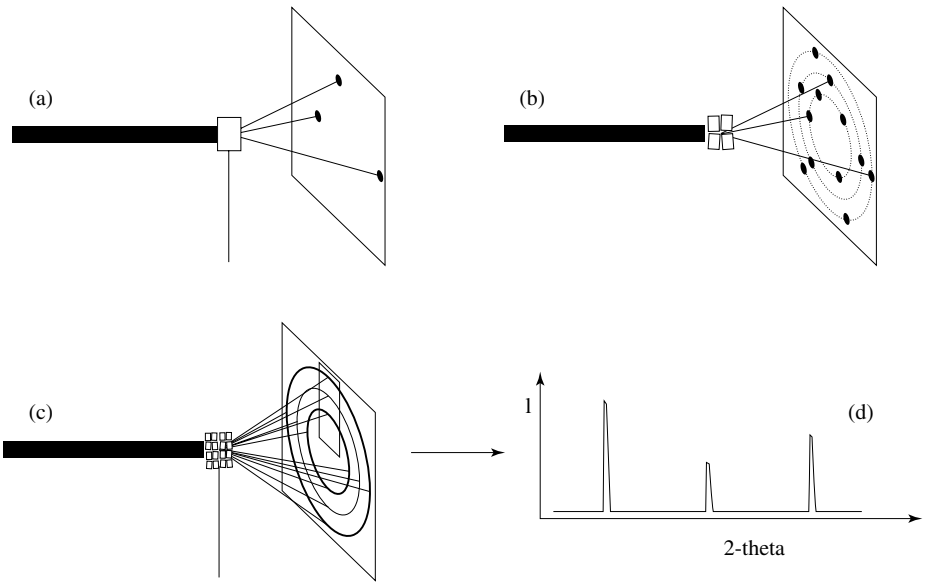

Fig. 17.1 (a) shows diffraction from an oriented single crystal, (b) from a collection of 4 crystals at different orientations with respect to the incident beam and (c) from a polycrystalline material. (d) shows the resulting I versus 2θ plot obtained by scanning across the outlined rectangle of (c).

the diffraction data as a plot of total diffracted intensity against the diffraction angle 2θ.

Figure 17.1 immediately shows one of the inherent problems of powder diffraction. The 3D intensity distribution of a single-crystal experiment is compressed into the one dimension of 2θ space, leading to a vast loss of information due to peak overlap. In a metrically cubic crystal, for example, interplanar spacings are given by $d_{hkl} = a/(h^2+k^2+l^2)^{1/2}$. The (221) and (300) reflections (which will in general be of different intensity) will occur at identical values of 2θ and only information on their summed intensity is available from a powder diffraction experiment. For cells of lower symmetry one may get accidental overlap (partial or complete) of different *hkl* reflections. For a triclinic cell of the complexity that would be routine for modern single-crystal methods (3400 Å^3), using a typical laboratory powder diffractometer with $\lambda = 1.54$ Å there would be ~5500 reflections predicted between 0 and 90° 2θ($d_{\min} = 1.09$ Å). Even for a highly crystalline material this will lead to a considerable degree of peak overlap (Sivia, 2000; David, 1999). In order to minimize the effects of peak overlap it is important to choose an experimental setup (see Section 17.3) that gives peak widths that are as sharp as possible. In powder diffraction this is referred to as a 'high-resolution' experiment. Note that this is a different meaning from that typically implied in single-crystal studies (data recorded to high $\sin\theta/\lambda$ to allow high resolution in Fourier maps).

There are a number of methods that attempt to alleviate overlap problems. In one approach some independent information regarding overlapping peaks can be retrieved from intensity variations around the Debye–Scherrer rings of deliberately textured samples (Wessels *et al.*, 1999); in another one can make use of anisotropic thermal expansion to try to resolve different families of reflections at different temperatures. In the absence of such methods, overlap can be minimized only by recording the highest-resolution data attainable for a given sample.

The problems of peak overlap and the compression of 3D data into 1D are at the heart of the differences in data analysis between single-crystal and powder methods. Typically stages 2–4, and often stage 1, listed above are merged into one and one works with the whole experimentally recorded dataset throughout. The need for high resolution for many experiments also means that CCD detectors are not widely used, and point detectors or specially designed 1D/2D position-sensitive detectors are employed.

17.3 Experimental methods

There are a host of experimental methods available for recording powder diffraction data, each with its own inherent advantages and disadvantages. The two most commonly used geometries for obtaining X-ray diffraction data in home laboratories are shown in Fig. 17.2. In the simplest 'reflection' or Bragg–Brentano setup (Fig. 17.2a), one has an X-ray line source at **3**. A flat-plate sample is mounted at **4** and a point detector at **6**. The sample is scanned through an angle θ as the detector is moved through 2θ. The most common laboratory X-ray source is a sealed Cu tube. To produce monochromatic radiation (Cu$K\alpha_1\lambda = 1.540596$ Å) one can place the line source of the tube at position **1** and a curved focusing Johannsen monochromator (e.g. Ge 111) at position **2** to produce an effective line source at position **3**. Either a scintillation counter or a linear position-sensitive detector is commonly placed at position **6**. This arrangement gives high resolution, but can suffer from high backgrounds for samples that fluoresce under Cu irradiation (e.g. Co-containing materials). Fluorescence effects can be reduced by instead placing a monochromator between the sample and detector. Perhaps the most common laboratory setup uses a post-sample pyrolytic graphite monochromator at **5** and a point detector, giving an approximately 2:1 mixture of Cu$K\alpha_1$ ($\lambda = 1.540596$ Å) and $K\alpha_2$ ($\lambda = 1.544493$ Å) radiation.

It is also possible to use an energy-dispersive detector at **6** and dispense with the monochromator altogether. Commercially available detectors can eliminate $K\beta$ radiation, leaving an α_1/α_2 mix. The advantage of this is that a typical monochromator is only ~25–35% efficient, so its omission leads to dramatic gains in intensity. In the latest generation of laboratory instruments it is common to use silicon-strip-based linear detectors. This means that a post-sample monochromator is no

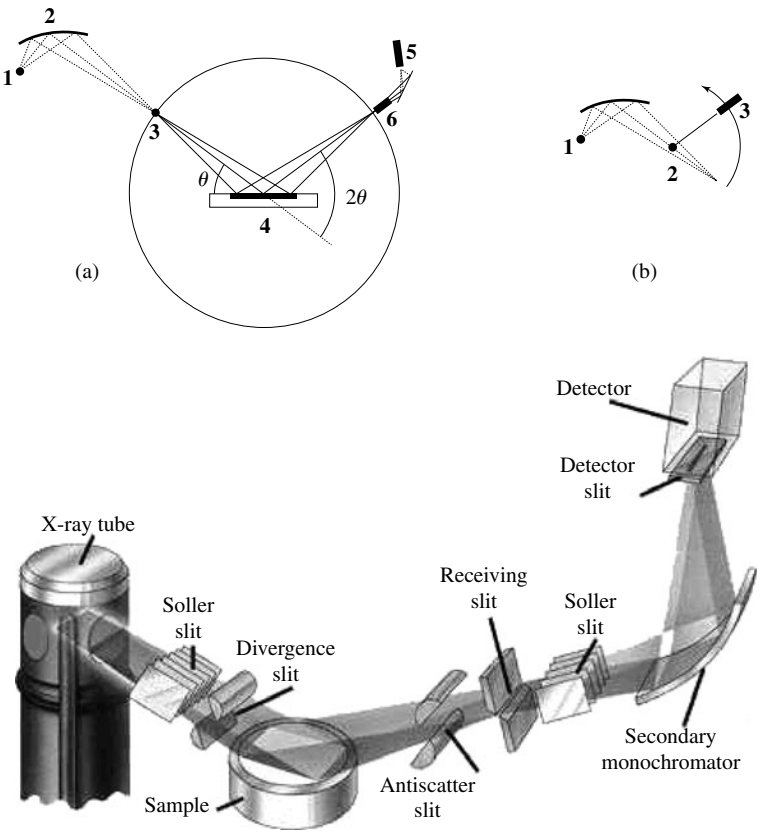

Fig. 17.2 (a) and (b) Typical laboratory powder diffraction setups (see text for details). Diagrams are not to scale; typical distances 1–3, 3–4 and 4–6 would be ∼200 mm, a sample area of ∼100 mm^2 would be illuminated. Below: schematic 3D view of a traditional flat-plate diffraction setup (reproduced from Philips publicity material).

longer employed and an Ni filter is placed in front of the detector to remove most of the $K\beta$ radiation. It should be noted that, with the high count rates achievable, significant discontinuities in background can be observed around strong reflections due to the absorption edge of the filter.

There are a host of other optical components present in a typical laboratory setup. Between the source and sample one uses a divergence slit to control the area of sample illumination. To obtain quantitatively useful intensities it is crucial that the beam remains smaller than the sample at all angles. To help achieve this, modern instruments may use a divergence slit that changes size with diffraction angle. This will lead to systematic changes in peak intensity with 2θ, which must be corrected in quantitative work. A similar antiscatter slit is often placed between the sample and detector. To reduce the effects of axial divergence, which can lead to significant peak asymmetry, Soller slits are

used. These are a series of thin metal plates placed in the beam parallel to the plane of Fig. 17.2. For a point detector one must also select a suitable detector slit. Each of the components in the system will influence the final peak shape in the diffraction pattern (see below), with finer Sollers or a smaller detector slit giving a better instrumental resolution. Each additional component will, however, lead to a significant loss in intensity. With a 0.05-mm detector slit one will get only ¼ of the count rate obtainable with a 0.2 mm slit. The optimal experimental setup will be dependent on the sample, the instrument and the information required. A typical 'quick' data collection covering 5−90° 2θ on a conventional laboratory instrument might take 30 min, a higher-quality scan for Rietveld refinement 12 h or more depending on the instrument configuration. Line/area detectors may reduce these times by a factor of 10–100.

Flat-plate samples can be prepared in a number of ways, either as bulk powders pressed into a recessed holder or sprinkled on an amorphous surface such as glass or (preferably) a 'zero-background' sample holder such as a 511-cut Si wafer. Flat-plate methods are, however, prone to problems due to preferred orientation, whereby a non-random arrangement of crystallites is presented to the beam. This can severely skew diffraction intensities – in extreme cases making experimental patterns appear completely different from calculated data or database standards. Several methods for reducing preferred orientation have been described in the literature (Klug and Alexander, 1974; www.mluri.sari.ac.uk/commercialservices/spraydrykit.html).

The positions and intensities of reflections are also influenced by factors such as the sample surface roughness and sample absorption properties. For organic samples low absorption can lead to a significant portion of the diffracted intensity occurring from below the ideal sample surface, leading to peak shifts and broadening. Surface roughness leads to peaks being artificially strong at high 2θ. This method of data collection is therefore perhaps best suited to relatively strongly absorbing samples or 'quick' qualitative measurements.

The transmission setup of Fig. 17.2b is particularly well suited for studies on low-absorbing organic/molecular materials. Here, the sample is placed at position **2**, usually mounted in a thin-walled glass capillary of 0.2–1.0 mm internal diameter and spun in the plane of the page (Fig. 17.3). Samples can also be mounted on thin mylar sheets. The use of capillaries significantly reduces preferred orientation effects, though sample mounting is slightly more time consuming. For highly absorbing samples unusual peak shapes may also be observed, but these can now be calculated/modelled during refinement.

As with any piece of scientific equipment, the performance of a powder diffractometer should be regularly checked. Various standard materials are available to check the alignment of and intensities recorded by the system (www.nist.gov). There are several commercial suppliers of powder diffractometers, with many of the modern designs allowing a number of different experimental configurations on the same basic

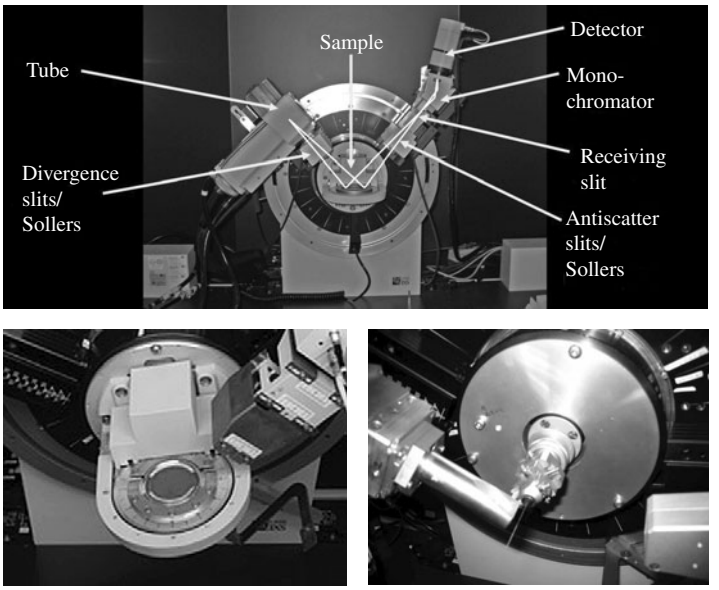

Fig. 17.3 Top: a typical laboratory instrument corresponding to the flat-plate setup of Fig. 17.2. Bottom: flat plate and capillary holders.

instrument. The introduction of new optical devices such as X-ray mirrors to replace monochromators gives further flexibility in experimental design.

Significantly higher fluxes and higher resolution is available at a synchrotron source. Diffractometers such as ID31 at the ESRF and I11 at Diamond receive a useful flux several orders of magnitude greater than a typical laboratory instrument and can give very high-resolution data. The range of energies emitted by a synchrotron source means that wavelengths can be selected for specific experiments. By selecting a short wavelength one can obtain data to higher values of $\sin\theta/\lambda$ with a shorter scan range; by choosing a longer wavelength the diffraction pattern is spread out in 2θ, potentially allowing better resolution of overlapping peaks. One can also select a wavelength close to an absorption edge to tune scattering factors (resonant or near-edge experiments). It is also possible to use the entire spectrum of radiation produced and perform energy-dispersive diffraction. In Bragg's law ($\lambda = 2d_{hkl}\sin\theta$) one is then measuring different d_{hkl} values by varying λ at fixed θ rather than varying θ at fixed λ. This can allow complex experimental setups to be used, but with current detectors gives lower-resolution data, which can also be harder to analyze quantitatively.

Powder neutron diffraction offers significant potential advantages over X-ray methods in some situations. In particular, since scattering occurs from the nucleus rather than electrons, one can detect light atoms in the presence of heavy atoms (e.g. O/H in the presence of metals). The penetrating nature of neutrons also gives more confidence that one is

studying the bulk of a sample rather than a thin surface layer and allows the use of more complex sample environment equipment. Neutrons are also scattered by magnetic moments in a material, giving the possibility of magnetic structure determination. Neutron diffraction can be performed either at a reactor (generally using constant λ neutrons) or at a spallation source (usually by the time-of-flight method that takes advantage of the full range of neutron wavelengths produced by the source). Perhaps the major drawback of this technique for the molecular chemist is the fact that H scatters neutrons incoherently. To avoid unreasonably high backgrounds it is often necessary to deuterate samples. However, with the high fluxes available for instruments such as GEM at ISIS and D20 at ILL (and becoming available on HRPD and at other facilities) studies on normal hydrogenated materials are becoming increasingly feasible.

17.4 Information contained in a powder pattern

The powder diffraction pattern of any material (or mixture of materials) contains information 'stored' in three distinct places. Peak positions are determined by the size, shape and symmetry of the unit cell. Peak intensities are determined by the arrangement of scattering density (i.e. atomic co-ordinates) within the unit cell. The peak shape is determined by a convolution of instrumental parameters (source, optics and detector contributions) and important information about the microstructure (domain size, strain) of the sample. This latter information is not usually considered in small-molecule crystallographic work, but is more noticeable in powder analysis as peak shapes are immediately apparent when one visualizes a dataset, and must be considered during many forms of data analysis.

One feature that distinguishes powder diffraction from single-crystal work is that structural analysis (i.e. the determination of fractional co-ordinates of the atoms in the material) is not always, indeed not normally, the goal of the experiment. The sections below describe some of the different applications of powder diffraction. They are arranged approximately in order of increasing complexity of analysis, and are the applications most likely to be of interest to the small-molecule/chemistry community.

17.4.1 Phase identification

Each (crystalline) phase present in a bulk sample will give rise to a characteristic set of peaks in a powder diffraction pattern. These can be compared to a database of known diffraction patterns or compared against patterns calculated from single-crystal diffraction data. Many powder diffractometer manufacturers supply search/match software to compare experimental datasets against the powder diffraction file

(PDF-2), a collection of around 186 000 (February 2007) datasets maintained by the International Centre for Diffraction Data (www.icdd.com). Very recently a large percentage of the Cambridge Structural Database (Allen, 2002) (approximately 400 000 entries in February 2007) have been made commercially available as calculated powder patterns in a format suitable for automated search/match algorithms. This so-called PDF-4/Organics contained 312 000 entries in February 2007. Many single-crystal refinement packages provide a facility for simulating a diffraction pattern from either a refined structural model or directly from experimental single-crystal data. These simulations can be compared with experimental data. Many other resources for calculating powder patterns are available via the web.

Perhaps the most important application of phase identification to the small-molecule crystallographer is in confirming whether the powder pattern of a bulk sample corresponds to a structure determined from a single crystal obtained during the same synthesis – there are innumerable examples where the few single crystals produced in a synthesis are due to minor products from side reactions or impurities. The presence of crystalline co-products (e.g. KCl from a salt-elimination reaction) can also be readily identified. A relatively quick powder diffraction experiment can often shed considerable light on otherwise conflicting pieces of analytical data.

With regard to synthesis, especially for solid-state syntheses of extended materials, powder diffraction provides a straightforward way of monitoring the course of reaction. Peaks due to starting materials and other impurities can be readily identified, allowing the progress of a reaction to be followed. In many ways powder diffraction is the solid-state chemist's equivalent of solution-state NMR.

17.4.2 Quantitative analysis

It is also possible to obtain quantitative information about the composition of a multiphase sample from powder diffraction data. Various techniques have been developed based on the analysis of intensities of individual peaks due to different phases contributing to the pattern, on whole-pattern intensity analysis, or on multiphase Rietveld refinement (see below). Specific details are beyond the scope of this chapter and the reader is referred elsewhere (Dinnebier and Billinge, 2008).

It is worth noting that extreme care should be taken when determining/interpreting quantitative composition. Results can be severely influenced by methods of sample preparation (see above), data collection and analysis. Careful calibration experiments on the system of interest are essential. It is also worth noting that it is possible to estimate the quantity of amorphous material in a sample by powder diffraction measurements (amorphous materials generally give rise to a gradually oscillating contribution to the background of the diffraction pattern and can easily be overlooked), by careful quantitative dilution of a powdered sample with an additional crystalline phase.

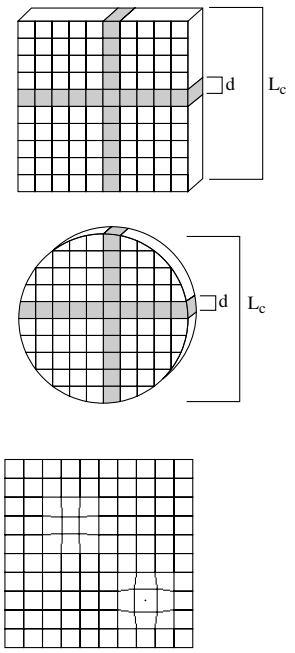

Fig. 17.4 Size-strain.

17.4.3 Peak-shape information

Whilst the position and intensity of peaks in a powder pattern are determined by the unit cell size and contents, their shape and width are determined by both instrumental effects (which can be corrected for or modelled) and sample properties such as the size and strain of crystallites and stacking faults (Fig. 17.4) (Klug and Alexander, 1974). The simplest expression for peak broadening due to sample size (the Scherrer formula) predicts that peak width and particle size are related by fwhm $= K\lambda/(\text{size} \times \cos\theta)$, where K is a shape factor (often 0.9), fwhm the peak full width at half-maximum in radians, and λ the wavelength; absolute numbers from this expression should be treated with caution. Sample strain leads to a peak-width dependence on $\tan\theta$. Note that, although size and strain both cause peaks to broaden with increasing 2θ, one can distinguish between these effects from their different 2θ dependence ($1/\cos\theta$ and $\tan\theta$, respectively). This does, however, need high-quality data recorded over a wide 2θ range. Practical guidance on determination of sample size and strain is given in a recent IUCr Round Robin (Balzar *et al.*, 2004).

Figure 17.5 illustrates the effects of sample size on peak shapes. Figure 17.5a shows the diffraction pattern of an FePt alloy that contains ~2.2 nm nanoparticles. Figure 17.5b shows a material with ~8 nm domains. It is worth remembering that there are many different ways of defining the 'size' of a material, and that diffraction methods report the volume-weighted mean column height of the crystallites present. The apparent 'size' of the sample is therefore dependent on the shape of the domains (only for $h00$ reflections of a perfect cube is the volume-weighted column height directly related to crystallite size). The apparent size determined will also be dependent on the size distribution (often log normal) present. If precise size information is required then supporting evidence from TEM/SEM is very important. In more sophisticated treatments hkl-dependent peak widths can be used to obtain information

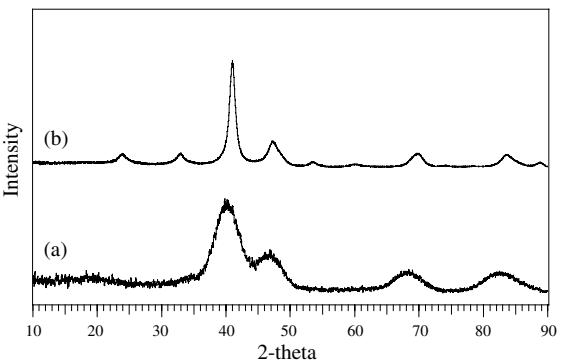

Fig. 17.5 Diffraction data from (a) ~2 nm FePt particles and (b) ~8 nm particles.

on the anisotropies of size and strain in a sample. More details on the interpretation of peak shapes are given elsewhere (Scardi and Leoni, 2002; Warren, 1969).

17.4.4 Intensity information

The intensities of peaks in a diffraction pattern contain information about atomic co-ordinates and displacement parameters, just as in a single-crystal experiment. Early structural work using powder diffraction data analyzed extracted intensities (e.g. by weighing carefully cut-out peaks in the early days!) and refinement methods essentially identical to those used in single-crystal work. Nowadays, it is more common to employ whole-pattern fitting methods to extract structural information – principally the Rietveld method discussed in Section 17.5. For any quantitative work involving powder diffraction intensities it is essential to consider how aspects of the experimental setup (use of variable slits, Lorentz-polarization factors, etc.) influence intensities. If the data are scaled in any way (e.g. to correct for variable slits) it is important to propagate the standard uncertainty of the intensity in an appropriate manner.

17.5 Rietveld refinement

One of the main factors that has driven the explosion of powder diffraction methods in recent years is the popularization of the Rietveld method (Rietveld, 1969; Young, 1995; McCusker *et al*., 1999). In this method a powder pattern is expressed in terms of y_{obs}, the intensity observed at a given value of 2θ. One can use a structural model (equivalent to that used in a single-crystal refinement), a model to describe how experimental peak shapes vary as a function of 2θ, and a model for the background, to determine the calculated intensity, y_{calc}, at each experimental value of 2θ. The most commonly used function for describing powder peaks is a pseudo-Voigt (a mixture of Gaussian and Lorentzian contributions), though more sophisticated approaches can model peak-shape contributions from the experimental setup and sample size/strain directly.

One then typically uses a least-squares method to adjust structural parameters such as unit cell dimensions, fractional atomic co-ordinates and displacement parameters, and instrument/experiment-related parameters to minimize the difference between y_{obs} and y_{calc} over the whole experimental pattern (Table. 17.1). The quality of a refinement can be monitored in terms of agreement factors R_{wp} or R_{Bragg} or goodness-of-fit/χ^2 (which compare the R_{wp} value to the statistically expected value R_{exp}). Standard expressions for agreement factors are given in (17.1)–(17.4); n is the number of observations, p the number of

Table 17.1. Parameters commonly refined during Rietveld analysis.

Sample-related	**Instrument-related**
scale factor	EITHER sample height error
unit cell parameters	OR zero-point error
fractional co-ordinates	wavelength?
atomic displacement parameters	
sample contribution to peak shape	instrument contribution to peak shape
preferred orientation correction	

parameters, and w_i a weighting factor.

$$R_{\mathrm{wp}} = \left\{ \frac{\sum_i w_i \left[y_i\,(obs) - y_i\,(calc) \right]^2}{\sum_i w_i \left[y_i\,(obs) \right]^2} \right\}^{\frac{1}{2}} \tag{17.1}$$

$$R_{\mathrm{exp}} = \left\{ \frac{(n-p)}{\sum_{i=1}^{n} w_i y_i (\mathrm{obs})^2} \right\}^{\frac{1}{2}} \tag{17.2}$$

$$\chi^2 = \left\{ \frac{R_{\mathrm{wp}}}{R_{\mathrm{exp}}} \right\}^2 \tag{17.3}$$

$$R_{\mathrm{Bragg}} = \frac{\sum_{hkl} \left| I_{hkl}\,('obs') - I_{hkl}\,(calc) \right|}{\sum_{hkl} I_{hkl}\,('obs')} \tag{17.4}$$

R_{wp} has the advantage that it represents directly the quantity minimized. It is, however, influenced by, e.g., background points and a high background can give a misleadingly low R_{wp} value – background-subtracted R_{wp} values are more useful. R_{Bragg} is most closely related to single-crystal R-factors. It is, however, biased by the structural model, which is used to partition intensities of overlapping reflections to obtain I_{hkl}('obs') values. The best indication of the quality of a structural refinement is often a visual inspection of the agreement of observed and calculated patterns and the difference profile.

An example of a Rietveld refinement of an inclusion compound is given in Fig. 17.6 (Evans *et al.*, 2001). A number of commercial and academic software packages are available for Rietveld refinement. The most widely used are GSAS, Fullprof, descendants of the DBWS code and Topas (Bruker, 2000; Larson and von Dreele, 1994; Wiles and Young, 1981; Rodriguez-Carvajal, 1990). Many of these packages offer the opportunity to refine a model simultaneously with both X-ray and neutron data, allowing one to utilize the often complementary information from the two techniques. They also allow fitting of multiple phases to each dataset, which can allow quantitative analysis or allow

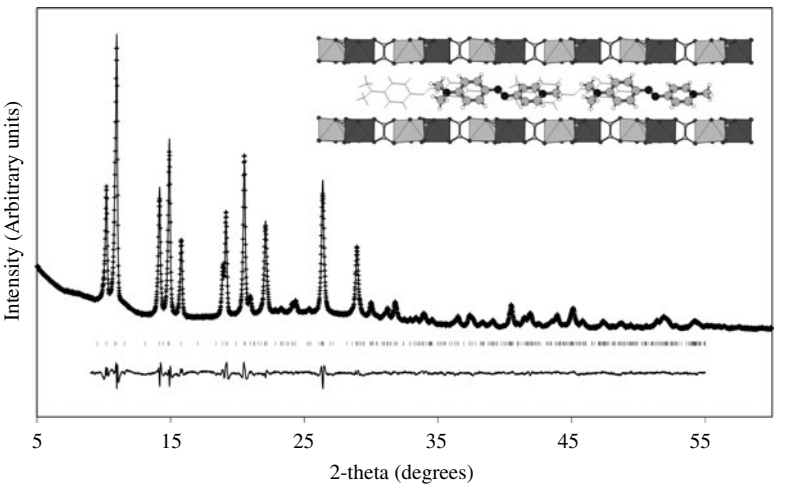

Fig. 17.6 A Rietveld refinement of an NLO-active layered inclusion compound DAZOP[$MnCr(ox)_3$]·0.6CH_3CN [DAZOP = 4-(4-dimethylamino-phenylazo)-1-methyl-pyridinium]. Observed data are shown as small crosses, calculated data as a solid line and the difference as the lower solid line. Small vertical tick marks show 2θ values where reflections are predicted.

for the presence of minor impurities during refinement of a phase of interest.

The practicalities of Rietveld refinement are beyond the scope of this text. Typically, though, in the early stages of a refinement one would want to adjust manually or refine the scale parameter and factors such as the detector zero-point error or sample height until predicted peak positions match those observed. Parameters describing the peak shape should then be adjusted until observed and calculated shapes match. Finally, factors affecting intensities (atomic co-ordinates and displacement parameters) should be refined. As the refinement improves (or with good software) one should be able to refine many of these parameters simultaneously. Details of parameters typically used in a Rietveld refinement are given in Table 17.1.

Rietveld refinement does contain many traps for the uninitiated. Refinements are far more likely to diverge compared to single-crystal refinements; one is far more likely to find false minima; it is much easier with powder work for a wrong model to fit the data well; many parameters are highly (sometimes completely) correlated so should not be refined together; there are many 'fudge factors' contained in software packages that may improve the quality of fit but have no physical meaning; there are many more refinement options ('buttons to click') than in single-crystal packages. Never refine any parameter unless you know exactly what it is doing! Finally, it is worth re-emphasizing that the information content in a powder pattern is almost always lower than in a single-crystal experiment. In all but the simplest systems one will not have the 10 observations per parameter that one would

like in single-crystal work. If you have a choice, do the single-crystal experiment!

17.6 Structure solution from powder diffraction data

It should be emphasized that the Rietveld technique is a refinement method – one needs an approximate set of starting co-ordinates from which to begin refinement. Until the late 1990s this meant that Rietveld refinement was largely confined to extended metal oxides and chalcogenides where starting models could be inferred from other known materials. In recent years there have, however, been dramatic breakthroughs in solving structures *ab initio* from powder data (Harris *et al.*, 2001, 2002; David *et al.*, 2006).

The process of structure solution of an unknown material from powder data can be divided into several steps. Firstly, one must record the highest-quality data possible on an (ideally) pure sample. One must then determine the unit cell parameters from observed peak positions. For simple systems indexing can be performed by hand (see problems at the end of the chapter). In most cases indexing is performed by software packages. Some operate along similar lines to those used in single-crystal work, others perform exhaustive searches of real space. Indexing powder data is by no means a trivial task and is often the bottleneck to structure solution. To maximize the chances of success peak positions must be determined with a high degree of accuracy (not just precision), for which the use of internal standards and careful peak fitting is recommended.

Next, the space group symmetry must be determined from systematic absences. This is again non-trivial, as peak overlap at high 2θ typically means that it is hard to tell if a particular reflection class is present or not. It may be easy to decide that the (010) reflection is absent and the (020) present, but gaining definitive information on higher-order reflections is hard. There are software packages that use intensity statistics from whole-pattern fitting to help with this (Markvardsen *et al.*, 2001).

Once the unit cell and space group are known it is often sensible to perform a Pawley (or Le Bail) refinement (Pawley, 1981; Le Bail *et al.*, 1988). These refinement methods are similar to Rietveld refinements but are performed without a structural model. They are essentially peak-fitting routines with allowed peak positions constrained by the unit cell size/shape (which is refined) and symmetry and a single 2θ-dependent peak shape for the whole pattern. If peaks are not fitted well during a Pawley refinement then either the cell or space group is wrong or impurities are present. The Pawley refinement also gives an indication of the best fit that will be achievable in the model-dependent Rietveld refinement. If the final Rietveld agreement factors are significantly higher than those for the Pawley refinement, or the fits visually worse, then the model should be examined carefully.

At this stage one of a number of different routes can be followed. One possibility is to extract integrated peak intensities from the pattern and use techniques similar to those employed in single-crystal studies such as direct methods or Patterson synthesis to solve the structure. Pawley/Le Bail refinements are the best way of obtaining these intensities. Various software packages exist for structure solution, some dedicated to overcoming the inherent uncertainties in intensities due to peak overlap and data shortage from a powder pattern. Very recently, so-called 'charge-flipping' algorithms have been applied to powder data with some success (Baerlocher *et al.*, 2007; Oszlanyi and Suto, 2004). Structure completion can then be performed via a series of Fourier difference maps and Rietveld refinement. For example the 33-atom structure of γ-ZrW_2O_8 was solved in this way (Fig. 17.7) (Evans *et al.*, 1997).

Alternatively (and perhaps more powerfully for molecular species where the connectivity of the molecule, or a significant part of it, is known), one can utilize information about the cell contents in the form of known molecular fragments and their geometric degrees of freedom and attempt direct-space structure solution. From the molecular cell contents one generates a trial structural model and compares its calculated diffraction pattern to the experimental data. Using a Monte-Carlo or simulated annealing approach one then adjusts the structural model in a random fashion and examines again the agreement between the observed and calculated patterns. The move is then accepted or rejected based on user-definable criteria and the process is repeated until the best agreement between model and experiment is obtained. With efficient algorithms many hundreds of thousands of trial structures can be generated and tested relatively rapidly even on desktop computers to produce a structural model that can be improved by Rietveld methods. Many variations on this general methodology and alternative genetic and differential evolution algorithms have been developed. Materials of remarkable complexity have been solved in this way. The 62-atom structure of the NLO-active inclusion compound of Fig. 17.6, for which single crystals could not be grown, was solved by a related technique (Evans *et al.*, 2001).

It should be noted that each stage of the structure solution pathway from indexing to refinement is complex and potentially insoluble. The range of techniques for overcoming each barrier is, however, expanding rapidly in what is a fast-moving research area.

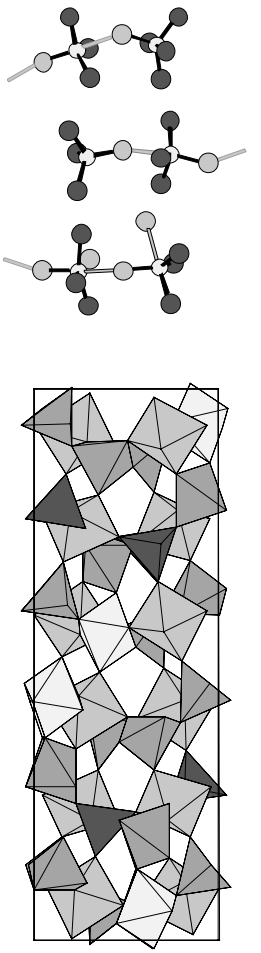

Fig. 17.7 The 33-atom structure of γ-ZrW_2O_8 solved by direct methods and Fourier maps.

17.7 Non-ambient studies

Experiments beyond a simple room-temperature diffraction pattern can yield considerable insight into the properties of materials. One of the most readily accessible thermodynamic variables experimentally is temperature. Commercial attachments are available for most diffractometers to cool/heat samples from liquid He temperatures to ~1600°C. Variable-temperature experiments allow one to follow, *inter alia*, phase

transitions in materials, study temperature-dependent polymorphism, follow hydration/dehydration pathways, and follow the synthesis of materials in real time (Evans and Evans, 2004).

The possibility of performing a powder diffraction experiment during more complex chemical reactions should not be overlooked. Various workers have shown that, using high-energy (and therefore highly penetrating) X-ray beams at synchrotrons, one can literally monitor reactions occurring in test tubes (or more sophisticated reactors!) in real time by powder diffraction methods (Evans *et al.*, 1998; Francis and O'Hare, 1998). By way of an example, O'Hare and co-workers have shown that one can record diffraction patterns of ~100 mg of a suspension of solid SnS_2 in toluene in as little as 5 s. One can then introduce a molecule such as cobaltocene and monitor in real time the structural changes and kinetics of the host-guest intercalation reaction.

The behaviour of materials under applied pressure is also readily studied by powder diffraction methods. Using small-volume diamond anvil cells most suitable for X-ray work, pressures of several hundred GPa at temperatures up to several thousand K can be achieved (Paszkowicz, 2002). Larger volumes of samples can be studied by neutron techniques using gas pressure cells (up to ~1 GPa on several cm^3 of sample) or more sophisticated designs such as the Paris–Edinburgh design cell (up to ~30 GPa/370 K on 30 mm^3). Such studies have revealed a wealth of important structural chemistry in a variety of molecular systems.

References

Allen, F. H. (2002). *Acta Crystallogr.* **B58**, 380–388.

Baerlocher, C., McCusker, L. M. and Palatinus, L. (2007). *Z. Kristallogr.* **222**, 47–53.

Balzar, D., Audebrand, N., Daymond, M. R., Fitch, A., Hewat, A., Langford, J. I., Le Bail, A., Louer, D., Masson, O., McCowan, C. N., Popa, N. C., Stephens P. W. and Toby, B. H. (2004). *J. Appl. Crystallogr.* **37**, 911–924.

Bruker (2000). *Topas: general profile and structure analysis software for powder diffraction data*. Bruker AXS, Karlsruhe, Germany.

Cullity, B. D. and Stock, S, (2001). *Elements of X-ray diffraction*. Prentice Hall: Upper Saddle River, New Jersey, USA.

David, W. I. F. (1999). *J. Appl. Crystallogr.* **32**, 654–663.

David, W. I. F., Shankland, K., McCusker, L. M. and Baerlocher, C. (2006). *Structure determination from powder diffraction data*. Oxford University Press, Oxford, UK.

Dinnebier, R. E. and Billinge, S. (2008). *Powder diffraction – theory and practice*. Royal Society of Chemistry, Cambridge.

Evans, J. S. O., Benard, S., Yu, P. and Clement, R. (2001). *Chem. Mater.* **13**, 3813–3816.

Evans, J. S. O. and Evans, I. R. (2004). *Chem. Soc. Rev.* **33**, 539–547.

Evans, J. S. O., Hu, Z., Jorgensen, J. D., Argyriou, D. N., Short, S. and Sleight, A. W. (1997). *Science*, **275**, 61–65.
Evans, J. S. O., Price, S. J., Wong, H. V. and O'Hare, D. (1998). *J. Am. Chem. Soc.* **120**, 10837–10846.
Francis, R. J. and O'Hare, D. (1998). *J. Chem. Soc. Dalton Trans.*, pp. 3133–3148.
Harris, K. D. M., Johnston, R. L., Cheung, E. Y., Turner, G. W., Habershon, S., Albesa-Jove, D., Tedesco, E. and Kariuki, B. M. (2002). *CrystEngComm*, pp. 356–367.
Harris, K. D. M., Tremayne, M. and Kariuki, B . M. (2001). *Angew. Chem. Int. Ed.* **40**, 1626–1651.
Jenkins, R. and Snyder, R. L. (1996). *Introduction to X-ray powder diffractometry*. Wiley-Interscience: New York, USA.
Klug, H. P. and Alexander, L. E. (1974). *X-ray diffraction procedures for polycrystalline and amorphous materials*, Wiley-Interscience: New York, USA.
Langford, J. I. and Louer, D. (1996). *Rep. Prog. Phys.*, **59**, 131–234.
Larson, A. C. and von Dreele, R. B. (1994). *Los Alamos Internal Report No. 86-748*.
Le Bail, A., Duroy, H. and Fourquet, J. L. (1988). *Mater. Res. Bull.* **23**, 447–452
Markvardsen, A. J., David, W. I. F., Johnson, J. C. and Shankland, K. (2001). *Acta Crystallogr.* **A57,** 47–54.
McCusker, L. B., Von Dreele, R. B., Cox, D. E., Louer, D. and Scardi, P. (1999). *J. Appl. Crystallogr.* **32**, 36–50.
Money, V. A., Evans, I. R., Halcrow, M. A., Goeta, A. E. and Howard, J. A. K. (2003). *Chem. Commun.* pp. 158–159.
Oszlanyi, G. and Suto, A. (2004). *Acta Crystallogr.* **60**, 134–141.
Paszkowicz, W. (2002). *Nucl. Instrum. Methods Phys. Res., Section B – Beam Interac. Mater. Atoms.* **198**, 142–182.
Pawley, G. S. (1981). *J. Appl. Crystallogr.* **14**, 357–361.
Pecharsky, V. K. and. Zavalij, P. Y. (2003). *Fundamentals of powder diffraction and structural characterization of materials.* Kluwer: Dordrecht, The Netherlands.
Rietveld, H. M. (1969). *J. Appl. Crystallogr.* **2**, 65–71.
Rodriguez-Carvajal, J. (1990). *Abstracts of the Satellite Meeting on Powder Diffraction of the XV Congress of the IUCr,* Toulouse, France, p. 127.
Scardi, P. and Leoni, M. (2002). *Acta Crystallogr.* **A58**, 190–200.
Sivia, D. S. (2000). *J. Appl. Crystallogr.* **33**, 1295–1301.
Warren, B. E. (1969). *X-ray diffraction.* Dover: New York.
Wessels, T., Baerlocher, C. and McCusker, L. B. (1999). *Science*, **284**, 477–479.
Wiles, D. B. and Young, R. A. (1981). *J. Appl. Crystallogr.* **14**, 149–151.
Young, R. A. (1995). *The Rietveld method*. Oxford University Press, Oxford, UK.

Exercises

1. Graphite is a layered material that undergoes intercalation chemistry with alkali metals. The first two reflections in the powder diffraction patterns of graphite and a K intercalation compound were observed at 26.58/54.76° and 16.56/33.47° 2θ, respectively. Calculate *d*-spacings for each reflection and suggest *hkl* indices. Why are only certain classes of *hkl* reflections typically seen in powder diffraction patterns of these materials? How might you try to observe other reflections? ($\lambda = 1.54$ Å).
2. Figure 17.8 shows powder diffraction patterns of two inorganic materials recorded with $\lambda = 1.54$ Å. Index

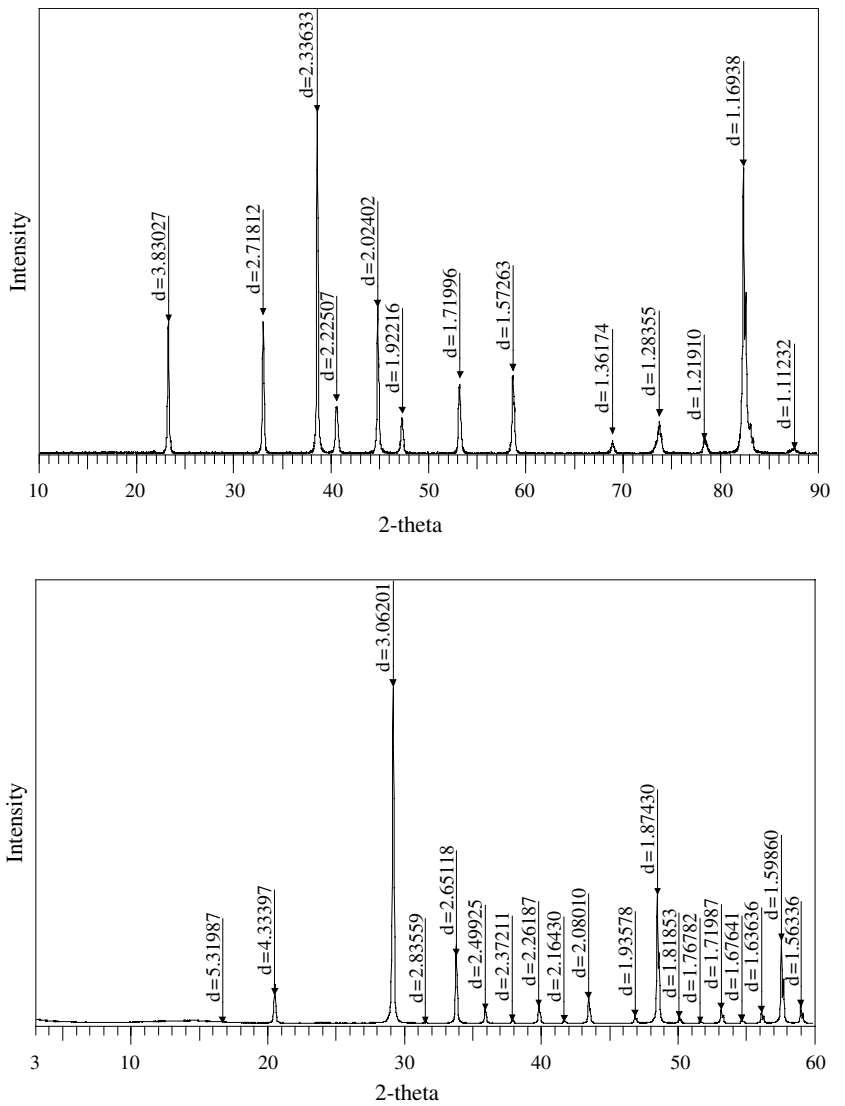

Fig. 17.8 Diffraction data recorded with $\lambda = 1.54$ Å for two materials. *d*-spacings are given in Å.

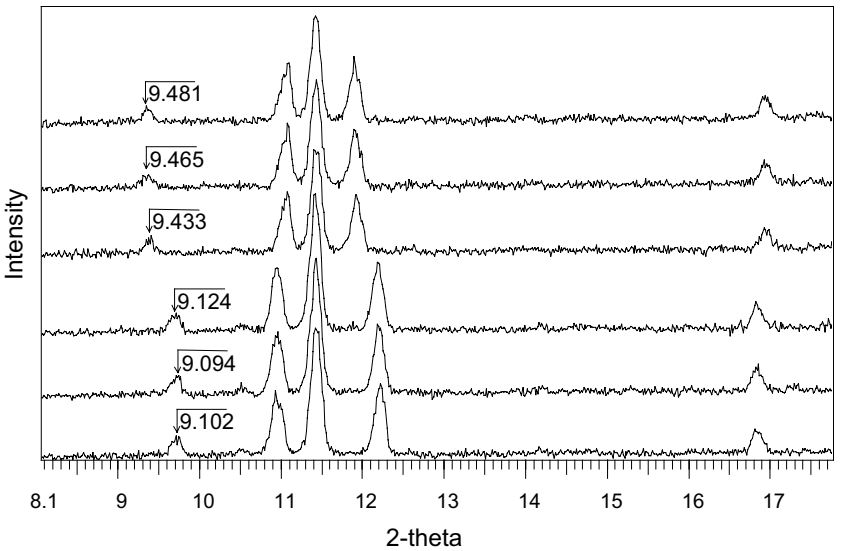

Fig. 17.9 Diffraction data recorded at $T = 237$, 248, 260, 271, 282 and 294 K for $[FeL_2](BF_4)_2$ (L = 2,6-di(pyrazol-1-yl)pyridine (Money *et al.*, 2003). Lowest temperature at the bottom of the figure. d-spacings are given in Å for one peak.

each and comment on their symmetry. Comment on any reflections you cannot index.

3. For the second example of exercise **2** calculate the cell parameter from each reflection indexed. Which data should be used to obtain precise cell parameters? Why?
4. What experimental factors can cause systematic errors in cell parameter determination? How would one obtain the most precise and most accurate cell parameters possible?
5. Figure 17.9 shows diffraction data recorded for an octahedral Fe^{II} complex (Fig. 17.10) at six different temperatures. Comment on these data.
6. Use the Scherrer formula (Section 17.4.3) to obtain a crude estimate of the size of the crystalline domains in Fig. 17.5(a) and (b).

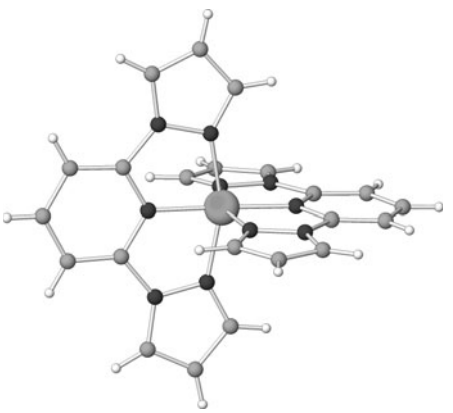

Fig. 17.10 The structure of $[FeL_2](BF_4)_2$.

This page intentionally left blank

Introduction to twinning

18

Simon Parsons

18.1 Introduction

Twinning is not an uncommon effect in crystallography, although it has long been considered to be one of the most serious potential obstacles to structure determination. Computer software has now been developed to such an extent that previously intractable twinning problems have yielded results of comparable precision to those obtained with untwinned samples. Structure determinations from twinned crystals are therefore now quite common, and the aim of this chapter is to present an introduction to the phenomenon of twinning.

18.2 A simple model for twinning

Twinning may occur when a unit cell (or a supercell) has higher symmetry than implied by the space group of the crystal structure. An example of a system that might be susceptible to twinning is a monoclinic crystal structure where the unique angle, β, is equal, or very close, to 90°. In this case the crystal structure has point group $2/m$, but the lattice has point group mmm. The elements of these point groups are:

$$2/m:\ 1, m\perp b, 2//b, \overline{1}$$

$$mmm:\ 1, m\perp a, 2//a, m\perp b, 2//b, m\perp c, 2//c, \overline{1}.$$

The important issue is that mmm contains symmetry elements that do not occur in $2/m$. Under these conditions 'mistakes' can occur during crystal growth such that different regions of the crystal (domains) have their unit cells related by symmetry operations that are elements of mmm but not of $2/m$ – a two-fold rotation axis about the a-axis direction for example.

This idea can be illustrated by building up a stack of bricks. The overall shape or outline of a brick has symmetry mmm, but if we consider the 'dent' (bricklayers call this the 'frog') on one side plus the words 'London Brick' the point symmetry is only 2. The most obvious way to build a stack of bricks is to place all the bricks in the same orientation, such as in Fig. 18.1*ii*: notice that the bricks are related to each other by the two-fold axes perpendicular to the page or simple translation – both are

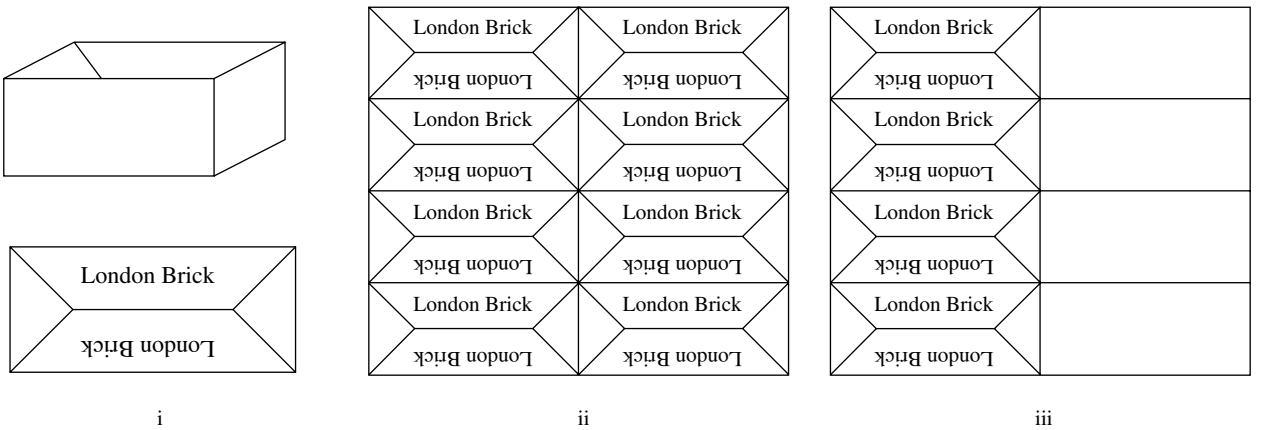

Fig. 18.1 A simple model for twinning. i. A brick; the top face of the brick has an indentation and the words London Brick embossed on two sides of the indentation. ii. A stack of bricks where all the bricks are related to one another by translation. This resembles the relationship between units cells making up a single crystal. iii. Here some of the bricks have been placed upside-down. The bricks still fit together, because in turning a brick upside-down we have used a symmetry element of the outline or overall shape of the brick. This resembles the relationship between unit cells in a twinned crystal. In both ii and iii the figures are intended to represent a whole crystal. Reproduced by permission of the International Union of Crystallography.

elements of the space group. The 'space group' of the stack of bricks in Fig. 18.1*ii* would be *P*2. However, it is also possible to stack the bricks in such a way that some of the bricks are placed upside-down (Fig. 18.1*iii*). The overall shape of the brick, with the 90° angles between the edges, allows this to happen without compromising the stacking of the bricks in any way. In turning some of the bricks upside-down we have used a two-fold axis that is a symmetry operation of point group *mmm*, but not of point group 2.

Figure 18.1*ii* is similar to a single crystal; Fig. 18.1*iii* resembles a twinned crystal. In Fig. 18.1*iii* bricks (which correspond to unit cells) within the same *domain* are related to each other by translation; bricks in different domains are related by a translation plus an additional symmetry element, such as a rotation, which occurs in the point symmetry of the outline or overall shape of the brick. This extra symmetry operation corresponds in crystallography to the *twin law*. Had the extra element been chosen to be a mirror plane the mirror image of the words 'London Brick' would have appeared in the second domain, and it is important to bear this in mind during the analysis of enantio-pure crystals of chiral compounds (for example, in protein crystallography the only possible twin laws are rotation axes). The fraction of the bricks in the alternative orientation corresponds to the *twin scale factor*, which in this example is 0.5.

18.3 Twinning in crystals

Monoclinic crystal structures sometimes have β very close to 90°. If twinning occurs the unit cells in one domain may be rotated by 180°

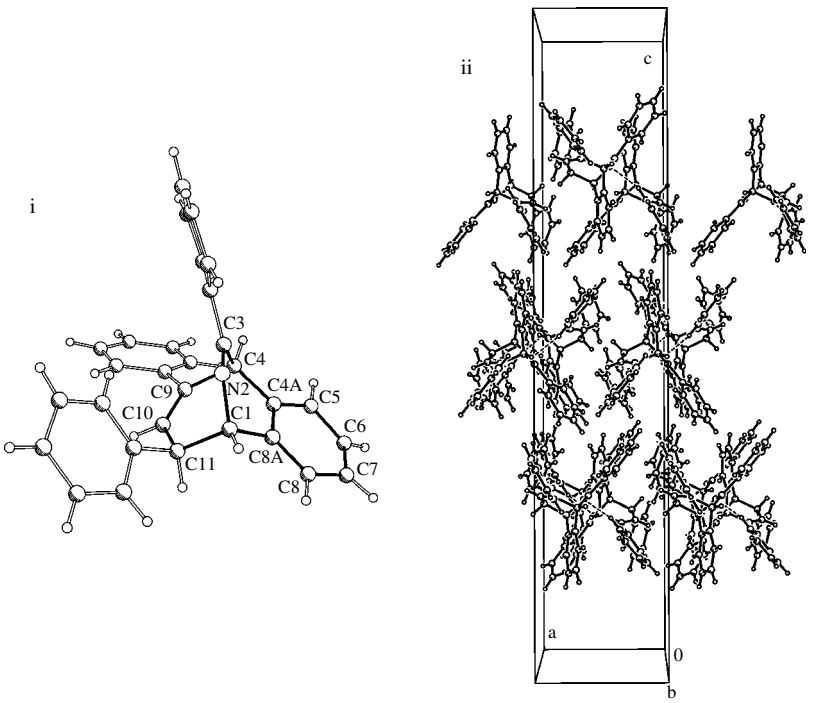

Fig. 18.2 Molecular structure (i) and crystal structure (ii) of compound 1. This is a monoclinic structure in which β was indistinguishable from 90°, twinned via a two-fold rotation about *a*. The labelled part of the molecule in (i) was used as a rigid fragment in a Patterson search to solve the structure.

about the *a*- or *c*-axes relative to those in the other domain in exactly the fashion described above for bricks. However, not all monoclinic crystal structures with $\beta \sim 90°$ form twinned crystals: twinning will be observed only if intermolecular interactions across a twin boundary are energetically competitive with those that would have been formed in a single crystal. For this reason, twinning very commonly occurs if a high-symmetry phase of a material undergoes a transition to a lower-symmetry form: a 'lost' symmetry element that made certain interactions equivalent in the high-symmetry form can act as a twin law in the low-symmetry form. Layered structures, such as the one shown in Fig. 18.2 (compound 1, see also Section 18.10), are also often susceptible to twinning if the interactions between layers are rather weak and non-specific: alternative orientations of successive layers are energetically similar. The total energy difference between intermolecular interactions that occur in a single, as opposed to a twinned, form of a crystal is one factor that controls the value of the domain scale factor, although in practice this may also be controlled kinetically, for example by the rate of crystal growth.

In the foregoing discussion the impression might have been given that a twinned crystal consists of just two domains. A monoclinic crystal with

$\beta \sim 90°$ twinned via a two-fold rotation about *a* may actually consist of very many domains, but the orientations of the unit cells in any pair of domains will be related either by the identity operator or by the twin law. Further examples have been illustrated by Giacovazzo (1992).

The twin law itself forms part of the model used to reproduce a diffraction pattern, and, as pointed out recently by Schwarzenbach *et al.* (2006) it is *'a purely formal description in terms of symmetry, [providing] no answer to important questions such as the origins of twinning and the interfaces between the domains'*. Although the properties of a material (e.g. mechanical and optical properties) can depend strongly on domain structure, it is usually not necessary to characterize this for the purposes of ordinary structure analysis. However, the twin scale factor may appear to vary when different regions of a crystal are sampled during data collection. This can give rise to non-isomorphism effects in protein structure determination (van Scheltinga, 2003).

18.4 Diffraction patterns from twinned crystals

Each domain of a twinned crystal gives rise to a diffraction pattern; what is measured on a diffractometer is a superposition of all these patterns with intensities weighted according to the domain scale factors. The relative orientations of the diffraction patterns from different domains are the same as the relative orientations of the domains. If the domains are related by a 180° rotation about the *a*-axis direction, then so too are their diffraction patterns. Figure 18.3 shows this for a twinned monoclinic crystal structure for which $\beta = 90°$. Twinning is a problem in crystallography because it causes superposition or overlap between symmetry-inequivalent reflections. In Fig. 18.3*iii* the reflection that would have been measured with indices 102 is actually a composite of the 102 reflection from domain 1 (Fig. 18.3*i*) and the $10\overline{2}$ reflection from domain 2 (Fig. 18-3*ii*). During structure analysis of a twinned crystal it is important to define exactly which reflections contribute to a given intensity measurement: this is the role of the twin law.

In order to treat twinning during refinement the twin law must obviously form part of the model. Usually it is input into a refinement program in the form of a 3×3 matrix. In the example shown in Fig. 18.3 the 2-fold axis about *a* will transform **a**, **b** into $-\mathbf{b}$, and **c** into $-\mathbf{c}$. This is the transformation between the cells in different domains of the crystal; written as a matrix this is

$$\begin{pmatrix} 1 & 0 & 0 \\ 0 & -1 & 0 \\ 0 & 0 & -1 \end{pmatrix}.$$

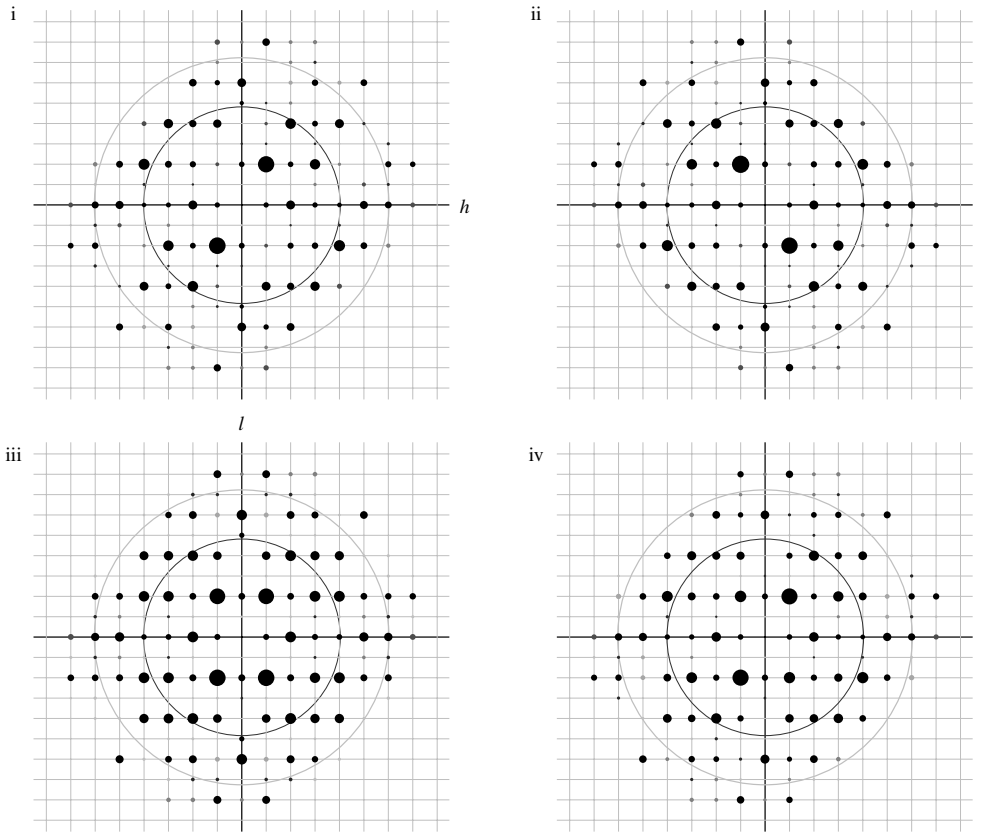

Fig. 18.3 The effect of twinning by a two-fold rotation about **a** on the diffraction pattern of a monoclinic crystal with $\beta = 90°$. Only the $h0l$ zone is illustrated; the space group is $P2_1/c$. i (top left): $h0l$ zones from a single crystal. This could represent the diffraction pattern from one domain of a twinned crystal. ii (top right): this is the same pattern as shown in i, but rotated about the a^* (or h) axis (which is parallel to the a-axis of the direct cell). This figure represents the diffraction pattern from the second domain of a twinned crystal. iii (bottom left): superposition of i and ii simulating a twin with a domain scale factor of 0.5 – that is, both domains are present in equal amounts. iv (bottom right): superposition of i and ii simulating a twin with a domain scale factor of 0.2 – the crystal consists of 80% of one domain (i) and 20% of the other (ii). The values of $|E^2-1|$ for each pattern are: i and ii 1.015; iii 0.674; iv 0.743. The ideal (untwinned) value of $|E^2 - 1|$ for this centrosymmetric crystal structure is 0.97, meaning that its diffraction pattern is characterized by the presence of both strong and weak reflections; intensities are more evenly distributed in acentric distributions, where $|E^2 - 1|$ has an ideal value of 0.74.

The same matrix relates the indices of pairs of overlapping reflections:[†]

$$\begin{pmatrix} 1 & 0 & 0 \\ 0 & -1 & 0 \\ 0 & 0 & -1 \end{pmatrix} \begin{pmatrix} h \\ k \\ l \end{pmatrix} = \begin{pmatrix} h \\ -k \\ -l \end{pmatrix}.$$

[†] Here, the triple hkl is represented as a column vector; if it is treated as a row vector (as it is in some software packages) the twin matrices discussed in this chapter should be transposed.

For the 102 reflection in our example

$$\begin{pmatrix} 1 & 0 & 0 \\ 0 & -1 & 0 \\ 0 & 0 & -1 \end{pmatrix} \begin{pmatrix} 1 \\ 0 \\ 2 \end{pmatrix} = \begin{pmatrix} 1 \\ 0 \\ \overline{2} \end{pmatrix}.$$

This two-component twin can be modelled using a quantity $|F_{\text{twin,calc}}|^2$ that is a linear combination (Equation 1; Pratt *et al.*, 1971) consisting of $|F|^2$ terms for each component reflection weighted according to the twin scale factor, x, which can be refined.

$$|F_{\text{twin,calc}}(h,k,l)|^2 = (1-x)|F_{\text{calc}}(h,k,l)|^2 + x|F_{\text{calc}}(h,-k,-l)|^2. \quad (18.1)$$

One striking feature of the reciprocal lattice plot shown in Fig. 18.3*iii* is that, while the single-crystal diffraction patterns lack any symmetry with respect to h- and l-axes (for example, the $10\overline{2}$ and 102 reflections have different intensities in Fig. 18.3*i*), the composite, twinned, pattern (Fig. 18.3*iii*) has mirror or two-fold symmetry in both these directions; that is, the composite pattern with equal domain volumes (that is $x = 0.5$, Fig. 18.3*iii*) appears to have orthorhombic Laue symmetry even though the crystal structure is monoclinic. In general, for a two-component twin, if x is near 0.5 then merging statistics will appear to imply higher point symmetry than that possessed by the crystal structure. As x deviates from 0.5 then the merging in the higher-symmetry point group gradually becomes poorer (Fig. 18.3*iv*); nevertheless, similar merging statistics for different Laue classes is a feature that is often taken to indicate twinning.

Another striking feature of the twinned diffraction pattern shown in Fig. 18.3*iii* is that it appears to have a more acentric intensity distribution than the component patterns. The superposition of the diffraction patterns arising from the different domains tends to average out intensities because strong and weak reflections sometimes overlap. The quantity $|E^2 - 1|$, which adopts values of 0.97 and 0.74 for ideal centric and acentric distributions, respectively, may assume a value in the range 0.4–0.7 for twinned crystal structures. Intensity statistics can therefore be a valuable tool for the diagnosis of twinning, although it is important to bear in mind all the usual caveats relating to the assumption of a random distribution of atoms, which is broken, for example, in the presence of heavy atoms or non-crystallographic symmetry. Rees (1980) has shown that an estimate of the twin scale factor, x, can be derived from the value of $|E^2 - 1|$. Other procedures have been developed by Britton (1972) and Yeates (1988), and these have been compared by Kahlenberg (1999). The latter statistical tests will fail, though, for twins with x near 0.5. If the value of x is known, and is not near 0.5, (18.1) can be used to 'de-twin' a dataset. This procedure may be useful for the purposes of structure solution, although it is generally preferable to refine the structure using the original twinned dataset.

Common signs of twinning have been given by Herbst-Irmer and Sheldrick (1998, 2002) and are listed in Section 18.9.

18.5 Inversion, merohedral and pseudo-merohedral twins

Twinning can occur whenever a compound crystallizes in a unit cell with a higher point group than that corresponding to the space group. This

can occur for crystal structures in non-centrosymmetric space groups, since all lattices have inversion symmetry. Thus, a crystal of a compound in a space group such as $P2_1$ may contain enantiomorphic domains. This type of twinning does not occur for an enantiopure compound, and it can therefore be ruled out in protein crystallography, for example. The twin law in this case is the inversion operator

$$\begin{pmatrix} -1 & 0 & 0 \\ 0 & -1 & 0 \\ 0 & 0 & -1 \end{pmatrix},$$

and is most commonly encountered in Flack's method for 'absolute structure' determination (Flack, 1983). The domain scale factor in this case is referred to as the Flack parameter.

Twinning may also occur in lower-symmetry tetragonal, trigonal and cubic systems. Thus, a tetragonal structure in point group $4/m$ may twin about the two-fold axis along [110], which is a symmetry element of the higher-symmetry tetragonal point group, $4/mmm$. The twin law in this case is

$$\begin{pmatrix} 0 & 1 & 0 \\ 1 & 0 & 0 \\ 0 & 0 & -1 \end{pmatrix},$$

and this matrix may also be used in the treatment of low-symmetry trigonal, hexagonal and cubic crystal structures, producing diffraction patterns with apparent $\bar{3}m1$, $6/mmm$ and $m\bar{3}m$ symmetry, respectively, when the domain scale factor, x, is 0.5.

Two further twin laws need to be considered in low-symmetry trigonal crystals. A two-fold rotation about $[1\bar{1}0]$, mimicking point group $\bar{3}1m$ when $x = 0.5$, is expressed by the matrix

$$\begin{pmatrix} 0 & -1 & 0 \\ -1 & 0 & 0 \\ 0 & 0 & -1 \end{pmatrix}.$$

By twinning via a 2-fold axis about [001] a trigonal crystal may also appear from merging statistics to be hexagonal if $x = 0.5$. The twin law in this case is

$$\begin{pmatrix} -1 & 0 & 0 \\ 0 & -1 & 0 \\ 0 & 0 & 1 \end{pmatrix}.$$

In rhombohedral crystal structures twinning of this type leads to obverse–reverse twinning (see below).

The point groups of the crystal lattices ($\bar{1}$ for triclinic, $2/m$ for monoclinic, mmm for orthorhombic, $4/mmm$ for tetragonal, $\bar{3}m$ for rhombohedral, $6/mmm$ for hexagonal and $m\bar{3}m$ for cubic) are referred to as the *holohedral* point groups. Those point groups that belong to

the same crystal family, but that are subgroups of the relevant holohedral point group, are referred to as *merohedral* point groups (Hahn and Klapper discuss this classification in detail in *International Tables for Crystallography, Volume A*). Thus, $4/m$ is a merohedral point group of $4/mmm$. With the exception of obverse-reverse twinning (see below), in all the cases described in the previous paragraphs in this section the twin law is a symmetry operation of the relevant holohedry (i.e. of the crystal lattice) that is not expressed in the point symmetry corresponding to the crystal structure. For this reason this type of phenomenon is referred to as *twinning by merohedry*. Such twins are often described as *merohedral* and, although this usage is occasionally criticised in the literature (Catti and Ferraris, 1976), it appears to have stuck.[†] Though it is quite rare in molecular crystals, twins containing more than two domain variants are sometimes observed; more commonly only two are present, however, and such twins are also described as *hemihedral* twins.

[†] *Holo* and *mero* are Greek stems meaning whole and part, respectively. This 'French School' nomenclature was originally devised to describe crystal morphology, and is used here because it is currently popular in the literature. Different nomenclature is also encountered; see, for example, Giacovazzo (1993) or van der Sluis (1989).

Twinning by merohedry should be carefully distinguished from the example described in Section 18.4, where a monoclinic crystal structure accidentally had a β angle near 90°; for example, there is nothing accidental about a low-symmetry tetragonal structure having a lattice with symmetry $4/mmm$: all low-symmetry tetragonal structures have this property. Put another way, the holohedry of the tetragonal lattice is $4/mmm$; the low-symmetry tetragonal structure might belong to point group $4/m$, 4, or $\bar{4}$, which are all, nevertheless, still tetragonal point groups; this is what would make this twinning by merohedry.

A monoclinic crystal structure that happens to have $\beta \sim 90°$ has a lattice with, at least approximately, the *mmm* symmetry characteristic of the orthorhombic crystal family. If twinning occurs by a two-fold axis along **a** or **c**, the crystal is not merohedrally twinned, since monoclinic and orthorhombic are two different crystal families. This type of effect is instead referred to as twinning by *pseudo-merohedry*. A further example might occur in an orthorhombic crystal where two axes (b and c, say) are of equal length (pseudo-tetragonal). The twin law in this case could be a four-fold axis along **a**:

$$\begin{pmatrix} 1 & 0 & 0 \\ 0 & 0 & 1 \\ 0 & -1 & 0 \end{pmatrix}.$$

A monoclinic crystal where $a \sim c$ and $\beta \sim 120°$ may be twinned by a three-fold axis along **b**. The clockwise and anticlockwise three-fold rotations (3^+ and 3^-) about this direction are:

$$\begin{pmatrix} 0 & 0 & 1 \\ 0 & 1 & 0 \\ -1 & 0 & -1 \end{pmatrix} \text{ and } \begin{pmatrix} -1 & 0 & -1 \\ 0 & 1 & 0 \\ 1 & 0 & 0 \end{pmatrix},$$

potentially yielding a three-component pseudo-merohedral twin appearing from the diffraction symmetry to be hexagonal.

A trigonal crystal structure may be merohedrally twinned via a two-fold axis along the [001] direction (parallel to the three-fold axis), because this is a symmetry element of the $6/mmm$ holohedry. However, the rhombohedral lattice holohedry is $\bar{3}m$, and this point group does not contain a two-fold axis parallel to the three-fold axis. Although twinning via a two-fold axis in this direction can certainly occur for rhombohedral crystal structures, it is not twinning by merohedry. It is, instead, referred to as obverse-reverse twinning or twinning by *reticular merohedry*; this is an important distinction, because overlap between reflections from different domain variants in obverse-reverse twins affects only one-third of the intensity data. This has recently been discussed in detail by Herbst-Irmer and Sheldrick (2002).

Note that higher symmetry may be 'hidden' in a centred setting of a unit cell, and not be immediately obvious from the cell dimensions, and it is necessary to inspect carefully the output from whichever program has been used to check the metric symmetry of the unit cell [Herbst-Irmer and Sheldrick (1998) have described two illustrations of this].

18.6 Derivation of twin laws

In Section 18.4 the case of a monoclinic crystal where $\beta \sim 90°$ was examined, and it was shown that twinning could occur about a two-fold axis in the a-axis direction. This leads to overlap between reflections with indices hkl and $h\,{-}k\,{-}l$. Twinning via a two-fold axis along c would lead to overlap between reflections with indices hkl and $-h\,{-}kl$. However, since reflections $h\,{-}k\,{-}l$ and $-h\,{-}kl$ are symmetry related by the monoclinic two-fold axis along b^*, which must be present if the crystal point group is 2 or $2/m$, these twin laws are equivalent. However, in the twinning about two three-fold axes described in Section 18.5 for a monoclinic crystal with $a \sim c$ and $\beta \sim 120°$, the rotations are not equivalent because they are not related by any of the symmetry operations of point group $2/m$.

It is usually the case that several equivalent descriptions may be used to describe a particular twin. However, several distinct twin laws may be possible, and they can be expressed simultaneously. There clearly exists a potential for possible twin laws to be overlooked during structure analysis. Flack (1987) has described the application of *coset decomposition* to this problem, enabling this danger to be systematically avoided. The procedure has been incorporated by Litvin and Boyle into the computer programs TWINLAWS (Schlessman and Litvin, 1995) and COSET (Boyle, 2007).[†]

Suppose that a crystal structure in point group G crystallizes in a lattice with higher point group symmetry H. The number of possible

[†]These programs are available free of charge to academic users from http://www.bk.psu.edu/faculty/litvin/Download.html, and http://www.xray.ncsu.edu/COSET/ or via the CCP14 website (http://www.ccp14.ac.uk).

Table 18.1. Coset decomposition of point group 422 with respect to point group 2. Output taken from the program TWINLAWS (Schlessman and Litvin, 1995). The four rows represent the four different domains; either symmetry operation in a row may be taken to generate that domain. Notes: a. The notation indicates a two-fold rotation about the [−110] direction. b. This is a 4^- or 4^3 rotation about [001]. c. This is a two-fold rotation about [110].

1	2(Y)
2(X)	2(Z)
2(X-Y)[a]	4(Z)
4(3)(Z)[b]	2(XY)[c]

twin laws is given by

$$n = \frac{h_H}{h_G} - 1, \tag{18.2}$$

where h_G and h_H are the orders of point groups G and H, respectively. For example, in a protein crystallizing in point group 2 (space group $P2$, $C2$ or $P2_1$) with a unit cell with dimensions $a = 30.5$, $b = 30.5$, $c = 44.9$ Å $\beta = 90.02°$, G is point group 2 and H is effectively point group 422 ($4/mmm$ in principle, but mirror symmetry is not permitted for an enantiopure protein crystal). The orders of G and H are 2 and 8, respectively, and so this crystal may suffer from up to three twin laws to form, at most, a four-domain twin (the reference domain plus three others).

Coset decomposition yields the symmetry elements that must be added to point group G to form the higher point group H. Table 18.1 shows the output of the program TWINLAWS, listing decomposition of point group 422 into cosets with point group 2. Possible twin laws are two-fold axes about the [1 0 0], [−1 1 0] and [1 1 0] directions. However, the two-fold rotation about [1 1 0] is an equivalent twin law to the 4^- (i.e. the 4^3) rotation about [001] and the two-fold axis about [1 0 0] is equivalent to that about [0 0 1].

18.7 Non-merohedral twinning

In merohedral and pseudo-merohedral twinning the nature of the twin law matrix means that all integral Miller indices are converted into other integer triples, so that all reciprocal lattice points overlap. This usually means that all reflections are affected by overlap, although reflections from one domain may overlap with systematic absences from another. Twins in which only certain zones of reciprocal lattice points overlap are classified as being non-merohedral. In these cases only reflections that meet some special conditions on h, k and/or l are affected by twinning.

A non-merohedral twin law is commonly a symmetry operation belonging to a higher-symmetry supercell. A simple example that might be susceptible to this form of twinning is an orthorhombic crystal structure where $2a \sim b$ (Fig. 18.4*i*). A metrically tetragonal supercell can be formed by doubling the length of a so that there is a pseudo-four-fold axis along c. The diffraction pattern from one domain of the crystal is related to that from the other by a 90° rotation about c^*. Superposition of the two diffraction patterns shows that data from the first domain are affected by overlap with data from the second domain only when k is even (Fig. 18.4*iv*).

For the purposes of structure analysis the relationship between the cells in Fig. 18.4*i* (the twin law) needs to be expressed with respect to the axes of the true orthorhombic cell.

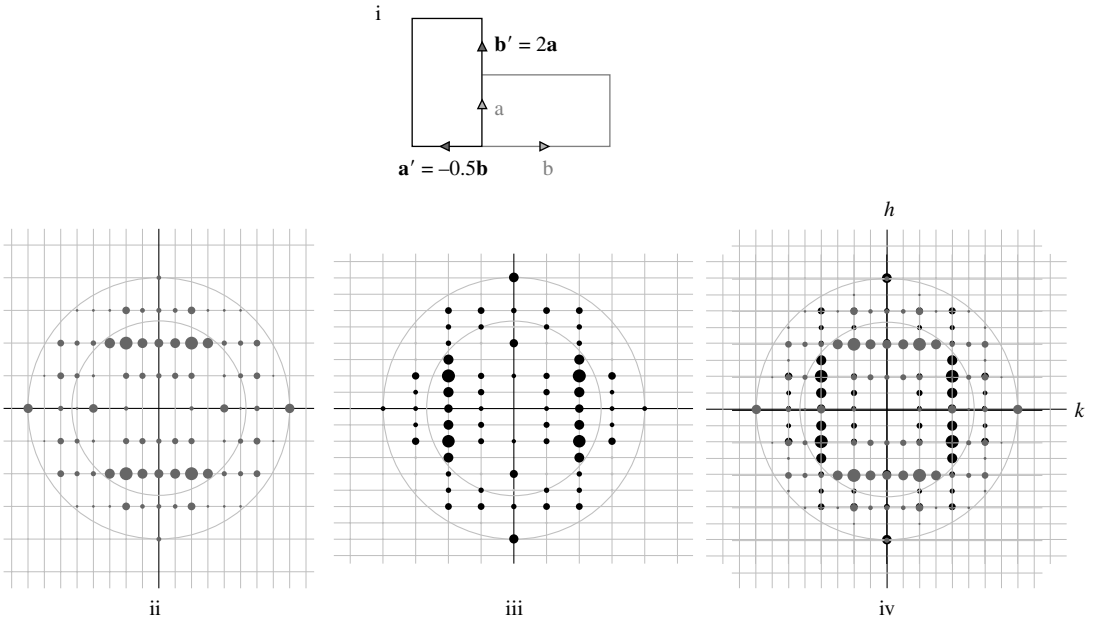

Fig. 18.4 Non-merohedral twinning in an orthorhombic crystal where $2a = b$. *i*: the relationship of the unit cells in different domains is a 90° rotation about **c**. *ii* and *iii*: diffraction patterns from the two different domains in the crystal. The grey spots in *ii* arise from cells in the orientation shown in the same grey shade in *i*; likewise the black spots in *iii* come from the darker orientation in *i*. *iv*: superposition of *ii* and *iii* to illustrate the diffraction pattern that would be measured for the twinned crystal. Note that black and grey spots overlap only where k is an even number. Both Fig. 18.3 and this figure were drawn using XPREP (Sheldrick, 2001).

From Fig. 18.4*i*,

$$\mathbf{a'} = -0.5\mathbf{b}$$
$$\mathbf{b'} = 2\mathbf{a}$$
$$\mathbf{c'} = \mathbf{c},$$

so that the twin law is:

$$\begin{pmatrix} 0 & -0.5 & 0 \\ 2 & 0 & 0 \\ 0 & 0 & 1 \end{pmatrix}.$$

The effect of this matrix on the data is:

$$\begin{pmatrix} 0 & -0.5 & 0 \\ 2 & 0 & 0 \\ 0 & 0 & 1 \end{pmatrix} \begin{pmatrix} h \\ k \\ l \end{pmatrix} = \begin{pmatrix} -k/2 \\ 2h \\ l \end{pmatrix},$$

confirming that only data with $k = 2n$ are affected by the twinning ($k/2$ is integral only if k is even). Thus, the 143 reflection from the first domain (grey) is overlapped with the $\bar{2}23$ reflection from the second (black)

domain. The 413 reflection in the grey domain would be unaffected by twinning.

It is likely that the example given here would index readily on the tetragonal supercell, but notice the bizarre systematic absences in Fig. 18.4*iv*. Zones of unusual systematic absences are frequently a sign that a crystal is non-merohedrally twinned. This pseudo-translational symmetry should enable the true orthorhombic cell to be inferred, and it can be characterized by a strong non-origin peak in a Patterson synthesis (see Section 18.10, Example 8).

In orthorhombic and higher systems potential non-merohedral twin laws can often be derived from inspection of the unit cell dimensions. In low-symmetry crystals the twin law is usually less obvious (general procedures are given below), but it is possible to make a few general observations that apply to monoclinic crystals. In these cases the twin law is often found to be a 2-fold axis along the unit cell *a*- or *c*-axes. The matrix for a two-fold rotation about the *a*-axis is:

$$\begin{pmatrix} 1 & 0 & 0 \\ 0 & -1 & 0 \\ \dfrac{2c\cos\beta}{a} & 0 & -1 \end{pmatrix}.$$

The corresponding rotation about *c* is:

$$\begin{pmatrix} -1 & 0 & \dfrac{2a\cos\beta}{c} \\ 0 & -1 & 0 \\ 0 & 0 & 1 \end{pmatrix}.$$

Likely twin laws can be derived for monoclinic crystals by evaluating the off-diagonal terms in these matrices; if near-rational values are obtained the corresponding matrix should be investigated as a possible twin law.

18.8 The derivation of non-merohedral twin laws

Diffraction patterns from non-merohedrally twinned crystals contain many more spots than would be observed for an untwinned sample. Since individual spots may come from different domains of the twin such diffraction patterns are frequently difficult to index. Overlap between reflections may be imperfect in some or all zones of data affected, and integration and data reduction needs to be performed carefully. Software for integrating datasets from non-merohedral twins and performing absorption corrections has recently become available [for example, SAINT version 7 (Bruker-Nonius, 2002); TWINABS (Sheldrick, 2002)].

Excellent programs such as DIRAX (Duisenberg, 1992) and CELL_NOW (Sheldrick, 2005) have been developed to index diffraction patterns from non-merohedral twins. In many cases a pattern can be completely indexed with two orientation matrices, and both these programs offer procedures by which the relationship between these alternative matrices is analyzed to suggest a twin law: if two domains are indexed with orientation matrices $\mathbf{A_1}$ and $\mathbf{A_2}$ the twin law is given by the product $\mathbf{A_2^{-1}A_1}$.

It is usually the case that twinning can be described by a two-fold rotation about a direct or reciprocal lattice direction. Indeed, it has been shown by Le Page and Flack that, if two such directions are parallel, and the vectors describing them have a dot product greater than two, then a higher-symmetry supercell can be derived. The program CREDUC (Le Page, 1982) is extremely useful for investigating this; it is available in the Xtal suite of software (Hall *et al*., 1992), which can be downloaded from http://www.ccp14.ac.uk. The same procedure is available in the LePage routine in PLATON (Spek, 2003).

It is sometimes the case that the first intimation the analyst has that a crystal is twinned is during refinement. Symptoms such as large, inexplicable difference peaks and a high R factor may indicate that twinning is a problem, while careful analysis of poorly fitting data reveals that they belong predominantly to certain distinct zones in which $|F_{\rm obs}|^2$ is systematically larger than $|F_{\rm calc}|^2$. If twinning is not taken into account it is likely that these zones are being poorly modelled, and that trends in their indices may provide a clue as to a possible twin law. The computer program ROTAX (Cooper *et al*., 2002; also available from http://www.ccp14.ac.uk) makes use of this idea to identify possible twins laws. A set of data with the largest values of $[|F_{\rm obs}|^2 - |F_{\rm calc}|^2]/\sigma(|F_{\rm obs}|^2)$ is identified and the indices transformed by two-fold rotations or other symmetry operations about possible direct and reciprocal lattice directions. Matrices that transform the indices of the poorly fitting data to integers are identified as possible twin laws. The analyst then has a set of potential matrices that might explain the source of the refinement problems described above. A related procedure, TwinRotMat, available in PLATON (Spek, 2003), works by identifying reflections with very similar d-spacings.

18.9 Common signs of twinning

The following list of common signs of twinning is based on that originally given by Herbst-Irmer and Sheldrick (1998). Use of these signs in diagnosing twinning problems is illustrated in Section 18.10.

1. *The metric symmetry of the lattice is higher than the Laue symmetry of the diffraction pattern.*
   The reasons for this were discussed in Section 18.4. Three common cases in small-molecule crystallography are as follows.

- Monoclinic P with β near 90° (metrically orthorhombic); use a two-fold axis along either a or c as the twin law.
- Triclinic, but transformable to monoclinic C; use a two-fold rotation about the pseudo-monoclinic b-axis direction as the twin law.
- Monoclinic P, but transformable to orthorhombic C; use a two-fold rotation about one of the pseudo-orthorhombic cell axes as the twin law. (The axis chosen should not correspond to the monoclinic b-axis!)

If the twin scale factor is near 0.5, $R_{\rm int}$ in the high-symmetry group will be the same or only slightly higher than in the lower-symmetry group. Even when the twin scale factor deviates significantly from 0.5 the higher symmetry $R_{\rm int}$ may still be less than about 0.4; values of 0.60 or higher might be expected for untwinned samples (although pseudo-symmetry in, for example, heavy-atom positions can give rise to a similar effect).

2. *The space group can not be determined, or, if it can, it is unusual.*
   Zones of systematic absences can be contaminated by overlap with reflections from another domain in the twin.

   What constitutes 'unusual' depends on the material being studied. For example, space group $C2/m$ is uncommon for molecular compounds but not uncommon at all for 'extended' or 'inorganic' structures. In the author's experience of molecular crystal structures, however, crystals appearing to be C-centred orthorhombic are often (though not always) twinned monoclinic P, and those appearing from systematic absences to be in $C2$, Cm or $C2/m$ are triclinic twins in $P\bar{1}$. Note that, even here, space group $C2$ is quite common for enantiopure compounds, and $C2$, Cm or $C2/m$ are not uncommon at all for 'inorganic' compounds such as metal oxides. Finally, of course, some compounds really do crystallize in unusual space groups. Unusual zones of absences may not be revealed by a space group determination program, but can be identified by a large peak in a Patterson map or by inspection of reciprocal lattice plots.
3. *High symmetry.*
   Low-symmetry tetragonal, trigonal, rhombohedral, hexagonal and cubic crystals are always potentially twinned by merohedry; low-symmetry trigonal crystals seem to be particularly prone. It is good practice to test such structures for twinning as a matter of routine: possible twin laws are given in Section 18.5. 95% of molecular crystal structures are either triclinic, monoclinic or orthorhombic, and so pseudo-merohedral twinning should always be kept in mind when such a material appears to be tetragonal or higher symmetry. High symmetry is common for 'inorganic' structures.
4. *The value of* $|E^2 - 1|$ *is low.*
   The reasons for this were discussed in Section 18.4.
5. *The sample being studied has undergone a phase transition.*

This was briefly discussed in Section 18.3; and examples are available in Gaudin *et al.* (2000) and Guelylah *et al.* (2001).

6. *Indexing problems.*
   Perhaps the diffraction pattern did not index using default procedures. Alternatively, the unit cell volume may seem too high (implying $Z' > 3$) or there is a very long cell axis; though both of these features are possible for untwinned crystals, they are unusual. Close inspection of peak profiles is a useful diagnostic tool: twinning may be evidenced by a mixture of sharp and split peaks in the diffraction pattern. Indexing problems are a very common warning sign of non-merohedral twinning. Pseudo-merohedral twins may be difficult to index if peaks from different domains overlap well at low resolution but not at high resolution: this may occur, for example, in a monoclinic crystal where β deviates by more than $\sim$0.5° from 90°.
7. *The structure does not appear to solve.*
   Most small-molecule structures solve readily with modern software, and twinning should be considered in cases where automatic solution fails (especially if the dataset appears to be of good quality). The possibility that the crystal being studied is very different in composition from that intended should also be carefully explored.

   Twinning reveals itself in the Patterson function, which becomes a weighted superposition of the function derived from each domain; this is discussed by Dauter (2003).
8. *The refinement is unsatisfactory.*
   The R factor may stick at a value much higher than $R_{\rm int}$; the difference map may show inexplicable peaks; $F_{\rm o}^2$ may be consistently higher than $F_{\rm c}^2$ for poorly fitting data; or $\langle F_{\rm o}^2\rangle/\langle F_{\rm c}^2\rangle$ may be systematically high for the weakest data.

18.10 Examples

Example 1. This example illustrates items 1, 2 and 7 in Section 18.9. Crystals of the compound $C_{30}H_{27}N$ (Fig. 18.2) diffracted rather weakly. The unit cell appeared to be orthorhombic with dimensions $a = 8.28$, $b = 12.92$, $c = 41.67$ Å. The volume fits for $Z = 8$, the value of $|E^2 - 1|$ was 0.725. $Z = 8$ is not unusual for orthorhombic crystals; the c-axis is long, but there were no other indexing solutions that were able to account for all the reflections in the diffraction pattern. Although the crystal was twinned the mean value of $|E^2 - 1|$ is not abnormal for a non-centrosymmetric structure. However, the space group assuming orthorhombic symmetry appeared to be $P22_12$, which is very rare.

Merging statistics ($R_{\rm int}$) were as follows: *mmm*, 0.14; 2/*m* with *a* unique, 0.13; 2/*m with b* unique 0.06, 2/*m* with *c* unique 0.09. The lowest $R_{\rm int}$ assumed monoclinic symmetry with the *b*-axis of the orthorhombic cell corresponding to the unique axis of the monoclinic cell. Notice,

though, that merging in the higher-symmetry Laue class (*mmm*) yields $R_{\rm int}$ that is only moderately higher than in $2/m$.

Taken with the space group information described above this seemed to be a twin. The twin law used was

$$\begin{pmatrix} 1 & 0 & 0 \\ 0 & -1 & 0 \\ 0 & 0 & -1 \end{pmatrix},$$

and space group $P2_1$ was assumed. The symmetry of the lattice is *mmm* (the order of this group is 8); the crystal structure belongs to point group $2/m$ (order 4). Hence, we need to specify $(8/4) - 1 = 1$ twin law (Eqn. 18.2).

The structure was difficult to solve, and repeated attempts to find a solution in different direct methods packages were unsuccessful. The molecule contains a rigid fragment, and a position and orientation for one molecule (there are four in the asymmetric unit) was obtained by Patterson search methods (DIRDIF, Beurskens *et al.*, 1996) using the rigid part of the molecule as a search fragment. The structure was completed by iterative cycles of least-squares and Fourier syntheses (SHELXL97; Sheldrick, 2008). A search for missed space-group symmetry did not reveal any glide or mirror planes: the final R factor was 0.1, and the twin scale factor was 0.392(5).

Patterson methods are normally applied to the solution of heavy-atom structures, but they are a valuable alternative to direct methods when the latter fail for light-atom structures containing a rigid fragment. Solution packages do not, as a rule, enable a twin law to be applied during structure solution. The exception to this is the program SHELXD (Sheldrick, 2008), which has proved to be very useful for solution of twinned structures.

Example 2. This is an example of an apparently 'impossible' space group (item 2 in Section 18.9), and also illustrates the comments made about twinning in Sections 18.2 and 18.3. A nickel complex was apparently orthorhombic P with cell dimensions $a = 9.93$, $b = 10.95$, $c = 14.14$ Å; all three cell angles were indistinguishable from 90°, and $R_{\rm int}$ was 0.079 for *mmm* symmetry. However, only the following systematic absences were observed: $h00$ with h odd; $0k0$ with k odd; $00l$ with l odd, and $hk0$ with $h + k$ odd – a pattern that is not consistent with any orthorhombic space group. If the crystal system is taken to be monoclinic, with the original c-axis corresponding to the unique monoclinic b direction, the space group is $P2_1/n$. $R_{\rm int}$ for $2/m$ symmetry is 0.039. The structure solved for Ni and a few light-atom positions by direct methods. The twin law

$$\begin{pmatrix} 1 & 0 & 0 \\ 0 & -1 & 0 \\ 0 & 0 & -1 \end{pmatrix}$$

was applied, and the remaining atoms were located in a difference map. The symmetry of the lattice is effectively *mmm*, and the crystal structure

belongs to point group $2/m$, and as in example 1 we need to specify $(8/4) - 1 = 1$ twin law. The final R factor [based on F and data with $F > 4\sigma(F)$] was 0.061, and the twin scale factor was 0.373(3).

Example 3. This example also illustrates a structure in which correct space group determination was hindered by twinning. Twinning can cause systematic absences from one domain to overlap with reflections from a second domain, and this may yield a pattern of absences that is inconsistent with any known space group (as we saw in Example 2), or that leads to an incorrect space group assignment (as is illustrated here).

The diffraction pattern of a palladium complex was found to index on a primitive monoclinic unit cell with dimensions $a = 3.84$, $b = 9.73$, $c = 21.20$ Å, $\beta = 95.4°$; $R_{\rm int} = 0.037$ for point group $2/m$. This cell can be transformed using the matrix

$$\mathbf{M} = \begin{pmatrix} 1 & 0 & 0 \\ -1 & 0 & -2 \\ 0 & 1 & 0 \end{pmatrix}$$

to a metrically orthorhombic C cell with dimensions $a = 3.84$, $b = 42.20$, $c = 9.73$ Å, $\alpha = \beta = 90°$, $\gamma = 89.8°$, but $R_{\rm int}$ for mmm symmetry was 0.434. The merging statistics imply that the crystal is monoclinic. The systematic absence data are summarized in Table 18.2.

The data in Table 18.2 appear to show a 'clean' set of absences for the $0k0$ zone, but significant intensity for the three $h0l$ zones, indicating that the space group is $P2_1$. Notice the values of $\langle I \rangle$ for the different conditions on $h0l$: that for $h + k$ odd is over ten times smaller than either h odd or l odd. In fact, the crystal is twinned, and the space group is $P2_1/n$, but the n-glide absences are contaminated by overlap of reflections from the different domains.

As in the previous examples, we need to specify one twin law. A two-fold rotation about either the a- or b-axis of the orthorhombic cell could be used, but it is not necessary to use both (this can be proved using coset decomposition). A two-fold rotation about the orthorhombic c-axis should not be used as a twin law as this corresponds to the b-axis

Table 18.2. Systematic absence data for the palladium complex in Example 3. N is the number of data meeting the condition indicated in the first row; N $(I > 3\sigma)$ is the number of these with significant intensity; I and σ are the intensity and uncertainty of the intensity, respectively. $\langle I \rangle$ indicates the mean value of I. Data calculated using XPREP.

Condition	***0k0*, *k* odd**	***h0l*, *h* odd**	***h0l*, *l* odd**	***h0l*, *h* + *k* odd**
N	24	437	431	432
N $(I > 3\sigma)$	1	323	195	128
$\langle I \rangle$	2.6	326.8	310.5	23.9
$\langle I/\sigma \rangle$	0.5	7.6	5.4	2.8

of the monoclinic cell, and a two-fold axis about this direction is part of the monoclinic symmetry already.

With respect to the orthorhombic cell axes, a two-fold rotation about the orthorhombic *a*-axis direction is given by the matrix

$$\mathbf{R} = \begin{pmatrix} 1 & 0 & 0 \\ 0 & -1 & 0 \\ 0 & 0 & -1 \end{pmatrix}.$$

However, it is necessary to express this operation with respect to the monoclinic axis system because this is being used to describe the structure. The matrix **M**, which transforms the monoclinic cell to the orthorhombic cell, was defined above, and the required twin law is given by the triple matrix product $\mathbf{M^{-1}RM}$:

$$\begin{pmatrix} 1 & 0 & 0 \\ 0 & 0 & 1 \\ -0.5 & -0.5 & 0 \end{pmatrix} \begin{pmatrix} 1 & 0 & 0 \\ 0 & -1 & 0 \\ 0 & 0 & -1 \end{pmatrix} \begin{pmatrix} 1 & 0 & 0 \\ -1 & 0 & -2 \\ 0 & 1 & 0 \end{pmatrix} = \begin{pmatrix} 1 & 0 & 0 \\ 0 & -1 & 0 \\ -1 & 0 & -1 \end{pmatrix}.$$

This procedure can be used whenever it is necessary to transform an operation from one axis system to another.

Consider the effect of the twin law on the *h*0*l* reflections:

$$\begin{pmatrix} 1 & 0 & 0 \\ 0 & -1 & 0 \\ -1 & 0 & -1 \end{pmatrix} \begin{pmatrix} h \\ 0 \\ l \end{pmatrix} = \begin{pmatrix} h \\ 0 \\ -h-l \end{pmatrix}.$$

For example, the systematically absent 102 reflection will overlap with the $10\bar{3}$ reflection from the second domain: the $10\bar{3}$ reflection is *not* systematically absent. This explains why the systematic absences for the *n*-glide appear to have some intensity in Table 18.2.

Even though it was twinned this crystal structure solved easily, and refined to $R = 0.042$; the twin scale factor was only 0.07, which explains the very different merging statistics in 2/*m* and *mmm*.

This structure could have been solved in $P2_1$, but refinement would have been unstable; the extra symmetry could have been located by a program such as PLATON/ADDSYM or MISSYM. Symmetry checking should be carried out as a matter of routine for all crystal structures, but it is particularly important to do this for twinned structures because of the extra pitfalls attendant on space group determination.

Example 4. The diffraction pattern measured from a crystal of a nickel complex of composition $C_{17}H_{30}N_6NiO_6$ indexed on the monoclinic *C*-centred unit cell $a = 15.20$, $b = 54.49$, $c = 10.14$ Å, $\beta = 90.73°$. R_{int} for 2/*m* symmetry was 0.076. The space group appeared to be one of *C*2, *Cm* or *C*2/*m*; solution in each of these was attempted, but no recognizable structure solution was obtained. Merging in Laue class $\bar{1}$ yielded $R_{\text{int}} = 0.038$, which is somewhat better than in 2/*m*, and this indicated that the structure was really triclinic.

The conventional triclinic setting of the unit cell is $a = 10.14, b = 15.20$, $c = 28.29$ Å, $\alpha = 74.42$, $\beta = 89.80$ and $\gamma = 89.27°$, and transformation is accomplished with the matrix:

$$\begin{pmatrix} 0 & 0 & -1 \\ 1 & 0 & 0 \\ 0.5 & -0.5 & 0 \end{pmatrix}$$

(a cell reduction program, such as XPREP, will provide this information).

The twin law is a two-fold rotation about the pseudo-monoclinic b direction, but this needs to be expressed with respect to the triclinic axes. As in Example 3, this requires the formation of a triple matrix product:

$$\begin{pmatrix} 0 & 0 & -1 \\ 1 & 0 & 0 \\ 0.5 & -0.5 & 0 \end{pmatrix} \begin{pmatrix} -1 & 0 & 0 \\ 0 & 1 & 0 \\ 0 & 0 & -1 \end{pmatrix} \begin{pmatrix} 0 & 1 & 0 \\ 0 & 1 & -2 \\ -1 & 0 & 0 \end{pmatrix} = \begin{pmatrix} -1 & 0 & 0 \\ 0 & -1 & 0 \\ 0 & -1 & 1 \end{pmatrix},$$

where the three matrices to be multiplied are (from right to left) the triclinic to monoclinic transformation, a two-fold axis about b in the monoclinic cell and the monoclinic to triclinic transformation. Note that the first and third matrices are the inverses of each other.

The crystal structure solved readily by direct methods in $P\bar{1}$, and refined to $R = 0.037$, with a twin scale factor of 0.2668(7). Z' for this structure was 4, which is unusually high, though symmetry checking using PLATON/ADDSYM did not indicate any missed translational or other symmetry.

An alternative, but equivalent strategy in this example would have been to work in the non-standard setting $C\bar{1}$, using the pseudo-monoclinic axis system and the twin law

$$\begin{pmatrix} -1 & 0 & 0 \\ 0 & 1 & 0 \\ 0 & 0 & -1 \end{pmatrix}.$$

This might have been preferred on the grounds that use of the non-standard space group setting made the choice of twin law more obvious.

Example 5. The crystal structure of $B_{10}F_{12}$ is tetragonal. R_{int} was 0.020 in point group $4/m$, but 0.060 in $4/mmm$. The absences were consistent with space group $I4_1/a$; even though this space group is centrosymmetric the mean value of $|E^2 - 1|$ was only 0.686. The ambiguous Laue symmetry, the high metric symmetry and low mean value of $|E^2-1|$ were taken as signs that the structure could be twinned (signs 1, 3 and 4 in Section 18.9).

The structure was solved easily by direct methods (SIR92) in default mode in $I4_1/a$ but, on refining the structure, R appeared to stick at 0.23, even with anisotropic displacement parameters for all atoms. Low-symmetry tetragonal structures are always susceptible to twinning via

Table 18.3. Coset decomposition of $4/mmm$ with respect to $4/m$ (calculated using TWINLAWS). The notation $2_{[100]}$ indicates a two-fold axis along [100], $m_{[100]}$ is a mirror plane perpendicular to [100] and $4^{+}_{[001]}$ is a rotation of $+90°$ about [001].

1	$2_{[001]}$	$4^{+}_{[001]}$	$4^{-}_{[001]}$	-1	$m_{[001]}$	$-4^{+}_{[001]}$	$-4^{-}_{[001]}$
$2_{[100]}$	$2_{[010]}$	$2_{[-110]}$	$2_{[110]}$	$m_{[100]}$	$m_{[010]}$	$m_{[-110]}$	$m_{[110]}$

one of the symmetry elements of point group $4/mmm$ that is not present in $4/m$. One such operator is a two-fold axis about [110], expressed by the matrix

$$\begin{pmatrix} 0 & 1 & 0 \\ 1 & 0 & 0 \\ 0 & 0 & -1 \end{pmatrix}.$$

Application of this matrix as a twin law, together with refinement of the twin scale factor, caused R to drop immediately to 0.023; the twin scale factor was 0.416(2).

The orders of $4/mmm$ and $4/m$ are 16 and 8, respectively. Therefore we need to consider $(16/8) - 1 = 1$ twin law (Eqn. 18.2). Coset decomposition of $4/mmm$ with respect to $4/m$ yields the data in Table 18.3. The elements in the first line of the table are those of point group $4/m$; any of the elements in the second line of the table could have been used as a twin law: the two-fold axis along [110] was used above, but use of a two-fold axis along [100] or [010], or a mirror perpendicular to [−1 1 0] would have modelled the data equally well.

Example 6. The compound $Et_3NH^+Cl^-$ crystallizes with a metrically hexagonal unit cell, of dimensions $a = 8.254$ and $c = 6.996$ Å (Churakov and Howard, 2004). The systematic absences were consistent with space groups $P6_3mc$ and $P31c$, and merging in $6mm$ and $31m$ yielded similar statistics. The mean value of $|E^2 - 1|$ was 0.678, slightly lower than expected for a non-centrosymmetric space group. The data could be modelled in $P6_3mc$, though the structure was disordered; R was 0.054, though the Flack parameter was rather imprecise [0.0(4)], and the highest difference map peak was $+0.82$ eÅ^{-3}, which is high for a compound of this composition.

The high symmetry, refinement statistics, the low mean value of $|E^2 - 1|$ and the similar merging in $6mm$ and $31c$ point to twinning (1, 3, 4, and 8 in Section 18.9), and so the structure was also solved and refined in $P31c$. This yielded an ordered model. The R factor was 0.072 before twinning was modelled, but application of a twin law (see below) caused R to drop to 0.019, with difference map extremes of $+0.18$ and -0.09 eÅ^{-3}. These statistics are clearly superior to those obtained in $P6_3mc$, and illustrate the comment made by Herbst-Irmer and Sheldrick (1998) that it is worth investigating the possibility of twinning before investing time and effort in disorder modelling.

Table 18.4. Coset decomposition of $6/mmm$ with respect to $31m$ (calculated using TWINLAWS). The notation used is similar to that in Table 18.3.

1	$3^{+}_{[001]}$	$3^{-}_{[001]}$	$m_{[210]}$	$m_{[120]}$	$m_{[-110]}$
$6^{+}_{[001]}$	$2_{[001]}$	$6^{-}_{[001]}$	$m_{[110]}$	$m_{[100]}$	$m_{[010]}$
$2_{[210]}$	$2_{[120]}$	$2_{[-110]}$	-1	$-3^{+}_{[001]}$	$-3^{-}_{[001]}$
$2_{[100]}$	$2_{[010]}$	$2_{[110]}$	$-6^{+}_{[001]}$	$-6^{-}_{[001]}$	$m_{[001]}$

The orders of $6/mmm$ (the lattice holohedry) and $31m$ are 24 and 6, respectively, and so to investigate twinning completely we need to consider $(24/6) - 1 = 3$ different twin laws (i.e. the crystal could consist of up to four domains). Table 18.4 shows coset decomposition of $6/mmm$ and $31m$. The first line in the table shows the elements of $31m$, and the second line a set of possible merohedral twin laws that could model a second domain; Churakov and Howard used the mirror perpendicular to [100], expressed by the matrix

$$\begin{pmatrix} -1 & 0 & 0 \\ 1 & 1 & 0 \\ 0 & 0 & 1 \end{pmatrix},$$

but any of the other elements in row two of Table 18.4 would have worked equally well.

$31m$ is a non-centrosymmetric point group, and so the 'absolute structure' should be determined: *two* Flack parameters are needed, one for each of the domains so far identified. It is easy to forget to do this, but use of coset decomposition ensures the absolute structure will be correctly treated! The third line of Table 18.4 contains the element $\overline{1}$: inclusion of the inversion operator (or any other other elements in row 3) as a second twin law would model twinning by inversion (i.e. the Flack parameter) in the first domain of the crystal. The elements in the fourth row would enable the Flack parameter in the second domain to be refined. In the widely used program SHELXL the instructions

```
TWIN −1 0 0 1 1 0 0 0 1 −4
BASF 0.25 0.25 0.25
```

would ensure that all twin laws were included in the model; other programs may need each twin law matrix to be input explicitly.

After refinement, the scale factors for the four domains of the crystal were 0.46(4), 0.48(4), 0.05(5) and 0.01(4). The last two scale factors are the Flack parameters for the first two domains; the fact that they are very near zero with small standard uncertainties shows that the absolute structures of the first and second domains are correct.

Example 7. A further example of the importance of coset decomposition in the analysis of twinned crystals is found in the crystal structure of the

energetic material α-NTO (Bolotina *et al.*, 2005). The unit cell dimensions of this compound are $a = 5.12$, $b = 10.31$, $c = 17.99$ Å, $\alpha = 106.6$, $\beta = 97.8$, $\gamma = 90.1°$, and the space group is $P\overline{1}$. Symmetry checking shows that the triclinic unit cell can be transformed to a metrically nearly orthorhombic unit cell with dimensions $a = 5.12$, $b = 10.31$, $c = 31.14$ Å by the matrix

$$\begin{pmatrix} 1 & 0 & 0 \\ 0 & 1 & 0 \\ 1 & 1 & 2 \end{pmatrix}.$$

Table 18.5. Coset decomposition of mmm with respect to $\overline{1}$ (calculated using TWINLAWS). The notation used is similar to that in Table 18.3.

1	-1
$2_{[100]}$	$m_{[100]}$
$2_{[010]}$	$m_{[010]}$
$2_{[001]}$	$m_{[001]}$

The lattice effectively has *mmm* symmetry (order 8), but the space group belongs to point group $\overline{1}$ (order 2). There are therefore three twin laws ($8/2 - 1 = 3$) to consider. A unique set of twin laws can be obtained by decomposing *mmm* into cosets with $\overline{1}$ (Table 18.5); we shall use the two-fold rotations about the [100], [010] and [001] directions of the orthorhombic cell as the twin laws. These operations need to be expressed with respect to the triclinic axes, and this is achieved by forming triple matrix products as in examples 3 and 4; in each case the three matrices are (from right to left) the triclinic to orthorhombic transformation, a two-fold axis in the orthorhombic cell and the orthorhombic to triclinic transformation:

$$\begin{pmatrix} 1 & 0 & 0 \\ 0 & 1 & 0 \\ -0.5 & -0.5 & 0.5 \end{pmatrix} \begin{pmatrix} 1 & 0 & 0 \\ 0 & -1 & 0 \\ 0 & 0 & -1 \end{pmatrix} \begin{pmatrix} 1 & 0 & 0 \\ 0 & 1 & 0 \\ 1 & 1 & 2 \end{pmatrix} = \begin{pmatrix} 1 & 0 & 0 \\ 0 & -1 & 0 \\ -1 & 0 & -1 \end{pmatrix}$$

$$\begin{pmatrix} 1 & 0 & 0 \\ 0 & 1 & 0 \\ -0.5 & -0.5 & 0.5 \end{pmatrix} \begin{pmatrix} -1 & 0 & 0 \\ 0 & 1 & 0 \\ 0 & 0 & -1 \end{pmatrix} \begin{pmatrix} 1 & 0 & 0 \\ 0 & 1 & 0 \\ 1 & 1 & 2 \end{pmatrix} = \begin{pmatrix} -1 & 0 & 0 \\ 0 & 1 & 0 \\ 0 & -1 & -1 \end{pmatrix}$$

$$\begin{pmatrix} 1 & 0 & 0 \\ 0 & 1 & 0 \\ -0.5 & -0.5 & 0.5 \end{pmatrix} \begin{pmatrix} -1 & 0 & 0 \\ 0 & -1 & 0 \\ 0 & 0 & 1 \end{pmatrix} \begin{pmatrix} 1 & 0 & 0 \\ 0 & 1 & 0 \\ 1 & 1 & 2 \end{pmatrix} = \begin{pmatrix} -1 & 0 & 0 \\ 0 & -1 & 0 \\ 1 & 1 & 1 \end{pmatrix}.$$

All four domains (i.e. the reference domain and the three generated by the three twin laws above) were found to be significantly populated, though the populations were found to be different in different crystals. R converged to ~0.04. Further details of this structure determination are given in Bolotina *et al.* (2005) and in Schwarzenbach *et al.* (2006), where the twinning is interpreted in terms of layer stacking faults.

Example 8. The following exemplifies analysis of a non-merohedrally twinned crystal. Trimethyltin hydride (Me_3SnH) is a gas under ambient conditions, and its melting point is ~160 K. A sample was crystallized

in situ in a capillary. The diffraction pattern failed to index using routine procedures, but was indexed using the twin-indexing package DIRAX. Indexing problems are the most common sign of non-merohedral twinning, but it is often also clear from features such as split peaks in the diffraction pattern itself that a crystal is not single.

The unit cell chosen for data collection (on a four-circle instrument with a point detector) was a metrically monoclinic *C*-centred cell with dimensions $a = 6.255(2)$, $b = 12.113(4)$, $c = 15.963(6)$ Å, $\beta = 91.66(6)^\circ$, although it was noted that γ was significantly different from 90° at 90.10(3)°. After data collection it was clear from the Laue symmetry of the data set that the true crystal system was triclinic. These data imply $Z' = 4$, which is high. In addition, the dataset showed strong pseudo-translational symmetry of the form $(h + k + 2l) = 4n$, this information being readily available in the output of SIR97 (Altomare *et al*., 1999), and in a Patterson map that showed a very large peak at (¼, ¼, ½).

Non-merohedral twinning occurs when a metrically higher-symmetry supercell exists. Sometimes (though quite rarely in the author's experience) this supercell, rather than the true cell, is identified on indexing, and this is what occurred here. Strong pseudo-translational effects and a high implied Z' usually indicate that this has occurred, and a Patterson synthesis is a useful tool to identify the correct cell.

The unit cell was transformed with the matrix

$$\begin{pmatrix} 1 & 0 & 0 \\ 0.5 & 0.5 & 0 \\ 0.25 & 0.25 & 0.5 \end{pmatrix},$$

and re-refined to give the triclinic setting $a = 6.262$, $b = 6.822$, $c = 8.640$ Å, $\alpha = 67.41^\circ$, $\beta = 80.92^\circ$, $\gamma = 62.62^\circ$. The structure solved easily by Patterson methods, and the carbon atoms were located in a subsequent difference map. Isotropic refinement converged to $R = 0.068$, $R_w = 0.081$ with unit weights, anisotropic refinement led one C atom to become non-positive-definite. The difference map showed a very large peak (+6.42 eÅ^{-3}) in a chemically unreasonable position. Application of ROTAX identified a two-fold axis along the [−1 2 0] direct lattice direction (or alternatively the (021) reciprocal lattice direction) as a potential twin law. This is described by the matrix

$$\begin{pmatrix} -1 & 0 & 0 \\ -1 & -1 & 0 \\ -0.5 & 1 & -1 \end{pmatrix}.$$

This matrix can also be derived by recognising that twinning may occur by two-fold rotation about the *b*-axis of the monoclinic supercell. In terms of the triclinic axis system this symmetry operation is given by a triple matrix product consisting of the transformation from the triclinic to the monoclinic cell, the two-fold about the monoclinic *b* axis, and the

monoclinic to triclinic transformation:

$$\begin{pmatrix} 1 & 0 & 0 \\ 0.5 & 0.5 & 0 \\ 0.25 & 0.25 & 0.5 \end{pmatrix} \begin{pmatrix} -1 & 0 & 0 \\ 0 & 1 & 0 \\ 0 & 0 & -1 \end{pmatrix} \begin{pmatrix} 1 & 0 & 0 \\ -1 & 2 & 0 \\ 0 & -1 & 2 \end{pmatrix}.$$

Incorporation of the twin law into the model gave an R factor of 0.031 and even allowed H atoms to be located in a difference map.

The dataset used for this example was collected using a point detector, though this is unusual nowadays. Although twinning can be applied to a dataset collected with an area detector and integrated as though the crystal were single, it is almost always better to take twinning into account during integration, using more than one orientation matrix. This feature is available in modern integration packages such as SAINT v7, EVALCCD and TWINSOLVE.

An extensive database of papers describing twinning has been assembled by Spek and Lutz (Utrecht University, The Netherlands), and is available on the internet at http://www.cryst.chem.uu.nl/lutz/twin/gen_twin.html.

Worked examples for several twinning problems have been assembled by Herbst-Irmer, and are available from http://shelx.uni-ac.gwdg.de/~rherbst/twin.html. Further examples of non-merohedral twinning problems are given by Dauter (2003), Choe *et al.* (2000), Colombo *et al.* (2000), Gaudin *et al.* (2000), Guelylah *et al.* (2001), Cooper *et al.* (2002) and Tang *et al.* (2001). A worked example (Herbst-Irmer and Sheldrick, 1998) is available from http://shelx.uni-ac.gwdg.de/~rherbst/twin.html.

References

Beurskens, P. T., Beurskens, G., Bosman, W. P., de Gelder, R., Garcia-Granda, S., Gould, R. O., Israel, R. and Smits, J. M. M. (1996). The DIRDIF96 Program System, Technical Report of the Crystallography Laboratory, University of Nijmegen, The Netherlands.

Bolotina, N., Kirschblaum, K. and Pinkerton, A. A. (2005). *Acta Crystallogr.* **B61**, 577–584.

Boyle, P. D. (2007) COSET. A program for deriving potential merohedral and pseudomerohedral twin laws by coset decomposition. North Carolina State University, Raleigh, NC, USA.

Britton, D. (1972). *Acta Crystallogr.* **A28**, 296–297.

Bruker-Nonius (2002). SAINT, version 7. Bruker-Nonius, Madison, Wisconsin, USA.

Catti, M. and Ferraris, G. (1976). *Acta Crystallogr.* A**32**, 163–165.

Choe, W. V., Pecharsky, K., Pecharsky, A. O., Gschneidner, K. A., Young, V. G. and Miller, G. J. (2000). *Phys. Rev. Lett.* **84**, 4617–4620.

Churakov, A. V. and Howard, J. A. K. (2004). *Acta Crystallogr.* **C60**, o557–o558.

Colombo, D. G., Young, V. G. and Gladfelter, W. L. (2000). *Inorg. Chem.* **39**, 4621–4624.
Cooper, R. I., Gould, R. O., Parsons, S. and Watkin, D. J. (2002). *J. Appl. Crystallogr.* **35**, 168–174.
Dauter, Z. (2003). *Acta Crystallogr.* **D59**, 2004–2016.
Duisenberg, A. J. M. (1992). *J. Appl. Crystallogr.* **25**, 92–96.
Flack, H. D. (1983). *Acta Crystallogr.* **A39**, 876–881.
Flack, H. D. (1987). *Acta Crystallogr.* **A43**, 564–568.
Gaudin, E., Petricek, V., Boucher, F., Taulelle, F. and Evain, M. (2000). *Acta Crystallogr.* **B56**, 972–979.
Giacovazzo, C. (1992). (ed.) *Fundamentals of crystallography*. Oxford University Press, Oxford, UK.
Guelylah, A., Madariaga, G., Petricek, V., Breczewski, T., Aroyo, M. I. and Bocanegra, E. H. (2001). *Acta Crystallogr.* **B57**, 221–230.
Hall, S. R., Flack, H. and Stewart, R. F. (1992). Xtal3.2, University of Western Australia.
Herbst-Irmer, R. and Sheldrick, G. M. (1998). *Acta Crystallogr.* **B54**, 443–449.
Herbst-Irmer, R. and Sheldrick, G. M. (2002). *Acta Crystallogr.* **B58**, 477–481.
Jameson, G. B. (1982). *Acta Crystallogr.* **A38**, 817–820.
Kahlenberg, V. (1999). *Acta Crystallogr*. **B55**, 745–751.
Le Page, Y. (1982). *J. Appl. Crystallogr*. **15**, 255–259.
Le Page, Y. (1999). *Acta Crystallogr*. **A55**, Supplement, Abstract M12.CC.001; this refers to a lecture given by Le Page at the IUCr Conference in Glasgow, 1999.
Pratt, C. S., Coyle, B. A. and Ibers, J. A. (1971). *J. Chem. Soc.* pp. 2146–2151.
Rees, D. C. (1980). *Acta Crystallogr.* **A36**, 578–581.
Schlessman, J. and Litvin, D. B. (1995). *Acta Crystallogr.* **A51**, 947–949.
Schwarzenbach, D., Kirschblaum, K. and Pinkerton, A. A. (2006). *Acta Crystallogr. B***62**, 944–948.
Sheldrick, G. M. (2001). XPREP. Bruker AXS Inc., Madison, Wisconsin, USA.
Sheldrick, G. M. (2002). TWINABS. Bruker AXS Inc., Madison, Wisconsin, USA.
Sheldrick, G. M. (2005). CELL_NOW. Bruker AXS Inc., Madison, Wisconsin, USA.
Sheldrick, G. M. (2008). *Acta Crystallogr.* **A64**, 112–122.
Spek, A. L. (2003). *J. Appl. Crystallogr.* **36**, 7–13
Tang, C. Y., Coxall, R. A., Downs, A. J., Greene, T. M. and Parsons, S. (2001). *J. Chem. Soc. Dalton Trans.* pp. 2141–2147.
van der Sluis, P. (1989). *Thesis*, University of Utrecht, The Netherlands.
van Scheltinga, A. T., Valegard, K., Haidu, J. and Andersson, I. (2003). *Acta Crystallogr.* **D59**, 2017–2022.
Yeates, T. O. (1988). *Acta Crystallogr.* **A44**, 142–144.

Exercises

1. To which point groups do the following space groups belong?
   $P\bar{1}$, $P2_1/c$, $P2_12_12_1$, $Cmca$, $I\bar{4}$, $P3_121$, $R\bar{3}m$, $P6_3/mmc$, $Pa\bar{3}$.
2. Explain why it is often stated that a low value for $\langle|E^2 - 1|\rangle$ can indicate twinning. What values of this parameter are expected for untwinned structures, and what values might be expected for a twinned structure? Under what circumstances might this parameter be misleading?
3. Suggest twin laws that might arise from structures with the following unit cells. In each case state which reflections would be affected and what features would help diagnose the twinning.
   (a) Monoclinic, with $\beta \sim 90°$.
   (b) Monoclinic P with $a \sim c$.
   (c) Orthorhombic with two edges approximately equal.
4. Consider a triclinic crystal structure with a unit cell with approximately orthorhombic metric symmetry.
   (a) How many domains are possible if the crystal forms a twin and the space group is $P\bar{1}$?
   (b) What twin laws are possible if the space group is $P\bar{1}$?
   (c) How many domains are possible if the space group is $P1$?
5. In *Example* 6 a mirror perpendicular to [100] was used to model twinning. Write down in matrix form the twin laws corresponding to $6^+_{[001]}$ and $m_{[110]}$ that are equivalent to this operation.
6. Which reflections would be affected in the presence of the following twin laws?

$$\begin{pmatrix} -1 & 0 & 0 \\ 0 & -1 & 0 \\ 0 & 0 & 1 \end{pmatrix}$$

$$\begin{pmatrix} -1 & 0 & -0.33 \\ 0 & -1 & 0 \\ 0 & 0 & 1 \end{pmatrix}$$

7. Suggest twin laws that might arise from structures with the following unit cells. In each case state which reflections would be affected and what features would help diagnose the twinning.
   (i) Orthorhombic P, $a = 4.49$, $b = 16.74$, $c = 9.01$ Å.
   (ii) Monoclinic P, $a = 5.50$, $b = 11.49$, $c = 6.34$ Å, $\beta = 98.3°$.
8. Diffraction data were collected on the low-temperature phase of oxalyl chloride, $(COCl)_2$. A frame from the diffraction pattern is shown in Fig. 18.5.
   (a) Comment on the appearance of this diffraction pattern.
   (b) Discuss strategies that might be used to index this pattern.
   (c) The pattern was indexed with the metrically orthorhombic unit cell $a = 5.342(4)$, $b = 7.270(5)$, $c = 16.676(11)$ Å. The following (next page) was found assuming orthorhombic symmetry using XPREP. Show that these data are consistent with the correct space group $P2_1/c$ with $a = 16.67$, $b = 5.34$, $c = 7.26$ Å, $\beta = 90°$.

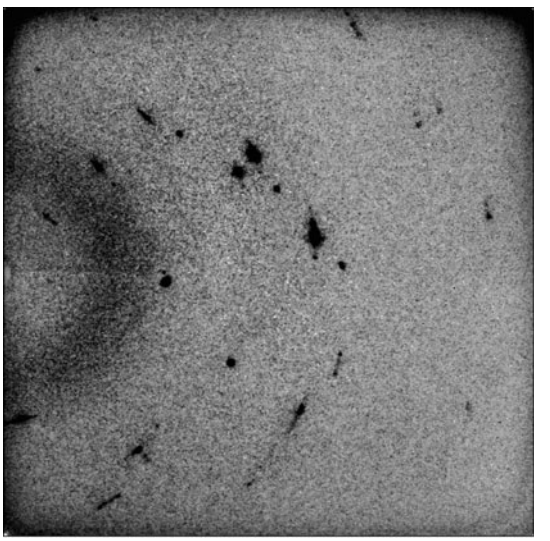

Fig. 18.5 A frame of diffraction from oxalyl chloride.

```
    b--   c--   n--  21--  -c-  -a-  -n-  -21-  --a  --b  --n  --21
N   347   317   316     7  240  235  239    12   85   97   94    26
NI>3s 4    70    68     0   79   72   73     0   28   26   22     8

<I> 0.4  115.8 116.2 0.2 204.6 335.6 275.4 0.2 59.9 40.3 78.9 347.8
<I/s>0.5   1.9   1.8 0.2   2.6   2.6   2.5 0.4  2.3  2.1  2.0   2.8

Identical indices and Friedel opposites combined before calculating
R(sym)
No acceptable space group - change tolerances or unset chiral flag
or possibly change input lattice type, then recheck cell using H-option
Mean |E*E-1| = 1.327 [expected .968 centrosym and .736 non-centrosym]
```

(d) Calculate Z' and comment on the mean value $\langle|E^2 - 1|\rangle = 1.327$.

(e) A Patterson map calculated using the second cell given in part (c) showed a very strong non-origin peak at [⅓ 0 ⅔]. Suggest a transformation to a smaller unit cell.

(f) What are the dimensions of this smaller cell?

(g) The structure of oxalyl chloride was successfully modelled as a twin. What is the likely twin law?

This page intentionally left blank

The presentation of results

19

Alexander Blake

19.1 Introduction

The final stage of a crystal-structure analysis is its presentation. This can occur within your own research group, as a conference poster or oral contribution, on the internet, or as a refereed article in a journal. In each case the requirements are different and you must tailor the presentation to the medium used. As with all communication skills the presentation of crystallographic results improves with practice. The reporting of structural results in crystallographic or chemical journals is usually guided by the relevant *Notes*, *Instructions* or *Guidance for Authors* published in these journals. Some journals accept only electronic submissions via a web interface (or possibly by e-mail, FTP or on a disk) in a specific computer-readable format. Since April 1996 *Section C* of *Acta Crystallographica* has accepted submissions only as Crystallographic Information Files (CIF); since its launch in 2001 *Section E* of *Acta Crystallographica* has required CIF submissions, as does the *New Crystal Structures* section of *Zeitschrift für Kristallographie*.

Even among crystallographic journals there has been a marked trend away from publishing primary data (co-ordinates and displacement parameters). Greater selectivity in the choice of molecular geometry parameters to be published is also being encouraged. Even when journals did publish extensive information it did not always convey the structural information effectively, but now it is even more important to include effective graphical representations of your structures. With the spread of graphical abstracts in the contents pages of journals, a picture that is clear and attractive can be effective in attracting the attention of a reader browsing a hardcopy journal or an index on the web.

This section will deal first with molecular graphics, then with the production of tables, and finally with the different methods of delivering your results. Archiving will also be briefly mentioned. The use of the CIF will be referred to here as necessary but will be covered in more detail in the following chapter.

19.2 Graphics

Although most obviously associated with the production of high-quality views of the final structure, molecular graphics are also used as an aid in initial structure determination, in the interpretation of difference electron density maps and to investigate disorder and other situations requiring modelling. Here, we are concerned only with the first of these, and the main consideration is the quality of the resulting illustration in terms of its clarity, effectiveness and information content. Early graphics programs [e.g. *ORTEP* (Johnson, 1965, 1976)] were not interactive and the program had to be re-run every time a new view was required. Happily, modern programs are interactive [e.g. *XP* (Sheldrick, 2001), *CAMERON* (Pearce *et al*., 1996), *Mercury* (Macrae *et al*., 2006)], allowing continuous or stepped rotation of the molecule.

19.3 Graphics programs

The range of graphics programs is vast and it is not practical to offer a comprehensive survey here: an excellent source of information on potentially useful programs is the CCP14 website (http://www.ccp14.ac.uk). The majority are free (at least to academic users) or cost very little. A major factor in your choice of program is its range of features and how these match your needs. Are atomic displacement ellipsoids required? Are polyhedral representations important? Do you want to display a ball-and-stick drawing of a molecule within its van der Waals envelope? A further point concerns the ability of the program to read and write data in certain formats. For example, if you regularly need to represent the data in files from the Cambridge Structural Database it is desirable that your program can do this without manual editing of the input file. More generally, a program's ability to generate plot files in standard formats such as HPGL, PostScript, TIFF or JPEG makes it possible to incorporate these into documents or transmit them by e-mail or FTP, or to a networked printer or plotter.

There are also commercially available programs, usually supplied by diffractometer manufacturers as a complete package for structure analysis, but in some cases these can be purchased separately from the instrumentation. Such packages have the advantage of integration: for example, the solution and refinement programs communicate directly with the graphics module and the problems that can arise due to incompatible data formats are avoided. Integration is also available in freely available software [e.g. *WinGX* (Farrugia, 1999)] that provides a graphical interface linking various programs.

The increasing power of desktop computers and the availability of cheap laser printers with 600 dpi or higher resolution means that publication-quality illustrations can be produced with what is now very standard and affordable hardware. If you are considering the purchase of a system for structure analysis the advice is the same as for

any computer-related purchase. First choose the software you need, then select hardware you know will run it. Buy the fastest processor (for structure solution and refinement), the best screen (for viewing the structure), and the best printer (for hardcopy output) you can afford. Of course, if you plan to submit only electronic versions of your illustrations, then a printer with adequate features to allow proof checking is all you will need.

19.4 Underlying concepts

The positions of the atoms in a structure are derived from their fractional co-ordinates (x, y, z) on the crystal unit cell axes. Any graphics program needs to read these, along with the cell parameters required to convert to the orthogonal co-ordinate system in which the necessary calculations will be performed. The actual orthogonal axis set (x_o, y_o, z_o) is arbitrary and is not important. Provided that the program accepts and can use symmetry operators, it is necessary to read in only those atoms comprising the crystallographic asymmetric unit: symmetry-equivalent parts of the structure, whether for a molecule straddling a special position or for a packing diagram, can then be generated by the program. If the program cannot handle symmetry then all the atoms required for a particular drawing must be generated before being input. (One reason for doing this could be to exploit a particular drawing style not available in the graphics routine you normally use.) For the drawing itself the program uses a separate co-ordinate system (x_p, y_p, z_p) in which the axes are defined relative to the drawing medium (usually a screen) and co-ordinates are generated only in order to produce the plot. The axes of this co-ordinate system are variously defined in different programs and this represents a minor source of possible confusion if you use a number of these.

The rotation (or view) matrix transforms the initial arbitrary view defined by the orthogonal co-ordinates (x_o, y_o, z_o) into the plotting co-ordinates (x_p, y_p, z_p) corresponding to the viewing direction required. Much of the ease of use of a program is associated with the flexibility and simplicity with which this can be done. The following options may be available:

- direct input of the nine elements of a rotation matrix – of limited interest;
- along cell axes or other crystallographic directions;
- with respect to molecular features such as
  - (i) the direction perpendicular to the mean plane through selected (or all) atoms;
  - (ii) along the vector between two atoms (which need not be bonded together).

A good general approach is to start by looking along the direction perpendicular to the mean plane through all the non-H atoms, then

make small rotations to refine this view. It is always a good idea to explore a range of views in case a less obvious one proves to be the best. Most programs will allow you to do this either by continuous rotation or in small incremental steps and, unless you have a very large structure or a really slow computer, the default rotation speed should be acceptable. In fact, with faster processors you may need to slow the rotation rate for smaller molecules to prevent their spinning too rapidly.

Most drawings are composed from atoms and the bonds linking them. The connectivity information, which tells the program which atoms to draw bonds between, can be input explicitly along with the co-ordinates, but it is more common for the program to calculate the connectivity array using values for covalent or other radii appropriate to each atom. For example, the program may consider that two atoms are bonded if their separation is less than the sum of their covalent radii (plus a 'fudge factor' to ensure that slightly longer bonds are not missed): if the stored default covalent radius for carbon is 0.70 Å and the default 'fudge factor' is 0.40 Å then any pair of carbon atoms will be deemed to be bonded if they are within (0.70 + 0.70 + 0.40) = 1.80 Å of each other. This approach is generally valid for organic compounds, where covalent radii are well defined, and many users may be unaware of the default values simply because they never need to change them. With organometallic and inorganic compounds more care must be taken to ensure that all relevant interatomic distances are considered. It may be necessary to edit the connectivity list in order to add or remove specific entries. There will be limits on the numbers of atoms and bonds that can be handled within any particular program: these limits may be set within the program, perhaps at compilation, or they may be determined by the memory available.

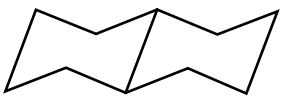

Fig. 19.1 A simple stick drawing.

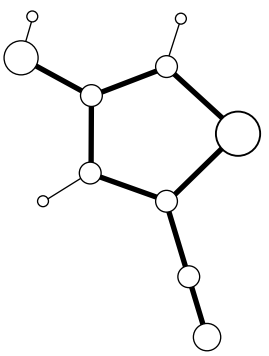

Fig. 19.2 A ball-and-spoke model.

19.5 Drawing styles

A wide range of representations is possible and it is important to choose appropriately. The simplest is a stick drawing, where bonds are represented by straight lines: atoms are implied by bond intersections or termini (Fig. 19.1). Some programs use this representation for rapid preliminary assessment of the best viewing direction as it is the least demanding in terms of computing power (and is therefore faster). It may also be the best way to display some large molecules, where drawing atoms as spheres or ellipsoids would seriously obscure the features behind them.

A more usual style (ball-and-spoke, Fig. 19.2) involves displaying atoms as spheres (circles in projection) with the bonds shown as rods. The user can select the radii of the spheres and the width of the bonds, alter the bond style and add shading or other effects to the atoms: Figure 19.3 shows the styles available in *SHELXTL/PC* (Sheldrick, 2001). Such features can be used to emphasize features of importance, such as the co-ordination sphere in a metal complex (Fig. 19.4). Different bond

types can be used to indicate π-bonded ligands in metal complexes, or interactions such as intramolecular hydrogen bonds.

A highly informative type of plot, colloquially referred to as an 'ORTEP' after its best-known implementation (Johnson, 1965, 1976), depicts atomic displacements as displacement ellipsoids. If the program offers a range of ellipsoid styles (e.g. those labelled –4 to –1 in Fig. 19.3) it will be possible to represent atomic motion and (to a limited extent) differentiate atom types in the same drawing (Fig. 19.5). The ellipsoids can be scaled in size to represent the percentage probability of finding within them the electrons around the atom as it vibrates: this probability level must always be quoted in the figure caption and a value of 50% is typical, although values such as 20% or 70% are sometimes used to obtain reasonable views of structures with particularly high or low U^{ij} values, respectively. Ellipsoid plots are uniquely helpful in highlighting possible problems such as disorder that may not be obvious from

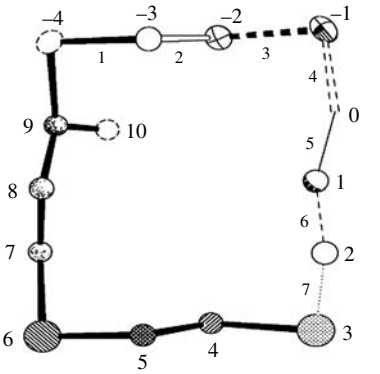

Fig. 19.3 A range of style for atoms and bonds.

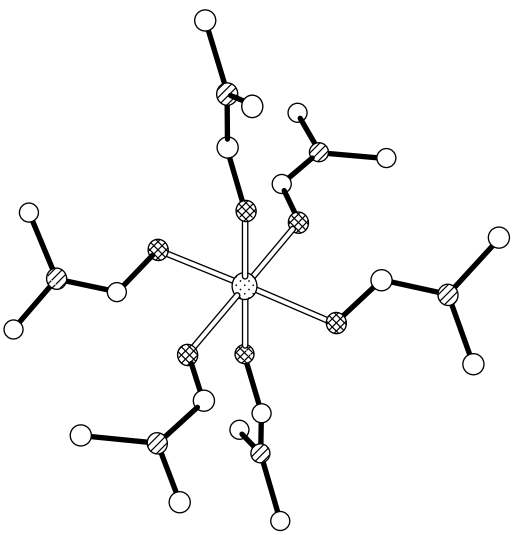

Fig. 19.4 The use of different styles for a metal complex.

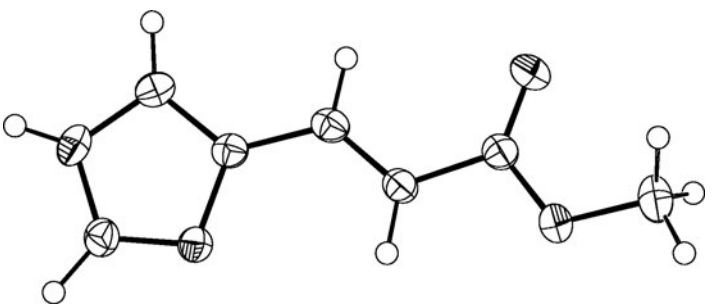

Fig. 19.5 Different style for displacement ellipsoids.

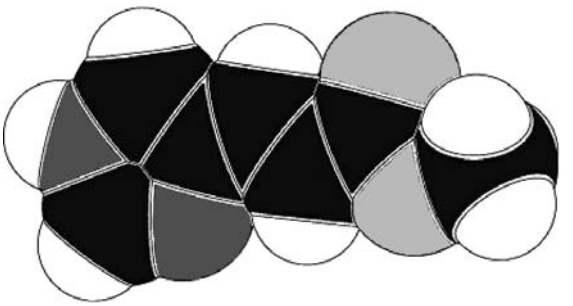

Fig. 19.6 A space-filling model.

the numerical U^{ij} values, even when these are available. In fact, some crystallographers are suspicious of ball-and-spoke plots because disorder and other potential problems such as incorrect atom assignments can be hidden, by either accident or intent.

In reality, of course, molecules do not consist of balls and spokes, and these give a poor idea of the external shape and steric requirements of a molecule. A more realistic representation is provided by a plot such as Fig. 19.6, where the atoms are shown as spheres having van der Waals radii rather than much smaller, arbitrary radii. These are referred to as 'van der Waals' or 'space-filling' plots and can be used to investigate questions such as whether a central metal atom is fully enclosed by its ligand array or exposed and therefore more likely to undergo reaction. The program *SCHAKAL* (Keller, 1989) was the first to allow you to display a composite picture of a ball-and-stick drawing of your molecule within its van der Waals envelope.

The molecules to be included can be selected automatically by the program (using criteria such as distance from a reference point or a certain number of unit cells) but the default selection may not give the best diagram. It is important to select and design packing diagrams in order to bring out the points you wish to illustrate without introducing unnecessary clutter. For this reason, the alternative approach of explicitly generating the required symmetry-equivalent molecules by the use of symmetry operations and cell translations has much to recommend it, even although it demands a higher level of understanding of crystal symmetry and expertise in using the more advanced features of graphics programs. Packing diagrams are frequently of poor quality and low information content and suggest that to the maxim 'one picture is worth a thousand words' should be added 'but only if it is a good one'. If the point of your packing diagram is merely to show that your molecules form typical linear chains it may be more effective to convey this in words. With some journals adopting a policy that only one illustration of a structure is normally published, the ability to produce plots with high information content is very useful. For example, it may be possible to show both a single molecule and the salient features of its environment in a single illustration (e.g. Fig. 19.7) rather than as two separate ones.

When adjusting the size of your graphics, take care to not change it unequally in two dimensions as it gives a distorted picture that can be misleading:

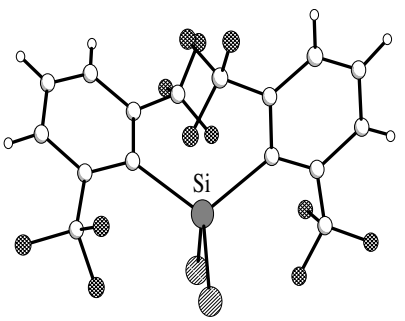

Notice how much more acute the C–Si–C angle looks above than below. To stop this from happening, ensure that you always have 'Lock Aspect Ratio' switched on:

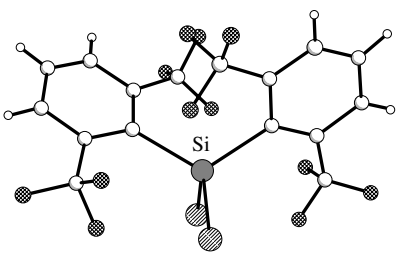

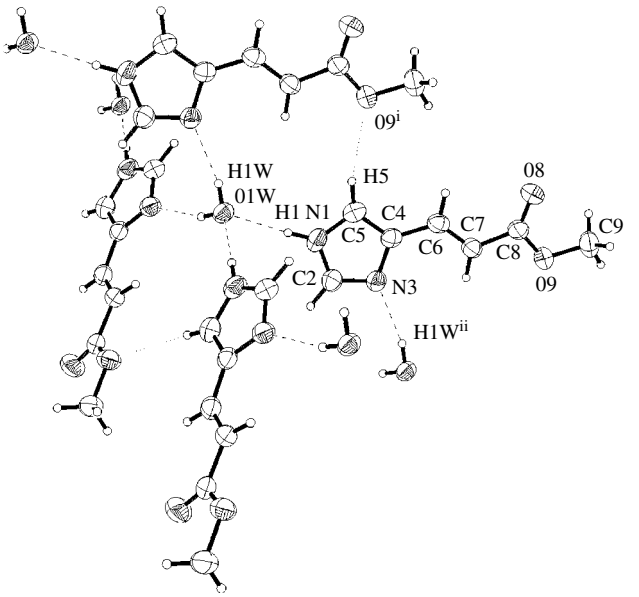

Fig. 19.7 A view of the environment of a reference molecule (labelled) showing the hydrogen-bonding network. The symmetry codes need to be defined in the text or caption.

The important interactions between molecules should be made as clear as possible, typically by the use of different bond types: for example, in a structure containing two types of hydrogen bond these could be differentiated using dashed and dotted lines while normal (intramolecular) bonds are shown by solid lines. If your figure is to be a representation of the packing you will probably want to include the outline of the unit cell, with the axes labelled. The labelling of symmetry-related atoms is a slightly difficult area, as the method recommended by many journals (superscripted lower-case Roman numerals) is not easily available in many graphics programs. Fortunately, it is usually possible to work round this with a little ingenuity.

The captions to packing diagrams are probably one of the least exploited ways to convey structural information. They are often limited to 'Fig. 2: a view of the crystal packing' when they could contain concise information about the view direction, the most important contacts and distances and the resulting arrangement of molecules (see Fig. 19.8).

If you work with inorganic compounds, molecular representations may be less appropriate than polyhedral plots in which groups of atoms form polyhedral shapes (e.g. six oxygen atoms around a metal centre can be linked to generate an octahedron), which are shown as opaque solid shapes. Neighbouring polyhedra are linked through their vertices, edges or faces to build up the structure. As with packing diagrams of molecules the selection of suitable symmetry-equivalents is important to the effectiveness of the illustration.

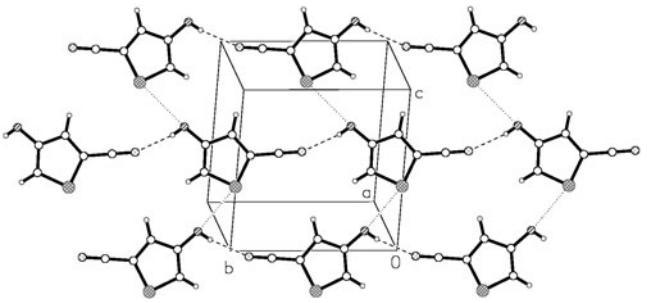

Fig. 19.8 What would you suggest as a caption?

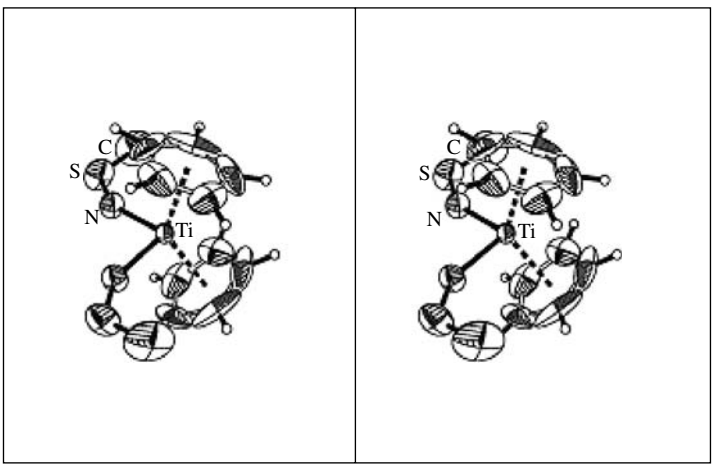

Fig. 19.9 A stereo pair, with separate left- and right-eye views.

19.6 Creating three-dimensional illusions

When even a simple three-dimensional structure is represented in two dimensions there is loss of information and for more complex cases this can be quite misleading. Various techniques have been developed to give an illusion of depth on the screen or on paper, including depth cueing, the use of perspective, bond tapering, hidden-line removal and the use of shading and highlights. Some techniques (e.g. depth cueing) work better on a screen than on paper because of the different background colours used. You may find that your graphics program has the required parameters already optimized, but conversely it may be rewarding to adjust these so as to produce the best effects for your example. However, beware of overdoing effects such as perspective or bond tapering to such an extent that the result looks ridiculous.

The traditional way to restore some depth to a flat molecular plot is by inducing stereopsis. A 'stereo pair' (Fig. 19.9) consists of two drawings, one for each eye, with a suitable separation and slightly different

rotations. When viewed, the two drawings should merge to give a complete three-dimensional effect. Such pairs are not universally effective, as a substantial proportion of the population literally cannot see the point of them (they cannot get the two images to merge) and the effectiveness should be compared with that of a 'mono' plot occupying a similar area.

19.7 The use of colour

In the last few years colour plots of crystal structures have become much more accessible, due to the wider availability of suitable software, the falling price of high-quality colour printers and the greater readiness with which many journals will publish colour plots, often at no charge but only where referees are convinced that they enhance the presentation significantly. The use of colour is most effective where it illuminates features that could not otherwise be easily identified: for example, in a polymeric structure two different metal atoms may have similar-looking high co-ordination and it might be impossible to find room for adequately sized labels to differentiate them. Colour codes can be defined in the figure caption or by means of a key panel. Other applications include colour coding of different bonds or atoms; highlighting of important features; colour coding of different molecules or structural motifs such as planes in packing diagrams; and sometimes just because colour looks wonderful on a poster. As with many good things, there are advantages in moderation: overuse of colour can be distracting and, if all or most of the atoms are coloured, many of the benefits of its use may be lost. Note that there are certain loose conventions about atom colours that you can use to convey more information: orange for B, black for C, light blue for N, red for O, light green for F, brown for Si, yellow for S, a darker green for Cl, and blue, green or red for metals. You are under no obligation to use these colours, but using other colour schemes will confuse at least some of those looking at the plot. Colour is probably least effective if only thin atom outlines are coloured and the colours are weak (yellow can be particularly problematic): it is better to fill the atom with a strong, vibrant colour. The use of colour opens up the possibility of using variations in intensity to convey depth information (depth cueing).

19.8 Textual information in drawings

Although the main constituents of a molecular plot will be atoms and bonds, it is normal (but not always essential) to include text, most commonly atom labels such as C1, N2 or O(3), or atom types (C/N/O). Unless colour or shading has been used to identify atom types, a drawing consisting only of chemically indistinguishable atoms and bonds is of limited use. Make sure that any labels are of a sufficient size that they will be legible at their final reduced size (but not so huge that they

overwhelm the structure) and placed so that they will not overlap or merge with any atoms or bonds. Obviously, make sure the labels refer to the correct atoms and do not leave any ambiguity. If the graphics program inserts them automatically, do check their placement. One decision is whether to have parentheses in your atom labels or not [e.g. C24 or C(24)]: the latter require more space but in some circumstances can help to avoid confusion [e.g. using some fonts the labels C11 and Cl1 may look very similar, while C(11) and Cl(1) are clearly distinguished]. If the program really cannot provide the text you need, you may be able to transfer the plot into a graphical manipulation program (e.g. *Adobe Photoshop*, *Corel Paint Shop Pro*). Journals now refuse to transfer hand-written labels onto an unlabelled copy of the plot. It is not always necessary to label every last atom, but any atoms referred to in the text or in a table of selected molecular geometry parameters should be identified: for example, in a co-ordination compound labelling the central metal and the ligand donor atoms may suffice. (You can always include a fully labelled version for the referees and possibly for deposition.) Unless they are of special significance (e.g. involved in H-bonding) hydrogen atoms are not normally labelled.

Other text may be included: this can be excellent on large posters, but where figures will undergo reduction it is likely to become hard to read. For example, adding bond lengths and angles to a drawing may help interpretation, but only if they are legible. To avoid cluttered drawings, some journals expressly forbid these additions and insist that you relegate such text to the figure caption.

19.9 Some hints for effective drawings

(a) Decide on the content: this is usually obvious for a single molecule but there is much more choice for packing diagrams. In some cases the hydrogen atoms make it impossible to see the rest of the structure and can be omitted, although you may wish to include those on O or N atoms, for example. You can sometimes reduce clutter by devices such as drawing a single bond (in a different style) from the metal to the centroid of a co-ordinated benzene (or cyclopentadiene) ring rather than the six (or five) bonds to the individual carbon atoms. Sometimes you need to omit peripheral groups, or show only the *ipso* carbon of an aryl ring, before you can see the salient parts of the molecule (you must state in the figure caption that you have done this). In some cases you may find it impossible to show all the important features in a single view.

(b) Invest some time looking for the best viewing direction with the minimum of overlap, especially where important atoms are concerned. If an atom really cannot be manoeuvred into view you could add a phrase such as 'C8 is wholly obscured by C7' to the figure caption.

(c) If the important features are still not obvious, can you emphasize them by using a distinct style for the atoms or bonds involved? For example, you can identify a metal's co-ordination sphere by having

a distinct style for the ligand–metal bonds. If an atom has additional co-ordination at a greater distance, the bonds involved can be shown differently.

(d) If colour is effective use it in moderation to draw attention to selected features of the structure.

(e) Choose the most effective representation to convey the information you want, bearing in mind that some journals may have specific requirements. Displacement ellipsoid plots certainly contain a lot of information, but it may not be the information you want to convey. Often, the most significant atoms appear smallest because they have higher atomic and co-ordination numbers and consequently have lower displacement parameters. Furthermore, there is limited scope for differentiating atom types (but see Fig. 19.5), whereas a ball-and-spoke model allows more freedom to assign atomic radii and drawing styles. Avoid the use of similar styles for different atoms as far as possible: for example, styles 7, 8 and 9 in Fig. 19.3 may look identical if the circle representing the atom is very small (e.g. in a packing diagram) or after reduction.

(f) Avoid clutter. In some cases you have to add atom labels but it may be possible to be selective. Omitting parentheses may help, as will calling the only phosphorus atom in the structure P1 or even P rather than P01 or P001. Also, you may be able to label the carbon atoms using only their numbers (i.e. omitting the atom type and any parentheses). If there is no room to place a label close enough to an atom to identify it uniquely, consider placing the label some distance away with a line or arrow pointing to the atom.

(g) Take particular care with stereo views. Do they constitute a good view? Most importantly, are they better than a larger mono view occupying the same space?

(h) As mentioned earlier, different criteria apply for different publication formats. Are you preparing an illustration for a journal, a thesis, a poster, a web page, or an overhead transparency? Do not unthinkingly transfer a figure between formats without assessing its suitability. For example, a web graphic that is so complex that it takes a long time to download, or that is effective only on a very high resolution monitor, is unlikely to reach a wide audience.

(i) If you are submitting results to a journal that allows only a limited number of views (e.g. one) of any single structure, consider whether figures can be combined without loss of information.

(j) Be creative and have fun – this part of crystallography allows you more choice than any other. The original *ORTEP* manual (Johnson, 1965) exhorted users to improve on the standard views produced from the program – that is now easier than ever.

19.10 Tables of results

The main tables produced at the end of the structure refinement will comprise all or most of the following:

• fractional atomic co-ordinates (with s.u.s) – and possibly U_{eq} or B_{eq} values – for the non-H atoms: the values may be multiplied by a convenient factor (given in the table heading) to give integers, or expressed as decimal numbers;

• atomic displacement parameters – normally as U^{ij} or B^{ij} – with s.u.s;

• fractional atomic co-ordinates – and possibly U_{iso} or B_{iso} values – for H atoms that have not been refined freely (those that have could either be given here, with s.u.s, or moved into the first table);

• molecular geometry parameters (bond lengths, valence angles, torsion angles, intermolecular contacts, least-squares mean plane data, *etc.*) – there will usually be two versions of these tables, a shorter list of selected parameters for publication and a fuller listing (of the bonds and angles at least) for refereeing and deposition;

• structure-factor tables.

It is also possible to tabulate crystal data and details of the structure determination, although this is not efficient in terms of space unless you can combine data for at least two or three structures in one table. Journals may have particular requirements, but if none are specified (perhaps because the journal rarely publishes crystal structures), those of the journals of the Royal Society of Chemistry or the American Chemical Society seem to be widely accepted.

Journals still vary enormously in their policies on crystallographic data – what they will publish, what they require as supplementary data and what they will deposit. Before you start to prepare a submission, study the relevant instructions for authors (traditionally published in the first issue of each year but now available on the journal's web pages) and follow them closely. There is, however, a strong trend towards publishing less, and many journals stopped publishing structure factors, displacement parameters, fractional co-ordinates and full molecular geometry (more or less in that chronological order) so that the selection of results for publication assumes greater importance (see below). Many journals will require supplementary data in CIF format rather than hard-copy, although for a time some remained a little suspicious of electronic data and demanded both! Some refinement programs will produce tables of results automatically and, although these are useful, they almost always benefit from critical inspection and sometimes manual adjustment of content and format, but you must exercise extreme care not to introduce numerical or other errors.

19.11 The content of tables

19.11.1 Selected results

Selection almost always involves molecular geometry parameters as co-ordinate data are usually complete – it is definitely not permissible to include only the co-ordinates of what you consider the 'interesting' atoms. The selection of geometry parameters depends on the chemical nature of the compound and the structural features that you want to emphasize. These are often obvious: in a co-ordination compound you

might want to include only bonds involving a central metal and angles subtended at it (torsion angles involving such metals may be produced automatically but in most cases are not even worth archiving), but each structure should be considered individually. There is no point in trying to publish bond lengths that have been constrained during refinement, or that are unreliable because they fall in a region affected by disorder. Extensive listing of the internal molecular geometry of typical benzene rings, whether constrained or not, is useful only for refereeing purposes and deposition. In many organic compounds there are no interesting or unusual bond lengths or angles that merit publication, but a selection of torsion angles might be worth including. Mean values or ranges may usefully supplant large numbers of individual values for similar parameters.

19.11.2 Redundant information

Where a molecule lies on a crystallographic symmetry element, some of its molecular geometry parameters will be equal or simply related to each other and therefore not all need to be given. Strictly speaking, only the unique set should be given and automatic table-generating routines may not be able to cope with this requirement. It may, however, be sensible to include some redundant information to make the situation clearer, especially for a non-crystallographic audience. For example, molecules of doubly bridged dinuclear metal complexes $M_2(\mu - L)_2$ contain four-membered rings and these are often found lying across crystallographic inversion centres: by symmetry, the opposite M–L bond lengths are equal; the two M–L–M angles are equal; the two L–M–L angles are equal; the MLML rings are strictly planar; and adjacent pairs of M–L–M and L–M–L angles add up to exactly 180°. The independent parameters are two adjacent M–L bond lengths and one angle within the ring. A mirror plane or a two-fold rotation axis instead of an inversion centre will involve different relationships among the parameters, and these relationships will depend on the orientation of these symmetry elements. Similar arguments apply to the more common situation where a structure contains a central, often metal, atom on a special position. For example, a four-co-ordinate palladium atom on an inversion centre has only two independent bond lengths and one independent angle.

When tables contain atoms that are related by symmetry to those in the original asymmetric unit, for example in order to give a bond length between two atoms related by a mirror plane, these atoms must be clearly identified (e.g. C5′, C5* and C5^{i} could be symmetry-equivalents of atom C5) and the symmetry operations denoted by ′, * or ^{i} defined in a footnote.

19.11.3 Additional entries

Not all entries required for a molecular geometry table are necessarily produced automatically. ‘Long’ bonds may be missed and have to be inserted manually; short contacts such as those in hydrogen bonding

may be calculated elsewhere but not transferred automatically. You may even want to include non-existent 'bonds', for example to demonstrate that two atoms are not close enough to interact. These values and their s.u.s should be calculated by the refinement program.

19.12 The format of tables

Journals tend to have their own requirements for tables that you must follow or risk objections from the referees or editors. The precision to which results are required does vary: *Acta Crystallographica* prefers s.u.s in the range 2–19, while *Dalton Transactions* have preferred 2–14 in the past, and some referees and editors object to s.u.s of 1. This can mean allowing more significant figures for the co-ordinates of heavier elements. Make sure the s.u.s look sensible and that any redundant data (such as the U^{ij} components for atoms on special positions other than inversion centres) have the correct relationships between their values (and among their s.u.s).

Ensure that the table headings are informative and correct: are the powers of ten quoted there actually those used in the table? Are the displacement parameters correctly identified as *U* or *B*? Are the headings on the structure-factor tables correct, with any reflections not used in the refinement flagged? If it is possible, I suggest having a compound code or other identifier on every page of tables so that structures cannot be mixed up.

While one program might produce geometric parameters based on the order in which atoms occur in the refinement model, another might give the bonds in ascending order of length, and so on. It is worth looking at the tables to see whether this can be improved. In my opinion, the clarity of this table of selected bond lengths (in Å):

```
Pd–N6   1.996(8)   Pd–N2   2.017(7)
Pd–N4   2.001(6)   Pd–N5   2.035(6)
Pd–N1   2.008(7)   Pd–N3   2.057(7)
```

is much improved by re-ordering to give:

```
Pd–N1   2.008(7)   Pd–N4   2.001(6)
Pd–N2   2.017(7)   Pd–N5   2.035(6)
Pd–N3   2.057(7)   Pd–N6   1.996(8)
```

19.13 Hints on presentation

19.13.1 In research journals

This has mostly been covered already. Follow the instructions to authors for submitting papers, including experimental data, tables, figures and supplementary data. What is the policy on colour plots? The range of formats for literature references can appear overwhelming, and if you

submit to a wide range of journals the use of reference management software may be worthwhile. If you regularly use the same references in the same format they could simply be stored in a standard ASCII or word processor file.

19.13.2 In theses and reports

Here you have much more freedom, but you have to be careful that the result is appropriate in style and length to the purpose in hand: a thesis that runs to 300 pages may be acceptable but an interim report of that size is ridiculous. Fortunately, guidelines are normally available at each institution, so consult them before you write a word.

Don't overdo the tables: it is seldom necessary to include structure-factor tables, even in an appendix. However, you could put co-ordinate data and full molecular geometry tables in appendices and retain only selected information in the main body: this will cause less disruption to the flow of your report. These appendices do not necessarily even have to be in hard copy: does your institution allow you to include appendices on a CD or DVD?

You can be more generous with diagrams than when publishing in a journal, but remember that there must always be a good reason for including any diagram.

19.13.3 On posters

Select the most important points you want to get across. Save yourself time by planning what you are going to present – there is no point in producing material you don't have space for. (Do you know the size and orientation of the poster display area available to you?) Text must be readable from a distance of one to two metres – you may not always attract a crowd but the poster will make a greater impact if it can be viewed from a comfortable distance. Keep any tabulated information short and relevant. (Are the crystal data really needed on the poster, or is it sufficient to have these to hand in case someone asks?) Posters are one place where colour can be exploited to the full, and not only in figures but in text, backing material and surrounds. It is harder to overdo it here, but still possible! You should keep the information density relatively low: this has the additional advantage that you will have something more to tell those who express an interest in your work.

19.13.4 As oral presentations

Many of the points mentioned in respect of posters apply here too: avoid high-density slides or overhead transparencies that nobody will have time to read. Don't be tempted to use that convenient table prepared for publication if it consists mostly of values that are not relevant to your lecture.

An important function of your visual aids can be to remind you what to say next, so they must be 'in phase' with your talk; they must not let the audience see your final results while you are still outlining the problem! If you need to refer to the same slide or transparency at two points in your talk, it is better to make two copies than to waste time rummaging around for the single copy you last saw ten minutes before. If you have just covered the material outlined on a slide and made a point that requires the audience to absorb information from the slide, do not immediately proceed to the next one. This point is particularly relevant if the slide contains a crystal structure diagram.

Compose your visual aids carefully. Try to find out the size of the auditorium and about its facilities. Mixing slides and transparencies requires some planning to ensure you don't lose track of what you are saying. If you are inexperienced it is safer to have all your visuals in the same format if at all possible. Colour can be extremely powerful, especially when used in bold, simple illustrations.

Do not try to cover too much material. Your audience will be less familiar with your material than you are and it will not help if you speak too quickly. Time your talk in advance – a practice session with a sympathetic (and constructively critical) audience is a good idea if you are unused to speaking in public. You should assess the composition of your audience in advance. If they are not experts in your own field, you will need to give more background information so that they understand the context, before you begin to describe your own work and its results.

Humour can be a good way to engage the audience's attention but it needs to be used carefully and sparingly. In some circumstances it is wholly inappropriate. If in any doubt, avoid it.

19.13.5 On the web

The web is an excellent medium for disseminating research results but it has its own special requirements. The speed at which data can be transferred is limited: as faster networks are installed these are required to carry ever more demanding applications. Combined with a constant increase in the number of users this ensures that bandwidth is always restricted in some way. As a result, the most effective web pages are often those that do not involve large-scale data transfer in order to be useful. Authors need to bear in mind that many of their potential audience may be using modest hardware and not-so-recent software, and they must ensure that using new features in the latest version of their web authoring software does not restrict this audience. On a related point, any web page should at the very least be viewable with the most common web browsers such as Microsoft Internet Explorer or Mozilla Firefox.

It might seem obvious that any website should be designed so that the visitor can find information easily, yet many impressive-looking corporate sites are so poorly structured that finding what you want is time consuming, inefficient and frustrating. If you have an extensive website you should give serious thought to how it is constructed, and

in particular whether your homepage allows a visitor easily to begin navigating it. As well as hyperlinked text and graphics, web publishing offers the possibility of illustrations that can be rotated or otherwise moved, either according to your pre-programmed instructions or in response to user input. This allows the visualization of complex structures and packing diagrams, for example. These features are usually implemented by means of Virtual Reality Modelling Language (VRML) extensions to your browser.

Publishing results on the web is quite different from displaying them on a poster that you can take down at the end of a conference. Once placed on the web, material assumes a substantial degree of permanence as it is accessed, stored in various caches, copied to other formats and printed. On the other hand, such results can be more ephemeral that those printed in a journal, as it is possible to remove, modify or update them. The copyright implications of publishing your results on the web are often far from clear, but these are likely to become more serious with the spread of electronic publishing. As with other forms of publication, placing results on the web should be done only with the knowledge and consent of all those contributing to the work, and only when the consequences of doing so have been fully explored.

19.14 Archiving of results

Although some of the results of your structure determinations will end up in a database after publication, you must keep your own copies of all relevant files and other information safely and in an accessible form. Most crystallographers know the frustration of setting out to prepare a structure for publication, only to find that some experimental parameter such as the colour of the crystal or the type of diffractometer used is not immediately available and has to be ferreted out. In the not-so-distant past the only safe way seemed to be to keep every piece of hard-copy output ever generated for a structure, but now archiving and transmission tools such as the CIF format allow this to be done much more concisely. The 'paperless office' once promised by the advocates of information technology may have proved illusory elsewhere, but in the modern crystallography laboratory it has largely materialized. The CIF and its uses are described in detail in the next chapter.

When archiving data the main considerations are safety and accessibility. To address the first, you need to keep backup copies of your files, possibly on tape, including a set that will survive fire, flood and theft at your workplace. This could involve a fireproof safe, but keeping a backup in a safe place at home is probably as reliable. Keeping all the files for one structure together aids organisation, and utilities such as *PKZIP*, *WinZIP*, *PowerArchiver* or *WinRAR* allow these to be compressed within a single archive file, with the bonus of a considerable saving on disk space. For accessibility, you need some form of indexing so that the structures you require can be quickly and uniquely identified. Before

starting to rely on it, you must check the backup procedure works by restoring some typical files from the archive. Most backup devices come not only with software to drive them but also with documentation that includes advice on how to implement a suitable and effective backup regime. This documentation should include explanations of how to use both full and incremental backups, the latter referring to the procedure whereby only those files that have changed since the last backup are transferred to the archive.

There are two distinct aspects to backing up a particular computer. The first requires an archive medium capacious enough to allow you to back up everything on that computer, including operating system, applications and data. This would allow you to re-create your working environment in the event of the computer or its hard disk failing totally, and requires a backup medium with the same capacity as your hard disk. The best solution used to be some kind of tape drive, and models with capacities of up to many tens of gigabytes are currently available, but there is an increasing view that the only effective, convenient backup medium for a hard disk is another hard drive. An additional level of security could be provided by backing up your working hard disk to another *physical* hard disk (not a different *logical* drive on the same disk) on the computer. Such a backup will survive any failure of the working disk, and most disasters short of theft or outright destruction of your computer. If the computer is automatically backed up over a network you may be content to rely on this, but make sure that the frequency of backup is appropriate and that the backup files are accessible. Remember to update the backup files whenever you make significant changes to the computer, for example after a major new application has been installed and configured.

The second aspect is the regular backup of new data and the media that can be used will depend on the volume of these data. The essential files to be kept at the end of a structure analysis may well amount to only a few hundred kilobytes after compression and several structures could be archived on a standard 3.5″ floppy disk. In contrast, the frames for one data collection using an area-detector diffractometer occupy several hundred Mbytes and, while archiving to CD-ROM is a possibility, each CD will hold only two or three sets of frames at most. However, with DVD writers costing from less than £50 per unit, and each disk holding 15–40 sets, this seems a sensible backup medium. Two rival formats (Blu-ray and HD DVD, see Table 19.1) were in competition to succeed DVD, but in 2008 it became clear that Blu-ray had won. For data transfer, solid-state drives are now available with sufficient capacities (e.g. 8 Gb) and have the advantage of simplicity.

When you are planning a backup regime, ease of use is an important factor. You are unlikely to regularly use any method that is cumbersome or time consuming. Archive media can change and develop as rapidly as other aspects of computer hardware, and factors such as capacity, cost, convenience and durability need to be considered. It is not necessarily best to adopt the latest technology: in fact it may be safer to select one

Table 19.1. Data storage capacity.

Medium	**Capacity**
3.5" disk	1.44 Mb
super-floppy	120 Mb
cartridges	100 Mb–2 Gb
solid state drives	1–128 Gb
CD-ROM	550 Mb
DVD	4.7–8.5 Gb
HD DVD	30 Gb
Blu-ray disk	50 Gb
tape	400 Mb–120+ Gb
portable hard disk	40–500 Gb

that has gained reasonably wide acceptance so that consumables such as tapes are likely to remain available for the useful life of the computer. Table 19.1 gives (sometimes rather approximate) current capacities for various storage media.

References

Farrugia, L. J. (1999). *J. Appl. Crystallogr*. **32**, 837–838.

Johnson, C, K. (1965). *ORTEP*. Report ORNL-3794. Oak Ridge National Laboratory, Oak Ridge, Tennessee, USA.

Johnson, C. K. (1976). *ORTEPII*. Report ORNL-5138. Oak Ridge National Laboratory, Oak Ridge, Tennessee, USA.

Keller, E. (1989). *J. Appl. Crystallogr*. **22**, 19–22.

Macrae, C. F., Edgington, P. R., McCabe, P., Pidcock, E., Shields, G. P., Taylor, R., Towler, M. and van de Streek, J. (2006). *J. Appl. Crystallogr.* **39**, 453–457.

Pearce, L. J., Watkin, D. J. and Prout, C. K. (1996). *CAMERON*. Chemical Crystallography Laboratory, University of Oxford, UK.

Sheldrick, G. M. (2001). *SHELXTL XP* graphics module: various versions, and for different platforms (e.g. PC, Unix, Linux).

This page intentionally left blank

The crystallographic information file (CIF)

20

Alexander Blake

20.1 Introduction

The crystallographic information file (CIF) is an archive file for the transmission of crystallographic data: this transfer can be between different laboratories or computer programs, or to a journal or database. The file is free-format, flexible and designed to be read by both computer programs and humans (the latter require a little practice at the start). The specification of the CIF standard has been published and the same article provides information on its evolution (Hall *et al.*, 1991). It is based around the self-defining text archive and retrieval (STAR) procedure (Hall, 1991), and consists of data names and the corresponding data items with a loop facility to handle repeated items such as the author/address list or the fractional co-ordinates. The format is extensible, so that data names covering new developments such as area detectors can easily be accommodated. However, once a data name is included it is never removed, otherwise portions of those archives written in the interim would be undefined.

20.2 Basics

The CIF is an ASCII file, such that only the following characters are allowed:

```
abcdefghijklmnopqrstuvwxyz ABCDEFGHIJKLMNOPQRSTUVWXYZ
0123456789  !@#$%^&*()_+{}:"~<>?|\-=[];'',/.
```

Any others that you may want to include in a manuscript (such as Å,°, é, ø, subscripts and superscripts, Greek letters, mathematical symbols such as ±, and chemical multiple bonds) require special codes that are detailed in the *Notes for Authors* for *Acta Crystallographica, Section C*. Do not attempt to show italicized, bold or underlined text (e.g. in space group symbols) as these attributes

should be added automatically. Many data names have implicit units (e.g. Å for `_cell_length_a`; Å^3 for `_cell_volume`; minutes for `_diffrn_standards_interval_time`) and these units must not be appended; thus

```
_cell_volume    2367.5(8)
```

is correct but

```
_cell_volume    2367.5(8)\%A^3^
```

is not.

If you prepare your CIF using a word processor rather than a text editor you must make sure that the output file is ASCII, that there are no (hidden?) embedded codes and that lines do not exceed 80 characters in length. If you are exporting an ASCII file from a word processor it is best to have used a large fixed font (e.g. Courier 12 point or larger) so that any lines that are part of blocks of text do not overrun upon conversion. Do not include any non-ASCII characters in the word processor file as these will be lost or corrupted upon writing the ASCII file and, even if they survived unchanged, the CIF processing software will not recognize them correctly. It is much safer to use a dedicated CIF editor such as *enCIFer* (Allen *et al*., 2004; see http://www.ccdc.cam.ac.uk/free_services/encifer/ for the *enCIFer* home page) or *publCIF* (Westrip, 2009; see http://journals.iucr.org/services/cif/publcif), because these programs also check the CIF for syntax errors and whether the data names and items correspond to valid CIF dictionary entries. *EnCIFer* can also display the structure graphically.

The following CIF terminology is used.

text string	a string of characters delimited by blanks, quotes, or semi-colons (;) as the first character on the line
data name	a text string starting with an underline (_) character
data item	a text string not starting with an underline, but preceded by a data name
data loop	a list of data names, preceded by _loop and followed by a repeated list of data items
data block	a collection of data names and data items (which may be looped) preceded by a data_code statement and terminated by another data_ statement or the end of the file. A data name may only occur once within any one data block.
data file	a collection of data blocks: no two data block codes may have the same name

CIF data name and data block code definitions are restricted to a maximum of 76 characters, but their hierarchical construction and careful design mean that they are largely self-explanatory: e.g.

```
_publ_author_name
_exptl_crystal_colour
_computing_structure_solution.
```

The term 'CIF' has acquired a range of informal meanings: it is used to describe the format, the data output by a control or refinement program, as well as the data file (comprising two or more data blocks) submitted as a manuscript for electronic publication.

20.3 Uses of CIF

(a) Your own local archive. A CIF produced by a refinement program upon convergence of your structure can be edited and augmented so that all the relevant results and details of procedures can be stored. As with other uses, the degree of manual editing required will depend on the extent to which your data collection and reduction programs produce relevant output in CIF format.
(b) A standard method of transmitting data between crystallographic programs (an increasing number of which read files in CIF format) or to colleagues in other laboratories.
(c) An efficient method of providing supplementary data for papers containing crystal-structure determinations.
(d) A standard route for deposition into structural databases.
(e) A route to standard printed tables (e.g. via the *SHELXL* ancillary program *CIFTAB* or *XCIF*).
(f) Direct electronic submission of manuscripts to journals such as *Sections C* and *E* of *Acta Crystallographica* or *Zeitschrift für Kristallographie*. The required data file will consist of a number of data blocks. One, perhaps called `data_global` and possibly prepared by manual editing of a template, will contain author contact information, submission information, an author/affiliation/address list, a title, a synopsis, an abstract, a comment (discussion) section, experimental details, references, figure captions and acknowledgements. This block will be followed by one data block for each structure to be included, perhaps called `data_compound1, data_compound2`, etc.

20.4 Some properties of the CIF format

(a) Within any data block, the ordering of the associated pairs of data names and data items is not important, as file integrity does not depend on finding these in a particular sequence. However, human readers will find it easier to read the CIF if they are grouped logically. Furthermore, there are no restrictions on the ordering of the data blocks.

(b) Each data name must have its corresponding data item, but the latter need not contain real information. Sometimes a placeholder such as `?` or `.` is used as in

```
_chemical_name_common ?
```

These placeholders are used within loop structures when some data items are not relevant to every line of the loop. In the following example the fourth data name in the loop applies only in the second line.

```
loop_
        _geom_bond_atom_site_label_1
        _geom_bond_atom_site_label_2
        _geom_bond_distance
        _geom_bond_site_symmetry_2
        _geom_bond_publ_flag
          Ni  N1  2.036(2)   .  Yes
          Ni  N1  2.054(2)   2_555  Yes
          Ni  S2  2.421(10)  .  Yes
          C   S2  1.637(3)  .  Yes
          N1  C1  1.327(3)  .  ?
          N1  C5  1.358(4)  .  ?
          N2  C12 1.309(3)  .  ?
```

Some items are mandatory for certain CIF applications: for example, the list of data items required for a submission to *Acta Crystallographica Sections C* and *E* is given in these journals' *Notes for Authors*.

(c) Certain data items can be specified as standard codes and these must be used wherever possible. For example, there are now seven standard codes for the treatment of H atoms during refinement associated with the data name

```
_refine_ls_hydrogen_treatment
```

and these include `refall` (all H parameters refined) and `constr` (e.g. a riding model). If the standard codes are inappropriate or inadequate then a fuller explanation can be given as part of an experimental section.

(d) There are now a large number of ancillary programs available for preparing, checking, manipulating and extracting CIF data. Some of these will be mentioned later and others are given on the IUCr website (www.iucr.org).

(e) Additional tables can be created within the CIF format. The most common of these contain hydrogen-bonding parameters and there are now standard `geom_hbond_` data items to facilitate their input. However, it is possible to set up tables of non-standard parameters by defining additional data items; the following example sets up a comparison table of molecular geometry parameters.

```
loop_
_publ_manuscript_incl_extra_item
'_geom_extra_tableA_col_1'
'_geom_extra_tableA_col_2'
'_geom_extra_tableA_col_3'
'_geom_extra_tableA_col_4'
'_geom_extra_tableA_col_5'
'_geom_extra_tableA_col_6'  # up to 14 columns allowed
'_geom_extra_table_head_A'  # for table heading

'_geom_table_headnote_A'    # for headnote if needed
'_geom_table_footnote_A'    # for footnote if needed

_geom_extra_table_head_A
;
Table 3.
Comparison of molecular geometry parameters (\%A,\%) for
    1,3-dioxolan-2-ones
;

loop_
_geom_extra_tableA_col_1
_geom_extra_tableA_col_2
_geom_extra_tableA_col_3
_geom_extra_tableA_col_4
_geom_extra_tableA_col_5
_geom_extra_tableA_col_6

Parameter^a^   (I)      (II)       (III)      (IV)      (V)
O1---C2        1.33   1.327(2)   1.316(6)   1.34(2)   1.323(5)
"C2\\db O2"    1.15   1.207(2)   1.192(6)   1.21(2)   1.200(6)
C2---O3        1.33   1.341(2)   1.316(6)   1.28(2)   1.348(6)
O3---C4        1.40   1.447(2)   1.443(5)   1.42(2)   1.460(6)
C4---C5        1.52   1.531(2)   1.498(7)   1.53(2)   1.527(6)
O1---C5        1.40   1.448(2)   1.420(6)   1.46(2)   1.456(5)
O1---C2---O3   111    112.7(1)   111.9(4)   113(1)    112.0(4)

_geom_table_footnote_A
;
(I) 1,3-dioxolan-2-one (Brown, 1954)
(II) D-erythronic acid 3,4-carbonate (Moen, 1982)
(III)  4-p-chlorophenyloxymethyl-1,3-dioxolan-2-one
      (Katzhendler et al.,1989)
(IV) 4-(5-(2-iodo-1-hydroxyethyl)-5-methyl-tetrahydro-2-
     furyl)-4-methyl-1,3-dioxolan-2-one (Wuts, D'Costa &
     Butler, 1984)
(V) 1,6-bis(1,3-dioxolan-2-one)-2,5-dithiahexane (this
    work)

^a^ Atom numbering scheme has been standardised as for (V)
;
```

20.5 Some practicalities

20.5.1 Strings

The correct handling of strings throughout the CIF is vital. There are three ways to supply the information in these and examples of each follow.

(a) Delimitation by blanks – the data item is effectively a word or a number without any spaces within it. The data item cannot extend beyond the end of a line. Examples are:

```
_publ_contact_author_email      J.O-Groats@north.ac.uk
_cell_length_a                  10.446(3)
_diffrn_standards_number        3
```

Note that

```
J. O-Groats@north.ac.uk
```

and

```
10.446 (3)
```

are not allowed because they contain spaces.

(b) Delimitation by quotation marks (single or double) – the data item may now contain spaces. It is limited to one line, but it can be on the line following the data name if required. For example:

```
_exptl_crystal_density_method   'not measured'

_chemical_formula_moiety 'C12 H24 S6 Cu 2+, 2(P F6 -)'

_publ_section_acknowledgements
  "We thank EPSRC for support (to J.O'G.)."
```

(c) Delimitation by semi-colons as the first character in a line – this is necessary for blocks of text that exceed one line in length. For example:

```
_publ_section_abstract
;
In the title compound C~12~H~22~O~7~, (1), molecules
occur exclusively as the cis geometric isomer and are
linked by hydrogen bonding to form helices running
parallel to the crystallographic c direction.
;
```

20.5.2 Text

(a) When preparing a data file for publication, most effort will be devoted to the textual sections, in particular `_publ_section_abstract`, `_publ_section_comment` and `_publ_section_references`. Much of this may appear as normal text, but certain special character codes are commonly required. Subscripted and superscripted text is delimited by pairs of tilde (~) and caret (^) characters, respectively; for example, if you want `[Cu(H2O)4]2+` to appear in your paper, you need to enter it as `[Cu(H~2~O)~4~]^2+^`. Note that these must not be used in `_chemical_formula_moiety`, etc. In discussing molecular geometry you will need the symbols Å and °, the codes for which are `\%A` and `\%` (not `^o^`), respectively. You will occasionally need

other codes – see the appropriate page in the IUCr journals website for the full list.

(b) Certain trivial errors occur frequently and can cause a great deal of annoyance because the CIF processing software does exactly what you tell it to, rather than what you want. CIF checking software (see below) will strive to return helpful reports on the location of errors in the data file, but sometimes the results of the fault are so pervasive, or appear so far removed from the original error, that a manual search is necessary. Some of the most common and irritating faults arise from the simplest of causes, such as the failure to have matching subscript and superscript codes: forgetting to 'switch off' these features means that subsequent information in the CIF is misinterpreted. Another frequent mistake is not terminating text strings or text blocks correctly.

(c) Within a CIF, the selection of molecular geometry parameters for publication depends on the setting of the `_geom_`*`type`*`_publ_flag` for each parameter, where *`type`* is `bond`, `angle` or `torsion`. Setting a flag to `Yes` (or `y`) indicates that the corresponding parameter should be published: anything else (`No`, `n` or `?`, for example) means that it will not. Make sure that this editing does not disrupt the number of data items (including placeholders), as doing so will create problems for any program attempting to read the CIF.

20.5.3 Checking the CIF

Before a CIF is used, for whatever purpose, it is ***essential*** to submit it for automated checking. The *checkCIF* procedure tests for valid CIF data names, correct syntax, missing IUCr Journals Commission requirements, consistency of crystal data, correct space group, unusual atomic displacement parameter values, completeness of diffraction data, etc. It is available through the IUCr website (www.iucr.org), and the current version returns reports within a few seconds. Depending on the intended purpose of the CIF, failure to satisfy certain of these tests (e.g. missing Journals Commission requirements) may not be important as they are designed primarily as a check on a data file before electronic submission to *Acta Crystallographica*. If you have a way of reading PDF files, such as the free program *Adobe Reader*, you should take advantage of another utility: *printCIF*, also available through the IUCr website, returns a preprint of your paper for checking. This is valuable because some errors, especially formatting ones, may not be detected by *checkCIF* but they are usually horribly obvious on a preprint. The IUCr program *publCIF* (Westrip, 2009) includes the same functionality as *printCIF* but, like *enCIFer*, it is interactive, offering an HTML representation of the required CIF publication data. You can also carry out useful additional checks with programs such as *PLATON* (Spek, 2003) running on your own computer: these include not only numerical checks but also visual checks of conformation, ellipsoid plots and other

features. It is worthwhile checking whether chemically equivalent geometric parameters are equal within the relevant standard uncertainty limits; for example, in a tertiary butyl substituent are all three C–CH_3 bond distances close to 1.52 Å, and is there tetrahedral geometry around the central carbon atom? If not, you should check for disorder or other problems.

References

Allen, F. H., Johnson, O., Shields, G. P., Smith, B. R. and Towler, M. (2004). *J. Appl. Crystallogr.* **37**, 335–338.

Hall, S. R. (1991). *J. Chem. Inf. Comput. Sci.* **31**, 326–333.

Hall, S. R., Allen, F. H. and Brown, I. D. (1991). *Acta Crystallogr.* A**47**, 655–685. Reprints are available from the International Union of Crystallography, 5 Abbey Square, Chester CH1 2HU, England.

Spek, A. L. (2003). *J. Appl. Crystallogr.* **36**, 7–13.

Westrip, S. P. (2009). In preparation.

In 2006 the IUCr published *Volume G* of *International Tables for Crystallography* (S.R. Hall and B. McMahon (eds.); ISBN 1-4020-3138-6). This deals with the definition and exchange of crystallographic data by means of the CIF format.

Crystallographic databases

21

Jacqueline Cole

21.1 What is a database?

A database is a collection of related data along with tools for amending, updating and adding records and selectively extracting information. Crystallographic databases generally contain basic crystallographic data (unit cell dimensions, space group, atomic co-ordinates and perhaps atomic displacement parameters) and may also carry derived information on connectivity or atom and bond properties. Bibliographic information such as author names, the journal and year of publication will be stored. A compound's formula and systematic name, absolute configuration, polymorphic form and pharmaceutical or biological activity may be indicated where applicable. Experimental details such as the temperature and radiation used in the experiment may be available. Entries may carry flags indicating the level of precision for each structure, the presence of disorder, and there may even be comments about problems or unresolved queries regarding the structure. The exact contents depend on the database.

21.2 What types of search are possible?

Depending on the database, it may be possible to carry out searches based on a structure fragment, compound name, compound formula, compound properties, experimental conditions, space group, unit cell dimensions or bibliographic criteria – or some combination of these. For molecular compounds the ability to sketch or define a structure fragment whose occurrence within the database can then be probed is a powerful and intuitive tool for chemists. Whereas details of the internal structure of a database are not generally of interest, a good knowledge of the search facilities available is essential in order to best exploit the stored information.

21.3 What information can you get out?

- bibliographic data,
- space group and cell dimensions,
- atomic co-ordinates,
- atomic displacement parameters (maybe),
- molecular geometry parameters,
- intermolecular geometry parameters,
- analyses of the above, etc.

21.4 What can you use databases for?

- finding out what has been done before – surveying the field,
- determining if specific compounds have been reported,
- checking if a unit cell is known – diagnostic for the *phase*,
- obtaining parameters to assist structure solution or refinement (e.g. geometrical restraints),
- validation and comparison of your structure against published ones,
- deriving typical bonds lengths or other parameters,
- as a source of parameters for calculations or simulations,
- as a research tool for structure correlation, identifying trends or relationships, data mining,
- etc.

21.5 What are the limitations?

You need to be aware that there can be a considerable delay between the appearance of a structure in the literature and its inclusion in a database, although the availability of data in standard electronic format should reduce this delay. Such delays may result from a number of factors; perhaps the required data have not been (automatically) sent to the database, or database updates may not be distributed frequently. Structures that have been determined but neither published nor deposited will obviously not be included, but structures that form part of conference proceedings, including poster presentations, may be represented only by very basic data. For these reasons you should also check non-crystallographic databases such as *Chemical Abstracts*, which are more current (but may contain little or no crystallographic data).

21.6 Short descriptions of crystallographic databases

The Cambridge Structural Database (CSD) is the comprehensive collection of small-molecule organic and organometallic crystal structures. It does not contain structures of inorganic compounds like NaCl, PtS or

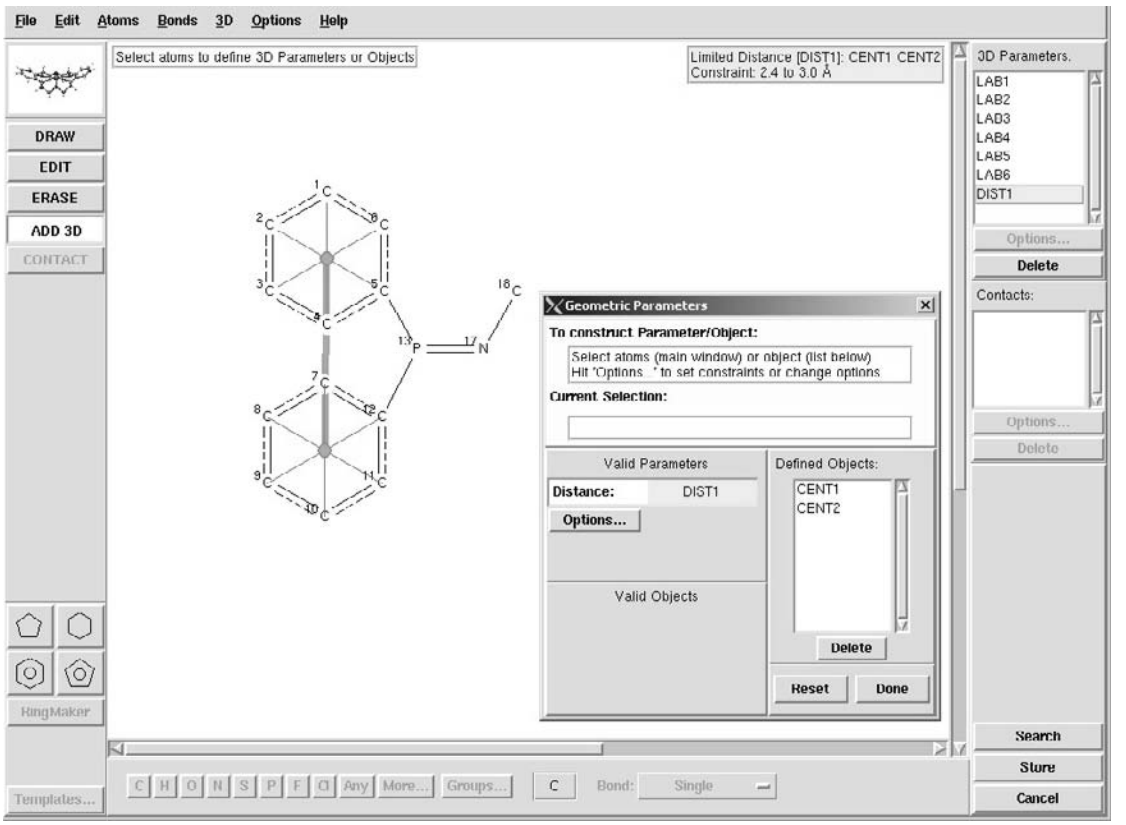

Fig. 21.1 ConQuest (CSD)

$CuSO_4 \cdot 5H_2O$; metals or their alloys; or macromolecular structures such as proteins or nucleic acids. The ConQuest (and earlier Quest) software has been developed for the search, retrieval, display and analysis of CSD information and its particular strength is the ability to search for structures on the basis of a chemical diagram, although text-based searches are also possible (Fig. 21.1). At the beginning of 2009 the CSD contained crystal structure data for over 460 000 organic and organometallic compounds. The CSD is updated through a full release every year, with approximately quarterly interim updates via the internet for registered users. There are a number of related programs such as Vista (graphical display of results, statistical analysis), Isostar (CSD-derived library of non-bonded contacts), Mogul (library of molecular geometries) and Mercury (advanced graphical visualization of structures). See *http://www.ccdc.cam.ac.uk* for further details.

The Inorganic Crystal Structure Database (ICSD) provides fast retrieval of structural and bibliographic information, allows logical manipulation of retrieved material and display of results, and is complementary to the CSD (Fig. 21.2). By late 2008, the ICSD contained over 108 000 entries. It is searchable by using either a command-line or

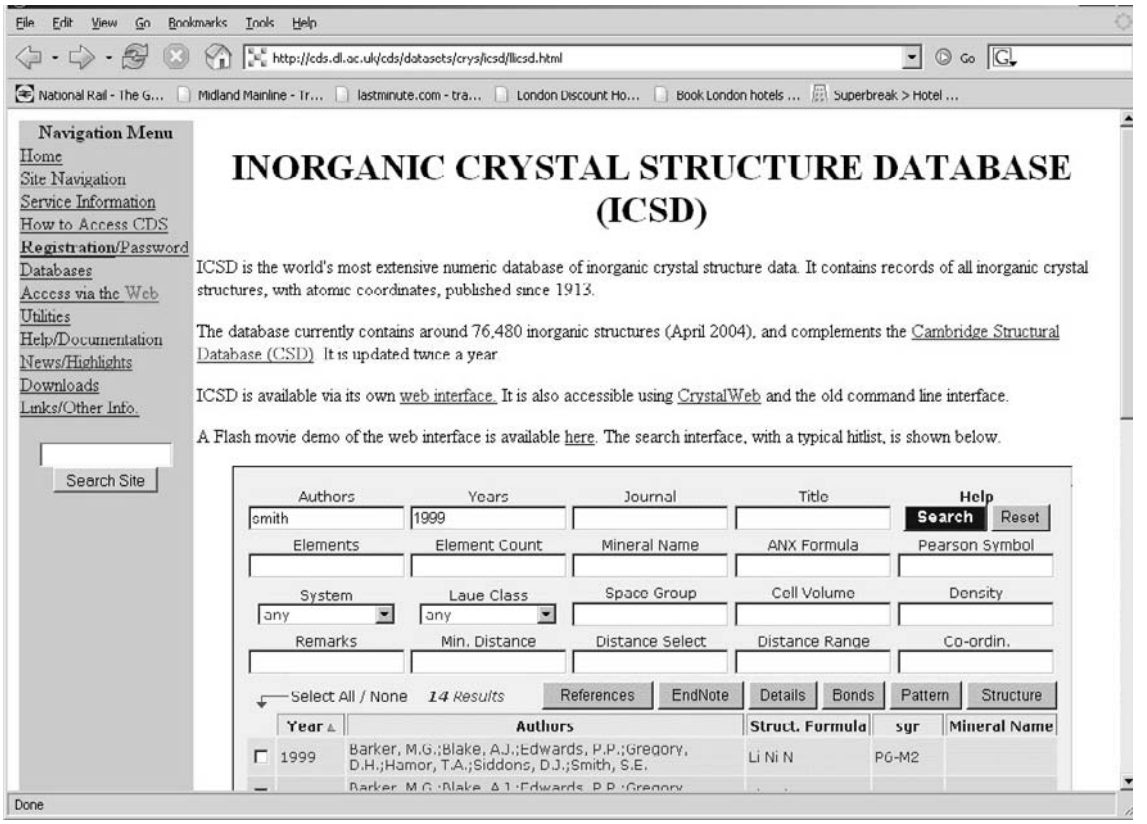

Fig. 21.2 ICSD

a web interface and contains two types of data: (1) bibliographic information about each entry, giving authors, journal reference, compound name, formula, mineral name (if any), etc.; (2) numeric information from the crystal structure analysis (if it is available), giving cell parameters, space group, atomic co-ordinates and displacement parameters. Because of the nature of the structures, connectivity searching is not appropriate.

See *http://cds.dl.ac.uk/cds/datasets/crys/icsd/llicsd.html* for further information.

The Metals Data File or CrystMet (MDF) provides fast retrieval of structural and bibliographic information for metals and alloys. For searching, the MDF uses a set of instructions similar to ICSD. It contains two types of data: (1) bibliographic information about each entry, giving authors, journal reference, compound name, formula, mineral name (if any) etc.; (2) numeric data from the crystal structure analysis (if it is available), giving cell parameters, space group, atomic co-ordinates and displacement parameters. The MDF currently contains around 100 000 entries for metals, alloys and intermetallics.

See *http://cds.dl.ac.uk/cds/datasets/crys/mdf/llmdf.html* for further information.

CDIF was an online retrieval package using the National Institute of Standards and Technology (NIST, Washington) Crystal Data Identification File. Entries in this file comprised unit cell data for some 237 000 organic, inorganic and metal crystal structures, some 72 000 of which did not appear in any other database. Each entry gave details of cell dimensions, crystal class, name and formula of the substance, and journal reference. CDIF has been superseded by the Daresbury CrystalWeb interface that allows searches of the CSD, the ICSD, CrystMet and CDIF on the basis of bibliographic, unit cell, reduced cell, formula, database code or combined queries.

See *http://cds.dl.ac.uk/cweb/* for information on CrystalWeb.

The Protein DataBank (PDB) contains bibliographic and co-ordinate details for proteins and other biological macromolecules. At the beginning of 2009, the PDB contained over 56 000 entries, of which most were derived from X-ray studies and others from NMR work. See *http://www.rcsb.org/pdb/* for further information. There is also a companion nucleic acid database.

With the exception of the PDB, these databases are available free of charge to UK academic researchers through the Chemical Database Service (CDS) at STFC Daresbury Laboratory. The CDS homepage is at *http://cds.dl.ac.uk/*. This Service has also provided access to a range of databases for organic chemistry, physical chemistry and spectroscopy but some of these services have been discontinued. Access to CSD, ICSD and DETHERM (a thermophysical properties database) is currently guaranteed until 2011. See *http://cds.dl.ac.uk* for up-to-date information.

This page intentionally left blank

X-ray and neutron sources

22

William Clegg

22.1 Introduction

The main topic of this book is the analysis of crystal structures using diffraction of X-rays by single crystals. Most such experiments are carried out in local research laboratories, either in Universities or in industry, and make use of commercial X-ray diffractometers that are equipped with 'X-ray tubes' of various designs. These involve the generation of X-rays by directing fast-moving beams of electrons at metal targets, and typically consume electrical power in the range from tens of watts to tens of kilowatts.

Much higher X-ray intensities are available from large-scale national and international storage-ring facilities (more commonly, if strictly incorrectly, known as synchrotron facilities), and there are ways other than the enhanced intensity in which the properties of these X-rays differ from those from laboratory X-ray tubes.

Furthermore, diffraction from crystals can occur with fast-moving beams of subatomic particles, particularly neutrons and electrons, which have wave properties and interact with the investigated crystalline material on quite different physical bases from X-rays, giving diffraction patterns with different information content.

In this chapter we consider the conventional and synchrotron sources of X-rays and their different properties and uses, then we discuss the application of neutron diffraction. Electron diffraction by solids, because it involves a much stronger interaction with the sample, is normally confined to thin specimens and surfaces, and it finds wide application in electron microscopy. It, and the use of electrons for diffraction by gas samples, lie outside the scope of this text, and will not be considered.

22.2 Laboratory X-ray sources

Most laboratory X-ray diffractometers, whether fitted with serial detectors or area detectors, operate with a conventional sealed X-ray tube, the

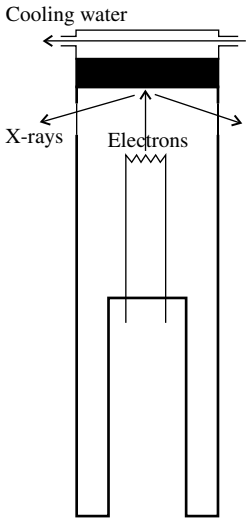

Fig. 22.1 Schematic diagram of a sealed X-ray tube.

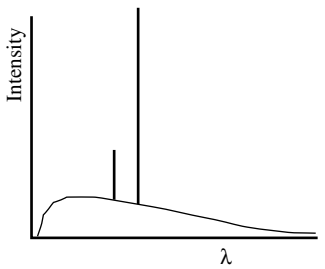

Fig. 22.2 The spectrum of X-rays generated by a sealed tube.

basic design of which has not changed for a long time, though ceramic insulating materials are increasingly being used instead of glass. The principle of operation of an X-ray tube is simple (Fig. 22.1). Electrons are generated in a vacuum by passing an electric current through a wire filament and are accelerated to a high velocity by an electric potential of tens of thousands of volts across a space of a few millimetres. The filament is held at a large negative potential and the electrons are attracted to an earthed and water-cooled metal block, where they are brought to an abrupt halt. Most of the kinetic energy of the electrons is converted to heat and carried away in the cooling water, but a small proportion generates X-rays by interaction with the atoms in the metal target. Some of the interactions produce a broad range of wavelengths of X-rays, with a minimum wavelength (maximum photon energy) set by the kinetic energy of the electrons. For our purposes, however, the most important process is the ionization of an electron from a core orbital, followed by relaxation of an electron from a higher orbital to fill the vacancy. This electron transition leads to loss of excess energy by radiation, and the emitted radiation, with a definite wavelength, is in the X-ray region of the spectrum. Several different transitions are possible, so a number of intense sharp maxima (in wavelength terms) are superimposed on the broad output of the overall spectrum of radiation produced (Fig. 22.2).

Since we use monochromatic X-rays for most purposes, one particular intense line of the output spectrum is selected and the rest discarded. The usual way of achieving this is to use diffraction itself: the X-rays emerging from a thin beryllium window in the X-ray tube are passed through a single crystal of a strongly diffracting material set at an appropriate angle. The (002) reflection of graphite is very widely used, with a 2θ angle of just over 12° for Mo-$K\alpha$ radiation ($\lambda = 0.71073$ Å, the most intense line from a target consisting of molybdenum metal) and about 26.5° for Cu-$K\alpha$ radiation ($\lambda = 1.54184$ Å, from a copper target). All other wavelengths pass undeflected through the monochromator crystal, leaving a single wavelength for the diffraction experiment.

Various developments of the basic X-ray tube produce higher intensities. The main limitation is the amount of heat produced, which can damage or even melt the target if it is excessive. One way to reduce the heat loading, and hence allow larger electron beam currents and more intense X-rays, is to keep the target moving in its own plane by rotating it, so that the target spot is constantly replaced. Rotating-anode sources require continuous evacuation because of the moving parts, and their use involves much more maintenance as well as higher energy consumption than sealed tubes. The increase in intensity can be up to about a factor of ten.

Another approach is to collect and concentrate more of the X-rays generated instead of just the narrow beam taken from a standard tube. Recent technological advances have produced extremely well polished mirrors giving glancing-angle total reflection of X-rays, and devices consisting of variable-thickness layers of materials with different crystal

lattice spacings to give a focusing effect through diffraction (also referred to, not strictly correctly, as mirrors). X-rays can also be concentrated and focused through glass capillaries. Each of these devices can give a significant increase in intensity from a suitable X-ray tube (whether sealed or rotating anode). Some of them can be combined with X-ray tubes in which the electron beam is magnetically focused to give a very small target spot, reducing heat loading, and these are known as micro-focus tubes. They typically operate with power consumption of tens of watts, compared with 1–3 kW for conventional sealed tubes and 5–30 kW for rotating-anode sources. Overall, the developments in X-ray generation and focusing have led to increases of 1–2 orders of magnitude for laboratory X-ray sources.

22.3 Synchrotron X-ray sources

When moving charged particles are deflected by a magnetic field, they emit electromagnetic radiation and hence lose energy. The radiation wavelength depends on the particles (charge, mass and velocity) and on the magnetic field strength. This effect was found to occur in synchrotrons, particle accelerators with a closed path (pseudo-circular, actually polygonal resulting from an array of magnets), and is an undesirable feature in the orginal primary purpose of such devices. However, the radiation has special properties and can be exploited for diffraction, spectroscopy and other uses. The first such experiments were carried out around 1970 on the NINA accelerator at Daresbury, UK, and gave rise to the term 'first-generation' synchrotron radiation source, referring to parasitic use of a synchrotron that was designed for other purposes.

Such a radiation source is far from ideal, being erratic and unstable through rapid acceleration, deceleration and deliberate collisions of the particles; a storage ring, with a stable circulating particle beam, is much better suited as a reliable source of electromagnetic radiation. Once the usefulness of synchrotron radiation (SR) had been established, storage rings were designed and built, dedicated to the production of SR, with the aim of stability in terms of intensity, position and direction of the radiated beams. These are called second-generation SR sources, and initially the SR was generated exclusively by the bending magnets that keep the particles in their circulating motion. The energy of the particles is maintained by the inclusion of microwave cavities at one or more positions in the ring, compensating for the energy loss associated with SR emission. The first second-generation SR source was the UK Synchrotron Radiation Source (SRS), built at Daresbury to replace NINA, and operational from 1980 to 2008.

Even greater intensity (and some other useful properties) can be achieved by putting more complex arrays of magnets in the straight sections between bending magnets. These 'insertion devices' include wigglers and undulators, which induce a series of sideways oscillations in the particle beam path; each wiggle generates SR and the individual

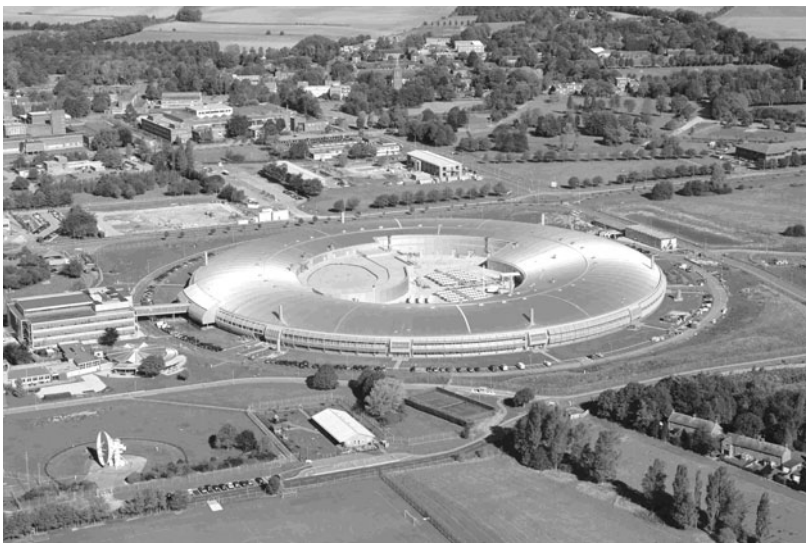

Fig. 22.3 Diamond Light Source. Copyright Diamond Light Source, reproduced with permission.

contributions combine in different ways depending on the precise arrangements of the magnets. Some insertion devices were added to second-generation sources such as SRS, but they provide the main SR output of third-generation sources, the bending magnets of which can also be used, of course. Most SR sources now operational are of this third generation, including Diamond (Fig. 22.3), the UK replacement for SRS, many other national facilities, and international sources such as the European Synchrotron Radiation Source (ESRF) in Grenoble, France. The fourth generation of SR sources, currently under development, is based on the free-electron laser.

The precise properties of SR depend on a combination of factors, including

(a) the energy of the stored particle beam (several GeV, with essentially the speed of light, resulting in relativistic behaviour);
(b) the size of the storage ring, the number of bending magnets, and details of other magnetic components for controlling and focusing the particle beam;
(c) the types and specifications of insertion devices;
(d) the structure of the particle beam, which usually consists of discrete bunches rather than a continuous stream, giving rise to a rapid pulse behaviour of the SR output;
(e) the way in which beam-current loss (inevitable through collisions, imperfect vacuum and other effects) is dealt with, in various 'top-up' and refill operations;
(f) optical components for conditioning the SR, including monochromators and mirrors for wavelength selection, harmonic rejection and focusing.

SR is produced tangentially every time the particle beam changes direction in bending magnets or insertion devices (Fig. 22.4). As a result of relativity, it is strongly concentrated in a single forward direction, giving a very highly collimated beam of radiation. It is almost completely polarized in the plane of the storage ring, has a very high intensity compared with conventional X-ray sources, and covers a continuous wide spectrum from infrared to hard X-rays (undulators give a jagged stepped X-ray spectrum), with a maximum photon energy (minimum wavelength) dictated by the operating conditions. For the purposes of X-ray crystallography, we can think of a synchrotron storage ring in simple terms as a large device that exploits relativity to convert microwave energy into X-rays by a massive doppler shift. Any wavelength can be selected from the broad spectrum by a monochromator, or the continuous 'white' X-ray spectrum can be used for the Laue diffraction technique, which is not discussed in this book.

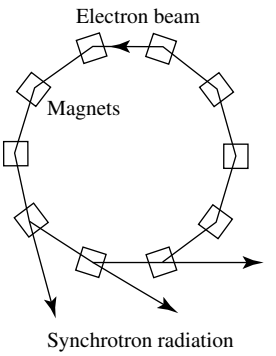

Fig. 22.4 The principle of operation of a synchrotron storage ring.

The very high intensity, several orders of magnitude greater than from conventional sources, is the most obvious and desirable feature of SR X-rays. It allows diffraction patterns to be measured quickly, even from tiny crystals (down to micrometre dimensions, depending on the chemical composition and crystal quality of the sample), or from other samples giving relatively weak diffraction as a result of structural faults such as disorder. Obviously this is useful when larger single crystals can not be obtained, and individual powder grains can be treated as single crystals, though the requirements of crystal mounting and diffractometer mechanical precision are demanding; it is also an advantage for chemically unstable and sensitive materials, and makes it possible (in combination with the pulsed nature of SR and the use of lasers) to investigate short-lived excited states.

The advantages of the high intensity of SR are further enhanced by the high degree of collimation, which makes individual reflections from single-crystal samples stand out more clearly from the background because of their sharper profiles; these are dictated largely by the sample quality rather than a non-parallel incident X-ray beam. This can also help in the spatial resolution of reflections from a sample with a large unit cell, or if a short wavelength is selected. A short wavelength gives access to higher-resolution data for charge-density studies, can reduce some systematic errors such as absorption and extinction, and can allow more of the diffraction pattern to be measured from a sample in a diamond anvil high-pressure cell or other special environment. Conversely, a longer wavelength spreads out a dense diffraction pattern for a large structure. A particular wavelength might also be chosen to minimize or to maximize special effects such as anomalous scattering. Bent monochromators and mirrors (giving total external reflection of X-rays at a glancing angle) can be used to focus and concentrate the available X-rays to match the sample size, so that the high flux is more effectively used as high brilliance (flux in a given cross-sectional area or solid angle).

The pulsed nature of SR is exploited in special time-resolved studies, but is not relevant to most crystallographic users. The polarization

properties mean that diffractometers have to be operated 'on their side', with diffraction measured in a vertical rather than a horizontal plane, making synchrotron installations look rather strange compared with standard laboratory setups.

SR sources are large national and international facilities providing equipment and support for a wide range of scattering, spectroscopy, imaging and other applications. Modes of access vary, but usually include some form of peer-reviewed application process on a regular basis (often twice per year), leading to use that is 'free at the point of access' to successful academic research groups, and charged for commercial users. There may be service modes of operation, or users may have to carry out their own experiments after appropriate training for safety and other aspects.

Structure determination with SR single-crystal diffraction facilities has been particularly important in certain research areas where small crystals and other weakly scattering samples frequently occur. These include microporous materials, often synthesized solvothermally; polymeric co-ordination networks; other supramolecular assemblies with weak intermolecular interactions; pharmaceuticals; pigments; low-yield products of reactions; and structures with several molecules in the asymmetric unit ($Z' > 1$).

A particular problem frequently encountered is of crystals that grow to a reasonable size in one or two dimensions, but form only very thin needles or plates with a total volume, and hence scattering power, below acceptable levels for laboratory study. In addition, there are applications where it is an advantage to select as small a crystal as possible to avoid other problems (e.g. in high-pressure studies, or to reduce absorption and extinction effects). The use of synchrotron radiation opens up the possibility of determining a complete structure from a single powder grain and thus investigating the homogeneity of a microcrystalline sample.

Some materials form only very small crystals because of poor crystallinity, but even large crystals may be of inferior quality, with a large mosaic spread, and so give broad and weak reflections. Synchrotron radiation can give adequate diffracted intensities, and the low intrinsic beam divergence also minimizes the breadth of observed reflections. Weak diffraction may be caused particularly by various types of disorder in the structure, and cooling of the sample is also important. A somewhat related topic is the study of substructure/superstructure relationships. Resolution of such structures depends critically on the measurement of very weak reflections that alone distinguish different possible space groups.

For unstable species and time-resolved studies, very high intensity means that data can be collected at maximum speed while still achieving an acceptable precision of measurement. The combination of synchrotron radiation and high-speed area detectors provides a means of doing this type of experiment. Rapid data collection is essential for unstable samples, but can also be very useful in collecting multiple data

sets for a sample under different conditions of temperature or pressure in order to investigate the effects of varying these conditions. It may be possible to follow solid-state reactions, where the reactant and product have related structures and crystal integrity is maintained in the reaction; these may include phase transitions, polymerization, and reactions related to catalysis.

Although SR facilities are expensive to build and operate, their use in structure determination can be very cost effective, with rapid throughput of samples, data and results. Typical use of station 9.8 at Daresbury SRS (finally closed in August 2008 after about 12 years of operation) by the UK National Crystallography Service has given around 12–15 full data sets in each 24-hour period, investigating samples that had been previously screened and found to be beyond the capabilities of even the most powerful conventional laboratory sources, and results have been published in leading international journals. Even higher productivity is expected at Diamond beamline I19.

For a historical survey of SR work, see Helliwell (1998). For a more extensive account of SR in crystal structure determination, see Clegg (2000), and for information on the use of SR in the UK National Crystallography Service, see http://www.ncl.ac.uk/xraycry.

22.4 Neutron sources

X-rays are used for crystal-structure determination because they have a wavelength comparable to the size of molecules and their separation in solids, so they give measurable diffraction effects from crystals. By definition, they are the only region of the electromagnetic spectrum with an appropriate wavelength. However, a beam of neutrons can have a similar associated wavelength, related to its velocity v and momentum mv (where m is the neutron mass) by $\lambda = h/mv$. Such neutrons may be generated by nuclear reactors and by spallation sources, which are described later. Such large-scale facilities are, of course, an expensive way to produce neutron radiation, so it is worthwhile only if there are clear advantages over X-rays. In the case of scattering and diffraction this is true in certain cases, and the two techniques are complementary.

X-rays are scattered by the electron density of atoms, so the scattering is proportional to atomic number. This means that 'heavy atoms' (those with many electrons) dominate X-ray diffraction by crystals, and lighter atoms are relatively difficult to see and imprecisely located. It also means that neighbouring elements in the periodic table give almost identical X-ray scattering and can not easily be distinguished on this basis alone.

Neutrons, by contrast, are scattered by atomic nuclei. There is no simple dependence on atomic number, and the variation of neutron scattering across the whole periodic table is much smaller than that of X-ray scattering. Neutron scattering by neighbouring elements can be very different; the variation from element to element is quite erratic, and

Table 22.1. Selected X-ray and neutron scattering factors (electrons and fm, respectively)

Element	X-ray	Neutron
H	1	−3.74
D	1	6.67
O	8	5.81
V	23	−0.38
Fe	26	9.45
Co	27	2.78
Ba	56	5.28
U	92	8.42

different isotopes of a given element usually have quite different neutron scattering powers, while they are completely indistinguishable to X-rays. These differences are illustrated by some examples in Table 22.1. Note that some nuclei have a negative neutron scattering factor (usually expressed as a scattering length with units of fm); they scatter exactly out of phase with other nuclei. In general, neutron scattering is much weaker than X-ray diffraction (the two sets of values in Table 22.1 are not on the same scale). The adjacent elements Co and Fe have very different neutron scattering factors, while their X-ray scattering factors differ by only a few per cent. Deuterium scatters neutrons almost as strongly as does uranium, but is essentially invisible to X-rays when both elements are in the same material, and it is dramatically different from its lighter isotope H for neutron diffraction.

These features of neutron scattering by nuclei lead to a number of practical advantages over X-ray diffraction in certain types of studies.

(a) It is often easier to locate light atoms precisely in the presence of heavier ones. For example, the exact positions of oxide anions in complex metal-oxide structures can be very important in understanding properties such as superconductivity and unusual magnetism. If heavy metals are present, this is a serious challenge for X-ray diffraction, especially if the oxide positions display any disorder. Oxygen has a relatively large neutron scattering length; it is very similar to that of barium (Table 22.1) – in fact a little higher – but with X-rays Ba scatters seven times as strongly as O.

(b) The most extreme case of this is the location of H atoms, for which X-ray diffraction is not the ideal technique in view of the low electron density of H. Neutron diffraction is very much more effective here (even more so if D replaces H), in cases where it is important to find H atoms reliably, such as in metal-hydride complexes, agostic interactions, and unusual hydrogen-bonding patterns. The problem for X-ray diffraction is made worse by the fact that the electron density of the H atom is involved in bonding; it is not centred on the nucleus, but is distorted towards the adjacent atom, leading to a systematic apparent shortening of X–H bonds in X-ray diffraction studies. Neutron diffraction is not affected by the bonding or by other valence-electron density features such as lone pairs, and it determines accurate nuclear positions and hence internuclear distances.

(c) In some cases the ability of neutrons to distinguish clearly between atoms of neighbouring elements in the periodic table is important for a reliable structure determination, such as in mixed-metal complexes or metal alloys.

(d) Isotopes of the same element appear quite different in neutron diffraction, in most cases, whereas they are completely identical in X-ray diffraction. This may be useful, for example, in establishing the positions of isotopically labelled atoms in a product as part of an investigation of the reaction mechanism.

The weak interaction of neutrons with nuclei in a crystalline sample, compared with the rather stronger interaction of X-rays with electrons, means that larger crystals are usually required for neutron diffraction, though this limitation of the technique is mitigated to some extent with more intense modern neutron sources and more sensitive detectors. On the other hand, it means that neutrons are generally more penetrating than X-rays, giving lower absorption, allowing the study of materials in containers through which X-rays would not pass, and leading to little radiation damage (except in cases where neutrons react with some nuclei to generate new nuclei). Nuclei are also effectively point scatterers in contrast to the finite size of the electron distribution in an atom, so neutron scattering from a stationary atom does not fall off with increasing angle as does X-ray diffraction – the θ dependence is due only to atomic displacements, which are reduced at low temperature.

One other special property of neutrons is that they have an instrinsic magnetic moment, or spin. This can be exploited to investigate magnetic properties such as ferromagnetism, ferrimagnetism and antiferromagnetism, which involve regular arrangements of atomic magnetic moments (and these are due to unpaired electrons, so this is a neutron-electron interaction) in a solid material.

Two main types of neutron sources are used for crystallography. A nuclear reactor uses neutrons to maintain its activity, but more are produced by ^{235}U fission than are needed for the continued nuclear chain reaction, so the excess can be extracted in a continuous supply. The Institut Laue-Langevin (ILL) in Grenoble is an example, and serves as a European international facility, adjacent to ESRF.

A spallation source generates rapid pulses of neutrons (and other subatomic particles) by accelerating protons in a synchrotron and directing them at a target containing heavy-metal atoms such as tungsten. The wavelength of each neutron can be determined by measuring its 'time of flight' between the source and detector, as an alternative to selecting a monochromatic beam. An example of a spallation source is ISIS at the Rutherford Appleton Laboratory in Oxfordshire, UK, adjacent to Diamond.

For both types of neutron source, diffraction equipment is similar to that used with X-rays, but it tends to be larger and more heavily shielded for radiation. The greater penetrating power of neutrons means that samples can be held in larger and thicker containers, including closed low-temperature and high-pressure devices.

Finally, we note that combining X-ray and neutron diffraction for the same sample material can exploit the complementary advantages of the two techniques, for example in obtaining reliable structural information when a wide range of elements is present, simultaneously investigating geometrical and magnetic structural features, or decoupling valence and atomic displacement effects in accurate high-resolution charge-density studies of bonding.

For more detailed accounts of neutron diffraction, see Wilson (2000); Piccoli *et al*. (2007).

References

Clegg, W. (2000). *J. Chem. Soc., Dalton Trans.* 3223–3232.
Helliwell, J. R. (1998). *Acta Crystallogr.* A**54**, 738–749.
Piccoli, P. M., Koetzle, T. F. and Schultz, A. J. (2007). *Comments Inorg. Chem.* **28**, 3–38.
Wilson, C. C. (2000). *Single crystal neutron diffraction from molecular materials*, World Scientific: Singapore.

Appendix A: Useful mathematics and formulae

A

Peter Main

A.1 Introduction

To paraphrase Lord Kelvin, when you cannot express your observations in numbers, your knowledge is of a meagre and unsatisfactory kind. The use of scientific observation to add to our knowledge inevitably means we need to express both observations and deductions mathematically. The link between the two is mathematical also. We present here some mathematics and a few formulae that are important in X-ray crystallography.

A.2 Trigonometry

Trigonometry means 'measurement of triangles', but its use goes far beyond what its name suggests. Many properties of triangles can be summarized in terms of the ratios of the sides of the right-angled triangle in Fig. A.1, giving:

$$\cos\theta = a/c \quad \sin\theta = b/c \quad \tan\theta = b/a$$
$$\text{so that } \tan\theta = \sin\theta/\cos\theta.$$

The symmetry of the sine and cosine functions shows that $\cos(-\theta) = \cos(\theta)$ and $\sin(-\theta) = -\sin(\theta)$.

Another relationship among these functions is obtained from Pythagoras' theorem:

$$a^2 + b^2 = c^2$$
$$\text{giving } \cos^2\theta + \sin^2\theta = 1.$$

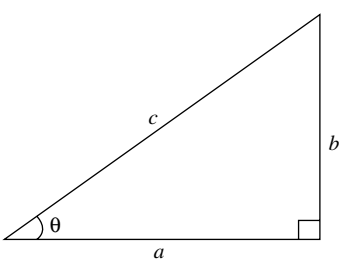

Fig. A.1 A right-angled triangle for defining trigonometric ratios.

Also useful in crystallography are the multiple angle formulae, which are given without derivation as:

$$\cos(\theta + \phi) = \cos\theta\cos\phi - \sin\theta\sin\phi$$
$$\text{and } \sin(\theta + \phi) = \sin\theta\cos\phi + \cos\theta\sin\phi.$$

These come into their own in the manipulation of the electron-density equation for numerical calculation. For example, by putting $\theta = 2\pi(hx + ky)$ and $\phi = 2\pi lz$ in the above expressions, $\cos 2\pi(hx + ky + lz)$ can be changed into:

$$\cos 2\pi(hx + ky + lz) = \cos 2\pi(hx + ky)\cos 2\pi lz - \sin 2\pi(hx + ky)\sin 2\pi lz.$$

A similar operation gives

$$\cos 2\pi(hx + ky) = \cos(2\pi hx)\cos(2\pi ky) - \sin(2\pi hx)\sin(2\pi ky)$$
$$\sin 2\pi(hx + ky) = \sin(2\pi hx)\cos(2\pi ky) + \cos(2\pi hx)\sin(2\pi ky),$$

so that

$$\begin{aligned}\cos 2\pi(hx + ky + lz) = {} & \cos(2\pi hx)\cos(2\pi ky)\cos(2\pi lz) \\ & - \sin(2\pi hx)\sin(2\pi ky)\cos(2\pi lz) \\ & - \sin(2\pi hx)\cos(2\pi ky)\sin(2\pi lz) \\ & - \cos(2\pi hx)\sin(2\pi ky)\sin(2\pi lz).\end{aligned}$$

It looks as if we have made things far more complicated by doing this. However, these expressions usually simplify enormously in different ways according to space group symmetry and are useful in the Beevers–Lipson factorization of the electron-density equation, which is how many computer programs handle Fourier transform summations.

A.3 Complex numbers

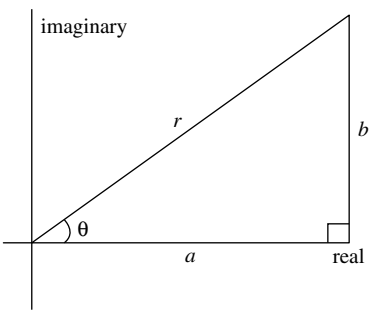

Fig. A.2 The complex number $a+ib$ plotted on an Argand diagram.

Much of the mathematics dealing with structure factors and discrete Fourier transforms makes use of complex numbers. It is a pity these numbers have the name they do, because it has the connotation of being complicated. Complex numbers are simply numbers with two components instead of the usual one. The components are called the real and imaginary parts of the number and can be plotted on a two-dimensional diagram, called an Argand diagram, as shown in Fig. A.2. The number plotted has real and imaginary parts of a and b, respectively, and can be written algebraically as $a + ib$ where $i^2 = -1$. You may regard the imaginary constant i as a mathematical curiosity, but the important property of its square given in the previous sentence enables complex numbers to be multiplied and divided in a completely consistent way.

An equivalent way to represent a complex number is in polar form, i.e. in terms of r and θ in Fig. A.2. These are called the modulus and argument of the number respectively. A knowledge of trigonometry allows us to write

$$a + ib = r\cos\theta + i\,r\sin\theta = r(\cos\theta + i\sin\theta) = r\,\mathrm{e}^{i\theta}.$$

The last relationship used in this equation is

$$\cos\theta + i\sin\theta = \mathrm{e}^{i\theta},$$

which is one of the most amazing relationships in the whole of mathematics. Pythagoras' theorem tells us that $r^2 = a^2 + b^2$ and we also have $\tan\theta = b/a$.

Some properties of complex numbers are important for the manipulation of structure factors. A simple operation is to take the complex conjugate, which means changing the sign of the imaginary part. Thus, the complex conjugate of the complex number $a+ib$ is written as $(a+ib)^*$ and it is equal to $a - ib$. You should be able to confirm that multiplying a complex number by its complex conjugate gives a real number that is the square of the modulus:

$$\begin{aligned}(a + i\,b)(a + i\,b)^* &= (a + i\,b)(a - i\,b)\\ &= a^2 - i\,a\,b + i\,a\,b - i^2b^2 = a^2 + b^2 = r^2.\end{aligned}$$

A.4 Waves and structure factors

X-rays are waves and we must be able to deal with them mathematically. The obvious wavy functions are sines and cosines, so these are used in the mathematical description of waves. It is an enormous convenience to combine both sines and cosines into the single term $\exp(i\theta)$ as seen in the last equation but one above. This is the main reason why you find complex exponentials in the structure factor and electron-density equations ((1.1) and (1.2), respectively, in Chapter 1).

Similarly, the structure factors $F(hkl)$ are the mathematical representation of diffracted waves. When they are combined to form an image of the electron density (which represents adding waves together), their relative phases are important. The mathematical construction in Fig. A.2 allows both the amplitude of the wave, $|F(hkl)|$, and its relative phase, $\phi(hkl)$, to be represented by the modulus and argument of a single complex number. This leads us to write a structure factor in various ways such as:

$$\begin{aligned}F(\mathbf{h}) = A(\mathbf{h}) + i\,B(\mathbf{h}) &= |F(\mathbf{h})|\cos(\phi(\mathbf{h})) + i|F(\mathbf{h})|\sin(\phi(\mathbf{h}))\\ &= |F(\mathbf{h})|\exp(i\phi(\mathbf{h})),\end{aligned}$$

where the diffraction indices (*hkl*) are represented by the components of the vector **h**.

The structure-factor equation, (1.1) in Chapter 1, shows that $F(\mathbf{h}) = F^*(\overline{\mathbf{h}})$, i.e. structure factors that are Friedel opposites are complex conjugates of each other. This leads immediately to the relationship $F(\mathbf{h}) \times F(\overline{\mathbf{h}}) = |F(\mathbf{h})|^2$. In addition, we find that the product of any two structure factors can be written as:

$$F(\mathbf{h}) \times F(\mathbf{k}) = |F(\mathbf{h})|\, e^{i\phi(\mathbf{h})} \times |F(\mathbf{k})|\, e^{i\phi(\mathbf{k})} = |F(\mathbf{h})F(\mathbf{k})|\, e^{i(\phi(\mathbf{h})+\phi(\mathbf{k}))},$$

showing that the structure factor magnitudes multiply and the phases add. This is of importance when applying direct methods of phase determination.

A.5 Vectors

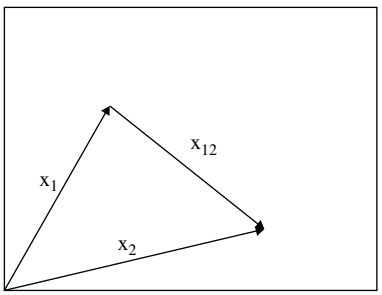

Fig. A.3 Addition of vectors: $x_1 + x_{12} = x_2$.

A vector is often described as a quantity that has magnitude and direction, as opposed to a scalar quantity that has only magnitude. This definition is sufficient for the present purpose and we shall see how useful the directional properties of vectors are. One of the consequences of this is that vectors can be added together as shown in Fig. A.3. The vectors $\mathbf{x}_1$ and $\mathbf{x}_{12}$ are added together to give the resultant $\mathbf{x}_2$. This is expressed algebraically as:

$$\mathbf{x}_1 + \mathbf{x}_{12} = \mathbf{x}_2.$$

Note that vectors are conventionally written in bold characters, as are matrices when we come to them. If the vectors $\mathbf{x}_1$ and $\mathbf{x}_2$ give the positions of two atoms in the unit cell, they are known as position vectors; $\mathbf{x}_{12}$ is known as a displacement vector, giving the displacement of atom 2 relative to atom 1. A rearrangement of the above equation expresses the displacement vector as $\mathbf{x}_{12} = \mathbf{x}_2 - \mathbf{x}_1$ and these displacement vectors arise in the description of the Patterson function (see Chapter 9).

In the unit cell, the position vector **x** has components (x, y, z) such that

$$\mathbf{x} = \mathbf{a}x + \mathbf{b}y + \mathbf{c}z,$$

where **a**, **b** and **c** are the lattice translation vectors (the edges of the unit cell) and x, y and z are the fractional co-ordinates of the point. The vector displacement of atom 2 from atom 1 can therefore be written as

$$\begin{aligned}\mathbf{x}_{12} = \mathbf{x}_2 - \mathbf{x}_1 &= (\mathbf{a}x_2 + \mathbf{b}y_2 + \mathbf{c}z_2) - (\mathbf{a}x_1 + \mathbf{b}y_1 + \mathbf{c}z_1) \\ &= \mathbf{a}(x_2 - x_1) + \mathbf{b}(y_2 - y_1) + \mathbf{c}(z_2 - z_1).\end{aligned}$$

Similarly, the position of a point in reciprocal space is given by the vector **h**, which has components (*h*,*k*,*l*) such that:

$$\mathbf{h} = \mathbf{a}^*h + \mathbf{b}^*k + \mathbf{c}^*l,$$

where **a*****, **b*** and **c*** are the reciprocal lattice translation vectors (the edges of the reciprocal unit cell) and h, k and l are usually integers giving the diffraction indices of the structure factor $F(\mathbf{h})$ at that point in the reciprocal lattice.

The scalar (dot) product of the two vectors **x** and **h** is:

$$\mathbf{h}.\mathbf{x} = hx + ky + lz,$$

which is an expression to be found in both the structure factor and electron-density equations. The vector (cross) product is used in the relationships between the direct and reciprocal lattices:

$$\mathbf{a}^* = \frac{\mathbf{b} \times \mathbf{c}}{V} \quad \mathbf{b}^* = \frac{\mathbf{c} \times \mathbf{a}}{V} \quad \mathbf{c}^* = \frac{\mathbf{a} \times \mathbf{b}}{V} \quad V = \mathbf{a}.\mathbf{b} \times \mathbf{c},$$

where V is the volume of the unit cell. It should be remembered that

$$\mathbf{a} \times \mathbf{b} = ab \sin \gamma \mathbf{n},$$

where γ is the angle between the vectors and **n** is a unit vector perpendicular to both **a** and **b**, such that **a**, **b** and **n** are a right-handed set. It should be clear from these relationships that **a*** is perpendicular to the **bc**-plane; similarly, **b*** and **c*** are perpendicular to the **ac**- and **ab**-planes, respectively. If you need convincing that vectors are the most convenient way of expressing these relationships, here is the volume of the unit cell without using vectors:

$$V = abc\sqrt{1 - \cos^2 \alpha - \cos^2 \beta - \cos^2 \gamma + 2 \cos \alpha \cos \beta \cos \gamma}.$$

The angles of the reciprocal lattice can be obtained from the relationships above but, to save you the trouble, they are:

$$\cos \alpha^* = \frac{\cos \beta \cos \gamma - \cos \alpha}{\sin \beta \sin \gamma},$$

with corresponding expressions for $\cos \beta^*$ and $\cos \gamma^*$ obtained by cyclic permutation of α, β, and γ.

The calculation of a Bragg angle is commonly required, for example to calculate structure factors or the setting angles on a diffractometer. In the triclinic system, the formula is:

$$\frac{4 \sin^2 \theta}{\lambda^2} = h^2 a^{*2} + k^2 b^{*2} + l^2 c^{*2} + 2hka^* b^* \cos \gamma^* + 2klb^* c^* \cos \alpha^* + 2lhc^* a^* \cos \beta^*,$$

and this simplifies enormously for other crystal systems.

A.6 Determinants

Determinants feature in inequality relationships among structure factors, are needed in matrix inversion, and form a useful diagnostic tool when your least-squares refinement runs into trouble. A determinant is a square array of numbers that has a single algebraic value. An order two determinant is written and evaluated as:

$$\begin{vmatrix} a & b \\ c & d \end{vmatrix} = ad - bc,$$

and an order three determinant is:

$$\begin{vmatrix} a & b & c \\ d & e & f \\ g & h & i \end{vmatrix} = aei + bfg + cdh - ceg - bdi - afh.$$

In general, a determinant can be expressed in terms of determinants of order one less than the original. For an order n determinant, this is expressed as

$$\Delta = \sum_{i=1}^{n} (-1)^{i+j} a_{ij} \Delta_{ij},$$

where a_{ij} is the ij element of Δ and Δ_{ij} is the determinant formed from Δ by missing out the ith row and the jth column. The summation can equally well be carried out over j instead of i and gives the same answer. However, this is useful only for determinants of small order. Evaluation of high-order determinants is best done using the process of Gauss elimination (a standard mathematical procedure not discussed here) to reduce the determinant to triangular form, then taking the product of the diagonal elements.

A.7 Matrices

Matrices are used for a number of tasks in X-ray crystallography. Typically, they represent symmetry operations, describe the orientation of a crystal on a diffractometer, and are heavily used in the least-squares refinement of crystal structures. A brief refresher course will therefore not be out of place. A matrix is a rectangular array of numbers or algebraic expressions and matrix algebra gives a very powerful way of manipulating them.

One of the operations often required is to transpose a matrix. This exchanges columns with rows so that, if **A** is the matrix

$$\begin{pmatrix} a & b \\ c & d \\ e & f \end{pmatrix},$$

its transpose, $\mathbf{A}^T$, is

$$\begin{pmatrix} a & c & e \\ b & d & f \end{pmatrix}.$$

If a square matrix is symmetric, it is equal to its own transpose.

Matrix multiplication is carried out by multiplying the elements in a row of the first matrix by the elements in a column of the second and adding the products. This forms the element in the product matrix on the same row and column as those used in its calculation:

$$\begin{pmatrix} a & b & c \\ d & e & f \end{pmatrix} \begin{pmatrix} u & x \\ v & y \\ w & z \end{pmatrix} = \begin{pmatrix} au + bv + cw & ax + by + cz \\ du + ev + fw & dx + ey + fz \end{pmatrix}$$

Multiplication can only be carried out if the number of columns in the first matrix is the same as the number of rows in the second. For example, you may wish to verify that

$$\begin{pmatrix} 2 & 3 \\ -1 & 4 \end{pmatrix} \begin{pmatrix} 3 & -2 & 1 \\ 4 & 5 & -3 \end{pmatrix} = \begin{pmatrix} 18 & 11 & -7 \\ 13 & 22 & -13 \end{pmatrix}$$

Multiplication of a matrix by its own transpose always produces a symmetric matrix.

A.8 Matrices in symmetry

Matrix multiplication is useful for representing symmetry operations. For example, the operation of the 2_1 axis relating (x, y, z) to $(\frac{1}{2}+x, \frac{1}{2}-y, -z)$ may be written as:

$$\begin{pmatrix} 1 & 0 & 0 \\ 0 & -1 & 0 \\ 0 & 0 & -1 \end{pmatrix} \begin{pmatrix} x \\ y \\ z \end{pmatrix} + \begin{pmatrix} \frac{1}{2} \\ \frac{1}{2} \\ 0 \end{pmatrix},$$

and this form of expression is used to represent symmetry operations in a computer.

It is sometimes useful to be able to deal with symmetry operations in reciprocal space also. The operation above can be written in terms of matrix algebra as

$$\mathbf{x}' = \mathbf{C}\mathbf{x} + \mathbf{d},$$

where $\mathbf{C}$ is the 3×3 matrix and $\mathbf{d}$ the translation vector. If a space group symmetry operation is carried out on the whole crystal, by definition

the X-rays see exactly the same structure. The structure-factor equation may then be written as

$$F(\mathbf{h}) = \sum_{j=1}^{N} f_j \exp(2\pi i \mathbf{h}.(\mathbf{C}\mathbf{x}_j + \mathbf{d}) = \sum_{j=1}^{N} f_j \exp(2\pi i \mathbf{h}^{\mathrm{T}}\mathbf{C}\mathbf{x}_j) \times \exp(2\pi i \mathbf{h}.\mathbf{d})$$
$$= F(\mathbf{h}^{\mathrm{T}}\mathbf{C}) \exp(2\pi i \mathbf{h}.\mathbf{d}).$$

That is, the two reflections $F(\mathbf{h})$ and $F(\mathbf{h}^T\mathbf{C})$ are symmetry related. Their magnitudes are the same and there is a phase difference between them of $2\pi\,\mathbf{h}.\mathbf{d}$.

This is easier to understand if we continue with the example above. The 2_1 axis is one of those that occur in the space group $P2_12_12_1$. The symmetry-related reflections that it produces are given by

$$\mathbf{h}^{\mathrm{T}}\mathbf{C} = \begin{pmatrix} h & k & l \end{pmatrix} \begin{pmatrix} 1 & 0 & 0 \\ 0 & -1 & 0 \\ 0 & 0 & -1 \end{pmatrix} = \begin{pmatrix} h & \bar{k} & \bar{l} \end{pmatrix}.$$

That is, $F(hkl)$ is related by symmetry to $F(h\bar{k}\bar{l})$. Their magnitudes must be the same and there is a phase shift between them of

$$2\pi\,\mathbf{h}.\mathbf{d} = 2\pi(h\ k\ l).(\tfrac{1}{2}\ \tfrac{1}{2}\ 0) = \pi(h+k).$$

Putting this all together gives the relationships $|F(hkl)| = |F(h\bar{k}\bar{l})|$ and $\phi(hkl) = \phi(h\bar{k}\bar{l}) + \pi(h+k)$. Thus, the phase is the same if $h+k$ is even, but shifted by π if $h+k$ is odd.

Even with anomalous scattering, these relationships are strictly true. It is only when structure factors are related by a complex conjugate that they are affected differently by anomalous scattering. For example, in $P2_12_12_1$, we have already seen that $|F(hkl)|$ and $|F(h\bar{k}\bar{l})|$ are always the same, but $|F(hkl)|$ and $|F(\bar{h}kl)|$ will be affected differently, as will $|F(hkl)|$ and $|F(\bar{h}\bar{k}\bar{l})|$.

A.9 Matrix inversion

The inverse of the square matrix $\mathbf{A}$ is the matrix $\mathbf{A}^{-1}$ that has the property that

$$\mathbf{A}\mathbf{A}^{-1} = \mathbf{A}^{-1}\mathbf{A} = \mathbf{I},$$

where $\mathbf{I}$ is the identity matrix (1s down the diagonal and 0s everywhere else).

Operations performed by multiplying by a matrix, $\mathbf{A}$, can be undone by multiplying by the inverse of the matrix, $\mathbf{A}^{-1}$. For an order 2 square

matrix, the recipe for inversion is:

$$\text{if } \mathbf{A} = \begin{pmatrix} a & b \\ c & d \end{pmatrix} \quad \text{then} \quad \mathbf{A}^{-1} = \frac{1}{\det(\mathbf{A})} \begin{pmatrix} d & -b \\ -c & a \end{pmatrix},$$

where $\det(\mathbf{A})$ is the determinant of the matrix $\mathbf{A}$.

Inversion of an order three matrix is achieved by the following recipe: if $\mathbf{A} = \begin{pmatrix} a_{11} & a_{12} & a_{13} \\ a_{21} & a_{22} & a_{23} \\ a_{31} & a_{32} & a_{33} \end{pmatrix}$, then form $\mathbf{C} = \begin{pmatrix} c_{11} & c_{12} & c_{13} \\ c_{21} & c_{22} & c_{23} \\ c_{31} & c_{32} & c_{33} \end{pmatrix}$, where c_{ij} is the determinant obtained from $\mathbf{A}$ by removing the ith row and jth column and multiplying by $(-1)^{i+j}$. We then have:

$$\mathbf{A}^{-1} = \frac{1}{\det(\mathbf{A})} \mathbf{C}^{\mathrm{T}}.$$

This recipe will work for any order of matrix, but it is extremely inefficient for orders higher than three. Larger matrices are best inverted using Gauss elimination, as mentioned earlier. It is a commonly believed fallacy that matrix inversion is necessary for solving systems of linear simultaneous equations. Since it is quicker to solve equations than to calculate an inverse matrix, the inverse should be calculated only if it is specifically required, for example, to estimate standard uncertainties of parameters determined by the equations.

A.10 Convolution

Convolution is an operation that affects the lives of all scientists. Since no measuring or recording instrument is perfect, it will affect the quantity that is detected before the recording takes place. For example, loudspeakers change the signal that is fed to them from an amplifier, thus altering (hopefully slightly) the sound that you hear. The mathematical description of this is called convolution. It also appears in the mathematics of crystallography, although many people function quite adequately as crystallographers without knowing much about it.

The simplest example of convolution is in the description of a crystal. The convolution of a lattice point with anything at all, e.g. a single unit cell, leaves that object unchanged. However, the convolution of two lattice points with a unit cell gives two unit cells, one at the position of each lattice point. A complete crystal, therefore, can be described as the convolution of a single unit cell with the whole crystal lattice. This would seem to be an unnecessary complication except for the intimate association of convolution with Fourier transforms.

The convolution theorem in mathematics states that: "the Fourier transform of a product of two functions is given by the convolution of their respective Fourier transforms." That is, if $c(x)$, $f(x)$ and $g(x)$ are Fourier transforms of $C(S)$, $F(S)$ and $G(S)$, respectively, the theorem may

be expressed mathematically as:

$$\text{if} \quad C(S) = F(S).G(S) \quad \text{then} \quad c(x) = f(x)^* g(x),$$

where * is the convolution operator.

This leads to the description of the X-ray diffraction pattern of a crystal as the product of the X-ray scattering from a single unit cell and the reciprocal lattice, seen in the following relationships:

unit cell	$*$	crystal lattice	=	crystal
⇳ F.T.		⇳ F.T.		⇳ F.T.
unit cell scattering pattern	$\times$	reciprocal lattice	=	X-ray diffraction pattern.

This allows us to deal with a single unit cell instead of the millions of cells that make up the complete crystal.

Appendix B: Questions and answers

B

Chapter 1

No exercises.

Chapter 2

1. You are provided in Fig. 2.3 and Fig. 2.4 with four two-dimensional repeating patterns (Traidcraft gift wrapping paper!). For each one, identify lattice points and outline a unit cell (possible shapes are oblique, rectangular, square, and hexagonal; a rectangular unit cell can be primitive or centred). Find the symmetry elements; for a 2D pattern the following are possible: 2-, 3-, 4- and 6-fold rotations, mirror lines, and glide lines (mirrors with a half-unit-cell translation component parallel to the reflection line); in 2D inversion symmetry is the same as a 2-fold rotation. Show what fraction of the unit cell is the asymmetric unit.

See the diagrams provided on the next page; note that a lot of 2D patterns such as wallpapers have higher metric symmetry than true symmetry, because a rectangular shape is convenient for printing, but the contents often have lower symmetry than this. Here are some useful notes for discussion.

In 1, there are normal reflections in one direction and glides in the other. There are also two-fold rotations. The unit cell is primitive rectangular (the conventional origin being chosen on a two-fold rotation point), and the asymmetric unit is one quarter of this.

In 2, all the individual rectangular blocks are identical; note here that the directions 'up' and 'down' are different, so this is a polar group; there are vertical mirrors (and glides), but no horizontal ones. The asymmetric unit is one quarter of the centred rectangular unit cell.

For 3, no reflection is possible, because the spiral shapes are chiral and are all of the same hand; all the small rectangular blocks are identical. Although a rectangular unit cell can be selected, it is centred and there is no good reason for this. The diamond shape is the most convenient unit cell, and this is also the asymmetric unit.

For 4, the basic repeat pattern is a pair of rounded triangles, but the mirror symmetry demands a rectangular cell, so this is centred; it is conventional to put the cell origin on one of the 2-fold axes (on an inversion centre in 3D); as well as mirrors there are also glide lines (a general feature of centred unit cells with reflection symmetry). The asymmetric unit is half of a rounded triangle, one eighth of the rectangular centred unit cell.

2. The point group of a ferrocene molecule [$Fe(C_5H_5)_2$] is D_{5h}, assuming an eclipsed conformation of the two rings. This point group symmetry is not possible in the crystalline solid state (no 5-fold rotation axes!). The symmetry elements of D_{5h} are: a five-fold rotation axis, 5 two-fold rotation axes perpendicular to this, 5 'vertical' mirror planes each containing Fe and 2 C atoms, and one 'horizontal' mirror plane through Fe and lying between the two rings (there is also an S_5 improper rotation axis). Which of these symmetry elements could be retained in the site symmetry of a ferrocene molecule in a crystal structure, and what is the highest possible point group symmetry for ferrocene in the crystal (the maximum number of symmetry elements that can be retained simultaneously)?

Each of the symmetry elements other than the five-fold proper and improper rotations is possible in the solid state, but not all at once (since this would retain the five-fold symmetry also). Only one two-fold rotation

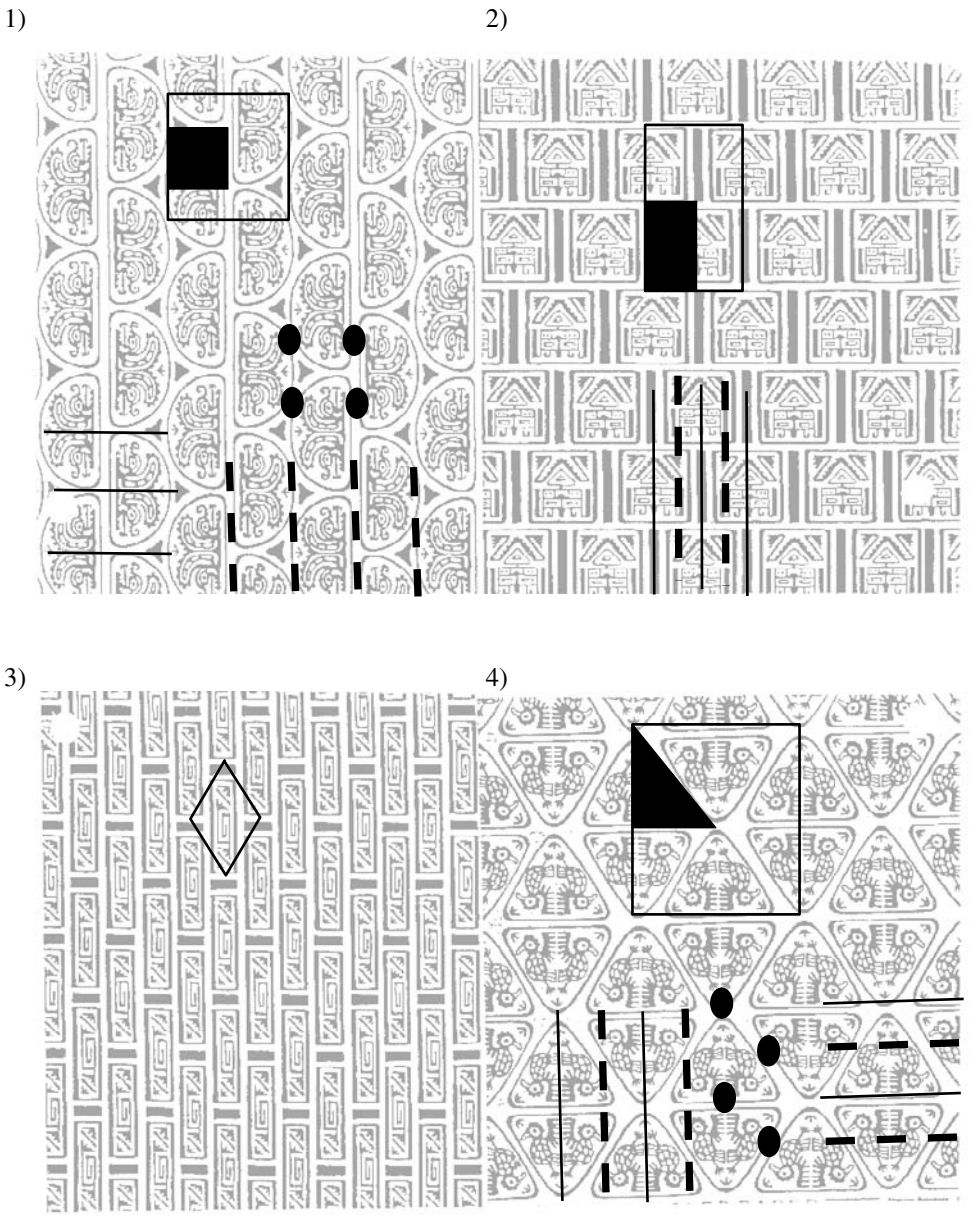

Patterns for Exercise 1.

axis can be retained, because the others are all at 'crystallographically impossible' angles to this one. Together with this axis, we can retain two mirror planes: the one relating the two rings to each other, and one other perpendicular to this, the two planes intersecting in the line of the two-fold rotation axis. This point group symmetry is C_{2v} (*mm*2).

3. Why does the list of conventional Bravais lattices not include any centred unit cells in the triclinic system, tetragonal *C*, or cubic *C*?

Triclinic centred cells are unnecessary, as it is always possible then to choose a smaller unit cell with the centring points taken as corners, because there are no requirements for special values of the cell axes or angles;

try it in 2D for an arbitrary centred oblique cell. For tetragonal *C*, the square base can be halved in area (choose two lattice points separated by one unit cell *a* or *b* edge and two centring points to make a smaller square), and this retains the conventional square-prism shape for tetragonal symmetry; in the same way tetragonal *I* and *F* can be converted into each other. Cubic *C* is ***impossible***, because this would make one pair of opposite cell faces different from the other two pairs, i.e. it makes the *c*-axis different from *a* and *b*; the same would apply to tetragonal *A* or *B* centring.

4. **Work out the point group and the Laue class corresponding to the following space groups: (a) *C*2; (b) *Pna*2_1; (c) *Fd*$\bar{3}$*c*; (d) *I*4_1*cd*.**
(a) *C*2 is point group 2, Laue group 2/*m*; (b) *Pna*2_1 is point group *mm*2, Laue group *mmm*; (c) *Fd*$\bar{3}$*c* is point group *m*$\bar{3}$*m* and this is also the Laue group, since it is centrosymmetric; (d) *I*4_1*cd* is point group 4*mm* and Laue group 4/*mmm*.

5. **From the space group symbols alone, what (if any) special positions would you expect to find for (a) *P*$\bar{1}$; (b) *C*2; (c) *P*$2_12_12_1$?**
(a) The only symmetry here is inversion, and inversion centres are the special positions (there are actually 8 per unit cell; by conventional cell origin choice, they lie at the corners, the middle of all edges, the middle of all faces, and the body centre – it is a useful exercise to demonstrate that this does give 8 per unit cell, since most of them are shared by two or more cells!). (b) The only symmetry elements are 2-fold rotation axes, and any position on one of these is a special position. (c) The only symmetry elements here are screw axes, and these do not provide any special positions, since any atom on a screw axis is shifted to another position by operation of the screw; this space group has no special positions.

Chapter 3

No exercises.

Chapter 4

1. **The following unit cell volumes and densities have been measured for the given compounds. Calculate *Z* for the crystal, and comment on how well (or badly) the '18 Å^3 rule' works for each compound:**
   a) **methane (CH_4) at 70 K: $V = 215.8$ Å^3, $D = 0.492$ g cm^{-3};**
   b) **diamond (C): $V = 45.38$ Å^3, $D = 3.512$ g cm^{-3};**
   c) **glucose ($C_6H_{12}O_6$): $V = 764.1$ Å^3, $D = 1.564$ g cm^{-3};**
   d) **bis(dimethylglyoximato)platinum(II) ($C_8H_{14}N_4O_4Pt$): $V = 1146$ Å^3, $D = 2.46$ g cm^{-3}.**

   Use $Z =$ density × Avogadro's number × cell volume/formula mass (with correct units!). The first two are far from typical organic or co-ordination compounds!

   a) methane ($M = 16.04$), $Z = 4$, 54 Å^3 per non-H atom;
   b) diamond ($M = 12.01$), $Z = 8$, 5.7 Å^3 per non-H atom;
   c) glucose ($M = 180.1$), $Z = 4$, 15.9 Å^3 per non-H atom;
   d) Pt complex ($M = 425.3$), $Z = 4$, 16.9 Å^3 per non-H atom.

2. **A unit cell has three different axis lengths and three angles all apparently equal to 90°. What is the metric symmetry? The Laue symmetry, however, does not agree with this; equivalent intensities are found to be**

$$hkl \equiv hk\bar{l} \equiv \overline{hk}l \equiv \overline{hk\bar{l}}$$

$$\bar{h}kl \equiv \bar{h}k\bar{l} \equiv h\bar{k}l \equiv h\bar{k}\bar{l}.$$

   What is the true crystal system and its conventional axis setting?
   The metric symmetry is orthorhombic. However, true orthorhombic symmetry would make all 8 reflections equivalent, not two sets of 4. The Laue symmetry is monoclinic, but the unique axis here is *c* instead of the conventional *b* setting, as shown by the fact that the index *l* is the one that can change its sign alone and still give an equivalent reflection; the other two have to change sign together.

3. **What are the systematic absences for the space groups *I*222 and *I*$2_12_12_1$?**
   Because of the *I* centring, $h+k+l$ must be even for a reflection intensity to be observed, for both space groups. This affects all subsets of the reflections with one or with two indices equal to zero. The systematically absent reflections with one index equal to zero do not, then, prove that glide planes are present (they are not for these space groups, but they are for *Ibca*, which has the same systematic absences but should have a different statistical distribution of intensities because it is centrosymmetric), and similarly the presence of screw axes can not be deduced. In fact, both space groups have screw axes and normal rotation axes parallel to all three cell axes, but they are arranged in different relative positions; 2-fold rotation axes in all three directions intersect each other in *I*222, but not in *I*$2_12_12_1$ in the way these two space group symbols are conventionally assigned.

4. **Deduce as much as you can about the space groups of the compounds for which the following data were obtained.**
Systematic absences for general reflections give the unit cell centring; other absences give glide planes and screw axes; centric or acentric statistics indicate the presence or absence of inversion centres.

   a) **Monoclinic. Conditions for observed reflections: *hkl*, none; *h*0*l*, *h*+*l* even; *h*00, *h* even; 0*k*0, *k* even; 00*l*, *l* even. Centric distribution for general reflections.**
   Monoclinic, *P*; *h*0*l* absences show *n* glide plane perpendicular to *b* and include *h*00 and 00*l*; 0*k*0 shows 2_1 parallel to *b*. This uniquely identifies $P2_1/n$ (alternative setting of $P2_1/c$ with different choice of *a*,*c* axes), which is centrosymmetric in accord with statistics.

   b) **Orthorhombic. Conditions for observed reflections: *hkl*, all odd or all even; 0*kl*, $k + l = 4n$ and both *k* and *l* even; *h*0*l*, $h + l = 4n$ and both *h* and *l* even; *hk*0, $h + k = 4n$ and both *h* and *k* even; *h*00, $h = 4n$, 0*k*0, $k = 4n$; 00*l*, $l = 4n$. Centric distribution for general reflections.**
   Orthorhombic *F* (this condition can be expressed in equivalent terms as: $h + k$, $k + l$, $h + l$ all even, and it includes all the all-even index observations for reflections with one index zero); the various $4n$ observations for relections with one index equal to zero show *d* glide planes perpendicular to all three cell axes, and these include all the axial reflection conditions (so no deduction of four-fold screw axes!). This uniquely identifies *Fddd*, which is centrosymmetric.

   c) **Orthorhombic. Conditions for observed reflections: *hkl*, none; 0*kl*, $k + l$ even; *h*0*l*, *h* even; *hk*0, none; *h*00, *h* even; 0*k*0, *k* even; 00*l*, *l* even. Acentric distribution for general reflections, centric for *hk*0.**
   Orthorhombic *P*; 0*kl* absences show *n* glide perpendicular to *a*-axis; *h*0*l* absences show *a* glide perpendicular to *b*-axis; no glide plane perpendicular to *c*-axis and absences say nothing about mirror planes; all axial absences are contained within the glide plane conditions, so prove nothing. Acentric distribution indicates no inversion symmetry, so there can not be a mirror plane perpendicular to *c* (this would give the centrosymmetric point group *mmm* and space group *Pnam*, an alternative setting of the conventional *Pnma* with a change of axes). Point group must be *mm*2, with either 2 or 2_1 parallel to *c*-axis. In fact it is 2_1 and the space group is $Pna2_1$ (there is no *Pna*2, this is an impossible combination of symmetry elements).

   d) **Tetragonal. Reflections *hkl* and *khl* have the same intensity. Conditions for observed reflections: *hkl*, none; 0*kl*, none; *h*0*l*, none; *hk*0, none; *h*00, *h* even; 0*k*0, *k* even; 00*l*, $l = 4n$; *hh*0, none. Acentric distribution for general reflections; centric for 0*kl*, *h*0*l*, *hk*0, and *hhl* subsets of data.**
   Tetragonal *P*; the equivalence of *hkl* and *khl* shows mirror symmetry in the *ab* diagonal for the Laue group, which is $4/mmm$ rather than $4/m$; there are no glide planes, from reflections with one zero index; 00*l* absences show either 4_1 or 4_3 along *c*-axis; *h*00 and 0*k*0 show 2_1 parallel to both *a* and *b* (which are equivalent in tetragonal symmetry); no absences for *hh*0, so no 2_1 in the *ab* diagonal direction. Space group is either $P4_12_12$ or $P4_32_12$; these are an enantiomorphous pair, and are non-centrosymmetric.

Chapter 5

1. **State which of the following represent real-space or reciprocal-space quantities:**

   a) **the structure factor, *F*;**
   Reciprocal.

   b) **a space in which Miller indices, h, k, l are labelled;**
   Reciprocal.

   c) **the measured intensity of a diffraction spot;**
   Real.

   d) **unit cell parameters, $a, b, c, \alpha, \beta, \gamma$;**
   Real.

   e) **the representation of a part of a crystal structure via a 2D diffraction pattern;**
   Reciprocal.

   f) **diffractometer axes, *x*, *y*, *z*;**
   Real.

2. **Below are the crystal data for a given compound.**
Crystal data for $C_{26}H_{40}N_2Mo$, $M_r = 476.54$, orange spherical crystal (0.4 mm diameter), monoclinic, space group $C2/c$, $a = 20.240(2)$, $b = 6.550(1)$, $c = 19.910(4)$ Å, $\beta = 90.101(3)°$, $V = 2640.4(3)$ Å^3, $T = 150$ K. 2253 unique reflections were measured on a Bruker CCD area diffractometer, using graphite-monochromated Mo K_α radiation ($\lambda = 0.71073$ Å). Lorentz and polarization corrections were applied. Absorption corrections were made by Gaussian integration using the calculated attenuation coefficient, $\mu = 0.44$ mm^{-1}. The structure was solved using direct methods and refined by full-matrix least-squares refinement using *SHELXL*97 with 2253 unique reflections. During the refinement, an extinction correction was applied. Refinement of

302 positional and anisotropic displacement parameters converged to $R_1[I > 2\sigma(I)] = 0.1654$ and $wR_2[I > 2\sigma(I)] = 0.3401$ [$w = 1/\sigma^2(F_o)^2$] with $S = 2.31$ and residual electron density, $\rho_{min\,/\,max} = -5.43/4.30$ eÅ^{-3}.

(a) Calculate F(000).
Assuming F_o is on an absolute scale, $F(000)$ has an amplitude equal to the total number of electrons in the unit cell:

$$F(000) = \sum_{j=1}^{N} z_j$$

$C2/c \rightarrow Z = 8$. $V = 2640.4(3)$ Å
$C_{26}H_{40}N_2Mo \rightarrow$ 29 non-hydrogen atoms $\therefore$ molecular volume = 580 Å $\therefore$ $Z' = 0.5$. Total number of electrons $= 4((6 \times 26) + (1 \times 40) + (7 \times 2) + (42)) = 1008$.

(b) Using Bragg's law, calculate *d* when the detector lies at $2\theta = 20°$.
$\lambda = 2d \sin\theta \qquad \lambda = 0.71073$Å $\qquad \theta = 10.$
$\therefore d = 2.046$ Å.

(c) Confirm the result in (b) by using the Ewald construction, and the cosine rule to derive the value of *d*.

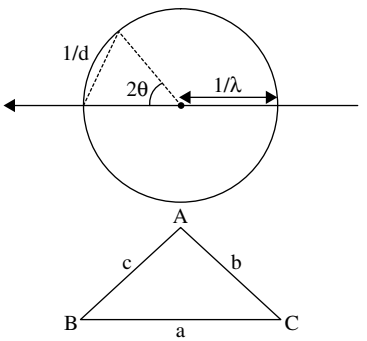

Cosine rule:
$a^2 = b^2 + c^2 - 2bc\cos A$
$1/d = a$
$a^2 = (1.407)^2 + (1.407)^2 - (2 \times 1.407 \times 1.407 \times \cos 20) = 0.23877.$
$a = 0.4886$
$d = 1/a = 2.046$

(d) What percentage of the X-ray beam is absorbed by the crystal? (Assume that, on average, the X-ray path through a crystal diffracts at its centre).
$\mu = 0.44$ mm^{-1}
Spherical crystal ($r = 0.4$)
$I_t = I_o \exp(-\mu t)$, so $I_t/I_o = 0.84$

(e) When indexing the crystal, the experimenter could not be sure if the crystal was orthorhombic or monoclinic. Given this, which crystal system should the experimenter assume when setting up the data-collection strategy? Explain why.
Monoclinic $-$ ¼ of a sphere is unique for monoclinic compared with orthorhombic, where ⅛ of the sphere is unique. Assuming monoclinic gives enough data for either system.

(f) The residual electron density is significant; indeed, the refined model is poor. Assuming that the problem lay at the data-reduction stage, describe possible causes for this.
Incorrect space group or incorrect centring for data integration are possibilities; however, R_{int} is not high, which would be expected. Other possibilities include a variety of twinning as $\beta = 90°$, $a \approx c$ and $3b \approx c$.

3. From the orientation matrix

$$\mathbf{A} = \begin{pmatrix} 0 & 0.250 & 0 \\ 0.125 & 0 & 0 \\ 0 & 0 & -0.100 \end{pmatrix}$$

calculate the unit cell parameters. About which axis is the crystal mounted? Is this desirable?
The unit cell parameters are $a = 8$, $b = 4$, $c = 10$ Å. The crystal is mounted exactly along c. This would be fine on a diffractometer with a fixed non-zero χ circle but not on a four-circle (favours multiple diffraction effects) or a single-axis diffractometer (minimizes coverage).

Chapter 6

1. Assuming both are available, which of Cu or Mo radiation would you use to determine the following problems, and why? (a) $C_6H_4Br_2$; (b) $C_6Cl_4Br_2$; (c) $C_{36}H_{12}O_{18}Ru_6$; (d) absolute configuration of $C_{24}H_{42}N_2O_8$; (e) absolute configuration of $C_{24}H_{40}Br_2N_2O_8$.
(a) Although absorption is lower with Mo radiation the difference is rather small (about 20%). If the crystal is weakly diffracting you should use Cu radiation.
(b) Absorption is more than twice as serious with Cu, due to the high chlorine content. Mo is clearly better.
(c) Ru is beyond the Mo absorption edge and absorption has dropped off, so Mo is strongly preferred.
(d) **Must** use Cu as N and O have almost no anomalous scattering with Mo.
(e) Either could be used.

2. A crystal indexed to give a metrically orthorhombic unit cell. After processing the frameset, the reflection file was examined in order to establish the true diffraction symmetry, and the measurements below are representative of the pattern found. There were no major absorption effects. Is the crystal system really orthorhombic?

h	*k*	*l*	Intensity
10	2	4	258.2
−10	2	4	187.4
10	−2	4	267.4
10	2	−4	216.4
−10	−2	−4	245.2
10	−2	−4	200.9
−10	2	−4	264.6
10	−2	4	208.3

If this pattern is repeated throughout the full set of measurements, the answer is no. The reflections divide into two sets of monoclinic equivalents with intensities grouped around 260 and 200.

3. A compound $C_{32}H_{31}N_3O_2$ crystallized from tetrahydrofuran (thf) (C_4H_8O) solution gives a primitive monoclinic unit cell of 1850 Å^3. What are the likely unit cell contents?

There is no mathematically unique answer to this question. The compound and thf have 37 and five non-H atoms requiring 666 Å^3 and 90 Å^3, respectively. The unit cell could contain three molecules of the compound (1998 Å^3) and no thf but the agreement is not good and $Z = 3$ is unlikely. If it held two molecules of the compound (1332 Å^3) that would leave 518 Å^3, enough for about six molecules of thf per unit cell. Such a crystal would most likely lose solvent unless protected.

4. Estimate the range of absorption correction factors for the following crystals with $\mu = 1.0$ mm^{-1}.
(a) a thin plate 0.02 × 0.4 × 0.4 mm; (b) a tabular crystal 0.2 × 0.4 × 0.4 mm; (c) a needle 0.06 × 0.08 × 0.40 mm, mounted parallel to the fibre; d) a needle 0.06 × 0.08 × 0.40 mm, mounted across the fibre. Repeat the calculations with $\mu = 0.1$ and 5.0 mm^{-1}.

Method: consider the likely paths the beams will follow and calculate $\exp(-\mu x)$ for each case. [The maximum and minimum paths will be (a) 0.02 and 0.4 mm; (b) 0.2 and 0.4 mm; (c) 0.06 and 0.08 mm; (d) 0.06 or 0.08 and 0.40 mm.] Note the advantages of (c) over (d), especially with the higher values of μ.

5. Two estimates were made of a set of unit cell parameters a…γ: (a) 8.364(12), 10.624(16), 16.76(5) Å, 89.61(8), 90.24(8), 90.08(6)°; (b) 8.327(4), 10.622(6), 16.804(8) Å, 90, 90, 90°. The first estimate was derived from the original orientation matrix refinement using 67 reflections, while the second was obtained by a final constrained refinement using 5965 reflections from the entire frameset. Estimate the approximate contribution in each case to the uncertainty in a C–C bond of 1.520 Å.

This calculation involves some approximations and assumptions, the point being to get a reasonable estimate of the uncertainties involved and decide whether these are important. Consider case (b) first: you need to calculate the relative uncertainties in the three cell dimensions and realize that these are roughly the same [the error is about 1 part in 2000]. Next, proceed on the basis that cell standard uncertainties are isotropic. You can then use the figure of 1 in 2000 to get a contribution to the uncertainty in the C–C bond of 1.520 Å /2000 = 0.0008 Å, which will not be significant in any but the most accurate determinations. The calculation is valid for all orientations of the C–C bond.

The cell in (a) is obviously poorer. Work out the relative uncertainties in *a*, *b* and *c* [1 in 700, 1 in 650 and 1 in 350, respectively]. The errors are much higher and not isotropic. Next, work out the contribution to the uncertainty for a C–C bond lying parallel to each of the (100), (010) and (001) directions. [Answers are 0.002, 0.002 and 0.004 Å, respectively.] These, especially the last, would add significantly to the uncertainty of a typical structure determination. Note that the values are probably an underestimate as we have ignored any contribution from the unconstrained angles.

Chapter 7

1. Measuring a reflection for twice the time doubles the observed intensity *I*. What is the effect on $\sigma(I)$ and on $I/\sigma(I)$?

$\sigma(I)$ is increased by $\sqrt{2}$; $I/\sigma(I)$ is increased by $\sqrt{2}$ ($2/\sqrt{2}$).

2. An area detector with diameter *a* of 6.0 cm normally sits at a distance *D* of 5.0 mm from the crystal. Calculate the 2θ ranges that would be recorded with θ_c set at 28.0° if *D* was increased to (a) 6.0 cm; (b) 7.0 cm; (c) 8.0 cm. Assuming Mo $K\alpha$ radiation, at what point should you consider using two settings for θ_c?

Using the expression $\tan^{-1}(a/2D)$ for the range on either side of θ_c, the upper and lower 2θ limits are (a) 1.4–54.6; (b) 4.8–51.2; (c) 7.5–48.5°. Given that an upper 2θ limit of around 50° is acceptable to all journals, you might decide to use two detector settings when the distance *D* is more than 7 cm.

3. A frameset was processed satisfactorily as orthorhombic, except for consistently high values of around 0.25 for the merging *R* index. Although the resulting dataset led to a plausible-looking solution, the subsequent refinement stalled at $R = 0.19$. There are no significant absorption effects. Suggest a possible solution.

The crystal system would most likely have been assigned as orthorhombic on metric considerations, but these may have been misleading. Orthorhombic and monoclinic are differentiated by whether the third cell angle is also exactly 90°: a monoclinic β angle close to this value may lead to an incorrect assignment of the crystal system as orthorhombic. The slightly poor agreement between the intensities under orthorhombic symmetry is not definitive, but the frameset should be re-processed under monoclinic symmetry and the corresponding structure solution and refinement investigated. The plausibility of the solution under orthorhombic symmetry may be a sign that some form of pseudo-symmetry is present.

Chapter 8

1. In Fig. 8.3, assign the correct atom types, the H atoms, and the appropriate bond types (single, double, or aromatic). The correct formula is $C_{13}H_{12}N_2O$. Why is there only one peak visible for the ethyl group H atoms?

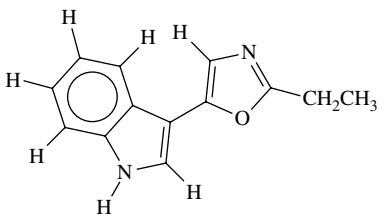

Correct assignment of atom and bond types.

One C should be N, and one N should be O, because of extra electron density needed. H atoms on rings all show clearly. From number of H atoms and chemical sense, the chain must be ethyl. All bond types follow from valency considerations. Only one H atom of the ethyl group lies in this plane; the other four are above and below it, so are not seen in this 2D section of the full 3D map.

2. What would be the effect on a Fourier synthesis of:

a) omitting the term *F*(000);
All values of the electron density are reduced by this value. This will make the electron density negative in many regions, but relative values are still correct.

b) omitting the 20% of reflections with highest values of $(\sin\theta)/\lambda$;
This would increase the usual series termination error, introducing greater ripples into the electron density; there will be additional spurious peaks as a result.

c) omitting the 5% of reflections with lowest values of $(\sin\theta)/\lambda$;
These reflections contribute broad low-resolution features to the electron density, so there will be a distortion of the general level of electron density around the unit cell; individual peaks will probably still be recognizable, but with the wrong relative heights. A few very low-angle reflections are sometimes missing, especially for large unit cells, because they lie partly or fully behind the X-ray beam stop. This is not usually a problem.

d) setting all phases equal to zero?
This is effectively the same as a Patterson function, but using amplitudes instead of their squares. The appearance will be very similar, but there will be less variation in the peak heights.

Chapter 9

1. Generate the 4 × 4 vector table for space group $P2_1/n$. The general positions are as follows.

$$x, y, z \qquad \tfrac{1}{2} + x, \tfrac{1}{2} - y, \tfrac{1}{2} + z$$
$$\tfrac{1}{2} - x, \tfrac{1}{2} + y, \tfrac{1}{2} - z \qquad -x, -y, -z.$$

The required table is shown on the next page. The construction principles are just the same as for the tables in Chapter 9.

2. For a compound of formula $BiBr_3(PMe_3)_2$ with Z = 4 in $P2_1/n$, the largest independent Patterson peaks are shown in Table 9.6 (below). Propose co-ordinates for one Bi atom. Give the corresponding positions of the other 3 Bi atoms in the unit cell. The next highest peaks in the Patterson map include some with vector lengths 2.8–3.3 Å. To what features in the molecular structure do these peaks correspond? Deduce whether the molecule is likely to be monomeric or dimeric, and give the expected co-ordination number of bismuth.

Peak height	Co-ordinates			Vector length (Å)
999	0.000	0.000	0.000	0.00
383	0.500	0.150	0.500	8.96
361	0.460	0.500	0.586	10.12
194	0.040	0.350	0.914	4.46

$P2_1/n$	x, y, z	$-x, -y, -z$	$½ + x, ½ - y, ½ + z$	$½ - x, ½ + y, ½ - z$
x, y, z	$0, 0, 0$	$-2x, -2y, -2z$	$½, ½ - 2y, ½$	$½ - 2x, ½, ½ - 2z$
$-x, -y, -z$	$2x, 2y, 2z$	$0, 0, 0$	$½ + 2x, ½, ½ + 2z$	$½, ½ + 2y, ½$
$½ + x, ½ - y, ½ + z$	$½, ½ + 2y, ½$	$½ - 2x, ½, ½ - 2z$	$0, 0, 0$	$-2x, 2y, -2z$
$½ - x, ½ + y, ½ - z$	$½ + 2x, ½, ½ + 2z$	$½, ½ - 2y, ½$	$2x, -2y, 2z$	$0, 0, 0$

Vectors between general positions in $P2_1/n$ for Exercises 1 and 2.

One Bi is at 0.020, 0.175, 0.457 (half the numbers for the fourth peak, which is $2x$, $2y$, $2z$, and consistent with the second and third peaks if allowed shifts and inversions are applied). There are actually a lot of possible correct answers, by choosing different unit cell origins and inverting either y or both x and z together. Co-ordinates of the other 3 Bi atoms are obtained by applying the general position transformations to the first atom. The next highest peaks will be due to vectors between Bi and Br atoms; some of these are intermolecular, and others are intramolecular and will have vector lengths equal to Bi–Br bond lengths, around 3 Å. The shortest Bi…Bi distance is 4.46 Å and is appropriate for the diagonal of a Bi_2Br_2 four-membered ring with two bromides bridging two Bi atoms. This would give each Bi atom 2 terminal phosphine and 2 terminal bromide ligands, and a share in 2 bridging bromides, so the co-ordination number is 6 instead of the 5 indicated by the monomer formula. The structure is dimeric with the ring on an inversion centre.

3. For a compound of formula $C_{21}H_{24}FeN_6O_3$ with $Z = 8$ in *Pbca*, the largest independent Patterson peaks are shown in Table 9.7 (below). Propose co-ordinates for one Fe atom.

Peak height	Co-ordinates			Vector length (Å)
999	0.000	0.000	0.000	0.00
241	0.000	0.172	0.500	12.03
240	0.500	0.000	0.088	11.42
213	0.243	0.500	0.000	6.68
107	0.243	0.327	0.500	13.38
104	0.500	0.176	0.412	14.99
103	0.257	0.500	0.088	7.24
51	0.257	0.327	0.412	11.69

Again, there are many possible correct answers. Co-ordinates are obtained singly from peaks 2, 3 and 4; in pairs from peaks 5, 6 and 7; and all together from peak 8. Note how all the co-ordinates of peaks in any column are zero, half, or one of two values adding up to ½. This shows that they are all due to pairs of the same set of 8 symmetry-equivalent heavy atoms. One possible answer is obtained by just halving the co-ordinates of peak 8: 0.129, 0.164, 0.206 (keeping to 3 decimal places). It really is as easy as this!

4. For a compound of formula $C_{14}H_{19}FeNO_3$ with $Z = 4$ (two molecules in the asymmetric unit) in $P\bar{1}$, the largest independent Patterson peaks are shown in Table 9.8 (below). Propose co-ordinates for two independent Fe atoms.

Peak height	Co-ordinates			Vector length (Å)
999	0.000	0.000	0.000	0.00
270	0.136	0.008	0.506	6.50
234	0.492	0.295	0.151	6.39
144	0.644	0.715	0.350	5.64
130	0.370	0.705	0.343	5.59

Peaks 2 and 3 are the sums and differences of the co-ordinates of the two heavy atoms in the asymmetric unit. Peaks 4 and 5 are vectors between pairs of atoms related by the inversion symmetry ($2x$, $2y$, $2z$). There are several ways of solving this. One is to find one of the heavy atoms from either peak 3 or peak 4 as for the single-heavy-atom situation, and then use the sum and difference peaks to locate the second atom, checking the answer against the remaining peak. Another is to solve peaks 2 and 3 as a pair of simultaneous equations and

check the answers against peaks 4 and 5. Yet another method is to find one atom from peak 4 and provisional co-ordinates for the other from peak 5, then use peaks 2 and 3 to decide how to resolve the sign and $\pm$½ ambiguities for this second atom to give consistent answers. One of many correct answers (co-ordinates to 2 decimal places) is: Fe1 at 0.32, 0.36, 0.18; Fe2 at 0.18, 0.35, 0.67. The first of these is just half the co-ordinates of peak 4, the other is half the co-ordinates of peak 5, except that ½ must be added to the z co-ordinate to obtain a result consistent with peaks 2 and 3.

Chapter 10

1. **Set up the order 3 Karle–Hauptman determinant for a centrosymmetric structure whose top row contains the reflections with indices 0, h, and 2h. Hence, obtain a constraint on the sign of E(2h). What is the sign of E(2h) if E(0) = 3, |E(h)| = |E(2h)| = 2?**
The required determinant is:

$$\begin{vmatrix} E(0) & E(h) & E(2h) \\ E(-h) & E(0) & E(h) \\ E(-2h) & E(-h) & E(0) \end{vmatrix},$$

which can be expanded to give the inequality relationship:

$$E(0)\left[E^2(0) - |E(2h)|^2 - 2|E(h)|^2\right] + 2|E(h)|^2 E(2h) \geq 0.$$

This can be simplified by cancelling out a common factor of $[E(0) - E(2h)]$ and rearranging to give:

$$|E(h)|^2 \leq \frac{1}{2}E(0)\left[E(0) + E(2h)\right].$$

With the given amplitudes, the left-hand side of the inequality is 4 and the right-hand side is 15/2 or 3/2 for $E(2h)$ positive or negative, respectively. The sign of $E(2h)$ must, therefore, be positive.

2. **Verify (10.8). What sign information does it contain under the conditions E(0) = 3, |E(h)| = |E(2h)| = 2, |E(h − k)| = 1?**
Equation (10.8) comes directly from the expansion of the determinant in (10.7). With the given amplitudes, the inequality becomes $8 \geq 0$ or $-8 \geq 0$ depending on the sign of $E(-h)E(h-k)E(k)$. The sign of $E(-h)E(h-k)E(k)$ must, therefore, be positive.

3. **Expand the order 4 Karle–Hauptman determinant for a centrosymmetric structure whose top row contains the reflections with indices 0, h, $h+k$, and $h+k+l$ and for which $E(h+k) = E(k+l) = 0$. Interpret your expression in terms of the sign information to be obtained and under which conditions it occurs.**
The order four determinant is:

$$\begin{vmatrix} E(0) & E(h) & E(h+k) & E(h+k+l) \\ E(-h) & E(0) & E(k) & E(k+l) \\ E(-h-k) & E(-k) & E(0) & E(l) \\ E(-h-k-l) & E(-k-l) & E(-l) & E(0) \end{vmatrix}.$$

With $E(h+k) = E(k+l) = 0$, this forms the inequality relationship:

$$E^2(0)[E^2(0) - |E(h)|^2 - |E(k)|^2 - |E(l)|^2 - |E(-h-k-l)|^2] + |E(h)E(l)|^2 + |E(k)E(-h-k-l)|^2 - 2E(h)E(k)E(l)E(-h-k-l) \geq 0,$$

and with suitably large amplitudes, this can be used to prove that the sign of $E(h)E(k)E(l)E(-h-k-l)$ must be negative; this is a negative quartet relationship.

4. **Compare the Karle–Hauptman determinants with the following reflections in the top row: 0, h, $h+k$, $h+k+l$; 0, k, $k+l$, $k+l+h$; 0, l, $l+h$, $l+h+k$. Summarize the sign information they contain when $E(h)$, $E(k)$, $E(l)$, $E(h+k+l)$ are all strong and $E(h+k) = E(k+l) = E(l+h) = 0$.**
The three determinants are obtained from the one in Exercise 3 by cyclic permutation of indices. Together they give a stronger indication of the negative quartet provided that $E(h+k) = E(k+l) = E(h+l) = 0$.

5. **Symbolic addition applied to a projection. Ammonium oxalate monohydrate gives orthorhombic crystals, $P2_12_12$, with a = 8.017, b = 10.309, c = 3.735 Å (at 30 K). The short c–axis projection makes this an ideal structure for study in projection, as there can be little overlap of atoms. Data for the projection have been sharpened to point atoms at rest (i.e. converted to E-values) and are shown in Fig. 10.5 (below). Note the *mm* symmetry and the fact that data are only present for h00 and 0k0 for even orders, consistent with the screw axes. Find the especially strong data 5,7; −14, 5; 9, −12, which have indices summing to zero, as an example of a triple phase relationship (we omit the l index, since it is always zero for these reflections).**

   The problem is that phases must be assigned to the structure factors before they can be added up. Since this projection is centrosymmetric, phases must be 0 or π radians (0 or 180°), i.e. E must be given a sign + or −, but there are 228 combinations of these values, and

your chance of getting an interpretable map is small! Fortunately, the planes giving strong $|E|$ values are related by enough relationships to give us a unique, or almost unique, solution. The main relationship used is that for large values of $|E|$, say $|E1|$, $|E2|$ and $|E3|$ all > 1.5, if: $h1+h2+h3 = k1+k2+k3\ (= l1+l2+l3) = 0$, then: $\phi 1+\phi 2+\phi 3 \approx 0$. Additional help is given by the symmetry of the structure, illustrated in the figure.

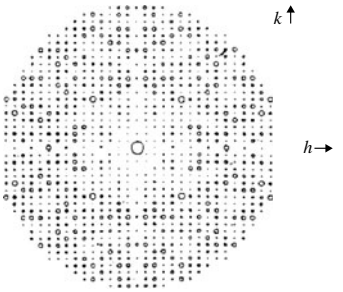

c-Axis projection data for ammonium oxalate monohydrate for Exercise 5

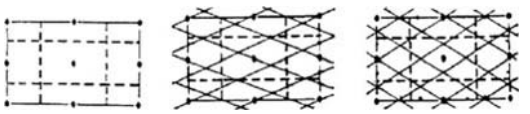

Plane group symmetry for the ammonium oxalate monohydrate structure projection, together with two sets of lines (equivalent to planes in three dimensions) for Exercise 5.

The plane group (two-dimensional space group) is *pgg*, with glide lines perpendicular to both axes, and there are four alternative positions for the origin: 0, 0; 0, ½; ½, 0; and ½, ½. This means that two phases may be arbitrarily fixed from any two of the parity groups g, u; u, g; or u, u (g and u mean even and odd, respectively, for the indices h and k), since, for example, shifting the origin by half a unit cell along a will shift the phase of all structure factors with h odd by π. Another result of the symmetry is that planes with indices h, k are related to $h, -k$ or $-h, k$ by the glide lines. The structure amplitudes must be the same for these, and the phases must be related, although they are not always the same. If h and k are both even or both odd, $\phi(h,k) = \phi(-h,k)$. If, however, one is odd and one even, $\phi(h,k) = \pi + \phi(-h,k)$. See the examples given for (2,3) and (3,3) in the diagrams. In other words, if we have a sign for a particular reflection h, k and we want the sign for either $-h, k$ or $h, -k$, then we must change the sign if $h + k$ is odd, but not if $h + k$ is even. Such sign changes are marked * in the list below.

To get started, assign arbitrary signs to 5,7 and 14,5, and give 8,8 the symbol A (unknown, to be determined). Data marked * have opposite signs to those that have both indices positive. Triples are arranged from left to right and downwards in order of decreasing reliability. Note $A^2 = 1$ whatever the sign of A. For brevity, use B to stand for $-A$.

To get started, arbitrary signs (+) have been assigned to 5,7 and 14,5 and the symbol A to 8,8. B means the opposite to sign A. Alternative solutions may be obtained with other combinations of signs. The fact that A = + is shown by the alternative values found for 8,13, here B and –.

5	7+	−5	7+	5	7+	14	5+
5	−7+	14	5+	10	0+	−9	12*−
10	0+	9	12+	15	7+	5	17−
5	17−	−5	7+	14	−5*−	5	7+
5	−17−	8	8A	−8	8A	6	−3*A
10	0+	3	15A	6	3B	11	4A
−5	7+	9	−12*−	5	17−	−5	17−
6	3B	−3	15A	6	−3*A	6	−3*A
1	10B	6	3B	11	14B	1	14B
11	14B	−1	14*A	−1	10*A	14	5+
−10	0+	10	0+	−8	−8A	−7	−2+
1	14B	9	14A	7	2+	7	3+
5	7+	−5	17−	11	−4*B	14	5+
7	3+	7	2+	1	14B	−9	14*B
12	10+	2	19−	12	10+	5	19B
5	19B	11	−4*B	−3	15A	9	9A
5	−19B	1	10B	12	−6+	−8	8A
10	0+	12	6+	9	9A	1	17+
6	3B	6	3B	5	−7+	−9	12*−
6	3B	7	3+	13	6B	1	17+
12	6+	13	6B	8	13B	10	5−
−3	15A	−5	7+	5	−7+	−7	10*B
10	−5*+	7	10A	−2	17*B	10	0+
7	10A	2	17A	3	10B	3	10B
10	5−	9	−9A	5	19B	−5	19B
−9	9A	−2	19*+	2	−17*B	13	−6*A
1	14B	7	10A	7	2+	8	13−
−2	17*B	−1	−10B				
9	−14*B	8	13B				
7	3+	7	3+				

	Determined	Signs
1	10	B
1	14	BBB
1	17	+
2	17	A
2	19	-
3	10	BB
3	15	A
5	7	+
5	17	-
5	19	B
6	3	BB
7	2	++
7	3	+++
7	10	AA
8	8	A
8	13	B-
9	9	A
9	12	+
9	14	A
10	0	+++
10	5	-
11	4	A
11	14	B
12	6	++
12	10	++
13	6	B
14	5	+
15	7	+

If you had to look at the solution in order to decide what to do, try again with another starting set, say $5, 7 = +$ and $14, 5 = -$. You should still get a consistent set and the symbol A should still come out as $+$.

Chapter 11

No exercises.

Chapter 12

1. Show how (12.13) was derived and verify the least-squares solution.

The expected error in α is half that of the others so the weight is twice that of the others: instead of $\alpha = 73$, we have $2\alpha = 146$. The stronger application of the restraint changes the equation $\alpha + \beta + \gamma = 180$ into $2\alpha + 2\beta + 2\gamma = 360$ (the factor of 2 is arbitrary).

The normal equations are $\mathbf{A^T A x = A^T b}$, i.e.:

$$\begin{pmatrix} 2 & 0 & 0 & 2 \\ 0 & 1 & 0 & 2 \\ 0 & 0 & 1 & 2 \end{pmatrix} \begin{pmatrix} 2 & 0 & 0 \\ 0 & 1 & 0 \\ 0 & 0 & 1 \\ 2 & 2 & 2 \end{pmatrix} \begin{pmatrix} \alpha \\ \beta \\ \gamma \end{pmatrix} = \begin{pmatrix} 2 & 0 & 0 & 2 \\ 0 & 1 & 0 & 2 \\ 0 & 0 & 1 & 2 \end{pmatrix} \begin{pmatrix} 146 \\ 46 \\ 55 \\ 360 \end{pmatrix},$$

which gives:

$$\begin{pmatrix} 8 & 4 & 4 \\ 4 & 5 & 4 \\ 4 & 4 & 5 \end{pmatrix} \begin{pmatrix} \alpha \\ \beta \\ \gamma \end{pmatrix} = \begin{pmatrix} 1012 \\ 766 \\ 775 \end{pmatrix}.$$

Confirm the solution $\alpha = 73.6°$, $\beta = 48.4°$, $\gamma = 57.4°$ by showing that this satisfies the equations.

2. Determine the slope and intercept of the line of linear regression through the points (1, 2), (3, 3), (5, 7), giving equal weight to each point.

Observational equations are:

$$\begin{pmatrix} 1 & 1 \\ 3 & 1 \\ 5 & 1 \end{pmatrix} \begin{pmatrix} m \\ c \end{pmatrix} = \begin{pmatrix} 2 \\ 3 \\ 7 \end{pmatrix}.$$

Normal equations are:

$$\begin{pmatrix} 1 & 3 & 5 \\ 1 & 1 & 1 \end{pmatrix} \begin{pmatrix} 1 & 1 \\ 3 & 1 \\ 5 & 1 \end{pmatrix} = \begin{pmatrix} m \\ c \end{pmatrix} = \begin{pmatrix} 1 & 3 & 5 \\ 1 & 1 & 1 \end{pmatrix} \begin{pmatrix} 2 \\ 3 \\ 7 \end{pmatrix},$$

which gives

$$\begin{pmatrix} 35 & 9 \\ 9 & 3 \end{pmatrix} \begin{pmatrix} m \\ c \end{pmatrix} = \begin{pmatrix} 46 \\ 12 \end{pmatrix},$$

and the solution is $m = 5/4$, $c = 1/4$, so the line of regression is $y = 5/4x + 1/4$.

3. Using data from Exercise 12.2, invert the normal matrix and, from this, calculate the correlation coefficient μ_{mc} between the slope m and intercept c.

The matrix of normal equations is:

$$\begin{pmatrix} 35 & 9 \\ 9 & 3 \end{pmatrix}.$$

Its inverse is:

$$\frac{1}{24} \begin{pmatrix} 3 & -9 \\ -9 & 35 \end{pmatrix}.$$

This gives values proportional to:

$$\begin{pmatrix} \sigma_m^2 & \sigma_m \sigma_c \mu_{mc} \\ \sigma_m \sigma_c \mu_{mc} & \sigma_c^2 \end{pmatrix}.$$

So that $\mu_{mc} = -9/\sqrt{(3 \times 35)} = -0.86$.

4. In the triangle problem, let the expected errors in α, β, γ be in the ratio 1:2:1.

a) Set up the weighted observational equations for α, β, γ and include the restraint $\alpha + \beta + \gamma = 180°$ at half the weight of the equation $\alpha = 73°$.

b) Set up the normal equations of least squares from the observational and restraint equations.

c) Confirm that the solution of the normal equations is $\alpha = 73.6°$, $\beta = 48.4°$, $\gamma = 55.6°$.

The weighted observational equations are:

$$\begin{pmatrix} 2 & 0 & 0 \\ 0 & 1 & 0 \\ 0 & 0 & 2 \\ 1 & 1 & 1 \end{pmatrix} \begin{pmatrix} \alpha \\ \beta \\ \gamma \end{pmatrix} = \begin{pmatrix} 146 \\ 46 \\ 110 \\ 180 \end{pmatrix}.$$

The normal equations are:

$$\begin{pmatrix} 5 & 1 & 1 \\ 1 & 2 & 1 \\ 1 & 1 & 5 \end{pmatrix} \begin{pmatrix} \alpha \\ \beta \\ \gamma \end{pmatrix} = \begin{pmatrix} 472 \\ 226 \\ 400 \end{pmatrix}.$$

5. In the triangle problem, let the observational equations be $\alpha = 73°$, $\beta = 46°$, $\gamma = 55°$, $a = 21$ m, $b = 16$ m, $c = 19$ m, and use the two restraint equations $a^2 = b^2 + c^2 + 2bc\cos\alpha$ and $\alpha + \beta + \gamma = 180°$. Set up the matrix of derivatives needed to calculate shifts to the parameters.

All equations are linear except the cosine rule. Write this as:

$$f(\alpha, \beta, \gamma, a, b, c) = b^2 + c^2 - a^2 + 2bc\cos\alpha = 0.$$

Then, the derivatives are:

$$\frac{df}{d\alpha} = -2bc\sin\alpha \quad \frac{df}{da} = -2a$$
$$\frac{df}{d\beta} = 0 \quad \frac{df}{db} = 2b + 2b\cos\alpha$$
$$\frac{df}{d\gamma} = 0 \quad \frac{df}{dc} = 2c + 2b\cos\alpha.$$

The matrix of derivatives is therefore:

$$\begin{pmatrix} 1 & 0 & 0 & 0 & 0 & 0 \\ 0 & 1 & 0 & 0 & 0 & 0 \\ 0 & 0 & 1 & 0 & 0 & 0 \\ 0 & 0 & 0 & 1 & 0 & 0 \\ 0 & 0 & 0 & 0 & 1 & 0 \\ 0 & 0 & 0 & 0 & 0 & 1 \\ -2bc\sin\alpha & 0 & 0 & -2a & 2b+2c\cos\alpha & 2c+2b\cos\alpha \\ 1 & 1 & 1 & 0 & 0 & 0 \end{pmatrix}.$$

Chapter 13

In these model answers, Y_o and Y_c are used to represent either F_o and F_c, or their squared values (F_o^2, F_c^2).

General

1. List some of the important differences between $P2_1/m$, $P2_1$ and Pm.

All three space groups are monoclinic. $P2_1/m$ is centrosymmetric. Removal of the centre creates either of two non-centrosymmetric space groups. Pm is achiral (contains both hands if the molecule is chiral), and has two floating origin axes. $P2_1$ is chiral and has one floating origin axis.

2. Give some reasons for wishing to publish structures in $P2_1/a$ or $P2_1/n$; $Pnma$, $Pnam$ or $Pna2_1$.

Both $P2_1/a$ and $P2_1/n$ refer to the same arrangement of symmetry operators. Only the orientation of the cell axes differs. The most stable refinement is achieved by choosing the setting with a monoclinic angle closest to 90°. *Pnam* and *Pnma* are the same centrosymmetric space group but with the axes differently labelled. *Pnma* is the 'standard setting', but *Pnam* preserves the axis notation of the corresponding non-centrosymmetric space group, $Pna2_1$.

3. A structure could be published in $P1$, or in $A1$ with a cell of twice the volume. Could this be valid, how many parameters would be involved in each refinement, and how might the observation to parameter ratio alter?

$A1$ is a centred non-standard setting of $P1$. Though the cell is bigger, the number of reflections is the same (because of the systematic absences), and the extra atoms in the cell are generated from the asymmetric unit by the additional symmetry operator. The observation-to-parameter ratio is unaltered. Non-standard settings may be chosen either to achieve a cell with angles close to 90°, or to preserve a relationship with another material or phase.

4. A synthetic organic material yields a good triclinic dataset. The structure will not solve in $P\bar{1}$, but solves easily in $P1$. What should one do next?

This situation is not uncommon if the cell contains two molecules – the absence of restrictions on the phase angles in the non-centrosymmetric space group permits effective tangent refinement. The resulting structure should be examined for a centre of symmetry, since the synthesis would normally be expected to produce a racemic mixture. If an approximate centre is found, the structure should be shifted so that the pseudo-centre lies on a true centre in $P\bar{1}$.

5. Imagine an organometallic compound with potentially 3-fold molecular rotation symmetry. Would you be worried if the diffractometer proposed the space group $C2/c$?

$C2/c$ is a subgroup of $R\bar{3}c$, so one should be alert to the possibility that the true symmetry is rhombohedral, with the molecule actually lying on a 3-fold rotation axis.

6. **An organolead compound crystallizes in *Pc*, and solves in that space group. Comment on origin-fixing techniques, and their effect on atomic and molecular parameter s.u.s.**
   Pc is non-centrosymmetric with two floating directions (both in the unique plane). Singularity of the normal equations can be avoided by shift-limiting (Marquardt) restraints, by restraining the centre of gravity, or by eigenvalue filtering (all of which produce evenly distributed s.u.s). Older programs may fix the x and z co-ordinates of one atom. The s.u.s that should be associated with these co-ordinates appear as increased s.u.s in all the other atoms. It is obviously better to fix a heavy atom than a light one. Molecular parameter s.u.s will be correct under all regimes if the full variance–covariance matrix is used, but over-estimated by the atom-fixing method if only the variances are used.

7. **Explain what happens during refinement given the following scenarios: a) a few structurally important C atoms have been omitted; b) an ethanol molecule of solvation has been omitted; c) an oxygen and a nitrogen atom have been interchanged; d) the chemist is uncertain if a terminal group is CN or NC; the crystallographer is sent some data without an indication as to whether they are F, F^2 or I; somehow the user loses ⅓ of the reflections during a file transfer without getting a warning message.**

   a) The R-factor remains unexpectedly high, a difference map should show the additional atoms, the ratio F_o/F_c is not approximately unity over the whole F_o (or F_c) range, bond lengths in the rest of the structure are distorted.

   b) As above, but less evident.

   c) The displacement parameters will be anomalous – the N in place of O will have reduced parameters, and vice versa

   d) As above, but less evident, especially if there is substantial motion.

   e) The structure may well solve, but will not refine. Refinement of F^2 as F will lead to large displacement parameters, and small ones for the opposite confusion.

   f) If the losses are random, there may be no evident effect except that the observation-to-parameter ratio will be low. Systematic loss of high- or low-angle data will affect the displacement parameters. Loss of data in a particular direction in reciprocal space will lead to unusual adps.

8. **For a material in $P222_1$ we measure and keep separate the h and the $-h$ reflections. How does the number of independent observations we have depend upon the material and the diffraction experiment?**
   If the material contains any elements with substantial anomalous scattering, the h and $-h$ data must be treated as individual, and the absolute configuration determined. If there are no strong anomalous scatterers, h and $-h$ cease to be independent, and can be either kept separate or merged.

9. **The 112 reflection for an 'ordinary' material has $F_o = 10$, $F_c = 500$. What should we do? If F_o were 400, what should we expect?**
   If the R factor is reasonably low – say less than 15% – there is a good probability that F_c is of the right order of magnitude, and that there is something wrong with the measurement of F_o. In the first case it might possibly be partially obscured by the beam-stop and so should be discarded. In the second case it might be the effects of extinction, and an extinction parameter should be refined.

10. **Suggest different restraint regimes for PF_6^- under different patterns of disorder. Suggest some suitable constraints.**
    Bond, angle and adp restraints, or rigid group constraints. If fully disordered, use group electron density models (spherical shells or SQUEEZE).

11. **Why do we bother fiddling with a) hydrogen atoms; b) disordered solvent? Comment on different techniques available for dealing with the problems.**

    a) We may have a scientific reason for wanting to locate them. Even if not, approximate placement is necessary since they contribute to F_c.

    b) To keep referees happy, and to avoid substantial bias in F_c.

12. **Are there any reasons why a laboratory might want both Cu and Mo data-collection capabilities?**
    The diffraction experiment is more efficient with long wavelengths, so smaller crystals can be used with Cu. In general, Mo is less strongly absorbed, so larger crystals containing absorbing elements can be handled. The major reason is that usually anomalous dispersion differences can be measured with Cu radiation from materials containing only C, H, N and O, so that the absolute configuration can be determined from native pharmaceutical (organic) materials.

13. For a chirally pure material in $P6_1$, the Flack parameter has an s.u. of 0.03 and a value of 0.98. What should be done?

If the material is unquestionably ***chirally pure***, an s.u. as large as 0.1 can be safely used to evaluate the parameter. In this case the model needs inverting, and the space group changing to $P6_5$.

14. Imagine a drug compound for which the diffractometer proposes the space group $I4_1$. The Flack parameter refines to about 1.0, with an s.u. of 0.01. What should you do next?

A drug can be expected to be chiral, but there is always risk of contamination by the opposite enantiomer. S.u.s need to be below 0.04 to give a definitive answer. In this case, the structure needs inverting and the space group needs changing. Note that an origin shift is also required ($-$x, ½ $-y$, $-z$ in $I4_3$).

15. A novel inorganic phosphate in $P2_1$ gives a Flack parameter of 0.47 and an s.u. of 0.40. What do we know about the material? What would we know if the s.u. was 0.05?

An s.u. of 0.5 means that the data contain no useful anomalous scattering information, so we know nothing about the hand of the structure. An s.u. of 0.05 means that there is a reasonable anomalous signal, giving us confidence in the calculated value of the Flack parameter, which corresponds to a 50:50 twin by inversion.

16. Give the relationship between the number of parameters and execution time in least squares.

In the matrix accumulation every derivative in the matrix must be multiplied by every other derivative, so the time is proportional to n^2. Matrix inversion depends on the method but is generally of the order of n^3.

17. Explain the derivation of the symmetry constraints for the parameters of atoms on special positions.

$\mathbf{x}' = \mathbf{R}.\mathbf{x} + \mathbf{t}$. If $\mathbf{x}' = \mathbf{x}$ the atom has folded back onto itself, and so is on a special position. Try with operator $x, -y, z$ an atom at 0.3, 0.5, 0.3.

18. Why does the least-squares-determined scale factor ($k.\boldsymbol{F_c} = \boldsymbol{F_o}$) rarely make $\Sigma \boldsymbol{F_o} = \Sigma \boldsymbol{F_c}$?

Least-squares minimises $\Sigma w(Y_o - k.Y_c)^2$, i.e. is a quadratic function, while $\Sigma F_o = k\Sigma$ is linear.

19. Why is the Hamilton '*R*' factor usually higher than the conventional '*R*' factor?

The Hamilton weighted *R* factor (which should always be used in statistical tests) depends on the weights and uses the coefficient $(Y_o - Y_c)^2$, rather than moduli, which are statistically difficult to handle. The square of a large residual is a very large number.

20. What is 'the variance of a reflection of unit weight'?

This is the square of the 'goodness of fit' defined by $S^2 = (\Sigma[w(Y_o - Y_c)^2])/(n - m)$, with n observations and m variables. The squared observations may also be used.

Note that this can easily be fiddled by fiddling the weights, fiddling the number of reflections used, or leaving out of m any parameters that were refined in previous cycles, but not in the last.

21. What is the effect of unaveraged reflections (multiple observations) on least-squares refinement?

There is no objection to the use of unaveraged reflections provided that they are correctly weighted. The weight is (theoretically) proportional to the inverse of the variance, and while averaging reflections reduces the number of observations used in the refinement, the variance of the average will be reduced, so that its weight may be increased. It is therefore possible to mix averaged and unaveraged data. ***This is not true for Fourier calculations***.

22. What is the effect on *R* and bond length s.u.s of ignoring 'weak' reflections?

Sketch *R* versus F_o, and number of reflections versus F_o. A large number of weak reflections usually raises the *R* factor, but has no substantial effect on positional parameters. They may affect displacement parameters, and are important for the determination of absolute configuration (sketch variation of f and f'' versus θ, and $\langle I \rangle$ versus θ). They are also important for distinguishing centrosymmetric and non–centrosymmetric space groups.

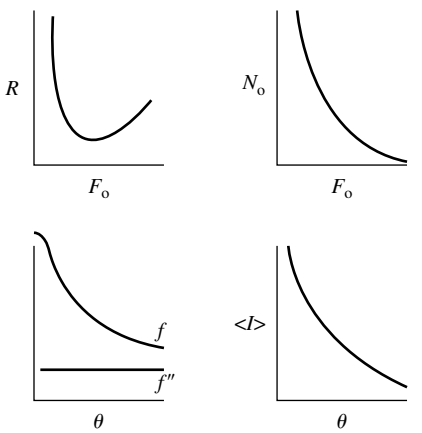

23. What is the effect on *R* and bond length s.u.s of anisotropic refinement?

Refinement is of parameters against $Y_o - Y_c$, where Y_c is based on the current model. If the model is too simple, Y_c cannot be computed to correspond to Y_o, so $Y_o - Y_c$ must be incorrect. The remaining parameters may take on invalid values. R should decrease as the model has more degrees of freedom. Bond-length s.u.s are related to the 'goodness of fit', and will decrease if the residual $(Y_o - Y_c)$ drops more rapidly than the number of degrees of freedom, $(n-m)$. Note that, if too many new parameters are introduced into a refinement, the analysis becomes 'under–determined', and the parameters may take on unrealistic values. Chemical or physical restraints may be useful.

24. What is the effect on *R* and bond-length s.u.s of using block diagonal refinement?
Bond-length s.u.s depend on atomic variances *and covariances*. Block diagonal refinements exclude the covariances, so that molecular parameter s.u.s are usually underestimated. Note that, even if the refinement is correctly performed, geometry programs may leave out the covariances. Block diagonal refinement is more prone to falling into false minima.

25. What is the effect on *R* and bond-length s.u.s of missing solvent molecules?
As in 23 above, an inappropriate or incomplete model will adversely affect the remaining parameters. If solvent can be modelled by discrete atoms (i.e. is not seriously disordered), then that sort of model may be used. If the disorder is more severe, then multiply disordered pseudo-atoms may be used to try to model the diffuse electron density in the disordered region (as in SHELXL97), or the discrete Fourier transform of the region may be computed and added to the values of F_c computed from the atomic model. The important thing is to add into Y_c as much as is reasonable, since refinement is against $Y_o - Y_c$, not just simply Y_o.

Matrix

26. What are the design matrix and the normal matrix?
The design matrix encodes the relationship between the unknown parameters and the conditions at which observations are made. In crystallography it is difficult to predict in advance which observations will be most useful, so it is usual to measure all 'observable' reflections. This usually means up to the diffractometer's θ limit for Cu radiation, but the operator must generally choose a limit for Mo radiation. Don't stop collecting data just because you 'have enough' reflections. You don't yet know which will be important. The normal matrix is a transform of these data, and shortcomings in the choice of reflections to measure (which may also include the consequences of the choice of a wrong crystal system, or pseudo-symmetry) become apparent in processing this matrix.

27. What are some uses in crystallography of the eigenvalues and eigenvectors of a symmetric matrix?
Ellipsoids are common features in crystallography (e.g. atomic-displacement parameters, formerly known as anisotropic temperature factors). In their normal form (arbitrarily orientated and evaluated with respect to a non-orthogonal co-ordinate system) they are difficult to visualize. The eigenvalues of the tensor representation of the ellipsoid are a measure of the principal axes, and the eigenvectors are a measure of the orientation of these axes. A rare use (found in some versions of ORFLS, and in CRYSTALS) is in the inversion of the normal matrix. More common uses are in the solution of the equations in DIFABS, and in TLS analysis. Both of these procedures involve the analysis of systems in which the user may be unaware of exactly which variables are important. Matrix inversion involving selection of eigenvalues often automatically selects the most appropriate parameters for evaluation.

28. What is the 'riding' model in parameter refinement?
'Riding' refinement is usually associated with the refinement of hydrogen atoms. In the crudest implementations the associated heavy-atom co-ordinate shifts are computed, and the same shifts applied to the hydrogen atoms. (Sketch this, and deduce the effect on bond angles.) In better implementations, the derivatives of the heavy atom and the hydrogen atom are added together, and composite shifts computed and applied to the parameters, so that all riding atoms contribute to the computed shift. However, the concept can be applied to any parameter combinations, so that it is simple to construct 'fragment' anisotropic displacement parameters, in which all the atoms in a fragment have the same U_{aniso} values. Imagine some other situations, including ones in which the derivatives are inverted in sign before being added into the normal equations.

29. How can the problem of pseudo-doubled cells be ameliorated?
If, by accident, a cell parameter is taken to be twice its true value, then on solution of the structure two motifs will be found lying parallel to that direction, with co-ordinates differing by exactly ½. Refinement will be difficult because the 'independent' parameters are in fact 100% correlated. The situation should become clear because of the absence of reflections in the odd layers perpendicular to that direction. Situations

exist in which the reflections in these planes are not absent, but just very weak, indicating that the corresponding atoms are not separated by exactly half a cell. Refinement may be possible using eigenvalue filtering, or by transforming the co-ordinate system, $\mathbf{x}' = \mathbf{x}_1 + \mathbf{x}_2, \mathbf{x}'' = \mathbf{x}_1 - \mathbf{x}_2$, and refining the transformed co-ordinates. Sketch a contour of constant minimization function versus two uncorrelated parameters, and versus two highly correlated parameters, and indicate how the correlation may be reduced.

Errors in data

Discuss:

30. the symptoms of applying the Lp correction twice, or not at all;
($L = 1/\sin(2\theta)$, $p = \frac{1}{2}(1 + \cos^2(2\theta))$.) Sketch the Lp correction versus θ, and $\langle I \rangle$ versus θ. Sketch f, an atomic scattering factor, and $\exp(-U \sin\theta)$ for small U.

31. the effect of neglecting reflections with negative net intensity;
Goodness-of-fit $S^2 = \Sigma(w\Delta^2)/(n - m)$, n = number of observations, m = number of variables. Sketch histogram of number of reflections versus $I/\sigma(I)$ (often masses of weak reflections). What about weights of weak reflections? (Generally very small.) Very negative reflections are probably outliers.

32. the effect on structural parameters of ignoring absorption effects;
Refinement is of parameters against $Y_o - Y_c$. If there is a systematic error in Y_o then the model will be modified to try to model this error. This will only be valid if the model contains appropriate parameters (e.g. DIFABS), otherwise other parameters may be perturbed in an unpredictable way.

33. the effect of ignoring the θ-dependent component of the absorption correction;
Sketch $I(= I_o \exp(-\mu t))$ and compare with isotropic displacement parameter sketch in 1 above. Sketch absorption correction versus $\sin\theta$ for spherical samples and relate to U_{iso}.

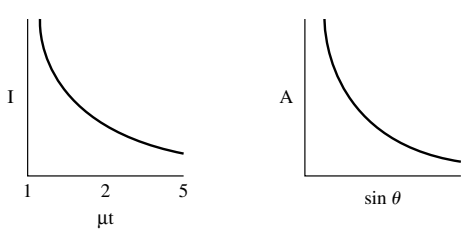

Failure to apply the correction makes low-angle reflections too weak (i.e., high-angle too strong after scaling) which depresses the temperature factors.

34. the errors introduced by ignoring anomalous dispersion;
Even in centrosymmetric structures there is a phase shift (phase angles not exactly 0 or 180°) so parameters are incorrect if f'' is ignored. Particularly important are polar space groups. Note that if f' or f'' are large and omitted, the adps will be affected, possibly leading to failure of the Hirshfeld test.

35. 'robust–resistant' refinement.
Robust implies that the refinement produces useful estimates of the parameter variances for a wide range of (possibly unknown) distributions of errors in the data. Resistant implies that the refinement is insensitive to a concentration of errors in a small subset of the data. Robust/resistant refinements converge to a 'best' model.

Origin fixing

36. Give example of space groups with origins not fixed in 1, 2 and 3 dimensions.
See also 34 above. $P4_1$, Pm, $P1$.

37. Give three methods of fixing the origin in $P1$ in least squares.

a) Hold all three co-ordinates of one atom (preferably heavy) unrefined.

b) Keep the centre of gravity of the structure fixed (i.e. $\Sigma(\Delta\mathbf{x}) = 0$).

c) Invert the normal matrix using eigenvalue filtering.

38. How do these three methods affect atomic parameter s.u.s?

a) The unrefined atom has zero s.u.s, other atoms have increased s.u.s. There will be significant covariances between atoms.

b) The s.u.s are correctly distributed, and have the correct covariances between directions and between atoms.

c) As in b.

39. How do these three methods affect molecular parameter (e.g. bond length) s.u.s?

a) Molecular parameter s.u.s will be correct if (and only if) the full covariance matrix is used in their computation.

b) As in 38b above, but the reduced covariance terms mean that 'fair' s.u.s may sometimes be computed from co-ordinate s.u.s alone.

c) As in 38c above.

Centres of symmetry

40. What is the effect of refining a centrosymmetric structure in a non–centrosymmetric space group?
There is always high correlation between related atoms, which will lead to a singular or near-singular matrix. Molecular parameters (bond lengths) are often 'curious'.

41. Why are pseudo-symmetric structures difficult to refine?
There is high correlation between related parameters, so that the matrix inversion is unreliable, and parameters may shift to unreasonable but complementary values. See 29 above.

Refinement

42. Discuss uses in refinement of a weighting scheme that is a direct function of $(\sin\theta)/\lambda$.
A scheme that is a direct function of θ will upweight the high-angle data, which depends on 'core' electrons, and may thus position heavy atoms so that difference Fourier syntheses reveal hydrogen atoms or anomalous electron-density distributions.

43. Discuss uses in refinement of a weighting scheme that is an inverse function of $(\sin\theta)/\lambda$.
The low-order reflections depend only on the gross details of the structure, so that this weighting scheme may help in the initial development of a structure.

44. Under what conditions will F and F^2 refinements converge to the same parameter values?
Only if the weights used are suitable ($w' = w/2F^2$). However, it is worth asking why we should aim for the same minimum.

45. What is refinement using rigid-body CONSTRAINTS?
The relative spatial disposition of the atoms in the group cannot change, but the group may translate or rotate as an inflexible body.

46. List some uses of this technique.
The refinement of structures containing rigid subunits, in particular during early development of large structures, or when the X–ray data are sparse or of poor quality. To accelerate the initial stages of routine refinement. Often used in powder data refinement. The normal matrix is reduced in size, but the chain rule must be used in computing group derivatives.

47. List some problems with this technique.
The rigid groups cannot flex during the refinement, so they cannot adapt to fine changes in structure due to chemical or physical effects.

48. What is refinement using rigid-body RESTRAINTS?
Estimates are made of the likely values for molecular parameters (bond lengths, angle, planarity, etc.) together with estimates of possible deviations from these values, and these estimates are used as supplemental observations to guide the refinement.

49. List some uses of this technique.
As in 46 above, with the addition that more or less flexibility can be built into the group depending on the target molecular parameters and their estimated validity. Totally rigid bodies can be simulated by sufficient very tightly defined restraints.

50. List some problems with this technique.
Almost none, except that the size of the normal matrix is not reduced. If the restraints are assigned very small uncertainties, derived parameter uncertainties may be anomalously small. PLATON will spot this.

51. What are similarity restraints, and how are they used?
Similarity restraints require that atomic or molecular parameters in a structure should have similar values, but without knowing in advance what these values are; e.g. displacement parameters of bonded atoms should have similar values, and bonds in similar environments should have similar lengths.

Absolute configuration

52. Give three methods for the determination of absolute configuration.

a) Comparing the signs of the differences of very carefully measured Friedel pairs of reflections with the computed Bijvoet differences.

b) Comparing the weighted R factor of a refined structure with that of its opposite enantiomer.

c) Refinement of the Rogers η parameter, which should take the value 1 if the model has the correct hand, otherwise -1.

d) Refinement of the Flack 'enantiopole' parameter, which has the value 0 if the model is of the correct hand, otherwise 1.

53. Is inverting the co-ordinates of all atoms always sufficient to correct an error in enantiomer assignment?
No. There are pairs of space groups in which the space group must also be changed if the hand of the model is changed (e.g. $P4_1$ and $P4_3$).

Standard uncertainties

54. Why can we NOT compute reliable molecular parameter s.u.s from atomic parameter s.u.s only?
The s.u.s on x, y and z do not contain information about the correlation between the uncertainties for the parameters of a single atom, nor for the correlation between atoms. In the event of correlation (which is inevitable in non–orthogonal unit cells, in the case of pseudo-symmetry and polar space groups, and when constraints or restraints are used), molecular parameter s.u.s are miscalculated.

Chapter 14

1. As part of an undergraduate practical class a student was asked to record powder diffraction patterns of the compounds BaS and SrSe, both of which have the rock salt structure. Ionic radii (Å) are Ba 1.49, Sr 1.32, S 1.70, Se 1.84. Unfortunately, the student has forgotten to label the patterns (which are shown in Fig. 14.13). Can you help?
The first thing to notice is that the ionic radii are such that the two compounds will have similar cell parameters. For rock salt you would expect the cubic cell parameter to be twice the sum of the ionic radii (6.38 and 6.32 Å). Given the uncertainty in additivities of ionic radii, peak positions in the powder pattern will not help desperately. You could calculate where you would expect reflections for these cell parameters and therefore index the powder pattern. $d^2_{hkl} = a^2/(h^2 + k^2 + l^2)$. The peaks expected (for a cell parameter of 6.359 Å and F centring) are:

h	k	l	d_{hkl} (Å)	2θ(°)
1	1	1	3.67137	24.22268
0	0	2	3.17950	28.04113
0	2	2	2.24825	40.07337
3	1	1	1.91731	47.37645
2	2	2	1.83569	49.62173
0	0	4	1.58975	57.96472
3	3	1	1.45885	63.74295
0	4	2	1.42192	65.60332
4	2	2	1.29803	72.80276
5	1	1	1.22379	78.01710
3	3	3	1.22379	78.01710
0	4	4	1.12412	86.50952

Alternatively, you could start with the experimental data and index the pattern by hand (easiest way is to make a table of $1/d^2$ values and look for ratios to determine $h^2 + k^2 + l^2$). The table below contains the relevant numbers. As the first peak is the 111 reflection $1/d^2$ ratios should be multiplied by 3.

d_{obs}	d^2	$1/d^2$	/0.074	×3	h^2	k^2	l^2	h^2+ k^2+l^2
3.6708	13.475	0.07421	1.000	3.000	1	1	1	3
3.1792	10.107	0.09893	1.333	3.999	0	0	2	4
2.2485	5.0560	0.19778	2.665	7.995	0	2	2	8
1.9175	3.6768	0.27196	3.664	10.99	3	1	1	11
1.8355	3.3693	0.29679	3.999	11.99	2	2	2	12
1.5895	2.5266	0.39578	5.333	15.99	0	0	4	16
1.4588	2.1283	0.46984	6.331	18.99	3	3	1	19
1.4219	2.0217	0.49460	6.664	19.99	0	4	2	20
1.2979	1.6847	0.59354	7.998	23.99	4	2	2	24
1.2239	1.4979	0.66758	8.995	26.98	5	1	1	27
1.1240	1.2635	0.79140	10.66	31.99	0	4	4	32

In the case of SrSe the only peaks observed are 002, 022, 222, 044, 042, 422, 044. One could therefore index the whole pattern on a primitive cubic cell of $a = 3.18$ Å. This is an example of how X-rays can give misleading answers. This is because the scattering factors for Sr^{2+} (atomic number 38) and Se^{2-} (atomic number 34) are essentially identical. You can explain this by sketching a plan view of the rock salt structure and then shading both atoms the same colour ('colour-blind X-rays'). You could also work through structure-factor calculations, which for rock salt end up as:

h, k, l all even, $F_{hkl} = 4(f^+ + f^-)$

h, k, l all odd, $F_{hkl} = 4(f^+ - f^-)$

1 odd, 2 even or 2 even, 1 odd, $F_{hkl} = 0$.

This shows directly why certain reflections disappear if the scattering power of cation (f^+) and anion (f^-) are identical.

2. The structure of $MnRe_2O_8$ has been reported in space group $P\bar{3}$ with unit cell parameters $a = b = 5.8579$ Å, $c = 6.0665$ Å and fractional co-ordinates as shown in Table 14.3 (next page). Draw a plan view of the structure and determine the co-ordination environment of Mn and Re atoms. Given bond distances of 2.179 Å for Mn1–O1, 1.704 Å for both Re1–O1 and Re1–O2 and R_{ij} values of 1.79 and 1.97 Å for Mn(II)/Re(VII), determine bond-valence sums for Mn and Re. Do you think the published structure is correct? What error could have been made when solving/refining the structure?
The figure opposite shows views of the structure. The first figure is the published structure viewed down c. The other two are views of what the true structure

probably is. $MnRe_2O_8$ can be described as MnO_6 octahedra, which share corners with ReO_4 tetrahedra. It might help to think of an octahedron in terms of two staggered triangles (one above and one below the plane of the metal). The octahedra are then generated directly by the $\bar{3}$ site on which Mn sits.

	x	*y*	*z*
Mn1	0	0	0
Re1	⅓	⅔	0.2891
O1	0.135	0.349	0.206
O2	⅓	⅔	0.57

Literature co-ordinates of $MnRe_2O_8$

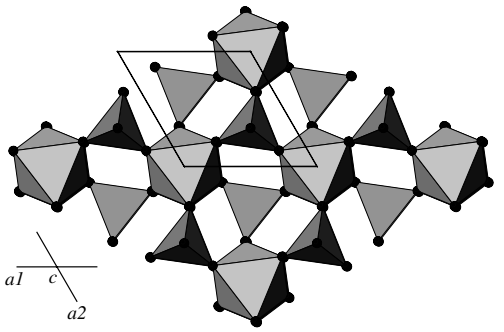

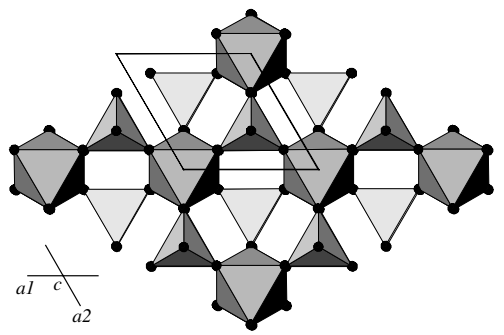

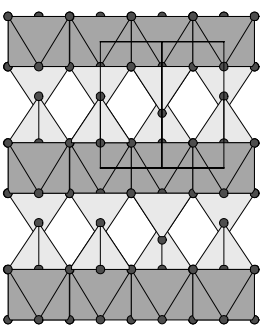

Bond-valence sums for the 4 atoms are:

Mn 2.1

Re 8.2

O1 2.4

O2 2.1

Clearly these values are not particularly good. This is a classic case in which the oxygen positions are hard to determine in the presence of heavy-metal atoms, particularly as this structure was determined from laboratory X-ray data. One problem you might notice with a half-decent sketch is that the published structure is very close to having more symmetry than expected for $P\bar{3}$. In particular, youshould be able to spot an approximate mirror plane (in the 2nd figure you have rectangles between polyhedra, not parallelograms). In fact, X-ray/neutron studies on closely related materials have shown that their symmetry is $P\bar{3}m1$. This would require O1 to be on the mirror plane (an x, $2x$ type position). It is not far off that in the co-ordinate table above! In the related better-characterized structures this oxygen atom is found at (0.166, 0.332, z). $P\bar{3}m1$ diagram below.

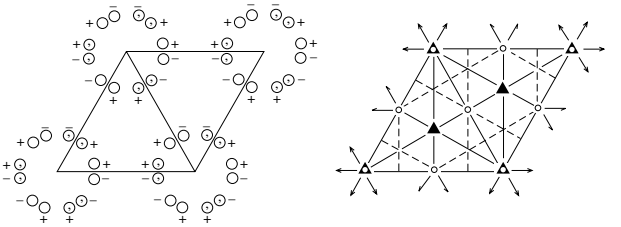

3. As described in Case history 2, the structure of $Mo_2P_4O_{15}$ was originally described using an incorrect unit cell with $a = 8.3065$, $b = 6.5154$, $c = 10.7102$ Å, $\beta = 106.695°$, $V = 555.20$ Å^3. From the information below calculate the transformation matrix required to convert to the correct cell. Calculate the volume of the true cell.

A classic transformation matrix problem. From the reflection lists given it should be clear to the reader that there are often lots of possible choices for which reflections might be equivalent – especially if one cell is large so reflections are closely spaced in d. Here, it should be obvious from the intensities which reflections are equivalent for the first two reflections. If you notice that there is a 2:6:1 approximate relationship between the supercell reflection intensities you should be able to decide that (4,6,−6) is equivalent to (2,2,−2) rather than

```
Strong Supercell Reflections
-3 -3  1 d = 5.0378 2-th = 17.5904 I =  352.05 sigI =  7.90
-2  3 -4 d = 4.0281 2-th = 22.0493 I =  965.51 sigI = 28.70
 4  6 -6 d = 2.4436 2-th = 36.7491 I =  152.14 sigI =  4.46
Selected Subcell Reflections
 0  0  2 d = 5.1294 2-th = 17.2739 I =  154.96 sigI =  6.38
-1 -1  0 d = 5.0531 2-th = 17.5367 I = 2356.06 sigI = 15.64
-1  0  2 d = 5.0172 2-th = 17.6633 I =  392.77 sigI =  2.91
-2  0  1 d = 4.1308 2-th = 21.4946 I =    1.98 sigI =  0.25
 0  1 -2 d = 4.0365 2-th = 22.0030 I = 6739.94 sigI = 17.90
-1  1  2 d = 3.9811 2-th = 22.3129 I = 1233.35 sigI =  5.97
-3  0  3 d = 2.4669 2-th = 36.3908 I =    0.55 sigI =  0.30
 3  1  0 d = 2.4580 2-th = 36.5273 I = 1989.42 sigI = 11.78
 2  2 -2 d = 2.4507 2-th = 36.6401 I = 1048.92 sigI =  9.43
 3  0  1 d = 2.4059 2-th = 37.3473 I =    0.11 sigI =  0.29
```

Transformation matrix data for Exercise 3.

(3,1,0). The matrices can then be set up as **C** = **AB** and solved for **A**, i.e. $\mathbf{CB}^{-1} = \mathbf{A}$.

$$\begin{pmatrix} 4 & -3 & -2 \\ 6 & -3 & 3 \\ -6 & 1 & -4 \end{pmatrix} = A \begin{pmatrix} 2 & -1 & 0 \\ 2 & -1 & 1 \\ -2 & 0 & -2 \end{pmatrix}$$

Determinant of $\mathbf{B} = 2$

Matrix of cofactors of **B** is:

$$\begin{pmatrix} 2 & -2 & -2 \\ 2 & -4 & -2 \\ -1 & 2 & 0 \end{pmatrix}.$$

$\mathbf{B}^{-1}$ is:

$$\begin{pmatrix} 1 & -1 & -0.5 \\ 1 & -2 & -1 \\ -1 & 1 & 0 \end{pmatrix}.$$

$\mathbf{CB}^{-1} = \mathbf{A}$

$$\begin{pmatrix} 4 & -3 & -2 \\ 6 & -3 & 3 \\ -6 & 1 & -4 \end{pmatrix} \begin{pmatrix} 1 & -1 & -0.5 \\ 1 & -2 & -1 \\ -1 & 1 & 0 \end{pmatrix} = \begin{pmatrix} 3 & 0 & 1 \\ 0 & 3 & 0 \\ -1 & 0 & 2 \end{pmatrix}.$$

Thus:

$$a_{\text{sup}} = 3a_{\text{sub}} + c_{\text{sub}}$$

$$b_{\text{sup}} = 3b_{\text{sub}}$$

$$c_{\text{sup}} = -a_{\text{sub}} + 2c_{\text{sub}},$$

leading to a picture like the one below. The determinant of the transformation matrixis 21, allowing the volume of the new cell to be calculated directly from that of the subcell. Alternatively, it could be verified from $V = abc \sin\beta$.

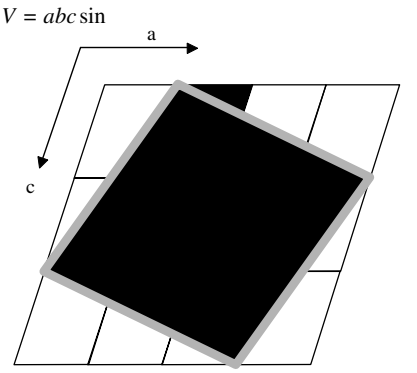

4. A layered form of SiP_2O_7 containing corner-linked SiO_6 tetrahedra and P_2O_7 tetrahedra has been reported in space group $P6_3$ with $a = 4.7158$, $c = 11.917$ Å and fractional co-ordinates as shown in Table 14.4. Sketch the structure. Bond distances are 3 × Si–O1 1.768 Å, 3 × Si–O3 1.701 Å, 3 × P2–O1 1.476 Å, P2–O2 1.525 Å, P1–O2 1.585 Å and 3 × P1–O3 1.481 Å. Do you think this structure is correct? See Fig. 14.14 for space group symmetry.

From the co-ordinates you should realize that P1–O2–P2 lies along the 3-fold axis in the structure. As such,

the P–O–P bond angle has to be linear. However, P–O–P linkages should be bent, like the water molecule H_2O, because of lone pairs on the O atom. It is therefore unlikely that the published structure is completely correct. Either the authors could have missed a superstructure (which would allow P–O–P to bend) or the oxygen is disordered around the published position.

Bond-valence sums probably are not really necessary here but are:

Si 4.47

P1 5.23

P2 5.48

O1 2.09

O2 2.29.

5. **$RbMn[Cr(CN)_6].xH_2O$ is a framework material related to the Prussian Blues. What methods would you use to probe its structure? What are the potential problems of each approach?**
The material's structure can be thought of as being like WO_3 /perovskite (see figures in Chapter 14) but with CN groups linking the Mn- and Cr-centred octahedra. Cr and Mn ($Z = 24/25$) and C/N ($Z = 6/7$) will be very hard to distinguish by X-ray diffraction, particularly if there is any disorder. Problem of CN versus NC bonding. Neutrons might help (Mn/Cr/C/N have neutron scattering lengths of $-0.373/0.3635/0.6646/0.936 \times 10^{-14}$ m); however, if you had a powder you would have to be careful of the xH_2O as H gives large incoherent scattering. You might want to think about other analytical methods.

Chapter 15

1. **The following (top of the next page) was given in the output of CELL_NOW after indexing a twinned crystal. The twin law is described as a two-fold rotation about the reciprocal lattice vector (1 0 0) and the direct lattice vector [3 0 1] (which is parallel to [1 0 ⅓]). Show that these are equivalent descriptions of the same vector.**
Direct and reciprocal lattice vectors are transformed to each other using the metric tensors:
   - to transform reciprocal lattice axes to direct lattice axes use **G** (i.e. $\mathbf{A} = \mathbf{GA}^*$);
   - to transform reciprocal lattice vector components to direct lattice vector components use $\mathbf{G}^*$ (formally $\mathbf{G}^{*T}$, but $\mathbf{G}^*$ is symmetric);
   - to transform direct lattice axes to reciprocal lattice axes use $\mathbf{G}^*$ (i.e. $\mathbf{A}^* = \mathbf{G}^*\mathbf{A}$);
   - to transform direct lattice vector components to reciprocal lattice vector components use **G**.

$$\mathbf{G} = \begin{pmatrix} 6.05^2 & 6.05\times5.34\times\cos90 & 6.05\times7.24\times\cos113.5 \\ 6.05\times5.34\times\cos90 & 5.34^2 & 5.34\times7.24\times\cos90 \\ 6.05\times7.24\times\cos113.5 & 5.34\times7.24\times\cos90 & 7.24^2 \end{pmatrix} = \begin{pmatrix} 36.6 & 0 & -17.6 \\ 0 & 28.5 & 0 \\ -17.6 & 0 & 52.4 \end{pmatrix}.$$

Here, it is probably simplest to transform the direct vector to the reciprocal as this involves **G**, and we do not have to deal with reciprocal lattice constants.

$$\begin{pmatrix} 36.6 & 0 & -17.6 \\ 0 & 28.5 & 0 \\ -17.6 & 0 & 52.4 \end{pmatrix} \begin{pmatrix} 3 \\ 0 \\ 1 \end{pmatrix} = \begin{pmatrix} 92.2 \\ 0 \\ -0.4 \end{pmatrix} \sim \begin{pmatrix} 1 \\ 0 \\ 0 \end{pmatrix}.$$

Hence, the [3 0 1] direct lattice direction is the same as the (1 0 0) reciprocal lattice direction, as shown in the CELL_NOW output. Note that when specifying a direction the length of the vector is immaterial, and the components can be multiplied by any common factor.

2. **A structure has been solved in $Pna2_1$, but symmetry checking shows that the correct space group is *Pnma*. What matrices should be used to transform the reflection indices and the co-ordinates?**
In going from $Pna2_1$ to *Pnma* the *a*-glide changes from being perpendicular to *b* to being perpendicular to *c*, while the *n*-glide remains perpendicular to the *a*-axis. Therefore, the required transformation will do something like this:

$$\mathbf{a}\ (Pnma) = \mathbf{a}\ (Pna2_1)$$
$$\mathbf{b}\ (Pnma) = \mathbf{c}\ (Pna2_1)$$
$$\mathbf{c}\ (Pnma) = \mathbf{b}\ (Pna2_1),$$

for which the matrix would be

$$\begin{pmatrix} 1 & 0 & 0 \\ 0 & 0 & 1 \\ 0 & 1 & 0 \end{pmatrix}.$$

However, this matrix has a determinant of -1, meaning that we would have changed from a right-handed axis set to a left-handed one, and this is not allowed. The problem can be solved by simply converting one of the entries 1 into -1:

$$\begin{pmatrix} 1 & 0 & 0 \\ 0 & 0 & 1 \\ 0 & -1 & 0 \end{pmatrix}.$$

The matrices that transform direct cell axes and Miller indices are always the same.

```
Cell for domain 2:  6.055   5.340   7.235   89.82  113.51  90.11
Figure of merit: 0.432  %(0.1): 36.1   %(0.2): 38.9 %(0.3): 49.7
Orientation matrix:  0.03526080  0.18122675  -0.01073746
                    -0.17602921  0.03347900  -0.07420789
                    -0.01420090  0.03333605   0.13075234
Rotated from first domain by 179.9 degrees about
reciprocal axis 1.000 -0.001 0.001 and real axis
1.000 -0.001 0.334
Twin law to convert hkl from first to this domain
(SHELXL TWIN matrix):
 0.999  -0.002   0.668
-0.003  -1.000  -0.002
 0.002   0.003  -0.999
```

CELL_NOW output for Exercise 1.

(ii) To transform co-ordinates the inverse transpose of this matrix is needed. The inverse is

$$\begin{pmatrix} 1 & 0 & 0 \\ 0 & 0 & -1 \\ 0 & 1 & 0 \end{pmatrix},$$

and so the required co-ordinate transformation is just the same as the axis transformation in this case.

3. Two metal–oxygen bond lengths were found to be 2.052(5) and 2.032(4) Å. Are these significantly different?

$$\frac{2.052 - 2.032}{\sqrt{0.005^2 + 0.004^2}} = 3.1.$$

Since this is > 3, then the difference could be significant. However, based on experience of numerous re-determinations of the same structure, it is generally thought that s.u.s are underestimated. Strict adherence to the '3σ-rule' is dangerous, and one might look for a 5σ difference before being really confident that a difference is real.

4. Oxalyl chloride is monoclinic, with cell dimensions a = 6.072(4), b = 5.345(3), c = 7.272(4) Å, β = 113.638(7)°. The fractional co-ordinates of the C and O atoms are:

O(1)	**0.3854(2)**	**0.2109(2)**	**0.3029(2)**
C(1)	**0.5256(3)**	**0.1173(2)**	**0.4497(2).**

Evaluate the C(1)–O(1) distance. Do not attempt to evaluate the s.u.

Using the metric tensor method:

$(\Delta x, \Delta y, \Delta z) = (-0.140.09 - 0.15).$

$$\begin{pmatrix} -0.14 & 0.09 & -0.15 \end{pmatrix} \begin{pmatrix} 36.8 & 0 & -17.7 \\ 0 & 28.5 & 0 \\ -17.7 & 0 & 52.8 \end{pmatrix} \begin{pmatrix} -0.14 \\ 0.09 \\ -0.15 \end{pmatrix}$$

$= 1.397$

$(1.397)^{1/2} = 1.18$Å.

5. Which of these symmetry elements make a four-membered MLML ring strictly planar? In each case, how many bond lengths are independent?

a) a centre of symmetry;

b) a two-fold axis normal to the mean plane of the ring;

c) a two-fold axis through the two M atoms;

d) a mirror plane through the M atoms but not through the L atoms;

e) a mirror plane through all four atoms.

a) Planar; 2
b) Non-planar; 2
c) Planar; 2
d) Non-planar; 2
e) Planar; 4

6. A six-co-ordinate atom lies on an inversion centre. How many independent bond lengths and angles are there around this atom?
3 lengths (opposite ones are equal); three angles, all the others are equal to 180–these or exactly 180°.

7. If an atom resides on a mirror plane perpendicular to [1 0 0] (i.e. the a-axis) what constraints should be applied to its anisotropic displacement parameters?

$$\begin{pmatrix} -1 & 0 & 0 \\ 0 & 1 & 0 \\ 0 & 0 & 1 \end{pmatrix} \begin{pmatrix} \beta_{11} & \beta_{12} & \beta_{13} \\ \beta_{12} & \beta_{22} & \beta_{23} \\ \beta_{13} & \beta_{23} & \beta_{33} \end{pmatrix} \begin{pmatrix} -1 & 0 & 0 \\ 0 & 1 & 0 \\ 0 & 0 & 1 \end{pmatrix}$$
$$= \begin{pmatrix} \beta_{11} & -\beta_{12} & -\beta_{13} \\ -\beta_{12} & \beta_{22} & \beta_{23} \\ -\beta_{13} & \beta_{23} & \beta_{33} \end{pmatrix}.$$

Hence, $\beta_{12} = \beta_{13} = 0$: two axes must lie in the mirror plane.

8. **Discuss the placement of H-atoms on (i) terminal hydroxyl groups; (ii) ligating water molecules; (iii) unco-ordinated molecules of water of crystallization.**
One answer to all parts is to find the H atoms in a difference map, or do a neutron-diffraction experiment. These may not be possible, of course. Another option is not to place the offending H atoms at all. Otherwise, geometrical considerations have to be used, but this still leaves the orientations of O–H bonds ambiguous, apart from the expected bond angles at O. For a terminal OH group, positions could be considered that make it staggered with respect to whatever is bonded to it. Possible hydrogen-bonding interactions should also be investigated in each case, and these may help to define a unique orientation.

Chapter 16

1. **Show that (16.1) and (16.2) can be derived from Equations (16.3) and (16.5) if unit weights are used.**
Unit weights mean $w_i = 1$ always. Remember that $\sum_{i=1}^{N} 1 = N$.

2. **The data in Table 16.4 (below) are H…O distances taken from structures determined with neutron diffraction, containing a certain type of hydrogen bond.**

x_i	$\sigma(x_i)$
1.814	0.0015
1.844	0.003
1.728	0.003
1.832	0.003
2.121	0.003
1.997	0.0075
1.808	0.0075
1.833	0.009
1.739	0.009
1.772	0.009
1.742	0.0105
1.877	0.012
1.948	0.012

(a) Calculate the weighted value of χ^2 and χ^2_{red} using $w_i = 1/\sigma^2(x_i)$.
From the table on page 376 $\chi^2 = 11245$. The number of degrees of freedom is $13 - 1 = 12$, so $\chi^2_{\text{red}} = 937$.

(b) Is calculation of a mean justified for these data? Discuss your answer in terms of the likely effects of environmental factors on hydrogen bonds.
937 is a long way from 1.0, and so the data are not drawn from the same parent distribution, and environmental effects are important. This is expected as H-bond distances are likely to be strongly dependent on 'environmental effects' such as the pK_a of the HX group.

(c) Your supervisor looks blank when you tell him about χ^2, and says that you must calculate an average. What standard deviation should you quote?
The mean is $24.055/13 = 1.85$. $\sigma^2 = 0.154/12$, so $\sigma = 0.11$.

3. **The data in Table 16.5 (copied here) were measured at points x giving measured values y.**

x	y
1	7.1
2	34.9
3	111.2
4	258.7

(a) Fit these data to an equation of the form $y = a + bx^3$, finding the values of a and b by least squares.
The least-squares equations are:

$$\begin{pmatrix} 1 & 1 \\ 1 & 8 \\ 1 & 27 \\ 1 & 64 \end{pmatrix} \begin{pmatrix} a \\ b \end{pmatrix} = \begin{pmatrix} 7.1 \\ 34.9 \\ 111.2 \\ 258.7 \end{pmatrix}$$
$$\begin{pmatrix} 4 & 100 \\ 100 & 4890 \end{pmatrix} \begin{pmatrix} a \\ b \end{pmatrix} = \begin{pmatrix} 411.9 \\ 19845.5 \end{pmatrix}$$
$$\begin{pmatrix} a \\ b \end{pmatrix} = \begin{pmatrix} 0.5115 & -0.01046 \\ -0.01046 & 0.000418 \end{pmatrix} \begin{pmatrix} 411.9 \\ 19845.5 \end{pmatrix} = \begin{pmatrix} 3.101 \\ 3.995 \end{pmatrix}.$$

(b) Work out an R factor. Hint: The crystallographic R factor is

$$R = \frac{\Sigma|F_o - F_c|}{\Sigma|F_o|}.$$

See second table on the next page.

$x(N=3)$	σ	$1/\sigma^2$	x/σ^2	$(x-1.847)^2/\sigma^2$	$(x-1.85)^2$
1.814	0.0015	444 444	806 222	484.00	0.001296
1.844	0.0030	111 111	204 889	1.00	0.000036
1.728	0.0030	111 111	192 000	1573.44	0.014884
1.832	0.0030	111 111	203 556	25.00	0.000324
2.121	0.0030	111 111	235 667	8341.78	0.073441
1.997	0.0075	17 778	35 502	400.00	0.021609
1.808	0.0075	17 778	32 142	27.04	0.001764
1.833	0.0090	12 346	22 630	2.42	0.000289
1.739	0.0090	12 346	21 469	144.00	0.012321
1.772	0.0090	12 346	21 877	69.44	0.006084
1.742	0.0105	9 070	15 800	100.00	0.011664
1.877	0.0120	6 944	13 035	6.25	0.000729
1.948	0.0120	6 944	13 528	70.84	0.009604
24.055		**984 441**	**1 818 316**	**11 245**	**0.154045**

Results for Exercise 2a.

x	y_{calc}	y_{obs}	$\lvert y_c - y_o\rvert$	$\lvert y_c - y_o\rvert^2$
1	7.096	7.1	0.004	1.6×10^{-5}
2	35.061	34.9	0.161	0.02592
3	110.966	111.2	0.234	0.05476
4	258.781	258.7	0.081	6.561×10^{-3}
		411.9	**0.48**	**0.087254**

$R = 0.48/411 = 0.0012$ or 0.12%.

(c) Work out the standard uncertainties of a and b.
The variances are

$$\sigma^2(a) = \frac{0.0873}{4-2}0.5115 = 0.0223$$
$$\sigma^2(b) = \frac{0.0873}{4-2}0.000418 = 1.824\times10^{-5}$$
$$a = 3.10(15) \text{ and } b = 3.995(4).$$

Notice that b is more precisely determined than a because it is multiplied by a large number (x^3). You may like to consider the precision of H-atom parameters after refinement with X-ray data.

(d) For a particular application the quantity $c = a + b^2$ is important. Compare the standard uncertainties in c obtained if covariance terms are included or excluded.

Note: For a function $f(x_1, x_2, x_3, \ldots x_n)$ the full propagation of error formula is

$$\sigma^2(f) = \sum_{i,j=1}^{N} \frac{\partial f}{\partial x_i} \cdot \frac{\partial f}{\partial x_j} \cdot \mathrm{cov}(x_i, x_j),$$

where $\mathrm{cov}(x_i, x_i)$ are variances $[\sigma^2(x_i)]$, and $\mathrm{cov}(x_i, x_j)$ are covariances.

$$c = a + b^2$$
$$\frac{\partial c}{\partial a} = 1$$
$$\frac{\partial c}{\partial b} = 2b$$
$$\sigma^2(c) = \left(\frac{\partial c}{\partial a}\right)^2 \sigma^2(a) + \left(\frac{\partial c}{\partial b}\right)^2 \sigma^2(b) + 2\left(\frac{\partial c}{\partial a}\right)\left(\frac{\partial c}{\partial b}\right)\mathrm{cov}(a,b)$$
$$\mathrm{cov}(a,b) = \frac{0.0873}{4-2}(-0.01046) = -4.56\times10^{-4}$$

$$\sigma^2(c) = (0.15)^2 + (2\times3.995)^2(0.004)^2 + 2(3.995)(-4.56\times10^{-4})$$

$\sigma(c) = 0.13$ with the last covariance term and 0.15 without it.

4. **The following ALERT was issued by CHECKCIF after a refinement where restraints had been applied:**

```
732_ALERT_1_B Angle      Calc    105(4),
Rep     104.9(8)          5.00 su-Rat
N2    -O1    -H1   1.555   1.555   1.555.
```

What response might be given?
Restraints increase correlation between parameters, and so off-diagonal terms in the inverse normal matrix must be taken into account. CHECKCIF does not have access to these, though, and bases its calculation on the variances only.

5. **In a particular structure determination the bond angles in a nitrate anion were found to be 120.1(2), 119.4(2) and 119.5(2)°. What is the sum of the angles and its s.u.?**

$$\sigma^2(f) = \sigma^2(x_1) + \sigma^2(x_2) + \cdots .$$

The sum is therefore 359.0(4)°.

6. **Bond angles in a substituted cyclopropane ring are reported as 59.3(2), 59.6(2), 61.0(2) . What is the sum of the angles and its s.u.?**
180° with an uncertainty of exactly zero. The sum of the angles in a triangle must come to 180° – this question illustrates the danger of excluding correlations. Note that the angles in question 5 are also highly correlated (though the sum does not have to be exactly 360°, unless the group lies on an appropriate symmetry element), so the s.u. calculated by the simple formula is almost certainly over-estimated.

Chapter 17

1. **Graphite is a layered material that undergoes intercalation chemistry with alkali metals. The first two reflections in the powder diffraction patterns of graphite and a K intercalation compound were observed at 26.58/54.76° and 16.56/33.47° 2θ, respectively. Calculate *d*-spacings for each reflection and suggest *hkl* indices. Why are only certain classes of *hkl* reflections typically seen in powder diffraction patterns of these materials? How might you try to observe other reflections? ($\lambda = 1.54$ Å).**
d-Spacings should be 3.35 and 1.675 and 5.35/2.675 Å for graphite and the intercalation compound. Note that 26.6° is the setting angle you need for a graphite monochromator in powder diffraction (and therefore the angle that would appear in any *Lp* correction). You should be able to index the reflections as 001/002. In fact, graphite has space group $P6_3/mmc$ so the reflections are 002/004. Graphite will show extreme preferred orientation in a flat-plate reflection powder pattern as the plate-like crystals will lie with their *c*-axes perpendicular to the sample holder, meaning only (00*l*) reflections are seen. If you run a flat-plate transmission experiment you would see (*hk*0) reflections. It is essentially impossible to make a 'good' powder sample of a material like this. Capillary measurements or spray drying might help. Graphite also shows turbostratic disorder such that there is little order along the stacking axis. You therefore see broad, asymmetric peaks in the powder pattern.

2. **Figure 17.8 shows powder diffraction patterns of two inorganic materials recorded with $\lambda = 1.54$ Å. Index each and comment on their symmetry. Comment on any reflections you cannot index.**

d	$1/d^2$	ratio to peak 1	*h*	*k*	*l*	$h^2+k^2+l^2$	a_{calc}
3.83027	0.06816	1	1	0	0	1	3.8303
2.71812	0.13535	1.98574	1	1	0	2	3.8440
2.3363	***0.1832***	***2.6878***					
2.22507	0.20198	2.96327	1	1	1	3	3.8539
2.024	***0.2441***	***3.5812***					
1.92216	0.27066	3.97082	2	0	0	4	3.8443
1.71996	0.33804	4.95932	2	1	0	5	3.8459
1.57263	0.40434	5.93206	2	1	1	6	3.8521
1.36174	0.53928	7.91171	2	2	0	8	3.8516
1.28355	0.60698	8.90499	3	0	0	9	3.8507
1.2191	0.67285	9.87143	3	1	0	10	3.8551
1.1694	***0.7313***	***10.729***	***3***	***1***	***1***	***11***	***3.8784***
1.11232	0.80824	11.8577	2	2	2	12	3.8532

d	$1/d^2$	ratio x 3	*h*	*k*	*l*	$h^2+k^2+l^2$	a_{calc}
2.33633	0.1832	3	1	1	1	3	4.0466
2.02402	0.2441	3.99724	2	0	0	4	4.0480
1.16938	0.73129	11.9751	2	2	2	12	4.0509

This pattern is of Na_xWO_3, which is essentially cubic: $d_{hkl} = a/(h^2 + k^2 + l^2)^{1/2}$. You should produce a table of *d* and $1/d^2$ as above and divide each $1/d^2$ value by the value for the first peak (0.06816). This assumes the first peak is (100) and gives you values of $(h^2 + k^2 + l^2)$ for every other peak. You should be able to assign *hkl* values to give these sums. Note that 9 is given by (300) or (221); these peaks will overlap perfectly.

d	$1/d^2$	ratio	$4 \times$ ratio	h	k	l	$(h^2+k^2+l^2)$/ratio	a_{calc}
5.31987	1.03533	1.000	4.000	2	0	0	1.0000	10.6397
4.33397	0.5324	1.507	6.027	2	1	1	0.9955	10.6160
3.0619	0.10666	3.019	12.075	2	2	2	0.9938	10.6067
2.83559	0.12437	3.520	14.079	3	2	1	0.9944	10.6098
2.65118	0.14227	4.026	16.106	4	0	0	0.9934	10.6047
2.49925	0.16010	4.531	18.124	4	1	1	0.9932	10.6034
2.37211	0.17772	5.030	20.118	4	2	0	0.9941	10.6084
2.26187	0.19546	5.532	22.127	3	3	2	0.9943	10.6091
2.1643	0.21348	7.042	24.167	4	2	2	0.9931	10.6029
2.0801	0.23112	6.541	26.163	4	3	1	0.9938	10.6065
1.93578	0.26686	7.552	30.210	5	2	1	0.9931	10.6027
1.8743	0.28466	8.056	32.224	4	4	0	0.9930	10.6026
1.81853	0.30238	8.558	34.231	5	3	0	0.9932	10.6038
1.76782	0.31998	9.056	36.223	6	0	0	0.9938	10.6069
1.71987	0.33807	9.568	38.271	5	3	2	0.9929	10.6020
1.67641	0.35583	10.070	40.281	6	0	2	0.9930	10.6025
1.63636	0.37346	10.569	42.277	5	4	1	0.9934	10.6048
1.5986	0.39131	11.074	44.298	6	2	2	0.9933	10.6039
1.56336	0.40915	11.579	46.317	6	3	1	0.9931	10.6032
1.53034	0.42700	12.084	48.338	4	4	4	0.9930	10.6025
1.49953	0.44472	12.586	50.344	5	4	3	0.9932	10.6033
1.47019	0.46265	13.093	52.374	6	0	4	0.9929	10.6017
1.44306	0.48021	13.590	54.362	5	5	2	0.9933	10.6043
1.41678	0.49819	14.099	56.397	6	4	2	0.9930	10.6022
1.34645	0.55159	15.611	62.443	6	5	1	0.9929	10.6020

Table for Exercise 3.

The peaks at 38, 44 and 82° are due to the Al sample holder used for the experiment. You might be able to guess this from the fact that, e.g., the 82° peak is so strong (normally intensities fall off with 2θ). You may be able to index the Al peaks as well. Al is fcc so you only expect all odd/all even hkl combinations. Indexing of the Al peaks is included in the table above.

The second pattern is Y_2O_3, which is body centred ($Ia\bar{3}$). If you try the same method for WO_3, and assume the first peak is (100) you will get stuck when you find that the second reflection has a ratio of 1.5. If you double the value of all ratios it is the same as saying the first peak is 110 ($h^2+k^2+l^2=2$) and not 100. You will then be able to index reflections until the fourth peak, for which $h^2+k^2+l^2$ is 7 (for which there are no valid indices). To get round this you have to multiply the ratio by 4 instead. This is the same as assuming the first peak is (200). If you then index everything you will see that reflections observed all have $h+k+l$ even – the condition for body centring. To save time just work with the first 10 peaks.

3. **For the second example of exercise 2 calculate the cell parameter from each reflection indexed. Which data should be used to obtain precise cell parameters? Why?** Use $a = d(h^2+k^2+l^2)^{1/2}$. For accurate cell parameters it is best to use high 2θ values. Many systematic errors (e.g. zero point) are linear in $2\theta - d$-spacing is not! From a table like the one above you should be able to see that cell parameters converge to an approximately consistent value for the high-angle data. The Rietveld-refined cell parameter of this sample is 10.602 Å.

   The following graphs plot this for both data sets. Rietveld refinement for the Na_xWO_3 example suggests that the sample was actually mounted with a height error of 0.16 mm and had a cell parameter of 3.8548 Å. Peak shapes also show the material is probably actually tetragonal.

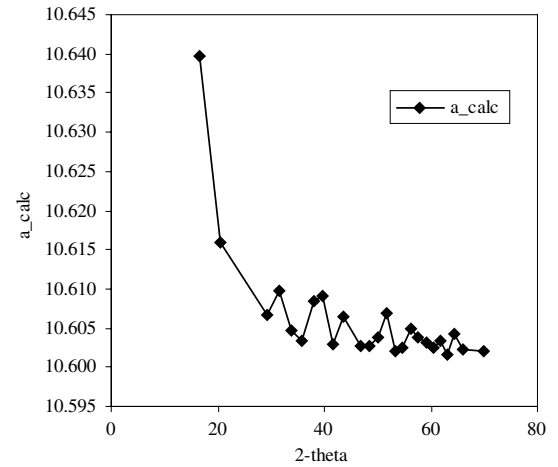

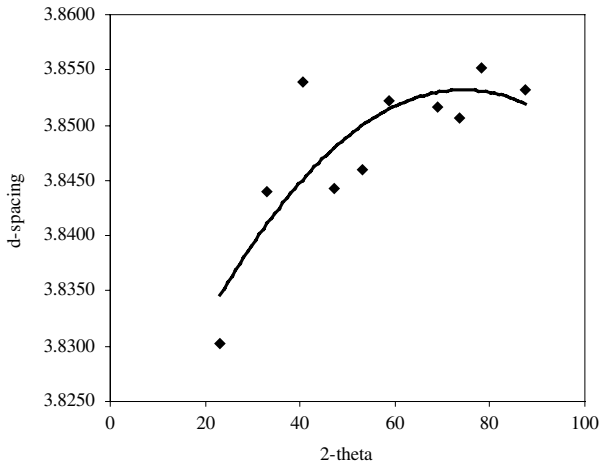

4. What experimental factors can cause systematic errors in cell parameter determination? How would one obtain the most precise and most accurate cell parameters possible?

2θ zero errors; sample height errors; sample absorption leading to an effective height error; axial divergence leading to peak asymmetry causes peak maxima not to be in the correct place; α_1/α_2 splitting is not resolved at low 2θ and is at high 2θ so be careful when peak picking; temperature errors; the best way is to use an internal standard (e.g. NBS Si) that has a known cell parameter and calibrate accordingly.

5. Figure 17.9 shows diffraction data recorded for an octahedral Fe^{II} complex (Fig. 17.10) at six different temperatures. Comment on these data.

These data show a phase transition in an iron co-ordination compound as it undergoes a high-spin to low-spin phase transition (Fe^{II} d^6). From the powder data you should be able to infer that there are no major structural changes that occur as intensities do not change hugely. With good-quality data one should be able to refine a change in Fe–L bond distances but the intensity changes would not be noticeable by eye. You should be able to plot a very rough sketch of thermal expansion from the peak d-spacings given and convince yourself that it is a first-order transition, as there is an abrupt change in volume at the transition. You would expect to see hysteresis in the cell volume as a function of temperature as it is first-order.

6. Use the Scherrer formula (Section 17.4.3) to obtain a crude estimate of the size of the crystalline domains in Figs. 17.5(a) and (b).

The values derived from whole-pattern fitting using an empirical instrumental function and convoluting terms to describe size broadening are given in the text.

Approximate sizes can be derived from the figure and the Scherrer equation. For Fig. 17.5(a) the peak width is around 4°, which is 0.070 radians. Assuming the peak is at $2\theta = 40°$ the formula gives 21 Å or around 2 nm. For (b) the width is around 1° or 0.0175 radians, giving a size of 84.5 Å or 8.5 nm. These data are verified by TEM measurements (see below), suggesting one has single-domain nanoparticles.

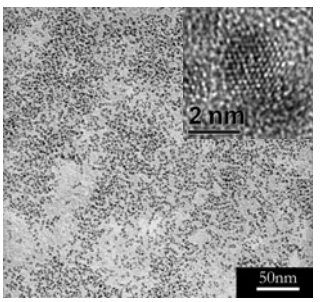

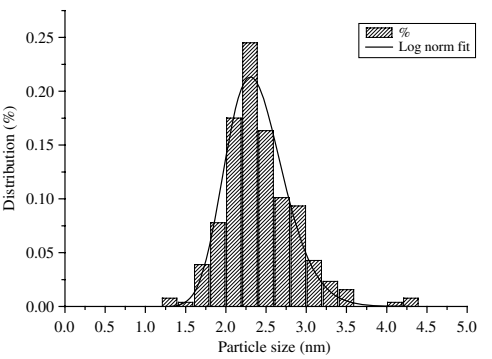

Chapter 18

1. To which point groups do the following space groups belong? $P\bar{1}$, $P2_1/c$, $P2_12_12_1$, $Cmca$, $I\bar{4}$, $P3_121$, $R\bar{3}m$, $P6_3/mmc$, $Pa\bar{3}$?

$P\bar{1}$, $\bar{1}$; $P2_1/c$, $2/m$; $P2_12_12_1$, 222; $Cmca$, mmm; $I\bar{4}$, $\bar{4}$; $P3_121$, 321; $R\bar{3}m$, $\bar{3}m$; $P6_3/mmc$, $6/mmm$; $Pa\bar{3}$, $m\bar{3}$.

2. Explain why it is often stated that a low value for $\langle|E^2-1|\rangle$ can indicate twinning. What values of this parameter are expected for untwinned structures, and what values might be expected for a twinned structure? Under what circumstances might this parameter be misleading?

*E*s are *F*s corrected for finite atomic size and vibrational motion. Wilson statistics show that, if a structure is centrosymmetric, then $\langle|E^2-1|\rangle$ is expected to be about 0.97; if it is non-centrosymmetric then this parameter should be about 0.74. A twin might have a value 0.2 or so below these values, although this varies from system to system. A value of 0.4 would look suspicious. Reason: twinning causes reflections to overlap, thus averaging their intensities out a little; this gives a low $\langle|E^2-1|\rangle$ value. Wilson statistics assume a random distribution of scattering power in the unit cell. If this is not the case, e.g. in a heavy-atom structure, the value of $\langle|E^2-1|\rangle$ may be much lower than expected. Consider α-Po for example: Po scatters into all reflections and $\langle|E^2-1|\rangle$ is zero!

3. Suggest twin laws that might arise from structures with the following unit cells. In each case state which reflections would be affected and what features would help diagnose the twinning.

(a) Monoclinic, with $\beta \sim 90°$.

(b) Monoclinic *P* with $a \sim c$.

(c) Orthorhombic with two edges approximately equal.

a) Pseudo-orthorhombic and so 2-fold rotations about **a** and **c**, and mirrors perpendicular to **a** and **c** would work. Only the 2-fold axes would be relevant if the compound were chirally pure. A 2-fold rotation about **a** would be (1 0 0 / 0 −1 0/ 0 0 −1). All reflections would overlap, so this would not be spotted at the data-collection stage. If the twin scale factor was 50% the Laue symmetry would appear to be *mmm*. Merging in *mmm* would get progressively worse as the scale factor drops. Just how much worse it gets can be used to estimate the scale factor. If this information is available and the scale factor is significantly less than 0.5 an attempt can be made to untwin the data set and so solve the structure. There would be problems determining the space group if orthorhombic symmetry was assumed. For example, if the true space group was $P2_1$, assumption of orthorhombic symmetry would imply space group $P22_12$ (no absences along a^* or c^*), which is rather unusual. A low $\langle|E^2-1|\rangle$ value may indicate twinning. The structure would probably be difficult to solve, especially if no heavy atoms were present. A Patterson search would be well worth a try.

b) This cell can be transformed into orthorhombic *C*. A 2-fold axis along the [101] direction would work:

$$\begin{pmatrix}0&0&1\\0&-1&0\\1&0&0\end{pmatrix}\begin{pmatrix}h\\k\\l\end{pmatrix}=\begin{pmatrix}l\\-k\\h\end{pmatrix}.$$

All reflections affected, and so the comments made above apply. Note that if the space group were $P2_1/c$ the ($h0l$) absences would overlap with ($l0h$) reflections from the other domain, and so the space group would appear to be $P2_1$.

c) Pseudo-tetragonal, and so a 4-fold rotation about one axis or a 2-fold rotation about the square-face diagonal would work. All data are affected.

4. Consider a triclinic crystal structure with a unit cell with approximately orthorhombic metric symmetry.

(a) How many domains are possible if the crystal forms a twin and the space group is $P\bar{1}$?

The lattice has *mmm* symmetry (order = 8), the point group of the crystal structure is only $\bar{1}$ (order 2). Therefore four domains are possible.

(b) What twin laws are possible if the space group is $P\bar{1}$?

Two-fold rotations about the three unit cell axes would generate *mmm*.

(c) How many domains are possible if the space group is *P*1?

If the crystal structure belongs to point group 1 then in principle eight domains are possible. If the material is enantiopure, however, inversions and mirrors are not allowed, so the number of domains would still be 4.

5. In Example 6 a mirror perpendicular to [100] was used to model twinning. Write down in matrix form the twin laws corresponding to $6^+_{[001]}$ and $m_{[110]}$ that are equivalent to this operation.

$6^+_{[001]}$ and $m_{[110]}$ are:

$$\begin{pmatrix}1&1&0\\-1&0&0\\0&0&1\end{pmatrix}\text{ and }\begin{pmatrix}0&-1&0\\-1&0&0\\0&0&1\end{pmatrix}.$$

6. Which reflections would be affected in the presence of the following twin laws?

(a) $\begin{pmatrix} -1 & 0 & 0 \\ 0 & -1 & 0 \\ 0 & 0 & 1 \end{pmatrix}$

(b) $\begin{pmatrix} -1 & 0 & -0.33 \\ 0 & -1 & 0 \\ 0 & 0 & 1 \end{pmatrix}$.

(a) $\begin{pmatrix} -1 & 0 & 0 \\ 0 & -1 & 0 \\ 0 & 0 & 1 \end{pmatrix} \begin{pmatrix} h \\ k \\ l \end{pmatrix} = \begin{pmatrix} -h \\ -k \\ l \end{pmatrix}$.

All the transformed indices (which correspond to indices from the second domain) are integers and so all reflections from the first domain overlap.

(b) $\begin{pmatrix} -1 & 0 & -\frac{1}{3} \\ 0 & -1 & 0 \\ 0 & 0 & 1 \end{pmatrix} \begin{pmatrix} h \\ k \\ l \end{pmatrix} = \begin{pmatrix} -h - \frac{l}{3} \\ -k \\ l \end{pmatrix}$.

The transformed indices are integral only when $l = 3n$. So only $l = 0, \pm 3, \pm 6 \ldots$ layers will be affected.

7. Suggest twin laws that might arise from structures with the following unit cells. In each case state which reflections would be affected and what features would help diagnose the twinning.

(a) Orthorhombic P, $a = 4.49$, $b = 16.74$, $c = 9.01$ Å.

(b) Monoclinic P, $a = 5.50$, $b = 11.49$, $c = 6.34$ Å, $\beta = 98.3°$.

(a) Notice that $c \sim 2a$, so there is a pseudo-tetragonal supercell. There are various possibilities for the symmetry element of this; if we use the 4-fold rotation (about **b**), the twin law would be:

$$\begin{pmatrix} 1/2 & 0 & 0 \\ 0 & 1 & 0 \\ 0 & 0 & 1 \end{pmatrix} \begin{pmatrix} 0 & 0 & 1 \\ 0 & 1 & 0 \\ -1 & 0 & 0 \end{pmatrix} \begin{pmatrix} 2 & 0 & 0 \\ 0 & 1 & 0 \\ 0 & 0 & 1 \end{pmatrix} = \begin{pmatrix} 0 & 0 & 1/2 \\ 0 & 1 & 0 \\ -2 & 0 & 0 \end{pmatrix}.$$

Thus, the $l = 2n$ data are affected. Probably the crystal would appear to be tetragonal at the data-collection stage, but, provided the scale factor was significantly less than 0.5, pseudo-translational symmetry would be evident in the dataset.

(b) It is much harder to see this one by inspection. Actually, most monoclinic twins are affected by 2-fold rotations about **a** and **c**. The matrices for these are given in Chapter 18, so a good strategy is to work out the ratios $-2a\cos\beta/c$ and $-2c\cos\beta/a$. If either is nearly rational then the corresponding rotation is a likely twin law. Here, $-2a\cos\beta/c = -0.25$ and $-2c\cos\beta/a = -0.33$, and both are nearly rational ($-\frac{1}{4}$ and $-\frac{1}{3}$). The matrix for a 2-fold rotation about **a** is (1 0 0/ 0 −1 0/ −0.33 0 −1). This will affect the $h = 3n$ data. That for a 2-fold rotation about **c** is: (−1 0 −0.25/ 0 −1 0/ 0 0 1). This would affect the $l = 4n$ data.

These could be distinguished by looking at the poorly fitting data. If these tend to have $h = 3n$ then the first matrix is likely, if they have $l = 4n$ the second is more likely. A twin like this would probably be difficult to index. The simplest method here is to allow your indexing program to tell you what the twin law is! However, if the data are from a four-circle diffractometer where the initial search found only a few reflections and the scale factor is small, this might not work.

8. Diffraction data were collected on the low-temperature phase of oxalyl chloride, $(COCl)_2$. A frame from the diffraction pattern is shown below.

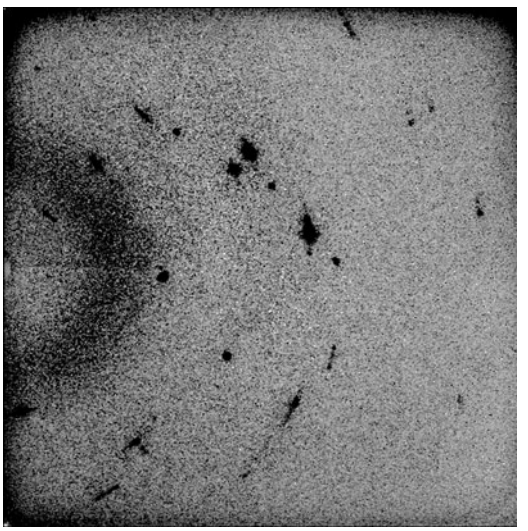

(a) Comment on the appearance of this diffraction pattern.

Note the generally nasty appearance of the pattern, particularly the split peaks.

(b) Discuss strategies that might be used to index this pattern.

Use a twin-indexing package such as CELL_NOW. Alternatively, a reciprocal lattice viewer, such as RLATT, could also be used to pick out a lattice.

(c) The pattern was indexed with the metrically orthorhombic unit cell $a = 5.342(4)$, $b = 7.270(5)$,

```
Mean |E*E-1| = 1.327 [expected .968 centrosym and .736 non-centrosym]
Systematic absence exceptions:
        b--     c--     n--   21--     -c-     -a-     -n-   -21-    --a    --b    --n    --21
N     347     317     316      7     240     235     239     12     85     97     94      26
NI>3s   4      70      68      0      79      72      73      0     28     26     22       8
<I>     0.4   115.8   116.2    0.2   204.6   335.6   275.4    0.2   59.9   40.3   78.9   347.8
<I/s>   0.5     1.9     1.8    0.2     2.6     2.6     2.5    0.4    2.3    2.1    2.0     2.8

Identical indices and Friedel opposites combined before calculating R(sym)
No acceptable space group - change tolerances or unset chiral flag
or possibly change input lattice type, then recheck cell using H-option
```

XPREP output for oxalyl chloride

$c = 16.676(11)$ Å. The following (table above) was found assuming orthorhombic symmetry using XPREP. Show that these data are consistent with the correct space group being $P2_1/c$ with $a = 16.67$, $b = 5.34$, $c = 7.26$ Å, $\beta = 90°$.

There are absences in the $0kl$ (k odd, b–) and $h00$ (2_1–) index classes. The absences in the $–2_1–$ class are just a subset of the former. These absences do not correspond to any orthorhombic space group, but do correspond to the monoclinic space group $P2_1/b11$. This is just a non-standard setting of $P2_1/c$, with the new b = old a and new c = old a.

(d) Calculate Z' and comment on the mean value $\langle|E^2 - 1|\rangle = 1.327$.

The volume of the cell is 646.3 Å^3. Applying the 18 Å^3 rule gives six molecules per cell. This is relatively unusual, though not impossible here, as the oxalyl chloride molecule is centrosymmetric, and so $Z' = 1.5$ is possible. The value of $\langle|E^2 - 1|\rangle$ is unusually high, and implies a distribution comprising both strong data and weak (or absent) data.

(e) A Patterson map calculated using the second cell given in part (c) showed a very strong non-origin peak at [1/3 0 2/3]. Suggest a transformation to a smaller unit cell.

$$\begin{pmatrix} 1/3 & 0 & 2/3 \\ 0 & 1 & 0 \\ 0 & 0 & 1 \end{pmatrix}$$

is possible, though this would give a very acute β angle (cell OABC in the diagram), and it is better to use

$$\begin{pmatrix} 1/3 & 0 & -1/3 \\ 0 & 1 & 0 \\ 0 & 0 & 1 \end{pmatrix} \text{ cell 0ACD.}$$

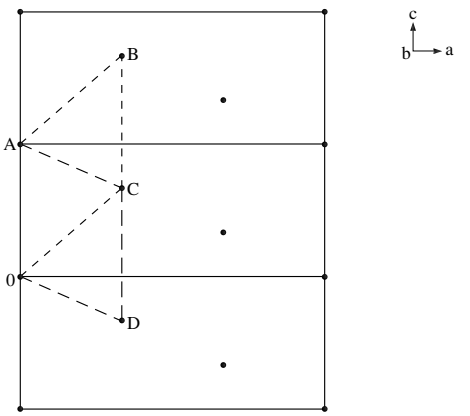

(f) What are the dimensions of this smaller cell?

From the figure above

a' = length of the vector $(1/3\ 0\ -1/3) = [(16.67/3)^2 + (7.26/3)^2]^{1/2} = 6.06$ Å

$b' = b = 5.34$ Å

$c' = c = 7.26$ Å.

β can be obtained from the dot product

$$(\mathbf{a}/3 - \mathbf{c}/3).\mathbf{c} = \mathbf{a}.\mathbf{c}/3 - \mathbf{c}.\mathbf{c}/3$$
$$= (16.67 \times 7.26 \times \cos 90)/3 - (7.26^2/3)$$
$$= 0 - (7.26^2/3)$$
$$= 6.06 \times 7.26 \times \cos\beta$$

so $\beta = 113.5°$.

(g) The structure of oxalyl chloride was successfully modelled as a twin. What is the likely twin law?

The likely twin law is a two-fold rotation about the a- or c-axis of the larger pseudo-orthorhombic cell. This can be expressed on the axes of the small

monoclinic cell by forming a triple matrix product:

$$\begin{pmatrix} 1/3 & 0 & -1/3 \\ 0 & 1 & 0 \\ 0 & 0 & 1 \end{pmatrix} \begin{pmatrix} 1 & 0 & 0 \\ 0 & -1 & 0 \\ 0 & 0 & -1 \end{pmatrix} \begin{pmatrix} 3 & 0 & 1 \\ 0 & 1 & 0 \\ 0 & 0 & 1 \end{pmatrix} = \begin{pmatrix} 1 & 0 & 2/3 \\ 0 & -1 & 0 \\ 0 & 0 & -1 \end{pmatrix}.$$

Chapter 19

No exercises.

Chapter 20

No exercises.

Chapter 21

No exercises.

Chapter 22

No exercises.

This page intentionally left blank

Index

$\alpha-$doublet 254–5
absences, systematic 44–7, 49, 51, 61, 94, 176, 184, 264, 280, 282, 284, 286, 287–8
absorption 43, 75, 174, 189, 197, 233–4, 243, 247–8, 256, 341
absorption correction 41, 65, 70, 75, 90, 94–5, 177, 198–9, 282
absorption edge 1, 191, 255, 257
accuracy, *see* precision and accuracy
amplitudes 4, 5, 54–5, 170
  in direct methods 133–4, 140
  in Fourier syntheses 104–9, 110–14, 117–18, 172–3
  normalized, *see* structure factors, normalized
analogue of diffraction, optical, *see* microscope, analogy for X-ray diffraction
analysis of variance 234, 236, 245
angle, dihedral 211–13
area detector 41, 53, 54, 62, 65, 67, 70, 73–75, 77–82, 90, 98–9

body, rigid 217–8
bond valence 195–6, 201–2
Bragg angle 6, 71, 80, 95, 175
Bragg–Brentano geometry 254
Bragg's law (Bragg equation) 6, 7, 55–6, 170, 257
Bravais lattice, *see* unit cell centring

capillary tubes 34, 37–8, 256–7
cell, unit 2, 3, 11–12, 51, 104–5, 118–19, 209, 271–2
  centring 14–15, 19, 22, 45–6, 61, 120, 197, 279
  contents 21, 43–4, 88, 247, 265
  determination 58–64, 84–8, 94, 264, 283
  origin 18, 51, 122, 129–30, 140–1, 144
  parameters 2–3, 14, 49, 56, 57, 62–3, 211, 243
Central Limit Theorem 227–9, 233
chirality 13–14, 22–3, 42, 48–9, 184, 207, 272
CIF (crystallographic information file) 299, 310, 315, 319–26
configuration, absolute, *see* structure, absolute
conformation 207, 213, 246
constraints
  in direct methods 134–41
  in refinement 21, 160–2, 180, 184, 191, 192, 210, 214, 216, 245, 248, 311
convolution 3, 119, 133–4, 135, 258, 351–2
correlation, *see* covariance and correlation
coset decomposition 279–80, 290, 291, 291–2
covariance and correlation 158, 160, 178, 191, 209–11, 216, 240–2, 263
crystal growth 28–34, 189, 271
crystal morphology (shape) 19, 42, 90
crystal mounting, sample mounting 36–9, 62, 254–6
crystal packing 18, 232, 304–5
crystal screening, crystal evaluation 35–36, 42–3, 82–4
crystal, single 9, 28, 33, 34, 35, 42
crystal system 14–15, 17–20, 22, 35, 43–4, 51, 54

damping, *see* restraints, shift-limiting
databases 34, 87–8, 195, 230, 258–9, 294, 321, 327–31
data collection 41–2, 56, 61–2, 64–7, 73–90
data completeness 64–5, 89–90, 95, 176
data reduction 67–71, 93–8
data, unique, *see* set of data, unique
Debye–Scherrer rings 254
degrees of freedom 158, 224, 231, 239
density of crystals 43–44, 192
design matrix 157, 159, 180
deviation, estimated standard, *see* uncertainty, standard
deviation, standard 155–6, 222, 224–5, 229–30, 232, 236
difference electron density 110–13, 114, 172–3, 174, 245, 248
diffraction, multiple, *see* Renninger reflection
diffraction pattern 2, 3, 4–5, 9–10, 18–20, 54, 64–5, 74, 99, 104–5, 110, 170, 192, 193, 194–5, 252–3, 257, 258–65, 274–6, 280–1, 282
diffractometer 36, 39, 62–4, 65–6, 73–5, 80, 243, 254–8
diffusion, liquid 30–1
diffusion, reactant 31–2
diffusion, vapour 31
disorder 28, 50, 76, 104, 108, 174, 176, 182–3, 189, 190–4, 197–8, 214, 215, 218, 246
dispersion, anomalous, *see* scattering, anomalous
displacement ellipsoid 215, 303–4
displacement parameters 103–4, 172, 181–2, 214–8, 243
  anisotropic 103, 215–6
displacements, atomic, *see* displacement parameters
distribution, normal (or Gaussian) 155, 211, 225–7, 230–1
distributions, statistical 47–8, 222–9, 233

electron density 5, 6, 7–8, 103, 134–5, 135–40, 170–2, 182–3, 184
  from direct methods 141, 145–6
  from Fourier synthesis 105–7, 108, 109–10, 113–14, 170, 172–3
  and maximum entropy 150, 151, 153–4
ellipsoid, thermal, *see* displacement ellipsoid
entropy, maximum 140, 149–54
equations, normal 157, 161, 162, 166, 183
equations, observational 156–7, 158, 159, 162–4, 165–6
errors, random 177, 178, 221–2, 221–32
errors, systematic 76, 145, 174, 176, 178, 214, 221–2, 242–7
E-map 109, 145
E values, *see* structure factor, normalised
Ewald sphere 56–8, 69
extinction (optical) 35–6, 42–3
extinction (primary and secondary) 70, 94, 181, 182, 243

figures of merit 141, 144–5
Flack parameter, *see* structure, absolute
Fourier transform, Fourier synthesis 6, 9, 54–5, 64, 103–14, 133–4, 135, 146
  in structure refinement
  in structure solution 117–19, 126–7, 133–4
Friedel pairs 183
Friedel's law 4, 19–20, 64–5

Gaussian distribution, *see* distribution, normal
gel crystallization 32–3
geometry of diffraction 9–10, 55–8, 254
geometry of molecular structure 128, 181, 205–7, 209, 210–11, 217, 232, 242, 245, 310–12, 328
goniometer head 36–7, 39, 62
goodness of fit 173, 183, 235–6, 261
graphics, molecular 300–9
group, rigid 128, 210–11

Harker lines and planes (sections) 123–6
Hermann–Maugin notation 13–14
high-pressure data collection 77, 266
hydrogen atoms 47, 111–13, 182, 210, 213–14, 245, 308, 340
hydrogen bonding 213–4, 303, 305, 311–12

ill-conditioning and singular matrix 164–5, 180, 246
indices, indexing 6, 55–62, 85–7, 104, 106, 264, 282–3, 285
inequality relationships 136, 138, 140
integration, *see* data reduction
intensity 3, 4, 5, 9–10, 44, 54–5, 64, 65–7, 67–71, 81, 88–90, 93–4, 142, 170, 175 252–4, 255–6, 257, 259, 261, 262, 265, 274, 337
intensity statistics 47–8, 141, 228–9, 264, 275–6, 284
interactions, intermolecular 213, 273
International Tables for Crystallography 17, 50–1, 122, 278

Karle-Hauptmann determinants 136–7

Lagrange multipliers 160–1
lattice 2–3, 11–12, 14–15, 45, 58–9, 69
lattice centring, *see* cell, unit
lattice planes 6, 55–8, 69, 70, 71, 136–7
lattice, reciprocal 2–3, 36, 45, 57, 58–62, 87, 170, 208
Laue class, Laue symmetry 19–20, 21–22, 41, 43–4, 48–9, 61–2, 64–5, 89–90, 120, 276, 283
least-squares planes 211–13, 310
least-squares refinement 156–66, 169–85, 200–1, 232–4, 240, 261
leverage 176
libration 182, 217–18
Lorentz-polarization corrections 69–70, 94, 261
low-temperature (and high-temperature) data collection 38–9, 76–7, 176, 197–8, 200, 218, 243, 246, 265–6

matrix, singular, *see* ill-conditioning
mean 155–6, 224–5, 229–30, 231–3
methods, direct 133–46
microscope 35–36, 42
  analogy for X-ray diffraction 7, 9, 53–55, 105–6
Miller indices, *see* indices
minimum, false 180, 263
model, riding 210
monochromator 69–70, 254–5, 257, 334, 337
mosaic spread, mosaicity 35, 89
mother liquor, *see* solvent
multiplicity of atom site, *see* site occupancy factor

neutron diffraction 191, 214, 257–8, 266, 339–41

orientation matrix 62–4, 84–7, 93
origin, floating, *see* polarity
outliers 178, 179, 225, 233–5

parameters, in refinement 104, 155–8, 161–6, 172–3, 175, 178, 182–3, 205, 231, 240–1, 261–3
parameters, thermal, see displacement parameters
Patterson search 128–30
Patterson synthesis, Patterson map 109, 117–30
phase change, phase transition 38, 77, 99, 176, 189, 190–1, 194–5, 265–6, 273, 284
phase identification and analysis 258–9, 262–3
  phases (of reflections) 1–2, 4, 5, 6, 8, 54–5, 104–14, 133–5, 142–4, 170, 172–3
  determination 134–46
point group 10, 12, 14, 19–20, 21, 22–3, 42, 51, 213
polarity, floating origin 22–3, 51, 125, 126–7, 129–30, 165, 210, 244
polarization of light, *see* microscope
positions, general and special 21, 23, 44, 51, 122–7, 210, 216
powder diffraction 99, 194, 251–67
precipitant (antisolvent) 28, 30–1
precision and accuracy 183, 205, 210, 211, 213–14, 218, 222, 240, 242, 264
probability distribution function (pdf) 138, 225–6
probability plot, normal 236–8
pseudo-symmetry 49, 50, 126–7, 183–4, 190, 194–5, 196–9, 199–202, 271–2, 280–2, 283, 284, 293–4
publication 299, 304, 307, 309, 310, 311, 315, 321

quartets, negative 137, 144

recrystallization, *see* crystal growth
refinement
  of crystal structure, *see* least-squares refinement
  of unit cell 87, 94
reflection profiles 65–7, 68–9, 93, 260–1, 263
reflections, equivalent (by symmetry) 43, 61–2, 64–5, 90, 95, 105, 107, 194, 222–3
Renninger reflection (multiple diffraction) 49, 94, 176
replacement, molecular 140
residuals, *see R* indices
resolution, series termination 7–8, 108, 114, 135, 173, 175–6, 253
restraints 158–60, 180, 181, 182, 183, 184, 191, 192, 201, 210, 214, 218, 245, 248
  shift-limiting 180, 181
Rietveld refinement 261–4
R indices, *R* factors 174, 177, 181, 191, 198–9, 238–9, 261–2
rule, 18Å^3 44

samples, air-sensitive 38–9
Sayre's equation 139–40, 146
scattering, anomalous 1, 2, 4, 19, 48–9, 183, 191, 243–4, 257
  use in absolute structure determination, *see* structure, absolute
scattering factor, atomic 1–2, 4, 103–4, 112, 135, 139, 172, 189, 215, 243, 245, 339–41; *see also* scattering, anomalous
scattering, (thermal) diffuse 71, 94, 100, 176, 193–4, 243
series termination, *see* resolution
set of data, unique 41, 56, 61–2, 64–5, 90, 107
significance level in statistical tests 239
site occupancy factor 104, 182, 183, 190, 191–2

solvent 28–32, 33, 39
  of crystallization 27–8, 29, 35, 38, 44, 88, 182
Soxhlet apparatus 30
space group 17–18, 18–20, 21, 22–23, 41–51, 121–8, 190, 192, 197, 200, 246, 264
  of Patterson function 119–20
stereoscopy 306–7, 309
strain 196, 260–1
structure, absolute 75, 182, 183, 248, 276–7
structure factor 4, 5, 6, 54–5, 64, 68–9, 104–6, 109, 117, 133–4, 170, 172, 178, 345–6
  calculated 105, 110
  normalized (*E*-value) 47–8, 121, 135–6, 137–8, 139, 140–1, 142
  observed 105
structure, incommensurate 74, 99, 190, 194–5
structure invariants 140–1, 143
structure, model 103, 110–14, 172–3, 175, 177, 178–9, 180–3, 190, 191–2, 195, 196, 200–1, 215, 221, 236, 238, 239, 244–7, 259, 261, 262, 264–5
structure validation 173–4, 195–6, 201–2, 247–8, 325–6
subcell, supercell, *see* pseudo-symmetry
sublimation 33
substructure, superstructure, *see* pseudo-symmetry
symmetry element, symmetry operation 12–14, 15, 16–18, 19, 21, 42, 47, 51, 123, 210, 216, 242, 246, 271–3, 280
symmetry, metric 21–2, 43, 49, 61–2, 253, 279, 283–4
symmetry, molecular 12–15, 20, 311
synchrotron radiation 71, 76, 257, 266, 335–9

tangent formula 139–40, 141, 142–3, 144
tensor, metric 208
temperature factors, *see* displacement parameters
Thomson scattering 1
torsion angle 207, 212, 213
translation symmetry 10–12, 16–17
twin law 272, 274–6, 279–80, 282–3
twinning 28, 29, 42–3, 49, 74, 85, 98–9, 170, 179, 189, 192, 194, 271–95
  by inversion 276–7
  merohedral 277–8, 279, 289–91
  non-merohedral 280–3, 292–4
  pseudo-merohedral 278, 285–9, 291–2
twin scale factor 272, 276

uncertainty, standard 205, 222
  in data 177, 261
  in molecular structure 209–10, 211, 242
  in refined parameters 178, 210–11, 240
unit, asymmetric 20, 21, 51, 103–4, 107, 121–6, 140, 195, 199–200

variance 143–4, 151, 155–6, 158, 165, 212, 224, 229

weights
  in direct methods 144
  in Fourier syntheses 112–13
  in least-squares refinement 157–8, 159–60, 161–3, 178–9, 183, 197, 212, 214, 232–8, 240, 244, 261–2
  in mean values 155–6, 224–5, 229–31
Wilson plot 142

X-ray photographs 36
X-ray sources 75–6, 254, 333–9
X-ray wavelength 6, 12, 55–6, 70, 75–6, 257, 334, 337

Z and *Z*′ (unit cell contents) 21, 43–4, 51, 183–4, 247